



UNIVERSITAT<sup>DE</sup>  
BARCELONA

## Polycyclic group optimization in 11 $\beta$ -HSD1 inhibitors and their pharmacological evaluation

Rosana Leiva Martínez



Aquesta tesi doctoral està subjecta a la llicència **Reconeixement 3.0. Espanya de Creative Commons.**

Esta tesis doctoral está sujeta a la licencia **Reconocimiento 3.0. España de Creative Commons.**

This doctoral thesis is licensed under the **Creative Commons Attribution 3.0. Spain License.**



UNIVERSITAT DE  
BARCELONA

UNIVERSITAT DE BARCELONA  
FACULTAT DE FARMÀCIA I CIÈNCIES DE L'ALIMENTACIÓ

**POLYCYCLIC GROUP OPTIMIZATION IN 11 $\beta$ -HSD1 INHIBITORS  
AND THEIR PHARMACOLOGICAL EVALUATION**

Rosana Leiva Martínez

2017



UNIVERSITAT DE BARCELONA  
FACULTAT DE FARMÀCIA I CIÈNCIES DE L'ALIMENTACIÓ

PROGRAMA DE DOCTORAT DE  
QUÍMICA ORGÀNICA EXPERIMENTAL I INDUSTRIAL

**POLYCYCLIC GROUP OPTIMIZATION IN 11 $\beta$ -HSD1 INHIBITORS  
AND THEIR PHARMACOLOGICAL EVALUATION**

Memòria presentada per Rosana Leiva Martínez per optar al títol de  
Doctora per la Universitat de Barcelona

Director i tutor: Dr Santiago Vázquez Cruz

Doctoranda: Rosana Leiva Martínez

Rosana Leiva Martínez

2017



A la meva família, als meus pares i germà.

I a *tu*, la meva família escollida.



Follow the problem. Not the subject.

‘We are not students of some subject matter, but students of problems.  
And problems may cut right across the borders of any subject matter or discipline.’

Karl Popper, 1963





Las primeras páginas de esta tesis van a ser las que dedique a todas aquellas personas que me han ayudado y apoyado durante estos años y que de una manera u otra han hecho posible este trabajo.

Y qué mejor que empezar con mi director; a Santi, a la vez compañero de este viaje, al que le debo tanto y del que he aprendido mucho más. Se quedan cortas las palabras para expresar lo agradecida que estoy, por haberme *captado* en segundo de carrera, por haberme invitado rápidamente a unirme a tu grupo, por transmitirme esa pasión por la investigación, ese afán de querer más. Siempre disponible, siempre atento, siempre protegiendo a la vez que dando alas para crecer. Gracias por la confianza, el aprecio, ya sabes que es mutuo, y que esto no es un punto final.

Continuaré con el resto de profesores del laboratorio. A Pelayo, por ser el referente y maestro de la *familia Química Farmacèutica*, agradeciéndole sus ánimos siempre con una sonrisa cuando quedábamos de los últimos del laboratorio y se preocupaba que no nos quedara demasiado para irnos a casa. A Diego, por sus ganas de ayudar, de escuchar, por aportar su rigurosidad en momentos necesarios y, especialmente, por aceptar rápidamente a formar parte de mi tribunal de tesis. A Carmen, última incorporación del grupo a nivel formal, aunque ya la teníamos medio *fichada* con nuestras comidas en la biblioteca que no serían lo mismo sin ella, sin sus risas, sin sus *zascas*. Las comidas diarias de todos juntos son un claro ejemplo de la *familia* que habéis creado, fomentado y cuidado siempre.

Querría resaltar el agradecimiento a otros grupos de investigación que han colaborado en este trabajo. En primer lugar al Dr. Scott Webster y su grupo en el QMRI de la University of Edinburgh. Thanks Margaret and Andrew for testing the compounds of this Thesis and Scott for accepting me in your research group to understand the whole process and learn more about 11 $\beta$ -HSD1 from an expert like you. Also thanks to Roberta for her support and our walks around Edinburgh. En segundo lugar pero no menos importante, al grupo del profesor Dr. F. Javier Luque del Departament de Nutrició, Ciències de l'Alimentació i Gastronomia. A Constantí, Axel y Javi por realizar los ensayos computacionales de esta tesis; por lidiar con esta proteína tan *difícil* y siempre estar dispuestos a ayudar y explicar de la forma más didáctica posible sus cálculos. Y por último al grupo de la profesora Dra. Mercè Pallàs de la Unitat de Farmacologia. A Christian, Dolors i Mercè por realizar los ensayos *in vivo*; por su eficacia y afán por aportar al proyecto su amplio conocimiento en el tema de neurodegeneración; ha sido el inicio de muchas otras colaboraciones en curso, gracias!

Aunque no ha sido incorporado en esta tesis, mi trabajo realizado durante la estancia en el laboratorio de la profesora Dra. Helma Wennemers del ETH Zürich ha sido clave para mi formación y me gustaría tener unas palabras para la gente que fue partícipe de ello. First of all, thanks to Helma for accepting me so quickly in her *group-family*; since the moment I met you in La Coruña, your enthusiasm and charm *captured* me and I knew that I wanted to be part of your group during some time. I enjoyed a lot my time there, I learnt a lot and I met wonderful people who make me remember my stay with lovely memories. Rüdiger, my supervisor and a friend at the same time, who could transmit

me his fascination for chemistry. My other labmates Patrick and Carla, thanks for all the support, conversations, recommendations, the bike... and staying right up to the end my last night. Last but not least, all the rest of the *family* who greeted me so warmly in the lab activities and also in the outside plans: lunches, dinners, aperos, the hicking, the volleyball :) Bartosz, Ula, Matt, Mattia, Jessica, Michal, Carlotta, Stefano, Stefanie, Oli, Elena, Andy, Nellie, Jasmine, Tobi, Rebecca, Nina, Cedric, Andreas, Raffa and Esther. Thank you all very much and I wish you all the best!

Al personal Científico-Tècnic de la Universitat de Barcelona que con su trabajo ha posibilitado la realización de esta tesis. Al equipo de la Unitat de RMN y la Unitat de masses, con especial énfasis en Ana por su siempre disponibilidad para ayudar; y al Servei de Microanàlisi por la realización de los análisis elementales. A Maite, por su ayuda y eficiencia en cuestiones más allá de la ciencia; y a Javier, porque no deja a nadie indiferente. A Josep, por siempre tener unas palabras simpáticas al cruzarnos por la facultad y por coordinar el equipo *bricomanía* siempre tan resolutivo liderado por Armando.

Porque esta tesis y todo el periodo detrás vivido no sería para nada lo mismo sin la *familia Química Farmacèutica*. Los compañeros que crean el ambiente en el lab, que te apoyan, te enseñan, y te regalan su amistad, una amistad que perdura; eso no tiene precio y es lo mejor que me llevo de esta etapa. Las personas que estaban cuando empecé, las que vinieron y se fueron, y las que se quedaron; un ambiente de cambio constante pero que te transmite una sensación siempre de estar en casa.

Empezar por el grupo SVC, al que le debo tanto. A l'Eva, per ensenyar-me, per guiar-me, per ser com una germana gran, el meu referent, dins i fora del lab; per la seva amistat i els seus consells des de l'apreci i amb el millor dels seus desitjos. Ets una crack i arribaràs on tu vulguis, ho sé! Al Matu, el meu segon mentor al laboratori, *dueño de sabios consejos*, pura bondat i sempre plena disponibilitat per ajudar i parlar de qualsevol cosa. A l'Elena, compi de vitrina en els meus inicis, de la que vaig heretar el projecte d'aquesta tesi i la seva *SEH*, apreciand així la seva dedicació per la resta, el seu suport i professionalitat. Agrair-los també als dos la seva càlida i genial acollida a Tokio, gràcies a ells recordarem el viatge sempre amb molt de carinyo. A la Marta, amiga i companya de penes i glòries, entre *estreses*, confesions i reggaetones hem crescut juntes; una font d'energia interminable, que et motiva quan penses que ja no et queden forces, que ets un *mapache* perdut. A Sandra y Eugènia, mis *mindus* que después se han convertido en amigas y compañeras de viaje de mil proyectos y desafíos, desde *persecuciones* a fármaco a bailoteos incansables; vuestro apoyo es siempre un gran pilar para mí. A Andreea, por su energía y risas que siempre animan a todo el lab. A la Jèssica, última *mindu*, pel seu compromís, eficiència i sempre amb un bon somriure. Finalment als que han passat uns mesos pel grup però que també han deixat la seva empremta: la Marta Frigolé –amb qui vaig començar i amb qui sempre podem parlar d'inquietuts i plans de futur-, la Marta M., l'Enric –sempre disposat per un sopar i una festa- i l'Olga.

Seguir con los otros dos grupos de la *familia Química Farmacèutica*, FPL y DMT por orden de aparición. A qui vaig conèixer més *senior* al lab, la Tània, gràcies per ser un referent

per a tots. Al Carles, pels seus consells tant científics com culinaris de gran xef. A l'Eli, per la paciència, l'ajuda i el saber fer que transmet. A la Irene, per ser única, per ser la *gold sponsor* dels *DailyLabs*! A Ornella, por su gran ayuda *arriba* cuando estuve entre PDBs y dockings, y por su pasión por la ciencia que siempre nos ha transmitido a todos. A l'Ane, per la confiança, les converses de present i futur, i de cotis, és clar! Al David, per tantes discussions de *tot*, pel seu suport i bons consells, qui t'escolta i et dóna la calma que necessites; i per les farres i riures. Perquè et mereixes el millor en aquesta *supra* etapa! A Javi, por el buen rollo que desprende, por estar siempre disponible para una conversación de crisis o enviar un audio de *rescate*, por ayudarme a relativizar y a valorar las cosas. Mucha suerte en los nuevos proyectos que se acercan, que las fuerzas, ganas y energía sé que las tienes! A la Katia, per tots els moments al lab i al congrés que vam anar de *parejita* a GSK Madrid; i per la seva paciència amb els *azucarillos*, perquè les seves columnes *infern* mostraven que tota la resta eren possibles. Al Toni i a l'Albert, encara que no us quedessiu no us ho tenim en compte, sou part de la família! A les recents incorporacions Sònia i *niño* Sergio, tots els ànims per una que acaba –és l'últim sprint- i l'altre que tot just comença!

Als estudiants d'aquí i d'allà que han passat pel lab i han aportat el seu granet de sorra i la seva ajuda sempre d'agrair moltíssim: Deborah, Nunzia, Carla, Eduard, Natàlia, Anna, Chiara C., Chiara R.

Finalmente, al mundo exterior más allá del laboratorio que me ha permitido desconectar del mundillo y mantener mi cordura difícil de controlar en una tesis.

Sólo tengo palabras de agradecimiento para las dos familias que me han acogido durante mis estancias. Thank you very much to Elspeth and Douglas, you are amazing! I was very lucky to stay at your home and to meet your children David and Rousy. I enjoyed a lot our musical evenings, your delicious dinners and bread and the walks outside Edinburgh. You are always invited to return the visit and discover Barcelona! Muchas gracias también a Eva y Jacob, por acogerme en vuestra casa y ayudarme a situar en Zürich. Por las noches de series, las raclettes y por dejarnos el coche para nuestro viajecillo. Tengo muchas ganas de volver y conocer vuestro nuevo hogar!

Agradecer también su acogida a Claudia y Nikole en Edinburgh y Zürich, respectivamente. A Claudia, –ya doctora!- por las comidas en el QMRI, las cenas en tu casa o en las de tus amigos, por descubrirme unos cuantos pubs de Edinburgh y por la energía y positivismo que transmites. A Nikole, por nuestros paseos por el Christmas market, por los glühweins y raclettes, e incluso antes de llegar por la ayuda y recomendaciones para buscar casa en una ciudad tan difícil como Zürich!

A todos mis amigos y amigas –imposible mencionar a todos- que con conversaciones, reflexiones y ánimos me han ayudado durante la realización de este trabajo. Als de la *Uni*, per les paraules de suport sempre i perquè no hi ha millor teràpia que llegir el nostre grup de WhatsApp. A las del ballet, por compartir una gran pasión que nos une y que nos ha hecho vivir tantos buenos momentos fuera y dentro. A Alba Calvo, por su apoyo

con sus *Rousy tú puedes!* A las marbit, por estar siempre ahí y ayudarme a relativizar en momentos necesarios.

A mi familia, mi apoyo incondicional. A mi abuela, por confiar en mí, dispuesta siempre a preparar unos boquerones o un arroz con leche para darme fuerzas. A mis tíos y primos, desde las *filiales* Cunit y Cambrils, por siempre montar findes familiares; la unión hace la fuerza! A mi hermano, a veces tan lejos pero también tan cerca cuando nos necesitamos; por tu forma de ser que me transmite calma y felicidad. Muchos ánimos también para tu último año de tesis! Y a mis padres, a quienes les debo todo; eso sí que es un apoyo absoluto. Ya sé que la familia es lo que tiene, que siempre está tu lado, que siempre te respalda, pero no tiene por qué no agradecerse un apoyo que para mí es tan importante. Gracias y mil gracias!

Me siento muy afortunada de poder seguir dando gracias por tener una segunda familia –la de *Deivid*- y poder agradecerle todo su cariño durante este tiempo. Gràcies Family!

Y por último, como ya he mencionado antes, a mi familia escogida, a *Deivid*. Por hacerme sentir tan arropada, que alguien cuida de ti hasta el último detalle. Por entender lo importante que era esto para mí y siempre recordármelo para animarme cuando las fuerzas aflojaban. Porque ahora cierro una etapa y comienzo una nueva, y como siempre quiero que vayamos de la mano.

El treball experimental recollit en aquesta memòria s'ha realitzat al Laboratori de Química Farmacèutica del Departament de Farmacologia, Toxicologia i Química Terapèutica de la Facultat de Farmàcia i Ciències de l'Alimentació de la Universitat de Barcelona.

Aquest treball ha estat finançat pel *Ministerio de Ciencia e Innovación* (projecte CTQ-2011-22433), pel *Ministerio de Economía y Competitividad* (projecte SAF2014-57094-R) i per CIDQO 2012 i Generalitat de Catalunya (ACC10) (projecte UBAR 012688). Per a la realització de la present Tesi Doctoral he gaudit d'una beca predoctoral d'Ajuts de Formació de Personal Investigador (FI, Generalitat de Catalunya) l'any 2014 i d'una beca del Programa de Formació de Professorat Universitari (FPU, *Ministerio de Educación, Cultura y Deporte*) durant els anys 2015-2017. Part dels resultats experimentals recollits en aquesta memòria es van realitzar durant una estada de tres mesos realitzada al *BHF Centre for Cardiovascular Science, Queen's Medical Research Institute (University of Edinburgh)* amb un ajut de mobilitat de la Fundació Pedro i Pons (2015).



## PROLOGUE

The present PhD Thesis is presented as a compendium of publications and divided in 8 chapters. In accordance with the current regulation, the following chapters include: an introduction to the topic and the framework of the research gathered in the following manuscripts (Chapter 1); a section with the listed objectives of the Thesis (Chapter 2); a descriptive and discussion section before each publication of its framework and unpublished results, arranged chronologically (Chapters 3-7); and finally a conclusions and closing section of the Thesis (Chapter 8).

In Chapter 3, the manuscript "Ritter reaction-mediated syntheses of 2-oxaadamantan-5-amine, a novel amantadine analog" (Leiva, R.; Gazzarrini, S.; Esplugas, R.; Moroni, A.; Naesens, L.; Sureda, F. X.; Vázquez, S. *Tetrahedron Lett.* **2015**, *56*, 1272-1275) is included and discussed. In the next Chapter 4, the manuscript "Novel 11 $\beta$ -HSD1 inhibitors: effects of the C-1 vs C2-substitution and of the introduction of an oxygen atom in the adamantane scaffold" (Leiva, R.; Seira, C.; McBride, A.; Binnie, M.; Luque, F. J.; Bidon-Chanal, A.; Webster, S. P.; Vázquez, S. *Bioorg. Med. Chem. Lett.* **2015**, *25*, 4250-4253) is included and discussed. In Chapter 5, the manuscript "Design, synthesis and *in vivo* study of novel pyrrolidine-based 11 $\beta$ -HSD1 inhibitors for age-related cognitive dysfunction" (Leiva, R.; Griñan-Ferré, C.; Seira, C.; Valverde, E.; McBride, A.; Binnie, M.; Pérez, B.; Luque, F. J.; Pallàs, M.; Bidon-Chanal, A.; Webster, S. P.; Vázquez, S. *Eur. J. Med. Chem.* **2017**, *139*, 412-428) is included and discussed. In Chapter 6, the manuscript "Exploring *N*-acyl-4-azatetracyclo[5.3.2.0<sup>2,6</sup>.0<sup>8,10</sup>]dodec-11-enes as 11 $\beta$ -HSD1 inhibitors" (Leiva, R.; McBride, A.; Binnie, M.; Webster, S. P.; Vázquez, S. *Bioorg. Med. Chem.* (submitted)) is included and discussed. Finally, in Chapter 7, the draft manuscript "Rational design as an ally to discover novel *N*-acylpyrrolidine-based 11 $\beta$ -HSD1 inhibitors" (Leiva, R.; C.; Seira, C.; McBride, A.; Binnie, M.; Luque, F. J.; Bidon-Chanal, A.; Webster, S. P.; Vázquez, S.) is included and discussed.

This report also includes a results dissemination section where the publications of the present Thesis appear together with others besides this research work that are outcomes from additional collaborative projects.





## RESULTS DISSEMINATION

The present PhD Thesis and additional collaborations had led to the publication of several scientific papers, patent applications and conference communications listed hereunder.

### Scientific papers

1. **“Exploring *N*-acyl-4-azatetracyclo[5.3.2.0<sup>2,6</sup>.0<sup>8,10</sup>]dodec-11-enes as 11 $\beta$ -HSD1 inhibitors”**. Rosana Leiva, Andrew McBride, Margaret Binnie, Scott P. Webster, Santiago Vázquez. *Bioorg. Med. Chem.* (submitted 25-Aug-2017).
2. **“Aniline-based inhibitors of influenza H1N1 virus acting on hemagglutinin-mediated fusion”**. Rosana Leiva, Marta Barniol-Xicota, Sandra Codony, Tiziana Ginex, Evelien Vanderlinden, Marta Montes, Michael Caffrey, F. Javier Luque, Lieve Naesens, Santiago Vazquez. *J. Med. Chem.* (submitted 20-Jun-2017, revision requested by the editor 11-Aug-2017).
3. **“Design, synthesis and *in vivo* study of novel pyrrolidine-based 11 $\beta$ -HSD1 inhibitors for age-related cognitive dysfunction”**. Rosana Leiva, Christian Griñan-Ferré, Constantí Seira, Elena Valverde, Andrew McBride, Margaret Binnie, Belén Pérez, F. Javier Luque, Mercè Pallàs, Axel Bidon-Chanal, Scott P. Webster, Santiago Vázquez. *Eur. J. Med. Chem.* **2017**, *139*, 412-428.
4. **“Mechanism of the pseudoirreversible binding of amantadine to the M2 proton channel”**. Salomé Llabrés, Jordi Juárez-Jiménez, Matteo Masetti, Rosana Leiva, Santiago Vázquez, Sabrina Gazzarrini, Anna Moroni, Andrea Cavalli, F. Javier Luque. *J. Am. Chem. Soc.* **2016**, *138*, 15345-15358.
5. **“Heme-regulated inhibitor eIF2 $\alpha$  kinase modulates hepatic FGF21 and is activated by PPAR $\beta$ / $\delta$  deficiency”**. Mohammad Zarei, Emma Barroso, Rosana Leiva, Marta Barniol-Xicota, Eugènia Pujol, Carmen Escolano, Santiago Vázquez,

Xavier Palomer, Virginia Pardo, Águeda González-Rodríguez, Ángela M. Valverde, Walter Wahli, Manuel Vázquez-Carrera. *Diabetes* **2016**, *65*, 3185-3199.

6. **“Syntheses of cinacalcet”**. Marta Barniol-Xicota,<sup>1</sup> Rosana Leiva,<sup>1</sup> Carmen Escolano, Santiago Vázquez. *Synthesis* **2016**, *48*, 783-803. [<sup>1</sup>These authors contributed equally to this work]
  
7. **“Novel 11 $\beta$ -HSD1 inhibitors: effects of the C-1 vs C2-substitution and of the introduction of an oxygen atom in the adamantane scaffold.”** Rosana Leiva, Constantí Seira, Andrew McBride, Margaret Binnie, Axel Bidon-Chanal, F. Javier Luque, Scott P. Webster, Santiago Vázquez. *Bioorg. Med. Chem. Lett.* **2015**, *25*, 4250-4253.
  
8. **“Ritter reaction-mediated syntheses of 2-oxadamantan-5-amine, a novel amantadine analog”**. Rosana Leiva, Sabrina Gazzarrini, Roser Esplugas, Anna Moroni, Lieve Naesens, Francesc X. Sureda, Santiago Vázquez. *Tetrahedron Lett.* **2015**, *56*, 1272-1275.
  
9. **“Azapropellanes with Anti-Influenza A Virus activity”**. Eva Torres, Rosana Leiva, Sabrina Gazzarrini, Matías Rey-Carrizo, Marta Frigolé-Vivas, Anna Moroni, Lieve Naesens, Santiago Vázquez. *ACS Med. Chem. Lett.* **2014**, *5*, 831–836.

#### Patent applications

10. **“HRI activators useful for the treatment of cardiometabolic diseases”**. Mohammad Zarei, Manuel Vázquez Carrera, Santiago Vázquez Cruz, Rosana Leiva Martínez, Eugènia Pujol Bech. PCT/EP2017/057398. Filing date: 29 March 2017. Universitat de Barcelona.

11. **"Analogos of adamantylureas as soluble epoxide hydrolase inhibitors"**. Santiago Vázquez Cruz, Elena Valverde Murillo, Rosana Leiva Martínez, Manuel Vázquez Carrera, Sandra Codony Gisbert. WO 2017/017048 A1. Publication date: 2 February 2017; filing date: 25 July 2016. Universitat de Barcelona.
12. **"New azatetra-cyclo derivatives"**. Santiago Vázquez Cruz, Rosana Leiva Martínez, Elena Valverde Murillo. PCT/EP2017/059178 □ Filing date: 18 April 2017. Universitat de Barcelona and CIDQO 2012.

#### Conference communications

I. Oral communication. Leiva, R.; Seira, C.; McBride, A.; Binnie, M.; Bidon-Chanal, A.; Luque, F. J.; Webster, S. P.; Vázquez, S. *Novel polycyclic N-acylpyrrolidines as 11 $\beta$ -HSD1 inhibitors*.

10<sup>th</sup> Joint Meeting on Medicinal Chemistry. Dubrovnik (Croatia), 25<sup>th</sup> -28<sup>th</sup> June **2017**.

II. Flash oral communication. Leiva, R.; Rubí, J.; Taylor, M. C.; Pérez, B.; Kelly, J. M.; Vázquez, S. *Novel thiazoles as trypanocidal agents*.

Medicinal Chemistry of Tropical Diseases: XII SEQT Mini Symposium. III<sup>rd</sup> Spanish/Portuguese/Brazilian Meeting. Tres cantos (Madrid), 17<sup>th</sup>-18<sup>th</sup> November **2016**.

III. Poster. Codony, S.; Pizarro, J.; Valverde, E.; Pujol, E.; Ginex, T.; Loza, M. I.; Brea, J. M.; Pérez, B.; Sáez, E.; Oyarzabal, J.; Luque, F. J.; Leiva, R.; Vázquez-Carrera, M.; Vázquez, S. *Exploring 2-oxadamantylureas as novel soluble epoxide hydrolase inhibitors I: piperidine derivatives*.

XIII Simposio de Investigadores Jóvenes Químicos RSEQ-Sigma Aldrich. Logroño, 8<sup>th</sup>-11<sup>th</sup> November **2016**.

IV. Poster. Pujol, E.; Pizarro, J.; Valverde, E.; Codony, S.; Ginex, T.; Loza, M. I.; Brea, J. M.; Pérez, B.; Sáez, E.; Oyarzabal, J.; Luque, F. J.; **Leiva, R.**; Vázquez-Carrera, M.; Vázquez, S. *Exploring 2-oxaadamantylureas as novel soluble epoxide hydrolase inhibitors II: aromatic derivatives.*

XIII Simposio de Investigadores Jóvenes Químicos RSEQ-Sigma Aldrich. Logroño, 8<sup>th</sup>-11<sup>th</sup> November **2016**.

V. Poster. Puigoriol-Illamola, D.; Griñan-Ferré, C.; Vasilopoulou, F.; **Leiva, R.**; Webstrer, S. P.; Vázquez, S.; Pallàs, M. *Neuroprotective effect of 11 $\beta$ -HSD1 inhibition through autophagy activation in SAMP8 mouse model.*

X Symposium of Neurobiology. Barcelona, 6<sup>th</sup>-7<sup>th</sup> October **2016**.

VI. Poster. Ginex, T.; **Leiva, R.**; Codony, S.; Barniol-Xicota, M.; Santiago Vázquez, S.; Luque, F. J. *Preventing HA-mediated Influenza A virus infection: new H1-subtype selective fusion inhibitors from hybrid in vitro-in silico MM/MD studies.*

21st European Symposium on Quantitative Structure-Activity Relationship. Verona, 4<sup>th</sup>-8<sup>th</sup> September **2016**.

VII. Flash oral communication and poster. **Leiva, R.**; Griñan-Ferré, C.; Valverde, E.; Seira, C.; McBride, A.; Binnie, M.; Pérez, B.; Bidon-Chanal, A.; Pallàs, M.; Luque, F. J.; Webster, S. P.; Vázquez, S. *Novel 11 $\beta$ -HSD1 inhibitors for age-related cognitive disorders and Alzheimer's disease.*

XXIV EFMC International Symposium on Medicinal Chemistry. Manchester, 28<sup>th</sup> August - 1<sup>st</sup> September **2016**. Granted by the EFMC and RSC.

VIII. Poster. **Leiva, R.**; Sureda, F. X.; Soto, D.; Kurnikova, M.; Johnson, J. W.; Vázquez, S. *Novel memantine-like compounds and their binding mode study with the recent available crystallographic structure of the NMDA receptor.*

17th Tetrahedron Symposium. Sitges (Barcelona), 28<sup>th</sup> June - 1<sup>st</sup> July **2016**.

**IX.** Poster. Barniol-Xicotà, M.; Torres, E.; Rey-Carrizo, M.; **Leiva, R.**; Codony, S.; Montes, M.; Naesens, L.; Ginex, T.; Juárez-Jiménez, J.; Llabrés, S.; Luque, F. J.; DeGrado, W. J.; Wu, Y.; Moroni, A.; Vázquez, S. *Influenza A drugs: Towards monotherapy*.  
17th Tetrahedron Symposium. Sitges (Barcelona), 28<sup>th</sup> June - 1<sup>st</sup> July **2016**.

**X.** Poster. Codony, S.; Valverde, E.; **Leiva, R.**; Ginex, T.; Luque, F. J.; Hammock, B. D.; Morisseau, C.; Vázquez, S. *Exploring the size limit of the hydrophobic unit of soluble epoxide hydrolase inhibitors*.  
III SEQT Young Researchers' Symposium. Barcelona, 17<sup>th</sup> June **2016**.

**XI.** Oral communication and poster. **Leiva, R.**; Griñan, C.; Valverde, E.; Seira, C.; McBride, A.; Binnie, M.; Pérez, B.; Bidon-Chanal, A.; Pallàs, M.; Luque, F. J.; Webster, S. P.; Vázquez, S. *Design, synthesis and in vivo proof of concept of novel pyrrolidine-based 11 $\beta$ -HSD1 inhibitors for age-related cognitive dysfunction*.  
V SEQT Summer School "Medicinal Chemistry in Drug Discovery: the Pharma Perspective". Sant Feliu de Llobregat (Barcelona), 14<sup>th</sup>-16<sup>th</sup> June **2016**. **Best oral communication award**. Granted by the SEQT.

**XII.** Flash oral communication and poster. Barniol-Xicotà, M.; **Leiva, R.**; Codony, S.; Montes, M.; Luque, F. J.; Ginex, T.; Naesens, L.; Vázquez, S. *New horizons in Influenza A therapeutics. Hemagglutinin: the unexplored promising target*.  
V SEQT Summer School "Medicinal Chemistry in Drug Discovery: the Pharma Perspective". Sant Feliu de Llobregat (Barcelona), 14<sup>th</sup>-16<sup>th</sup> June **2016**.

**XIII.** Oral communication. **Leiva, R.**; Vázquez, S. *Design, synthesis and pharmacological evaluation of novel 11 $\beta$ -HSD1 inhibitors*.  
IX Research Workshop of the Faculty of Pharmacy of the University of Barcelona. Barcelona, 13<sup>th</sup> June **2016**. **3<sup>rd</sup> oral communication Fedefarma Award**.

**XIV.** Poster. García-Montoya, E.; Suñe-Negre, J. M.; Suñe-Pou, M.; Pérez-Lozano, P.; Vázquez, S.; **Leiva, R.**; Escolano-Mirón, C.; Pallàs-Lliberia, M. *When Academy and Industry walk together*.

8<sup>th</sup> International Conference and Exhibition on Pharmaceuticals & Novel Drug Delivery Systems. Madrid, 7<sup>th</sup>-9<sup>st</sup> March **2016**.

**XV.** Oral communication and poster. Leiva, R.; Sureda, F. X.; Soto, D.; Webster, S. P.; Wang, J.; Vázquez, S. *Is Adamantane the best lipophilic bullet in Medicinal Chemistry? Exploring alternative polycyclic scaffolds.*

III Annual Chemistry Learnings and Achievements Meeting and Early Career Researcher Event of the European Lead Factory. Barcelona, 21<sup>st</sup>-22<sup>nd</sup> January **2016**. **Selected as an external early career researcher.**

**XVI.** Poster. Leiva, R.; Valverde, E.; Barroso, E.; McBride, A.; Binnie, M.; Vázquez-Carrera, M.; Webster, S. P.; Vázquez, S. *Bridging the gap: Successful enzymatic inhibitor projects to reach tech transfer agreements.*

VII Spanish Drug Discovery Network Meeting. Barcelona, 12<sup>th</sup>-13<sup>th</sup> November **2015**.

**XVII.** Poster. Codony, S.; Leiva, R.; Naesens, L.; Vázquez, S. *Synthesis of novel anilines with anti-Influenza activity.*

XII Simposio de Investigadores Jóvenes Químicos RSEQ-Sigma Aldrich. Barcelona, 3<sup>rd</sup>-6<sup>th</sup> November **2015**.

**XVIII.** Poster. Leiva, R.; Seira, C.; McBride, A.; Bidon-Chanal, A.; Luque, F. J.; Webster, S. P.; Vázquez, S. *Adamantane and 11 $\beta$ -HSD1: a perfect match?*

XXXV Bienal Real Sociedad Española de Química. La Coruña, 12<sup>th</sup>-17<sup>th</sup> July **2015**.

**XIX.** Poster. García, E.; Pérez, P.; Suñé, J. M.; Escolano, M. C.; Leiva, R.; Vázquez, S. *Sinergia industria farmacéutica y academia: proyectos y servicios para la industria de la Facultad de Farmacia de Barcelona.*

35<sup>o</sup> Symposium Asociación Española de Farmacéuticos de la Industria. Barcelona, 12<sup>th</sup>-13<sup>th</sup> May **2015**.

**XX.** Poster. Leiva, R.; Gazzarrini, S.; Torres, E.; Rey-Carrizo, Barniol-Xicota, M.; Ma, C.; Moroni, A.; Naesens, L.; Vázquez, S. *Hemagglutinin as a new target to fight the flu.*

I SEQT Young Researchers' Symposium. Madrid, 9<sup>th</sup> May **2014**.

**XXI.** Flash oral communication. **Leiva, R., Barniol-Xicota, M.** *Fighting the flu: Design of new potential antiviral compounds.*

2<sup>nd</sup> Interdisciplinary Conference of Predoctoral Researchers. Barcelona, 6<sup>th</sup> February **2014**.





## RESEARCH STAYS

1. **Swiss Federal Institute of Technology in Zurich (ETHZ).** Supervisor: Prof. Helma Wennemers. Research topic: Synthesis and Application of Oxygenated Monothiomalonates in organocatalysis.  
FPU Travel Grant. (20/09/2016 - 20/12/2016)
2. **BHF Centre for Cardiovascular Science, Queen's Medical Research Institute** (University of Edinburgh). Supervisor: Dr Scott P. Webster. Research topic: *In vitro* pharmacological profiling of new 11 $\beta$ -HSD1 inhibitors as drug candidates.  
Pedro i Pons Travel Grant. (01/09/2015 – 30/10/2015)



# **Table of Contents**



<b>Summary</b>	1
<b>Chapter 1. Introduction</b>	3
1.1 Glucocorticoid physiology	5
1.1.1 GC actions	6
1.1.2 Stress, aging and disease	10
1.1.3 Gating GC access to its receptors: the discovery of 11 $\beta$ -HSD	11
1.1.4 One enzyme or two?	14
1.2 11 $\beta$ -Hydroxysteroid dehydrogenase type 1	15
1.2.1 Gene structure and main regulation	15
1.2.2 Protein structure	17
1.2.3 Distribution	18
1.2.4 Physiological functions and its role in pathogenesis	19
1.3 Development of 11 $\beta$ -HSD1 inhibitors	25
1.3.1 Type 2 diabetes mellitus and other cardiometabolic disorders	27
1.3.2 Glaucoma	33
1.3.3 Cognitive impairment and Alzheimer's disease	33
1.4 Framework and previous work of our group	36
<b>Chapter 2. Objectives</b>	41
<b>Chapter 3. Synthesis and evaluation of the novel 2-oxadamant-5-amine</b>	47
3.1 Rationale and previous work	49
3.2 Theoretical discussion	51
3.3 <u>Journal article</u> : <i>Ritter reaction-mediated syntheses of 2-oxadamant-5-amine, a novel amantadine analog</i>	59
3.4 Supporting information	63
<b>Chapter 4. Study of C-1 vs C-2 substitution in adamantyl derivatives and introduction of oxadamantyl groups in 11<math>\beta</math>-HSD1 inhibitors</b>	67
4.1 Rationale and previous work	69
4.2 Theoretical discussion	69
4.3 <u>Journal article</u> : <i>Novel 11<math>\beta</math>-HSD1 inhibitors: C-1 vs C-2 substitution and effect of the introduction of an oxygen atom in the adamantane scaffold</i>	71

4.4 Supporting information	75
<b>Chapter 5. Polycycle optimization in 11<math>\beta</math>-HSD1 inhibitors. Evaluation of unexplored pyrrolidine-based polycyclic hydrocarbons</b>	101
5.1 Rationale and previous work	103
5.2 Theoretical discussion	106
5.3 <u>Journal article</u> : <i>Design, synthesis and in vivo study of novel pyrrolidine-based 11<math>\beta</math>-HSD1 inhibitors for age-related cognitive dysfunction</i>	115
5.4 Supporting information	133
<b>Chapter 6. Exploring novel 11<math>\beta</math>-HSD1 inhibitors containing the optimized 4-azatetracyclo[5.3.2.0<sup>2,6</sup>.0<sup>8,10</sup>]dodec-11-ene polycycle</b>	163
6.1 Rationale and previous work	165
6.2 Theoretical discussion	166
6.3 <u>Draft manuscript</u> : <i>Exploring N-acyl-4-azatetracyclo[5.3.2.0<sup>2,6</sup>.0<sup>8,10</sup>]dodec-11-enes as 11<math>\beta</math>-HSD1 inhibitors</i>	167
<b>Chapter 7. Rationally designed 4-azatetracyclo[5.3.2.0<sup>2,6</sup>.0<sup>8,10</sup>]dodec-11-ene-containing derivatives as 11<math>\beta</math>-HSD1 inhibitors</b>	175
7.1 Rationale and previous work	177
7.2 Theoretical discussion	178
7.3 <u>Draft manuscript</u> : <i>Rational design as an ally to discover novel N-acylpyrrolidine-based 11<math>\beta</math>-HSD1 inhibitors</i>	179
7.4 Additional results: Dealing with selectivity. Synthesis and evaluation of additional biaryl amides	203
<b>Chapter 8. Conclusions</b>	211
<b>Abbreviations</b>	219
<b>References</b>	221

## **SUMMARY**

The present PhD Thesis evolves around the design, synthesis and pharmacological evaluation of novel 11 $\beta$ -hydroxysteroid dehydrogenase type 1 (11 $\beta$ -HSD1) inhibitors. Given that the enzyme active site includes a hydrophobic pocket to accommodate bulky lipophilic scaffolds, the main objective was focused on the study of new 11 $\beta$ -HSD1 inhibitors exploring different hydrophobic polycyclic substituents.

11 $\beta$ -HSD1 catalyzes the cortisol regeneration from its inactive form cortisone in tissues mainly expressing glucocorticoid (GC) receptors, such as liver, adipose and brain. GCs are well known hormones that play a major role in our organism. It is well accepted that the GC concentration in peripheral tissues not only depends on the adrenal secretion but also on the intracellular metabolism in these tissues, namely by 11 $\beta$ -HSD1. During the last years, both academia and industry have made great efforts to develop 11 $\beta$ -HSD1 inhibitors to target diseases such as type 2 diabetes and Alzheimer's. The general structure of these molecules consists on a bulky lipophilic group –usually an adamantyl-linked by an amide core to a right-hand side (RHS) substituent.

The first goal was the development of a new polycyclic amine, the 2-oxadamantan-5-amine, to add to our library of polycyclic substituents (Chapter 3). The target amine was envisioned to contain an oxygen atom in its hydrophobic skeleton to mimic the structure of some hydroxylated adamantyl derivatives in development. Its synthesis involved consecutive Criegee rearrangements on 2-methyl-2-adamantanol to deliver the 2-oxadamantane, which was then functionalized by C-H activation using phase-transfer catalysis. Finally, a Ritter reaction followed by deprotection with thiourea delivered the desired 2-oxadamantan-5-amine.

The second objective of the present thesis was the synthesis of a small series of 1- and 2-adamantyl-based 11 $\beta$ -HSD1 inhibitors, as most of the 11 $\beta$ -HSD1 inhibitors evaluated are 2-adamantyl substituted derivatives and no comparison with their C-1 isomers was available. Moreover, considering that very few heteroadamantanes have been studied in 11 $\beta$ -HSD1 inhibitors, we also evaluated the introduction of the previously synthesized 5-substituted 2-oxadamantane (Chapter 4).



Focusing on the main goal, it is reported the exploration of other hydrophobic polycyclic substituents as replacement of adamantane with a design supported by molecular modeling studies in order to optimize the filling of the hydrophobic pocket in the binding site (Chapter 5). This work led us to a new family of potent 11 $\beta$ -HSD1 inhibitors featuring unexplored pyrrolidine-based polycyclic substituents. The *in vitro* biological profiling of the compounds permitted us to select a proper candidate for an *in vivo* study in a rodent model of cognitive dysfunction. The results supported the neuroprotective effect of 11 $\beta$ -HSD1 inhibition in cognitive decline related to the aging process, since the treatment prevented memory deficits through a reduction of neuroinflammation and oxidative stress, and an increase of the abnormal proteins degradation in the brain. An additional *in vivo* study in a model of cognitive dysfunction and metabolic disease is currently ongoing to study how 11 $\beta$ -HSD1 inhibition can modulate these two linked disorders, as so-called type 3 diabetes.

Finally, the focus was on the exploration of different substituents in the RHS of the molecule to further improve potency, selectivity and metabolic stability. The endeavour started integrating different aromatic, heteroaromatic, heterocycloalkyl and branched alkyl substituents generating diversity to build some structure-activity relationship (SAR) information (Chapter 6). From this work we obtained potent nanomolar inhibitors but still without the needed selectivity and stability properties. In light of these results, we started a rational design of new substitution patterns in order to establish additional interactions that would deliver more potent and selective inhibitors (Chapter 7). The pharmacological tests revealed some low nanomolar activities together with good metabolic stabilities, although selectivity over the isoenzyme 11 $\beta$ -HSD2 remains a challenge to be accomplished.

## CHAPTER 1

# **Introduction**



### 1.1 Glucocorticoid Physiology

Glucocorticoids (GCs) are well known steroid hormones that play a vital role in all vertebrate animals. The etymology of the name glucocorticoid leaves no room for doubt since it is composed from its role in regulation of glucose metabolism, its synthesis in the adrenal cortex and its steroidal structure.

Despite this etymological definition, the role of GCs is primarily to modulate and control the *stress response* which deals with challenging situations after the onset of a stressor. This response begins within seconds with the first wave releasing the catecholamines (epinephrine and norepinephrine) of the sympathetic nervous system (SNS), the hypothalamic corticotropin-releasing hormone (CRH) that triggers the secretion of the pituitary corticotropin (ACTH), the prolactin (PRL) and growth hormone (GH) in primates, and the pancreatic glucagon. In parallel, there is also a decrease in secretion of the hypothalamic gonadotropin-releasing hormone (GnRH) with the subsequent decreased release of the pituitary gonadotropins. A massive secretion of arginine vasopressin (AVP) from the pituitary and renin from the kidney are also present in case of haemorrhage. The second wave involves the steroid hormones, being stimulated the GC secretion and suppressed the gonadal steroid secretion. Since the majority of steroid actions are genomic, its actions are accomplished over a longer timeframe in the minutes to hours following the stressor.<sup>1</sup>

The abovementioned hormone changes bring about the major physiological changes of the stress response. On the scale of seconds to a few minutes, these include:

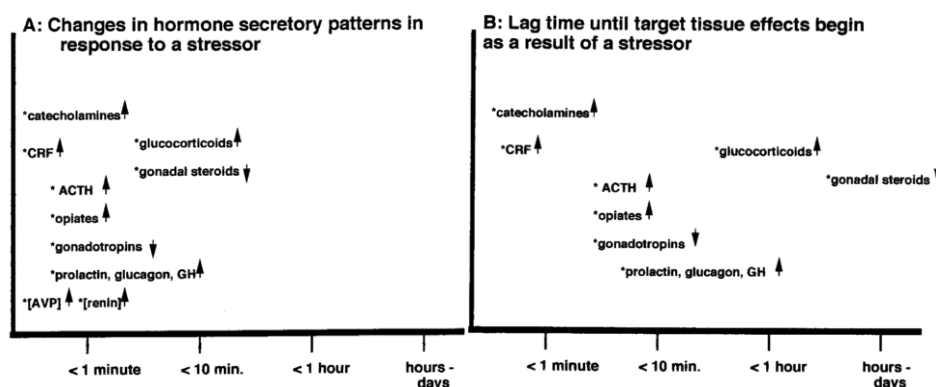
- 1) mobilization of energy stores from adipose and liver, inhibition of subsequent energy storage, and gluconeogenesis;
- 2) enhanced substrate delivery to muscle via increased cardiovascular tone;
- 3) stimulation of immune function;
- 4) inhibition of reproductive physiology and behavior;
- 5) decreased feeding and appetite;

---

<sup>1</sup> Sapolsky, R.M.; Romero, L.M.; Munck, A.U. *Endocr. Rev.* **2000**, *21*, 55–89.

6) sharpened cognition and increased cerebral perfusion rates and local cerebral glucose utilization.

In case of haemorrhage, responses also include water retention through both renal and vascular mechanisms.<sup>1</sup>



**Figure 1.** Schematic overview of the typical endocrine stress response. A) The time course of changes in hormone-secretory patterns in response to a stressor. B) The lag time until target tissue effects begin as a result of a stressor.<sup>1</sup>

### 1.1.1 GC actions

GCs have two classes of actions depending on the nature of the stressor. Modulating actions are those which alter the response to a stressor, whereas preparative actions alter the organism's response to a subsequent stressor or contribute to a chronic stressor. Not only stimulants and perceived threats stress our body, but also toxin and drug exposure, infections, poor nutrition, sleep deprivation and fake sugars.

Modulating GC actions can be classified in three groups: permissive, suppressive and stimulating. Permissive actions are due to GC basal levels present before the stressor, therefore previous to the stress response, and emerge during its initial phase. Stimulating and suppressive actions are imputable to the stress-induced rise in GC concentrations, so have a delay with reference to the onset of the stressor. Stimulating actions enhance the effects of the first wave of faster hormones, while suppressive ones prevent the response to be overshoot.

With this classification in hand and accepting the idea that GCs keep the primary defences from overshooting and help recovery, GC actions are discussed in each physiological system in order to better understand its role.<sup>1</sup>

- a) **Cardiovascular effects.** Activation of the cardiovascular system is primarily mediated by the SNS through catecholamines.<sup>2</sup> GCs enhance these first effects helping permissively the stress response since its effect is prompt and the removal does not cause overshooting.<sup>3,4</sup>
- b) **Fluid volume.** A haemorrhage stressor leads to an immediate explosion of vasoconstrictive hormones, namely AVP and renin. GCs inhibit the release of these mediators, increase glomerular filtration and secretion of atrial natriuretic polypeptide, enhancing this way water excretion.<sup>5,6</sup> These events act as a protective down-regulation from a fatal ischemia episode, restoring homeostasis through suppressive actions on the stress response.
- c) **Immunity and inflammation.** A rapid activation of the immune system not only is due to an infectious stressor but also to a variety of generalized stressors via diverse hormones of the first wave such as CRH.<sup>7,8</sup> This immune activation through various cytokines also contributes to the subsequent GC release, as IL-1 can release CRH from the hypothalamus and ACTH from the pituitary.<sup>9,10</sup> The role of GCs is to inhibit synthesis, release and efficacy of immune and inflammatory mediators and enzymes (IL-1, IL-2, IL-3, IL-4, IL-5, IL-6, IL-12, GM-CSF, IFN- $\gamma$ , TNF- $\alpha$ , histamine, bradykinin, eicosanoids, nitric oxide, collagenase, elastase, plasminogen activator). These effects explain the immunosuppressive and anti-inflammatory actions of GCs that are used in the clinics and mediate

---

<sup>2</sup> Galosy, R. A.; Clarke, L. K.; Vasko, M. R.; Crawford, I. L. *Neurosci. Biobehav. Rev.* **1981**, *5*, 137–175.

<sup>3</sup> Krakoff, L. *Cardiol. Clin.* **1988**, *6*, 537–545.

<sup>4</sup> Little, G. The adrenal cortex. **1981** In: Wilson J., Foster D. (eds) *Williams Textbook of Endocrinology*, ed. 7. W. B. Saunders Co., Philadelphia, 249–292.

<sup>5</sup> Orth, D.; Kovacs, W.; DeBold, C. The adrenal cortex. **1992** In: Wilson J., Foster D. (eds) *Williams Textbook of Endocrinology*, ed. 8. W. B. Saunders Co., Philadelphia, 518–519.

<sup>6</sup> Hayamizu, S.; Kanda, K.; Ohmori, S.; Murata, Y.; Seo, H. *Endocrinology* **1994**, *135*, 2459–2464.

<sup>7</sup> Jain, R.; Zwickler, D.; Hollander, C.; Brand, H.; Saperstein, A.; Hutchinson, B.; Brown, C.; Audhya, T. *Endocrinology* **1991**, *128*, 1329–1336.

<sup>8</sup> Pawlikowski, M.; Zelazowski, P.; Dohler, K.; Stepien, H. *Brain. Behav. Immun.* **1988**, *2*, 50–56.

<sup>9</sup> Sapolsky, R.; Rivier, C.; Yamamoto, G.; Plotsky, P.; Vale, W. *Science* **1987**, *238*, 522–524.

<sup>10</sup> Bernton, E.; Beach, J.; Holaday, J.; Smallridge, R.; Fein, H. *Science* **1987**, *238*, 519–521.

the recovery and prevent overshooting of the stress response.<sup>11</sup> In fact, GC deficiency is associated with pathological overshoot disorders such as autoimmune diseases.<sup>12</sup> Thus, most stress-induced GC actions on immune and inflammatory response are suppressive, although basal GC concentrations have shown permissive actions during the first moments of response to a stressor.<sup>13</sup> This picture raise the question of how GCs can both stimulate and suppress the immune system, although at different times. The answer lies on the different affinity of GCs to their receptors that causes the concentration-dependent differences in GC actions: GCs bind to mineralocorticoid receptor (MR) with much higher affinity than do to glucocorticoid (GR). Thus, MR are occupied at low basal concentrations and saturated in the early stage of a stressor, mediating the permissive effects, whereas GR are saturated only with stress-induced high GC levels and mediate suppressive actions.<sup>1,11,14</sup>

- d) **Metabolism.** During the first wave of hormones in the stress response, basal levels of GCs permissively synergize with catecholamines, GH and glucagon to stimulate lipolysis and proteolysis, and to elevate circulating glucose levels by stimulating glycogenolysis and gluconeogenesis.<sup>15,16,17</sup> Then, stress-induced GCs act slowly stimulating gluconeogenesis and inhibition of peripheral glucose utilization, supplementing permissive actions and being responsible for prolonging the stress response with stimulatory actions. Finally, the slow stimulation of liver glycogen deposition has a little influence on the stress response, but restores glycogen levels for the next one, being a preparative action.
- e) **Neurobiology.** Some neurobiological and behavioral effects of GCs during stress have suppressing elements. In case of cerebral glucose transport and utilization, stress-induced GCs inhibit local cerebral utilization and transport in

---

<sup>11</sup> Munck, A.; Guyre, P.M.; Holbrook, N. J. *Endocr. Rev.* **1984**, *5*, 25–44.

<sup>12</sup> Wick, G.; Hu, Y.; Schwarz, S.; Kroemer, G. *Endocr. Rev.* **1993**, *14*, 539–563.

<sup>13</sup> Barber, A. E.; Coyle, S. M.; Marano, M. A.; Fischer, E.; Calvano, S. E.; Fong, Y.; Moldawer, L. L.; Lowry, S. F. *J. Immunol.* **1993**, *150*, 1999–2006.

<sup>14</sup> De Kloet, E. R.; Vreugdenhil, E.; Oitzl, M. S.; Joels, M.; *Endocr. Rev.* **1998**, *19*, 269–301.

<sup>15</sup> Munck, A.; Naray-Fejes-Toth, A. Glucocorticoid action. *Physiology*. **1995** In: DeGroot L. J. (ed) *Endocrinology*. W.B. Saunders Co., Philadelphia, 1642–1656.

<sup>16</sup> Eigler, N.; Sacca, L.; Sherwin, R. S. *J. Clin. Invest.* **1979**, *63*, 114–123.

<sup>17</sup> DeFronzo, R.; Sherwin, R.; Felig, P. *Acta. Chir. Scand.* [Suppl] **1980**, *498*, 33–39.

many cell types through GRs.<sup>18,19</sup> Regarding appetite, CRH quickly suppresses feeding during the stress response,<sup>20</sup> while GCs stimulate appetite. Thus, GC actions are suppressive and preparative since help the recovery from the anorectic facet of the stress response. Finally, enhanced stress memory formation is mediated by catecholamines and permissively stimulated by basal levels of GCs through MRs.<sup>21</sup> In contrast, stress levels of GCs via GRs disrupt synaptic plasticity and hippocampal excitability, ultimately causing atrophy and neuron loss, and consequently disrupting memory.<sup>22</sup>

- f) **Reproductive physiology.** The first wave of hormonal mediators of the stress response is central to its reproductive suppression, being the CRH the key player as an inhibitor of reproductive physiology and behavior.<sup>23</sup> Stress-induced GCs stimulate this response decreasing the hypothalamic GnRH secretion and reducing gonadal responsiveness to luteinizing hormone (LH) and concentrations of LH receptors.<sup>24,25</sup> These antireproductive effects are logical since the associated physiology is far an expensive process. Furthermore, GCs have some integrative endpoints, such as disruption of ovulation, leading to preparative actions of the prolonged stress-induced GCs levels.

To summarize and to try to assimilate these heterogenous GC actions into a physiological whole, one could understand that GCs help to mediate the stress response to a “generic” stressor (e.g., the sprint across the savannah), whereas GCs appear to suppress responses to some specific stressors in order to avoid consequences of overshooting (e.g., haemorrhage, infection). In this way, immediate effects of the anticipatory permissive GC actions on cardiovascular and metabolism are beneficial in front a generic stressor, while preventive suppressive actions occur in case of a specialized stressors.

---

<sup>18</sup> Doyle, P.; Guillaume-Gentile, C.; Rohner-Jeanrenaud, F.; Jeanrenaud, B. *Brain Res.* **1994**, *645*, 225–230.

<sup>19</sup> Horner, H. C.; Packan, D. R.; Sapolsky, R. M. *Neuroendocrinology* **1990**, *52*, 57–63.

<sup>20</sup> Arase, K.; York, D.; Shimizu, H.; Shargill, N.; Bray, G. *Am. J. Physiol.* **1988**, *255*, E255–259.

<sup>21</sup> Pavlides, C.; Kimura, A.; Magarinos, A. M.; McEwen, B. S. *Neuroreport* **1994**, *5*, 2673–2677.

<sup>22</sup> Kerr, D. S.; Campbell, L. W.; Thibault, O.; Landfield, P. W. *Proc. Natl. Acad. Sci. USA* **1992**, *89*, 8527–8531.

<sup>23</sup> Sirinathsinghji, D.; Rees, L.; Rivier, J.; Vale, W. *Nature* **1983**, *305*, 232–235.

<sup>24</sup> Bambino, T.; Hsueh, A. *Endocrinology* **1981**, *108*, 2142–2147.

<sup>25</sup> Sapolsky, R. *Endocrinology* **1985**, *116*, 2273–2278.



### **1.1.2 Stress, aging and disease**

The link between stress and aging has been broadly studied, through the capacity of aged organisms to respond to stress and the damage caused on tissues by this stress. One idea is that senescence has been understood as a decreased adaptation to stress, since many physiological systems operate well under basal conditions but do not appropriately respond to a challenge.<sup>26</sup> The second idea revolves around chronic stress as an accelerator of the aging process, and derived from an earlier hypothesis that the *rate of living* could be a pacemaker of aging.<sup>27</sup> Different approaches have experimentally supported this idea with some biomarkers of age being accelerated by stress.<sup>28,29</sup>

Sapolsky and coworkers found a feed-forward cascade with GCs at the core of it in aged rat that is impaired in terminating the secretion of GCs at the end of stress. This hormonal excess is likely to be caused by degenerative changes in the brain, which in turn is due to cumulative exposure to GCs.<sup>30</sup>

As commented above (see section 1.1), GCs are secreted by the adrenal cortex as the final step of a neuroendocrine cascade triggered by a stressor. The GC actions in the physiological systems mentioned in the previous section are central to successful adaptation to acute physical stress, as they promote readily available energy and supportive metabolism. However, as these responses are mainly catabolic, excessive GC exposure –during prolonged stress or in the pathology of Cushing’s syndrome– produces myopathy, steroid diabetes, hypertension, immunosuppression, cognitive dysfunction, infertility and inhibition of growth, among others.<sup>31</sup> These observations started the suspicions that GCs contribute to the pathophysiology of typically diseases associated with age-related decline.

---

<sup>26</sup> Selye, H.; Tuchweber, B. Stress in relation to aging and disease. **1976** In: Everitt A, Burgess J (eds) Hypothalamus, Pituitary and Aging. Charles C Thomas, Springfield, IL, 557-573.

<sup>27</sup> Pearl, R. The Rate of Living. **1929** Alfred Knopf, New York.

<sup>28</sup> Curtis, H. *Science* **1963**, *141*, 686-694.

<sup>29</sup> Pare, W. J. *Gerontol.* **1965**, *20*, 78-84.

<sup>30</sup> Sapolsky, R.; Krey, L.; McEwen, B. *Exp. Gerontol.* **1983**, *18*, 55-64.

<sup>31</sup> Krieger, D. Cushing's Syndrome In: Monographs in Endocrinology. **1982** Springer-Verlag, Berlin, vol 22.

Both facts that plasma GCs become elevated in aging and that attempts of reducing circulating GCs ameliorate age-related pathologies have established the *GC hypothesis of age-related pathogenesis* in the brain, immune and cardiovascular systems.<sup>32,33,34</sup> In the brain, for example, prolonged GC exposure has diverse deleterious effects mediated by high GR occupancy, including impaired cognition and synaptic plasticity, inhibition of neurogenesis, atrophy of dendritic arbors and a reduction in spine density.<sup>35</sup>

Once discussed overabundance of GCs, one can appreciate that the pathophysiological consequences of the incapacity of ending GC secretion are as damaging as those from its inappropriate secretion at the onset of a stressor.

### 1.1.3 Gating GC access to its receptors: the discovery of 11 $\beta$ -HSD

1950 was the start of the GC physiology when Kendall, Hench and Reichstein were awarded with the Nobel Prize for the isolation of cortisone (“compound E”) and its impressive therapeutic effects in patients with rheumatoid arthritis.<sup>36</sup> Just three years after, Amelung and coworkers discovered the enzyme reaction catalyzing GC metabolism, when administered cortisone to rats and incubated cortisone with homogenates of various organs and found conversion to “compound F”, cortisol. They localized the highest conversion in microsomes and in liver followed by kidney and muscle.<sup>37</sup> This activity was due to 11 $\beta$ -hydroxysteroid dehydrogenase (11 $\beta$ -HSD). The following years this reaction was only of interest to steroid aficionados, with no concern for the medical community.

The renaissance of this enzyme activity arrived in the mid 1980s, when Carl Monder and coworkers characterized biochemically an 11 $\beta$ -HSD activity and subsequently

---

<sup>32</sup> Sapolsky, R. M.; Krey, L. C.; McEwen, B. S. *Endocr. Rev.* **1986**, *7*, 284–301.

<sup>33</sup> Bauer, M. E. *Stress* **2005**, *8*, 69–83.

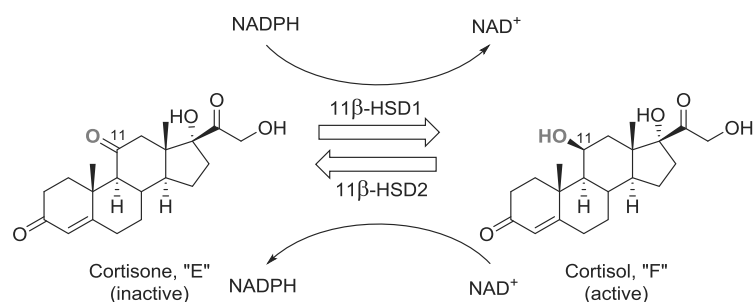
<sup>34</sup> Rosmond, R.; Dallman, M. F.; Bjorntorp, P. *J. Clin. Endocrinol. Metab.* **1998**, *83*, 1853–1859.

<sup>35</sup> McEwen, B. S.; Magarinos, A. M. *Hum. Psychopharmacol.* **2001**, *16*, S7–S19.

<sup>36</sup> Hench, P. S.; Kendall, E. C.; et al., *Proc. Staff Meet. Mayo Clin.* **1949**, *24*, 181–197.

<sup>37</sup> Amelung, D.; Hubener, H. J.; Roka, L.; Meyerheim, G. *J. Clin. Endocrinol. Metab.* **1953**, *13*, 1125–1126.

purified the enzyme from rat liver and isolated the encoding cDNA.<sup>38,39</sup> The enzymatic reaction was bidirectional in tissue homogenates, with both 11 $\beta$ -dehydrogenase and 11 $\beta$ -reductase activities using NADP(H) as cosubstrate.



**Figure 2.** Interconversion of cortisone to cortisol in humans catalyzed by 11 $\beta$ -HSD enzymes. In rodents, the corresponding pair is consisted of 11-dehydrocortisone and corticosterone (not shown).

In the late 1980s, Edwards and coworkers in Edinburgh studied a unique adult patient with “apparent mineralocorticoid excess” (AME) syndrome and solved its aetiology.<sup>40</sup> AME is marked by hypertension, sodium retention, potassium loss, metabolic alkalosis and suppressed plasma renin activity, characteristics compatible with mineralocorticoid excess. However, although undetectable levels of all mineralocorticoids were found, urinary cortisol metabolites were elevated. Inspired by the recent cloning of the human MR by Arriza and coworkers showing similar affinities *in vitro* for aldosterone, corticosterone and cortisol,<sup>41</sup> the Edinburgh group, together with Funder and colleagues in Melbourne, postulated that the oxidation of cortisol to cortisone by the renal 11 $\beta$ -HSD is critical in determining the intrarenal concentration of

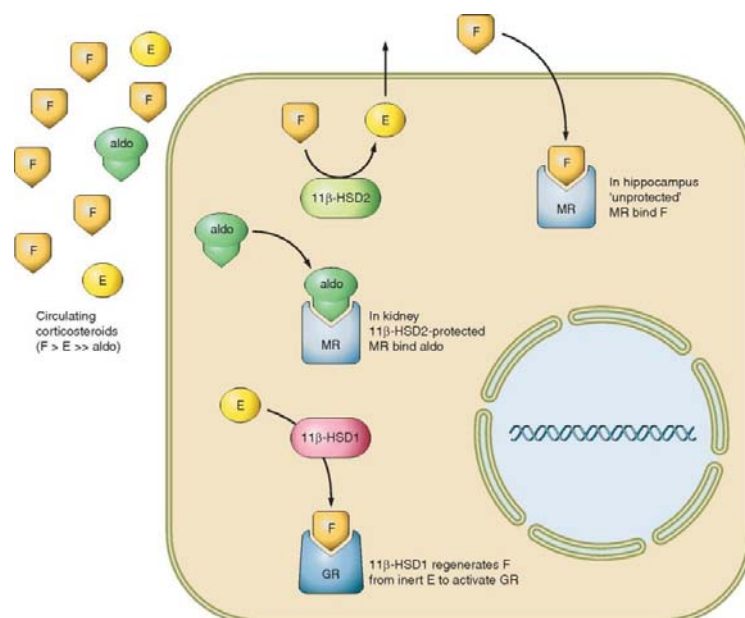
<sup>38</sup> Lakshmi, V.; Monder, C. *Endocrinology*, **1988**, *123*, 2390–2398.

<sup>39</sup> Agarwal, A. K.; Monder, C.; Eckstein, B.; White, P. C. *J. Biol. Chem.* **1989**, *264*, 18939–18943.

<sup>40</sup> Stewart, P. M.; Corrie, J. E.; Shackleton, C. H. Edwards, C. R. *J. Clin. Invest.* **1988**, *82*, 340–349.

<sup>41</sup> Arriza, J. L.; Weinberger, C.; Cerelli, G.; Glaser, T. M.; Handelin, B. L.; Housman, D. E.; Evans, R. M. *Science* **1987**, *237*, 268–275.

active GC and hence the specificity of the MR for aldosterone (Figure 3).<sup>42,43</sup> In this way, deficiency of renal 11 $\beta$ -HSD allows cortisol to mediate mineralocorticoid actions causing hypertension and hypokalemia. In addition to this, the Scottish investigators also recognized that the AME syndrome was analogous of liquorice effects, which derive from the 11 $\beta$ -HSD inhibition allowing cortisol to bypass the *enzymatic barrier* to bind to MR.<sup>44</sup> This was the first example of prereceptor metabolism gating GC access to its receptors. Same biology system was previously described for thyroid hormone receptors with mono-deiodinase isoenzymes.<sup>45</sup>



**Figure 3.** Diagrammatic representation of the reactions catalyzed by 11 $\beta$ -HSDs.<sup>46</sup> E = cortisone, F = cortisol, aldo = aldosterone.

<sup>42</sup> Edwards, C. R.; Stewart, P. M.; Burt, D.; Brett, L.; McIntyre, M. A.; Sutanto, W. S.; de Kloet, E. R.; Monder, C. *Lancet* **1988**, *2*, 986–989.

<sup>43</sup> Funder, J. W.; Pearce, P. T.; Smith, R.; Smith, A. I. *Science* **1988**, *242*, 583–585.

<sup>44</sup> Stewart, P. M.; Wallace, A. M.; Valentino, R.; Burt, D.; Shackleton, C. H.; Edwards, C. R. *Lancet* **1987**, *2*, 821–824.

<sup>45</sup> Gereben, B.; Zavacki, A. M.; Ribich, S.; Kim, B. W.; Huang, S. A.; Simonides, W. S.; Zeold, A.; Bianco, A. C. *Endocr. Rev.* **2008**, *29*, 898–938.

<sup>46</sup> Chapman, K.; Holmes, M.; Jonathan Seckl, J. R. *Physiol. Rev.* **2013**, *93*, 1139–1206.

#### 1.1.4 One enzyme or two?

In 1993, Seckl and coworkers isolated and characterized a novel 11 $\beta$ -HSD enzyme from human placenta<sup>47</sup> and Naray-Fejed-Toth's group from rat kidney<sup>48</sup>. The physicochemical characteristics and apparent molecular weight of this protein were different from Monder's enzyme, and being a high affinity exclusive dehydrogenase activity using NAD<sup>+</sup> as cosubstrate instead of NADP(H). The next year, Krozowski and colleagues isolated a cDNA encoding this renal enzyme from human kidney,<sup>49</sup> White and coworkers from sheep kidney,<sup>50</sup> also the rodent homologues were soon cloned<sup>51</sup> and an identical enzyme purified in the human placenta<sup>47</sup>. This new enzyme was named 11 $\beta$ -HSD type 2 in order to differentiate it from Monder's 11 $\beta$ -HSD type 1, and is highly expressed in aldosterone-selective target tissues –distal nephron, colon, salivary glands and skin- serving to confer aldosterone specificity on MR.<sup>52,53,54,55</sup> Also, mutations in *HSD11B2* encoding 11 $\beta$ -HSD2 are found in AME patients.<sup>56</sup>

By contrast, 11 $\beta$ -HSD1 is highly expressed in liver, adipose tissue, immune system and brain. Seckl, Walker and their coworkers in Edinburgh showed that 11 $\beta$ -HSD1 acts as a predominant reductase in intact cells and *in vivo*, directionality that is dependent on levels of cosubstrate NADPH (an NADPH/NADP ratio >10).<sup>57</sup> In fact, 11 $\beta$ -HSD1 is associated with hexose-6-phosphate dehydrogenase (H6PDH), which is the main

---

<sup>47</sup> Brown, R. W.; Chapman, K. E.; Edwards, C. R.; Seckl, J. R. *Endocrinology* **1993**, *132*, 2614–2621.

<sup>48</sup> Rusvai, E.; Naray-Fejes-Toth, A. *J. Biol. Chem.* **1993**, *268*, 10717–10720.

<sup>49</sup> Albiston, A. L.; Obeyesekere, V. R.; Smith, R. E.; Krozowski, Z. S. *Mol. Cell Endocrinol.* **1994**, *105*, R11–R17.

<sup>50</sup> Agarwal, A. K.; Mune, T.; Monder, C.; White, P. C. *J. Biol. Chem.* **1994**, *269*, 25959–25962.

<sup>51</sup> Rajan, V.; Chapman, K. E.; Lyons, V.; Jamieson, P.; Mullins, J. J.; Edwards, C. R.; Seckl, J. R. *J. Steroid Biochem. Mol. Biol.* **1995**, *52*, 141–147.

<sup>52</sup> Roland, B. L.; Krozowski, Z. S.; Funder, J. W. *Mol. Cell Endocrinol.* **1995**, *111*, R1–R7.

<sup>53</sup> Whorwood, C. B.; Ricketts, M. L.; Stewart, P. M. *Endocrinology* **1994**, *135*, 2533–2541.

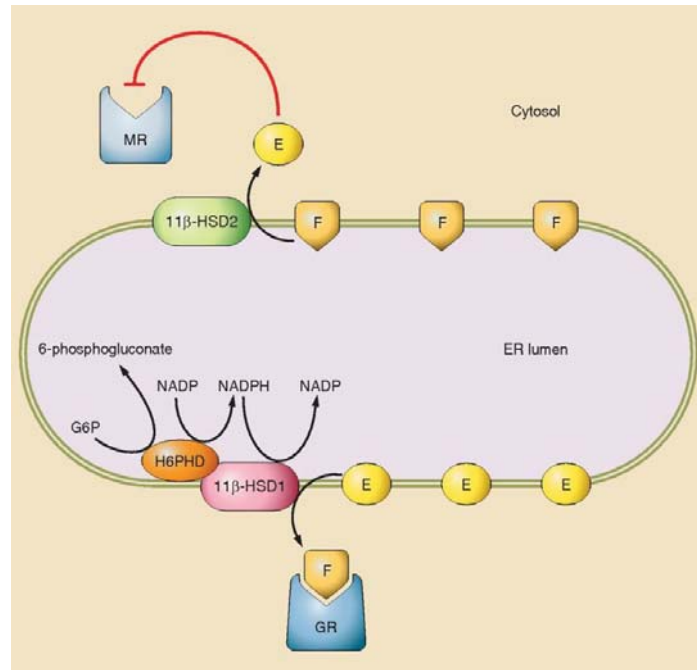
<sup>54</sup> Roland, B. L.; Funder, J. W. *Endocrinology* **1996**, *137*, 1123–1128.

<sup>55</sup> Kenouch, S.; Lombes, M.; Delahaye, F.; Eugene, E.; Bonvalet, J.P.; Farman, N. *J. Clin. Endocrinol. Metab.* **1994**, *79*, 1334–1341.

<sup>56</sup> Dave-Sharma, S.; Wilson, R. C.; Harbison, M. D.; Newfield, R.; Azar, M. R.; Krozowski, Z. S.; Funder, J. W.; Shackleton, C. H.; Bradlow, H. L.; Wei, J. Q.; Hertecant, J.; Moran, A.; Neiberger, R. E.; Balfe, J. W.; Fattah, A.; Daneman, D.; Akkurt, H. I.; De Santis, C.; New, M. I. *J. Clin. Endocrinol. Metab.* **1998**, *83*, 2244–2254.

<sup>57</sup> Jamieson, P. M.; Chapman, K. E.; Edwards, C. R.; Seckl, J. R. *Endocrinology* **1995**, *136*, 4754–4761.

source of NADPH regeneration, through protein-protein interactions in the endoplasmic reticulum (ER), driving this way its directionality (Figure 4).<sup>58</sup>



**Figure 4.** Cartoon of the likely intracellular relationships of 11 $\beta$ -HSDs.<sup>46</sup> E = cortisone, F = cortisol.

## 1.2 11 $\beta$ -HSD1 gene and protein structure, enzymology and its distribution

### 1.2.1 Gene structure and main regulation

11 $\beta$ -HSD1 is encoded in *HSD11B1* gene, located near the end of the long arm of chromosome 1 in humans and mice, and chromosome 13 in rats. It comprises seven exons, three promoters<sup>59,60</sup> and two highly conserved CCAAT/enhancer binding protein

<sup>58</sup> Dzyakanchuk, A. A.; Balazs, Z.; Nashev, L. G.; Amrein, K. E.; Odermatt, K. *Mol. Cell Endocrinol.* **2009**, *301*, 137–141.

<sup>59</sup> Bruley, C.; Lyons, V.; Worsley, A. G.; Wilde, M. D.; Darlington, G. D.; Morton, N. M.; Seckl, J. R.; Chapman, K. E. *Endocrinology* **2006**, *147*, 2879–2885.

<sup>60</sup> Moisan, M. P.; Edwards, C. R.; Seckl, J. R. *Mol. Endocrinol.* **1992**, *6*, 1082–1087.

(C/EBP) binding sites<sup>61</sup> (Figure 5). These sites are key for basal and regulated expression by transcription factors.



**Figure 5.** Schematic representation of the *HSD11B1* gene. Exonic sequences with the open reading frame (white boxes), the 5' leader and 3' untranslated sequences (red boxes and a blue box, respectively), promoters (arrows) and the two conserved C/EBP binding sites (green ovals) are shown.<sup>46</sup>

Among C/EBPs, C/EBP $\beta$  mediates 11 $\beta$ -HSD1 regulation by proinflammatory cytokines, GCs, diet, cAMP, ceramide and AMP-activated protein kinase (AMPK) in different cell types including adipocytes and fibroblasts.<sup>62,63,64,65,66</sup> C/EBP $\beta$  is a crucial regulator of inflammation and metabolism<sup>67</sup>, suggesting that *HSD11B1* may play an important down-stream role in these pleiotropic effects.<sup>46</sup> On top of this, C/EBP $\beta$  is itself GC induced, indicating a possible feed-forward loop-inflammation stimulating the HPA axis to secrete GCs that will increase 11 $\beta$ -HSD1 through C/EBP $\beta$ , further amplifying local GC signalling. Recently, the discovery of the opposite effects of posttranscriptional C/EBP $\beta$  isoforms, liver inhibitory protein (LIP) and liver activator protein (LAP), in mediating

<sup>61</sup> Williams, L. J.; Lyons, V.; MacLeod, I.; Rajan, V.; Darlington, G. J.; Poli, V.; Seckl, J. R.; Chapman, K. E. *J. Biol. Chem.* **2000**, *275*, 30232–30239.

<sup>62</sup> Yang, Z.; Zhu, X.; Guo, C.; Sun, K. *Endocrine* **2009**, *36*, 404–411.

<sup>63</sup> Ignatova, I. D.; Kostadinova, R. M.; Goldring, C. E.; Nawrocki, A. R.; Frey, F. J.; Frey, B. M. *Am. J. Physiol. Endocrinol. Metab.* **2009**, *296*, E367–E377.

<sup>64</sup> Sai, S.; Esteves, C. L.; Kelly, V.; Michailidou, Z.; Anderson, K.; Coll, A. P.; Nakagawa, Y.; Ohzeki, T.; Seckl, J. R.; Chapman, K. E. *Mol. Endocrinol.* **2008**, *22*, 2049–2060.

<sup>65</sup> Gout, J.; Tirard, J.; Thevenon, C.; Riou, J. P.; Begeot, M.; Naville, D. *Biochimie* **2006**, *88*, 1115–1124.

<sup>66</sup> Arai, N.; Masuzaki, H.; Tanaka, T.; Ishii, T.; Yasue, S.; Kobayashi, N.; Tomita, T.; Noguchi, M.; Kusakabe, T.; Fujikura, J.; Ebihara, K.; Hirata, M.; Hosoda, K.; Hayashi, T.; Sawai, H.; Minokoshi, Y.; Nakao, K. *Endocrinology* **2007**, *148*, 5268–5277.

<sup>67</sup> Arizmendi, C.; Liu, S.; Croniger, C.; Poli, V.; Friedman, J. E. *J. Biol. Chem.* **1999**, *274*, 13033–13040.

regulation in adipose tissue by high-fat diet –itself linked to adipose inflammation– added more questions in this complex system.<sup>68</sup>

### 1.2.2 Protein structure

11 $\beta$ -HSD1 has been broadly structurally studied with, to date, 42 crystal structures deposited in the Protein Data Bank. Of these, eight are from rodent enzyme (with and without substrate and inhibitor bound) and the remainder are human 11 $\beta$ -HSD1 with a vast variety of inhibitors bound, showing its interest as a pharmaceutical target.<sup>69,70</sup>

11 $\beta$ -HSD1 comprises 292 amino acids and has a predicted molecular weight of 34 kDa. It forms homodimers that is the functional unit *in vivo*.<sup>71</sup> The enzyme is structured in four main regions, 1) a transmembrane domain at the N-terminus linked to the ER membrane, 2) a cofactor binding domain, characterized by a Rossmann-fold, 3) a cluster of the key residues of the binding site, and 4) a region essential for enzyme dimerization at the C-terminus.

Like 11 $\beta$ -HSD2, it belongs to the large family of short-chain dehydrogenase/reductase,<sup>72</sup> whose members share the structurally conserved nucleotide cofactor-binding Rossmann-fold in the N-terminus region and an invariant Tyr-[Xaa]<sub>3</sub>-Lys motif in the binding site. Tyr183 and Lys187 are close to the conserved Asn143 and Ser170 in the catalytic site and are essential for the proton transfer between substrate and cofactor.<sup>73</sup> The Rossmann-fold structure consists of seven-stranded parallel  $\beta$ -sheets flanked by six  $\alpha$ -helices on the left and right sides each.<sup>74</sup>

---

<sup>68</sup> Esteves, C. L.; Kelly, V.; Begay, V.; Man, T. Y.; Morton, N. M.; Leutz, A.; Seckl, J. R.; Chapman, K. E. *PLoS One* **2012**, *7*, e37953.

<sup>69</sup> <http://www.rcsb.org/pdb/results/results.do?tabtoshow=Current&qrid=48A0266>, Accessed April 2017.

<sup>70</sup> Thomas, M. P.; Potter, B. V. L. *Future Med. Chem.* **2011**, *3*, 367-390.

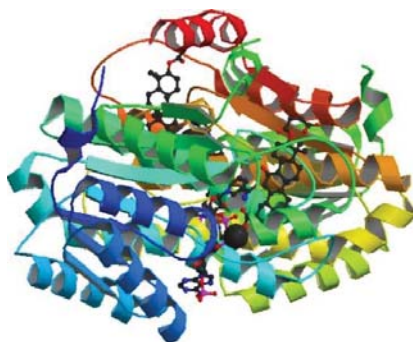
<sup>71</sup> Sandeep, T. C.; Walker, B. R. *Trends Endocrinol. Metab.* **2001**, *12*, 446-453.

<sup>72</sup> Persson, B.; Kallberg, Y.; Bray, J. E.; Bruford, E.; Dellaporta, S. L.; Favia, A. D.; Duarte, R. G.; Jornvall, H.; Kavanagh, K. L.; Kedishvili, N.; Kisiela, M.; Maser, E.; Mindnich, R.; Orchard, S.; Penning, T. M.; Thornton, J. M.; Adamski, J.; Oppermann, U. *Chem. Biol. Interact.* **2009**, *178*, 94–98.

<sup>73</sup> Obeid, J.; White, P. C. *Biochem. Biophys. Res. Commun.* 1992, *188*, 222–227.

<sup>74</sup> Schuster, D.; Maurer, E. M.; Laggner, C.; Nashev, L. G.; Wilckens, T.; Langer, T.; Odermatt, A. *J. Med. Chem.* **2006**, *49*, 3454-3466.





**Figure 6.** Structure of a dimer of human 11 $\beta$ -HSD1 with NADP cosubstrate (bottom middle) and the inhibitor carbenoxolone (top right) bound. [Image from the RCSB PDB ([www.rcsb.org](http://www.rcsb.org)) of PDB ID 2BEL]<sup>75</sup>

### 1.2.3 Distribution

In adult humans, non-humans primates and rodents, 11 $\beta$ -HSD1 is widely distributed, and as mentioned before the highest expression is in the liver.<sup>39,76,77</sup> 11 $\beta$ -HSD1 mRNA and enzyme activity is also found in adipose,<sup>78</sup> pancreas,<sup>79</sup> vasculature,<sup>80</sup> ovary,<sup>81</sup> testis,<sup>82</sup> brain,<sup>83,84,72</sup> uterus,<sup>85</sup> decidua of the placenta,<sup>86</sup> immune and inflammatory

<sup>75</sup> Kavanagh, K.; Wu, X.; Svensson, S.; Elleby, B.; Von Delft, F.; Debreczeni, J. E.; Sharma, S.; Bray, J.; Edwards, A.; Arrowsmith, C.; Sundstrom, M.; Abrahmsen, L.; Oppermann, U. PDB 2BEL, 2006. doi:10.2210/pdb2bel/pdb.

<sup>76</sup> Moisan, M. P.; Seckl, J. R.; Edwards, C. R. *Endocrinology* **1990**, *127*, 1450–1455.

<sup>77</sup> Tannin, G. M.; Agarwal, A. K.; Monder, C.; New, M. I.; White, P. C. *J. Biol. Chem.* **1991**, *266*, 16653–16658.

<sup>78</sup> Bujalska, I. J.; Kumar, S.; Stewart, P. M. *Lancet* **1997**, *349*, 1210–1213.

<sup>79</sup> Davani, B.; Khan, A.; Hult, M.; Martensson, E.; Okret, S.; Efendic, S.; Jornvall, H.; Oppermann, U. C. *J. Biol. Chem.* **2000**, *275*, 34841–34844.

<sup>80</sup> Walker, B. R.; Yau, J. L.; Brett, L. P.; Seckl, J. R.; Monder, C.; Williams, B. C.; Edwards, C. R. W. *Endocrinology* **1991**, *129*, 3305–3312.

<sup>81</sup> Benediktsson, R.; Yau, J. L. W.; Low, S.; Brett, L. P.; Cooke, B. E.; Edwards, C. R. W.; Seckl, J. R. *J. Endocrinol.* **1992**, *135*, 53–58.

<sup>82</sup> Phillips, D. M.; Lakshmi, V.; Monder, C. *Endocrinology* **1989**, *125*, 209–216.

<sup>83</sup> Lakshmi, V.; Sakai, R. R.; McEwen, B. S.; Monder, C. *Endocrinology* **1991**, *128*, 1741–1748.

<sup>84</sup> Moisan, M. P.; Seckl, J. R.; Brett, L. P.; Monder, C.; Agarwal, A. K.; White, P. C.; Edwards, C. R. *J. Neuroendocrinol.* **1990**, *2*, 853–858.

<sup>85</sup> Burton, P. J.; Krozowski, Z. S.; Waddell, B. J. *Endocrinology* **1998**, *139*, 376–382.

<sup>86</sup> Waddell, B. J.; Benediktsson, R.; Brown, R. W.; Seckl, J. R. *Endocrinology* **1998**, *139*, 1517–1523.

cells,<sup>87</sup> skeletal muscle<sup>88</sup> and heart.<sup>76</sup> During fetal life 11 $\beta$ -HSD1 is not expressed until late in gestation in organs where GC activity is required for late maturation prior to birth, namely lung and liver.<sup>89</sup>

#### 1.2.4 Physiological functions and its role in pathogenesis

Since its discovery, 11 $\beta$ -HSDs' biology has intrigued the researchers working on this topic. Although extensively studied, neither the physiological functions nor the role in pathogenesis are still fully understood.

Hereafter key points are highlighted in order to perceive the role of these enzymes at the level of some individual organs of interest for this Thesis.

- a) **Liver.** 11 $\beta$ -HSD1 exhibits net regeneration of cortisol from cortisone,<sup>57,80</sup> implying the increase of the GC action, stimulating gluconeogenesis and inhibiting  $\beta$ -oxidation of fats. In fact, in most cases of metabolic syndrome, 11 $\beta$ -HSD1 expression in liver is either maintained or modestly lowered, perhaps representing a homeostatic response to minimize GC-mediated insulin resistance. Furthermore, liver-specific deletion of 11 $\beta$ -HSD1 activity increases adrenal size,<sup>90</sup> suggesting HPA axis activation, and consequently a role for hepatic 11 $\beta$ -HSD1 in control of the HPA axis.<sup>91</sup> This idea of liver metabolism of GCs controlling the stress axis is enigmatic, plausibly being a key node in the intimate link between the essential organ of metabolic fuel availability and the major neuroendocrine control of fuel homeostasis. Finally, another intriguing point is the relationship with alternative substrates, such as 7-ketocholesterol -

---

<sup>87</sup> Gilmour, J. S.; Coutinho, A. E.; Cailhier, J. F.; Man, T. Y.; Clay, M.; Thomas, G.; Harris, H. J.; Mullins, J. J.; Seckl, J. R.; Savill, J. S.; Chapman, K. E. *J. Immunol.* **2006**, *176*, 7605–7611.

<sup>88</sup> Stewart, J. D.; Sienko, A. E.; Gonzalez, C. L.; Christensen, H. D.; Rayburn, W. F. *Am. J. Obstet. Gynecol.* **1998**, *179*, 1241–1247.

<sup>89</sup> Speirs, H. J.; Seckl, J. R.; Brown, R. W. *J. Endocrinol.* **2004**, *181*, 105–116.

<sup>90</sup> Kotelevtsev, Y.; Holmes, M. C.; Burchell, A.; Houston, P. M.; Schmoll, D.; Jamieson, P.; Best, R.; Brown, R.; Edwards, C. R. W.; Seckl, J. R.; Mullins, J. J. *Proc. Natl. Acad. Sci. USA* **1997**, *94*, 14924–14929.

<sup>91</sup> Lavery, G. G.; Zielinska, A. E.; Gathercole, L. L.; Hughes, B.; Semjonous, N.; Guest, P.; Saqib, K.; Sherlock, M.; Reynolds, G.; Morgan, S. A.; Tomlinson, J. W.; Walker, E. A.; Rabbitt, E. H.; Stewart, P. M. *Endocrinology* **2012**, *153*, 3236–3248.

involved in *de novo* cholesterol biosynthesis- and bile acids,<sup>92</sup> which are at the same time competitive inhibitors of the enzyme<sup>93,94</sup> and with GC-mediated homeostasis.<sup>95</sup>

- b) **Adipose tissue.** 11 $\beta$ -HSD1 exerts a key role on local adipocyte GC levels, since the access of circulating GCs to adipose tissue is restricted and slow.<sup>96</sup> Adipocytes taken from 11 $\beta$ -HSD1-deficient mice show reduced intra-adipose GC levels and greater insulin-mediated glucose uptake and triglyceride hydrolysis.<sup>97</sup> Therefore, it is produced a “favourable” metabolic state, particularly in the presence of obesity, since 11 $\beta$ -HSD1 activity is increased two- to threefold in subcutaneous adipose tissue in humans.<sup>98,99,100</sup> Masuzaki and coworkers generated a mouse model overexpressing the enzyme, increasing corticosterone levels twofold intra-adipose but without changing circulating GC concentration. The mice faithfully replicated metabolic syndrome with insulin resistance/impaired glucose tolerance, dyslipidemia, hypertension and hyperphagia.<sup>101,102</sup> These observations suggest that elevated 11 $\beta$ -HSD1 in adipose tissue seems to be pathogenic in metabolic disease associated with

---

<sup>92</sup> Odermatt, A.; Da Cunha, T.; Penno, C. A.; Chandsawangbhuwana, C.; Reichert, C.; Wolf, A.; Dong, M.; Baker, M. E. *Biochem. J.* **2011**, *436*, 621–629.

<sup>93</sup> Ackermann, D.; Vogt, B.; Escher, G.; Dick, B.; Reichen, J.; Frey, B. M.; Frey, F. J. *Hepatology* **1999**, *30*, 623–629.

<sup>94</sup> Diederich, S.; Grossmann, C.; Hanke, B.; Quinkler, M.; Herrmann, M.; Bahr, V.; Oelkers, W. *Eur. J. Endocrinol.* **2000**, *142*, 200–207.

<sup>95</sup> Rose, A. J.; Díaz, M. B.; Reimann, A.; Klement, J.; Walcher, T.; Kronen-Herzig, A.; Strobel, O.; Werner, J.; Peters, A.; Kleyman, A.; Tuckermann, J. P.; Vegiopoulos, A.; Herzig, S. *Cell Metab.* **2011**, *14*, 123–130.

<sup>96</sup> Hughes, K. A.; Reynolds, R. M.; Andrew, R.; Critchley, H. O.; Walker, B. R. *J. Clin. Endocrinol. Metab.* **2010**, *95*, 4696–4702.

<sup>97</sup> Morton, N. M.; Paterson, J. M.; Masuzaki, H.; Holmes, M. C.; Staels, B.; Fievet, C.; Walker, B. R.; Flier, J. S.; Mullins, J. J.; Seckl, J. R. *Diabetes* **2004**, *53*, 931–938.

<sup>98</sup> Goedecke, J. H.; Wake, D. J.; Levitt, N. S.; Lambert, E. V.; Collins, M. R.; Morton, N. M.; Andrew, R.; Seckl, J. R.; Walker, B. R. *Clin. Endocrinol.* **2006**, *65*, 81–87.

<sup>99</sup> Paulmyer-Lacroix, O.; Boullu, S.; Oliver, C.; Alessi, M. C.; Grino, M. *J. Clin. Endocrinol. Metab.* **2002**, *87*, 2701–2705.

<sup>100</sup> Rask, E.; Walker, B. R.; Soderberg, S.; Livingstone, D. E.; Eliasson, M.; Johnson, O.; Andrew, R.; Olsson, T. *J. Clin. Endocrinol. Metab.* **2002**, *87*, 3330–3336.

<sup>101</sup> Masuzaki, H.; Paterson, J.; Shinyama, H.; Morton, N. M.; Mullins, J. J.; Seckl, J. R.; Flier, J. S. *Science* **2001**, *294*, 2166–2170.

<sup>102</sup> Masuzaki, H.; Yamamoto, H.; Kenyon, C. J.; Elmquist, J. K.; Morton, N. M.; Paterson, J. M.; Shinyama, H.; Sharp, M. G.; Fleming, S.; Mullins, J. J.; Seckl, J. R.; Flier, J. S. *J. Clin. Invest.* **2003**, *112*, 83–90.

obesity. In contrast, much little is known about its evolutionary physiological function, but may be involved in the rapid storage of excess calories in visceral adipose to allow rapid delivery to the liver when it is required.<sup>46</sup>

- c) **Pancreas.** Since GCs directly inhibit beta-cell insulin secretion<sup>103,104</sup> and 11 $\beta$ -HSD1 activity is increased in islets from diabetic rodents<sup>105</sup>, it has been proposed that elevated islet 11 $\beta$ -HSD1 is involved in the pathogenesis of beta-cell failure.<sup>79</sup> However, moderate transgenic overexpression in beta cells is associated with enhanced glucose-stimulated insulin secretion, reflecting protection from apoptosis and cellular stress while facilitating secretion.<sup>106</sup> Intriguingly, greater beta-cell overexpression or lifelong deletion of 11 $\beta$ -HSD1 produces poor insulin secretion. These discrepancies could be explained by an inverted U-shaped relationship between 11 $\beta$ -HSD1 in beta cells and insulin secretion, as seen with the slight elevation in early diabetes associated with improved insulin secretory function.

This might be the first evidence of a physiological function for 11 $\beta$ -HSD1 in metabolic control. In normal weight, 11 $\beta$ -HSD1 performs a key endocrine role by regenerating GCs, thus contributing with approximately 40% of daily GC production. In addition, it has intracrine actions, amplifying the GC signal inside hepatocytes, pancreatic islets and adipocytes. Healthy mice fed with a high-fat diet show a compensatory insulin secretion probably promoted by the modest upregulation of beta-cell 11 $\beta$ -HSD1. Simultaneously, 11 $\beta$ -HSD1 is downregulated in adipose tissue, driving insulin sensitization in subcutaneous fat and “safe” storage of caloric excess, while AMPK-mediated beneficial metabolic and noninflammatory processes occur in visceral adipose.<sup>107</sup> Instead, in obesity, overexpressed adipose 11 $\beta$ -HSD1 provokes visceral obesity, insulin resistance and metabolic syndrome due to the release of proinflammatory/antimetabolic adipokines, and increase of

---

<sup>103</sup> Gremlich, S.; Roudit, R.; Thorens, B. *J. Biol. Chem.* **1997**, *272*, 3216–3222.

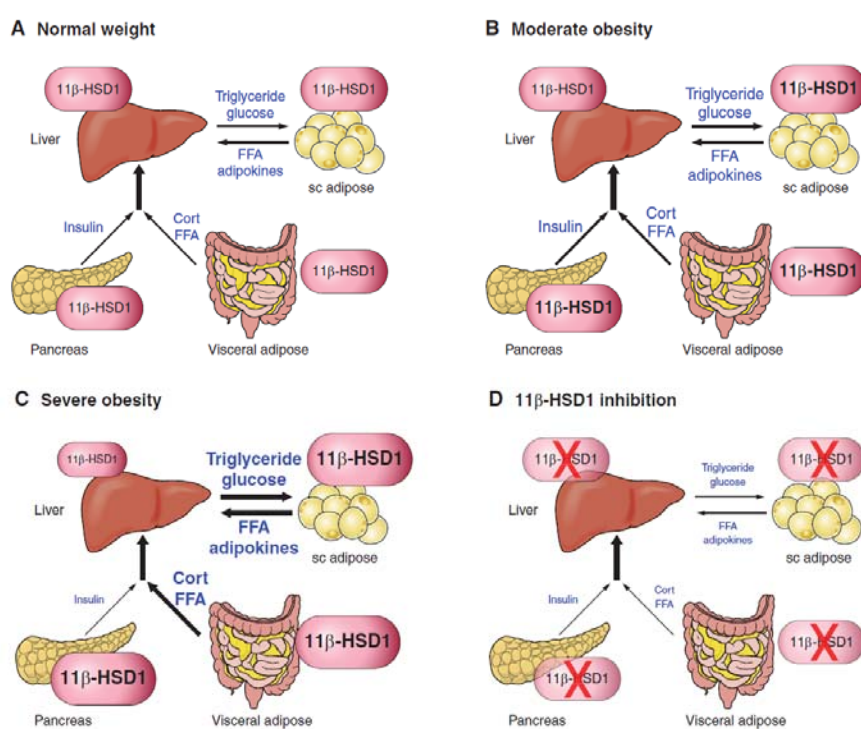
<sup>104</sup> Lambillotte, C.; Gilon, P.; Henquin, J. C. *J. Clin. Invest.* **1997**, *99*, 414–423.

<sup>105</sup> Duplomb, L.; Lee, Y.; Wang, M. Y.; Park, B. H.; Takaishi, K.; Agarwal, A. K.; Unger, R. H. *Biochem. Biophys. Res. Commun.* **2004**, *313*, 594–599.

<sup>106</sup> Turban, S.; Liu, X.; Ramage, L.; Webster, S. P.; Walker, B.; Dunbar, D.; Mullins, J.; Seckl, J. R.; Morton, N. *Diabetes* **2012**, *61*, 642–652.

<sup>107</sup> Morton, N. M.; Ramage, L.; Seckl, J. R. *Endocrinology* **2004**, *145*, 2707–2712.

portal blood GC and fatty acid deliver to the liver. Lastly, in severe obesity, exaggerated pancreatic 11 $\beta$ -HSD1 and consequent active GCs contributes to the beta-cell failure, and greater rise in adipose aggravate peripheral insulin resistance and metabolic disease despite potentially “compensatory” decline in hepatic GC regeneration, which might even contribute to HPA axis activation due to loss of bulk GC regeneration (Figure 7).



**Figure 7.** Cartoon of potential role of 11 $\beta$ -HSD1 in metabolic organ interrelationships in normal weight, obesity and 11 $\beta$ -HSD1 inhibition.<sup>46</sup>

These alterations in 11 $\beta$ -HSD1 in response to high-fat diet affecting the metabolism seem advantageous in a past environment with alternative feast and famine periods. The early calorie excess mediates insulin secretion facilitating fat storage that might help survival in the next famine period. When pronounced calorie excess, increased adipose tissue 11 $\beta$ -HSD1 may allow even more fat storage in

rapidly accessible visceral depot.<sup>46</sup> Nowadays, in the calorie abundance climate that we have, elevated adipose tissue 11 $\beta$ -HSD1 causes metabolic disease, instead of the homeostasis in metabolic tissues.

- d) **Immunity and inflammation.** As commented before (see Section 1.1), endogenous GCs have different effects, permissive, suppressive or stimulatory, depending on concentration and the cellular environment, hence shaping the immune and inflammatory responses. Also commented above, there is evidence suggesting 11 $\beta$ -HSD1 deficiency or inhibition diminish “metabolic inflammation”. In patients with inflammatory disease, increased whole body conversion of cortisone to cortisol suggests some alteration in 11 $\beta$ -HSD balance, and seems consequence of upregulation of 11 $\beta$ -HSD1 and downregulation of 11 $\beta$ -HSD2 by proinflammatory cytokines (e.g. TNF- $\alpha$  and IL-1) at sites of inflammation.<sup>108</sup> In addition to these cytokines, GCs themselves also induce 11 $\beta$ -HSD1 expression, this way amplifying intracellular GC-mediated attenuation of proinflammatory cytokine action in preparation for recovery in key tissues. This mechanism fails in synovial macrophages in rheumatoid arthritis when IL-10 does not increase 11 $\beta$ -HSD1 the same way that does in other macrophages, leading to a failure of the chronic inflammation resolution.<sup>109</sup>
- e) **Brain.** 11 $\beta$ -HSD1 is highly expressed in the hippocampus, cerebellum and cortex,<sup>76</sup> found both in neurons and glia,<sup>110</sup> significantly in microglia which express high levels of the enzyme especially when activated, acting as a regulator of central inflammatory signals.<sup>111</sup> Its activity is reductase exclusively, implying a role in amplification of intracellular GC action. Interestingly, 11 $\beta$ -HSD1 seems to be involved in the appetite regulation, since it is expressed in the arcuate nucleus, a key locus for appetite control.<sup>76</sup> This arcuate 11 $\beta$ -HSD1 is induced by high-fat feeding, suggesting being part of the acute inflammatory

---

<sup>108</sup> Ichikawa, Y.; Yoshida, K.; Kawagoe, M.; Saito, E.; Abe, Y.; Arikawa, K.; Homma, M. *Metabolism* **1977**, *26*, 989–997.

<sup>109</sup> Antoniv, T. T.; Ivashkiv, L. B. *Arthritis Rheum.* **2006**, *54*, 2711–2721.

<sup>110</sup> Sakai, R. R.; Lakshmi, V.; Monder, C.; McEwen, B. S. *J. Neuroendocrinol.* **1992**, *4*, 101–106.

<sup>111</sup> Gottfried-Blackmore, A.; Sierra, A.; McEwen, B. S.; Ge, R.; Bulloch, K. *Glia* **2010**, *58*, 1257–1266.

hypothalamic response to high-fat diet.<sup>112,113</sup> Regarding aging and cognitive decline, it is well established that chronic exposure to high concentrations of GCs is prone to cognitive and affective disorders,<sup>114</sup> and a key factor in cognitive decline in rodents and humans.<sup>115,116,117</sup> Hence, 11 $\beta$ -HSD1 activity, through local amplification of GC action, adversely impacts on cognitive function and the underlying biology.<sup>118</sup> In this regard, both 11 $\beta$ -HSD1 deficiency and pharmacological inhibition have shown improvement in memory retention and cognitive decline.<sup>119,120,121,122</sup> Referring to the mechanism, intrahippocampal GCs might be sufficiently reduced to minimize GR activation and its consequent anticognitive effects, while maintaining optimal MR-mediated procognitive effects. In addition to this, growing evidence suggests excessive GC activity may contribute to Alzheimer's disease (AD), since elevated levels of circulating cortisol in AD patients are associated with progression of the disease.<sup>123,124</sup> Moreover, administration of GCs to a rodent model of AD led to increases in  $\beta$ -amyloid and tau pathology, suggesting a relationship between

---

<sup>112</sup> Densmore, V. S.; Morton, N. M.; Mullins, J. J.; Seckl, J. R. *Endocrinology* **2006**, *147*, 4486–4495.

<sup>113</sup> Thaler, J. P.; Yi, C. X.; Schur, E. A.; Guyenet, S. J.; Hwang, B. H.; Dietrich, M. O.; Zhao, X.; Sarruf, D. A.; Izgur, V.; Maravilla, K. R.; Nguyen, H. T.; Fischer, J. D.; Matsen, M. E.; Wisse, B. E.; Morton, G. J.; Horvath, T. L.; Baskin, D. G.; Tsch, M. H.; Schwartz, M. W. J. *Clin. Invest.* **2012**, *122*, 153–162.

<sup>114</sup> Swaab, D. F.; Bao, A. M.; Lucassen, P. J. *Ageing Res. Rev.* **2005**, *4*, 141–194.

<sup>115</sup> Meaney, M. J.; O'Donnell, D.; Rowe, W.; Tannenbaum, B.; Steverman, A.; Walker, M.; Nair, N. P. V.; Lupien, S. *Exp. Gerontol.* **1995**, *30*, 229–251.

<sup>116</sup> Yau, J. L.; Olsson, T.; Morris, R. G.; Meaney, M. J.; Seckl, J. R. *Neuroscience* **1995**, *66*, 571–581.

<sup>117</sup> Lupien, S. J.; de Leon, M.; de Santi, S.; Convit, A.; Tarshish, C.; Nair, N. P. V.; Thakur, M.; McEwen, B. S.; Hauger, R. L.; Meaney, M. J. *Nat. Neurosci.* **1998**, *1*, 69–73.

<sup>118</sup> Seckl, J. R. *Front. Neuroendocrinol.* **1997**, *18*, 49–99.

<sup>119</sup> Yau, J. L.; McNair, K. M.; Noble, J.; Brownstein, D.; Hibberd, C.; Morton, N.; Mullins, J. J.; Morris, R. G.; Cobb, S.; Seckl, J. R. *J. Neurosci.* **2007**, *27*, 10487–10496.

<sup>120</sup> Yau, J. L.; Noble, J.; Kenyon, C. J.; Hibberd, C.; Kotelevtsev, Y.; Mullins, J. J.; Seckl, J. R. *Proc. Natl. Acad. Sci. USA* **2001**, *98*, 4716–4721.

<sup>121</sup> Sooy, K.; Webster, S. P.; Noble, J.; Binnie, M.; Walker, B. R.; Seckl, J. R.; Yau, J. L. *J. Neurosci.* **2010**, *30*, 13867–13872.

<sup>122</sup> Dhingra, D.; Parle, M.; Kulkarni, S. K. *J. Ethnopharmacol.* **2004**, *91*, 361–365.

<sup>123</sup> Peskind, E. R.; Wilkinson, C. W.; Petrie, E. C.; Schellenberg, G. D.; Raskind, M. A. *Neurology* **2001**, *56*, 1094–1098.

<sup>124</sup> Cernansky, J. G.; Dong, H.; Fagan, A. M.; Wang, L.; Xiong, C.; Holtzman, D. M.; Morris, J. C. *Am. J. Psychiatry* **2006**, *163*, 2164–2169.

elevated GC levels and AD pathology.<sup>125</sup> Overall, these data indicate that a reduction of GC levels in the brain may relieve cognitive dysfunction in both aging and AD.

### 1.3 Development of 11 $\beta$ -HSD1 inhibitors

Over 1400 scientific journals about 11 $\beta$ -HSD1 and more than 250 patent applications claiming 11 $\beta$ -HSD1 inhibitors from both academia and pharmaceutical industry evidence the high level of interest in this enzyme and its therapeutic inhibition value.<sup>126,127</sup> Although 11 $\beta$ -HSD1 has been linked with many diseases (e.g. type 2 diabetes, glaucoma, atherosclerosis, hypertension, cognitive dysfunction, osteoporosis, myopathy, hepatic steatosis), first and more fruitful research has been focused on metabolic disease since the resemblances between the phenotype of the hypercortisolism present in the Cushing's syndrome and the symptoms of the metabolic syndrome.<sup>128</sup>

Here below there is a brief review of the currently reported clinical data of the 11 $\beta$ -HSD1 inhibitors that have been developed by different organizations, first summarised in the following table.

---

<sup>125</sup> Green, K. N.; Billings, L. M.; Roozendaal, B.; McGaugh, J. L.; LaFerla, F. M. *J. Neurosci.* **2006**, *26*, 9047-9056.

<sup>126</sup> Scott, J. S.; Goldberg, F. W.; Turnbull, A. V. *J. Med. Chem.* **2014**, *57*, 4466–4486.

<sup>127</sup> Boyle, C. D.; Kowalski, T. J. *Expert Opin. Ther. Pat.* **2009**, *19*, 801–825.

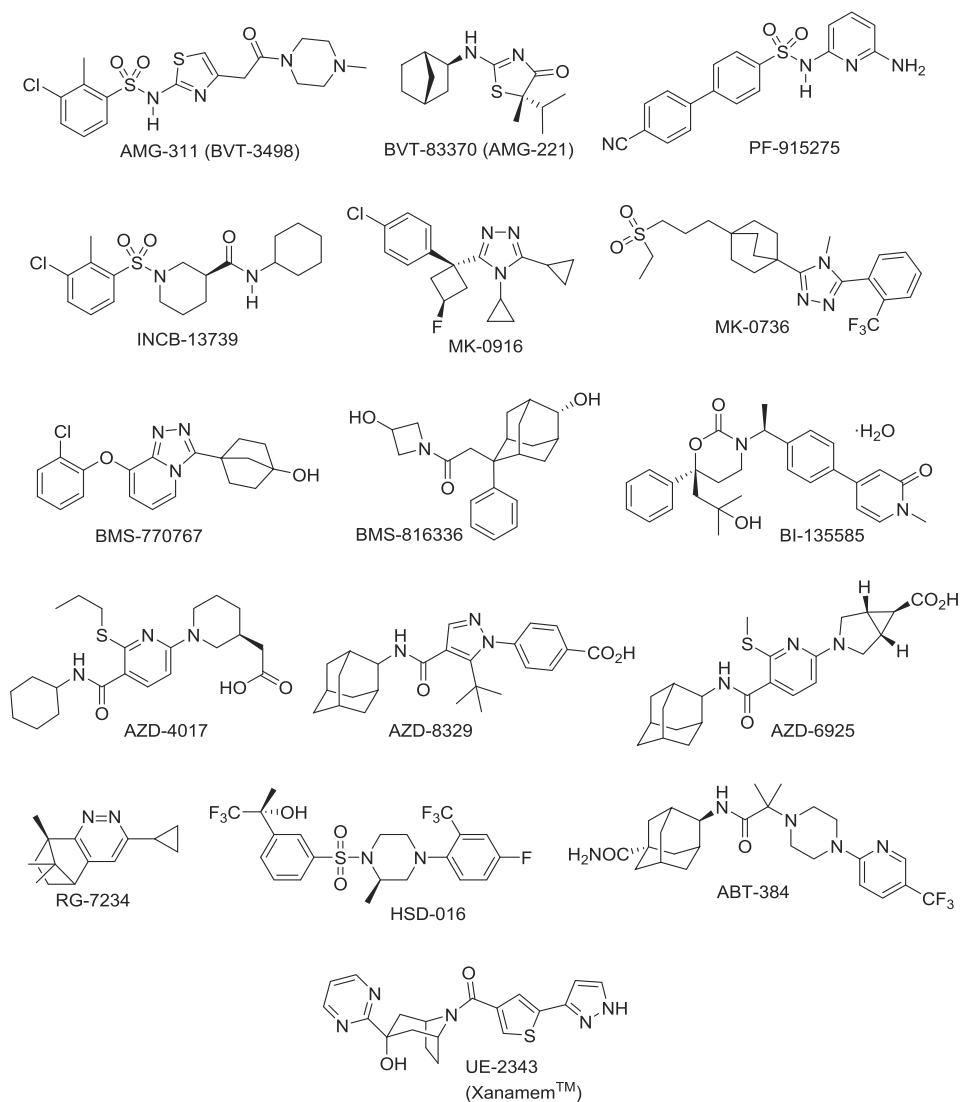
<sup>128</sup> Gathercole, L. L.; Lavery, G. G.; Morgan, S. A; Cooper, M. S.; Sinclair, A. J.; Tomlinson, J. W.; Stewart, P. M. *Endocr. Rev.* **2013**, *34*, 525-555.



Polycyclic group optimization in 11 $\beta$ -HSD1 inhibitors and their pharmacological evaluation

COMPANY	DRUG	INDICATION	PHASE	STATUS
Amgen/Biovitrum	BVT-3498 (AMB-311)	T2DM	II (2002)	Discontinued (2005)
Amgen/Biovitrum	AMG-221 (BVT-83370)	T2DM	I (2006)	Discontinued (2011)
Pfizer	PF-915275	T2DM	II (2007)	Discontinued (2007)
Incyte	INCB-13739	T2DM	II (2007)	No longer in pipeline
Incyte	INCB-20817*	T2DM	I (2008)	No longer in pipeline
Merck & Co	MK-0916	T2DM + MetS	II (2005)	No longer in pipeline
Merck & Co	MK-0736	Hypertension	II (2007)	No longer in pipeline
Bristol-Myers-Squibb	BMS-770767	T2DM + Dyslipidemia	II (2011)	No longer in pipeline
Bristol-Myers-Squibb	BMS-816336	T2DM + Dyslipidemia	I (2010)	Discontinued (2013)
Vitae/Boehringer Ingelheim	BI-135585	T2DM	I (2011)	No longer in pipeline
Vitae/Boehringer Ingelheim	BI-187004 CL*	T2DM	II (2015)	Discontinued (2015)
AstraZeneca	AZD-4017	T2DM	I (2010)	Switched indication
		Glaucoma	II (2012)	Discontinued (2012)
		Intracranial Hypertension	II (ongoing)	Active
Univ. Birmingham				
AstraZeneca	AZD-8329	T2DM + obesity	I (2010)	Discontinued (2011)
AstraZeneca	AZD-6925	T2DM	ND	No longer in pipeline
Roche	RG-7234 (RO5027838)	T2DM	I (2009)	Discontinued (2010)
Roche	RG-4929* (RO5093151)	T2DM NAFLD Glaucoma	II (2009) I (2012) I (2016)	Switched indication Switched indication No longer in pipeline
Wyeth (now Pfizer)	HSD-016	T2DM	I (2009)	Discontinued (2009)
Eli Lilly	LY-2523199*	T2DM	II (2011)	Discontinued (2013)
Piramal healthcare	P2202*	T2DM	II (2012)	Discontinued (2013)
Japan Tobacco	JTT-654*	T2DM	II (2010)	Discontinued (2010)
High Point Pharma	HPP-851*	Glaucoma	I (2010)	Discontinued (2016)
Abbott/Abbvie	ABT-384	AD	II (2011)	Discontinued (2012)
Univ. Edinburgh/ Actinogen Medical	UE-2343/ Xanamem™	AD	II (ongoing)	Active
Astellas	ASP-3662*	Agitation associated with AD	II (ongoing)	Active

**Table 1.** 11 $\beta$ -HSD1 inhibitors entered into clinical trials. \*Structure undisclosed.



**Chart 1.** Structures disclosed of 11 $\beta$ -HSD1 inhibitors entered into clinical trials.

### 1.3.1 Type 2 diabetes mellitus (T2DM) and other cardiometabolic disorders

Biovitrum started a collaboration with Amgen which led to the development of the first 11 $\beta$ -HSD1 inhibitor to enter clinical trials, BVT-3498 (AMG-311).<sup>129</sup> Its

<sup>129</sup> Abrahmsen, L.; Nilsson, J.; Opperman, U.; Svensson, S. WO Patent Application, WO2005068646, 2005.

development was discontinued in 2005 in phase II trials, and it was replaced by BVT-83370 (AMG-221) that was progressed into phase I trials but its development was stopped in 2011 for undisclosed reasons. AMG-221 was dosed to healthy, obese individuals in the range of 3-100 mg in order to shed light on pharmacokinetic/pharmacodynamic (PK/PD) relationships. The compound exhibited sustained inhibition of the enzyme over a 24 h period, but presented a delay between plasma and adipose tissue concentrations attributed to perfusion limited distribution to adipose.<sup>130</sup> An attempt to repurpose the compound for AD was done in 2011. The company disclosed that aged rats administered with its clinical candidate AMG-221 exhibited superior improvement in the Nobel Object Recognition Test (NORT) when compared to rats that had been administered galantamine.<sup>131</sup>

Compound PF-915275 from Pfizer entered in phase I trials in 2006 and after being well tolerated, at doses of 0.3-15 mg over 14 days, progressed to phase II next year;<sup>132</sup> however, its development was halted because of tablet formulation problems.<sup>133</sup> In the first study, PF-915275 presented dose-dependently inhibition of the prednisone/prednisolone conversion, reaching a 37% inhibition at the tope dose. Both free cortisol/cortisone ratio in urine and ACTH, adrenal androgens and urinary corticosteroid profile did not present significant changes, consistent with selectivity against 11 $\beta$ -HSD2 and no activation of the HPA axis.<sup>132</sup>

Incyte successfully completed phase I trials with INCB-13739 which then progressed into phase II trials in 2007. This efficacy study was performed in T2DM patients with metformin monotherapy, and resulted that after 12 weeks at doses of 200 mg of INCB-13739 there were significant metabolic improvements. In addition, a reversible, dose-dependent elevation in ACTH levels was present, indicting HPA axis activation,

---

<sup>130</sup> Gibbs, J. P.; Emery, M. G.; McCaffery, I.; Smith, B.; Gibbs, M. A.; Akrami, A.; Rossi, J.; Paweletz, K.; Gastonguay, M. R.; Bautista, E.; Wang, M.; Perfetti, R.; Daniels, O. *J. Clin. Pharmacol.* **2011**, *51*, 830–841.

<sup>131</sup> Wyszynski, M. WO Patent Application, WO2012/051139A1, 2012.

<sup>132</sup> Courtney, R.; Stewart, P. M.; Toh, M.; Ndongo, M. N.; Calle, R. A.; Hirshberg, B. *J. Clin. Endocrinol. Metab.* **2008**, *93*, 550–556.

<sup>133</sup>No safety issues were involved in the termination decision. See <http://clinicaltrials.gov/ct2/show/NCT00427401>, Accessed March 2017.

although down-stream hormones unchanged.<sup>134</sup> The investigators subsequently published a review highlighting the need of high doses of the compound to achieve efficacy, possibly attributed to the requirement of maximal inhibition of the enzyme. In addition to this, the authors also commented that the treatment is more effective in obese patients than in overweight ones, suggesting the importance of adipose tissue 11 $\beta$ -HSD1 activity to the cardiometabolic repercussion.<sup>135</sup> A structurally different back-up compound, INCB-20817, also completed phase I trials, though it does not appear on the company pipeline.<sup>136</sup>

Two compounds from Merck & Co entered to clinical trials, MK-0916 and MK-0736. A 12-week phase IIa study of MK-0916 in T2DM patients with metabolic syndrome at doses of 0.5 to 6 mg resulted in no significant improvement in fasting plasma glucose, although with some other modest significant improvements, such as decrease in blood pressure, body weight and haemoglobin A1C (HbA1c). By contrast, elevation of LDL cholesterol of 10% probably due to CYP3A4 induction and circulating adrenal androgens, though no clinically meaningful –indicating modest HPA axis activation– were observed.<sup>137</sup> A posterior phase II study of both MK-0916 and MK-0736 was performed in overweight and obese patients with hypertension. The new compound, MK-0736, was also well tolerated, although it did not achieve significant reduction in the diastolic blood pressure. Again, encouraging positive effects on some metabolic parameters (e.g. LDL cholesterol, body weight) and adrenal androgens elevation were also detected.<sup>138</sup> A subsequent report from the investigators stated that these effects were attributable to an unknown off-target activity rather than 11 $\beta$ -HSD1 inhibition

---

<sup>134</sup> Rosenstock, J.; Banarer, S.; Fonseca, V. A.; Inzucchi, S. E.; Sun, W.; Yao, W.; Hollis, G.; Flores, R.; Levy, R.; Williams, W. V.; Seckl, J. R.; Huber, R. *Diabetes Care* **2010**, *33*, 1516–1522.

<sup>135</sup> Hollis, G.; Huber, R. *Diabetes, Obesity Metab.* **2011**, *13*, 1–6.

<sup>136</sup> <https://www.incyte.com/what-we-do/develop.aspx>, Accessed March 2017.

<sup>137</sup> Feig, P. U.; Shah, S.; Hermanowski-Vosatka, A.; Plotkin, D.; Springer, M. S.; Donahue, S.; Thach, C.; Klein, E. J.; Lai, E.; Kaufman, K. D. *Diabetes, Obesity Metab.* **2011**, *13*, 498–504.

<sup>138</sup> Shah, S.; Hermanowski-Vosatka, A.; Gibson, K.; Ruck, R. A.; Jia, G.; Zhang, J.; Hwang, P. M. T.; Ryan, N. W.; Langdon, R. B.; Feig, P. U. *J. Am. Soc. Hypertens.* **2011**, *5*, 166–176.

since similar effects were observed in both wild-type and 11 $\beta$ -HSD1 knockout mice after administration of the compound.<sup>139</sup>

Bristol-Myers-Squibb has progressed two compounds into clinical trials. BMS-770767 completed phase II trials in subjects with T2DM and in hypercholesterolemic patients in 2011.<sup>140</sup> Then, without additional information, the compound no longer appeared in the company pipeline.<sup>141</sup> It could be hypothesized that some modest activity against 11 $\beta$ -HSD2 (IC<sub>50</sub> = 2.52  $\mu$ M, though >200 fold selectivity)<sup>142</sup> made the compound suboptimal for continuing its clinical development. Furthermore, compound BMS-816336<sup>143</sup> completed phase I for T2DM and dyslipidemia,<sup>144</sup> but it was discontinued in 2013.<sup>145</sup>

Vitae Pharmaceuticals and Boehringer Ingelheim collaborated since 2007 to develop a 11 $\beta$ -HSD1 inhibitor for the treatment of metabolic disorders. Compound BI-135585<sup>146</sup> entered in clinical trials and completed phase I trials in 2011 being safe and well tolerated.<sup>147,148</sup> However, it seems discontinued as it does not appear in the Report of

---

<sup>139</sup> Bauman, D. R.; Whitehead, A.; Contino, L. C.; Cui, J.; Garcia- Calvo, M.; Gu, X.; Kevin, N.; Ma, X.; Pai, L.; Shah, K.; Shen, X.; Stribling, S.; Zokian, H. J.; Metzger, J.; Shevell, D. E.; Waddell, S. T. *Bioorg. Med. Chem. Lett.* **2013**, *23*, 3650–3653.

<sup>140</sup> <https://clinicaltrials.gov/ct2/results?term=BMS-770767&Search=Search>, Accessed March 2017.

<sup>141</sup> <http://www.bms.com/research/pipeline/Pages/default.aspx>, Accessed March 2017.

<sup>142</sup> Wang, H.; Robl, J. A.; Hamann, L. G.; Simpkins, L.; Golla, R.; Li, Y.; Seethala, R.; Zvyaga, T.; Gordon, D. A.; Li, J. *Bioorg. Med. Chem. Lett.* **2011**, *21*, 4146–4149.

<sup>143</sup> Xiang-Yang, Y.; Chen, S. Y.; Wu, S.; Yoon, D. S.; Wang, H.; Hong, Z.; O'Connor, S. P.; Li, J.; Li, J. J.; Kennedy, L. L.; Walker, S. J.; Nayeem, A.; Sheriff, S.; Camac, D. M.; Ramamurthy, V.; Morin, P. E.; Zebo, R.; Taylor, J. R.; Morgan, N. N.; Ponticello, R. P.; Harrity, T.; Apedo, A.; Golla, R.; Seethala, R.; Wang, M.; Harper, T. W.; Slecicka, B. G.; He, B.; Kirby, M.; Leahy, D. K.; Li, J.; Hanson, R. L.; Guo, Z.; Li, Y.; DiMarco, J. D.; Scaringe, R.; Maxwell, B. D.; Moulin, F.; Barrish, J. C.; Gordon, D. A.; Robl, J. A. *J. Med. Chem.* **2017**, *60*, 4932-4948.

<sup>144</sup> <https://clinicaltrials.gov/ct2/show/NCT00979368?term=BMS-816336&rank=1>, Accessed March 2017.

<sup>145</sup> <http://adisinsight.springer.com/drugs/800027626>, Accessed March 2017.

<sup>146</sup> Zhuang, L.; Tice, C. M.; Xu, Z.; Zhao, W.; Cacatian, S.; Ye, Y. J.; Singh, S. B.; Lindblom, P.; McKeever, B. M.; Krosky, P. M.; Zhao, Y.; Lala, D.; Kruk, B. A.; Meng, S.; Howard, L.; Johnson, J. A.; Bukhtiyarov, Y.; Panemangalore, R.; Guo, J.; Guo, R.; Himmelsbach, F.; Hamilton, B.; Schuler-Metz, A.; Schauerte, H.; Gregg, R.; McGeehan, G. M.; Leftheris, K.; Claremon, D. A. *Bioorg. Med. Chem.* **2017**, *25*, 3649-3657.

<sup>147</sup> <https://clinicaltrials.gov/ct2/results?term=BI-135585&Search=Search>, Accessed March 2017.

<sup>148</sup> Freude, S.; Heise, T.; Woerle, H. J.; Jungnik, A.; Rauch, T.; Hamilton, B.; Schölch, C.; Huang, F.; Graefe-Mody, U. *Diabetes Obes. Metab.* **2016**, *18*, 483-490.

Medicines in Development for Diabetes 2014 of the America's Biopharmaceutical Research Companies and it did in the previous report of 2012.<sup>149,150</sup> In the later report, appeared a new compound, BI-187004 CL, another 11 $\beta$ -HSD1 inhibitor that replaced BI-135585.<sup>150</sup> This compound reached phase II trials but it did not meet the predefined efficacy regarding fasting glucose lowering. Consequently, Boehringer Ingelheim informed Vitae of its intention to end the program and the corresponding license agreement, being the compound discontinued at the end of 2015.<sup>151,152</sup>

Compound AZD-4017 from AstraZeneca was the first 11 $\beta$ -HSD1 inhibitor from this company to reach clinical trials in 2008 for diabetes and obesity.<sup>153</sup> After being safe and well tolerated, it switched indication to raised intraocular pressure for the phase II trials performed in 2012.<sup>154</sup> Although the company discontinued this program in 2013, the University of Birmingham planned other phase II trials for the next year.<sup>155</sup> According to EU Clinical Trials Register, the trials sponsored were for post-menopausal osteopenia and idiopathic intracranial hypertension, being the first prematurely ended and the later still ongoing.<sup>156,157,158</sup> Two back-up compounds generated from AZD-4017 were AZD-8329, that completed phase I trials for T2DM and obesity in 2010 but

---

<sup>149</sup> Report of Medicines in Development for Diabetes 2012, America's Biopharmaceutical Research Companies.

<sup>150</sup> Report of Medicines in Development for Diabetes 2014, America's Biopharmaceutical Research Companies.

<sup>151</sup> <http://ir.vitaepharma.com/phoenix.zhtml?c=219654&p=irol-newsArticle&ID=2123771>, Accessed March 2017.

<sup>152</sup> <http://adisinsight.springer.com/drugs/800036000>, Accessed March 2017.

<sup>153</sup> <https://clinicaltrials.gov/ct2/show/NCT00791752?term=AZD4017&rank=5>, Accessed March 2017.

<sup>154</sup> <https://clinicaltrials.gov/ct2/show/NCT01173471?term=AZD4017&rank=6>, Accessed March 2017.

<sup>155</sup> <http://adisinsight.springer.com/drugs/800029324>, Accessed March 2017.

<sup>156</sup> <https://www.clinicaltrialsregister.eu/ctr-search/trial/2013-003387-32/GB>, Accessed March 2017.

<sup>157</sup> <https://www.clinicaltrialsregister.eu/ctr-search/trial/2013-003643-31/GB>, Accessed March 2017.

<sup>158</sup> <https://clinicaltrials.gov/ct2/show/NCT02017444?term=AZD4017&rank=1>, Accessed March 2017.

discontinued the next year,<sup>159,160</sup> and AZD-6925, supposed to be a clinical candidate but not found in the clinical trials registers nor in the company pipeline.<sup>161</sup>

Roche entered two compounds in clinical trials. RG-7234 (RO5027838), that was selected due to its tissue selectivity in adipose over liver, and RG-4929 (RO5093151) completed a head to head, proof-of-concept study in 2009.<sup>162</sup> Slight metabolic improvements were observed, especially with RG-4929 high dose, although the changes did not present statistical significance and were not clearly dose dependent.<sup>163</sup> Subsequently, RG-7234 was discontinued at phase I the next year<sup>164</sup> and RG-4929 progressed into phase II trials, although its development was also interrupted for metabolic diseases in 2012.<sup>165</sup> Afterwards, this compound was switched its indication to non-alcoholic fatty liver disease (NAFLD) and completed a phase I trial for this condition in 2012.<sup>166</sup> The compound resulted effective in reducing liver-fat content, but did not improve systemic or hepatic insulin resistance, questioning the efficacy in NAFLD patients.<sup>167,168</sup> Again, the indication of RG-4929 was changed to glaucoma and a phase II trial at the end of 2012<sup>169</sup> and a phase I trial in 2016 were completed.<sup>170</sup> This compound was present in the company pipeline as indicated in the

---

<sup>159</sup> <https://clinicaltrials.gov/ct2/results?term=AZD8329&Search=Search>, Accessed March 2017.

<sup>160</sup> <http://adisinsight.springer.com/drugs/800030582>, Accessed March 2017.

<sup>161</sup> Scott, J. S.; Chooramun, J. RSC Drug Discovery Series No. 27, 2012. New Therapeutic Strategies for Type 2 Diabetes: Small Molecule Approaches. Chapter 5: 11 $\beta$ -Hydroxysteroid DehydrogenaseType1 (11 $\beta$ -HSD1) Inhibitors in Development.

<sup>162</sup> <https://clinicaltrials.gov/ct2/show/NCT00823680?term=RO5027838&rank=1>, Accessed March 2017.

<sup>163</sup> T. Heisel, L.; Morrow, M.; Hompesch, H.-U.; Häring, C.; Kapitza, M.; Abt, M.; Ramsauer, M.C.; Magnone, S.; Fuerst-Recktenwald, S. *Diabetes Obes. Metab.* **2014**, *16*, 1070-1077.

<sup>164</sup> Roche presentation, October 14, 2010, slide 37. See <http://www. Roche.com/irp3q10e.pdf>.

<sup>165</sup> Roche presentation, October 16, 2012, p 47. See <http://www. Roche.com/irp3q12e.pdf>.

<sup>166</sup> <https://clinicaltrials.gov/ct2/show/NCT01277094?term=RO5093151&rank=4>, Accessed March 2017.

<sup>167</sup> Stefan, N.; Ramsauer, M.; Jordan, P.; Nowotny, B.; Kantartzis, K.; Machann, J.; Hwang, J.; Nowotny, P.; Kahl, S.; Harreiter, J.; Hornemann, S.; Sanyal, A. J.; Stewart, P. M.; Pfeiffer, A. F.; Kautzky-Willer, A.; Roden, A.; Häring, H.; Fürst-Recktenwald, S. *Lancet Diabetes Endocrinol.* **2014**, *2*, 406-416.

<sup>168</sup> Ratziu, V. *Lancet Diabetes Endocrinol.* **2014**, *2*, 354-356.

<sup>169</sup> <https://clinicaltrials.gov/ct2/show/NCT01493271?term=RO5093151&rank=1>, Accessed March 2017.

<sup>170</sup> <https://clinicaltrials.gov/ct2/show/NCT02622334?term=RO5093151&rank=2>, Accessed March 2017.

first quartermaster 2016 report,<sup>171</sup> but discontinued some months after as indicated in the next report in October 2016.<sup>172</sup>

Wyeth entered a 11 $\beta$ -HSD1 inhibitor in clinic in 2008, named HSD-016. Although this compound completed phase I trials in 2009,<sup>173</sup> after the acquisition of Wyeth by Pfizer, this program does not appear in the company pipeline probably due to the overlap with its own program (PF-915275, see above).

Eli Lilly also had a 11 $\beta$ -HSD1 program in its development pipeline. Its compound LY-2523199 entered phase II trials in 2011 for T2DM in USA, although it was reported discontinued in the Second Quarter 2013 Financial Review of the company.<sup>174</sup> The compound P2202 originated by Eli Lilly has been developed by Piramal Enterprises for T2DM. Although a phase II study was terminated in the beginning of 2013,<sup>175</sup> a phase I pharmacokinetics trial was completed at the end of 2013 in India.<sup>176</sup> Since then, no further development has been reported, and the annual report of 2012 was the last one containing the status of P2202.

Japan Tobacco, through its pharmaceutical subsidiary Akros Pharma, progressed JTT-654 into phase II trials in 2009 for the treatment of T2DM.<sup>177</sup> However, accordingly to a company overview report with their updated pipeline in October 2010, the development of JTT-654 was terminated.<sup>178</sup>

---

<sup>171</sup> Roche presentation, April 19, 2016, page 50. <http://www.roche.com/dam/jcr:2a156912-eff5-4257-9547-fbd0623d9429/en/irp1q16e-a.pdf>.

<sup>172</sup> Roche presentation, October 20, 2016, page 50. <http://www.roche.com/dam/jcr:70fbe9e4-80d5-431c-9e78-eb12cf5ce087/en/irp161020-a.pdf>.

<sup>173</sup> <https://clinicaltrials.gov/ct2/results?term=HSD016&Search=Search>, Accessed March 2017.

<sup>174</sup> Lilly presentation 2Q 2013, page 12. [http://files.shareholder.com/downloads/LLY/2073248133x0x678669/d90dc9fa-da40-4bb3-82f6-02acaa752eb7/Q2\\_2013\\_Slides.pdf](http://files.shareholder.com/downloads/LLY/2073248133x0x678669/d90dc9fa-da40-4bb3-82f6-02acaa752eb7/Q2_2013_Slides.pdf).

<sup>175</sup> <https://clinicaltrials.gov/ct2/show/NCT01674348?term=P2202&rank=1>, Accessed March 2017.

<sup>176</sup> <http://www.ctri.nic.in/Clinicaltrials/pmaindet2.php?trialid=2394>, Accessed March 2017.

<sup>177</sup> <https://clinicaltrials.gov/ct2/show/NCT00997152?term=JTT-654&rank=1>, Accessed March 2017.

<sup>178</sup> Japan Tobacco presentation of the Consolidated Financial Results for the six months ended September 30, 2010, page 10. [http://www.jti.com/files/2713/2818/3505/JTs\\_Consolidated\\_Financial\\_Results\\_for\\_the\\_6\\_months\\_ended\\_September\\_30\\_2010.pdf](http://www.jti.com/files/2713/2818/3505/JTs_Consolidated_Financial_Results_for_the_6_months_ended_September_30_2010.pdf).



### 1.3.2 Glaucoma

Besides the previous compounds mentioned, AZD-4017 and RG-4929, compound HPP-851 from High Point Pharma entered in phase I trials for glaucoma in 2010.<sup>179</sup> This compound was evaluated in a phase Ib/Ila study in patients with elevated intraocular pressure or primary open-angle glaucoma,<sup>126</sup> but it is no longer in the company pipeline.

### 1.3.3 Cognitive impairment and Alzheimer's disease

Abbott focused its 11 $\beta$ -HSD1 program in developing a drug for the treatment of AD. The selected clinical candidate ABT-384 successfully completed phase I trials in 2010, after assessing the cerebral spinal fluid (CSF) pharmacokinetics and the plasma/CSF PK/PD relationship of the compound.<sup>180,181</sup> The next step was a phase II study in patients with mild-to-moderate AD during 12 weeks, which was completed in 2011.<sup>182</sup> ABT-384, when tested at doses associated with complete brain 11 $\beta$ -HSD1 inhibition, did not produce symptomatic improvement in AD, assessed by the Alzheimer's Disease Assessment Scale–Cognitive subscale (ADAS-Cog) and other secondary end points.<sup>183</sup> After this lack of efficacy, the compound was discontinued and it no longer appears in the company pipeline.

Researchers at the Centre for Cardiovascular Science of the University of Edinburgh also led this field of the discovery of 11 $\beta$ -HSD1 inhibitors and especially the target validation in Central Nervous System (CNS) disorders, since Prof. Jonathan Seckl discovered the role of this enzyme in the brain.<sup>118</sup> Prof. Brian Walker and Dr Scott Webster led the drug development program funded by the Wellcome Trust

<sup>179</sup> <http://www.businesswire.com/news/home/20101104007514/en/TransTech-Pharma-High-Point-Pharmaceuticals-Awarded-1.96>, Accessed March 2017.

<sup>180</sup> Katz, D. A.; Liu, W.; Locke, C.; Jacobson, P.; Barnes, D. M.; Basu, R.; An, G.; Rieser, M. J.; Daszkowski, D.; Groves, F.; Heneghan, G.; Shah, A.; Gevorkyan, H.; Jhee, S. S.; Ereshefsky, L.; Marek, G. J. *Transl. Psychiatry* **2013**, *3*, e295, 1-7.

<sup>181</sup> <https://clinicaltrials.gov/ct2/show/NCT01009216?term=ABT-384&rank=1>, Accessed March 2017.

<sup>182</sup> <https://clinicaltrials.gov/ct2/show/NCT01137526?term=ABT-384&rank=2>, Accessed March 2017.

<sup>183</sup> Marek, G. J.; Katz, D. A.; Meier, A.; Greco, N.; Zhang, W.; Liu, W.; Lenz, R. A. *Alzheimers Dement.* **2014**, *10*, (5 Suppl), S364-S373.

through a Seeding Drug Discovery award.<sup>184</sup> The great efforts put in this project permitted them to select their clinical candidate UE-2343 and to successfully complete single dose phase I study in healthy individuals in 2013.<sup>185</sup> In May 2014, they founded the spin-out company Corticrine Ltd.<sup>186</sup> to then being acquired by an Australian biotech company, Actinogen Medical.<sup>187,188</sup> In partnering, they completed phase I trials in 2015 with a CSF PK study of UE-2343 (whose brand name is Xanamem™).<sup>189,190</sup> After demonstrating well tolerability and sufficient brain concentrations to inhibit the target enzyme, the phase II study XanADu to assess efficacy in patients with mild dementia due to AD has already started (March 2017) and estimated to be completed in two years (May 2019).<sup>191</sup> Accordingly to the company website, they are currently conducting clinical research for other potential indications for Xanamem™, such as Diabetes Cognitive Impairment (DCI) and Post-Traumatic Stress Disorder (PTSD).<sup>192</sup>

Astellas Pharma entered its clinical candidate ASP-3662 into phase I trials in 2014.<sup>193</sup> The next year, they started a phase II trial for Painful Diabetic Peripheral Neuropathy (PDPN) which was terminated in 2016 due to futility analysis.<sup>194</sup> Currently, the compound is in phase II trials for agitation associated with AD accordingly to the company pipeline.<sup>195</sup>

---

<sup>184</sup> <https://wellcome.ac.uk/press-release/promising-drug-candidate-reverses-age-related-memory-loss-mice>, Accessed March 2017.

<sup>185</sup> <https://clinicaltrials.gov/ct2/show/NCT01770886?term=UE2343&rank=1>, Accessed March 2017.

<sup>186</sup> <https://beta.companieshouse.gov.uk/company/SC478733>, Accessed March 2017.

<sup>187</sup> <http://www.asx.com.au/asxpdf/20140827/pdf/42rs6xh1sx5rsm.pdf>.

<sup>188</sup> <http://www.edinburghbioquarter.com/news/item/actinogen-limited-to-acquire-corticrine-limited/>, Accessed March 2017.

<sup>189</sup> <https://clinicaltrials.gov/ct2/show/NCT02616445?term=UE2343&rank=2>, Accessed March 2017.

<sup>190</sup> Webster, S. P.; McBride, A.; Binnie, M.; Sooy, K.; Seckl, J. R.; Andrew, R.; Pallin, T. D.; Hunt, H. J.; Perrior, T. R.; Ruffles, V. S.; Ketelbey, J. W.; Boyd, A.; Walker, B. R. *British J. Pharmacol.* **2017**, *174*, 396-408.

<sup>191</sup> <https://clinicaltrials.gov/ct2/show/NCT02727699?term=UE2343&rank=3>, Accessed March 2017.

<sup>192</sup> <http://actinogen.com.au/research/#current>, Accessed March 2017.

<sup>193</sup> <https://clinicaltrials.gov/ct2/show/NCT02194491?term=ASP+3662&rank=1>, Accessed March 2017.

<sup>194</sup> <https://clinicaltrials.gov/ct2/show/NCT02372578?term=ASP+3662&rank=2>, Accessed March 2017.

<sup>195</sup> [https://www.astellas.com/en/ir/library/pdf/3q2017\\_rd\\_en.pdf](https://www.astellas.com/en/ir/library/pdf/3q2017_rd_en.pdf).

By way of conclusion, the efficacy of 11 $\beta$ -HSD1 inhibitors in clinics has still to be proven since no compounds have progressed beyond phase II, with insufficient efficacy being the main cause of attrition. In general, compounds were well tolerated and the concern about upregulation of the HPA axis has been mitigated since adrenal androgens and urinary corticosteroid profile have not presented significant changes or no clinically meaningful elevations.<sup>132,134,137</sup>

Regarding metabolic indications, the failure to achieve primary efficacy endpoints such as glycemic control or blood pressure were disappointing, but results at high dose INCB-13739 (200 mg) led to the hypothesis that a high drive on the target might be required (i.e. coverage of IC<sub>90</sub> rather than IC<sub>50</sub>). In addition to this, with this same compound, the greatest glucose- and lipid-lowering actions were seen in subjects with the highest plasma glucose and lipid levels, suggesting that subjects with elevated 11 $\beta$ -HSD1 in key target organs might represent the main beneficiaries.<sup>135</sup> Also, recent reports stating that some of the clinical observations may be in part off-target effects, have further complicated the development picture of 11 $\beta$ -HSD1 inhibitors for T2DM and metabolic syndrome.<sup>136,196</sup>

Finally, in relation to age-associated cognitive impairment and AD, inhibitors from Actinogen Medical and Astellas are still in active development, both of them in phase II trials. Although the failure of the Abbott compound ABT-384 in demonstrating efficacy, central 11 $\beta$ -HSD1 inhibition seems a promising approach to deal with cognitive dysfunction associated with AD. As Webster *et al.* highlighted in their last work reporting the selection and phase I trials of UE-2343, their data compare favourably with those published for ABT-384 in terms of CSF levels and the expected 11 $\beta$ -HSD1 inhibition in the brain, so they are keen to success in demonstrating efficacy with their compound.<sup>190</sup> Furthermore, in contrast with metabolic effects, previous preclinical studies have demonstrated that sub-maximal inhibition of the target in the brain is enough to reverse memory impairment in aging and AD.<sup>121</sup>

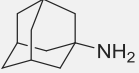
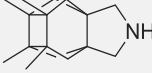

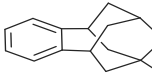
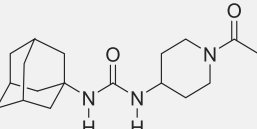
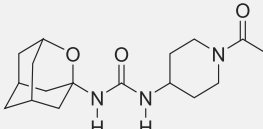
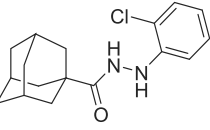
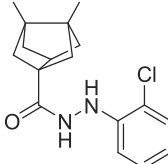
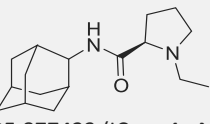
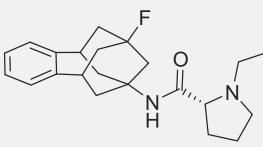
---

<sup>196</sup> Harno, E.; Cottrell, E. C.; Yu, A.; DeSchoolmeester, J.; Gutierrez, P. M.; Denn, M.; Swales, J. G.; Goldberg, F. W.; Bohlooly-Y, M.; Andersén, H.; Wild, M. J.; Turnbull, A. V.; Leighton, B.; White, A. *Endocrinology* **2013**, *154*, 4580-4593.

#### 1.4 Framework and previous work of our group

As the reader could appreciate in Chart 1 from the previous section, polycyclic and lipophilic groups are a common motif in 11 $\beta$ -HSD1 inhibitors entered in clinical trials, as well as in previous lead compounds not mentioned in this Thesis (i.e. MK-544, PF-877423). Among different structures, adamantyl and norbornyl are the most frequent motifs of the disclosed inhibitors (i.e. BMS-816336, AZD-8329, ABT-384, and AMG-221, BMS-770767, RG-7234, respectively), followed by bicyclo[2.2.2]octyl (MK-0736). The reason of these lipophilic groups is the filling of the hydrophobic cavity in the active site of the enzyme which is physiologically filled by the lipophilic GC skeleton.

This observation caught the attention of our research group, which is expert in polycyclic compounds and their potential use in medicinal chemistry as replacement of the adamantyl group. The work efforts put in the last years permitted us to discover potent channel inhibitors, such as M2 channel blockers (anti-Influenza A compounds), NMDA receptor antagonists (for AD) or P2X7 antagonists, as well as improved enzyme inhibitors with soluble epoxide hydrolase as the target enzyme. The following table intend to briefly summarize the last years' work replacing the adamantyl moiety in various reference compounds addressed to different targets (Table 2).

TARGET	REFERENCE COMPOUND	OUR COMPOUND
M2 channel of the influenza A virus	 Amantadine (wt IC <sub>50</sub> = 16 $\mu$ M, V27A inactive, L26F inactive)	 UB-MFV-3 (wt IC <sub>50</sub> = 18 $\mu$ M, V27A IC <sub>50</sub> = 0.7 $\mu$ M, L26F IC <sub>50</sub> = 8.6 $\mu$ M) <sup>197</sup>
NMDA receptor	 Memantine (IC <sub>50</sub> = 1.5 $\mu$ M)	 UB-EV-32 (IC <sub>50</sub> = 0.7 $\mu$ M) <sup>198</sup>
Soluble epoxide hydrolase (sEH)	 AR-9281 (IC <sub>50</sub> = 8 nM)	 UB-EV-53 (IC <sub>50</sub> = 1 nM) <sup>199</sup>
P2X7 receptor	 Abbott inhibitor (IC <sub>50</sub> = 11.5 nM)	 UB-EV-12 (IC <sub>50</sub> = 18 nM) <sup>200</sup>
11 $\beta$ -HSD1	 PF-877423 (IC <sub>50</sub> = 4 nM)	 UB-EV-57 (IC <sub>50</sub> = 350 nM) <sup>201</sup>

**Table 2.** Previous work of the group replacing the adamantyl group by other polycycles in different targets attractive for drug discovery. wt = wild type.

<sup>197</sup> Rey-Carrizo, M.; Barniol-Xicota, M.; Ma, C.; Frigolé-Vivas, M.; Torres, E.; Naesens, L.; Llabrés, S.; Juárez-Jiménez, J.; Luque, F. J.; DeGrado, W. F.; Lamb, R. A.; Pinto, L. H.; Vázquez, S. *J. Med. Chem.* **2014**, *57*, 5738–5747.

<sup>198</sup> Valverde, E.; Sureda, F. X.; Vázquez, S. *Bioorg. Med. Chem.* **2014**, *22*, 2678-2683.

<sup>199</sup> Vázquez S.; Valverde, E.; Leiva, R.; Vázquez-Carrera, M.; Codony, S. PCT Patent Application, WO2017017048.

<sup>200</sup> Barniol-Xicota, M.; Kwak, S.-H.; Lee, S.-D.; Caseley, E.; Valverde, E.; Jiang, L.-H.; Kim, Y.-C.; Vázquez, S. *Bioorg. Med. Chem. Lett.* **2017**, *27*, 759-763.

<sup>201</sup> Valverde, E.; Seira, C.; McBride, A.; Binnie, M.; Luque, F. J.; Webster, S. P.; Bidon-Chanal, A.; Vázquez, S. *Bioorg. Med. Chem.* **2015**, *23*, 7607-7617.

Although the research group had succeeded in finding suitable replacements for the adamantyl group against several targets,<sup>197,198,199,200</sup> in the case of 11 $\beta$ -HSD1, this strategy had not been successful. In the context of Dr Elena Valverde's PhD Thesis, new compounds featuring the benzohomoadamantane scaffold as adamantane surrogate were synthesized and evaluated.<sup>201</sup> Among thirteen new compounds prepared, with different right-hand side substituents and various groups in C-9 of the polycycle, only one presented a submicromolar 11 $\beta$ -HSD1 IC<sub>50</sub>, compound UB-EV-57 (last entry of Table 2), although two orders of magnitude above its adamantyl analog.

This work set the scene for the present PhD Thesis and the objectives thereof, resulting in the polycyclic group optimization in novel 11 $\beta$ -HSD1 inhibitors.



## CHAPTER 2

# **Objectives**

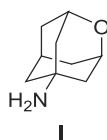




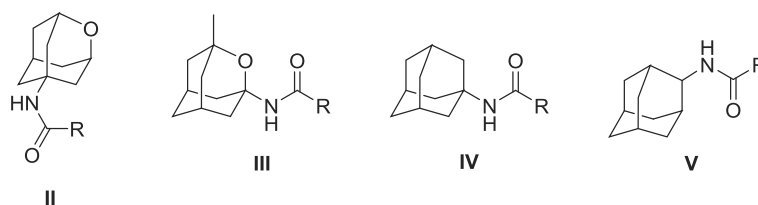
As mentioned in the last section of the Introduction chapter, the main goal of the present Thesis is the polycyclic group optimization in novel 11 $\beta$ -HSD1 inhibitors in order to improve the fit of the molecules in the enzyme binding site. After this, the structure-activity relationship (SAR) exploration of the rest of the structure is the ultimate objective to obtain suitable candidates to use them as investigational tools in rodent models of the diseases of interest.

Insightfully, the objectives are listed as follows:

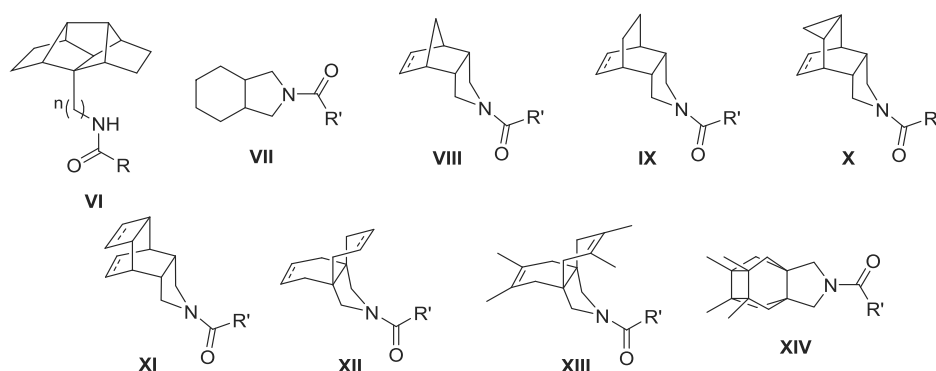
1. Synthesis and pharmacological evaluation of the novel oxapolycyclic amine 2-oxaadaman-5-amine, **I**, as a new polar analog of amantadine. (Chapter 3)



2. Synthesis of putative 11 $\beta$ -HSD1 inhibitors containing oxaadamantyl amines, the just mentioned 2-oxaadaman-5-amine, **II**, and the previously described by the group 3-methyl-2-oxaadaman-1-amine, **III**, and their pharmacological evaluation. By way of comparison, synthesis of a small series of 1- and 2-adamantyl derivatives, **IV** and **V**, also to compare the different substitution in the adamantyl moiety. (Chapter 4)

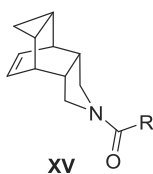


3. Synthesis and pharmacological evaluation of pentacyclododecyl-containing compounds, **VI**, and an array of pyrrolidine-based polycyclic amides, **VII-XIV**, in order to explore the pyrrolidine motif fused to the polycyclic moiety in 11 $\beta$ -HSD1 inhibitors. After an *in vitro* profiling, selection of a suitable compound to perform an *in vivo* study in a rodent model of cognitive dysfunction, the Senescence-Accelerated Mouse Prone 8 (SAMP8). (Chapter5)

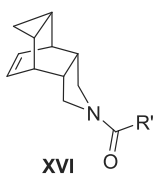


R = cyclohexyl or piperidine. n = 0 or 1. R' = cyclohexyl.

4. Due to the higher potency of the compound containing the 4-azapentacyclo[5.3.2.0<sup>2,6</sup>.0<sup>8,10</sup>]dodec-11-ene polycycle, **X**, the exploration of the right-hand side (RHS) substituent was the next objective in order to discover more potent and selective inhibitors. The synthesis and pharmacological evaluation of a family integrating different groups as RHS substituents, **XV**, was envisaged. (Chapter 6)



5. After the sub-optimal results of the previous compounds regarding selectivity and DMPK properties, a structure-based design of new substitution patterns of the RHS group in order to establish additional interactions in the binding site that would deliver more potent and selective inhibitors was planned. The synthesis and pharmacological evaluation of a new series of putative 11 $\beta$ -HSD1 inhibitors, **XVI**, following this methodology was arranged. (Chapter 7)





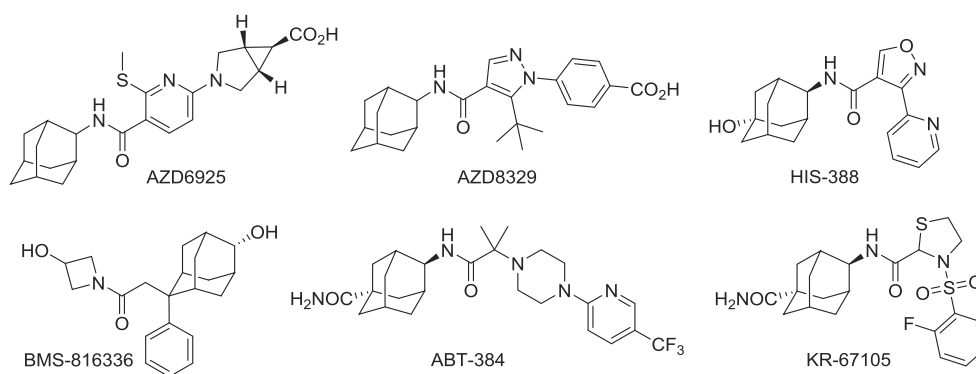
## CHAPTER 3

# **Synthesis and evaluation of the novel 2-oxadaman-5-amine**



### 3.1 Rationale and previous work

As previously mentioned in the Objectives section, the project presented in this chapter aimed to synthesize a novel cage amine in order to replace the aminoadamantyl group present in numerous 11 $\beta$ -HSD1 inhibitors (Chart 2). The target amine was envisioned to contain an oxygen atom in its hydrophobic skeleton to mimic the structure of some hydroxylated adamantyl derivatives developed by pharma companies such as HIS-388 and BMS-816336. It appears that the hydroxyl group as well as the carboxamide unit in C-5 of the adamantyl moiety confer well fit in the binding site together with proper DMPK characteristics.<sup>126</sup>



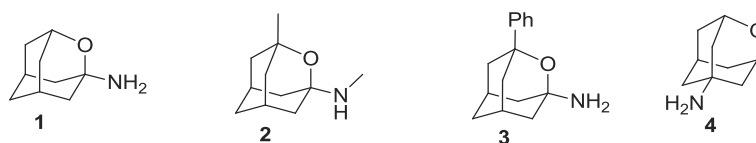
**Chart 2.** Structures of adamantyl-based 11 $\beta$ -HSD1 inhibitors.<sup>126</sup>

Taking into account the exposed reasons and the established expertise of the group with oxadamantyl compounds,<sup>202</sup> we proposed the synthesis of the novel 2-oxadamantan-5-amine, **4**, as the new cage amine to add to our library of polycyclic scaffolds (Chart 3).

<sup>126</sup> Scott, J. S.; Goldberg, F. W.; Turnbull, A. V. *J. Med. Chem.* **2014**, *57*, 4466–4486.

<sup>202</sup> Duque, M. D.; Camps, P.; Profire, L.; Montaner, S.; Vázquez, S.; Sureda, F. S.; Mallol, J.; López-Querol, M.; Naesens, L.; De Clercq, E.; Prathalingam, S. R.; Kelly, J. M. *Bioorg. Med. Chem.* **2009**, *17*, 3198–3206.





**Chart 3.** Structures of the previously described (2-oxaadaman-1-yl)amines, **1-3**<sup>202</sup>, and the target compound 2-oxaadaman-5-amine, **4**.

An additional driving force to prepare this novel oxapolycyclic amine **4** was its potential use as M2 channel inhibitor, of interest for the group as previously mentioned in the Introduction chapter. The foreseen blocking of the S31N mutant M2 channel of the Influenza A virus since its more polar nature was the attraction of this envisaged compound. The S31N is the most relevant mutation of the M2 channel, present in 95% cases of the current circulating infective viruses.<sup>203</sup>

Substitution of Serine 31 (-CH<sub>2</sub>OH as the side chain) with Asparagine (-CH<sub>2</sub>CONH<sub>2</sub> as the side chain) not only narrows the portion of the channel to which the adamantane-like drugs bind –providing steric hindrance that reduces the affinity- but also adds a hydrophilic atom to the site which interacts with the hydrophobic adamantyl cage (Figure 8a).

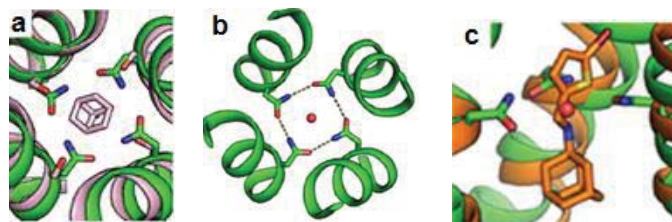
In light of this evidence, the introduction of an oxygen atom in the lipophilic structure of adamantane that could interact with these carboxamide groups seemed interesting to explore.

In addition to this, it has been recently reported that carboxamide nitrogen of each Asparagine (Asn) residue of the homotetramer forms a hydrogen bond with the carbonyl group of the neighbouring Asn31 side chain. At the centre of this cyclic hydrogen-bonding arrangement, a water molecule was observed bridging these interactions (Figure 8b).<sup>204</sup> In this same location, the nitrogen of a S31N mutant channel inhibitor was found in the solved inhibitor-bound solution NMR structure of

<sup>203</sup> Dong, G., Peng, C., Luo, J., Wang, C., Han, L., Wu, B., Ji, G. & He, H. *PLoS One* **2015**, *10*, e0119115.

<sup>204</sup> Thomaston, J. L.; DeGrado, W. F. *Protein Science* **2016**, *25*, 1551-1554.

S31N (Figure 8c).<sup>205</sup> These findings corroborate our hypothesis of trying to locate the oxygen atom of the oxadamantane structure in a convenient position to interact with the polar residues namely by hydrogen bonding.



**Figure 8.** (a) Overlay of S31N mutant structure 5C02 (green) onto the drug-bound structure 3C9J (pink) with Asn31, Ser31, and amantadine shown as sticks. (b) Top-down view of the channel pore; Asn31 residues form a network of hydrogen bonds (dashed lines). A single water (red sphere) is located in the middle of these residues. (c) Side view of *N*-[(5-bromothiophen-2-yl)methyl]adamantan-1-amine inhibitor from 2MUV in channel pore, with water from 5C02 shown as a red sphere.<sup>204, 205</sup>

### 3.2 Theoretical discussion

All the compounds described in the following manuscript and their precursors were prepared in the context of this Thesis.

The first goal of this project was the preparation of the 2-oxaadamantane nucleus, **8** (Scheme 1). Although its synthesis had been reported by other groups involving different synthetic routes, it was not straightforward and resulted in some interesting observations.

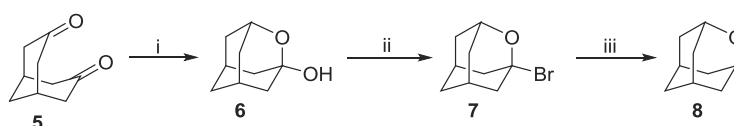
We initially envisaged the access to 2-oxaadamantane using the route previously reported by Stetter and coworkers from known diketone **5** since our group previously synthesized the 2-oxa-1-adamantanol **6** from it.<sup>206,207</sup> This approach revolves around a

<sup>205</sup> Wu, Y.; Canturk, B.; Jo, H.; Ma, C.; Gianti, E.; Klein, M. L.; Pinto, L. H.; Lamb, R. A.; Fiorin, G.; Wang, J.; DeGrado, W. F. *J. Am. Chem. Soc.* **2014**, *136*, 17987–17995.

<sup>206</sup> Stetter, H.; Tacke, P.; Gaertner, J. *Chem. Ber.* **1964**, *97*, 3480-3487.

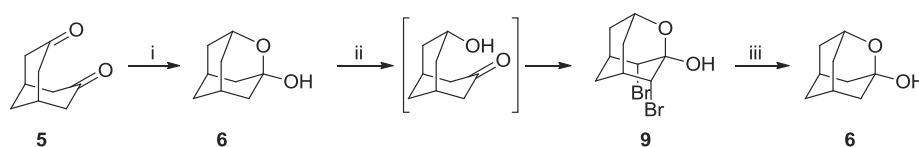
<sup>207</sup> Camps, P.; El Achab, R.; Font-Bardia, M.; Görbig, D. M.; Morral, J.; Muñoz-Torrero, D.; Solans, X.; Simon, M. *Tetrahedron* **1996**, *52*, 5867-5880.

bromide/hydroxy exchange with thionyl bromide on compound **6** followed by reduction to **8** (Scheme 1).



**Scheme 1.** Stetter's proposed synthesis for 2-oxaadmantane, **8**. (i) NaBH<sub>4</sub>, dry MeOH, r.t., 24 h, 92% yield. (ii) SOBr<sub>2</sub>, pyridine, 90 °C, 15 min, 10% yield. (iii) Raney-Nickel, NaOH, MeOH, 45 °C, 1 h.

In our hands, the reduction of the diketone **5** proceeded in very high yield, as previously reported.<sup>206</sup> Taking into account the very low yield reported by Stetter and coworkers for the exchange reaction (10% yield), we preferred to follow a different procedure previously applied by our group in a related compound.<sup>208</sup> However, this attempt was unsuccessful since our method did not use pyridine. Consequently, the bromination led to the 8,9-dibromo-2-oxaadmantan-1-ol, **9**, likely arising from the electrophilic bromination in the alpha positions of the ketone intermediate.<sup>209</sup> In this way, when we reduced the brominated compound **9** with sodium bis(2-methoxyethoxy)aluminum hydride (Red-Al®) we recovered the starting material **6** (Scheme 2).

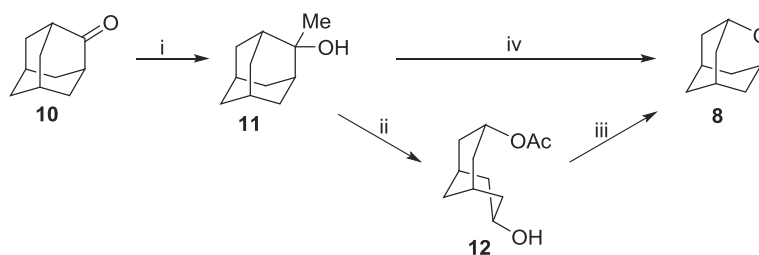


**Scheme 2.** First attempt to 2-oxaadmantane **8**. (i) NaBH<sub>4</sub>, dry MeOH, r.t., 24 h, 92% yield. (ii) SOBr<sub>2</sub>, r.t., 4 h, 75% yield. (iii) Red-Al®, dry toluene, reflux, 16 h, 70% yield.

<sup>208</sup> Valverde, E.; Sureda, F. X.; Vázquez, S. *Bioorg. Med. Chem. Lett.* **2014**, *22*, 2678-2683.

<sup>209</sup> Mc Donald, I. A.; Dreiding, A. S.; Hutmacher, H.; Musso, H. *Helv. Chim. Acta* **1973**, *56*, 1385-1395.

After that and considering the very low yield of the bromide/hydroxy exchange reaction, 2-oxaadamantane, **8**, was prepared using a previously described three-step synthesis involving a double Criegee rearrangement.<sup>210</sup> Commercially available 2-adamantanone, **10**, was treated with methylmagnesium bromide to give 2-methyl-2-adamantanol, **11**, in very high yield. Krasutsky and coworkers had reported consecutive Criegee rearrangements on the alcohol **11** to deliver the 2-oxaadamantane. As occurred to Alder and coworkers, the two-step procedure through the intermediate *endo,endo*-3-hydroxy-7-acetoxycyclo[3.3.1]nonane, **12**, seemed to be more efficient than the one-step photochemical procedure.<sup>211</sup> Thus, **11** was first treated with trifluoroacetic anhydride (TFAAn) and H<sub>2</sub>O<sub>2</sub> at -25 °C -generating *in situ* trifluoroperacetic acid (TFPAA) and trifluoroacetic acid (TFAA)- to give, after quenching with water, the acetate **12** (Scheme 3).

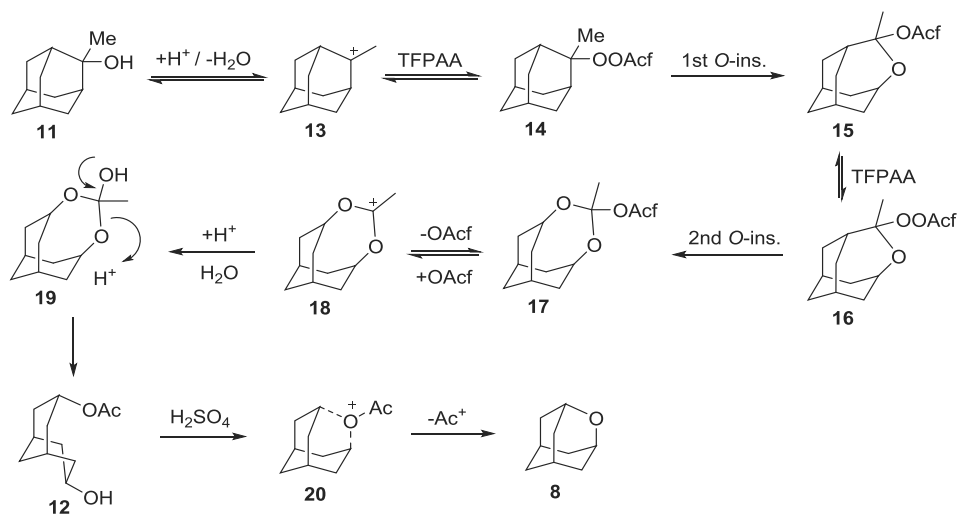


**Scheme 3.** Syntheses of 2-oxaadamantane, **8**. (i) MeMgBr, dry Et<sub>2</sub>O, r.t., 1.5 h, 97% yield. (ii) 1) TFAAn, H<sub>2</sub>O<sub>2</sub>, -25 °C, 2 h. 2) H<sub>2</sub>O. (iii) concd H<sub>2</sub>SO<sub>4</sub>, -10 °C, 1 h, 58% overall yield from **11**. (iv) HgO, I<sub>2</sub>, dry toluene, *hν*, 3 h, 12%.

Trifluoroacetate **14**, which could be formed from alcohol **11** through the intermediate carbocation **13**, is the obvious intermediate for the double *O*-insertion. Finally, acetate **12** was easily transformed to the required oxaadamantane in cold sulfuric acid by electrophilic cyclization (Scheme 4).

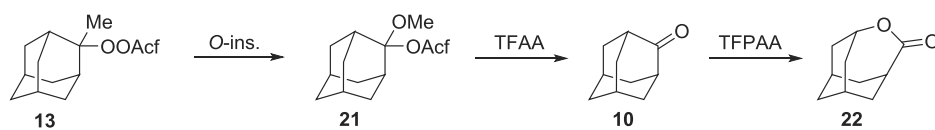
<sup>210</sup> Krasutsky, P. A.; Kolomitsin, I. V.; Kiprof, P.; Carlson, R. M.; Forkin, A. A. *J. Org. Chem.* **2000**, *65*, 3926-3933.

<sup>211</sup> Alder, R. W.; Carta, F.; Reed, C. A.; Stoyanova, I.; Willis, C. L. *Org. Biomol. Chem.* **2010**, *8*, 1551-1559.



**Scheme 4.** Proposed mechanism by Krasutsky and coworkers for the two-step procedure from 2-methyl-2-adamantanol, **11**, to 2-oxadamantane, **8**, involving a double Criegee rearrangement.<sup>209</sup>

Although the use of a methyl as the group least subject to rearrangement, the formation of small amounts of the lactone **22** together with the acetate **12** was evidence for a parallel *O*-insertion into the C2-CH<sub>3</sub> bond delivering the intermediate **21**. Subsequent hydrolysis of **21** to ketone **10** which undergoes a Baeyer-Villiger reaction in presence of TFPAA gave the stable lactone **22** (Scheme 5).



**Scheme 5.** Mechanism of the formation of lactone **22**, involving a Baeyer-Villiger reaction.

In parallel, we also tried the direct conversion from 2-methyl-2-adamantanol **11** to the desired 2-oxadamantane, **8**, through a previously described photochemical procedure

(Scheme 3).<sup>212</sup> We could not reproduce the moderate yield obtained by Suginome and Yamada (12% vs 43%), likely because of the lamp we used, a 100-W tungsten filament lamp instead of a 100-W high-pressure mercury arc.<sup>213</sup>

Once 2-oxadamantane in hand, we started working on the C-5 functionalization (Scheme 6). The successful method we used was the C-H activation of the oxadamantane nucleus by phase-transfer catalysis (PTC) in mixed aqueous/organic solvents previously described by Schreiner and coworkers.<sup>214</sup> The procedure uses tetrabromomethane and sodium hydroxide with benzyltriethylammonium chloride (BTEAC) as the catalyst delivering a high regioselectivity for the bromination at the bridgehead position 5. The reaction is likely to proceed by single-electron-transfer (SET) initiation of OH<sup>-</sup> by CBr<sub>4</sub> followed by a radical substitution that starts the chain reaction.

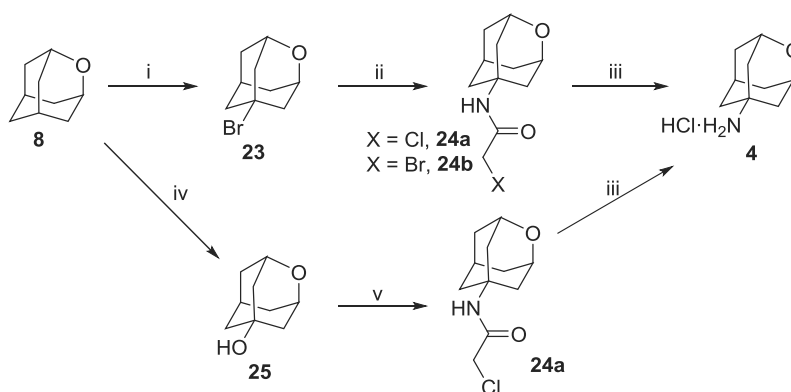
From the bromo derivative **23**, we envisaged the chloroacetamide **24a** as the key intermediate to finally get the desired 2-oxadamantane-5-amine, **4**. When we applied the Jirgensons' modification of the classical Ritter reaction to **23**, we recovered most of the starting material, together with an inseparable mixture of the expected chloroacetamide **24a** and the corresponding bromoacetamide **24b**, as evidenced by GC/MS analysis. Since alcohols perform better in the Ritter reaction, we attempted to obtain the chloroacetamide **24a** from the known alcohol **25**, which was prepared from **8** harshening the conditions increasing the temperature of the previous PTC reaction with the 50% NaOH solution. Satisfactorily, alcohol **25** furnished the chloroacetamide **24a** in high yield. Finally, cleavage of the haloacetamide group by using thiourea, either from pure **24a** or from the mixture of **24a** and **24b**, delivered the 2-oxadamantane-5-amine in good yield.

---

<sup>212</sup> Suginome, H.; Yamada, S. *Synthesis* **1986**, *9*, 741-743.

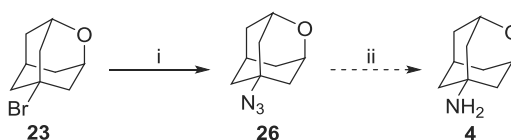
<sup>213</sup> After finishing this work, it has been recently reported a two-step synthesis of **8** from **6** in 36% overall yield, see Benneche, T.; Tius, M. A. *Tetrahedron Lett.* **2016**, *57*, 3150-3151.

<sup>214</sup> a) Schreiner, P. R.; Lauensteien, O.; Kolomitsyn, I. V.; Nadi, S.; Fokin, A. A. *Angew. Chem. Int. Ed.* **1998**, *37*, 1895-1897; b) Schreiner, P. R.; Lauensteien, O.; Butova, E. D.; Gunchenko, P. A.; Kolomitsyn, I. V.; Wittkopp, A.; Feder, F.; Fokin, A. A. *Chem. Eur. J.* **2001**, *7*, 4997-5003.



**Scheme 6.** Synthesis of 2-oxadamantan-5-amine, **4**. (i) 50% NaOH, CBr<sub>4</sub>, BTEAC, DCM, 40 °C, 90 h, 35% yield. (ii) Chloroacetonitrile, concd H<sub>2</sub>SO<sub>4</sub>, acetic acid, 0-50 °C, 40 h, 27% yield. (iii) Thiourea, acetic acid, EtOH, reflux, 16 h; then HCl/1,4-dioxane, 70% overall from the mixture **24a** and **24b**; 64% overall from **24a**. (iv) 50% NaOH, CBr<sub>4</sub>, BTEAC, DCM, 85 °C, 90 h, 54% yield. (v) Chloroacetonitrile, concd H<sub>2</sub>SO<sub>4</sub>, acetic acid, 0 °C to r.t., 70 h, 87% yield.

Alternatively, we tried to prepare the target compound **4** by reduction of the corresponding azide derivative **26** synthesized via azide/bromide exchange on **23** as previously reported by Alder and coworkers (Scheme7).<sup>210</sup>



**Scheme 7.** Proposed alternative synthesis for 2-oxadamantan-5-amine, **4**. (i) Me<sub>3</sub>SiN<sub>3</sub>, SnCl<sub>4</sub>, dry DCM, 0 °C, 4 h, 93% yield.<sup>210</sup> (ii) Reduction.

However, a complete exchange was not obtained, since a complex mixture of product, starting material and other side products was resulted. We later find out that these exchange reactions require reflux for completion as Davis and Nissan reported.<sup>215</sup>

<sup>215</sup> Davis, M. C.; Nissan, D. A. *Synth. Commun.* **2006**, *36*, 2113-2119.

As it was of interest for the research group, the novel oxanalog of the clinically approved drug amantadine was tested against two of its well-known targets, the M2 channel of the Influenza A virus and the NMDA receptor, in order to assess its behaviour as a bioisostere of amantadine. The results of these pharmacological evaluations are discussed in the manuscript that follows.

As an objective of the present Thesis, we used amine **4** as the starting product for the synthesis of a putative 11 $\beta$ -HSD1 inhibitor. This work is reported in the next Chapter 4.







Contents lists available at ScienceDirect

Tetrahedron Letters

journal homepage: [www.elsevier.com/locate/tetlet](http://www.elsevier.com/locate/tetlet)

## Ritter reaction-mediated syntheses of 2-oxaadaman-5-amine, a novel amantadine analog



Rosana Leiva<sup>a</sup>, Sabrina Gazzarrini<sup>b</sup>, Roser Esplugas<sup>c</sup>, Anna Moroni<sup>b</sup>, Lieve Naesens<sup>d</sup>, Francesc X. Sureda<sup>c</sup>, Santiago Vázquez<sup>a,\*</sup>

<sup>a</sup> Laboratori de Química Farmacèutica (Unitat Associada al CSIC), Facultat de Farmàcia, and Institute of Biomedicine (IBUB), Universitat de Barcelona, Av. Joan XXIII, s/n, Barcelona E-08028, Spain

<sup>b</sup> Department of Biosciences and National Research Council (CNR) Biophysics Institute (IBF), University of Milan, Via Celoria 26, 20133 Milan, Italy

<sup>c</sup> Unitat de Farmacologia, Facultat de Medicina i Ciències de la Salut, Universitat Rovira i Virgili, c/ St. Llorenç 21, Reus E-43201, Spain

<sup>d</sup> Rega Institute for Medical Research, KU Leuven, 3000 Leuven, Belgium

### ARTICLE INFO

#### Article history:

Received 24 December 2014

Revised 21 January 2015

Accepted 26 January 2015

Available online 31 January 2015

#### Keywords:

Adamantane

Amantadine

NMDA receptor antagonist

M2 channel

Ritter reaction

### ABSTRACT

Two alternative syntheses of 2-oxaadaman-5-amine, a novel analog of the clinically approved drug amantadine, are reported. The compound has been tested as an anti-influenza A virus agent and as an NMDA receptor antagonist. While the compound was not antivirally active, it displayed moderate activity as an NMDA receptor antagonist.

© 2015 Elsevier Ltd. All rights reserved.

### Introduction

The highly symmetrical structure of adamantane is a very common building block in organic chemistry. Among the several applications of adamantane derivatives, two are of the highest interest. First, the adamantane scaffold is used as a sterically demanding group in the synthesis of ligands for transition metal catalysts. Currently there are several adamantane-derived phosphines, such as Me-DalPhos<sup>®</sup>, Mor-DalPhos<sup>®</sup>, AdBrettPhos<sup>®</sup>, cataCXium<sup>®</sup> A, that are commercially available (Fig. 1).<sup>1</sup> Of note, the use of heteroadamantanes in catalysis has been less studied. The nitroxyl radical AZADO, a highly active catalyst for alcohol oxidation with superior catalytic proficiency to the well-known TEMPO, is a remarkable exception (Fig. 1).<sup>2</sup>

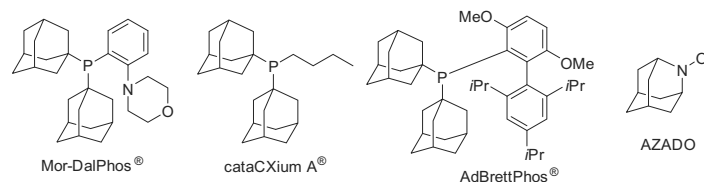
On the other hand, adamantane is of great interest in medicinal chemistry. The first clinically approved adamantane derivative, amantadine, was already introduced in the clinic in 1966.<sup>3</sup> Since then, thousands of adamantane derivatives have been pharmacologically evaluated and, so far, seven of them have been approved for clinical use (Fig. 2). Many more are in development as potential therapeutics against a plethora of targets.<sup>4</sup>

Although there are thousands of adamantyl derivatives that have been tested for biological activity, the number of heteroadamantanes that have been used in medicinal chemistry is only very small. Indeed, several oxaadamantanes, and azaadamantanes have been synthesized and pharmacologically tested, but no derivative has reached clinical trials so far. Some examples from either academic laboratories or the pharmaceutical industry are presented in Figure 3.<sup>5</sup>

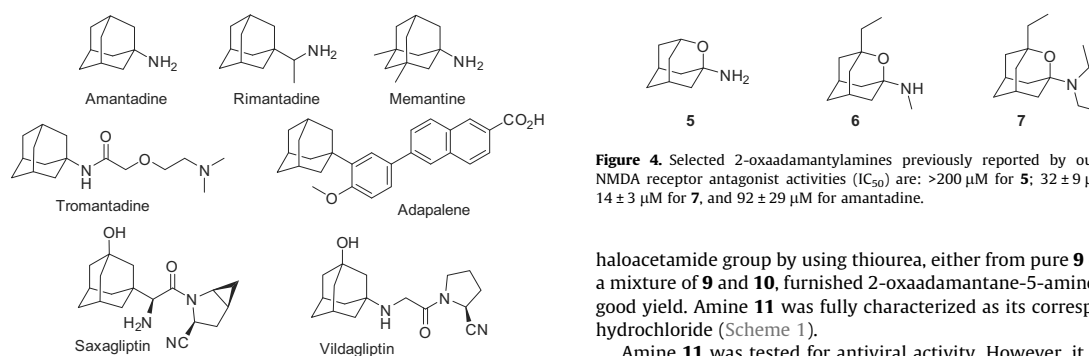
Some time ago, we reported the synthesis and pharmacological evaluation of several 2-oxaadaman-1-amines as analogs of amantadine (Fig. 4). Taking into account that amantadine shows NMDA receptor antagonist and anti-influenza A virus activities, we evaluated the 2-oxaanalogs for these two activities. We found that although all the compounds were devoid of antiviral activity, several of them displayed NMDA receptor antagonism, with some having lower IC<sub>50</sub> values than amantadine.<sup>6</sup>

In order to further explore the biological interest of heteroadamantanes, in this Letter we report the synthesis of a novel scaffold, 2-oxaadaman-5-amine, **11**, of potential interest in medicinal chemistry. We have found that **11** is devoid of any inhibitory activity against the M2 channel of influenza A virus, but displays activity as an NMDA receptor antagonist, albeit being less active than amantadine.

\* Corresponding author. Tel.: +34 934 024 533.  
E-mail address: [svazquez@ub.edu](mailto:svazquez@ub.edu) (S. Vázquez).

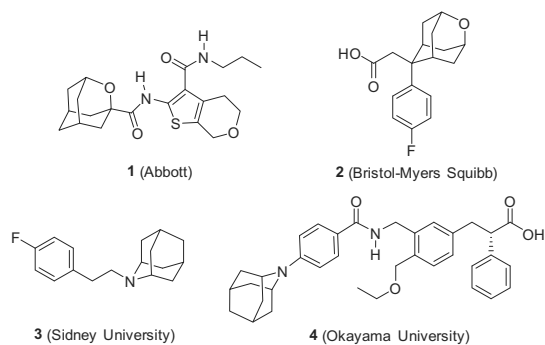


**Figure 1.** Structures of selected adamantyl- and heteroadamantyl-based compounds of interest in catalysis.



**Figure 4.** Selected 2-oxaadamantylamines previously reported by our group. NMDA receptor antagonist activities ( $IC_{50}$ ) are:  $>200 \mu\text{M}$  for **5**;  $32 \pm 9 \mu\text{M}$  for **6**,  $14 \pm 3 \mu\text{M}$  for **7**, and  $92 \pm 29 \mu\text{M}$  for amantadine.

**Figure 2.** Structures of adamantyl-based compounds in clinical use.



**Figure 3.** Selected heteroadamantyl-based compounds. **1** is a cannabinoid receptor 2 agonist; **2** an inhibitor of  $11\beta$ -hydroxysteroid dehydrogenase type 1 ( $11\beta$ -HSD1); **3** a low nanomolar inhibitor of  $\sigma$  receptors; and **4** a nanomolar agonist of the human peroxisome proliferator activated receptor- $\gamma$ .<sup>5</sup>

## Results and discussion

In order to synthesize the novel amantadine analog **11**, we envisaged chloroacetamide **9** as a key intermediate. In turn **9**, may be accessible from two already known 2-oxaadamantane derivatives, namely **8** and **12**.<sup>7,8</sup> When we applied the Jirgensons' modification of the classical Ritter reaction to **8**,<sup>9</sup> we recovered most of the starting material, along with an unseparable mixture of the expected chloroacetamide **9** and the corresponding bromoacetamide, **10**, as evidenced by GC/MS analysis. As it is known that alcohols behave better in the Ritter reaction, we attempted to obtain **11** from the known alcohol **12**.<sup>8</sup> To our satisfaction, reaction of **12** with chloroacetonitrile in acidic medium proceeded uneventfully to furnish **9** in high yield. Finally, cleavage of the

haloacetamide group by using thiourea, either from pure **9** or from a mixture of **9** and **10**, furnished 2-oxaadamantane-5-amine, **11**, in good yield. Amine **11** was fully characterized as its corresponding hydrochloride (Scheme 1).

Amine **11** was tested for antiviral activity. However, it did not display activity against the influenza viruses A/H1N1, A/H3N2 or B. Also, it was found to be inactive against the enveloped DNA viruses herpes simplex virus (type 1 or type 2) or vaccinia virus; the enveloped RNA viruses HIV-1, HIV-2, feline coronavirus, parainfluenza-3 virus, respiratory syncytial virus, vesicular stomatitis virus, sindbis virus or Punta Toro virus; or the non-enveloped RNA viruses Coxsackievirus B4 and Reovirus-1. Of interest, **11** did not show cytotoxicity ( $CC_{50} > 100 \mu\text{M}$ ) in the human MT4 lymphoblast cells; human embryonic lung (HEL) fibroblast cells; HeLa cervix carcinoma cells; or African green monkey Vero cells.

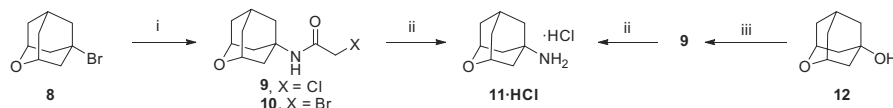
Previously, we had found that although **5** did not show any anti-influenza virus activity,<sup>6</sup> it was able to inhibit the wild-type (wt) M2 channel of influenza A virus, the target for the antiviral action of amantadine.<sup>10</sup> In order to assess if **11** was an inhibitor of the M2 protein, its inhibitory activity was tested on A/M2 channels expressed in *Xenopus* oocytes using the two-electrode voltage clamp (TEV) technique. At  $100 \mu\text{M}$ , amantadine was able to inhibit 91% of the activity of the wt A/M2 channel ( $IC_{50} = 16.0 \pm 1.2 \mu\text{M}$ ) and oxaamantadine **5** showed similar activity ( $IC_{50} = 29.2 \pm 1.2 \mu\text{M}$ ). On the other hand, the novel oxaamantadine **11**, at  $100 \mu\text{M}$ , produced only 18.9% inhibition of the activity of the wt M2 channel, and similar values were obtained when the compound was evaluated against the amantadine-resistant V27A (8.8% inhibition) and S31N (21.4% inhibition) M2 mutant channels.

Overall, taking into account the aforementioned pharmacological results, it seems that the introduction of the oxygen atom in the adamantane scaffold is much more deleterious for the anti-influenza A virus activity in **11** than in **5**.

Finally, we measured the effect of **11** on the increase in intracellular calcium evoked by NMDA (at a concentration of  $100 \mu\text{M}$  and in the presence of  $10 \mu\text{M}$  of glycine) on cultured rat cerebellar granule neurons. Although we indeed found some antagonistic activity, amine **11** was 2.5 fold less potent ( $IC_{50} = 258 \pm 93 \mu\text{M}$ ,  $n = 3$ ) than amantadine ( $IC_{50} = 92 \pm 29 \mu\text{M}$ ,  $n = 3$ ).<sup>11</sup>

## Conclusions

In conclusion, we have synthesized a novel heteroanalogue of amantadine. Although **11** does not behave as a bioisostere of



**Scheme 1.** Syntheses of 2-oxadamantan-5-amine, **11**, from known 2-oxadamantane derivatives **8** and **12**. (i) Chloroacetonitrile, acetic acid, concd  $\text{H}_2\text{SO}_4$ , 0–50 °C, 40 h, 27% yield. (ii) Thiourea, acetic acid, ethanol, reflux; then HCl/1,4-dioxane, 70% overall from the mixture of **9** and **10**; 64% overall from pure **9**. (iii) Chloroacetonitrile, acetic acid, concd  $\text{H}_2\text{SO}_4$ , 0 °C to room temperature, 70 h, 87% yield.

amantadine against two of its well-known targets, the potential of this novel amine in medicinal chemistry may still be very high, since adamantane-derived compounds can have activity against a broad and diverse panel of biological targets. Thus, we are currently further exploring the chemistry and biology of several derivatives of **11** with potential activity against several targets, such as the 11 $\beta$ -HSD1 or the soluble epoxide hydrolase enzymes.

## Experimental

### Chemistry: general

Melting points were determined in open capillary tubes. NMR spectra were recorded in the following spectrometers:  $^1\text{H}$  NMR (400 MHz),  $^{13}\text{C}$  NMR (100.6 MHz). Chemical shifts ( $\delta$ ) are reported in ppm related to internal tetramethylsilane (TMS) and coupling constants are reported in Hertz (Hz). Accurate mass measurements were obtained using ESI technic. Absorption values in the IR spectra [using the Attenuated Total Reflectance (ATR) technique] are given as wave-numbers ( $\text{cm}^{-1}$ ). Only the more intense bands are given. For the thin layer chromatography (TLC) aluminum-backed sheets with silica gel 60  $\text{F}_{254}$  were used and spots were visualized with UV light and/or 1% aqueous solution of  $\text{KMnO}_4$ .

### *N*-(2-Oxadmantan-5-yl)-2-chloroacetamide, **9**

- (a) From 5-bromo-2-oxadamantane, **8**: A solution of 5-bromo-2-oxadamantane, **8**, (593.5 mg, 2.74 mmol) in chloroacetonitrile (0.18 mL, 2.74 mmol) and glacial acetic acid (1.5 mL) was cooled to 0 °C. Then concentrated sulfuric acid (0.22 mL) was added dropwise. The reaction mixture was stirred at 50 °C for 40 h. The solution was added to ice (8 g) and the mixture stirred for few minutes.  $\text{CH}_2\text{Cl}_2$  (10 mL) was added, the layers separated and the aqueous layer extracted with further  $\text{CH}_2\text{Cl}_2$  ( $2 \times 10$  mL). The combined organics were dried over anhyd sodium sulfate and filtered. Evaporation in vacuo of the organics gave an orange oil (894.3 mg). Column chromatography (hexane/ethyl acetate mixture) gave *N*-(2-oxadamantan-5-yl)-2-chloroacetamide, **9**, and *N*-(2-oxadamantan-5-yl)-2-bromoacetamide, **10**, as a white solid (167.8 mg, approx. 26.7% yield).
- (b) From 2-oxadamantan-5-ol, **12**: A solution of 2-oxadamantan-5-ol, **12**<sup>8a</sup> (186 mg, 1.21 mmol) in chloroacetonitrile (0.08 mL, 1.21 mmol) and glacial acetic acid (0.8 mL) was cooled to 0 °C. Then concentrated sulfuric acid (0.1 mL) was added dropwise. The reaction mixture was stirred at room temperature for 70 h. The solution was added to ice (2 g) and the mixture stirred for few minutes.  $\text{CH}_2\text{Cl}_2$  (5 mL) was added, the layers separated and the aqueous layer extracted with further  $\text{CH}_2\text{Cl}_2$  ( $2 \times 5$  mL). The combined organics were dried over anhyd sodium sulfate and filtered. Evaporation in vacuo of the organics gave the *N*-(2-oxadamantan-5-yl)-2-chloroacetamide, **9**, as a white solid (239.9 mg, 86.5% yield), mp 105–106 °C. IR (ATR)  $\nu$ , 3272, 3082, 2937, 1661, 1556, 1441, 1414, 1358, 1315, 1271, 1234, 1193, 1150, 1107, 1076, 1017, 975, 961, 924,

817, 799, 777, 685  $\text{cm}^{-1}$ .  $^1\text{H}$  NMR (400 MHz,  $\text{CDCl}_3$ )  $\delta$ : 1.60 [dm, 2H, 8'(10')- $\text{H}_a$ ], 1.96–2.22 [complex signal, 8H, 4'(9')- $\text{H}_a$ , 4'(9')- $\text{H}_b$ , 8'(10')- $\text{H}_b$ , 6'- $\text{H}_2$ ], 2.27 [m, 1H, 7'-H], 3.94 [s, 2H,  $\text{CH}_2\text{Cl}$ ], 4.20 [br s, 2H, 1'(3')-H], 6.27 (s, 1H, NH).  $^{13}\text{C}$  NMR (100.6 MHz,  $\text{CDCl}_3$ )  $\delta$ : 27.2 (CH, C7'), 34.8 [ $\text{CH}_2$ , C8'(10')], 39.3 ( $\text{CH}_2$ , C6'), 40.2 [ $\text{CH}_2$ , C4'(9')], 42.7 ( $\text{CH}_2$ , C2), 51.1 (C, C5'), 69.0 [CH, C1'(3')], 164.9 (C, C1). HRMS-ESI+  $m/z$  [ $\text{M}+\text{H}$ ]<sup>+</sup> calcd for [ $\text{C}_{11}\text{H}_{16}\text{ClNO}_2+\text{H}$ ]<sup>+</sup>: 230.0942, found: 230.0951.

### 2-Oxadmantan-5- amine hydrochloride, **11-HCl**

- (a) From a mixture of **9** and **10**: To a solution of a mixture of *N*-(2-oxadamantan-5-yl)-2-chloroacetamide, **9**, and *N*-(2-oxadamantan-5-yl)-2-bromoacetamide, **10**, (113.6 mg, 0.49 mmol) in absolute ethanol (9.6 mL) was added thiourea (44.9 mg, 0.59 mmol) and glacial acetic acid (0.34 mL). The reaction mixture was stirred and heated at reflux overnight. The resulting mixture was allowed to reach room temperature and evaporated in vacuo. The residue was partitioned between  $\text{CH}_2\text{Cl}_2$  (10 mL) and water (10 mL) and the layers were separated. The aqueous layer was basified with 10 N NaOH to basic pH and extracted with  $\text{CH}_2\text{Cl}_2$  ( $3 \times 10$  mL). The combined organics were dried over anhyd sodium sulfate, filtered, and HCl/dioxane was added to form the hydrochloride salt. Evaporation in vacuo of the organics gave 2-oxadamantan-5-amine hydrochloride, **11-HCl**, as a white solid (55.8 mg, 70.0% yield).
- (b) From pure **9**: To a solution of *N*-(2-oxadamantan-5-yl)-2-chloroacetamide, **9**, (239.9 mg, 1.05 mmol) in absolute ethanol (20.3 mL) was added thiourea (95.2 mg, 1.25 mmol) and glacial acetic acid (0.72 mL). The reaction mixture was stirred and heated at reflux overnight. The resulting mixture was allowed to reach room temperature and evaporated in vacuo. The residue was partitioned between  $\text{CH}_2\text{Cl}_2$  (20 mL) and water (20 mL) and the layers were separated. The aqueous layer was basified with 10 N NaOH to basic pH and extracted with  $\text{CH}_2\text{Cl}_2$  ( $3 \times 20$  mL). The combined organics were dried over anhyd sodium sulfate, filtered, and HCl/dioxane was added to form the hydrochloride salt. Evaporation in vacuo of the organics gave 2-oxadamantan-5-amine hydrochloride, **11-HCl**, as a white solid (117.4 mg, 64.0% yield), mp 240 °C (sublimation). IR (ATR)  $\nu$ , 3361, 2893, 2609, 1657, 1625, 1525, 1443, 1383, 1364, 1322, 1197, 1172, 1120, 1095, 1062, 1009, 984, 933, 912, 896, 831, 811, 779, 717, 625  $\text{cm}^{-1}$ .  $^1\text{H}$  NMR (400 MHz,  $\text{CD}_3\text{OD}$ )  $\delta$ : 1.65 [dm, 2H, 8(10)- $\text{H}_a$ ], 1.89 [d,  $J = 12$  Hz, 2H, 4(9)- $\text{H}_a$ ], 1.98–2.12 [complex signal, 6H, 6- $\text{H}_2$ , 8(10)- $\text{H}_b$ , 4(9)- $\text{H}_b$ ], 2.35 [m, 1H, 7-H], 4.23 [br s, 2H, 1(3)-H], 4.86 (s, 3H,  $\text{NH}_3$ ).  $^{13}\text{C}$  NMR (100.6 MHz,  $\text{CD}_3\text{OD}$ )  $\delta$ : 28.4 (CH, C7), 35.0 [ $\text{CH}_2$ , C8(10)], 39.6 ( $\text{CH}_2$ , C6), 40.2 [ $\text{CH}_2$ , C4(9)], 51.8 (C, C5), 69.9 [CH, C1(3)]. Anal. Calcd for  $\text{C}_9\text{H}_{16}\text{ClNO} \cdot 0.75\text{H}_2\text{O}$ : C, 56.99; H, 8.50; N, 7.38; calcd for  $\text{C}_9\text{H}_{16}\text{ClNO} \cdot 0.75\text{H}_2\text{O}$ : C, 53.20; H, 8.68; N, 6.89. Found: C, 53.26; H, 8.40; N, 6.58.

### Antiviral activity

The antiviral activity of amine **11** was determined in established cell culture assays using a selection of DNA and RNA viruses, including four subtypes of influenza virus [A/Puerto Rico/8/34 (H1N1); A/Virginia/ATCC3/2009 (H1N1); A/Hong Kong/7/87 (H3N2) and B/Hong Kong/5/72].<sup>12</sup> The compound's inhibitory effect on virus replication (antiviral EC<sub>50</sub> >100 μM) as well as its cytotoxicity (CC<sub>50</sub> >100 μM) were monitored by microscopic inspection, and confirmed by the colorimetric MTS cell viability assay.

### Plasmid, mRNA synthesis, and microinjection of oocytes

The cDNA encoding the influenza A/Udorn/72 (A/M2) was inserted into pSUPER vector for expression in *Xenopus* oocyte plasma membrane. A/M2 S31N and A/M2 V27A mutants were generated by QuikChange site-directed mutagenesis kit (Agilent Technologies). The synthesis of crRNA and microinjection of oocytes have been described previously.<sup>13</sup>

### Two-electrode voltage clamp analysis

Macroscopic membrane current was recorded 24–72 h after injection as described previously.<sup>14</sup> Oocytes were perfused at room temperature in Barth's solution containing (in mM) 88 NaCl, 1 KCl, 2.4 NaHCO<sub>3</sub>, 0.3 NaNO<sub>3</sub>, 0.71 CaCl<sub>2</sub>, 0.82 MgCl<sub>2</sub>, and 15 HEPES for pH 8.5 or 15 MES for pH 5.5 at a rate of 2 mL/min. The tested compound was dissolved in DMSO and applied (100 μM) at pH 5.5 when the inward current reached a maximum. The compound was applied for 2 min, and residual membrane current was compared with the membrane current before the application of compounds. Currents were recorded at –20 mV and analyzed with pCLAMP 8 software package (Axon Instruments, Sunnyvale, CA).

### Antagonist activity against NMDA receptors

The functional assay for antagonist activity against NMDA receptors was performed using primary cultures of rat cerebellar granule neurons that were prepared according to established protocols.<sup>11</sup> Cells were grown on 10 mm poly-L-lysine coated glass cover slips, and used for the experiments after 6–10 days in vitro culture. Cells were loaded with 6 μM Fura-2 AM (Invitrogen-Molecular Probes) for 30 min. Then, the coverslip was mounted on a quartz cuvette containing a Locke–Hepes buffer using a special holder. Measurements were performed using a PerkinElmer LS-55 fluorescence spectrometer equipped with a fast-filter accessory, under mild agitation and at 37 °C. Analysis from each sample was recorded real-time during 1400 s. After stimulation with NMDA (100 μM, in the presence of 10 μM glycine), increasing cumulative concentrations of the compound to be tested were added. The percentages of inhibition at every tested concentration were analyzed using a non-linear regression curve fitting (variable slope) by using the software GraphPad Prism 5.0.

### Acknowledgments

R.L. thanks the Generalitat de Catalunya for a PhD Grant (FI). S.V. thanks financial support from *Ministerio de Ciencia e Innovación* (Project CTQ2011-22433) and the *Generalitat de Catalunya* (Grant 2014-SGR-00052). L.N. acknowledges the financial support from the KU Leuven Geconcerteerde Onderzoeksacties (GOA/15/019/TBA), and the technical assistance from W. van Dam.

### Supplementary data

Supplementary data (<sup>1</sup>H and <sup>13</sup>C NMR spectra of **9** and **11-HCl**) associated with this article can be found, in the online version, at <http://dx.doi.org/10.1016/j.tetlet.2015.01.160>.

### References and notes

- (a) Lundgren, R. J.; Peters, B. D.; Alsabeh, P. G.; Stradiotto, M. *Angew. Chem., Int. Ed.* **2010**, *49*, 4071–4074; (b) Lundgren, R. J.; Stradiotto, M. *Angew. Chem., Int. Ed.* **2010**, *49*, 8686–8690; (c) Lundgren, R. J.; Stradiotto, M. *Aldrichim. Acta* **2012**, *45*, 59–65; (d) Su, M.; Buchwald, S. L. *Angew. Chem., Int. Ed.* **2012**, *51*, 4710–4713; (e) Zapf, A.; Ehrentraut, A.; Beller, M. *Angew. Chem., Int. Ed.* **2000**, *39*, 4153–4155; (f) Zapf, A.; Jackstell, R.; Rataboul, F.; Riermeier, T.; Monsees, A.; Fuhrmann, C.; Shaikh, N.; Dingerdissen, U.; Beller, M. *Chem. Commun.* **2004**, 38–39; (g) Rataboul, F.; Zapf, A.; Jackstell, R.; Harkal, S.; Riermeier, T.; Monsees, A.; Dingerdissen, U.; Beller, M. *Chem. Eur. J.* **2004**, *10*, 2983–2990.
- (a) Shibuya, M.; Tomizawa, M.; Suzuki, I.; Iwabuchi, Y. *J. Am. Chem. Soc.* **2006**, *128*, 8412–8413; (b) Iwabuchi, Y. *Chem. Pharm. Bull.* **2013**, *61*, 1197–1213.
- Davies, W. L.; Grunert, R. R.; Haff, R. F.; McGahen, J. W.; Neumayer, E. M.; Paulshock, M.; Watts, J. C.; Wood, T. R.; Hermann, E. C.; Hoffmann, C. E. *Science* **1964**, *144*, 862–863.
- (a) Lamoureux, G.; Artavia, G. *Curr. Med. Chem.* **2010**, *17*, 2967–2978; (b) Liu, J.; Obando, D.; Liao, V.; Lifa, T.; Codd, R. *Eur. J. Med. Chem.* **2011**, *46*, 1949–1963; (c) Wanka, L.; Iqbal, K.; Schreiner, P. R. *Chem. Rev.* **2013**, *113*, 3516–3604.
- (a) Banister, S. D.; Yoo, D. T.; Chua, S. W.; Cui, J.; Mach, R. H.; Kassiou, M. *Bioorg. Med. Chem. Lett.* **2011**, *21*, 5289–5292; (b) Ye, X.-Y.; Chen, S. Y.; Nayeem, A.; Golla, R.; Seethala, R.; Wang, M.; Harper, T.; Slecicka, B. G.; He, B.; Gordon, D. A.; Robl, J. A. *Bioorg. Med. Chem. Lett.* **2011**, *21*, 6699–6704; (c) Nelson, D. W.; Frost, J. M.; Tietje, K. R.; Florjancic, A. S.; Ryther, K.; Carroll, W. A.; Dart, M. J.; Daza, A. V.; Hooker, B. A.; Grayson, G. K.; Fan, Y.; Garrison, T. R.; El-Kouhen, O. F.; Yao, B.; Pai, M.; Chandran, P.; Zhu, C.; Hsieh, G. C.; Meyer, M. D. *Bioorg. Med. Chem. Lett.* **2012**, *22*, 2604–2608; (d) Tanaka, Y.; Gamo, K.; Oyama, T.; Ohashi, M.; Waki, M.; Matsuno, K.; Matsuura, N.; Tokiwa, H.; Miyachi, H. *Bioorg. Med. Chem. Lett.* **2014**, *24*, 4001–4005.
- Duque, M. D.; Camps, P.; Profire, L.; Montaner, S.; Vázquez, S.; Sureda, F. S.; Mallol, J.; López-Querol, M.; Naesens, L.; De Clercq, E.; Prathalingam, S. R.; Kelly, J. M. *Bioorg. Med. Chem.* **2009**, *17*, 3198–3206.
- Schreiner, P. R.; Lauenstein, O.; Kolomitsyn, I. V.; Nadi, S.; Fokin, A. A. *Angew. Chem., Int. Ed.* **1998**, *37*, 1895–1897.
- (a) Duddeck, H.; Wagner, P. *Liebigs Ann. Chem.* **1984**, 1981–1988; (b) Alder, R. W.; Carta, F.; Reed, C. A.; Stoyanova, I.; Willis, C. L. *Org. Biomol. Chem.* **2010**, *8*, 1551.
- (a) Jirgensons, A.; Kauss, V.; Kalvinsh, L.; Gold, M. R. *Synthesis* **2000**, 1709–1712; (b) Jiang, D.; He, T.; Ma, L.; Wang, Z. *RSC Adv.* **2014**, *4*, 64936–64946.
- Duque, M. D.; Ma, C.; Torres, E.; Wang, J.; Naesens, L.; Juárez-Jiménez, J.; Camps, P.; Luque, F. J.; DeGrado, W. F.; Lamb, R. A.; Pinto, L. H.; Vázquez, S. *J. Med. Chem.* **2011**, *54*, 2646–2657.
- Canudas, A. M.; Pubill, D.; Sureda, F. X.; Verdagué, E.; Camps, P.; Muñoz-Torrero, D.; Jiménez, A.; Camins, A.; Pallàs, M. *Exp. Neurol.* **2003**, *180*, 123–130.
- (a) Setaki, D.; Tataridis, D.; Stamatou, G.; Kolocouris, A.; Foscolos, G. B.; Fytas, G.; Kolocouris, N.; Padalko, E.; Neyts, J.; De Clercq, E. *Bioorg. Chem.* **2006**, *34*, 248–273; (b) Naesens, L.; Vanderlinden, E.; Roth, E.; Jeko, J.; Andrei, G.; Snoeck, R.; Pannecouque, C.; Illyes, E.; Batta, G.; Herczegh, P.; Sztaricskai, F. *Antiviral Res.* **2009**, *82*, 89–94.
- Gazzarrini, S.; Kang, M.; Abenavoli, A.; Romani, G.; Olivari, C.; Gaslini, D.; Ferrara, G.; van Etten, J. L.; Kreim, M.; Kast, S. M.; Thiel, G.; Moroni, A. *Biochem. J.* **2009**, *420*, 295–303.
- Balannik, V.; Lamb, R. A.; Pinto, L. H. *J. Biol. Chem.* **2008**, *283*, 4895–4904.

# Supporting information

## Ritter reaction-mediated syntheses of 2-oxaadaman-5-amine, a novel amantadine analog

Rosana Leiva<sup>a</sup>, Sabrina Gazzarrini<sup>b</sup>, Roser Esplugas<sup>c</sup>, Anna Moroni<sup>b</sup>, Lieve Naesens<sup>d</sup>,  
Francesc X. Sureda<sup>c</sup>, and Santiago Vázquez<sup>a,\*</sup>

<sup>a</sup>*Laboratori de Química Farmacèutica (Unitat Associada al CSIC), Facultat de Farmàcia, and Institute of Biomedicine (IBUB),  
Universitat de Barcelona, Av. Joan XXIII, s/n, Barcelona, E-08028, Spain*

<sup>b</sup>*Department of Biosciences and National Research Council (CNR) Biophysics Institute (IBF), University of Milan, Via Celoria 26,  
20133 Milan, Italy*

<sup>c</sup>*Unitat de Farmacologia, Facultat de Medicina i Ciències de la Salut, Universitat Rovira i Virgili, c./ St. Llorenç 21, Reus E-43201,  
Spain*

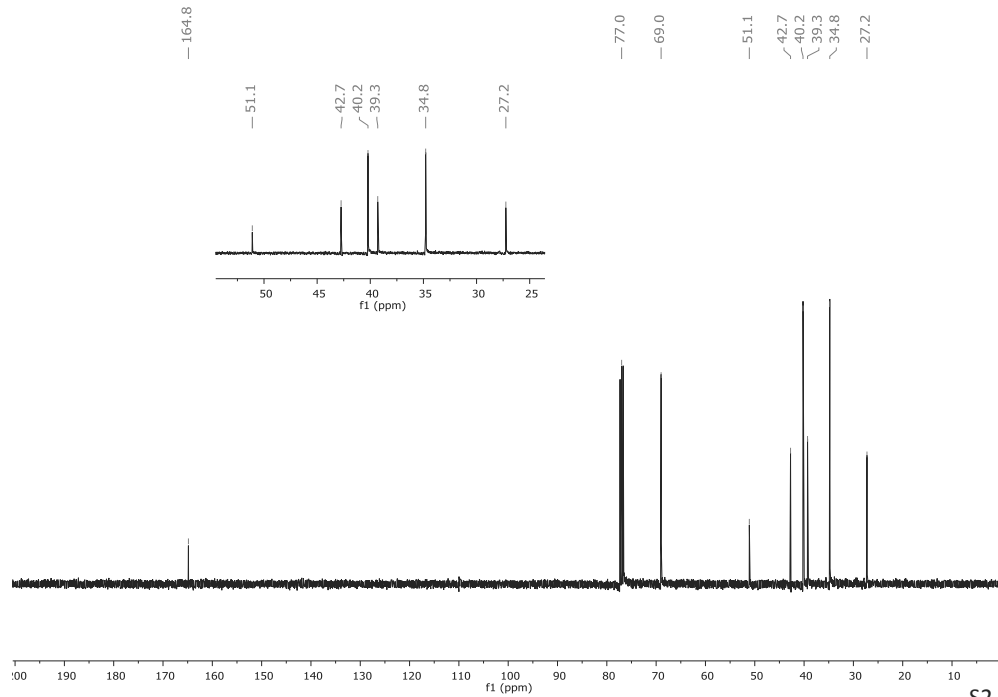
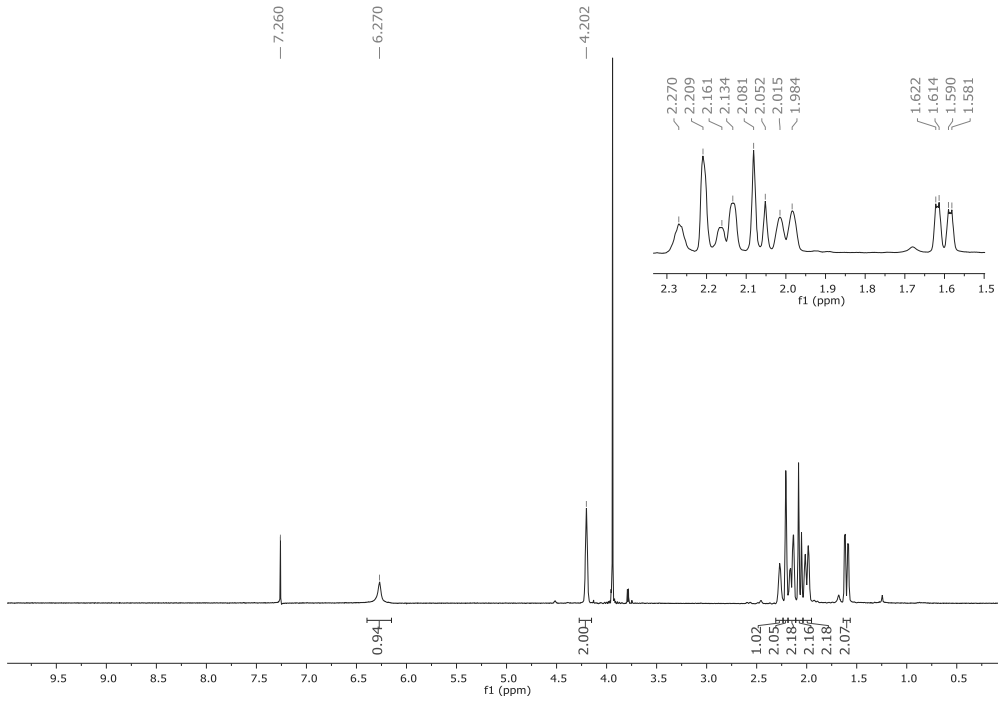
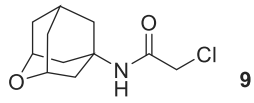
<sup>d</sup>*Rega Institute for Medical Research, KU Leuven, 3000 Leuven, Belgium*

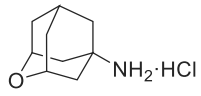
### Table of content:

<sup>1</sup> H and <sup>13</sup> C NMR spectra of <b>9</b>	S2
<sup>1</sup> H, <sup>13</sup> C NMR and HSQC spectra of <b>11·HCl</b>	S3

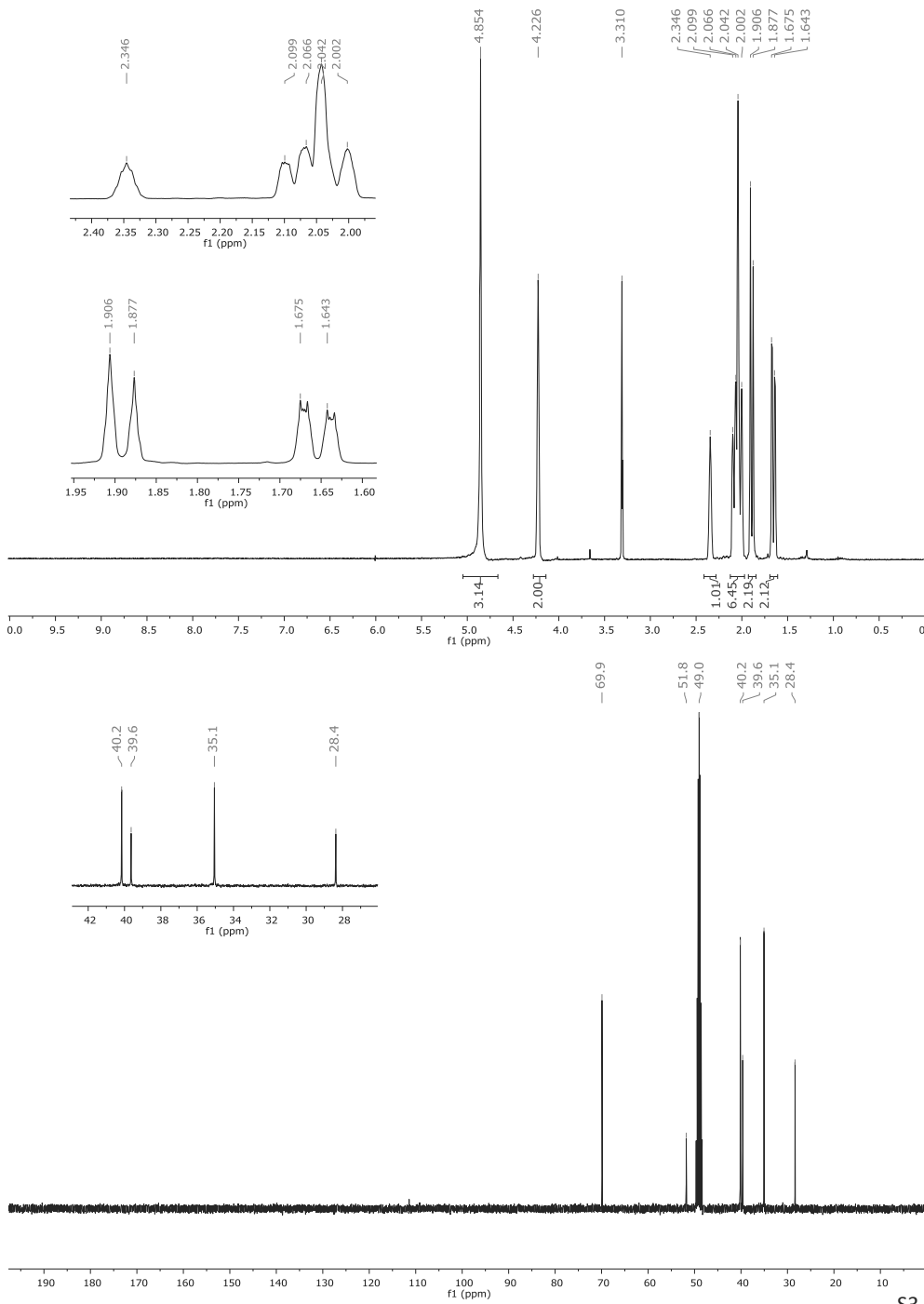
---

\* Corresponding author. Tel.: +34-934-024-533; e-mail: svazquez@ub.edu

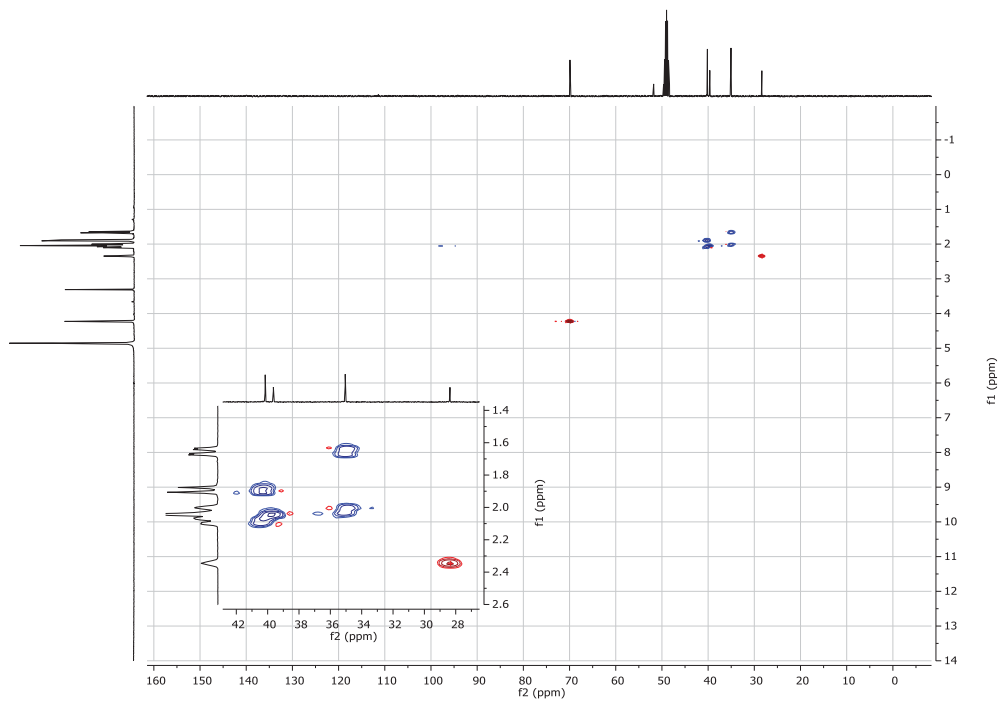




11·HCl







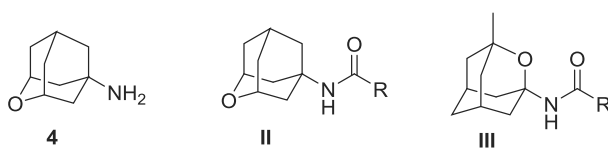
## CHAPTER 4

# **Study of C-1 vs C-2 substitution in adamantyl derivatives and introduction of oxaadamantyl groups in 11 $\beta$ -HSD1 inhibitors**



#### 4.1 Rationale and previous work

The project presented hereinafter is the follow-up work of the previous chapter. Therefore, after the preparation of the novel cage amine **4**,<sup>215</sup> the next step was introducing it in a potential 11 $\beta$ -HSD1 inhibitor structure, **II**, replacing the adamantyl group broadly used as the lipophilic motif of the molecule. As a comparison, another oxaamantadine previously described by the group, the 3-methyl-2-oxaadaman-1-amine, was used for the synthesis of other putative 11 $\beta$ -HSD1 inhibitors, **III**.<sup>202</sup>



**Chart 4.** Structures of the previously described 2-oxaadaman-5-amine, **4**, and the envisioned potential 11 $\beta$ -HSD1 inhibitors **II** and **III** featuring oxaadamantyl groups.<sup>202,215</sup>

In addition to this, the aim of this project was also the preparation of a small series of 1- and 2-adamantyl derivatives featuring fragments of proven 11 $\beta$ -HSD1 inhibitors in order to compare their potency, since some seemingly contradictory results and scarcity of data are present in this regard (see manuscript for further discussion).<sup>216,217</sup>

#### 4.2 Theoretical discussion

All the compounds described in the following manuscript were prepared in the context of this Thesis. Their design, synthesis and pharmacological results are discussed in the manuscript, and the experimental procedures and methods for the synthesis, characterization and biological evaluation are described in the accompanying supporting information.

<sup>215</sup> Leiva, R.; Gazzarrini, S.; Esplugas, R.; Moroni, A.; Naesens, L.; Sureda, F. X.; Vázquez, S. *Tetrahedron Lett.* **2015**, *56*, 1272-1275.

<sup>216</sup> Webster, S. P.; Ward, P.; Binnie, M.; Craigie, E.; McConnell, K. M. M.; Sooy, K.; Vinter, A.; Seckl, J. R.; Walker, B. R. *Bioorg. Med. Chem. Lett.* **2007**, *17*, 2838-2843.

<sup>217</sup> Xia, G.; Liu, L.; Liu, H.; Yu, J.; Xu, Z.; Chen, Q.; Ma, C.; Li, P.; Xiong, B.; Liu, X.; Shen, J. *Chem. Med. Chem.* **2013**, *8*, 577-581.





Contents lists available at ScienceDirect

## Bioorganic &amp; Medicinal Chemistry Letters

journal homepage: [www.elsevier.com/locate/bmcl](http://www.elsevier.com/locate/bmcl)

## Novel 11 $\beta$ -HSD1 inhibitors: C-1 versus C-2 substitution and effect of the introduction of an oxygen atom in the adamantane scaffold



Rosana Leiva<sup>a</sup>, Constantí Seira<sup>b</sup>, Andrew McBride<sup>c</sup>, Margaret Binnie<sup>c</sup>, F. Javier Luque<sup>b</sup>, Axel Bidon-Chanal<sup>b</sup>, Scott P. Webster<sup>c</sup>, Santiago Vázquez<sup>a,\*</sup>

<sup>a</sup> Laboratori de Química Farmacèutica (Unitat Associada al CSIC), Facultat de Farmàcia, and Institute of Biomedicine (IBUB), Universitat de Barcelona, Av. Joan XXIII, s/n, Barcelona E-08028, Spain

<sup>b</sup> Departament de Físicoquímica, Facultat de Farmàcia and Institute of Biomedicine (IBUB), Universitat de Barcelona, Av. Prat de la Riba, 171, 08921 Santa Coloma de Gramenet, Spain

<sup>c</sup> Endocrinology Unit, Centre for Cardiovascular Science, University of Edinburgh, Queen's Medical Research Institute, EH16 4TJ, United Kingdom

## ARTICLE INFO

## Article history:

Received 6 July 2015

Revised 27 July 2015

Accepted 29 July 2015

Available online 5 August 2015

## Keywords:

Adamantane

11 $\beta$ -HSD1 inhibitors

Drug discovery

Molecular modeling

## ABSTRACT

The adamantane scaffold is found in several marketed drugs and in many investigational 11 $\beta$ -HSD1 inhibitors. Interestingly, all the clinically approved adamantane derivatives are C-1 substituted. We demonstrate that, in a series of paired adamantane isomers, substitution of the adamantane in C-2 is preferred over the substitution at C-1 and is necessary for potency at human 11 $\beta$ -HSD1. Furthermore, the introduction of an oxygen atom in the hydrocarbon scaffold of adamantane is deleterious to 11 $\beta$ -HSD1 inhibition. Molecular modeling studies provide a basis to rationalize these features.

© 2015 Elsevier Ltd. All rights reserved.

Adamantane is a very common building block in medicinal chemistry.<sup>1</sup> So far, seven adamantane derivatives have been introduced in clinical use for a variety of diseases and molecular targets (Fig. 1) and hundreds of derivatives have been tested against different targets.

Interestingly, the rapid inspection of the structures of the adamantane derivatives shown in Figure 1 reveals as a general trend that the polycyclic scaffold is substituted at the C-1 position. Of note, the anti-influenza A activity of amantadine is significantly higher than that of its isomer, 2-aminoadamantane.<sup>2</sup>

In recent years, more than 25 pharmaceutical companies have been working on the synthesis of 11 $\beta$ -hydroxysteroid dehydrogenase type 1 (11 $\beta$ -HSD1) inhibitors, as a potential new candidates for the treatment of type II diabetes and metabolic syndrome.<sup>3</sup> On the one hand, contrary to the aforementioned trend observed in clinically approved adamantanes, most of the 11 $\beta$ -HSD1 inhibitors evaluated are 2-adamantyl substituted derivatives (Fig. 2).<sup>4,5</sup> However, for these derivatives no comparison between the activities of compounds substituted at the C-1 and C-2 positions is available. On the other hand, a potential advantage of positioning the substituent at the 1-position is that one of the metabolically labile positions of the adamantane would be blocked. Also, for any given

substituent, the theoretical *clogP* value of the 1-substituted analog is usually lower than that of the 2-substituted derivative.<sup>6</sup>

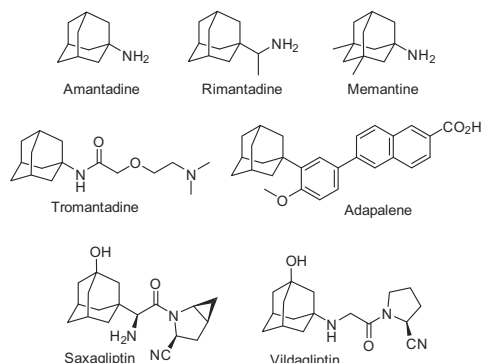
The synthesis and pharmacological evaluation of a series of 1-adamantyl amide 11 $\beta$ -HSD1 inhibitors has been previously reported by Webster et al.<sup>7</sup> Of note, inhibitors **1** and **2** were found to be equipotent compounds (Fig. 3). Later, Xia et al. reported that the C-2 substituted amide **3** was 20 times more potent than its 1-isomer, **4** (Fig. 3).<sup>8</sup>

Taking into account these seemingly contradictory results and the scarcity of data on 1-substituted adamantane derivatives evaluated as 11 $\beta$ -HSD1 inhibitors,<sup>5</sup> we decided to synthesize a small series of 1- and 2-adamantyl derivatives featuring fragments of proven inhibitors of 11 $\beta$ -HSD1 in order to compare their pharmacological behavior.

Moreover, considering that very few heteroadamantanes have been biologically tested as 11 $\beta$ -HSD1 inhibitors,<sup>9</sup> we also evaluated some 1- and 5-substituted 2-oxaadamantanes. The introduction of an oxygen atom in the scaffold increases the polar surface area and decreases the overall lipophilicity. Thus, if potency is retained, the lipophilic ligand efficiency, which is one of the most significant parameters that normalizes potency relative to lipophilicity, would increase.<sup>10</sup>

We started from known urea **5**, an 11 $\beta$ -HSD1 inhibitor reported by Vitae.<sup>11</sup> In our microsomal assay, **5** was shown to be a submicromolar inhibitor of the human 11 $\beta$ -HSD1 enzyme

\* Corresponding author. Tel.: +34 934 024 533.  
E-mail address: [svazquez@ub.edu](mailto:svazquez@ub.edu) (S. Vázquez).

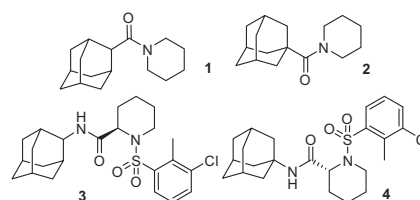


**Figure 1.** Clinically-approved adamantane derivatives. Amantadine, rimantadine and tromantadine are anti-virals, the first two are M2 channel blockers and are anti-influenza drugs, and tromantadine inhibits herpes virus simplex replication; memantine is a NMDA receptor antagonist used in the treatment of Alzheimer's disease; adapalene inhibits keratinocyte differentiation and proliferation and is used for the treatment of acne; and saxagliptin and vildagliptin are DPP-IV inhibitors used to treat type 2 diabetes.

( $IC_{50} = 0.87 \mu\text{M}$ ). Table 1 shows the structures and the percentage of inhibition of human  $11\beta$ -HSD1 at  $10 \mu\text{M}$  of the novel compounds. The  $IC_{50}$  value of the more potent derivatives is also included.

All the compounds were synthesized in medium to high yields using standard chemistry from four known amines: amantadine (1-aminoadamantane), 2-aminoadamantane, 5-amino-2-oxaadamantane,<sup>12</sup> and 3-methyl-2-oxaadamantane-1-amine<sup>13</sup> (see details in Supplementary material). Briefly, the reaction of amantadine with 1-piperidinecarbonyl chloride in dichloromethane in the presence of triethylamine furnished, after column chromatography, urea **6** in 31% yield.<sup>14</sup> In the same way, starting from the known 3-methyl-2-oxaadamantane-1-amine, urea **7** was obtained in 34% yield. We also synthesized amides **8** and **9** in high yields, by reaction of amantadine with 3,5-dichloro-4-aminobenzoic acid or cyclohexanecarboxylic acid, respectively.<sup>15</sup>

Surprisingly, in our microsomal assay ureas **6** and **7** and amide **8** did not inhibit the human  $11\beta$ -HSD1 enzyme. Under the same conditions, amide **9** only inhibited 20% the enzyme activity. Oxaadamantanes **10** and **11** were also very poor inhibitors.



**Figure 3.** Structures of  $11\beta$ -HSD1 inhibitors **1–4**.

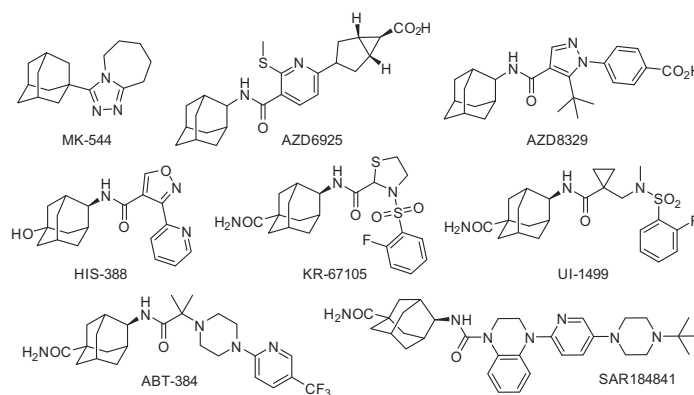
Taking into account the aforementioned results and that the corresponding C-2 isomers of **8** and **9** had not been previously tested, we synthesized both amides from 2-aminoadamantane. By way of contrast with the lack of inhibitory activity of their C-1 isomers, amides **12** and **13** displayed potent, nanomolar inhibition. Also, in agreement with the previous trend observed in going from ureas **6** and **7** to their corresponding amides **9** and **10**, the novel amide **12** was more potent than our previous hit **5**. It was noteworthy that ring contraction from **12** to **14** led to a less potent inhibitor.

Overall, for the three pairs of isomers evaluated here, substitution in position 2 of the adamantyl scaffold consistently leads to more potent inhibitory activity of human  $11\beta$ -HSD1.

The introduction of an oxygen atom in the adamantane does not improve the activity within the series of the C-1 substituted adamantanes. As Ye et al. found, within a series of 2,2-disubstituted oxaadamantanes, that the corresponding oxaadamantane analogs performed poorly,<sup>9b</sup> we have not evaluated oxaadamantane derivatives with the amino group attached to a methylene group of the polycyclic ring.<sup>16</sup>

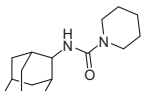
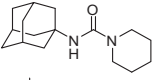
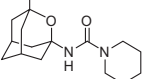
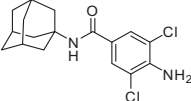
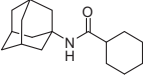
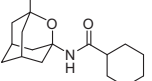
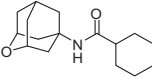
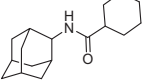
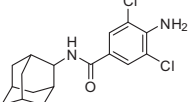
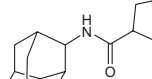
In order to rationalize these results we combined docking studies with molecular dynamics simulations to examine the structural integrity of the binding of compounds **5**, **6**, and **12**. Let us note that the inhibitory activities of **5** and **6**, which only differ in the substitution at positions C1 and C2, vary from 87% (**5**) to 3% (**6**). On the other hand, compound **12** involves the replacement of the piperidine moiety present in **5** by the cyclohexyl one in **12**, leading to a moderate increase of the inhibitory activity from 87% (**5**) to 100% (**12**).

Compounds were docked in the binding cavity of human  $11\beta$ -HSD1 using Glide.<sup>17</sup> In all cases the best scored poses mimicked the binding mode of PF-877423 (Fig. S1 in Supporting information), which is a potent adamantyl-based inhibitor against the human



**Figure 2.** Selected adamantyl-based  $11\beta$ -HSD1 inhibitors.

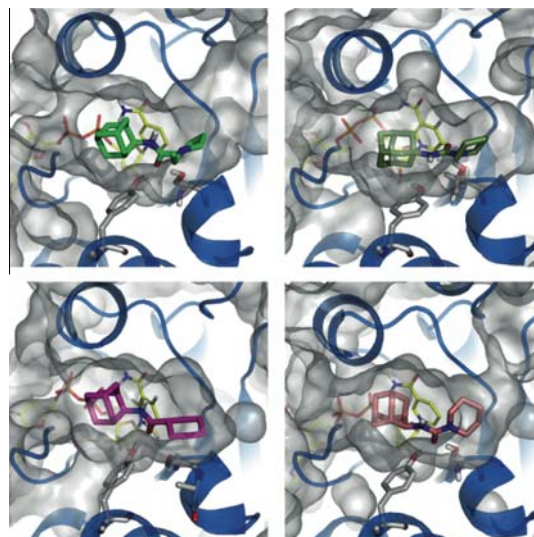
**Table 1**  
Structures and human 11 $\beta$ -HSD1 inhibitory activities of compounds **5–14**

Product	11 $\beta$ -hHSD1 inhibition at 10 $\mu$ M <sup>a</sup>	11 $\beta$ -hHSD1IC <sub>50</sub> (nM) <sup>a</sup>
	87	873
	3	ND
	0	ND
	0	ND
	20	ND
	9	ND
	9	ND
	100	86
	86	74
	76	520

<sup>a</sup> 11 $\beta$ -HSD1 inhibition was determined in mixed sex, Human Liver Microsomes (Celsis In-vitro Technologies) by measuring the conversion of <sup>3</sup>H-cortisone to <sup>3</sup>H-cortisol in a cortisol-Scintillation Proximity Assay. Percentage inhibition was determined relative to a no inhibitor control.

enzyme ( $K_i = 1.4$  nM).<sup>18</sup> Thus, all the compounds retained the hydrogen bond formed between the carbonyl oxygen of the amide/urea moiety with the hydroxyl group of Ser170 and the adamantyl cage filled a common site in the binding pocket.

Three independent 50 ns MD simulations were run for each ligand–receptor complex, and additional runs were performed for the complex with PF-877423, which was used as a reference system. All the simulations were stable except that of the complex with the C1-substituted compound **6**, since the ligand was released from the binding site in one simulation. Upon exclusion of this latter trajectory, the root-mean square deviation (RMSD) profiles were similar in all cases. Thus, the RMSD of the protein backbone varied from 1.5 to 2.2 Å, whereas the residues in the binding site



**Figure 4.** Last snapshot of a representative molecular dynamics simulation for the complexes between human 11 $\beta$ -HSD1 and compounds PF-877423 (top left), **6** (top right), **12** (bottom left) and **5** (bottom right). In all cases residues Tyr183 and Ser170, the NADP cofactor and the ligand are represented as sticks and only the polar hydrogens are shown. The shape of the binding cavity is shown as a white contour.

showed a larger RMSD (2.5–3.7 Å) due to the enhanced flexibility of the loops that enclose the binding pocket.

The hydrogen bond formed between the inhibitor and the hydroxyl group of Ser170 was retained in all cases (average distance of 2.8 Å). Often, an additional hydrogen bond with the hydroxyl unit of Tyr183 was transiently formed. Nevertheless, compound **6** consistently showed a higher root-mean square fluctuation (1.4 Å) compared to inhibitors **5** and **12** (RMSF of 0.8 Å), suggesting a poorer fit of the hydrophobic cage in the binding cavity due to the change in the substitution pattern from position C1 in **6** to position C2 in **5** and **12**. This reflects the larger steric hindrance of the adamantyl cage with the NADP nicotinamide ring arising from the C1-substitution, because C2-derived compounds are found to adopt a configuration where the C2-H unit is primarily oriented toward the nicotinamide ring (Fig. 4).

Finally, the moderate increase in the inhibitory activity of compound **12** relative to **5** may be ascribed to the enhanced hydrophobicity afforded by the cyclohexane unit, as noted in their respective clogP values of 4.5 and 3.6, determined from quantum mechanical IEF/MST continuum solvation calculations.<sup>19</sup> This trend agrees with similar findings reported for series of structurally related compounds.<sup>20</sup>

In conclusion, bearing in mind the aforementioned pharmacological results, it is clear that for potent 11 $\beta$ -HSD1 inhibitory activity, 2-substituted adamantanes are preferred over their corresponding 1-substituted counterpart. Also, the introduction of an oxygen atom in the polycyclic scaffold did not improve the activity (compare **9** vs **10** and **11**).

#### Acknowledgments

R.L. thanks the *Ministerio de Educación, Cultura y Deporte* for a PhD Grant (FPU program). We thank financial support from *Ministerio de Economía y Competitividad* (Project SAF2014-57094-R) and the *Generalitat de Catalunya* (Grants 2014-SGR-00052 and



2014-SGR-1189) and the *Consorci de Serveis Universitaris de Catalunya* for computational resources. F.J.L. acknowledges the support from ICREA Academia. We thank ACCIÓ (*Generalitat de Catalunya*) and CIDQO 2012 SL for financial support (*Programa Nucleis*, RD14-1-0057, SAFNAD).

### Supplementary data

Supplementary data (experimental and computational procedures. NMR spectra for all the new compounds) associated with this article can be found in the online version, at <http://dx.doi.org/10.1016/j.bmcl.2015.07.097>.

### References and notes

- (a) Lamoureux, G.; Artavia, G. *Curr. Med. Chem.* **2010**, *17*, 2967; (b) Liu, J.; Obando, D.; Liao, V.; Lifa, T.; Codd, R. *Eur. J. Med. Chem.* **1949**, *2011*, 46; (c) Wanka, L.; Iqbal, K.; Schreiner, P. R. *Chem. Rev.* **2013**, *113*, 3516.
- Zoidis, G.; Kolocouris, N.; Foscolos, G. B.; Kolocouris, A.; Fytas, G.; Karayannis, P.; Padalko, E.; Neyts, J.; DeClercq, E. *Antiviral Chem. Chemother.* **2003**, *14*, 153; For another, non-related example, see: Lee, W.-G.; Lee, S.-D.; Cho, J.-H.; Jung, Y.; Kim, J.-H.; Hien, T. T.; Kang, K.-W.; Ko, H.; Kim, Y.-C. *J. Med. Chem.* **2012**, *55*, 3687.
- (a) Scott, J. S.; Chooramun, J. 11 $\beta$ -Hydroxysteroid Dehydrogenase Type 1 (11 $\beta$ -HSD1) inhibitors in Development. In *New Therapeutic Strategies for Type 2 Diabetes*; Jones, R. M., Ed.; Small Molecule Approaches, RSC Drug Discovery Series No. 27; Royal Society of Chemistry: Cambridge, 2012; pp 109–141; (b) Gathercole, L. L.; Lavery, G. G.; Morgan, S. A.; Cooper, M. S.; Sinclair, A. J.; Tomlinson, J. W.; Stewart, P. M. *Endocrine Rev.* **2013**, *34*, 525; (c) Scott, J. S.; Goldberg, F. W.; Turnbull, A. V. *J. Med. Chem.* **2014**, *57*, 4466.
- (a) Olson, S.; Aster, S. D.; Brown, K.; Carbin, L.; Graham, D. W.; Hermanowski-Vosatka, A.; LeGrand, C. B.; Mundt, S. S.; Robbins, M. A.; Schaeffer, J. M.; Slossberg, L. H.; Szymonifka, M. J.; Thieringer, R.; Wright, S. D.; Balkovec, J. M. *Bioorg. Med. Chem. Lett.* **2005**, *15*, 4359; (b) Sorensen, B.; Rohde, J.; Wang, J.; Fung, S.; Monzon, K.; Chiou, W.; Pan, L.; Deng, X.; Stolarik, D.; Frevert, E. U.; Jacobson, P.; Link, J. T. *Bioorg. Med. Chem. Lett.* **2006**, *16*, 5958; (c) Becker, C. L.; Engstrom, K. M.; Kerdesky, F. A.; Tolle, J. C.; Wagaw, S. H.; Wang, W. *Org. Process Res. Dev.* **2008**, *12*, 1114; (d) Scott, J. S.; Barton, P.; Bennett, S. N. L.; deSchoolmeester, J.; Godfrey, L.; Kilgour, E.; Mayers, R. M.; Packer, M. J.; Rees, A.; Schofield, P.; Selmi, N.; Swales, J. G.; Whittamore, P. R. *O. Med. Chem. Commun.* **2012**, *3*, 1263; (e) Scott, J. S.; deSchoolmeester, J.; Kilgour, E.; Mayers, R. M.; Packer, M. J.; Hargreaves, D.; Gerhardt, S.; Ogg, D. J.; Rees, A.; Selmi, N.; Stocker, A.; Swales, J. G.; Whittamore, P. R. *O. J. Med. Chem.* **2012**, *55*, 10136; (f) Venier, O.; Pascal, C.; Braun, A.; Namane, C.; Mougnot, P.; Crespin, O.; Pacquet, F.; Mougnot, C.; Monseau, C.; Onofri, B.; Dadji-Faihun, R.; Leger, C.; Ben-Hassine, M.; Van-Pham, T.; Ragot, J.-L.; Philippo, C.; Farjot, G.; Noah, L.; Maniani, K.; Boutarfa, A.; Nicolai, E.; Guillot, E.; Pruniaux, M.-P.; Güssregen, S.; Engel, C.; Coutant, A.-L.; de Miguel, B.; Castro, A. *Bioorg. Med. Chem. Lett.* **2013**, *23*, 2414; (g) Park, S. B.; Jung, W. H.; Kang, N. S.; Park, J. S.; Bae, G. H.; Kim, H. Y.; Rhee, S. D.; Kang, S. K.; Ahn, J. H.; Jeong, H. G.; Kim, K. Y. *Eur. J. Pharmacol.* **2013**, *721*, 70; (h) Okazaki, S.; Takahashi, T.; Iwamura, T.; Nakaki, J.; Sekiya, Y.; Yagi, M.; Kumagai, H.; Sato, M.; Sakami, S.; Nitta, A.; Kawai, K.; Kainoh, M. *J. Pharmacol. Exp. Ther.* **2014**, *351*, 181; (i) Byun, S. Y.; Shin, Y. J.; Nam, K. Y.; Hong, S. P.; Ahn, S. K. *Life Sci.* **2015**, *120*, 1.
- For some examples of 1-substituted adamantane evaluated as 11 $\beta$ -HSD1 inhibitors see: (a) Olson, S.; Aster, S. D.; Brown, K.; Carbin, L.; Graham, D. W.; Hermanowski-Vosatka, A.; LeGrand, C. B.; Mundt, S. S.; Robbins, M. A.; Schaeffer, J. M.; Slossberg, L. H.; Szymonifka, M. J.; Thieringer, R.; Wright, S. D.; Balkovec, J. M. *Bioorg. Med. Chem. Lett.* **2005**, *15*, 4359; (b) Su, X.; Pradaux-Caggiano, F.; Thomas, M. P.; Szeto, M. W. Y.; Halem, H. A.; Culler, M. D.; Vicker, N.; Potter, B. V. L. *Chem. Med. Chem.* **2010**, *5*, 1026; (c) Su, X.; Vicker, N.; Thomas, M. P.; Pradaux-Caggiano, F.; Halem, H. A.; Culler, M. D.; Potter, B. V. L. *Chem. Med. Chem.* **2011**, *6*, 1439; (d) Su, X.; Pradaux-Caggiano, F.; Vicker, N.; Thomas, M. P.; Halem, H. A.; Culler, M. D.; Potter, B. V. L. *Chem. Med. Chem.* **2011**, *6*, 1616; (e) Wang, H.; Robl, J. A.; Hamann, L. G.; Simpkins, L.; Golla, R.; Li, Y.-X.; Seethala, R.; Zvyaga, T.; Gordon, D. A.; Li, J. *Bioorg. Med. Chem. Lett.* **2011**, *21*, 4146; (f) Kim, S. H.; Kwon, S. W.; Chu, S. Y.; Lee, J. H.; Narsaiah, B.; Kim, C. H.; Kang, S. K.; Kang, N. S.; Rhee, S. D.; Bae, M. A.; Ahn, S. H.; Ha, D. C.; Kim, K. Y.; Ahn, J. H. *Chem. Pharm. Bull.* **2011**, *59*, 46; (g) Su, X.; Halem, H. A.; Thomas, M. P.; Moutrille, C.; Culler, M. D.; Vicker, N.; Potter, B. V. L. *Bioorg. Med. Chem.* **2012**, *20*, 6394.
- For example, the clogP of amide **2** (2.64) is 1 unit lower than that of amide **1** (3.68). Calculated using BioByte software: BioLoom 5.0 BioByte Co., Claremont, CA, USA. <http://www.biobyte.com>
- Webster, S. P.; Ward, P.; Binnie, M.; Craigie, E.; McConnell, K. M. M.; Sooy, K.; Vinter, A.; Seckl, J. R.; Walker, B. R. *Bioorg. Med. Chem. Lett.* **2007**, *17*, 2838.
- Xia, G.; Liu, L.; Liu, H.; Yu, J.; Xu, Z.; Chen, Q.; Ma, C.; Li, P.; Xiong, B.; Liu, X.; Shen, J. *Chem. Med. Chem.* **2013**, *8*, 577.
- (a) Yeh, V. S. C.; Kurukulasuriya, R.; Madar, D.; Patel, J. R.; Fung, S.; Monzon, K.; Chiou, W.; Wang, J.; Jacobson, P.; Sham, H. L.; Link, J. T. *Bioorg. Med. Chem. Lett.* **2006**, *16*, 5408; (b) Ye, X.-Y.; Chen, S. Y.; Nayeem, A.; Golla, R.; Seethala, R.; Wang, M.; Harper, T.; Slecza, B. G.; He, B.; Gordon, D. A.; Robl, J. A. *Bioorg. Med. Chem. Lett.* **2011**, *21*, 6699.
- (a) Freeman-Cook, K. D.; Hoffman, R. L.; Johnson, T. W. *Future Med. Chem.* **2013**, *5*, 113; (b) Murray, C. W.; Erlanson, D. A.; Hopkins, A. L.; Keseru, G. M.; Leeson, P. D.; Rees, D. C.; Reynolds, C. H.; Richmond, N. J. *J. Med. Chem.* **2014**, *5*, 616.
- Tice, C. M.; Zhao, W.; Xu, Z.; Cacatian, S. T.; Simpson, R. D.; Ye, Y.-J.; Singh, S. B.; McKeever, B. M.; Lindblom, P.; Guo, J.; Krosky, P. M.; Kruk, B. A.; Berbaum, J.; Harrison, R. K.; Johnson, J. J.; Bukhtiyarov, Y.; Panemangalore, R.; Scott, B. B.; Zhao, Y.; Bruno, J. G.; Zhuang, L.; McGeehan, G. M.; He, W.; Claremont, D. A. *Bioorg. Med. Chem. Lett.* **2010**, *20*, 881.
- Duque, M. D.; Camps, P.; Profire, S.; Vázquez, S.; Sureda, F. S.; Mallol, J.; López-Querol, M.; Naesens, L.; De Clercq, E.; Prathalingam, S. R.; Kelly, J. M. *Bioorg. Med. Chem.* **2009**, *17*, 3198.
- Leiva, R.; Gazzarrini, S.; Esplugas, R.; Moroni, A.; Naesens, L.; Sureda, F. X.; Vázquez, S. *Tetrahedron Lett.* **2015**, *56*, 1272.
- Urea **6** had been synthesized previously using a Pd-catalyzed carbonylation reaction: Orito, K.; Miyazawa, M.; Nakamura, T.; Horibata, A.; Ushito, H.; Nagasaki, H.; Yuguchi, M.; Yamashita, S.; Yamazaki, T.; Tokuda, M. *J. Org. Chem.* **2006**, *71*, 5951.
- The *N*-methyl derivative of **8** is reported to be a submicromolar inhibitor of 11 $\beta$ -HSD1. See, Richards, S.; Sorensen, B.; Jae, H.; Winn, M.; Chen, Y.; Wang, J.; Fung, S.; Monzon, K.; Frevert, E. U.; Jacobson, P.; Sham, H.; Link, J. T. *Bioorg. Med. Chem. Lett.* **2006**, *16*, 6241.
- For further related 2,2-disubstituted adamantanes that led to the discovery of the clinical candidate BMS-816336 see: (a) Ye, X.-Y.; Yoon, D.; Chen, S. Y.; Nayeem, A.; Golla, R.; Seethala, R.; Wang, M.; Harper, T.; Slecza, B. G.; Apedo, A.; Li, Y.-X.; He, B.; Kirby, M.; Gordon, D. A.; Robl, J. A. *Bioorg. Med. Chem. Lett.* **2014**, *24*, 654; (b) Ye, X.-Y.; Chen, S. Y.; Wu, S.; Yoon, D. S.; Wang, H.; Hong, Z.; Oconnor, S. P.; Li, J.; Li, J.; Walker, S.; Kennedy, L. J.; Apedo, A.; Nayeem, A.; Sheriff, S.; Morin, P.; Camac, D.; Harrity, T.; Zebo, R.; Taylor, J.; Morgan, N.; Ponticciello, R.; Golla, R.; Seethala, R.; Wang, M.; Harper, T.; Slecza, B. G.; He, B.; Kirby, M.; DiMarco, J.; Scaringe, R.; Hanson, R. L.; Guo, Z.; Li, J.; Sun, J.-H.; Wong, M. K.; Chen, B.-C.; Haque, L.; Leahy, D. K.; Chan, C.; Li, Y.-X.; Zvyaga, T.; Hansen, L.; Patel, C.; Gordon, D. A.; Robl, J. A. *Chem. Abstr.* **2015**, 477592.
- Friesner, R. A.; Murphy, R. B.; Repasky, M. P.; Frye, L. L.; Greenwood, J. R.; Halgren, T. A.; Sanschagrin, P. C.; Mainz, D. T. *J. Med. Chem.* **2006**, *49*, 6177.
- Cheng, H.; Hoffman, J.; Le, P.; Nair, S. K.; Cripps, S.; Matthews, J.; Smith, C.; Yang, M.; Kupchinsky, S.; Dress, K.; Edwards, M.; Cole, B.; Walters, E.; Loh, C.; Ermolieff, J.; Fanjul, A.; Bhat, G. B.; Herrera, J.; Pauly, T.; Hosea, N.; Paderes, G.; Rejto, P. *Bioorg. Med. Chem. Lett.* **2010**, *20*, 2897.
- (a) Curutchet, C.; Orozco, M.; Luque, F. J. *J. Comput. Chem.* **2001**, *22*, 1180; (b) Kolar, M.; Fanfril, J.; Lepšik, M.; Fort, F.; Luque, F. J.; Hobza, P. *J. Phys. Chem. B* **2013**, *117*, 5950.
- Robb, G. R.; Boyd, S.; Davies, C. D.; Dossetter, A. G.; Goldberg, F. W.; Kemmitt, P. D.; Scott, J. S.; Swales, J. G. *Med. Chem. Commun.* **2015**, *6*, 926.

# Supporting information

## Novel 11 $\beta$ -HSD1 inhibitors: C-1 vs C-2 substitution and effect of the introduction of an oxygen atom in the adamantane scaffold

Rosana Leiva<sup>a</sup>, Constantí Seira<sup>b</sup>, Andrew McBride<sup>c</sup>, Margaret Binnie<sup>c</sup>, F. Javier Luque<sup>b</sup>, Axel Bidon-Chanal<sup>b</sup>, Scott P. Webster<sup>c</sup>, and Santiago Vázquez<sup>a</sup>

<sup>a</sup>Laboratori de Química Farmacèutica (Unitat Associada al CSIC), Facultat de Farmàcia, and Institute of Biomedicine (IBUB), Universitat de Barcelona, Av. Joan XXIII, s/n, Barcelona, E-08028, Spain

<sup>b</sup>Departament de Físicoquímica, Facultat de Farmàcia and Institute of Biomedicine (IBUB), Universitat de Barcelona, Av. Prat de la Riba, 171, 08921 Santa Coloma de Gramenet, Spain

<sup>c</sup>Endocrinology Unit, Centre for Cardiovascular Science, University of Edinburgh, Queen's Medical Research Institute, EH16 4TJ, United Kingdom

### Table of content:

List of abbreviations	S2
Chemical synthesis. General methods	S3
Synthetic experimental procedures	S4
Determination of the 11 $\beta$ -HSD1 inhibition	S12
Computational methods	S13
Figure S1.	S15
<sup>1</sup> H and <sup>13</sup> C NMR spectra of new compounds	S16

### **List of abbreviations**

ATR = Attenuated Total Reflectance

COSY = Correlation Spectroscopy

DCM = dichloromethane

EDC = 1-ethyl-3-(3-dimethylaminopropyl)carbodiimide

EtOAc = ethyl acetate

HOBt = 1-hydroxybenzotriazole

11 $\beta$ -HSD1 = 11 $\beta$ -HydroxySteroid Dehydrogenase type 1

HSQC = Heteronuclear Single Quantum Correlation

NMR = Nuclear Magnetic Resonance

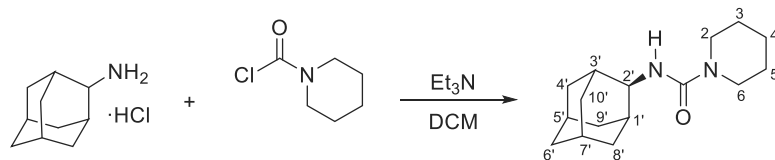
RESP = Restrained Electrostatic Potential

TIP3P = Transferable Intermolecular Potential 3P

### **Chemical Synthesis. General Methods**

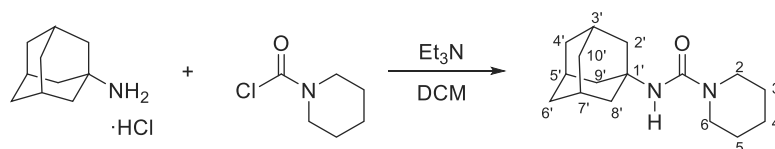
Melting points were determined in open capillary tubes with a MFB 595010M Gallenkamp melting point apparatus. 400 MHz  $^1\text{H}$  NMR and 100.6 MHz  $^{13}\text{C}$  NMR spectra were recorded on a Varian Mercury 400 spectrometer. The chemical shifts are reported in ppm ( $\delta$  scale) relative to internal tetramethylsilane, and coupling constants are reported in hertz (Hz). Assignments given for the NMR spectra of the new compounds is based on COSY  $^1\text{H}/^{13}\text{C}$  (gHSQC sequence) experiments. IR spectra were run on a Perkin-Elmer Spectrum RX I spectrophotometer. Absorption values are expressed as wavenumbers ( $\text{cm}^{-1}$ ). Column chromatography was performed on silica gel 60 Å (35-70 mesh, SDS, ref 2000027). Thin-layer chromatography was performed with aluminum-backed sheets with silica gel 60 F254 (Merck, ref 1.05554), and spots were visualized with UV light and 1% aqueous solution of  $\text{KMnO}_4$ . The analytical samples of all of the new compounds that were subjected to pharmacological evaluation possess a purity of >95%, as evidenced by results of their  $^1\text{H}$  NMR spectra and elemental analyses.

### Obtention of *N*-(2-adamantyl)piperidine-1-carboxamide (**5**)



To a solution of 2-adamantanamine hydrochloride (300 mg, 1.6 mmol) in DCM (15 mL) were added 1-piperidinecarbonyl chloride (0.30 mL, 2.4 mmol) and triethylamine (0.8 mL, 6.4 mmol). The reaction mixture was stirred at room temperature overnight. To the resulting suspension was then added saturated aqueous NaHCO<sub>3</sub> solution (15 mL) and the phases were separated. The aqueous phase was extracted with further DCM (2 x 15 mL), and the organics were dried over anh. sodium sulphate, filtered and concentrated in *vacuo* to give a white yellowish solid (507 mg). Column chromatography (hexane/ethyl acetate mixture) gave **5** as a white solid (298 mg, 71% yield), mp 183-184 °C. IR (ATR)  $\nu$ : 753, 993, 1030, 1056, 1116, 1193, 1218, 1250, 1261, 1506, 1534, 1558, 1606, 1640, 2901, 2918, 3415 cm<sup>-1</sup>. <sup>1</sup>H-NMR (400 MHz, CDCl<sub>3</sub>)  $\delta$ : 1.50-1.62 [c. s., 6 H, 4-H<sub>2</sub>, 3(5)-H<sub>2</sub>], 1.63 [m, 2 H, 8'(10')-H<sub>a</sub>], 1.69-1.78 [c. s., 4 H, 8'(10')-H<sub>b</sub>, 6'-H<sub>2</sub>], 1.82 [c. s., 6 H, 5'-H, 7'-H, 4'(9')-H<sub>2</sub>], 1.90 [m, 2 H, 1'(3')-H], 3.31 [c. s., 4 H, 2(6)-H<sub>2</sub>], 3.93 (m, 1 H, 2'-H), 4.74 (d,  $J$  = 4.8 Hz, 1 H, NH). <sup>13</sup>C-NMR (100.5 MHz, CDCl<sub>3</sub>)  $\delta$ : 24.4 (CH<sub>2</sub>, C4), 25.5 [CH<sub>2</sub>, C3(5)], 27.2 (CH, C5' or C7'), 27.3 (CH, C7' or C5'), 32.1 [CH<sub>2</sub>, C8'(10')], 32.4 [CH, C1'(3')], 37.2 [CH<sub>2</sub>, C4'(9')], 37.6 (CH<sub>2</sub>, C6'), 44.9 [CH<sub>2</sub>, C2(6)], 54.0 (CH, C2'), 157.1 (C, CO). Calcd for C<sub>17</sub>H<sub>27</sub>NO: C 73.24, H 9.99, N 10.68. Found: C 73.22, H 10.27, N 10.71.

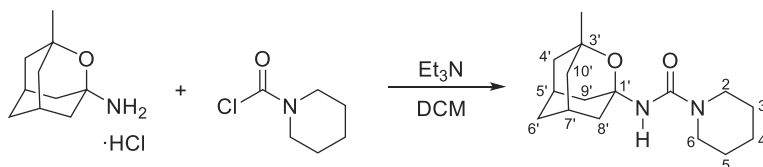
### Obtention of *N*-(1-adamantyl)piperidine-1-carboxamide (**6**)



To a solution of 1-adamantanamine hydrochloride (300 mg, 1.6 mmol) in DCM (15 mL) were added 1-piperidinecarbonyl chloride (0.30 mL, 2.4 mmol) and triethylamine (0.8 mL, 6.4 mmol). The reaction mixture was stirred at room

temperature overnight. To the resulting suspension was then added saturated aqueous NaHCO<sub>3</sub> solution (15 mL) and the phases were separated. The aqueous phase was extracted with further DCM (2 x 15 mL), and the organics were dried over anh. sodium sulphate, filtered and concentrated in *vacuo* to give a yellow solid (392 mg). Column chromatography (hexane/ethyl acetate mixture) gave **6** as a white solid (129 mg, 31% yield). The analytical sample was obtained by washing with pentane, mp 190-191 °C. IR (ATR)  $\nu$ : 756, 919, 982, 994, 1033, 1164, 1193, 1221, 1248, 1347, 1369, 1441, 1535, 1641, 2348, 2844, 2924, 3415 cm<sup>-1</sup>. <sup>1</sup>H-NMR (400 MHz, CDCl<sub>3</sub>)  $\delta$ : 1.47-1.60 [c. s., 6 H, 3(5)-H<sub>2</sub>, 4-H<sub>2</sub>], 1.61-1.71 [c. s., 6 H, 4'(6')(10')-H<sub>2</sub>], 1.94-2.00 [c. s., 6 H, 2'(8')(9')-H<sub>2</sub>], 2.05 [m, 3 H, 3'(5')(7')-H], 3.24 (m, 4 H, 2(6)-H<sub>2</sub>), 4.17 (b. s., 1 H, NH). <sup>13</sup>C-NMR (100.5 MHz, CDCl<sub>3</sub>)  $\delta$ : 24.4 (CH<sub>2</sub>, C<sub>4</sub>), 25.6 [CH<sub>2</sub>, C<sub>3</sub>(5)], 29.6 [CH, C<sub>3'</sub>(5')(7')], 36.5 [CH<sub>2</sub>, C<sub>4'</sub>(6')(10')], 42.4 [CH<sub>2</sub>, C<sub>2'</sub>(8')(9')], 44.9 [CH<sub>2</sub>, C<sub>2</sub>(6)], 51.0 (C, C<sub>1'</sub>), 156.8 (C, CO). Calcd for C<sub>17</sub>H<sub>20</sub>Cl<sub>2</sub>N<sub>2</sub>O: C 73.24, H 9.99, N 10.68. Found: C 73.22, H 10.26, N 10.73.

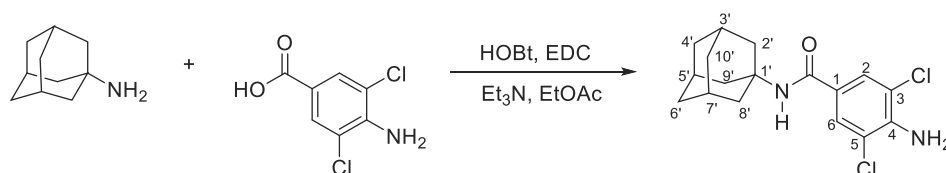
#### Obtention of *N*-(3-methyl-2-oxaadmant-1-yl)piperidine-1-carboxamide (**7**)



To a solution of (3-methyl-2-oxaadmant-1-yl)amine hydrochloride (137 mg, 0.7 mmol) in DCM (10 mL) were added 1-piperidinecarbonyl chloride (0.13 mL, 1 mmol) and triethylamine (0.34 mL, 2.7 mmol). The reaction mixture was stirred at room temperature overnight. To the resulting suspension was then added saturated aqueous NaHCO<sub>3</sub> solution (10 mL) and the phases were separated. The aqueous phase was extracted with further DCM (2 x 10 mL), and the organics were dried over anh. sodium sulphate, filtered and concentrated in *vacuo* to give an orange oil (374 mg). Column chromatography (hexane/ethyl acetate mixture) gave **7** as a white solid (64 mg, 34% yield), mp 116-117 °C. IR (ATR)  $\nu$ : 617, 672, 708, 764, 813, 852, 896, 922, 955, 964, 985, 995, 1037, 1067, 1144, 1166, 1195, 1220, 1253, 1349, 1374, 1392, 1443, 1538, 1632, 1643, 2847, 2922, 3322 cm<sup>-1</sup>. <sup>1</sup>H-NMR (400 MHz, CDCl<sub>3</sub>)  $\delta$ : 1.13 (s, 3 H, CH<sub>3</sub>-

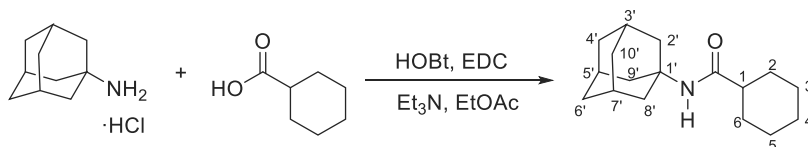
C3'), 1.46-1.60 [c. s., 8 H, 4-H<sub>2</sub>, 3(5)-H<sub>2</sub>, 4'(10')-H<sub>a</sub>], 1.61-1.70 [c. s., 3 H, 6'-H<sub>a</sub>, 4'(10')-H<sub>b</sub>], 1.72-1.80 (m, 1 H, 6'-H<sub>b</sub>), 1.86 [dm, *J* = 11.6 Hz, 2 H, 8'(9')-H<sub>a</sub>], 2.25 [m, 2 H, 5'(7')-H], 2.30 [dm, *J* = 11.6 Hz, 2H, 8'(9')-H<sub>b</sub>], 3.24 [c. s., 4 H, 2(6)-H<sub>2</sub>], 4.63 (b. s., 1 H, NH). <sup>13</sup>C-NMR (100.5 MHz, CDCl<sub>3</sub>) δ: 24.4 (CH<sub>2</sub>, C4), 25.6 [CH<sub>2</sub>, C3(5)], 28.7 [CH, C5'(7')], 29.2 (CH<sub>3</sub>, C3-CH<sub>3</sub>), 33.9 (CH<sub>2</sub>, C6'), 39.6 [CH<sub>2</sub>, C8'(9')], 41.0 [CH<sub>2</sub>, C4'(10')], 44.7 [CH<sub>2</sub>, C2(6)], 73.0 (C, C3'), 83.3 (C, C1'), 155.5 (C, CO). Calcd for C<sub>17</sub>H<sub>27</sub>NO: C 69.03, H 9.41, N 10.06. Found: C 68.91, H 9.40, N 9.82.

#### Obtention of *N*-(1-adamantyl)-4-amino-3,5-dichlorobenzamide (**8**)



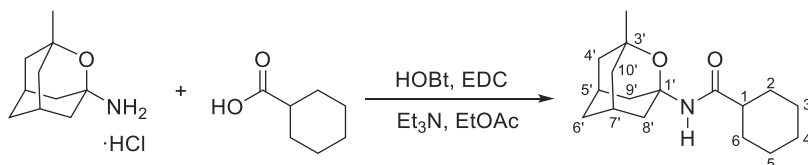
To a solution of 1-adamantanamine hydrochloride (207 mg, 1.1 mmol) in EtOAc (10 mL) were added 4-amino-3,5-dichlorobenzoic acid (206 mg, 1 mmol), HOBT (202.6 mg, 1.5 mmol), EDC (232 mg, 1.5 mmol) and triethylamine (0.6 mL, 4.4 mmol). The reaction mixture was stirred at room temperature for 22 hours. To the resulting suspension was then added water (20 mL) and the phases were separated. The organic phase was washed with saturated aqueous NaHCO<sub>3</sub> solution (15 mL) and brine (15 mL), dried over anh. sodium sulphate and filtered. Evaporation in *vacuo* of the organics gave **8** as a white yellowish solid (286 mg, 84% yield). The analytical sample was obtained by crystallization from ethyl acetate/pentane, mp 222-223 °C. IR (ATR)  $\nu$ : 648, 753, 799, 879, 907, 1027, 1053, 1087, 1107, 1250, 1306, 1321, 1483, 1533, 1569, 1600, 1638, 2353, 2844, 2901, 3381, 3729, 3832 cm<sup>-1</sup>. <sup>1</sup>H-NMR (400 MHz, CDCl<sub>3</sub>) δ: 1.65-1.76 [c. s., 6 H, 4'(6')(10')-H<sub>2</sub>], 2.07-2.11 [c. s., 6 H, 2'(8')(9')-H<sub>2</sub>], 2.11 [m, 3 H, 3'(5')(7')-H], 4.70 (b. s., 2 H, NH<sub>2</sub>), 5.62 (b. s., 1 H, NH), 7.56 [s, 2 H, 2(6)-H<sub>Ar</sub>]. <sup>13</sup>C-NMR (100.5 MHz, CDCl<sub>3</sub>) δ: 29.5 [CH, C3'(5')(7')], 36.3 [CH<sub>2</sub>, C4'(6')(10')], 41.6 [CH<sub>2</sub>, C2'(8')(9')], 52.4 (C, C1'), 118.8 [C, C3(5)], 125.8 (C, C1), 126.6 [CH, C2(6)], 142.3 (C, C4), 164.2 (C, CO). Calcd for C<sub>17</sub>H<sub>20</sub>Cl<sub>2</sub>N<sub>2</sub>O: C 60.19, H 5.94, N 8.26. Found: C 60.32, H 6.09, N 8.32.

### Obtention of *N*-(1-adamantyl)cyclohexanecarboxamide (9)



To a solution of 1-adamantanamine hydrochloride (207 mg, 1.1 mmol) in EtOAc (15 mL) were added cyclohexanecarboxylic acid (128 mg, 1 mmol), HOBt (203 mg, 1.5 mmol), EDC (232 mg, 1.5 mmol) and triethylamine (0.6 mL, 4.4 mmol). The reaction mixture was stirred at room temperature overnight. To the resulting suspension was then added water (15 mL) and the phases were separated. The organic phase was washed with saturated aqueous NaHCO<sub>3</sub> solution (15 mL) and brine (15 mL), dried over anhydrous sodium sulphate and filtered. Evaporation *in vacuo* of the organics gave **9** as a white solid (202 mg, 77% yield). The analytical sample was obtained by crystallization from ethyl acetate/pentane, mp 192-193 °C. IR (ATR)  $\nu$ : 665, 711, 762, 919, 950, 993, 1027, 1195, 1215, 1250, 1270, 1307, 1341, 1355, 1378, 1446, 1537, 1642, 2353, 2844, 2914, 3272, 3409 cm<sup>-1</sup>. <sup>1</sup>H-NMR (400 MHz, CDCl<sub>3</sub>)  $\delta$ : 1.12-1.31 [c. s., 3 H, 3(5)-H<sub>ax</sub> and 4-H<sub>ax</sub>], 1.32-1.46 [c. s., 2 H, 2(6)-H<sub>ax</sub>], 1.60-1.70 [c. s., 7 H, 4-H<sub>eq</sub>, 4'(6')(10')-H<sub>2</sub>], 1.72-1.82 [c. s., 4 H, 3(5)-H<sub>eq</sub> and 2(6)-H<sub>eq</sub>], 1.93 [tt, *J* = 11.6 Hz, *J'* = 3.6 Hz, 1 H, 1-H], 1.96-2.0 [c. s., 6 H, 2'(8')(9')-H<sub>2</sub>], 2.05 [m, 3 H, 3'(5')(7')-H], 5.07 (b. s., 1 H, NH). <sup>13</sup>C-NMR (100.5 MHz, CDCl<sub>3</sub>)  $\delta$ : 25.8 [CH<sub>2</sub>, C3(5) and C4], 29.4 [CH, C3'(5')(7')], 29.8 [CH<sub>2</sub>, C2(6)], 36.4 [CH<sub>2</sub>, C4'(6')(10')], 41.7 [CH<sub>2</sub>, C2'(8')(9')], 46.4 (CH, C1), 51.4 (C, C1'), 175.4 (C, CO). Calcd for C<sub>17</sub>H<sub>27</sub>NO: C 78.11, H 10.41, N 5.36. Found: C 78.26, H 10.29, N 5.27.

### Obtention of *N*-(3-methyl-2-oxaadamant-1-yl)cyclohexanecarboxamide (10)

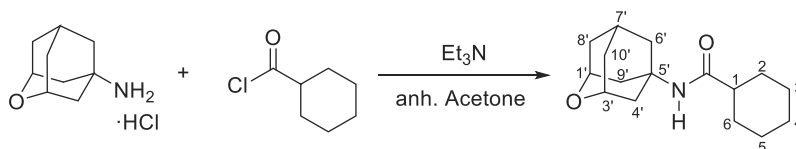


To a solution of (3-methyl-2-oxaadamant-1-yl)amine hydrochloride (120 mg, 0.6 mmol) in EtOAc (10 mL) were added cyclohexanecarboxylic acid (69 mg, 0.5 mmol), HOBt (111 mg, 0.8 mmol), EDC (127 mg, 0.8 mmol) and triethylamine



(0.3 mL, 2.4 mmol). The reaction mixture was stirred at room temperature overnight. To the resulting suspension was then added water (10 mL) and the phases were separated. The organic phase was washed with saturated aqueous NaHCO<sub>3</sub> solution (10 mL), brine (10 mL) and 2N HCl solution (2 x 10 mL), dried over anh. sodium sulphate and filtered. Evaporation in *vacuo* of the organics gave **10** as a white solid (59 mg, 39% yield), mp 101-102 °C. IR (ATR)  $\nu$ : 613, 642, 671, 714, 763, 797, 831, 890, 920, 953, 1000, 1037, 1074, 1100, 1146, 1204, 1217, 1255, 1302, 1319, 1338, 1374, 1445, 1540, 1662, 2850, 2918, 3316 cm<sup>-1</sup>. <sup>1</sup>H-NMR (400 MHz, CDCl<sub>3</sub>)  $\delta$ : 1.12 (s, 3 H, C3'-CH<sub>3</sub>), 1.15-1.29 [c. s., 3 H, 3(5)-H<sub>ax</sub> and 4-H<sub>ax</sub>], 1.38 [m, 2 H, 2(6)-H<sub>ax</sub>], 1.51 [dm,  $J$  = 12.4 Hz, 2 H, 4'(10')-H<sub>a</sub>], 1.60-1.88 [c. s., 11 H, 2(6)-H<sub>eq</sub>, 3(5)-H<sub>eq</sub>, 4-H<sub>eq</sub>, 6'-H<sub>2</sub>, 8'(9')-H<sub>a</sub>, 4'(10')-H<sub>b</sub>], 1.97 [tt,  $J$  = 11.6 Hz,  $J'$  = 3.6 Hz, 1 H, 1-H], 2.25 [m, 2 H, 5'(7')-H], 2.45 (dm,  $J$  = 12 Hz, 2 H, 8'(9')-H<sub>b</sub>), 5.54 (b. s., 1 H, NH). <sup>13</sup>C-NMR (100.5 MHz, CDCl<sub>3</sub>)  $\delta$ : 25.71 [CH<sub>2</sub>, C3(5)], 25.74 (CH<sub>2</sub>, C4), 28.6 [CH, C5'(7')], 29.1 (CH<sub>3</sub>, C3'-CH<sub>3</sub>), 29.6 [CH<sub>2</sub>, C2(6)], 33.6 (CH<sub>2</sub>, C6'), 39.0 [CH<sub>2</sub>, C8'(9')], 41.0 [CH<sub>2</sub>, C4'(10')], 46.2 (CH, C1), 73.2 (C, C3'), 83.4 (C, C1'), 174.4 (C, CO). Calcd for C<sub>17</sub>H<sub>27</sub>NO: C 73.61, H 9.81, N 5.05. Found: C 73.45, H 10.01, N 5.15.

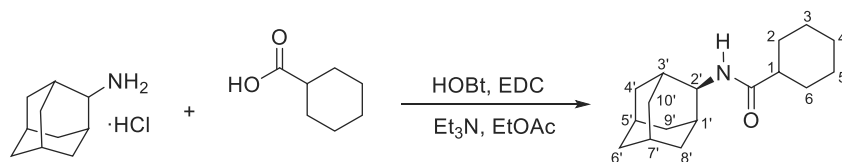
#### Obtention of *N*-(2-oxadamant-5-yl)cyclohexanecarboxamide (**11**)



A solution of cyclohexanecarbonyl chloride (87 mg, 0.59 mmol) in anhydrous acetone (0.5 mL) was added to a solution of the 2-oxadamantan-5-amine hydrochloride (86 mg, 0.49 mmol) and triethylamine in anhydrous acetone (0.5 mL). The reaction mixture was stirred at reflux for 3 hours. The residue was dissolved in DCM (5 mL) and 1N HCl solution (5 mL) and the phases were separated. The organic phase was washed with further 1N HCl solution (2 x 5 mL). The combined organic phases were dried, filtered and concentrated in *vacuo* to give RL-109 as a white solid (122 mg). Column chromatography (hexane/ethyl acetate mixture) gave **11** as a white solid (51 mg, 42% yield), mp 165-166 °C. IR (ATR)  $\nu$ : 675, 720, 733, 781, 803, 818, 847, 890, 924, 953, 972, 1002, 1015, 1073, 1106, 1144, 1190, 1217, 1249, 1273, 1315, 1347, 1357,

1438, 1548, 1639, 2847, 2899, 2933, 3073, 3267  $\text{cm}^{-1}$ .  $^1\text{H-NMR}$  (400 MHz,  $\text{CDCl}_3$ )  $\delta$ : 1.16-1.31 [c. s., 3 H, 3(5)- $\text{H}_{\text{ax}}$  and 4- $\text{H}_{\text{ax}}$ ], 1.39 [m, 2 H, 2(6)- $\text{H}_{\text{ax}}$ ], 1.59 [dm,  $J = 12.4$  Hz, 2 H, 8'(10')- $\text{H}_{\text{a}}$ ], 1.67 [m, 1 H, 4- $\text{H}_{\text{eq}}$ ], 1.74-1.86 [c. s., 4 H, 2(6)- $\text{H}_{\text{eq}}$ , 3(5)- $\text{H}_{\text{eq}}$ ], 1.90-2.03 [c. s., 3 H, 1-H, 8'(10')- $\text{H}_{\text{b}}$ ], 2.06 (c. s., 4 H, 4'(9')- $\text{H}_2$ ], 2.18-2.22 (c. s., 2 H, 6'- $\text{H}_2$ ), 2.23 (m, 1 H, 7'-H), 4.17 (m, 2 H, 1'(3')-H), 5.13 (b. s., 1 H, NH).  $^{13}\text{C-NMR}$  (100.5 MHz,  $\text{CDCl}_3$ )  $\delta$ : 25.7 [ $\text{CH}_2$ , C3(5), C4], 27.3 (CH, C7'), 29.7 [ $\text{CH}_2$ , C2(6)], 34.9 [ $\text{CH}_2$ , C8'(10')], 39.7 ( $\text{CH}_2$ , C6'), 40.7 [ $\text{CH}_2$ , C4'(9')], 46.2 (CH, C1), 50.2 (C, C5'), 69.2 [CH, C1'(3')], 175.6 (C, CO). Calcd for  $\text{C}_{16}\text{H}_{25}\text{NO}_2 \cdot 0.2 \text{H}_2\text{O}$ : C 71.98, H 9.59, N 5.25. Found: C 72.02, H 9.58, N 5.15.

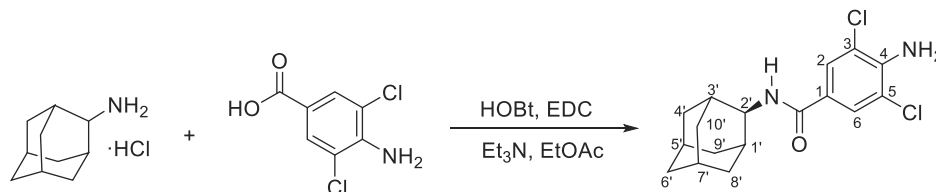
#### Obtention of *N*-(2-adamantyl)cyclohexanecarboxamide (**12**)



To a solution of 2-adamantanamine hydrochloride (207 mg, 1.1 mmol) in EtOAc (15 mL) were added cyclohexanecarboxylic acid (128 mg, 1 mmol), HOBt (203 mg, 1.5 mmol), EDC (232 mg, 1.5 mmol) and triethylamine (0.6 mL, 4.4 mmol). The reaction mixture was stirred at room temperature overnight. To the resulting suspension was then added water (15 mL) and the phases were separated. The organic phase was washed with saturated aqueous  $\text{NaHCO}_3$  solution (15 mL) and brine (15 mL). The aqueous phase was extracted with further EtOAc (2 x 15 mL) and the organics were dried over anhydrous sodium sulphate and filtered. Evaporation *in vacuo* of the organics gave **12** as a white solid (184 mg, 71% yield). The analytical sample was obtained by crystallization from DCM/diethyl ether, mp 201-202  $^\circ\text{C}$ . IR (ATR)  $\nu$ : 659, 919, 979, 993, 1030, 1195, 1218, 1248, 1367, 1441, 1536, 1609, 1641, 2365, 2844, 2923, 3415  $\text{cm}^{-1}$ .  $^1\text{H-NMR}$  (400 MHz,  $\text{CDCl}_3$ )  $\delta$ : 1.16-1.34 [c. s., 3 H, 3(5)- $\text{H}_{\text{ax}}$  and 4- $\text{H}_{\text{ax}}$ ], 1.42 [m, 2 H, 2(6)- $\text{H}_{\text{ax}}$ ], 1.60-1.94 [c. s., 18 H, 2(6)- $\text{H}_{\text{eq}}$ , 3(5)- $\text{H}_{\text{eq}}$ , 1'(3')-H, 4'(9')- $\text{H}_2$ , 5'(7')-H, 8'(10')- $\text{H}_2$ , 6'- $\text{H}_2$ ], 2.08 (tt,  $J = 11.6$  Hz,  $J' = 3.6$  Hz, 1 H, 1-H), 4.02 (m, 1 H, 2'-H), 5.75 (b. s., 1 H, NH).  $^{13}\text{C-NMR}$  (100.5 MHz,  $\text{CDCl}_3$ )  $\delta$ : 25.8 [ $\text{CH}_2$ , C3(5) and C4], 27.1 (CH, C5' or C7'), 27.2 (CH, C7' or C5'), 29.8 [ $\text{CH}_2$ , C2(6)], 31.8 [ $\text{CH}_2$ , C8'(10')],

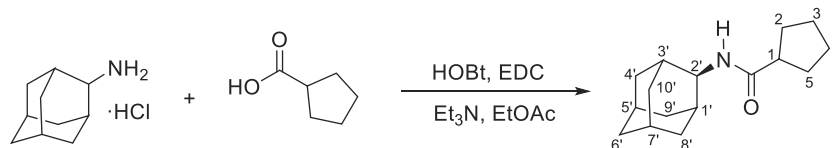
31.9 [CH, C1'(3')], 37.1 [CH<sub>2</sub>, C4'(9')], 37.5 (CH<sub>2</sub>, C6'), 45.8 (CH, C1), 52.7 (CH, C2'), 175.0 (C, CO). Calcd for C<sub>17</sub>H<sub>27</sub>NO: C 78.11, H 10.41, N 5.36. Found: C 78.23, H 10.52, N 5.30.

**Obtention of N-(2-adamantyl)-4-amino-3,5-dichlorobenzamide (13)**



To a solution of 2-adamantanamine hydrochloride (413 mg, 2.2 mmol) in EtOAc (20 mL) were added 4-amino-3,5-dichlorobenzoic acid (412 mg, 2 mmol), HOBT (405 mg, 3 mmol), EDC (464.6 mg, 3 mmol) and triethylamine (1.2 mL, 8.8 mmol). The reaction mixture was stirred at room temperature for 22 hours. To the resulting suspension was then added water (40 mL) and the phases were separated. The organic phase was washed with saturated aqueous NaHCO<sub>3</sub> solution (30 mL) and brine (30 mL), dried over anhydrous sodium sulphate and filtered. Evaporation *in vacuo* of the organics gave **13** as a white yellowish solid (686 mg, quantitative yield). The analytical sample was obtained by crystallization from hot EtOAc, mp 173-174 °C. IR (ATR)  $\nu$ : 632, 655, 718, 760, 789, 817, 845, 894, 905, 945, 982, 1019, 1056, 1078, 1102, 1224, 1279, 1300, 1341, 1358, 1375, 1470, 1481, 1531, 1606, 2848, 2903, 3298, 3391, 3490 cm<sup>-1</sup>. <sup>1</sup>H-NMR (400 MHz, CDCl<sub>3</sub>)  $\delta$ : 1.67-1.76 [m, 2 H, 8'(10')-H<sub>a</sub>], 1.77 (b. s., 2 H, 6'-H<sub>2</sub>), 1.81-1.94 [c. s., 8 H, 8'(10')-H<sub>b</sub>, 4'(9')-H<sub>2</sub>, 5'(7')-H], 2.01 [m, 2 H, 1'(3')-H], 4.20 (dm,  $J = 7.2$  Hz, 1 H, 2'-H), 4.74 (s, 2 H, NH<sub>2</sub>), 6.23 (d,  $J = 7.2$  Hz, 1 H, NH), 7.62 [s, 2 H, 2(6)-H<sub>Ar</sub>]. <sup>13</sup>C-NMR (100.5 MHz, CDCl<sub>3</sub>)  $\delta$ : 27.1 (CH, C5' or C7'), 27.2 (CH, C7' or C5'), 31.9 [CH, C1'(3')], 32.1 [CH<sub>2</sub>, C8'(10')], 37.1 [CH<sub>2</sub>, C4'(9')], 37.5 (CH<sub>2</sub>, C6'), 53.8 (CH, C2'), 118.9 [C, C3(5)], 125.0 (C, C1), 126.7 [CH, C2(6)], 142.6 (C, C4), 164.3 (C, CO). Calcd for C<sub>17</sub>H<sub>27</sub>NO: C 60.19, H 5.94, N 8.26. Found: C 60.25, H 6.11, N 8.26.

### Obtention of *N*-(2-adamantyl)cyclopentanecarboxamide (**14**)



To a solution of 2-adamantanamine hydrochloride (207 mg, 1.1 mmol) in EtOAc (10 mL) were added cyclopentanecarboxylic acid (0.11 mL, 1 mmol), HOBT (202.6 mg, 1.5 mmol), EDC (232 mg, 1.5 mmol) and triethylamine (0.6 mL, 4.4 mmol). The reaction mixture was stirred at room temperature for 22 hours. To the resulting suspension was then added water (20 mL) and the phases were separated. The organic phase was washed with saturated aqueous NaHCO<sub>3</sub> solution (15 mL) and brine (15 mL), dried over anhydrous sodium sulphate and filtered. Evaporation *in vacuo* of the organics gave **14** as a white solid (227 mg, 92% yield). The analytical sample was obtained by crystallization from hot EtOAc (180 mg), mp 203-204 °C. IR (ATR)  $\nu$ : 665, 797, 819, 862, 930, 963, 981, 1058, 1098, 1116, 1145, 1228, 1271, 1306, 1387, 1444, 1471, 1537, 1633, 2847, 2901, 3312 cm<sup>-1</sup>. <sup>1</sup>H-NMR (400 MHz, CDCl<sub>3</sub>)  $\delta$ : 1.54-1.60 [m, 2 H, 3(4)-H<sub>a</sub>], 1.61-1.87 [c. s., 18 H, 4'(9')-H<sub>2</sub>, 8'(10')-H<sub>2</sub>, 2(5)-H<sub>2</sub>, 5'-H, 7'-H, 6'-H<sub>2</sub>, 3(4)-H<sub>b</sub>], 1.90 [m, 2 H, 1'(3')-H], 2.53 (m, 1 H, 1-H), 4.04 (m, 1 H, 2'-H), 5.74 (b. s., 1 H, NH). <sup>13</sup>C-NMR (100.5 MHz, CDCl<sub>3</sub>)  $\delta$ : 25.9 [CH<sub>2</sub>, C3(4)], 27.1 (CH, C5' or C7'), 27.2 (CH, C7' or C5'), 30.5 [CH<sub>2</sub>, C2(5)], 31.9 [CH, C1'(3')], 32.0 [CH<sub>2</sub>, C8'(10')], 37.1 [CH<sub>2</sub>, C4'(9')], 37.5 (CH<sub>2</sub>, C6'), 46.2 (CH, C1), 52.9 (CH, C2'), 175.2 (C, CO). Calcd for C<sub>16</sub>H<sub>25</sub>NO·0.1 H<sub>2</sub>O: C 77.12, H 10.19, N 5.62. Found: C 77.05, H 10.16, N 5.52.

### **Determination of the 11 $\beta$ -HSD1 inhibition**

11 $\beta$ -HSD1 activity was determined in mixed sex, Human Liver Microsomes (Celsis In-vitro Technologies) by measuring the conversion of <sup>3</sup>H-cortisone to <sup>3</sup>H-cortisol. Percentage inhibition was determined relative to a no inhibitor control. 5 $\mu$ g of Human Liver microsomes was pre-incubated at 37°C for 15 minutes with inhibitor and 1mM NADPH in a final volume of 90 $\mu$ l Krebs buffer. 10 $\mu$ l of 200nM <sup>3</sup>H-cortisone was then added followed by incubation for at 37°C for a further 30 minutes. The assay was terminated by rapid freezing on dry ice and <sup>3</sup>H-cortisone to <sup>3</sup>H-cortisol conversion determined in 50 $\mu$ l of the defrosted reaction by capturing liberated <sup>3</sup>H-cortisol on anti-cortisol (HyTest Ltd)-coated scintillation proximity assay beads (protein A-coated YSi, GE Healthcare).

## **Computational methods**

### **Docking**

Taking advantage of the X-ray structures of the murine 11 $\beta$ -HSD1 (PDB ID 3LZ6)<sup>1</sup>, and the human enzyme (PDB IDs 4BB6<sup>2</sup> and 4BB5<sup>2</sup>) in complex with the known inhibitors PF-877423, HD1 and HD2, docking experiments were run to find the most appropriate orientation of compounds **5**, **6** and **12** in the binding site of human 11 $\beta$ -HSD1. The structures of the three complexes were used to restrict the position of the adamantyl amide group, and the protein coordinates were taken from X-ray structure 4BB6. NADP was also included in the docking experiment as it forms part of the binding site.

Glide<sup>3</sup> with the SP scoring function was used to perform the docking assays. Each molecule was energy minimized previously and the centroid of HD1 was used to generate the docking cavity by selecting all the residues located within 15 Å from the ligand. 100 poses were generated for each ligand and the best scored fulfilling the adamantyl amide group position requirement was selected.

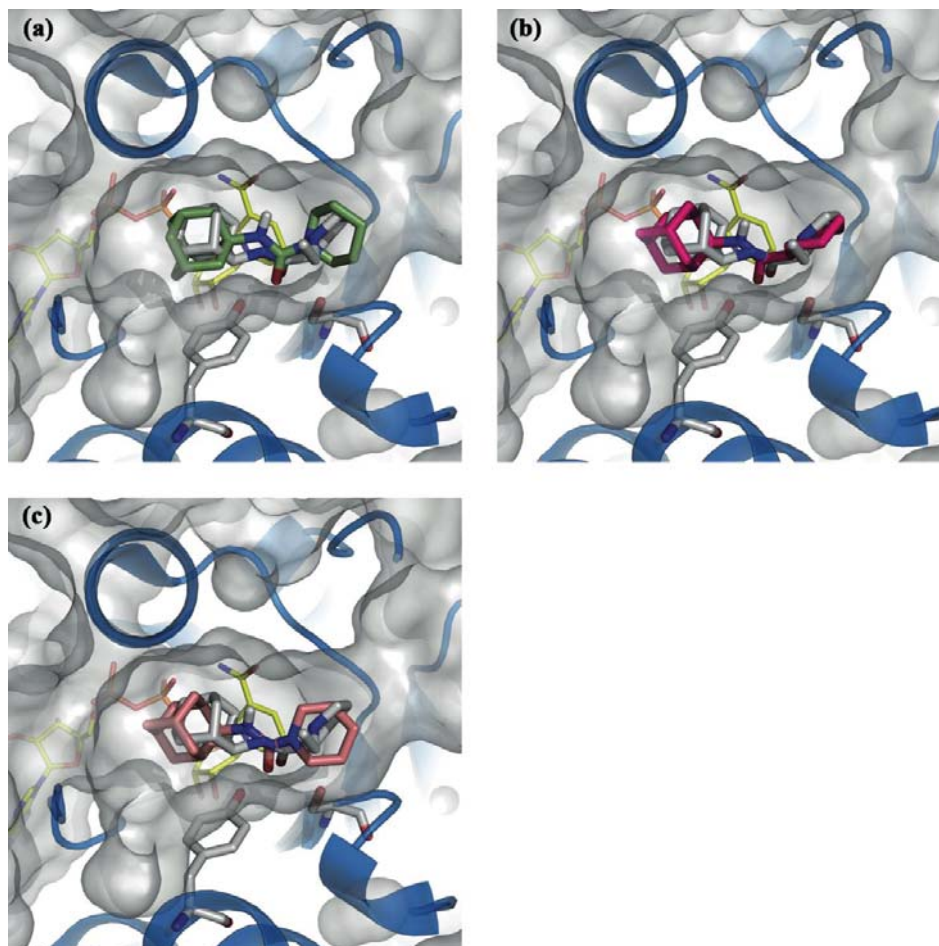
### **Molecular Dynamics**

For each compound (**5**, **6**, **12** and PF-877423) three independent 50 ns molecular dynamic simulations were run starting from the ligand-enzyme generated from docking calculations. Every complex was immersed in an octahedral box of TIP3P<sup>4</sup> water molecules and sodium ions were added to neutralize the system. The box size was selected so that 12 Å was the minimum distance between any atom of the protein and the box limits. The force field *ff99SBildn*<sup>5,6</sup> was used for the protein parameters and RESP charges at the HF/6-31G(d) level and the *gaff*<sup>7</sup> force field were used to build the ligand and NADP parameters.

The system was energy minimized following a three-step protocol. First, the hydrogens of the protein, the ligand and the cofactor were minimized. Second, the orientation of water molecules was optimized. Finally, a global minimization

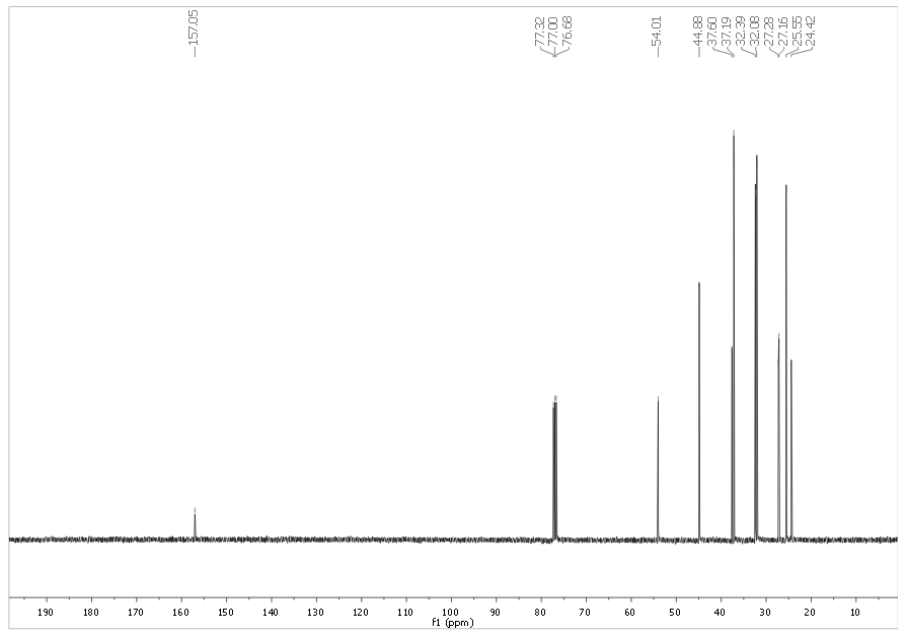
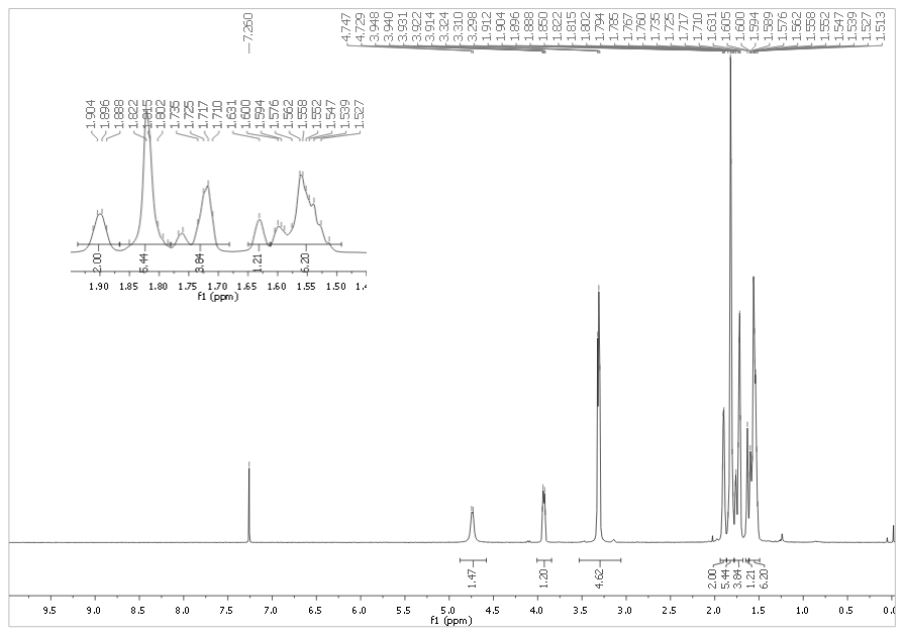
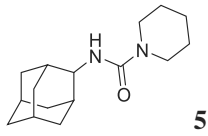
was run in which all the atoms were let free to move. At this point, the system was thermalized to 300K in 4 steps of 50 ps each from an initial temperature of 100K. The last snapshot from the thermalization procedure was used as starting point for the molecular dynamic simulations that were run in the NVT ensemble using a 2 fs timestep, periodic boundary conditions and keeping frozen all the bonds implicating hydrogen atoms using SHAKE.<sup>8</sup>

1. Cheng, H.; Hoffman, J.; Le, P.; Nair, S.K.; Cripps, S.; Matthews, J.; Smith, C.; Yang, M.; Kupchinsky, S.; Dress, K.; Edwards, M.; Cole, B.; Walters, E.; Loh, C.; Ermolieff, J.; Fanjul, A.; Bhat, G.B.; Herrera, J.; Pauly, T.; Hosea, N.; Paderes, G.; Rejto, P. *Bioorg. Med. Chem. Lett.* **2010**, *20*, 2897.
2. Goldberg, F.W.; Leach, A.G.; Scott, J.S.; Snelson, W.L.; Groombridge, S.D.; Donald, C.S.; Bennett, S.N.L.; Bodin, C.; Morentin Gutierrez, P.; Gyte, A.C. *J. Med. Chem.* **2012**, *55*, 10652.
3. Friesner, R. A.; Banks, J. L.; Murphy, R. B.; Halgren, T. A.; Klicic, J. J.; Mainz, D. T.; Repasky, M. P.; Knoll, E. H.; Shaw, D. E.; Shelley, M.; Perry, J. K.; Francis, P.; Shenkin, P. S., *J. Med. Chem.*, **2004**, *47*, 1739
4. Jorgensen, W. L.; Chandrasekhar, J.; Madura, J. D.; Impey, R. W.; Klein, M. L. *J. Chem. Phys.*, **1983**, *79*, 926.
5. Hornak, V.; Abel, R.; Okur, A.; Strockbine, B.; Roitberg, A.; Simmerling, C. *Proteins* **2006**, *65*, 712.
6. Lindorff-Larsen, K.; Piana, S.; palmo, K.; Maragakis, P.; Klepeis, J. L.; Dror, R. O.; Shaw, D. E. *Proteins* **2010**, *78*, 1950.
7. Wang, J.; Wolf, R. M.; Caldwell, J. W.; Kollman, P. A.; Case, D. A. *J. Comp. Chem.*, **2004**, *25*, 1157
8. Ryckaert, J.-P.; Ciccotti, G.; Berendsen, H.J.C. *J. Comput. Phys.*, **1977**, *23*, 327.

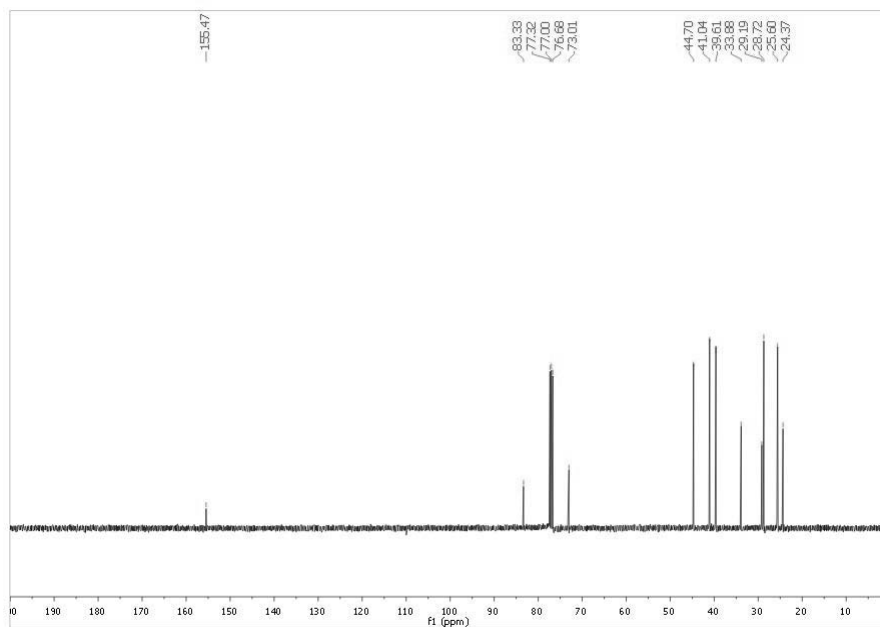
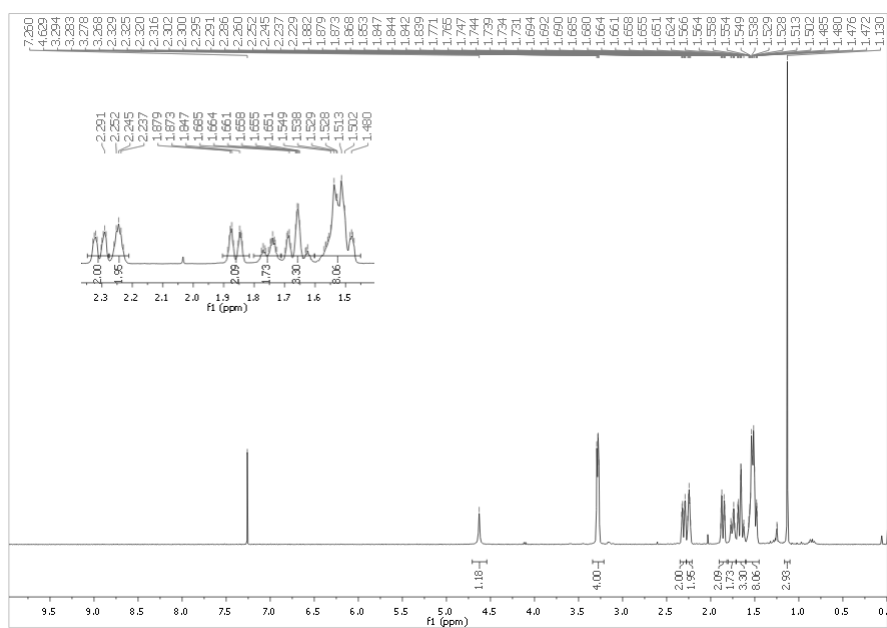
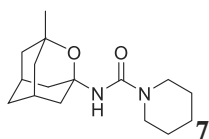


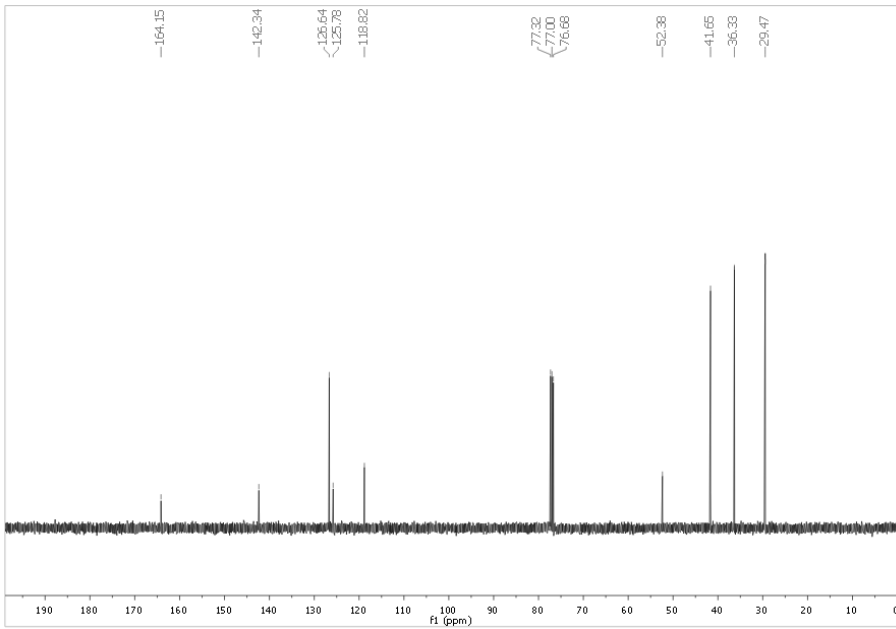
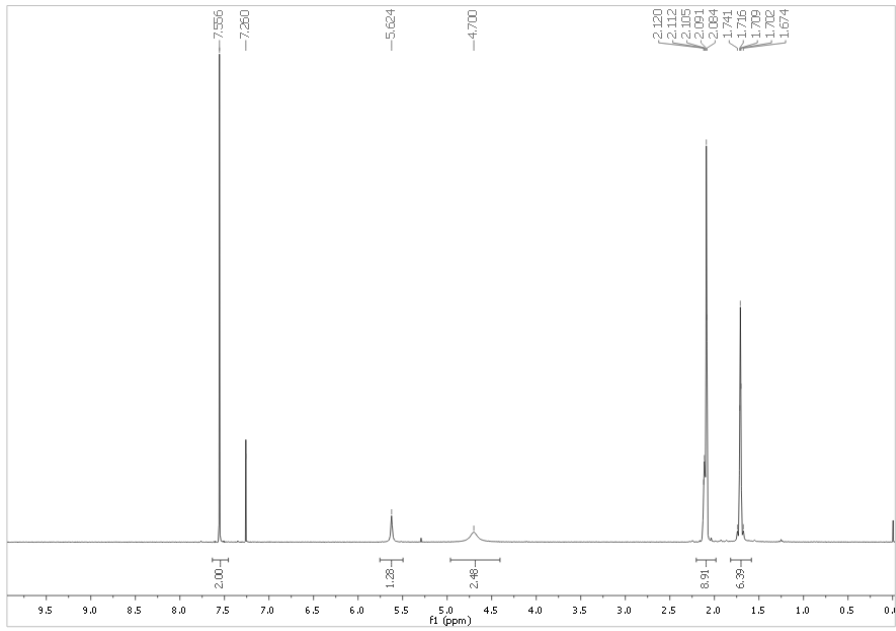
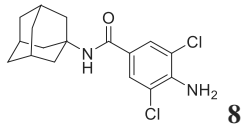
**Figure S1.** Best scoring complexes generated by docking for compounds **6** (a), **12** (b) and **5** (c) superposed to the crystallographic structure with PDB ID 3LZ6 containing the inhibitor PF-877423. The key residues Ser170 and Tyr183, NADP, PF-877423 and compounds **5**, **6** and **12** are shown as sticks. NADP carbons are colored in yellow, PF-877423 and the aminoacids carbons are colored in white. The secondary structure of the protein in the binding site region is shown as blue cartoon and the surface of the protein as transparent white contour.

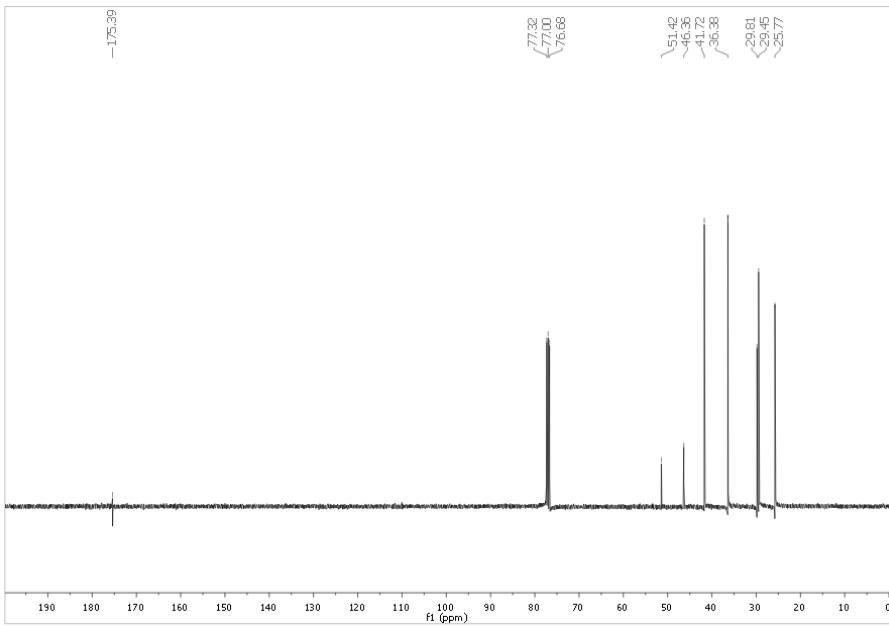
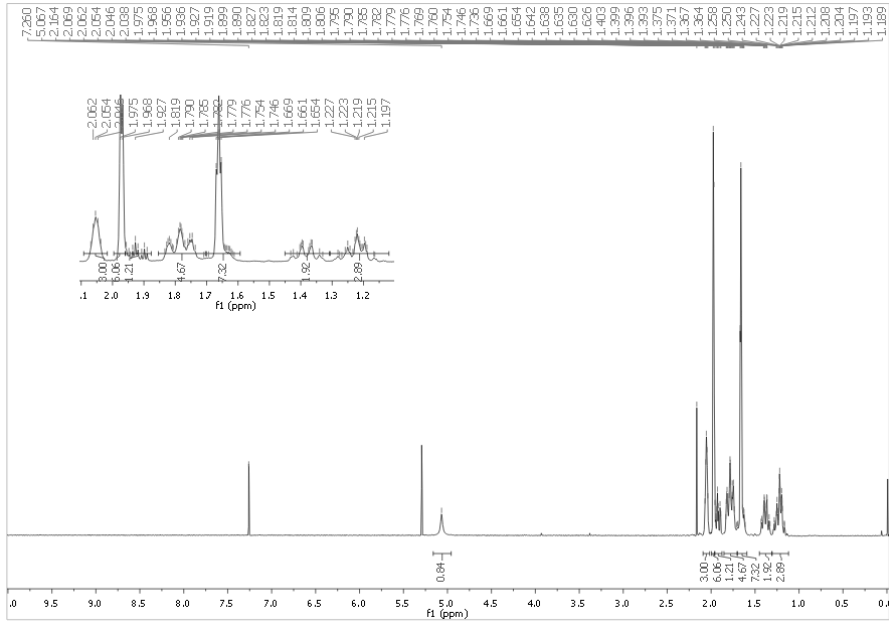
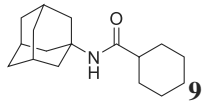


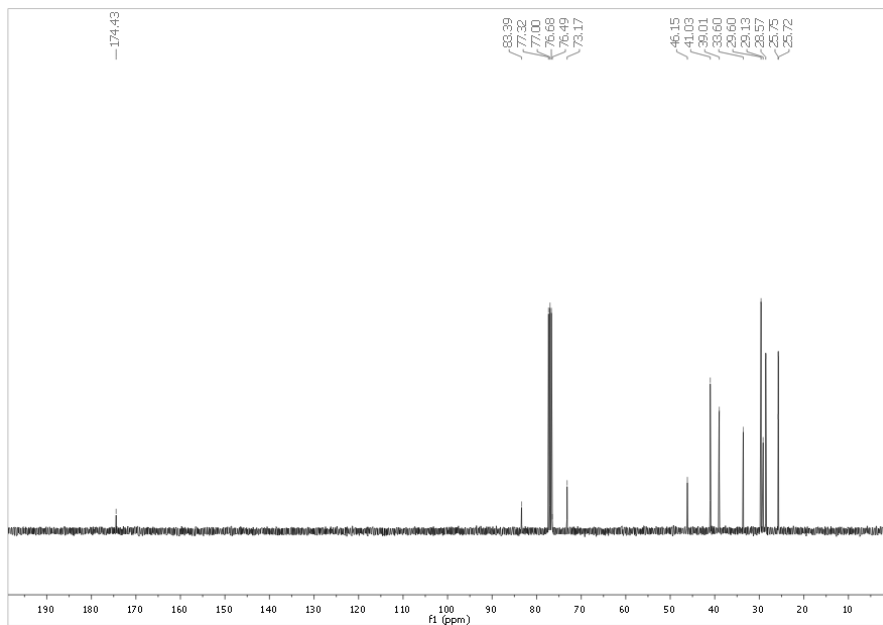
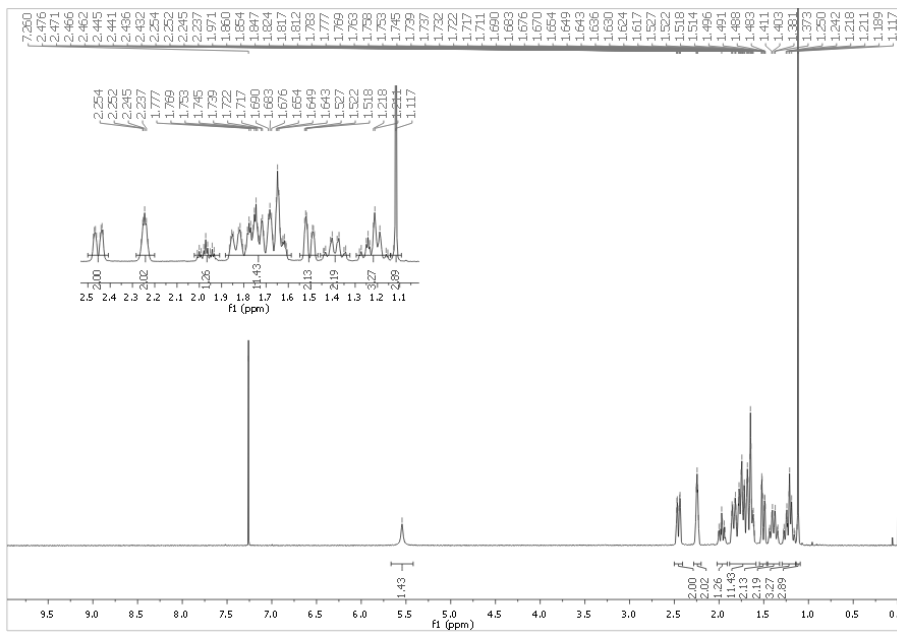
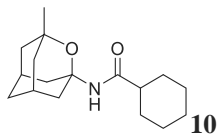




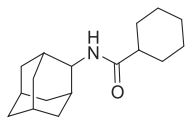




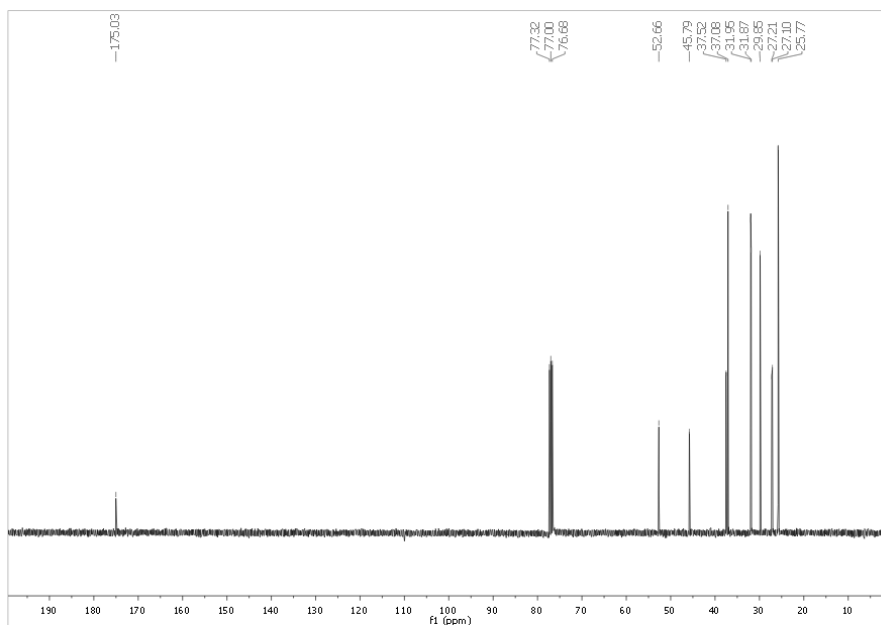
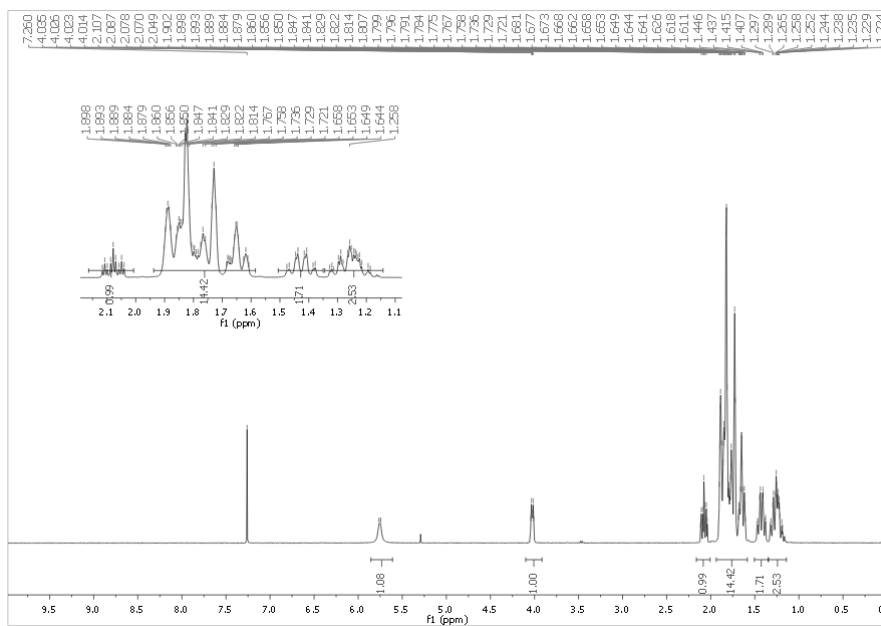




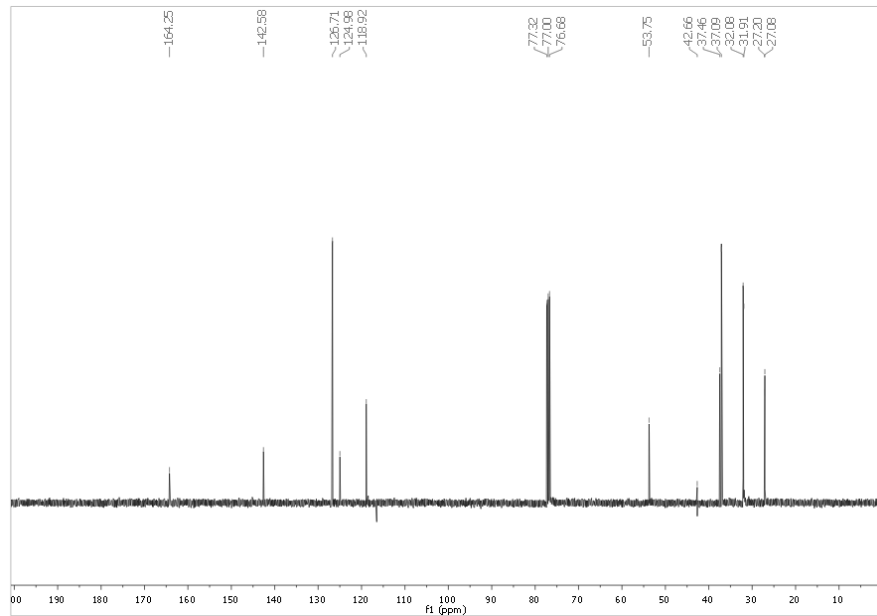
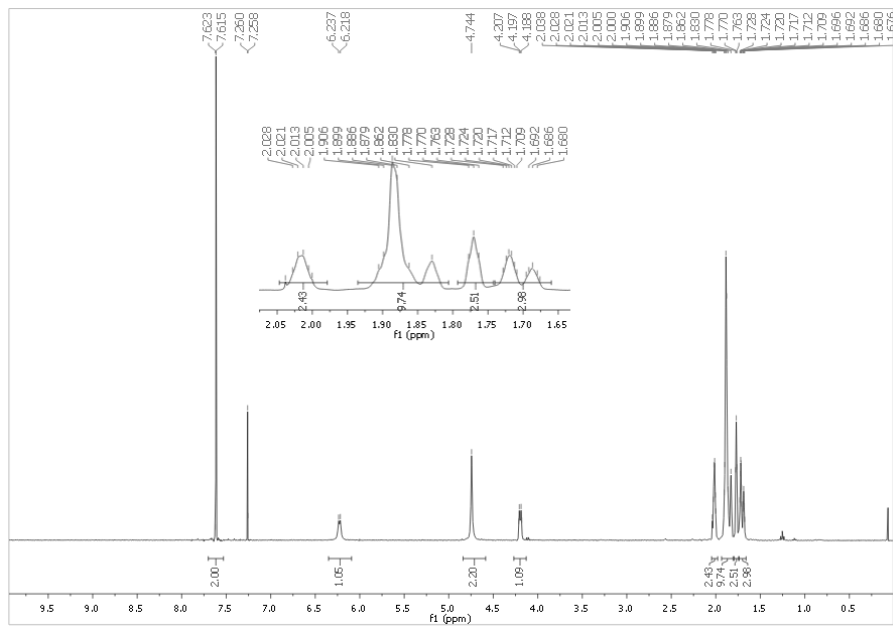
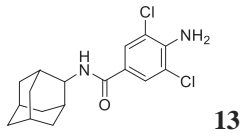


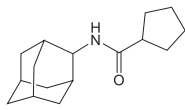


12

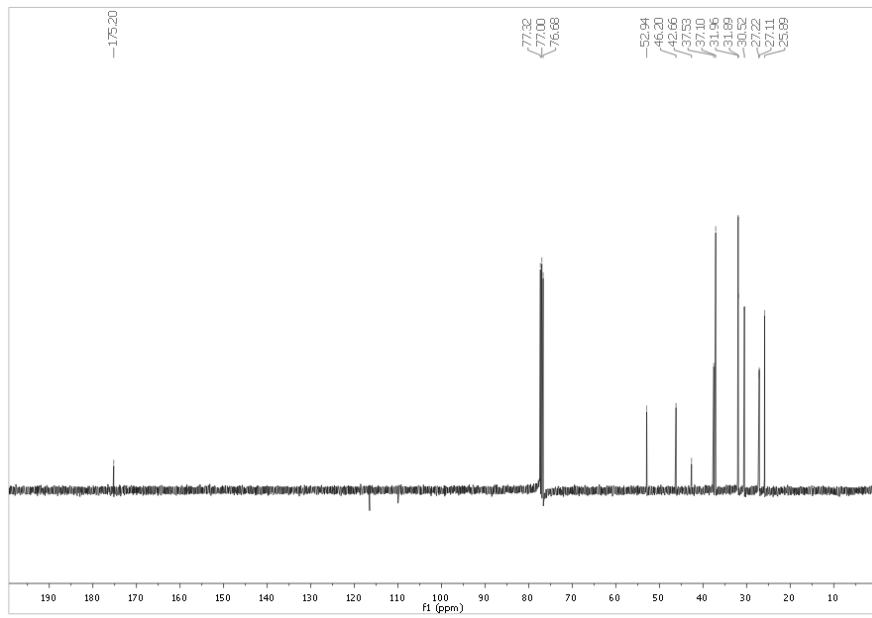
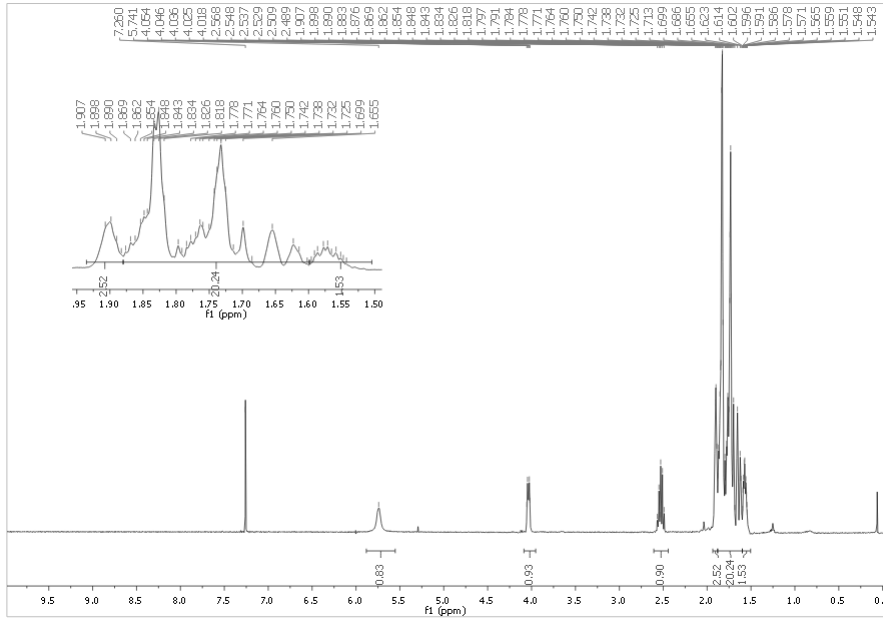








14





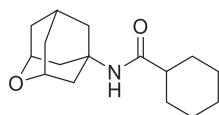
## CHAPTER 5

# **Polycycle optimization in 11 $\beta$ -HSD1 inhibitors. Evaluation of unexplored pyrrolidine-based polycyclic hydrocarbons**



### 5.1 Rationale and previous work

In the present chapter, the main goal of this Thesis is addressed as previously mentioned in the Objectives section. After the disappointing results of the new oxapolycycle whose synthesis is detailed in the Chapter 3 and its use in compound **27** in the fourth chapter (Figure 9), a polycyclic substituent optimization process supported by molecular modeling studies was implemented in order to improve the filling of the hydrophobic pocket in the binding site.



**27**  
hHSD1 (10  $\mu$ M) = 9% inh

**Figure 9.** Compound described in Chapter 4 featuring the 2-oxadaman-5-amine and its 11 $\beta$ -HSD1 inhibitory activity.<sup>218</sup>

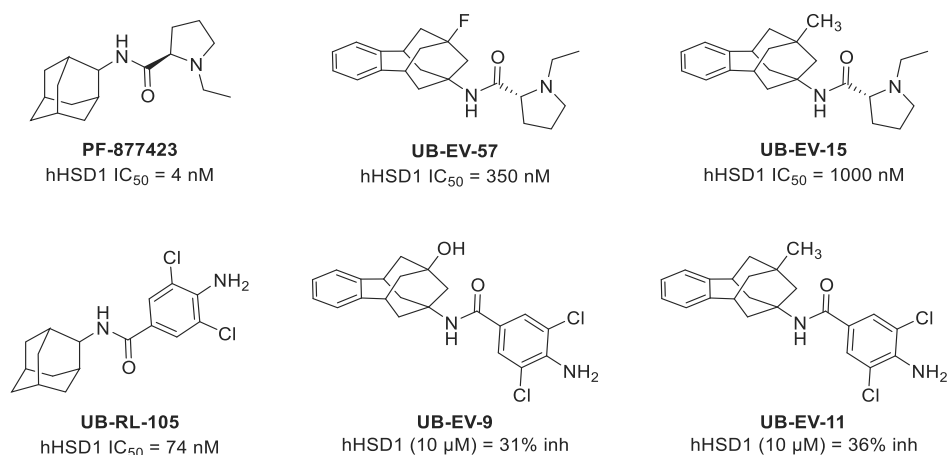
As noted in the final section of the Introduction chapter, a previous attempt in substituting the adamantyl moiety of numerous 11 $\beta$ -HSD1 inhibitors by one of *our* polycycles was conducted in the context of Dr Elena Valverde's PhD Thesis. The benzohomoadamantyl group succeed before in replacing the adamantyl scaffold in memantine delivering a potent NMDAR antagonist (see Table 2 in the Introduction chapter).<sup>198</sup> However, it did not deliver 11 $\beta$ -HSD1 inhibitors equal in potency when replaced the adamantyl moiety in a series of 11 $\beta$ -HSD1 inhibitors (Chart 5).<sup>201</sup>

<sup>218</sup> Leiva, R.; Seira, C.; McBride, A.; Binnie, M.; Bidon-Chanal, A.; Luque, F. J.; Webster, S. P.; Vázquez, S. *Bioorg. Med. Chem. Lett.* **2015**, *25*, 4250-4253.

<sup>198</sup> Valverde, E.; Sureda, F. X.; Vázquez, S. *Bioorg. Med. Chem.* **2014**, *22*, 2678-2683.

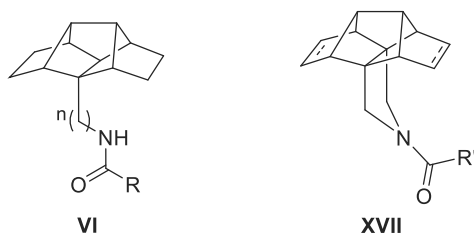
<sup>201</sup> Valverde, E.; Seira, C.; McBride, A.; Binnie, M.; Luque, F. J.; Webster, S. P.; Bidon-Chanal, A.; Vázquez, S. *Bioorg. Med. Chem.* **2015**, *23*, 7607-7617.

Polycyclic group optimization in 11 $\beta$ -HSD1 inhibitors and their pharmacological evaluation



**Chart 5.** Potent adamantyl-containing 11 $\beta$ -HSD1 inhibitors, **PF-877423** and **UB-RL-105**, and their analogs featuring the benzohomoadamantane moiety.<sup>219,218,201</sup>

Taking into account this previous work and the expertise of our group in multiple polycyclic groups, we envisioned further exploration of other cage structures detailed in this chapter. Our endeavour started with a series of compounds with the pentacyclic and hexacyclic amines contained in general structures **VI** and **XVII**, respectively.



**Chart 6.** General structures **VI** and **XVII** designed as putative 11 $\beta$ -HSD1 inhibitors.

R = cyclohexyl or piperidine. n = 0 or 1. R' = cyclohexyl, piperidine or 3,5-dichloro-4-aniline.

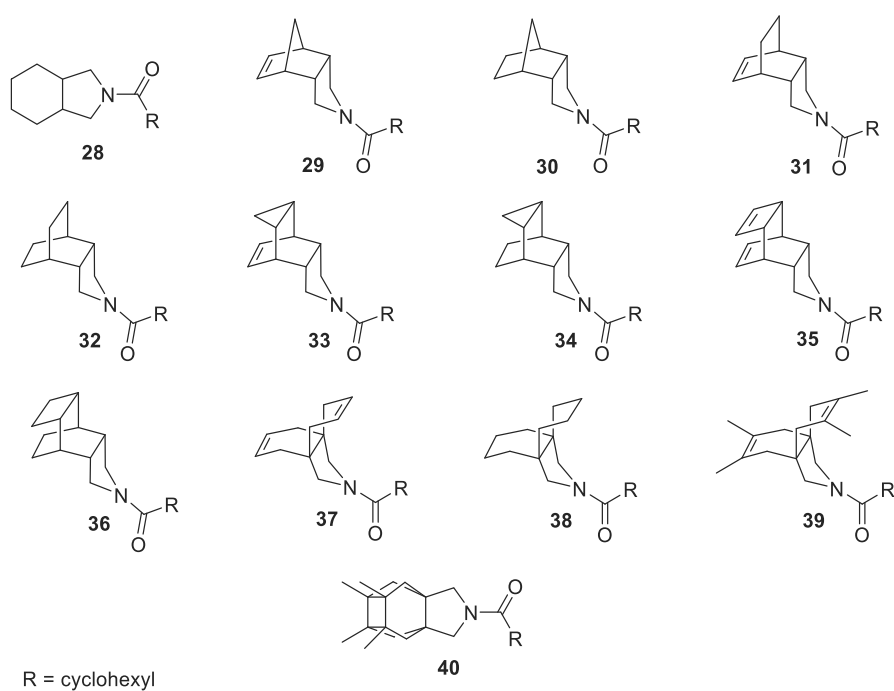
<sup>219</sup> Cheng, H.; Hoffman, J.; Le, P.; Nair, S. K.; Cripps, S.; Matthews, J.; Smith, C.; Yang, M.; Kupchinsky, S.; Dress, K.; Edwards, M.; Cole, B.; Walters, E.; Loh, C.; Ermolieff, J.; Fanjul, A.; Bhat, G. B.; Herrera, J.; Pauly, T.; Hosea, N.; Paderes, G.; Rejto, P. *Bioorg. Med. Chem. Lett.* **2010**, *20*, 2897-2902.

<sup>218</sup> Leiva, R.; Seira, C.; McBride, A.; Binnie, M.; Bidon-Chanal, A.; Luque, F. J.; Webster, S. P.; Vázquez, S. *Bioorg. Med. Chem. Lett.* **2015**, *25*, 4250-4253.

<sup>201</sup> Valverde, E.; Seira, C.; McBride, A.; Binnie, M.; Luque, F. J.; Webster, S. P.; Bidon-Chanal, A.; Vázquez, S. *Bioorg. Med. Chem.* **2015**, *23*, 7607-7617.

The pharmacological evaluation of the new compounds revealed that those of general structure **XVII** were more potent than their analogs of structure **VI** (see the following manuscript for further details). It seemed that the pyrrolidine ring is a favoured motif, likely reducing the contribution of the conformational penalty to the binding affinity of compounds containing it compared to the more flexible ones. Worthy of note is that this *N*-acylpyrrolidine motif fused to a polycycle has been barely explored in the design of 11 $\beta$ -HSD1 inhibitors.

In order to further improve the inhibitory potency of the previous compounds and to explore this peculiar motif, we envisage the preparation of an array of the following pyrrolidine-based polycyclic amides (Chart 7).



**Chart 7.** Designed pyrrolidine-based polycyclic amides as improved 11 $\beta$ -HSD1 inhibitors.



## 5.2 Theoretical discussion

Compounds featuring the general structure **VI** as well as all the compounds depicted in Chart 7 were prepared in the context of the present Thesis. Compounds of general structure **XVII** were prepared by Dr Elena Valverde in the context of her PhD Thesis.<sup>220</sup>

Here below the syntheses of the polycyclic amine precursors are detailed, with the exemption of the amine precursors of compounds **35** and **36** that were prepared in the context of Dr Marta Barniol-Xicota's PhD Thesis.<sup>221,197</sup>

To access the pentacyclo[6.4.0.0<sup>2,10</sup>.0<sup>3,7</sup>.0<sup>4,9</sup>]dodecane structure, a synthetic route previously conducted in the group was followed.<sup>222</sup> The synthetic pathway started with an elegant domino Diels-Alder reaction between 9,10-dihydrofulvalene and dimethyl acetylenedicarboxylate. Previously, freshly distilled cyclopentadiene was deprotonated by sodium hydride, whose anion **41** self-coupled through a low-temperature iodine-promoted oxidation, to generate *in situ* the 9,10-dihydrofulvalene **42**, which underwent double Diels-Alder reaction with the dimethyl acetylenedicarboxylate, yielding to a mixture of monoadducts **43** and **44**, and diadducts **45** and **46** (Scheme 8). This procedure was simultaneously described by Hedaya's and Paquette's research groups in 1974<sup>223,224</sup> and optimized later on by Paquette<sup>225</sup> (Scheme 8).

Taking advantage of the solubility properties of the products, **43** and **44** were isolated by precipitation the side-products **45** and **46** with diethyl ether. Hence, a simple filtration allowed the removal of the undesired diadducts. This procedure was scaled-up to 40 g of final mixture.

---

<sup>220</sup> Elena Valverde, PhD Thesis, Universitat de Barcelona 2015.

<sup>221</sup> Marta Barniol-Xicota, PhD Thesis, Universitat de Barcelona 2017.

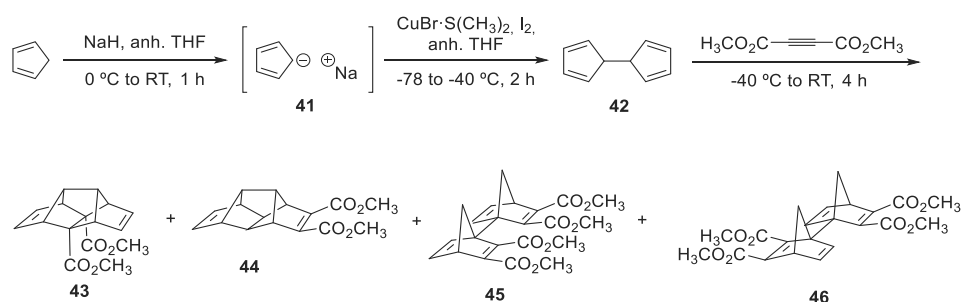
<sup>197</sup> Rey-Carrizo, M.; Barniol-Xicota, M.; Ma, C.; Frigolé-Vivas, M.; Torres, E.; Naesens, L.; Llabrés, S.; Juárez-Jiménez, J.; Luque, F. J.; DeGrado, W. F.; Lamb, R. A.; Pinto, L. H.; Vázquez, S. *J. Med. Chem.* **2014**, *57*, 5738–5747.

<sup>222</sup> Duque, M. D.; Ma, C.; Torres, E.; Wang, J.; Naesens, L.; Juárez-Jiménez, J.; Camps, P.; Luque, F. J.; DeGrado, W. F.; Lamb, R. A.; Pinto, L. H.; Vázquez, S. *J. Med. Chem.* **2011**, *54*, 2646–2657.

<sup>223</sup> Paquette, L. A.; Wyvratt, M. J. *J. Am. Chem. Soc.* **1974**, *96*, 4671-4673.

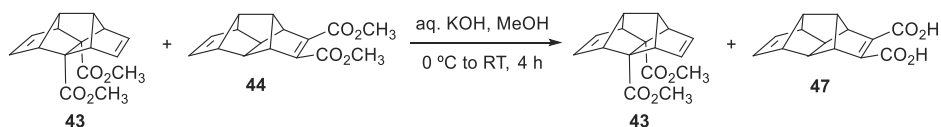
<sup>224</sup> McNeil, D.; Vogt, B. R.; Sudol, J. J.; Theodoropoulos, S.; Hedaya, E. *J. Am. Chem. Soc.* **1974**, *96*, 4673-4674.

<sup>225</sup> Taylor, R. J.; Welter, M. W.; Paquette, L. A. *Org. Synth. Coll. VIII* **1993**, 298-302.



**Scheme 8.** Domino Diels-Alder reaction of *in situ* prepared 9,10-dihydrofulvalene, **42**, and dimethyl acetylenedicarboxylate.<sup>223,224,225</sup>

Separation of the monoadducts **43** and **44** was achieved by selective hydrolysis of the less sterically hindered diester **44** to afford diacid **47**, which was removed from the intact diester **43** in the aqueous work-up (Scheme 9). In this way, 28 g of the desired pentacyclic diester **43** were prepared in 10% overall yield.



**Scheme 9.** Selective hydrolysis of **44** over **43**.<sup>223-225</sup>

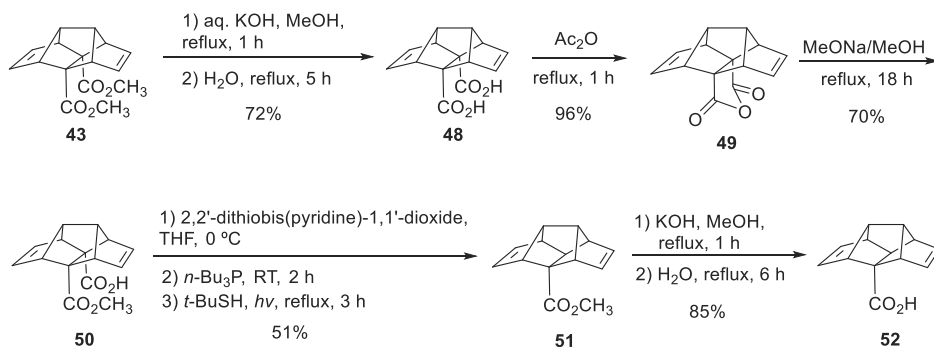
Pushing further the conditions, diester **43** was hydrolyzed providing its corresponding pentacyclic diacid **48**, which was subjected to dehydration leading the anhydride **49**.<sup>226</sup> This anhydride was then treated with sodium methoxide in anhydrous methanol to give the corresponding hemiester **50**.<sup>227</sup> Finally, **50** undergoes a Barton decarboxylation<sup>228,229</sup> to furnish the monoester **51** that via hydrolysis yields the monoacid **52** (Scheme 10).<sup>226</sup>

<sup>226</sup> Camps, P.; Pujol, X.; Rossi, R. A.; Vázquez, S. *Synthesis* **1999**, 854-858.

<sup>227</sup> Recently, our group has found that hemiester **50** can be obtained more easily just boiling anhydride **49** in methanol, without need of sodium methoxide neither anhydrous solvent.

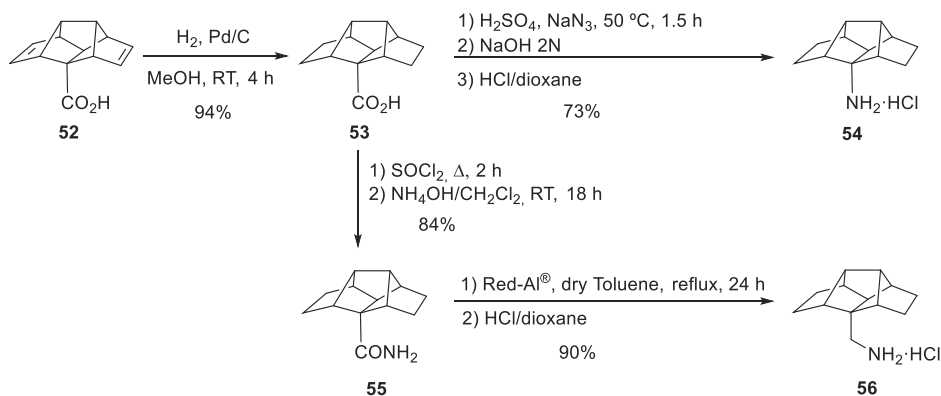
<sup>228</sup> Barton, D. H. R.; Crich, D.; Motherwell, W. B. *Tetrahedron*. **1985**, *41*, 3901-3924.

<sup>229</sup> Barton, D. H. R.; Samadi, M. *Tetrahedron* **1992**, *48*, 7083-7090.



**Scheme 10.** Preparation of monoacid **52** from pentacyclic diester **43**.<sup>223-226</sup>

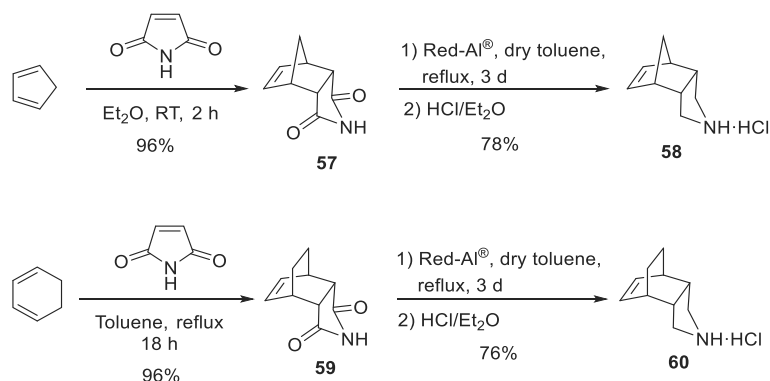
The monoacid **52** was then reduced applying a catalytic hydrogenation to yield its saturated analog **53**, the common precursor of both amines **54** and **56**.<sup>222</sup> The sooner was obtained through a Curtius rearrangement<sup>230</sup> on the *in situ* formed acyl azide; and the later was prepared following a two-step synthesis, starting with the formation of amide **55** and then its reduction with Red-Al® to deliver the amine **56** (Scheme 11).<sup>222</sup>



**Scheme 11.** Synthesis of amines **54** and **56** from the pentacyclic monoacid **52**.<sup>222</sup>

<sup>230</sup> Curtius, T. J. *Prakt. Chem.* **1894**, *50*, 275–294.

Tricyclic-based compounds **29-32** were prepared from their precursor amines **58** and **60**.<sup>231,232</sup> In the first case, imide **57** was prepared after Diels-Alder reaction between freshly distilled cyclopentadiene and maleimide, while the preparation of imide **59** involved cyclohexadiene and maleimide as well as dienophile. Afterwards, their reduction with Red-Al<sup>®</sup> gave the desired amines **58** and **60** (Scheme 12).



**Scheme 12.** Synthetic routes for the preparation of amines **58** and **60**.<sup>231,232</sup>

The synthesis of the tetracyclic amine precursors for the synthesis of **33-36** was previously described by our group, based on straightforward tandem electrocyclic/Diels-Alder reactions.<sup>197</sup>

For the preparation of amine **62**, the first step is a Diels-Alder reaction between norcaradiene, in turn obtained *in situ* by thermal electrocyclic ring closure of cycloheptatriene, and maleimide.<sup>233</sup> As expected, the *endo* product was obtained since there is a bonding interaction, stabilizing this isomer, between the carbonyl groups and the developing double bond at the back of norcaradiene. The synthetic route continued

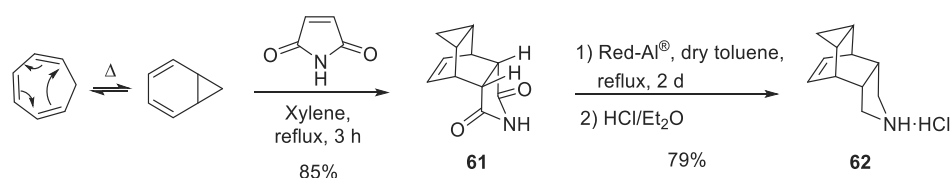
<sup>231</sup> Culberson, C. F.; Wilder Jr., P. J. *Org. Chem.* **1960**, *25*, 1358-1362.

<sup>232</sup> Fumimoto, M.; Okabe, K. *Chem. Pharm. Bull.* **1962**, *10*, 714-718.

<sup>197</sup> Rey-Carrizo, M.; Barniol-Xicotà, M.; Ma, C.; Frigolé-Vivas, M.; Torres, E.; Naesens, L.; Llabrés, S.; Juárez-Jiménez, J.; Luque, F. J.; DeGrado, W. F.; Lamb, R. A.; Pinto, L. H.; Vázquez, S. *J. Med. Chem.* **2014**, *57*, 5738-5747.

<sup>233</sup> Abou-Gharbia, M.; Patel, U. R.; Webb, M. B.; Moyer, J. A.; Andree, T. H.; Muth, E. A. *J. Med. Chem.* **1988**, *31*, 1382-1392.

with the reduction of the obtained imide **61** with Red-Al<sup>®</sup> to obtain the corresponding pyrrolidine derivative **62** (Scheme 13).<sup>197</sup>

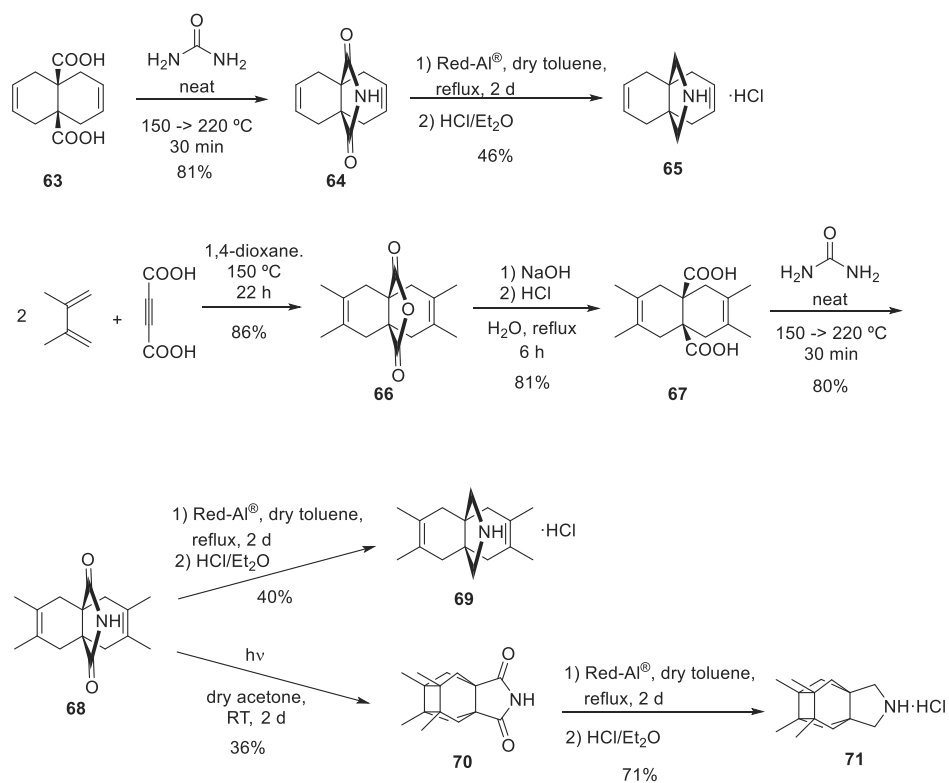


**Scheme 13.** Synthetic route for the preparation of amine **62**.<sup>233,197</sup>

Finally, for the synthesis of compounds **37-40**, two synthetic pathways were followed to access to their polycyclic amine precursors previously described by our group.<sup>197,234</sup> The bicyclic diacids, either the commercially available **63** or **67**, obtained from hydrolysis of the anhydride **66** prepared by a double Diels-Alder reaction, were subjected to imide cyclization with neat urea to afford imides **64** and **68** that were reduced with Red-Al<sup>®</sup> to get the corresponding amines **65** and **69**, respectively.<sup>197,234</sup>

Besides, the key step for the preparation of amine **71** was a [2+2] photocycloaddition. Imide **68** was submitted to UV radiation in order to form the cyclobutane derivative **70**. Then, a reduction procedure involving Red-Al<sup>®</sup> afforded the desired amine **71** (Scheme 14).<sup>197</sup>

<sup>234</sup> Torres, E.; Leiva, R.; Gazzarrini, S.; Rey-Carrizo, M.; Frigolé-Vivas, M.; Moroni, A.; Naesens, L.; Vázquez, S. *ACS Med. Chem. Lett.* **2014**, *5*, 831–836.

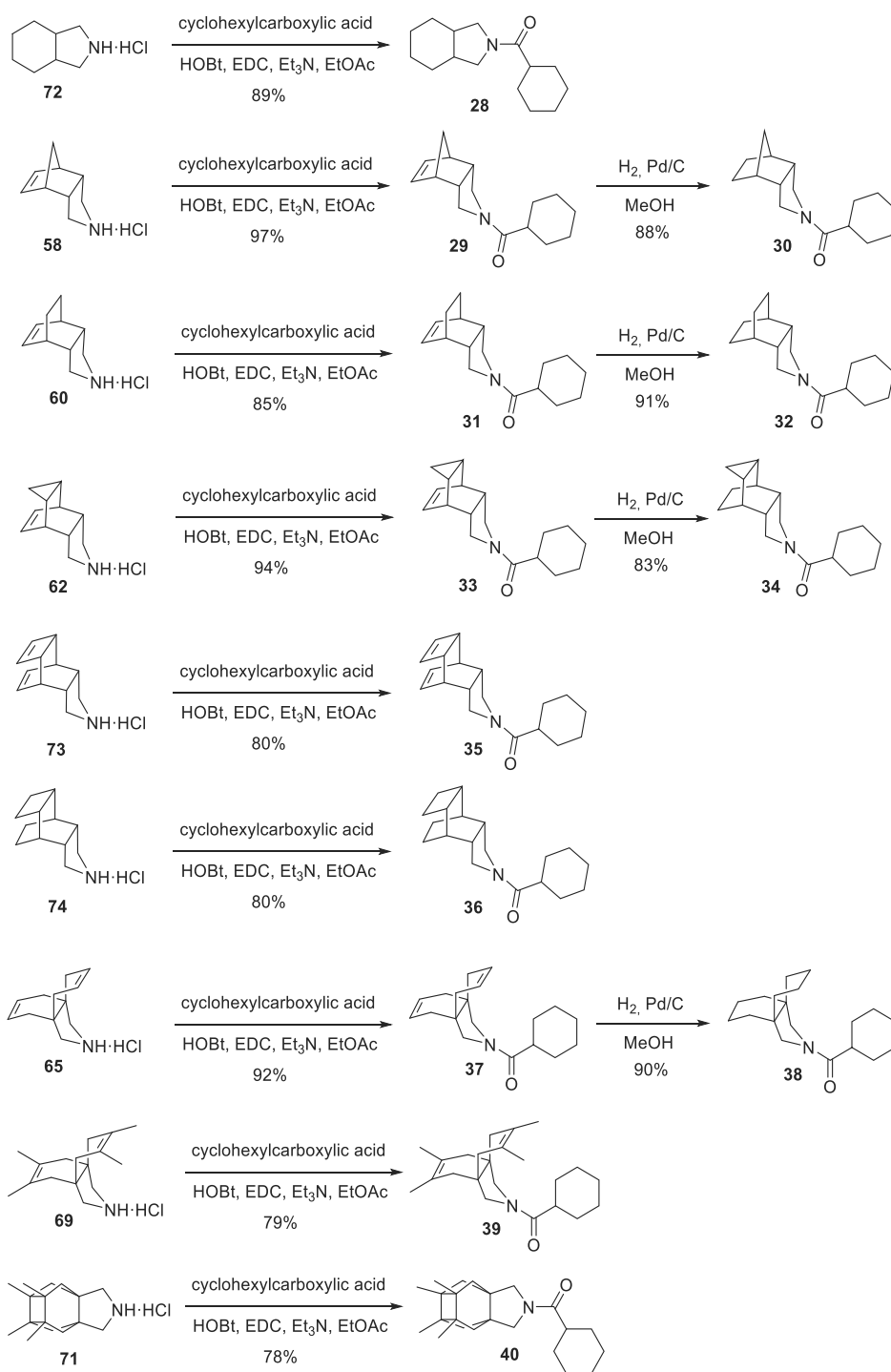


**Scheme 14.** Synthetic routes for the preparation of amines **65**, **69** and **71**.<sup>197,234</sup>

The preparation of the target amides is detailed in the following manuscript, as well as their pharmacological evaluation as 11 $\beta$ -HSD1 inhibitors.

Briefly, the synthesis of amides **28**, **29**, **31**, **33**, **35**, **36**, **37**, **39** and **40** involved a standard solution-phase peptide chemistry method employing 1-hydroxybenzotriazole (HOBt), water-soluble carbodiimide, EDC-HCl, and triethylamine. Then, the corresponding saturated analogs, **30**, **32**, **34** and **38**, were obtained by a reductive step using catalytic hydrogenation (Scheme 15).

Polycyclic group optimization in 11 $\beta$ -HSD1 inhibitors and their pharmacological evaluation



Scheme 15. Synthesis of amides 28-40.

Some of the compounds reported in the following manuscript along with those described in the next chapters 6 and 7 have been protected with a European patent application.<sup>235</sup> In such a way we have moved out of the current intellectual property protection for adamantyl-containing 11 $\beta$ -HSD1 inhibitors held by several of the big-pharma companies.<sup>236</sup>

In addition to the synthetic work, I also participated in the *in vitro* biological profiling of the compounds during my research stay in the BHF Centre for Cardiovascular Science of the Queen's Medical Research Institute (University of Edinburgh) under the supervision of our collaborator Dr Scott P. Webster. There, I learnt the basics of the pharmacological initial screening of the compounds and I conducted the activity evaluation in both human liver microsomes (HLM) and in transfected HEK293 cells, the selectivity over the isoform 11 $\beta$ -HSD2 in transfected HEK293 cells and the microsomal stability in HLM. The detailed procedures are described in the manuscript.

The *in vitro* characterization permitted us to select compound **34** to move forward to *in vivo* experiments. The Senescence-Accelerated Mouse Prone 8 (SAMP8) was used for the first time to investigate the effects of 11 $\beta$ -HSD1 pharmacological inhibition in this model of cognitive dysfunction.

The group of Prof. Mercè Pallàs (*Universitat de Barcelona*) with broad expertise in this model conducted two studies with the selected compound **34**, with one of those reported in the following manuscript. In this first analysis, behavioral tests were performed to assess cognitive changes, and biochemical assays of synaptic density, oxidative stress, inflammation and amyloid processing A $\beta$  clearance to shed light about the neuroprotective mechanism (if any) in the treated mice compared to control animals.

The second analysis, reported in a separated manuscript,<sup>237</sup> aimed to study the implications of the autophagy process in the neuroprotective effect observed in the

---

<sup>235</sup> Vázquez, S.; Leiva, R.; Valverde, E. PCT Patent Application, PCT/EP2017/059178, 2017.

<sup>236</sup> Boyle, C. D.; Kowalski, T. J. *Expert Opin. Ther. Patents* **2009**, *19*, 801-825.

<sup>237</sup> Puigoriol-Illamola, D.; Griñan-Ferre, C.; Vasilopoulou, F.; Leiva, R.; Vázquez, S.; Pallàs, M. Neuroprotective effect of RL-118, an 11 $\beta$ -HSD1 inhibitor: implication in autophagy and inflammaging processes in SAMP8 mouse model. *Neuropharmacology* (submitted).



previous work. The changes in behavior and cognition correlated with a decrease in mammalian target of rapamycin (mTOR) phosphorylation, without significant changes in phosphorylated AMP-activated protein kinase (pAMPK) activation, but an increase in *Beclin1* protein levels and changes in light chain 3 B (LC3B), indicating a progression in the autophagy process. In line with autophagy increase, a diminution in phosphorylated tau species (Ser396 and Ser404) jointly with an increase in the non-amyloidogenic pathway (a positive tendency in the  $\alpha$ -secretase *Adam10* and a significant increase in the secreted amyloid precursor protein- $\alpha$ , sAPP $\alpha$ ) indicated that an improvement in removing the abnormal proteins by autophagic process might be, in part, on the basis of the neuroprotective role of 11 $\beta$ -HSD1 inhibitor tested.

Additional *in vivo* studies in models of stress and cognitive dysfunction aggravated with metabolic disease are currently ongoing to study how 11 $\beta$ -HSD1 inhibition can modulate these linked disorders, as so-called type 3 diabetes in the second case.



## Research paper

Design, synthesis and *in vivo* study of novel pyrrolidine-based 11 $\beta$ -HSD1 inhibitors for age-related cognitive dysfunction

Rosana Leiva<sup>a</sup>, Christian Griñan-Ferré<sup>b</sup>, Constantí Seira<sup>c</sup>, Elena Valverde<sup>a</sup>, Andrew McBride<sup>d</sup>, Margaret Binnie<sup>d</sup>, Belén Pérez<sup>c</sup>, F. Javier Luque<sup>c</sup>, Mercè Pallàs<sup>b</sup>, Axel Bidon-Chanal<sup>c</sup>, Scott P. Webster<sup>d,\*</sup>, Santiago Vázquez<sup>a,\*\*</sup>

<sup>a</sup> *Laboratori de Química Farmacèutica (Unitat Associada al CSIC), Facultat de Farmàcia i Ciències de l'Alimentació, and Institute of Biomedicine (IBUB), Universitat de Barcelona, Av. Joan XXIII 27-31, Barcelona E-08028, Spain*

<sup>b</sup> *Unitat de Farmacologia, Farmacognòsia i Terapèutica, Facultat de Farmàcia i Ciències de l'Alimentació i Institut de Neurociències, Universitat de Barcelona, Av. Joan XXIII, 27-31, 08028 Barcelona, Spain*

<sup>c</sup> *Department of Nutrition, Food Science and Gastronomy, Faculty of Pharmacy and Institute of Biomedicine (IBUB), Universitat de Barcelona, Av. Prat de la Riba 171, Santa Coloma de Gramenet E-08921, Spain*

<sup>d</sup> *Centre for Cardiovascular Science, University of Edinburgh, Queen's Medical Research Institute, EH16 4TJ, United Kingdom*

<sup>e</sup> *Departament de Farmacologia, Terapèutica i Toxicologia, Universitat Autònoma de Barcelona, Bellaterra, Barcelona 08193, Spain*

## ARTICLE INFO

## Article history:

Received 25 June 2017

Received in revised form 30 July 2017

Accepted 2 August 2017

Available online xxx

## Keywords:

Glucocorticoids

11 $\beta$ -HSD1 inhibitors

Drug design

Adamantane

Polycyclic substituents

Aged-related cognitive dysfunction

Alzheimer's disease

SAMP8 mouse

## ABSTRACT

Recent findings suggest that treatment with 11 $\beta$ -HSD1 inhibitors provides a novel approach to deal with age-related cognitive dysfunctions, including Alzheimer's disease. In this work we report potent 11 $\beta$ -HSD1 inhibitors featuring unexplored pyrrolidine-based polycyclic substituents. A selected candidate administered to 12-month-old SAMP8 mice for four weeks prevented memory deficits and displayed a neuroprotective action. This is the first time that 11 $\beta$ -HSD1 inhibitors have been studied in this broadly-used mouse model of accelerated senescence and late-onset Alzheimer's disease.

© 2017.

## 1. Introduction

Elevated glucocorticoids (GCs) exposure is widely accepted as a key factor in age-related cognitive decline in rodents and humans [1–3]. High levels of GCs have been found in elderly individuals who exhibit learning and memory impairments. GC levels correlate with greater hippocampal atrophy, a region of the brain that is crucial for memory formation [3]. In contrast, low GC levels achieved through neonatal programming or adrenalectomy with exogenous steroid replacement in rats results in the prevention of memory impairments with aging [4].

Growing evidence also suggests that excessive glucocorticoid activity may contribute to Alzheimer's disease (AD), since elevated levels of circulating cortisol in AD patients are associated with more rapid disease progression [5,6]. In a rodent model of AD, systemic administration of GCs led to increases in  $\beta$ -amyloid and tau pathol-

ogy, the two major histopathologic hallmarks of AD, suggesting a relationship between elevated GC levels and AD pathology [7]. Overall, these data suggest that reducing GC levels in the brain may relieve cognitive dysfunction in both aging and AD.

As in other tissues, the presence of GCs in the brain is not only dependent on adrenal secretion and diffusion from the circulation but also on intracellular metabolism [8]. 11 $\beta$ -hydroxysteroid dehydrogenase type 1 (11 $\beta$ -HSD1) catalyzes the regeneration of active GCs (cortisol in humans, corticosterone in rodents) from their inactive forms (cortisone and 11-dehydrocorticosterone, respectively), providing a local amplification of GC action [9,10]. 11 $\beta$ -HSD1 is highly expressed in fundamental brain areas for cognition, such as the hippocampus, cortex and amygdala [11–13]. By contrast, the isoenzyme 11 $\beta$ -hydroxysteroid dehydrogenase type 2 (11 $\beta$ -HSD2), which catalyzes the opposite reaction, plays an important role during development, as expression of 11 $\beta$ -HSD2 is relevant in fetal brain and placenta, but it has very limited expression in the adult brain [14–16].

Recent studies have demonstrated that aged mice with cognitive deficits show increased 11 $\beta$ -HSD1 expression in the hippocampus and forebrain, and that overexpression of 11 $\beta$ -HSD1 leads to a similar premature memory decline [17]. Conversely, 11 $\beta$ -HSD1 knock-

\* Corresponding author.

\*\* Corresponding author.

Email addresses: scott.webster@ed.ac.uk (S.P. Webster); svazquez@ub.edu (S. Vázquez)

out mice and even heterozygous null mice performed better in different behavioural tests, which suggests resistance to cognitive decline due to a neuroprotective effect of 11 $\beta$ -HSD1 inhibition [18]. Accordingly, this protection correlates with loss of the age-associated rise in intrahippocampal corticosterone, insinuating a role for 11 $\beta$ -HSD1 in maintaining plasma corticosterone concentration [17]. Furthermore, acute and short-term treatments with 11 $\beta$ -HSD1 inhibitors have shown memory consolidation and improvements in cognitive function in aged mice and AD models [19–23]. Altogether, these findings suggest that 11 $\beta$ -HSD1 inhibitors provide a novel approach through a non-cholinergic mechanism to deal with these cognitive disorders.

In the present work, we report the results derived from a synthetic strategy, supported by molecular modeling studies, designed towards a novel family of potent 11 $\beta$ -HSD1 inhibitors, featuring unexplored pyrrolidine-based polycyclic substituents. The more potent compounds were characterized in terms of cellular potency, isoenzyme selectivity, human metabolic stability and predicted brain penetration to select a candidate for an *in vivo* study. For the first time in the context of 11 $\beta$ -HSD1 inhibitors, the Senescence Accelerated Mouse-Prone 8 (SAMP8) mice were used, as a naturally occurring mouse strain that displays a phenotype of accelerated aging as observed in AD and widely used as a robust rodent model of cognitive dysfunction [24,25].

## 2. Design, synthesis and *in vitro* evaluation of new inhibitors

Given that the 11 $\beta$ -HSD1 active site includes a hydrophobic pocket that can accommodate bulky lipophilic substituents, the introduction of a lipophilic group, such as adamantyl, has proven a successful strategy for the space filling of the cavity. Thus, several adamantyl-containing 11 $\beta$ -HSD1 inhibitors exhibit high affinity and potency and some of them (e.g. AZD8329 and ABT-384) have reached clinical trials (Fig. 1) [26–34]. Although the evaluation of alternative polycyclic hydrocarbons may offer further opportunities for optimizing the space filling of the hydrophobic cavity, the use of other polycyclic substituents featuring different size or shape has only been briefly scrutinized (e.g. AMG-221 and MK-0736) [35,36].

In the last few years, our research group has investigated new polycyclic substituents as surrogates of the adamantyl group, leading to inhibitors with promising results on multiple targets [37–45]. However, this strategy has not been successful yet in the case of human 11 $\beta$ -HSD1 inhibitors [46]. Very recently, we have found that the *N*-(2-adamantyl)amide derivatives **1** and **2** (Fig. 2), which are achiral analogues of PF-877423 (IC<sub>50</sub> = 4 nM) [47], are potent inhibitors of 11 $\beta$ -HSD1 (IC<sub>50</sub> = 86 and 74 nM, respectively) [48]. Interestingly, the corresponding urea analogue, **3**, was significantly less potent (IC<sub>50</sub> = 873 nM) [48]. Taking into account the simplicity of these three right-hand side (RHS) units, here we initially selected these

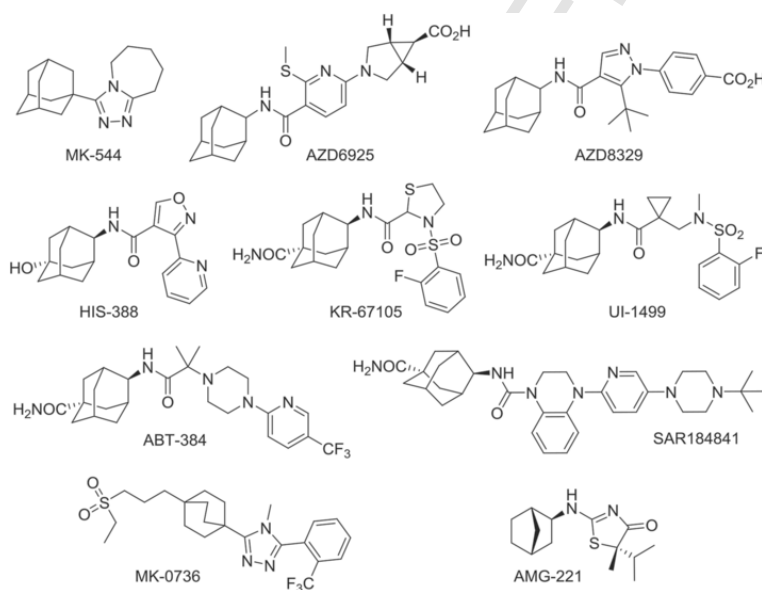


Fig. 1. Selected 11 $\beta$ -HSD1 inhibitors.

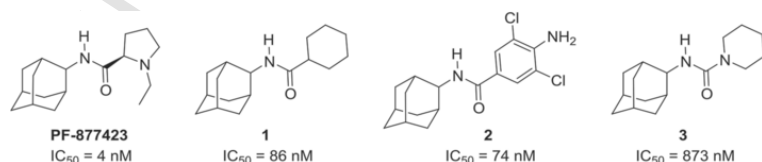


Fig. 2. PF-877423 and related inhibitors.

fragments for finding alternative polycyclic substituents able to successfully replace the adamantyl group in 11 $\beta$ -HSD1 inhibitors.

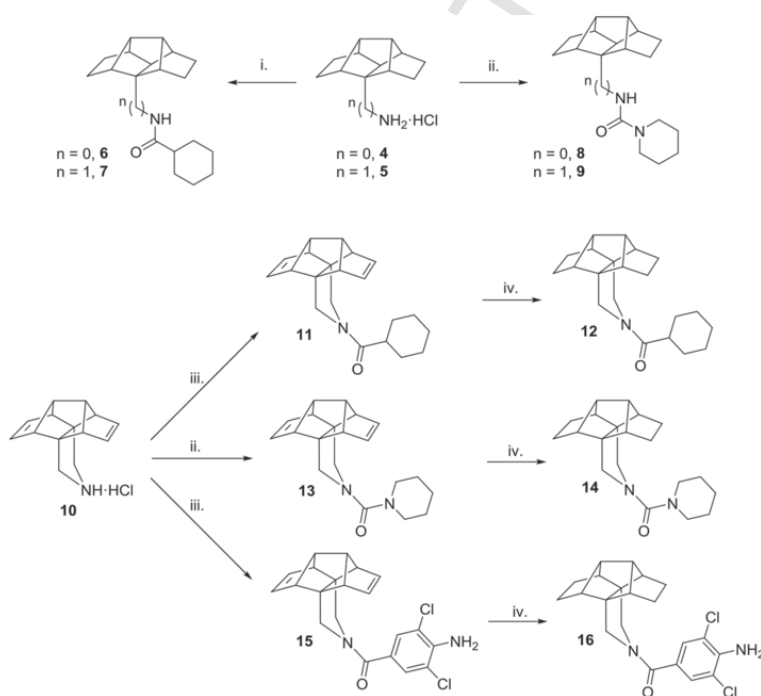
The design of new inhibitors was initially based on a structure-activity relationship (SAR) investigation we previously adopted [46]. The structure of the putative inhibitor was partitioned into two parts: the polycyclic substituent, a surrogate of adamantyl, and the carbocyclic or heterocyclic ring, linked by an amido or urea unit, respectively. Since inspection of the available X-ray structures and preliminary docking studies (see below) indicated that the enzyme active site is large enough to accommodate a polycycle bigger than adamantane, we started our endeavour with previously synthesized amines **4**, **5** and **10**, three compounds that were successfully used to replace 1-adamantylamine in other targets (Scheme 1) [38]. These amines were then combined with a common RHS moiety to shed light on the effect of key structural features on the inhibitory action: i) primary vs secondary amine (e.g. **4** vs **5**), ii) distance between the polycyclic ring and the nitrogen atom (e.g. **4** vs **5**), iii) restraint of the conformational freedom (e.g. **5** vs **10**), and iv) by incorporating two double bonds in the polycycle, which might form additional interactions in the binding site (e.g. derivatives of **10** vs its reduced analogues). Amides **6** and **7** were prepared in high yields by reaction of cyclohexane acyl chloride with amines **4** and **5**, respectively. From amine **10**, using either cyclohexanecarboxylic acid or 4-amino-3,5-dichlorobenzoic acid in combination with 1-hydroxybenzotriazole (HOBt) and *N*-(3-dimethylaminopropyl)-*N'*-ethylcarbodiimide (EDC) amides **11** and **15** were synthesized in moderate yields. Ureas **8**, **9** and **13** were prepared from the required amine and *N*-chloroformylpiperidine in moderate to excellent yields. Finally, catalytic

hydrogenation of **11**, **13** and **15** furnished **12**, **14** and **16**, respectively (Scheme 1).

A preliminary *in vitro* microsomal assay at 10  $\mu$ M compound concentration was performed to assess if the synthesized compounds were able to inhibit human 11 $\beta$ -HSD1, and the IC<sub>50</sub> values were determined for those compounds presenting an inhibition higher than 50% (Table 1).

The analysis of the inhibitory potencies disclosed some SAR. First, while amides **6** and **7** displayed poor inhibitory activity, derivatives **11** and **12**, featuring a pyrrolidine ring, showed low micromolar and sub-micromolar potency, respectively, reflecting a better fit within the hydrophobic pocket of the binding site. Second, replacement of the cyclohexyl ring of **12** by either a 1-piperidinyl substituent, as in **14**, or a 4-amino-3,5-dichlorophenyl group, as in **16**, retained the activity, further demonstrating that the adamantyl substituent may be replaced by other polycyclic groups. Third, no significant difference was found between the inhibitory activity of **12** and **14**, and hence the replacement of the amide bridge by a urea within this particular polycycle does not seem to affect the potency. Finally, saturated hexacyclic pyrrolidines were more potent than their diene analogues (compare **12** vs **11** and **16** vs **15**). Overall, aliphatic amides **11** and **12** were slightly more potent than aromatic amides **15** and **16** (compare **11** vs **15** and **12** vs **16**).

Docking studies were combined with molecular dynamics (MD) simulations to shed light into the inhibitory potencies of selected compounds. The structural integrity of the simulated systems was supported by the stability of the positional root-mean square deviation of the residues that define the binding site and the ligand, espe-



**Scheme 1. Amines **4**, **5** and **10**, and amides and ureas derived thereof.** Reagents and conditions: (i) cyclohexanecarbonyl chloride, anhydrous acetone, reflux, 3 h, 95% yield for **6**; 78% yield for **7**; (ii) 1-piperidinecarbonyl chloride, Et<sub>3</sub>N, DCM, rt, overnight, 54% yield for **8**; quant yield for **9**; 71% for **13**; (iii) cyclohexanecarboxylic acid for **11** or 4-amino-3,5-dichlorobenzoic acid for **15**, HOBt, EDC, Et<sub>3</sub>N, EtOAc, rt, overnight, 42% yield for **11**; 47% yield for **15**; (iv) H<sub>2</sub>, Pd/C, abs. EtOH, rt, 5 h for **12** and **16**, 3 h for **14**, 78% yield for **12**; 72% yield for **14**; 89% yield for **16**.

**Table 1**  
11 $\beta$ -HSD1 inhibition by compounds 6–9, 11, 12 and 14–16.<sup>a,b</sup>

Compound	hHSD1% inh at 10 $\mu$ M	hHSD1 IC <sub>50</sub> ( $\mu$ M)
6	41	ND
7	28	ND
8	50	ND
9	50	ND
11	95	1.08
12	100	0.29
14	100	0.32
15	98	2.77
16	98	0.41

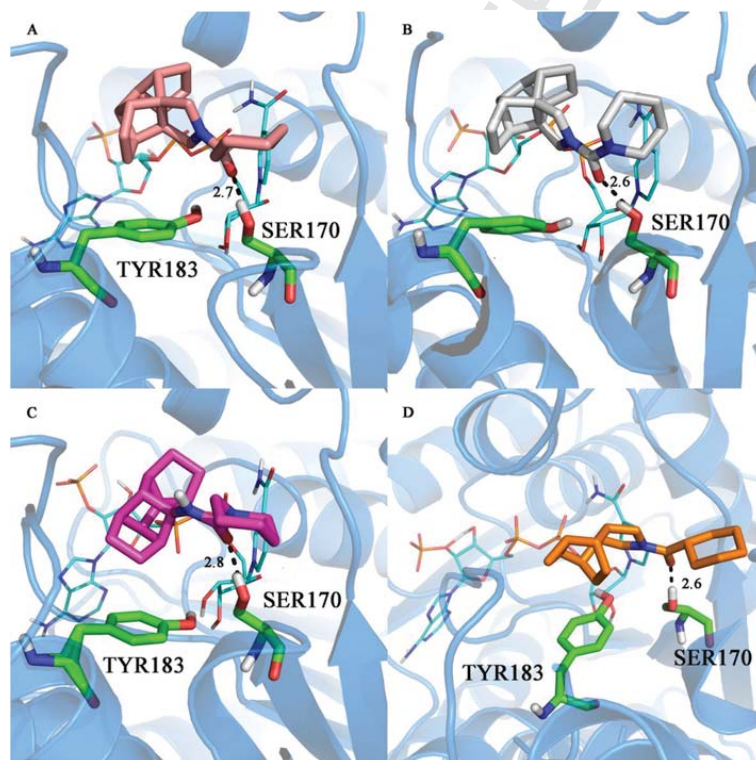
<sup>a</sup> 11 $\beta$ -HSD1 inhibition was determined in mixed sex, human liver microsomes (Celsis In-vitro Technologies) by measuring the conversion of <sup>3</sup>H-cortisone to <sup>3</sup>H-cortisol in a cortisol-scintillation proximity assay.

<sup>b</sup> Percentage inhibition was determined relative to a control system in the absence of inhibitor (see Experimental section for further details). ND, not determined.

cially for the most potent compounds (see Figs. S1–S3 in Supporting Information). A similar binding mode was found for compounds 8, 12 and 14 (see Fig. 3). In all cases the carbonyl group of the ligand formed a stable hydrogen bond with Ser170 (distances ranging from 2.6 to 3.0 Å). However, the hydrogen bond of the ligand's carbonyl group with the hydroxyl group of Tyr183, which was retained during the setup of the simulated systems, exhibited larger fluctuations and was eventually disrupted during the trajectories. Docking calculations

showed compounds 12 and 14 to have slightly better scores (–9.3 and –9.7 kcal/mol, respectively) than for 6 (–8.4 kcal/mol) and 8 (–9.0 kcal/mol). The higher inhibitory potency of 12 and 14 may also be explained by the fused pyrrolidine ring, which should reduce the contribution of the conformational penalty to the binding affinity of these compounds compared to the more flexible compounds 6 and 8. Although the results appear to support the ability of the size-expanded hydrophobic cage present in 12 and 14 to occupy the binding pocket, the lower inhibitory potency compared to 1 (IC<sub>50</sub> = 86 nM; Fig. 2) suggests that the size of the polycyclic substituent in 12 and 14 may be close to the upper limit allowed for ligand binding without triggering significant structural distortions in the pocket.

Of note, the *N*-acylpyrrolidine motif contained in 11, 12, 15 and 16 has scarcely been explored in the context of the design of 11 $\beta$ -HSD1 inhibitors [49]. However, the pyrrolidine 10 is not an ideal starting compound for a medicinal chemistry program, as its synthesis is tedious and very low-yielding [38]. For this reason, we explored the synthesis of alternative, easily synthesized, pyrrolidine derivatives. To this end, we followed a polycyclic substituent optimization process in which the cyclohexyl was selected as the RHS of the molecule, due to its simplicity (i.e. achiral, easy access) and good performance with both adamantyl (1, IC<sub>50</sub> = 0.09  $\mu$ M) and hexacyclic substituents (12, IC<sub>50</sub> = 0.29  $\mu$ M). An array of 13 pyrrolidine-based polycyclic amides was prepared from cyclohexanecarboxylic acid, HOBt, EDC, and a series of previously synthesized amines (Fig. 4). Our aim



**Fig. 3.** Representative snapshot of the binding mode of compounds 12 (A), 14 (B), 8 (C), and 23 (D) to the human 11 $\beta$ -HSD1 enzyme as determined from the analysis of the MD simulations. The protein backbone is shown as blue cartoon, the NADP cofactor, residues Tyr183 and Ser170, and the ligands are shown as atom-coloured sticks. The hydrogen bond between the ligand and the hydroxyl group of Ser170 is shown as a dashed line. (For interpretation of the references to colour in this figure legend, the reader is referred to the web version of this article.)

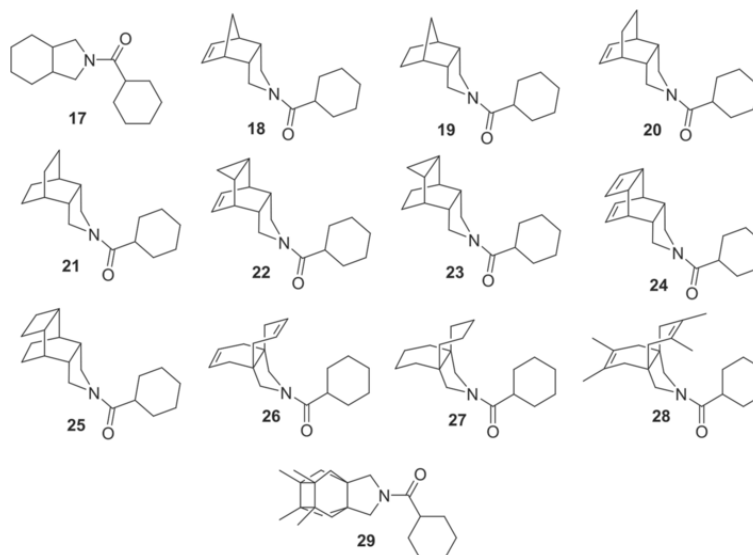


Fig. 4. Novel pyrrolidine-based polycyclic amides 17–29.

was to obtain different pyrrolidine-based polycyclic compounds, some of them simplified analogues of the hexacyclic unit contained in **10** but with higher conformational freedom, in order to find the optimal size and shape to deliver more potent 11 $\beta$ -HSD1 inhibitors.

Following the aforementioned preliminary *in vitro* microsomal assay, the IC<sub>50</sub> values were determined for compounds with an inhibitory activity higher than 50% at 10  $\mu$ M (Table 2). In general, compounds containing smaller polycyclic rings (i.e. **17–23**) were one order of magnitude more potent than our initially best inhibitors **12**, **14** and **16**, and some of them were also more potent than the adamantyl derivative **1** (IC<sub>50</sub> = 0.09  $\mu$ M). The most potent inhibitors were **18**, **20**, **21**, **22** and **23** (IC<sub>50</sub> values ranging from 0.02 to 0.03  $\mu$ M). MD simulations of the enzyme complex with compound **23** confirmed the stability of the binding mode (see Fig. 3D and Fig. S4), which resembled the arrangement of compound **12**, and the formation of the hydrogen-bond interaction with Ser170 (average dis-

tance of 2.8  $\pm$  0.3  $\text{Å}$ ). However, there was not a clear trend in terms of activity between the alkene/alkane pairs containing the same polycyclic ring system (compare **20** vs **21**, and **22** vs **23**). Thus, in the pair **18/19** the alkene derivative presented a slightly higher potency, but the bigger alkene derivatives **24** and **26** were significantly more potent than their alkane analogues **25** and **27** (IC<sub>50</sub> = 1.49  $\mu$ M vs 27% inhibition at 10  $\mu$ M, and 0.04  $\mu$ M vs 1.22  $\mu$ M, respectively). Finally, the introduction of four methyl groups, either in an extended (**28**) or compact (**29**) arrangement, was highly deleterious to the inhibitory activity (compare **26** vs **28** and **29**). Overall, these findings reinforce the assumption that the hexacyclic substituent reaches the upper-limit size to fill the hydrophobic pocket of the binding site.

### 3. Biological profiling of the more potent 11 $\beta$ -HSD1 inhibitors

The more potent inhibitors obtained by this polycyclic substituent optimization process have clogP values between 2.68 and 3.99, more desirable than that of the adamantyl-containing analogue **1** (clogP = 4.65). These new compounds were characterized in terms of cellular potency, selectivity over 11 $\beta$ -HSD2, human metabolic stability, cytochromes P450 (CYP) inhibition and predicted brain permeability, in order to select the best candidate to perform an *in vivo* study in a rodent model of cognitive dysfunction.

The cellular potency was assessed in Human Embryonic Kidney 293 (HEK293) cells stably transfected with the 11 $\beta$ -HSD1 gene. With the only exception of alkenes **18**, **20** and **26**, which showed a moderate inhibitory activity (55%, 64% and 64%, respectively), all compounds completely inhibited the enzyme at 10  $\mu$ M (Table 3).

Selectivity over 11 $\beta$ -HSD2 is required for 11 $\beta$ -HSD1 inhibitors progressing into clinical trials since 11 $\beta$ -HSD2 inhibition in the kidney can lead to sodium retention and increased blood pressure *via* cortisol stimulation of mineralocorticoid receptors. However, for the purposes of our *in vivo* study of cognitive dysfunction in rodents, high selectivity vs 11 $\beta$ -HSD2 was not required. Notwithstanding, 11 $\beta$ -HSD2 inhibition was assessed in a cellular assay with HEK293 cells stably transfected with the 11 $\beta$ -HSD2 gene at 10, 1 and 0.1  $\mu$ M in order to establish the selectivity of our compounds.

Table 2  
11 $\beta$ -HSD1 inhibition by compounds 17–29.<sup>a,b</sup>

Compound	hHSD1% inh at 10 $\mu$ M	hHSD1 IC <sub>50</sub> ( $\mu$ M)
<b>17</b>	85	0.05
<b>18</b>	89	0.02
<b>19</b>	92	0.09
<b>20</b>	96	0.03
<b>21</b>	95	0.02
<b>22</b>	100	0.02
<b>23</b>	100	0.03
<b>24</b>	83	1.49
<b>25</b>	27	ND
<b>26</b>	82	0.04
<b>27</b>	67	1.22
<b>28</b>	30	ND
<b>29</b>	42	ND

<sup>a</sup> 11 $\beta$ -HSD1 inhibition was determined in mixed sex, Human Liver Microsomes (Celsis In-vitro Technologies) by measuring the conversion of <sup>3</sup>H-cortisone to <sup>3</sup>H-cortisol in a cortisol-Scintillation Proximity Assay.

<sup>b</sup> Percentage inhibition was determined relative to a no inhibitor control (see Experimental section for further details). ND, not determined.

**Table 3**  
Biological profiling of the most potent compounds.<sup>a,b</sup>

Compound	hHSD1 IC <sub>50</sub> ( $\mu\text{M}$ )	HEK hHSD1% inh at 10 $\mu\text{M}$ <sup>c</sup>	HEK hHSD2 inhibition at 10 $\mu\text{M}$ or IC <sub>50</sub> ( $\mu\text{M}$ ) <sup>e</sup>	HLM % parent <sup>d</sup>	PAMPA-BBB P <sub>e</sub> ( $10^{-6} \text{ cm s}^{-1}$ ) <sup>e,f</sup>
<b>1</b>	0.09	100	88%	79	–
<b>18</b>	0.02	55	<0.1 $\mu\text{M}$	60	–
<b>19</b>	0.099	100	<0.1 $\mu\text{M}$	37	5.20 $\pm$ 0.1 (CNS $\pm$ )
<b>20</b>	0.03	64	0.1–1 $\mu\text{M}$	44	–
<b>21</b>	0.02	100	0.1–1 $\mu\text{M}$	17	ND <sup>g</sup>
<b>22</b>	0.02	100	1–10 $\mu\text{M}$	27	ND
<b>23</b>	0.03	100	<0.1 $\mu\text{M}$	94	>30 (CNS+)
<b>26</b>	0.04	64	100%	–	–

<sup>a</sup> See Experimental section for further details.

<sup>b</sup> Percentage inhibition was determined relative to a no inhibitor control.

<sup>c</sup> HEK293 cells stably transfected with the full-length gene coding for human either 11 $\beta$ -HSD1 or 11 $\beta$ -HSD2 were used.

<sup>d</sup> The microsomal stability of each compound was determined using human liver microsomes.

<sup>e</sup> Permeability values from PAMPA-BBB assay. Values are expressed as the mean  $\pm$  SD of three independent experiments. CNS+, predicted positive brain penetration.

<sup>f</sup> Calibration line between 0 and  $30 \times 10^{-6} \text{ cm s}^{-1}$ .

<sup>g</sup> ND, not detected.

Ideally, the 11 $\beta$ -HSD2 inhibition at 10  $\mu\text{M}$  should be lower than 50% to consider a compound sufficiently selective toward 11 $\beta$ -HSD1. None of our compounds achieved this threshold but some slightly improved the poor selectivity of the adamantyl-containing analogue **1**, such as amide **22** (88% vs 69% inhibition at 10  $\mu\text{M}$ , respectively, data not shown). Although **22** had an IC<sub>50</sub> between 1 and 10  $\mu\text{M}$ , so we cannot rigorously consider this compound to be selective against 11 $\beta$ -HSD1, its selectivity index was at least 50-fold compared to compounds **20** and **21**, which displayed selectivities less than 5-fold. Poor selectivity was observed for compounds **18**, **19** and **23**.

Microsomal stability was performed in human liver microsomes (HLM), which are widely used to determine the likely degree of primary metabolic clearance in the liver. Compounds **18**, **19** and **20** presented moderate microsomal stabilities between 36 and 60% of remaining parent compound after 30 min incubation, while amides **21** and **22** showed stabilities lower than 28%. Compound **23** displayed a high microsomal stability with 94% of remaining parent compound after the 30 min incubation period.

The active compounds in the 11 $\beta$ -HSD1 cellular assay (**19** and **21–23**) were further tested for predicted brain permeation using the widely used *in vitro* PAMPA-BBB model [50]. Unfortunately, the *in vitro* permeabilities (P<sub>e</sub>) for compounds **21** and **22** could not be determined due to their lack of UV absorption. Whereas **19** showed an uncertain BBB permeation [CNS  $\pm$  with  $5.179 > P_e$  ( $10^{-6} \text{ cm s}^{-1}$ )  $> 2.106$ ], compound **23** had P<sub>e</sub> clearly above the threshold established for a high blood-brain barrier (BBB) permeation ( $P_e > 30 \times 10^{-6} \text{ cm s}^{-1}$ ).

#### 4. *In vivo* study

Recent studies in rodents and humans with brain-penetrant 11 $\beta$ -HSD1 inhibitors have shown that they provide beneficial effects on the cognitive impairment associated with aging [13,18–23]. SAMP8 has been studied as a non-transgenic murine mouse model of accelerated senescence and late-onset AD [51,52]. These mice exhibit cognitive and emotional disturbances, probably due to early development of brain pathological hallmarks, such as oxidative stress (OS), inflammation, and activation of neuronal death pathways, which mainly affect cerebral cortex and hippocampus [24,53]. To date, this rodent

model has not been used to test 11 $\beta$ -HSD1 inhibitors, being this work the first investigation of the effects of 11 $\beta$ -HSD1 pharmacological inhibition in SAMP8.

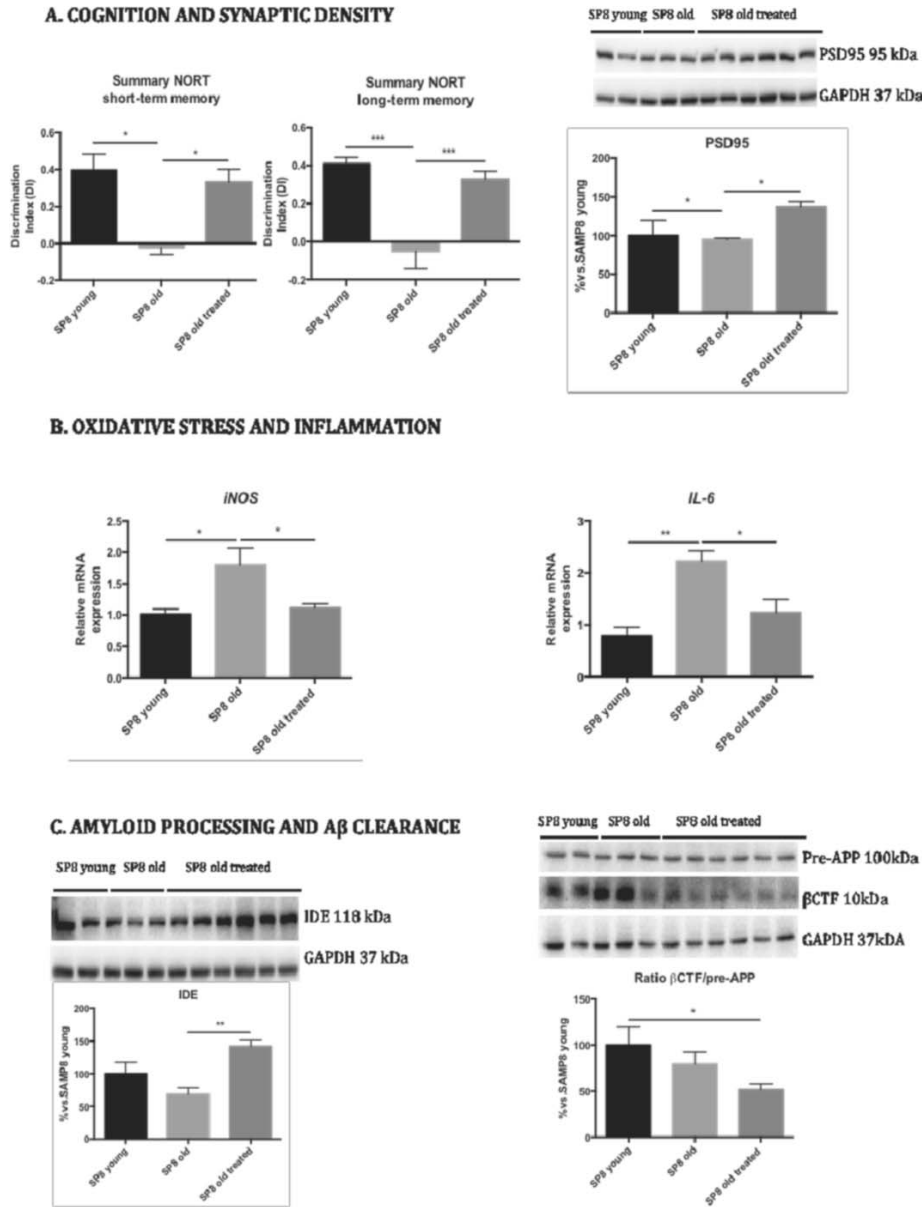
The *in vivo* study was performed with amide **23**, as this compound had low nanomolar potency against the murine 11 $\beta$ -HSD1 enzyme (mHSD1, IC<sub>50</sub> = 0.08  $\mu\text{M}$ ), high cellular potency, high microsomal stability (both in human and mouse liver microsomes, 94 and 93%, respectively) and positive predicted brain penetration. A pharmacokinetic study of compound **23** was performed in order to assess its oral administration. Although its clearance seems to be rapid, the concentration levels at 30 min post-administration are five fold the IC<sub>50</sub> (Table S1, Fig. S5 and Table S2). In addition, we could also measure compound concentration in brain tissue at 3 h post-administration (1.45 ng/mL), hint of *in vivo* BBB permeability. Then, compound **23** was administered to 12-month-old SAMP8 mice in drinking water during four weeks at a concentration of 105 mg/L (average body weight for 48-week-old mice is 25 g; fluid consumption is 5 mL, therefore the dose was 0.105 mg/mL  $\times$  5 mL/0.025 kg = 21 mg/kg). Compound **23** was dissolved in polyethylene glycol 400 (PEG400) and then diluted with water to a PEG400 final concentration of 2% (v/v) in drinking fluid. 2% PEG400 in water was given to the remaining mice in drinking fluid as a vehicle control.

Neuroprotective effects were investigated through a behavioural test, the novel object recognition test (NORT), as a common measure of cognition (short-term and long-term memory) [54], and biochemical analysis, which were made through Western blotting and quantitative real-time polymerase chain reaction (qPCR). Brain tissue was analysed upon termination of the study to determine compound levels and *ex vivo* inhibition of 11 $\beta$ -HSD1. Consistent with previous reports, we found that aged SAMP8 mice presented memory impairments in the NORT when compared to young animals [53]. Satisfactorily, treatment with **23** certainly prevented short-term and long-term memory deficits in SAMP8 mice (Fig. 5A).

Postsynaptic density 95 (PSD95) protein levels were evaluated as a measure of neuronal synapses, whereas gene expression for interleukin-6 (IL-6), which acts as a pro-inflammatory cytokine, and for inducible nitric oxide synthase (iNOS), an oxidative stress sensor that catalyzes the production of nitric oxide (NO), were also studied. Treatment with **23** prevented the reduction of PSD95 protein levels, while the oxidative stress and pro-inflammatory gene expression markers, such as iNOS and IL-6, were significantly decreased compared to untreated mice (Fig. 5A–B). These observations indicate a neuroprotective action of **23**, whereby reduced cognitive impairment in **23**-treated mice is mediated by a reduction of neuroinflammation and oxidative stress as confirmed by in the measurements of pro-inflammatory biomarkers (IL-6 and iNOS).

AD is characterized by the production and deposition of  $\beta$ -amyloid and it has been postulated that its reduction produces beneficial effects [55]. For these reasons, the effect of **23** in modifying amyloid processing pathways was also examined. No changes in amyloid beta A4 precursor (*PreAPP*),  $\beta$ -secretase 1 (*Bace1*), disintegrin and metalloproteinase 10 (*Adam 10*) gene expression levels were found (data not shown). Nevertheless, after treatment with **23**, we found a decrease of APP  $\beta$ -secretase C-terminal fragment ( $\beta$ CTF) protein levels without modification of those of *PreAPP*, together with an increase of the protein levels of insulin-degrading enzyme (IDE) (Fig. 1C), a zinc metalloprotease that degrades  $\beta$ -amyloid species. Several *in vitro* and *in vivo* studies have shown correlations between IDE,  $\beta$ -amyloid levels and AD [56].

In an attempt to elucidate the mechanisms underlying the beneficial effects of **23** and the relationship with cognitive amelioration in old SAMP8, we focused our study on amyloid processing and  $\beta$ CTF because of its implication in neurodegeneration and cognitive decline process in this strain [57]. Amide **23** did not alter the proamiloido-



**Fig. 5. Results of *in vivo* study. 2A. -Cognition and synaptic density:** -Left panel: Results. Discrimination index of Novel Object recognition test (NORT) obtained in young SAMP8, old SAMP8 and treated SAMP8, at 2 and 24 h. -Right Panel: Representative Western blot (wb) for PSD95 and quantification. **2B. -Oxidative stress and inflammation:** -Left Panel: Oxidative stress gene expression iNOS. -Right panel: pro-inflammatory gene expression for IL-6. Gene expression levels were determined by real-time PCR. **2C. -Amyloid processing and  $\beta$ -CTF clearance:** -Left panel: Representative Western blot (wb) for IDE and quantification. -Right panel: Representative Western blot (wb) for Pre-APP and  $\beta$ -CTF and  $\beta$ -CTF/APP ratio quantification. For Western blot, bars represent mean  $\pm$  standard error of the mean (SEM), and values are adjusted to 100% for levels SAMP8 young. For real-time PCR, mean  $\pm$  SEM from five independent experiments performed in triplicate are represented. The One-Way ANOVA analysis and Tukey post hoc analysis were conducted. Statistical outliers (Grubbs' test) were removed from the analyses. \* $p < 0.05$ ; \*\* $p < 0.01$ ; \*\*\* $p < 0.001$ .

genic pathway in SAMP8, as demonstrated by the lack of effect on *Pre-APP*, *Adam10* or *Bace1* gene expression (see Fig. S6 in the Supplementary material file). However, the capacity of the brain to re-

move proamiloidogenic species by activation of specific proteases, such as IDE or neprilysin, appeared greatly increased in treated SAMP8 with higher protein levels of IDE than in control animals and



consequently with substantially decreased  $\beta$ CTF protein levels. The results of the behavioural and biochemical studies in SAMP8 mice suggest that compound **23** acts centrally on 11 $\beta$ -HSD1.

Overall, behavioural tests and biochemical analyses confirmed a neuroprotective action of compound **23**, probably by reduction of inflammation and oxidative stress, as measured by reduction of IL-6 and iNOS.

## 5. Conclusions

We have found that adamantyl, widely used as a lipophilic substituent in 11 $\beta$ -HSD1 inhibitors, may successfully be replaced by other polycyclic hydrocarbons. The previously scarcely explored pyrrolidine-based polycyclic substituents presented here led to potent 11 $\beta$ -HSD1 inhibitors, and potentially these aliphatic ring-systems can serve as alternatives to adamantyl. Of note, the novel nanomolar inhibitors reported are achiral and easily synthesized in maximum four synthetic steps (compounds **19**, **21** and **23**) from commercially available starting materials. Biological profiling allowed us to select amide **23** for the first *in vivo* study in SAMP8 aiming to investigate the pharmacological effects of 11 $\beta$ -HSD1 inhibition in this model of cognitive dysfunction. In this study, prevention of cognitive impairment in aged SAMP8 after four-week treatment with **23** was demonstrated in comparison with control animals. The results provide further support for the neuroprotective effect of 11 $\beta$ -HSD1 inhibition, through reduction of neuroinflammation and oxidative stress, in cognitive decline related to the aging process. Due to the promising biological activity of **23**, further optimization is currently being carried out, with focus on modifying the RHS of the molecule to improve the selectivity and DMPK properties.

## 6. Experimental section

### 6.1. Chemistry

#### 6.1.1. General

Melting points were determined in open capillary tubes with a MFB 595010M Gallenkamp. 400 MHz  $^1\text{H}/100.6\text{ MHz }^{13}\text{C}$  NMR spectra, and 500 MHz  $^1\text{H}$  NMR spectra were recorded on Varian Mercury 400, and Varian Inova 500 spectrometers, respectively. The chemical shifts are reported in ppm ( $\delta$  scale) relative to internal tetramethylsilane, and coupling constants are reported in Hertz (Hz). Assignments given for the NMR spectra of the new compounds have been carried out on the basis of DEPT, COSY  $^1\text{H}/^1\text{H}$  (standard procedures), and COSY  $^1\text{H}/^{13}\text{C}$  (gHSQC and gHMBC sequences) experiments. IR spectra were run on Perkin-Elmer Spectrum RX I spectrophotometer. Absorption values are expressed as wave-numbers ( $\text{cm}^{-1}$ ); only significant absorption bands are given. Column chromatography was performed either on silica gel 60 Å (35–70 mesh) or on aluminium oxide, neutral, 60 Å (50–200  $\mu\text{m}$ , Brockmann I). Thin-layer chromatography was performed with aluminium-backed sheets with silica gel 60 F<sub>254</sub> (Merck, ref 1.05554), and spots were visualized with UV light and 1% aqueous solution of  $\text{KMnO}_4$ . The analytical samples of all of the new compounds which were subjected to pharmacological evaluation possessed purity  $\geq 95\%$  as evidenced by their elemental analyses.

#### 6.1.2. General procedures for the synthesis of the compounds

##### 6.1.2.1. General procedure A

A solution of cyclohexane acyl chloride (1.2 mmol) in anhydrous acetone was added to a solution of the amine hydrochloride (1 mmol) and triethylamine (2 mmol) in anhydrous acetone. The reaction mixture was stirred at 90° C for 3 h. The resulting residue was dissolved

with DCM (20 mL) and washed with 1 M aqueous solution of HCl (4  $\times$  25 mL), dried over anhydrous  $\text{Na}_2\text{SO}_4$  and filtered. The evaporation *in vacuo* of the organics gave the desired product.

##### 6.1.2.2. General procedure B

To a solution of the amine hydrochloride (1 mmol) in DCM (10 mL) were added 1-piperidinecarbonyl chloride (1.5 mmol) and triethylamine (4 mmol). The reaction mixture was stirred at rt overnight. To the resulting mixture was added saturated aqueous solution of  $\text{NaHCO}_3$  (10 mL) and the phases were separated. The aqueous layer was extracted with further DCM (2  $\times$  10 mL). The organics were washed with 10%  $\text{Na}_2\text{CO}_3$  solution (30 mL), dried over anhydrous  $\text{Na}_2\text{SO}_4$ , filtered and concentrated *in vacuo* to give the desired product.

##### 6.1.2.3. General procedure C

To a solution of amine hydrochloride (1.1 mmol) in EtOAc (15 mL) were added the carboxylic acid (1 mmol), HOBt (1.5 mmol), EDC (1.5 mmol) and triethylamine (4 mmol) and the reaction mixture was stirred at rt overnight. To the resulting suspension was then added water (15 mL) and the phases were separated. The organic phase was washed with saturated aqueous  $\text{NaHCO}_3$  solution (15 mL) and brine (15 mL), dried over anhydrous  $\text{Na}_2\text{SO}_4$  and filtered. The organic layer was concentrated *in vacuo* to give the desired product.

##### 6.1.2.4. General procedure D

A solution or suspension of the amide or urea (1 mmol) and 5 wt % palladium on carbon (50% in water, 10% of the weight) in absolute ethanol (ca 30 mL) was stirred at rt and atmospheric pressure under hydrogen for 3–72 h. The suspension was then filtered and the solids were washed with EtOH (10 mL). The solvents were removed *in vacuo* to give the desired reduced product.

#### 6.1.3. N-[[Pentacyclo[6.4.0.0<sup>2,10</sup>.0<sup>3,7</sup>.0<sup>4,9</sup>]dodec-8-yl]cyclohexanecarboxamide, (6)

From cyclohexane acyl chloride (128 mg, 0.88 mmol) in anhydrous acetone (0.6 mL) and amine **4** [38] (152 mg, 0.72 mmol) and triethylamine (0.25 mL, 1.74 mmol) in anhydrous acetone (0.9 mL) and following the general procedure A, amide **6** (215 mg, 95% yield) was obtained as a yellow solid. The analytical sample was obtained by crystallization from EtOAc/pentane (164 mg), mp 228–229 °C; IR (ATR)  $\nu$ : 580, 591, 604, 638, 663, 695, 722, 761, 824, 894, 933, 1143, 1194, 1221, 1277, 1304, 1336, 1386, 1448, 1547, 1639, 2851, 2923, 3271  $\text{cm}^{-1}$ ;  $^1\text{H}$  NMR (400 MHz,  $\text{CDCl}_3$ )  $\delta$ : 1.08 (t,  $J = 2.8\text{ Hz}$ , 1 H, 9'-H), 1.18–1.34 [complex signal, 3 H, 3(5)-H<sub>ax</sub> and 4-H<sub>ax</sub>], 1.39–1.55 [complex signal, 10 H, 5'(11')-H<sub>2</sub>, 6'(12')-H<sub>2</sub> and 2(6)-H<sub>ax</sub>], 1.66 (m, 1 H, 4-H<sub>eq</sub>), 1.79 [m, 2 H, 3(5)-H<sub>eq</sub>], 1.85 [m, 2 H, 2(6)-H<sub>eq</sub>], 2.08 (tt,  $J = 11.6\text{ Hz}$ ,  $J' = 3.4\text{ Hz}$ , 1 H, 1-H), 2.13 [b. s., 2 H, 4'(10')-H], 2.21 [m, 2 H, 2'(3')-H], 2.81 [b. s., 2 H, 1'(7')-H], 5.47 (s, 1 H, NH);  $^{13}\text{C}$  NMR (100.5 MHz,  $\text{CDCl}_3$ )  $\delta$ : 21.5 [ $\text{CH}_2$ , C5'(C11')], 24.4 [ $\text{CH}_2$ , C6'(C12')], 25.7 ( $\text{CH}_2$ , C4), 25.8 [ $\text{CH}_2$ , C3(5)], 30.1 [ $\text{CH}_2$ , C2(C6)], 45.8 (CH, C1), 46.9 [CH, C2'(3')], 52.8 [CH, C4'(10')], 53.4 [CH, C1'(7')], 54.8 (CH, C9'), 65.4 (C, C8'), 176.7 (C, CO). Anal. Calcd for  $\text{C}_{19}\text{H}_{27}\text{NO}$ : C 79.95, H 9.54, N 4.91. Found: C 79.73, H 9.75, N 4.82.

#### 6.1.4. N-[[Pentacyclo[6.4.0.0<sup>2,10</sup>.0<sup>3,7</sup>.0<sup>4,9</sup>]dodec-8-yl]methyl]cyclohexanecarboxamide, (7)

From cyclohexane acyl chloride (119 mg, 0.81 mmol) in anhydrous acetone (0.6 mL) and amine **5** [38] (150 mg, 0.67 mmol) and triethylamine (0.23 mL, 1.62 mmol) in anhydrous acetone (0.8 mL) and following the general procedure A, amide **7** (155 mg, 78% yield) was obtained as a dark solid. The analytical sample was obtained by crystallization from EtOAc/pentane (77 mg), mp 148–149 °C; IR

(ATR)  $\nu$ : 576, 589, 604, 621, 660, 672, 711, 800, 894, 956, 979, 1037, 1106, 1123, 1180, 1213, 1252, 1298, 1314, 1380, 1435, 1443, 1550, 1633, 1659, 2855, 2928, 3299  $\text{cm}^{-1}$ ;  $^1\text{H}$  NMR (400 MHz,  $\text{CDCl}_3$ )  $\delta$ : 1.05 (b. s., 1 H, 9'-H), 1.17–1.33 [complex signal, 3 H, 3(5)- $\text{H}_{\text{ax}}$  and 4- $\text{H}_{\text{ax}}$ ], 1.35–1.55 [complex signal, 8 H, 5'(11')- $\text{H}_{\text{exo}}$  or  $\text{endo}$ , 6'(12')- $\text{H}_2$  and 2(6)- $\text{H}_{\text{ax}}$ ], 1.56–1.70 [complex signal, 3 H, 5'(11')- $\text{H}_{\text{endo}}$  or  $\text{exo}$  and 4- $\text{H}_{\text{eq}}$ ], 1.74–1.87 [complex signal, 4 H, 2(6)- $\text{H}_{\text{eq}}$  and 3(5)- $\text{H}_{\text{eq}}$ ], 1.98 [b. s., 2 H, 4'(10')-H], 2.05 (tt,  $J = 11.6$  Hz,  $J' = 3.2$  Hz, 1 H, 1-H), 2.13 [b. s., 2 H, 1'(7')-H], 2.22 [m, 2 H, 2'(3')-H], 3.38 [d,  $J = 5.6$  Hz, 2 H,  $\text{NCH}_2$ ], 5.20 [b. s., 1H, NH];  $^{13}\text{C}$  NMR (100.5 MHz,  $\text{CDCl}_3$ )  $\delta$ : 22.3 [ $\text{CH}_2$ , C5'(C11')], 24.2 [ $\text{CH}_2$ , C6'(12')], 25.7 (3  $\text{CH}_2$ , C3, C4 and C5), 29.8 [ $\text{CH}_2$ , C2(6)], 36.9 ( $\text{CH}_2$ ,  $\text{NCH}_2$ ), 42.7 (C, C8'), 45.7 (CH, C1), 47.9 [CH, C2'(3')], 51.2 (CH, C9'), 53.1 [CH, C1'(7')], 53.5 [CH, C4'(10')], 175.6 (C, CO). Anal. Calcd for  $\text{C}_{20}\text{H}_{29}\text{NO}$ : 0.15 EtOAc: C 79.13, H 9.74, N 4.48. Found: C 79.03, H 9.88, N 4.52.

**6.1.5. N-[Pentacyclo[6.4.0.0<sup>2,10</sup>.0<sup>3,7</sup>.0<sup>4,9</sup>]dodec-8-yl]piperidine-1-carboxamide, (8)**

From amine **4** [38] (100 mg, 0.47 mmol), 1-piperidinecarbonyl chloride (0.09 mL, 0.71 mmol) and triethylamine (0.23 mL, 1.88 mmol) in DCM (5 mL) and following the general procedure B, amide **8** (72 mg, 54% yield) was obtained as a white solid. The analytical sample was obtained by crystallization from hot EtOAc (22 mg), mp 225–226 °C; IR (ATR)  $\nu$ : 700, 721, 734, 764, 794, 851, 866, 907, 954, 971, 1003, 1019, 1050, 1128, 1141, 1187, 1232, 1254, 1261, 1276, 1306, 1325, 1357, 1395, 1440, 1479, 1520, 1615, 2024, 2158, 2855, 2930, 3362  $\text{cm}^{-1}$ ;  $^1\text{H}$  NMR (400 MHz,  $\text{CDCl}_3$ )  $\delta$ : 0.99 (broad s, 1 H, 9'-H), 1.43–1.65 complex signal, 14 H, 5'(11')- $\text{H}_2$ , 6'(12')- $\text{H}_2$ , 3(5)- $\text{H}_2$  and 4- $\text{H}_2$ ], 2.13 [broad s, 2 H, 4'(10')-H], 2.21 [broad s, 2 H, 2'(3')-H], 2.78 [broad s, 2 H, 1'(7')-H], 3.31 [m, 4 H, 2(6)- $\text{H}_2$ ], 4.53 (broad s, 1 H, NH);  $^{13}\text{C}$  NMR (100.5 MHz,  $\text{CDCl}_3$ )  $\delta$ : 21.5 [ $\text{CH}_2$ , C5'(11')], 24.5 ( $\text{CH}_2$ , C4), 24.6 [ $\text{CH}_2$ , C6'(12')], 25.6 [ $\text{CH}_2$ , C3(5)], 45.2 [ $\text{CH}_2$ , C2(6)], 46.8 [CH, C2'(3')], 52.8 [CH, C4'(10')], 53.6 [CH, C1'(7')], 55.4 (CH, C9'), 65.8 (C, C8'), 157.4 (C, CO); HRMS-ESI +  $m/z$  [M+H]<sup>+</sup> calcd for  $[\text{C}_{18}\text{H}_{26}\text{N}_2\text{O} + \text{H}]^+$ : 287.2118, found: 287.2118.

**6.1.6. N-[[Pentacyclo[6.4.0.0<sup>2,10</sup>.0<sup>3,7</sup>.0<sup>4,9</sup>]dodec-8-yl)methyl]piperidine-1-carboxamide, (9)**

From amine **5** [38] (96 mg, 0.42 mmol), 1-piperidinecarbonyl chloride (0.08 mL, 0.63 mmol) and triethylamine (0.21 mL, 1.68 mmol) in DCM (5 mL) and following the general procedure B, amide **9** (125 mg, quantitative yield) was obtained as a white solid. The analytical sample was obtained by crystallization from hot EtOAc (25 mg), mp 144–145 °C; IR (ATR)  $\nu$ : 554, 572, 623, 637, 678, 734, 763, 851, 869, 900, 908, 945, 969, 992, 1023, 1107, 1155, 1232, 1253, 1261, 1340, 1397, 1438, 1451, 1475, 1524, 1614, 2018, 2158, 2842, 2860, 2930, 3378  $\text{cm}^{-1}$ ;  $^1\text{H}$  NMR (400 MHz,  $\text{CDCl}_3$ )  $\delta$ : 1.06 (broad s, 1 H, 9'-H), 1.40–1.70 [complex signal, 14 H, 5'(11')- $\text{H}_2$ , 6'(12')- $\text{H}_2$ , 3(5)- $\text{H}_2$  and 4- $\text{H}_2$ ], 2.00 [broad s, 2 H, 4'(10')-H], 2.13 [broad s, 2 H, 1'(7')-H], 2.22 [broad s, 2 H, 2'(3')-H], 3.28 [m, 4 H, 2(6)- $\text{H}_2$ ], 3.37 (d,  $J = 5.2$  Hz, 2 H,  $\text{NCH}_2$ ), 4.18 (broad s, 1H, NH);  $^{13}\text{C}$  NMR (100.5 MHz,  $\text{CDCl}_3$ )  $\delta$ : 22.4 [ $\text{CH}_2$ , C5'(11')], 24.3 [ $\text{CH}_2$ , C6'(12')], 24.4 ( $\text{CH}_2$ , C4), 25.6 [ $\text{CH}_2$ , C3(5)], 38.6 ( $\text{CH}_2$ ,  $\text{NCH}_2$ ), 44.5 (C, C8'), 45.0 [ $\text{CH}_2$ , C2(6)], 47.9 [CH, C2'(3')], 51.2 (CH, C9'), 53.1 [CH, C1'(7')], 53.6 [CH, C4'(10')], 157.8 (C, CO); HRMS-ESI +  $m/z$  [M+H]<sup>+</sup> calcd for  $[\text{C}_{19}\text{H}_{29}\text{N}_2\text{O} + \text{H}]^+$ : 301.2274, found: 301.2276.

**6.1.7. (3-Azahexacyclo[7.6.0.0<sup>1,5</sup>.0<sup>5,12</sup>.0<sup>6,10</sup>.0<sup>11,15</sup>]pentadeca-7,13-dien-3-yl)(cyclohexyl) methanone, (11)**

From amine **10** [38] (400 mg, 2.03 mmol), cyclohexanecarboxylic acid (237 mg, 1.85 mmol), HOBT (375 mg, 2.78 mmol), EDC

(430 mg, 2.78 mmol) and triethylamine (0.570 mL, 4.07 mmol) in ethyl acetate (30 mL) and following the general procedure C, an orange oil (627 mg) was obtained. Column chromatography ( $\text{Al}_2\text{O}_3$ , DCM/methanol) gave amide **11** (260 mg, 42% yield) as a white solid. The analytical sample was obtained by crystallization from *tert*-butanol, mp 111–113 °C; IR (ATR)  $\nu$ : 2961, 2930, 2853, 1630, 1443, 1425, 1347, 1305, 1223, 1194, 1138, 1067, 998, 897, 878, 830, 780, 749, 734, 696, 659, 646  $\text{cm}^{-1}$ ;  $^1\text{H}$  NMR (500 MHz,  $\text{CDCl}_3$ )  $\delta$ : 1.17–1.24 [complex signal, 3 H, 4'- $\text{H}_{\text{ax}}$ , 3'(5')- $\text{H}_{\text{ax}}$ ], 1.43 [complex signal, 2 H, 2'(6')- $\text{H}_{\text{ax}}$ ], 1.60–1.66 [complex signal, 3 H, 2'(6')- $\text{H}_{\text{eq}}$ , 4'- $\text{H}_{\text{eq}}$ ], 1.75–1.78 [complex signal, 2 H, 3'(5')- $\text{H}_{\text{eq}}$ ], 2.13 (tt,  $J = 12.0$  Hz,  $J' = 3.5$  Hz, 1 H, 1'-H), 2.67 [m, 2 H, 10(11)-H], 2.98 [complex signal, 4 H, 6(12)-H, 9(15)-H], 3.18 (s, 2 H, 2- $\text{H}_2$  or 4- $\text{H}_2$ ), 3.19 (s, 2 H, 4- $\text{H}_2$  or 2- $\text{H}_2$ ), 6.00 [ddd,  $J = 6$  Hz,  $J' = 3$  Hz,  $J'' = 1.5$  Hz, 2 H, 7(13)-H or 8(14)-H], 6.04 [ddd,  $J = 6$  Hz,  $J' = 3$  Hz,  $J'' = 1$  Hz, 2 H, 8(14)-H or 7(13)-H];  $^{13}\text{C}$  NMR (125.7 MHz,  $\text{CDCl}_3$ )  $\delta$ : 25.8 ( $\text{CH}_2$ , C4'), 25.9 [ $\text{CH}_2$ , C3'(5')], 28.7 [ $\text{CH}_2$ , C2'(6')], 42.5 (CH, C1'), 45.5 ( $\text{CH}_2$ , C2 or C4), 46.7 ( $\text{CH}_2$ , C4 or C2), 62.0 [CH, C6(12) and C9(15)], 62.8 [CH, C10(11)], 69.1 (C, C1 or C5), 70.8 (C, C5 or C1), 132.8 [CH, C7(13) or 8(14)], 134.1 [CH, C8(14) or C7(13)], 174.4 (C, CO); MS (EI), (rt = 25.4 min),  $m/z$  (%): significant ions: 308 (20), 307 ( $\text{M}^+$ , 83), 252 (16), 242 (25), 198 (17), 197 (100), 196 [ $(\text{C}_{14}\text{H}_{14}\text{N})^+$ , 39], 182 (19), 181 (15), 180 (41), 179 (16), 168 (24), 167 (25), 166 (15), 165 (38), 156 (21), 153 (23), 152 (27), 132 (64), 131 (100), 130 (64), 128 (17), 118 (19), 117 (19), 115 (23), 91 (18), 83 [ $(\text{C}_6\text{H}_{11})^+$ , 85], 77 (15), 55 (72); HRMS-ESI +  $m/z$  [M+H]<sup>+</sup> calcd for  $[\text{C}_{21}\text{H}_{25}\text{NO} + \text{H}]^+$ : 308.2009, found: 308.2003.

**6.1.8. (3-Azahexacyclo[7.6.0.0<sup>1,5</sup>.0<sup>5,12</sup>.0<sup>6,10</sup>.0<sup>11,15</sup>]pentadecane-3-yl)(cyclohexyl) methanone, (12)**

From amide **11** (118 mg, 0.40 mmol) and Pd/C (13 mg) and following the general procedure D (5 h), amide **12** (94 mg, 78% yield) was obtained as a white solid. The analytical sample was obtained by crystallization from DCM/diethyl ether, mp 134–135 °C; IR (ATR)  $\nu$ : 2932, 2851, 1621, 1463, 1426, 1357, 1286, 1202, 1120, 1104, 1036, 1013, 969, 925, 886, 860, 825, 768, 732, 702, 657, 627  $\text{cm}^{-1}$ ;  $^1\text{H}$  NMR (500 MHz,  $\text{CDCl}_3$ )  $\delta$ : 1.25 [complex signal, 3 H, 4'- $\text{H}_{\text{ax}}$ , 3'(5')- $\text{H}_{\text{ax}}$ ], 1.48–1.57 [complex signal, 10 H, 7(13)- $\text{H}_2$ , 8(14)- $\text{H}_2$ , 17(21)- $\text{H}_{\text{ax}}$ ], 1.68 (m, 1 H, 4'- $\text{H}_{\text{eq}}$ ), 1.75–1.82 [complex signal, 4 H, 2'(6')- $\text{H}_{\text{eq}}$ , 3'(5')- $\text{H}_{\text{eq}}$ ], 2.08 (broad signal, 4 H, 6(12)-H, 9(15)-H], 2.36 (tt,  $J = 12$  Hz,  $J' = 3.5$  Hz, 1 H, 1'-H), 2.41 [m, 2 H, 10(11)-H], 3.29 [s, 4 H, 2(4)- $\text{H}_2$ ];  $^{13}\text{C}$  NMR (125.7 MHz,  $\text{CDCl}_3$ )  $\delta$ : 21.5 [ $\text{CH}_2$ , C7(13) or C8(14)], 21.8 [ $\text{CH}_2$ , C8(14) or C7(13)], 25.8 ( $\text{CH}_2$ , C4'), 25.9 [ $\text{CH}_2$ , C3'(5')], 29.0 [ $\text{CH}_2$ , C2'(6')], 40.7 ( $\text{CH}_2$ , C2 or C4), 42.0 ( $\text{CH}_2$ , C4 or C2), 42.9 (CH, C1'), 49.6 [CH, C10(11)], 55.0 [CH, C6(12) or C9(15)], 55.1 [CH, C9(15) or C6(12)], 57.5 (C, C1 or C5), 59.3 (C, C5 or C1), 175.1 (C, CO); MS (EI), (rt = 26.7 min),  $m/z$  (%): significant ions: 312 (23), 311 ( $\text{M}^+$ , 100), 270 (14), 257 (19), 256 (99), 243 (12), 228 [ $(\text{C}_{15}\text{H}_{18}\text{NO})^+$ , 13], 202 (12), 201 (30), 184 (29), 129 (15), 128 (15), 91 (16), 83 [ $(\text{C}_6\text{H}_{11})^+$ , 24], 55 (25). Anal. Calcd for  $\text{C}_{21}\text{H}_{29}\text{NO}$ : C 80.98, H 9.39, N 4.50. Found: 80.76, H 9.61, N 4.33.

**6.1.9. (3-Azahexacyclo[7.6.0.0<sup>1,5</sup>.0<sup>5,12</sup>.0<sup>6,10</sup>.0<sup>11,15</sup>]pentadeca-7,13-diene-3-yl)(piperidin-1-yl) methanone, (13)**

From amine **10** [38] (400 mg, 2.03 mmol), 1-piperidinecarbonyl chloride (0.26 mL, 2.13 mmol) and triethylamine (0.56 mL, 4.06 mmol) in DCM and following the general procedure B amide **13** (443 mg, 71% yield) was obtained as a clear oil. Several attempts to crystallize this product met with failure. The product was used in the next step without further purification or characterization; MS (EI), (rt = 24.2 min),  $m/z$  (%): significant ions: 308 ( $\text{M}^+$ , 46), 196 [ $(\text{C}_{14}\text{H}_{14}\text{N})^+$ , 17], 165 (14), 130 (15), 112 [ $(\text{C}_6\text{H}_{10}\text{NO})^+$ , 100], 84 [ $(\text{C}_5\text{H}_{10}\text{N})^+$ , 17], 69 (41).

6.1.10. (3-Azahexacyclo[7.6.0.0<sup>1,5</sup>.0<sup>5,12</sup>.0<sup>6,10</sup>.0<sup>11,15</sup>]pentadeca-3-yl)(piperidin-1-yl) methanone, (**14**)

From urea **13** (235 mg, 0.76 mmol) and Pd/C (24 mg) and following the general procedure D (3 h), urea **14** (171 mg, 72% yield) was obtained as a white solid, mp 124–126 °C; IR (ATR)  $\nu$ : 3457, 3291, 2936, 2867, 2839, 1615, 1538, 1461, 1415, 1370, 1332, 1304, 1252, 1226, 1202, 1159, 1124, 1110, 1027, 991, 915, 882, 851, 767, 722, 632 cm<sup>-1</sup>; <sup>1</sup>H NMR (500 MHz, CDCl<sub>3</sub>)  $\delta$ : 1.47–1.58 [complex signal, 14 H, 7(8,13,14)-H<sub>2</sub>, 3'(5')-H<sub>2</sub>, 4'-H<sub>2</sub>], 2.05 [m, 4 H, 6(9,12,15)-H], 2.38 [m, 2 H, 10(11)-H], 3.19 [m, 8 H, 2(4)-H<sub>2</sub>, 2'(6')-H<sub>2</sub>]; <sup>13</sup>C NMR (125.7 MHz, CDCl<sub>3</sub>)  $\delta$ : 21.7 [CH<sub>2</sub>, C7(8, 13, 14)], 24.8 (CH<sub>2</sub>, C4'), 25.9 [CH<sub>2</sub>, C3'(5')], 43.3 [CH<sub>2</sub>, C2(4)], 47.8 [CH<sub>2</sub>, C16(20)], 49.6 [CH, C10(11)], 54.8 [CH, C6(9, 12, 15)], 58.8 [C, C1(5)], 163.3 (C, CO); MS (EI), (rt = 25.1 min),  $m/z$  (%); significant ions: 312 (M<sup>+</sup>, 100), 201 (15), 200 [(C<sub>14</sub>H<sub>18</sub>N)<sup>+</sup>, 82], 184 (33), 129 (36), 112 [(C<sub>6</sub>H<sub>10</sub>NO)<sup>+</sup>, 54], 91 (16), 84 [(C<sub>3</sub>H<sub>10</sub>N)<sup>+</sup>, 59], 69 (28). Anal. Calcd for C<sub>20</sub>H<sub>28</sub>N<sub>2</sub>O: C 76.88, H 9.03, N 8.97. Found: 76.60, H 9.21, N 8.74.

6.1.11. (4-Amino-3,5-dichlorophenyl)(3-azahexacyclo[7.6.0.0<sup>1,5</sup>.0<sup>5,12</sup>.0<sup>6,10</sup>.0<sup>11,15</sup>]pentadeca-7,13-dien-3-yl)methanone, (**15**)

From amine **10** [38] (400 mg, 2.03 mmol), 4-amino-3,5-dichlorobenzoic acid (380 mg, 1.85 mmol), 1-hydroxybenzotriazole (HOBt) (375 mg, 2.78 mmol), 1-ethyl-3-(3-dimethylaminopropyl)carbodiimide (EDC) (430 mg, 2.78 mmol) and triethylamine (0.560 mL, 4.07 mmol) in EtOAc (30 mL) and DMF (2 mL) and following the general procedure C, a yellow solid (677 mg) was obtained. Column chromatography (Al<sub>2</sub>O<sub>3</sub>, DCM/methanol) furnished **15** (332 mg, 47% yield) as a white solid, mp 236–238 °C; IR (ATR)  $\nu$ : 3449, 3306, 3250, 3204, 2954, 2867, 2150, 1597, 1538, 1501, 1456, 1410, 1384, 1342, 1316, 1295, 1244, 1225, 1192, 1054, 1002, 943, 896, 875, 791, 745, 733, 686, 667, 643 cm<sup>-1</sup>; <sup>1</sup>H NMR (500 MHz, CDCl<sub>3</sub>)  $\delta$ : 2.61 [m, 2 H, 10(11)-H], 2.85 [broad s, 2 H, 6(12)-H or 9(15)-H], 2.94 [broad s, 2 H, 9(15)-H or 6(12)-H], 3.13 [broad s, 2 H, 2-H or 4-H], 3.33 [broad s, 2 H, 4-H or 2-H], 5.91 [m, 2 H, 7(13)-H or 8(14)-H], 6.03 [m, 2 H, 8(14)-H or 7(13)-H], 7.19 (s, 2 H, Ar-H); <sup>13</sup>C NMR (125.7 MHz, CDCl<sub>3</sub>)  $\delta$ : 45.5 (CH<sub>2</sub>, C2 or C4), 49.9 (CH<sub>2</sub>, C4 or C2), 61.8 [CH, C6(12), C9(15)], 62.7 [CH, C10(11)], 68.8 (C, C1 or C5), 71.0 (C, C5 or C1), 118.7 (C, Ar-C<sub>meta</sub>), 126.7 (C, C<sub>ipso</sub>), 127.1 (CH, Ar-C<sub>ortho</sub>), 132.9 [CH, C7(13) or 8(14)], 133.9 [CH, C8(14) or C7(13)], 141.3 (C, Ar-C<sub>para</sub>), 166.8 (C, CO); GC/MS (EI), (rt = 30.7 min),  $m/z$  (%); significant ions: 388 [(C<sub>21</sub>H<sub>18</sub><sup>37</sup>Cl<sub>2</sub>N<sub>2</sub>O)<sup>+</sup>, 2], 386 [(C<sub>21</sub>H<sub>18</sub><sup>37</sup>Cl<sup>35</sup>ClN<sub>2</sub>O)<sup>+</sup>, 12], 384 [(C<sub>21</sub>H<sub>18</sub><sup>35</sup>Cl<sub>2</sub>N<sub>2</sub>O)<sup>+</sup>, 18], 192 [(C<sub>7</sub>H<sub>4</sub><sup>37</sup>Cl<sub>2</sub>NO)<sup>+</sup>, 10], 190 [(C<sub>7</sub>H<sub>4</sub><sup>37</sup>Cl<sup>35</sup>ClNO)<sup>+</sup>, 63], 188 [(C<sub>7</sub>H<sub>4</sub><sup>35</sup>Cl<sub>2</sub>NO)<sup>+</sup>, 100], 180 (12), 160 (12), 124 (16); HRMS-ESI<sup>+</sup>  $m/z$  [M+H]<sup>+</sup> calcd for [C<sub>21</sub>H<sub>18</sub>Cl<sub>2</sub>N<sub>2</sub>O + H]<sup>+</sup>: 385.0869, found: 385.0875.

6.1.12. (4-Amino-3,5-dichlorophenyl) (3-azahexacyclo[7.6.0.0<sup>1,5</sup>.0<sup>5,12</sup>.0<sup>6,10</sup>.0<sup>11,15</sup>]pentadeca-3-yl)methanone, (**16**)

From amide **15** (200 mg, 0.78 mmol) and Pd/C (24 mg) and following the general procedure D (5 h) a yellow solid (207 mg) was obtained. Column chromatography (Al<sub>2</sub>O<sub>3</sub>, DCM/methanol) gave the desired amide **16** (180 mg, 89% yield) as a white solid, mp 243–244 °C; IR (ATR)  $\nu$ : 3455, 3283, 3238, 3186, 2931, 2865, 1631, 1597, 1545, 1498, 1456, 1425, 1332, 1307, 1269, 1232, 1216, 1118, 1070, 1035, 944, 895, 789, 768, 745, 693, 647, 629 cm<sup>-1</sup>; <sup>1</sup>H NMR (500 MHz, CDCl<sub>3</sub>)  $\delta$ : 1.43–1.60 [complex signal, 8 H, 7(13)-H<sub>2</sub>, 8(14)-H<sub>2</sub>], 2.04 [broad s, 2 H, 6(12)-H or 9(15)-H], 2.12 [broad s, 2 H, 9(15)-H or 6(12)-H], 2.41 [m, 2 H, 10(11)-H], 3.29 (s, 2 H, 2-H<sub>2</sub> or 4-H<sub>2</sub>), 3.53 (s, 2 H, 4-H<sub>2</sub> or 2-H<sub>2</sub>), 7.40 (s, 2 H, Ar-H); <sup>13</sup>C NMR (125.7 MHz, CDCl<sub>3</sub>)  $\delta$ : 21.5 [CH<sub>2</sub>, C7(13) or C8(14)], 21.8 [CH<sub>2</sub>, C8(14) or C7(13)], 40.8 (CH<sub>2</sub>, C2 or C4), 45.5 (CH<sub>2</sub>, C4 or C2), 49.6

[CH, C10(11)], 54.8 [broad CH, C6(12) and C9(15)], 57.9 (C, C1 or C5), 59.6 (C, C5 or C1), 118.8 (C, Ar-C<sub>meta</sub>), 126.9 (C, C<sub>ipso</sub>), 127.2 (CH, Ar-C<sub>ortho</sub>), 141.4 (C, Ar-C<sub>para</sub>), 167.0 (C, CO); MS (EI), (rt = 32.3 min),  $m/z$  (%); significant ions: 392 [(C<sub>21</sub>H<sub>22</sub><sup>37</sup>Cl<sub>2</sub>N<sub>2</sub>O)<sup>+</sup>, 8], 390 [(C<sub>21</sub>H<sub>22</sub><sup>37</sup>Cl<sup>35</sup>ClN<sub>2</sub>O)<sup>+</sup>, 42], 388 [(C<sub>21</sub>H<sub>22</sub><sup>35</sup>Cl<sub>2</sub>N<sub>2</sub>O)<sup>+</sup>, 63], 200 (18), 192 [(C<sub>7</sub>H<sub>4</sub><sup>37</sup>Cl<sub>2</sub>NO)<sup>+</sup>, 11], 190 [(C<sub>7</sub>H<sub>4</sub><sup>37</sup>Cl<sup>35</sup>ClNO)<sup>+</sup>, 64], 188 [(C<sub>7</sub>H<sub>4</sub><sup>35</sup>Cl<sub>2</sub>NO)<sup>+</sup>, 100], 184 (33), 169 (13), 160 (12), 124 (13). Anal. Calcd for C<sub>21</sub>H<sub>22</sub>Cl<sub>2</sub>N<sub>2</sub>O·0.50H<sub>2</sub>O: C 63.32, H 5.82, Cl 17.80, N 7.03. Found: C 63.23, H 5.71, Cl 17.82, N 6.77.

6.1.13. (Cyclohexyl)(octahydro-2H-isoindol-2-yl)methanone, (**17**)

From octahydro-1H-isoindole hydrochloride (300 mg, 2.40 mmol), cyclohexanecarboxylic acid (279 mg, 2.18 mmol), HOBt (442 mg, 3.27 mmol), EDC (506 mg, 3.27 mmol) and triethylamine (0.7 mL, 4.80 mmol) in EtOAc (10 mL) and following the general procedure C, **17** (458 mg, 89% yield) was obtained as a white solid. The analytical sample was obtained by crystallization from hot EtOAc (82 mg), mp 67–68 °C; IR (ATR)  $\nu$ : 734, 890, 973, 1073, 1113, 1136, 1173, 1184, 1307, 1341, 1358, 1443, 1481, 1622, 2851, 2873, 2917 cm<sup>-1</sup>; <sup>1</sup>H NMR (400 MHz, CDCl<sub>3</sub>)  $\delta$ : 1.16–1.30 [complex signal, 3 H, 3-H<sub>ax</sub>, 4-H<sub>ax</sub> and 5-H<sub>ax</sub>], 1.31–1.63 [complex signal, 10 H, 2-H<sub>ax</sub>, 6-H<sub>ax</sub>, 4'-H<sub>2</sub>, 7'-H<sub>2</sub>, 5'-H<sub>2</sub>, 6'-H<sub>2</sub>], 1.64–1.84 [complex signal, 5 H, 2-H<sub>eq</sub>, 6-H<sub>eq</sub>, 3-H<sub>eq</sub>, 4-H<sub>eq</sub> and 5-H<sub>eq</sub>], 2.16 (m, 1 H, 3a'-H or 7a'-H), 2.24 (m, 1 H, 7a'-H or 3a'-H), 2.30 [tt,  $J = 11.6$  Hz,  $J' = 3.6$  Hz, 1 H, 1-H], 3.31 (dd,  $J = 10.0$  Hz,  $J' = 6.0$  Hz, 1 H, 1'-H<sub>a</sub> or 3'-H<sub>a</sub>), 3.36 (dd,  $J = 12.0$  Hz,  $J' = 6.6$  Hz, 1 H, 3'-H<sub>a</sub> or 1'-H<sub>a</sub>), 3.40 (dd,  $J = 12.0$  Hz,  $J' = 7.8$  Hz, 1 H, 3'-H<sub>b</sub> or 1'-H<sub>b</sub>), 3.45 (dd,  $J = 10.0$  Hz,  $J' = 7.0$  Hz, 1 H, 1'-H<sub>b</sub> or 3'-H<sub>b</sub>); <sup>13</sup>C NMR (100.5 MHz, CDCl<sub>3</sub>)  $\delta$ : 22.5 (CH<sub>2</sub>, C5' or C6'), 22.8 (CH<sub>2</sub>, C6' or C5'), 25.73 (CH<sub>2</sub>), 25.78 (CH<sub>2</sub>), 25.80 (CH<sub>2</sub>), 25.84 (CH<sub>2</sub>) and 25.91 (CH<sub>2</sub>) [C4', C7', C3, C4 and C5], 28.8 (CH<sub>2</sub>, C2 or C6), 29.0 (CH<sub>2</sub>, C6 or C2), 35.8 (CH, C3a' or C7a'), 37.6 (CH, C7a' or C3a'), 42.7 (CH, C1), 49.3 (CH<sub>2</sub>, C1' or C3'), 50.4 (CH<sub>2</sub>, C3' or C1'), 175.4 (C, CO). Anal. Calcd for C<sub>15</sub>H<sub>25</sub>NO: C 76.55, H 10.71, N 5.95. Found: 76.56, H 10.67, N 5.96.

6.1.14. (4-Azatricyclo[5.2.1.0<sup>2,6</sup>]dec-8-en-4-yl)(cyclohexyl)methanone, (**18**)

From 4-azatricyclo[5.2.1.0<sup>2,6</sup>]dec-8-ene hydrochloride [58] (240 mg, 1.40 mmol), cyclohexanecarboxylic acid (163 mg, 1.27 mmol), HOBt (258 mg, 1.91 mmol), EDC (296 mg, 1.91 mmol) and triethylamine (0.8 mL, 5.59 mmol) in EtOAc (8 mL) and following the general procedure C, amide **18** (304 mg, 97% yield) was obtained as a yellowish solid. Column chromatography (hexane/EtOAc) gave **18** as a white solid (209 mg), mp 77–78 °C; IR (ATR)  $\nu$ : 702, 731, 761, 793, 897, 987, 1216, 1256, 1332, 1347, 1428, 1621, 2850, 2920 cm<sup>-1</sup>; <sup>1</sup>H NMR (400 MHz, CDCl<sub>3</sub>)  $\delta$ : 1.12–1.29 [complex signal, 3 H, 3-H<sub>ax</sub>, 4-H<sub>ax</sub> and 5-H<sub>ax</sub>], 1.36–1.51 [complex signal, 3 H, 2-H<sub>ax</sub>, 6-H<sub>ax</sub> and 10'-H<sub>a</sub>], 1.54 (dt,  $J = 8.4$  Hz,  $J' = 1.6$  Hz, 1 H, 10'-H<sub>b</sub>), 1.60–1.70 [complex signal, 3 H, 2-H<sub>eq</sub>, 6-H<sub>eq</sub> and 4-H<sub>eq</sub>], 1.71–1.84 [complex signal, 2 H, 3-H<sub>eq</sub> and 5-H<sub>eq</sub>], 2.16 (tt,  $J = 11.6$  Hz,  $J' = 3.6$  Hz, 1 H, 1-H), 2.82–3.00 [complex signal, 4 H, 1'-H, 7'-H, 2'-H and 6'-H], 3.10 (dd,  $J = 10.8$  Hz,  $J' = 3.6$  Hz, 1 H, 3'-H<sub>a</sub> or 5'-H<sub>a</sub>), 3.21 (dd,  $J = 13.5$  Hz,  $J' = 3.6$  Hz, 1 H, 5'-H<sub>a</sub> or 3'-H<sub>a</sub>), 3.29 (dd,  $J = 13.5$  Hz,  $J' = 9.2$  Hz, 1 H, 5'-H<sub>b</sub> or 3'-H<sub>b</sub>), 3.43 (dd,  $J = 10.8$  Hz,  $J' = 9.2$  Hz, 1 H, 3'-H<sub>b</sub> or 5'-H<sub>b</sub>), 6.14 (dd,  $J = 6.0$  Hz,  $J' = 3.2$  Hz, 1 H, 8'-H or 9'-H), 6.19 (dd,  $J = 6.0$  Hz,  $J' = 3.2$  Hz, 1 H, 9'-H or 8'-H); <sup>13</sup>C NMR (100.5 MHz, CDCl<sub>3</sub>)  $\delta$ : 25.8 [CH<sub>2</sub>, C3(5)], 25.9 (CH<sub>2</sub>, C4), 28.69 (CH<sub>2</sub>, C2 or C6), 28.71 (CH<sub>2</sub>, C6 or C2), 42.7 (CH, C1), 43.8 (CH, C2' or C6'), 45.9 (CH, C6' or C2'), 46.66 (CH, C1' or C7'), 46.70 (CH, C7' or C1'), 48.0 (CH<sub>2</sub>, C3' or C5'), 48.8 (CH<sub>2</sub>, C5' or C3'), 51.9 (CH<sub>2</sub>, C10'), 134.7 (CH, C8' or C9'), 136.1 (CH, C9' or C8'), 173.9 (C, CO). Anal. Calcd for C<sub>16</sub>H<sub>23</sub>NO: C 78.32, H 9.45, N 5.71. Found: 78.03, H 9.41, N 5.58.

**6.1.15. (4-Azatricyclo[5.2.1.0<sup>2,6</sup>]dec-4-yl)(cyclohexyl)methanone, (19)**

From amide **18** (177 mg) and Pd/C (36 mg) and following the general procedure D (18 h), amide **19** (156 mg, 88% yield) was obtained as a white solid, mp 83–84 °C; IR (ATR)  $\nu$ : 611, 625, 642, 886, 1002, 1133, 1170, 1187, 1204, 1218, 1290, 1327, 1344, 1357, 1425, 1446, 1623, 2871, 2936, 2945 cm<sup>-1</sup>; <sup>1</sup>H NMR (400 MHz, CDCl<sub>3</sub>)  $\delta$ : 1.20–1.94 (complex signal, 16 H, 3-H<sub>2</sub>, 4-H<sub>2</sub>, 5-H<sub>2</sub>, 2-H<sub>2</sub>, 6-H<sub>2</sub>, 8'-H<sub>2</sub>, 9'-H<sub>2</sub> and 10'-H<sub>2</sub>), 2.18–2.27 (complex signal, 2 H, 1'-H and 7'-H), 2.37 (tt,  $J$  = 11.6 Hz,  $J'$  = 3.2 Hz, 1 H, 1-H), 2.52 (m, 1 H, 2'-H or 6'-H), 2.60 (m, 1 H, 6'-H or 2'-H), 3.03 (dd,  $J$  = 13.2 Hz,  $J'$  = 8.4 Hz, 1 H, 3'-H<sub>a</sub> or 5'-H<sub>a</sub>), 3.26 (dd,  $J$  = 11.6 Hz,  $J'$  = 7.6 Hz, 1 H, 5'-H<sub>a</sub> or 3'-H<sub>a</sub>), 3.57 (dd,  $J$  = 11.6 Hz,  $J'$  = 1.6 Hz, 1 H, 5'-H<sub>b</sub> or 3'-H<sub>b</sub>), 3.84 (dd,  $J$  = 13.2 Hz,  $J'$  = 1.6 Hz, 1 H, 3'-H<sub>b</sub> or 5'-H<sub>b</sub>); <sup>13</sup>C NMR (100.5 MHz, CDCl<sub>3</sub>)  $\delta$ : 22.1 (CH<sub>2</sub>, C8' or C9'), 22.8 (CH<sub>2</sub>, C9' or C8'), 25.79 (CH<sub>2</sub>), 25.86 (CH<sub>2</sub>) and 25.88 (CH<sub>2</sub>) (C3, C4 and C5), 28.87 (CH<sub>2</sub>, C2 or C6), 28.89 (CH<sub>2</sub>, C6 or C2), 41.2 (CH, C1' or C7'), 41.4 (CH, C7' or C1'), 42.0 (CH<sub>2</sub>, C2' or C6'), 42.1 (CH<sub>2</sub>, C10'), 42.9 (CH, C1), 44.0 (CH<sub>2</sub>, C6' or C2'), 45.7 (CH<sub>2</sub>, C3' or C5'), 46.9 (CH<sub>2</sub>, C5' or C3'), 174.4 (C, CO). Anal. Calcd for C<sub>16</sub>H<sub>25</sub>NO: 77.68, H 10.19, N 5.66. Found: C 77.55, H 10.05, N 5.54.

**6.1.16. (4-Azatricyclo[5.2.2.0<sup>2,6</sup>]undec-8-en-4-yl)(cyclohexyl)methanone, (20)**

From 4-azatricyclo[5.2.2.0<sup>2,6</sup>]undec-8-ene hydrochloride [59] (300 mg), 1.62 mmol), cyclohexanecarboxylic acid (188 mg, 1.47 mmol), HOBt (300 mg, 2.21 mmol), EDC (342 mg, 2.21 mmol) and triethylamine (0.9 mL, 6.47 mmol) in EtOAc (10 mL) and following the general procedure C, amide **20** (323 mg, 85% yield) was obtained as a yellowish solid. Column chromatography (hexane/EtOAc) gave **20** as a white solid (205 mg), mp 86–87 °C; IR (ATR)  $\nu$ : 703, 715, 849, 887, 986, 1044, 1132, 1165, 1216, 1239, 1307, 1347, 1357, 1375, 1431, 1625, 2850, 2921, 3037 cm<sup>-1</sup>; <sup>1</sup>H NMR (400 MHz, CDCl<sub>3</sub>)  $\delta$ : 1.15–1.34 (complex signal, 5 H, 10'-H<sub>ax</sub>, 11'-H<sub>ax</sub>, 3-H<sub>ax</sub>, 4-H<sub>ax</sub> and 5-H<sub>ax</sub>), 1.37–1.54 (complex signal, 4 H, 2-H<sub>ax</sub>, 6-H<sub>ax</sub>, 10'-H<sub>eq</sub>, 11'-H<sub>eq</sub>), 1.58–1.86 (complex signal, 5 H, 2-H<sub>eq</sub>, 6-H<sub>eq</sub>, 3-H<sub>eq</sub>, 4-H<sub>eq</sub> and 5-H<sub>eq</sub>), 2.23 (tt,  $J$  = 11.6 Hz,  $J'$  = 3.6 Hz, 1 H, 1-H), 2.42 (m, 1 H, 2'-H or 6'-H), 2.51–2.61 (complex signal, 3 H, 1'-H, 7'-H, 6'-H or 2'-H), 3.09 (d,  $J$  = 12.8 Hz, 1 H, 3'-H<sub>a</sub> or 5'-H<sub>a</sub>), 3.11 (d,  $J$  = 12.4 Hz, 1 H, 5'-H<sub>a</sub> and 3'-H<sub>a</sub>), 3.62 (dd,  $J$  = 12.4 Hz,  $J'$  = 9.2 Hz, 1 H, 5'-H<sub>b</sub> or 3'-H<sub>b</sub>), 3.65 (dd,  $J$  = 12.8 Hz,  $J'$  = 9.6 Hz, 1 H, 3'-H<sub>b</sub> and 5'-H<sub>b</sub>), 6.15–6.26 (complex signal, 2 H, 8'-H and 9'-H); <sup>13</sup>C NMR (100.5 MHz, CDCl<sub>3</sub>)  $\delta$ : 24.2 (CH<sub>2</sub>, C10' or C11'), 24.3 (CH<sub>2</sub>, C11' or C10'), 25.81 (CH<sub>2</sub>), 25.84 (CH<sub>2</sub>) and 25.9 (CH<sub>2</sub>) [C3, C4 and C5], 28.7 (CH<sub>2</sub>, C2 or C6), 28.8 (CH<sub>2</sub>, C6 or C2), 34.1 (CH, C1' and C7'), 41.9 (CH, C2' or C6'), 42.6 (CH, C1), 44.0 (CH, C6' or C2'), 50.8 (CH<sub>2</sub>, C3' or C5'), 51.6 (CH<sub>2</sub>, C5' or C3'), 132.9 (CH, C8' or C9'), 134.3 (CH, C9' or C8'), 173.9 (C, CO). Anal. Calcd for C<sub>17</sub>H<sub>25</sub>NO: C 78.72, 9.71, N 5.40. Found: C 78.82, H 9.71, N 5.30.

**6.1.17. (4-Azatricyclo[5.2.2.0<sup>2,6</sup>]undec-4-yl)(cyclohexyl)methanone, (21)**

From amide **20** (165 mg) and Pd/C (33 mg) and following the general procedure D (18 h) amide **21** (151 mg, 91% yield) was obtained as a white solid, mp 78–79 °C; IR (ATR)  $\nu$ : 622, 725, 868, 976, 1138, 1173, 1204, 1346, 1429, 1443, 1622, 2861, 2901, 2923 cm<sup>-1</sup>; <sup>1</sup>H NMR (400 MHz, CDCl<sub>3</sub>)  $\delta$ : 1.18–1.42 (complex signal, 5 H, 3-H<sub>ax</sub>, 4-H<sub>ax</sub>, 5-H<sub>ax</sub>, 8'-H<sub>ax</sub> and 9'-H<sub>ax</sub>), 1.44–1.90 (complex signal, 15 H, 3-H<sub>eq</sub>, 4-H<sub>eq</sub>, 5-H<sub>eq</sub>, 2-H<sub>2</sub>, 6-H<sub>2</sub>, 1'-H, 7'-H, 8'-H<sub>eq</sub>, 9'-H<sub>eq</sub>, 10'-H<sub>2</sub> and 11'-H<sub>2</sub>), 2.33 (m, 1 H, 2'-H or 6'-H), 2.37 (tt,  $J$  = 11.2 Hz,  $J'$  = 3.4 Hz, 1 H, 1-H), 2.43 (m, 1 H, 6'-H and 2'-H), 3.44–3.65 (complex signal, 4 H, 3'-H<sub>2</sub> and 5'-H<sub>2</sub>); <sup>13</sup>C NMR (100.5 MHz, CDCl<sub>3</sub>)  $\delta$ : 19.8 (CH<sub>2</sub>, C9' or C8'), 20.1 (CH<sub>2</sub>, C8' or C9'), 25.7 (CH, C1' and

C7'), 25.81 (CH<sub>2</sub>), 25.86 (CH<sub>2</sub>) and 25.91 (CH<sub>2</sub>) (C3, C4 and C5), 27.8 (CH<sub>2</sub>, C11' or C10'), 28.0 (CH<sub>2</sub>, C10' or C11'), 28.86 (CH<sub>2</sub>, C2 or C6), 28.92 (CH<sub>2</sub>, C6 or C2), 37.8 (CH<sub>2</sub>, C2' or C6'), 40.0 (CH<sub>2</sub>, C6' or C2'), 42.8 (CH, C1), 49.1 (CH<sub>2</sub>, C3' or C5'), 49.9 (CH<sub>2</sub>, C5' or C3'), 174.3 (C, CO). Anal. Calcd for C<sub>17</sub>H<sub>27</sub>NO: C 78.11, H 10.41, N 5.36. Found: C 78.14, H 10.35, N 5.14.

**6.1.18. (4-Azatetracyclo[5.3.2.0<sup>2,6</sup>.0<sup>8,10</sup>]dodec-11-en-4-yl)(cyclohexyl)methanone, (22)**

From 4-azatetracyclo[5.3.2.0<sup>2,6</sup>.0<sup>8,10</sup>]dodec-11-ene hydrochloride [40] (2.06 g, 10.6 mmol), cyclohexanecarboxylic acid (1.24 g, 9.67 mmol), HOBt (1.96 g, 14.5 mmol), EDC (2.25 g, 14.5 mmol) and triethylamine (5.9 mL, 42.5 mmol) in EtOAc (150 mL) and following the general procedure C, amide **22** (2.43 g, 94% yield) was obtained as a yellowish solid. The analytical sample was obtained by crystallization from hot EtOAc (2.04 g), mp 96–97 °C; IR (ATR)  $\nu$ : 560, 570, 587, 696, 718, 741, 767, 812, 829, 847, 894, 915, 942, 963, 991, 1036, 1089, 1134, 1167, 1209, 1217, 1242, 1272, 1299, 1361, 1380, 1432, 1624, 2849, 2925, 3002, 3040 cm<sup>-1</sup>; <sup>1</sup>H NMR (400 MHz, CDCl<sub>3</sub>)  $\delta$ : 0.12–0.16 (complex signal, 2 H, 9'-H<sub>2</sub>), 0.86–0.96 (complex signal, 2 H, 8'-H and 10'-H), 1.14–1.29 (complex signal, 3 H, 3-H<sub>ax</sub>, 4-H<sub>ax</sub> and 5-H<sub>ax</sub>), 1.36–1.53 (complex signal, 2 H, 2-H<sub>ax</sub> and 6-H<sub>ax</sub>), 1.60–1.70 (complex signal, 3 H, 2-H<sub>eq</sub>, 4-H<sub>eq</sub> and 6-H<sub>eq</sub>), 1.72–1.80 (complex signal, 2 H, 3-H<sub>eq</sub> and 5-H<sub>eq</sub>), 2.21 (tt,  $J$  = 11.6 Hz,  $J'$  = 3.4 Hz, 1 H, 1-H), 2.55 (dm,  $J$  = 12.8 Hz, 1 H, 2'-H or 6'-H), 2.67 (dm,  $J$  = 12.8 Hz, 1 H, 6'-H or 2'-H), 2.81–2.87 (complex signal, 2 H, 1'-H and 7'-H), 3.12 (dd,  $J$  = 11.0 Hz,  $J'$  = 5.0 Hz, 1 H, 3'-H<sub>a</sub> or 5'-H<sub>a</sub>), 3.15 (dd,  $J$  = 13.2 Hz,  $J'$  = 5.6 Hz, 1 H, 5'-H<sub>a</sub> or 3'-H<sub>a</sub>), 3.55 (t,  $J$  = 10.0 Hz, 1 H, 5'-H<sub>b</sub> or 3'-H<sub>b</sub>), 3.58 (t,  $J$  = 8.8 Hz, 1 H, 3'-H<sub>b</sub> or 5'-H<sub>b</sub>), 5.73 (ddd,  $J$  = 14.4 Hz,  $J'$  = 8.4 Hz,  $J''$  = 2.0 Hz, 1 H, 11'-H or 12'-H), 5.77 (ddd,  $J$  = 14.4 Hz,  $J'$  = 8.4 Hz,  $J''$  = 2.0 Hz, 1 H, 12'-H or 11'-H); <sup>13</sup>C NMR (100.5 MHz, CDCl<sub>3</sub>)  $\delta$ : 4.1 (CH<sub>2</sub>, C9'), 10.0 (CH, C8' or C10'), 10.2 (CH, C10' or C8'), 25.80 (CH<sub>2</sub>), 25.83 (CH<sub>2</sub>) and 25.9 (CH<sub>2</sub>) [C3, C4 and C5], 28.7 (CH<sub>2</sub>, C2 or C6), 28.8 (CH<sub>2</sub>, C6 or C2), 35.6 (CH, C1' or C7'), 35.7 (CH, 7' or C1'), 42.6 (CH, C1), 42.7 (CH, C2' or C6'), 44.8 (CH, C6' or C2'), 49.6 (CH<sub>2</sub>, C3' or C5'), 50.6 (CH<sub>2</sub>, C5' or C3'), 128.1 (CH, C11' or C12'), 129.6 (CH, C12' or C11'), 174.1 (C, CO). Anal. Calcd for C<sub>18</sub>H<sub>25</sub>NO: C 79.66, H 9.29, N 5.16. Found: C 79.64, H 9.24, N 5.21.

**6.1.19. (4-Azatetracyclo[5.3.2.0<sup>2,6</sup>.0<sup>8,10</sup>]dodec-4-yl)(cyclohexyl)methanone, (23)**

From **22** (500 mg) and Pd/C (100 mg) and following the general procedure D (72 h) amide **23** (426 mg, 83% yield) was obtained as a white solid, mp 74–75 °C; IR (ATR)  $\nu$ : 651, 679, 707, 729, 748, 789, 805, 826, 839, 865, 885, 950, 961, 988, 1016, 1030, 1082, 1113, 1133, 1171, 1205, 1213, 1234, 1264, 1295, 1325, 1346, 1358, 1427, 1471, 1486, 1623, 2846, 2897, 2928, 3009, cm<sup>-1</sup>; <sup>1</sup>H NMR (400 MHz, CDCl<sub>3</sub>)  $\delta$ : 0.45 (dt,  $J$  = 6.0 Hz,  $J'$  = 8.0 Hz, 1 H, 9'-H<sub>a</sub>), 0.78 (m,  $J$  = 6.0 Hz,  $J'$  = 3.6 Hz, 1 H, 9'-H<sub>b</sub>), 0.90–0.96 (complex signal, 2 H, 8'-H and 10'-H), 1.00–1.14 (complex signal, 2 H, 11'-H<sub>ax</sub> and 12'-H<sub>ax</sub>), 1.17–1.34 [complex signal, 5 H, 11'-H<sub>eq</sub>, 12'-H<sub>eq</sub>, 3-H<sub>ax</sub>, 4-H<sub>ax</sub> and 5-H<sub>ax</sub>], 1.42–1.61 (complex signal, 2 H, 2-H<sub>ax</sub> and 6-H<sub>ax</sub>), 1.67 (m, 1 H, 4'-H<sub>eq</sub>), 1.69–1.83 (complex signal, 4 H, 3-H<sub>eq</sub>, 4-H<sub>eq</sub>, 5-H<sub>eq</sub>, 6-H<sub>eq</sub>), 1.84–1.91 (complex signal, 2 H, 1'-H and 7'-H), 2.38 [tt,  $J$  = 11.6 Hz,  $J'$  = 3.6 Hz, 1 H, 1-H], 2.50 (dm,  $J$  = 12.8 Hz, 1 H, 2'-H or 6'-H), 2.55 (dm,  $J$  = 12.8 Hz, 1 H, 6'-H or 2'-H), 3.32 (dd,  $J$  = 12.8 Hz,  $J'$  = 8.8 Hz, 1 H, 3'-H<sub>a</sub> or 5'-H<sub>a</sub>), 3.52 (m, 2 H, 5'-H<sub>2</sub> or 3'-H<sub>2</sub>), 3.76 (dd,  $J$  = 12.8 Hz,  $J'$  = 3.0 Hz, 1 H, 3'-H<sub>b</sub> or 5'-H<sub>b</sub>); <sup>13</sup>C NMR (100.5 MHz, CDCl<sub>3</sub>)  $\delta$ : 4.7 (CH<sub>2</sub>, C9'), 14.9 (CH, C8' or C10'), 15.1 (CH, C10' or C8'), 17.3 (CH<sub>2</sub>, C11' or C12'), 17.9 (CH<sub>2</sub>, C12' or C11'), 25.8 (CH<sub>2</sub>, C4), 25.9 [CH<sub>2</sub>, C3(5)], 28.87 (CH<sub>2</sub>, C2 or C6), 28.92 (CH<sub>2</sub>, C6 or C2), 29.0 (CH, C1' or C7'), 29.4 (CH, C7' or C1'), 38.4 (CH, C2' or C6'), 40.5 (CH, C6' or C2'), 42.7 (CH, C1), 48.1

(CH, C3' or C5'), 49.3 (CH<sub>2</sub>, C5' or C3'), 174.4 (C, CO). Anal. Calcd for C<sub>18</sub>H<sub>27</sub>NO: C 79.07, H 9.95, N 5.12. Found: 79.15, H 9.88, N 5.29.

**6.1.20. (4-Azatetracyclo[5.4.2.0<sup>2,6</sup>.0<sup>8,11</sup>]trideca-9,12-dien-4-yl)(cyclohexyl)methanone, (24)**

From 4-azatetracyclo[5.4.2.0<sup>2,6</sup>.0<sup>8,11</sup>]trideca-9,12-diene hydrochloride [40] (139 mg, 0.66 mmol), cyclohexanecarboxylic acid (77 mg, 0.60 mmol), HOBt (122 mg, 0.90 mmol), EDC (139 mg, 0.90 mmol) and triethylamine (0.4 mL, 2.64 mmol) in EtOAc (6 mL) and following the general procedure C, amide **24** (151 mg, 80% yield) was obtained as a yellowish solid. The analytical sample was obtained by crystallization from hot EtOAc (97 mg), mp 120–121 °C; IR (ATR)  $\nu$ : 730, 760, 788, 808, 967, 994, 1173, 1187, 1214, 1235, 1294, 1361, 1442, 1463, 1617, 2860, 2901, 2922 cm<sup>-1</sup>; <sup>1</sup>H NMR (400 MHz, CDCl<sub>3</sub>)  $\delta$ : 1.15–1.30 [complex signal, 3 H, 3-H<sub>ax</sub>, 4-H<sub>ax</sub> and 5-H<sub>ax</sub>], 1.38–1.54 [complex signal, 2 H, 2-H<sub>ax</sub> and 6-H<sub>ax</sub>], 1.60–1.72 (complex signal, 3 H, 2-H<sub>eq</sub>, 4-H<sub>eq</sub> and 6-H<sub>eq</sub>), 1.73–1.82 (complex signal, 2 H, 3-H<sub>eq</sub> and 5-H<sub>eq</sub>), 2.24 [tt,  $J = 11.6$  Hz,  $J' = 3.6$  Hz, 1 H, 1-H], 2.37 (tdd,  $J = 9.6$  Hz,  $J' = 5.8$  Hz,  $J'' = 2.8$  Hz, 1 H, 2'-H or 6'-H), 2.50 (tdd,  $J = 8.8$  Hz,  $J' = 5.6$  Hz,  $J'' = 2.8$  Hz, 1 H, 6'-H or 2'-H), 2.60–2.66 (complex signal, 2 H, 1'-H and 7'-H), 2.67–2.70 (complex signal, 2 H, 8'-H and 11'-H), 3.17–3.24 (complex signal, 2 H, 3'-H<sub>a</sub> and 5'-H<sub>a</sub>), 3.63–3.73 (complex signal, 2 H, 3'-H<sub>b</sub> and 5'-H<sub>b</sub>), 5.84–5.87 (complex signal, 2 H, 9'-H and 10'-H), 5.89–5.99 (complex signal, 2 H, 12'-H and 13'-H); <sup>13</sup>C NMR (100.5 MHz, CDCl<sub>3</sub>)  $\delta$ : 25.81 (CH<sub>2</sub>), 25.84 (CH<sub>2</sub>) and 25.9 (CH<sub>2</sub>) (C3, C4 and C5), 28.7 (CH<sub>2</sub>, C2 or C6), 28.8 (CH<sub>2</sub>, C6 or C2), 39.36 (CH, C1' or C7'), 39.37 (CH, C7' or C1'), 41.1 (CH, C2' or C6'), 42.6 (CH, C1), 43.2 (CH, C6' or C2'), 44.9 (CH, C8' or C11'), 45.1 (CH, C11' or C8'), 50.7 (CH<sub>2</sub>, C3' or C5'), 51.5 (CH<sub>2</sub>, C5' or C3'), 129.0 (CH, C12' or C13'), 130.3 (CH, C13' or C12'), 137.7 (CH, C9' or C10'), 138.0 (CH, C10' or C9'), 174.0 (C, CO). Anal. Calcd for C<sub>19</sub>H<sub>25</sub>NO: C 80.52, H 8.89, N 4.94. Found: 80.31, H 8.81, N 4.97.

**6.1.21. (4-Azatetracyclo[5.4.2.0<sup>2,6</sup>.0<sup>8,11</sup>]tridec-4-yl)(cyclohexyl)methanone, (25)**

From 4-azatetracyclo[5.4.2.0<sup>2,6</sup>.0<sup>8,11</sup>]tridecane hydrochloride [40] (235 mg, 1.10 mmol), cyclohexanecarboxylic acid (128 mg, 1.0 mmol), HOBt (203 mg, 1.50 mmol), EDC (232 mg, 1.50 mmol) and triethylamine (0.6 mL, 4.40 mmol) in EtOAc (10 mL) and following the general procedure C, amide **25** (253 mg, 80% yield) was obtained as a yellowish solid. The analytical sample was obtained by crystallization from hot EtOAc (110 mg), mp 115–116 °C; IR (ATR)  $\nu$ : 658, 731, 887, 988, 1133, 1172, 1204, 1236, 1357, 1434, 1440, 1621, 2908, 2925 cm<sup>-1</sup>; <sup>1</sup>H NMR (400 MHz, CDCl<sub>3</sub>)  $\delta$ : 1.18–1.34 (complex signal, 3 H, 3-H<sub>ax</sub>, 4-H<sub>ax</sub> and 5-H<sub>ax</sub>), 1.42–1.62 (complex signal, 6 H, 1'-H, 7'-H, 2-H<sub>ax</sub>, 6-H<sub>ax</sub>, 12'-H<sub>a</sub> and 13'-H<sub>a</sub>), 1.64–1.92 (complex signal, 7 H, 2-H<sub>eq</sub>, 6-H<sub>eq</sub>, 3-H<sub>eq</sub>, 4-H<sub>eq</sub>, 5-H<sub>eq</sub>, 12'-H<sub>b</sub> and 13'-H<sub>b</sub>), 2.02–2.20 (complex signal, 5 H, 2'-H or 6'-H, 9'-H<sub>a</sub>, 9'-H<sub>b</sub>, 10'-H<sub>a</sub> and 10'-H<sub>b</sub>), 2.27 (m, 1 H, 6'-H or 2'-H), 2.34–2.44 (complex signal, 3 H, 1-H, 8'-H and 11'-H), 3.48–3.70 (complex signal, 4 H, 3'-H<sub>2</sub> and 5'-H<sub>2</sub>); <sup>13</sup>C NMR (100.5 MHz, CDCl<sub>3</sub>)  $\delta$ : 15.0 (CH<sub>2</sub>, C12' or C13'), 15.3 (CH<sub>2</sub>, C13' or C12'), 20.8 [CH<sub>2</sub>, C9'(10')], 25.82 (CH<sub>2</sub>), 25.88 (CH<sub>2</sub>) and 25.92 (CH<sub>2</sub>) (C3, C4 and C5), 28.88 (CH<sub>2</sub>, C2 or C6), 28.95 (CH<sub>2</sub>, C6 or C2), 31.2 (CH, C1' or C7'), 31.5 (CH, C7' or C1'), 36.37 (CH, C8' or C11'), 36.44 (CH, C11' or C8'), 37.4 (CH, C2' or C6'), 39.5 (CH, C6' or C2'), 42.8 (CH, C1), 48.8 (CH<sub>2</sub>, C3' or C5'), 49.7 (CH<sub>2</sub>, C5' or C3'), 174.4 (C, CO). Anal. Calcd for C<sub>19</sub>H<sub>29</sub>NO: C 79.39, H 10.17, N 4.87. Found: C 79.20, H 10.30, N 4.72.

**6.1.22. (12-Azatricyclo[4.4.3.0<sup>1,6</sup>]trideca-3,8-dien-12-yl)(cyclohexyl)methanone, (26)**

From 12-azatricyclo[4.4.3.0<sup>1,6</sup>]trideca-3,8-diene hydrochloride [41] (150 mg, 0.71 mmol), cyclohexanecarboxylic acid (82 mg, 0.64 mmol), HOBt (131 mg, 0.97 mmol), EDC (150 mg, 0.97 mmol) and triethylamine (0.4 mL, 2.82 mmol) in EtOAc (6 mL) and following general procedure C, amide **26** (185 mg, 92% yield) was obtained as a yellowish solid. The analytical sample was obtained by crystallization from hot EtOAc (106 mg), mp 116–117 °C; IR (ATR)  $\nu$ : 605, 676, 739, 813, 865, 1004, 1187, 1207, 1224, 1332, 1347, 1427, 1629, 2858, 2918 cm<sup>-1</sup>; <sup>1</sup>H NMR (400 MHz, CDCl<sub>3</sub>)  $\delta$ : 1.16–1.31 (complex signal, 3 H, 3(5)-H<sub>ax</sub> and 4-H<sub>ax</sub>), 1.51 [m, 2 H, 2(6)-H<sub>ax</sub>], 1.62–1.84 [complex signal, 5 H, 2(6)-H<sub>eq</sub>, 3(5)-H<sub>eq</sub> and 4-H<sub>eq</sub>], 1.92–2.10 [complex signal, 8 H, 2'(10')-H<sub>2</sub> and 5'(7')-H<sub>2</sub>], 2.29 [tt,  $J = 11.6$  Hz,  $J' = 3.6$  Hz, 1 H, 1-H], 3.35–3.37 (complex signal, 4 H, 3'-H<sub>a</sub>, 3'-H<sub>b</sub>, 5'-H<sub>a</sub> and 5'-H<sub>b</sub>), 5.48–5.57 [complex signal, 4 H, 3'(9')-H and 4'(8')-H]; <sup>13</sup>C NMR (100.5 MHz, CDCl<sub>3</sub>)  $\delta$ : 25.8 (CH<sub>2</sub>, C4), 25.9 [CH<sub>2</sub>, C3(5)], 28.9 [CH<sub>2</sub>, C2(6)], 32.1 [CH<sub>2</sub>, C2'(10') or C5'(7')], 32.2 [CH<sub>2</sub>, C5'(7') or C2'(10')], 37.3 (C, C1' or C6'), 39.2 (C, C6' or C1'), 42.6 (CH, C1), 55.3 (CH<sub>2</sub>, C11' or C13'), 56.1 (CH<sub>2</sub>, C13' or C11'), 123.3 (CH, C3' and C9'), 123.9 (CH, C4' and C8'), 176.3 (C, CO); HRMS-ESI +  $m/z$  [M+H]<sup>+</sup> calcd for [C<sub>19</sub>H<sub>27</sub>NO + H]<sup>+</sup>: 286.2165, found: 286.2176.

**6.1.23. (12-Azatricyclo[4.4.3.0<sup>1,6</sup>]tridec-12-yl)(cyclohexyl)methanone, (27)**

From **26** (362 mg) and Pd/C (72 mg) and following the general procedure D (24 h), amide **27** (330 mg, 90% yield) was obtained as a white solid. The analytical sample was obtained by crystallization from hot EtOAc (178 mg), mp 160–161 °C; IR (ATR)  $\nu$ : 670, 764, 874, 891, 976, 1157, 1290, 1343, 1360, 1435, 1623, 1635, 2850, 2907, 2921 cm<sup>-1</sup>; <sup>1</sup>H NMR (400 MHz, CDCl<sub>3</sub>)  $\delta$ : 1.18–1.29 [complex signal, 3 H, 3(5)-H<sub>ax</sub> and 4-H<sub>ax</sub>], 1.31–1.62 [complex signal, 18 H, 2'(6)-H<sub>ax</sub>, 3'(9')-H<sub>2</sub>, 4'(8')-H<sub>2</sub>, 5'(7')-H<sub>2</sub>, 10'(13')-H<sub>2</sub>], 1.64–1.84 [complex signal, 5 H, 2(6)-H<sub>eq</sub>, 3(5)-H<sub>eq</sub> and 4-H<sub>eq</sub>], 2.30 [tt,  $J = 11.6$  Hz,  $J' = 3.6$  Hz, 1 H, 1-H], 2.70–3.90 (complex signal, 4 H, 3'-H<sub>2</sub> and 5'-H<sub>2</sub>); <sup>13</sup>C NMR (100.5 MHz, CDCl<sub>3</sub>)  $\delta$ : 21.6 [CH<sub>2</sub>, C3'(9') or C4'(8')], 21.8 [CH<sub>2</sub>, C4'(8') or C3'(9')], 25.8 (CH<sub>2</sub>, C4), 25.9 [CH<sub>2</sub>, C3(5)], 28.9 [CH<sub>2</sub>, C2(6)], 39.8 (C, C1' and C6'), 41.7 [CH<sub>2</sub>, C2'(10') and C5'(7')], 42.6 (CH, C1), 55.1 (CH<sub>2</sub>, C11' or C13'), 55.8 (CH<sub>2</sub>, C13' or C11'), 176.0 (C, CO). Anal. Calcd for C<sub>19</sub>H<sub>31</sub>NO: C 78.84, H 10.80, N 4.84. Found: 78.83, H 10.74, N 4.75.

**6.1.24. (3,4,8,9-Tetramethyl-12-azatricyclo[4.4.3.0<sup>1,6</sup>]trideca-3,8-dien-12-yl)(cyclohexyl)methanone, (28)**

From 3,4,8,9-tetramethyl-12-azatricyclo[4.4.3.0<sup>1,6</sup>]trideca-3,8-diene hydrochloride [41] (136 mg, 0.51 mmol), cyclohexanecarboxylic acid (62 mg, 0.48 mmol), HOBt (111 mg, 0.82 mmol), EDC (127 mg, 0.82 mmol) and triethylamine (0.3 mL, 2.38 mmol) in EtOAc (6 mL) and following the general procedure C, amide **28** (138 mg, 79% yield) was obtained as a yellowish solid. Column chromatography (hexane/EtOAc) gave **28** as a white solid (74 mg), mp 162–163 °C; IR (ATR)  $\nu$ : 748, 785, 848, 973, 1118, 1358, 1434, 1441, 1603, 1613, 2861, 2931 cm<sup>-1</sup>; <sup>1</sup>H NMR (400 MHz, CDCl<sub>3</sub>)  $\delta$ : 1.40–1.54 [complex signal, 3 H, 3(5)-H<sub>ax</sub> and 4-H<sub>ax</sub>], 1.56 (s, 12 H, CH<sub>3</sub>), 1.62–1.98 [complex signal, 15 H, 3(5)-H<sub>eq</sub>, 4-H<sub>eq</sub>, 2-H<sub>2</sub>, 6-H<sub>2</sub>, 2'(10')-H<sub>2</sub>, 5'(7')-H<sub>2</sub>], 2.28 (tt, 1 H,  $J = 11.6$  Hz,  $J' = 3.2$  Hz, 1 H, 1-H), 3.28–3.34 (complex signal, 4 H, 11'-H<sub>2</sub> and 13'-H<sub>2</sub>); <sup>13</sup>C NMR (100.5 MHz, CDCl<sub>3</sub>)  $\delta$ : 18.68 [CH<sub>3</sub>, H<sub>3</sub>C-C3'(9') or H<sub>3</sub>C-C4'(8')], 18.71 [CH<sub>3</sub>, H<sub>3</sub>C-C4'(8') or H<sub>3</sub>C-C3'(9')], 25.8 (CH<sub>2</sub>, C4), 25.9 [CH<sub>2</sub>, C3(5)], 28.9 [CH<sub>2</sub>, C2(6)], 38.6 (CH<sub>2</sub>, C1' or C6'), 38.7 [CH<sub>2</sub>, C2'(10') or C5'(7')], 38.8 [CH<sub>2</sub>, C5'(7') or C2'(10')], 40.4 (CH<sub>2</sub>, C6' or C1'), 42.6 (CH, C1), 55.5 (CH<sub>2</sub>, C11' or C13'), 56.4 (CH<sub>2</sub>, C13' or C11'), 121.6 [C,

C3'(9') or C4'(8'), 122.2 (C, C4'(8') or C3'(9')), 176.4 (C, CO); HRMS-ESI +  $m/z$   $[M+H]^+$  calcd for  $[C_{23}H_{36}NO + H]^+$ : 342.2791, found: 342.2793.

6.1.25. (7,8,9,10-Tetramethyl-3-azapentacyclo[7.2.1.1<sup>5,8</sup>.0<sup>1,5</sup>.0<sup>7,10</sup>]tridec-3-yl) (cyclohexyl) methanone, (29)

From 7,8,9,10-tetramethyl-3-azapentacyclo[7.2.1.1<sup>5,8</sup>.0<sup>1,5</sup>.0<sup>7,10</sup>]tridecane hydrochloride [40] (145 mg, 0.54 mmol), cyclohexanecarboxylic acid (67 mg, 0.52 mmol), HOBt (105 mg, 0.78 mmol), EDC (121 mg, 0.78 mmol) and triethylamine (0.3 mL, 2.29 mmol) in EtOAc (6 mL) and following the general procedure C, amide **29** (143 mg, 78% yield) was obtained as a yellowish solid. Column chromatography (hexane/EtOAc) gave **29** as a white solid (101 mg), mp 100–101 °C; IR (ATR)  $\nu$ : 636, 747, 791, 829, 866, 891, 977, 1026, 1083, 1124, 1207, 1243, 1266, 1346, 1382, 1442, 1625, 2857, 2925  $cm^{-1}$ ;  $^1H$  NMR (400 MHz,  $CDCl_3$ )  $\delta$ : 0.84 [dd,  $J = 10.8$  Hz,  $J' = 4.8$  Hz, 4 H, 6'(13')-H<sub>2</sub> or 11'(12')-H<sub>2</sub>], 0.93 (d,  $J = 3.6$  Hz, 12 H, 7'(8')-CH<sub>3</sub> and 9'(10')-CH<sub>3</sub>), 1.18–1.34 [complex signal, 3 H, 3(5)-H<sub>ax</sub> and 4-H<sub>ax</sub>], 1.52 (m, 2 H, 2(6)-H<sub>ax</sub>), 1.64–1.84 [complex signal, 9 H, 3(5)-H<sub>eq</sub>, 4-H<sub>eq</sub>, 2(6)-H<sub>ax</sub> and 11'(12')-H<sub>2</sub> or 6'(13')-H<sub>2</sub>], 2.35 (tt, 1 H,  $J = 11.6$  Hz,  $J' = 3.2$  Hz, 1 H, 1-H), 3.59 (d,  $J = 15.6$  Hz, 4 H, 2'-H<sub>2</sub> and 4'-H<sub>2</sub>);  $^{13}C$  NMR (100.5 MHz,  $CDCl_3$ )  $\delta$ : 15.5 [CH<sub>3</sub>, H<sub>3</sub>C-C7'(8') or H<sub>3</sub>C-C9'(10')], 15.6 [CH<sub>3</sub>, H<sub>3</sub>C-C9'(10') or H<sub>3</sub>C-C7'(8')], 25.8 (CH<sub>2</sub>, C4), 25.9 [CH<sub>2</sub>, C3(5)], 29.0 [CH<sub>2</sub>, C2(6)], 42.4 (CH, C1), 42.9 [CH<sub>2</sub>, C6'(13') or C11'(12')], 43.0 [CH<sub>2</sub>, C11'(12') or C6'(13')], 45.3 [C, C7'(8') or C9'(10')], 45.4 [C, C9'(10') or C7'(8')], 47.0 (C, C1' or C5'), 48.9 (C, C5' or C1'), 51.6 [CH<sub>2</sub>, C2' or C4'], 53.1 [CH<sub>2</sub>, C4' or C2'], 174.6 (C, CO). Anal. Calcd for C<sub>23</sub>H<sub>35</sub>NO: C 80.88, H 10.33, N 4.10. Found: 80.97, H 10.27, N 4.00.

## 6.2. Molecular modeling

Docking calculations were carried out using Glide [60], with the X-ray structure of human enzyme 4BB6 [61]. The geometry of each ligand was energy minimized and the centroid of the inhibitor cocrystallised in 4BB6 was used to generate the docking cavity by selecting all the residues located within 20 Å from the ligand. Between 70 and 100 poses were generated for each ligand, and the best-scored poses (and the expected arrangement within the binding pocket) were chosen as starting structures for MD simulations.

For each ligand-protein complex two independent 50ns MD simulations were run to check the consistency of the binding mode. To this end, the ligand-protein complex was immersed in an octahedral box of TIP3P [62] water molecules and sodium ions were added to neutralize the system. The force field ff99SBildn [63,64] was used for the protein parameters, and RESP charges at the HF/6-31G (d) together with the gaff [65] force field were used to for the ligand and NADP parameters. All systems were refined using a three-step energy minimization procedure (involving first hydrogen atoms, then water molecules, and finally the whole system) and a six-step equilibration (heating the system from 0 K to 300 K in 6 steps of 20 ps, the first, 50 ps the next four, and 5 ns the last one).

## 6.3. Human 11 $\beta$ -HSD1 in vitro enzyme inhibition assay

11 $\beta$ -HSD1 activity was determined in mixed sex, human liver microsomes (Celsis In-vitro Technologies) by measuring the conversion of  $^3H$ -cortisone to  $^3H$ -cortisol. Percentage inhibition was determined relative to a no inhibitor control. 5  $\mu$ g of human liver microsomes were pre-incubated at 37 °C for 15 min with inhibitor and 1 mM NADPH in a final volume of 90  $\mu$ L Krebs buffer. 10  $\mu$ L of 200 nM  $^3H$ -cortisone was then added followed by incubation at 37 °C for a further 30 min. The assay was terminated by rapid freezing on dry ice and  $^3H$ -cortisone to  $^3H$ -cortisol conversion determined in 50  $\mu$ L of the defrosted reaction by capturing liberated  $^3H$ -cortisol on anti-corti-

sol (HyTest Ltd)-coated scintillation proximity assay beads (protein A-coated YSi, GE Healthcare). A nanomolar 11 $\beta$ -HSD1 inhibitor, UE2316, was added as a positive control within in each set of assays. IC<sub>50</sub> values for UE2316 were within the normal range across each test occasion [66].

## 6.4. Mouse 11 $\beta$ -HSD1 in vitro enzyme inhibition assay

11 $\beta$ -HSD1 activity was determined in pooled mouse (CD-1) liver microsomes (Celsis In-vitro Technologies) by measuring the conversion of cortisone to cortisol by LC/MS. Percentage inhibition was determined relative to a no inhibitor control. 5  $\mu$ g of mouse liver microsomes were pre-incubated at 37 °C for 15 min with inhibitor and 1 mM NADPH in a final volume of 90  $\mu$ L Krebs buffer. 10  $\mu$ L of 2  $\mu$ M cortisone was then added followed by incubation at 37 °C for a further 30 min. The assay was terminated by rapid freezing on dry ice and subsequent extraction with acetonitrile on thawing. Samples dried down under nitrogen at 65 °C and solubilised in 100  $\mu$ L 70:30 H<sub>2</sub>O:ACN and removed to a 96-well V-bottomed plate for LC/MS analysis. Separation was carried out on a sunfire 150  $\times$  2.1 mm, 3.5  $\mu$ M column using a H<sub>2</sub>O:ACN gradient profile. Typical retention times were 2.71 min for cortisone and 2.80 min for cortisone. The peak area was calculated and the concentration of each compound determined from the calibration curve.

## 6.5. Microsomal stability assay

The microsomal stability of each compound was determined using either human or mouse liver microsomes (Celsis In-vitro Technologies). Microsomes were thawed and diluted to a concentration of 2 mg/mL in 50 mM NaPO<sub>4</sub> buffer pH 7.4. Each compound was diluted in 4 mM NADPH (made in the phosphate buffer above) to a concentration of 10  $\mu$ M. Two identical incubation plates were prepared to act as a 0 min and a 30 min time point assay. 30  $\mu$ L of each compound dilution was added in duplicate to the wells of a U-bottom 96-well plate and warmed at 37 °C for approximately 5 min. Verapamil, lidocaine and propranolol at 10  $\mu$ M concentration were utilized as reference compounds in this experiment. Microsomes were also pre-warmed at 37 °C before the addition of 30  $\mu$ L to each well of the plate resulting in a final concentration of 1 mg/mL. The reaction was terminated at the appropriate time point (0 or 30 min) by addition of 60  $\mu$ L of ice-cold 0.3 M trichloroacetic acid (TCA) per well. The plates were centrifuged for 10 min at 112  $\times$  g and the supernatant fraction transferred to a fresh U-bottom 96-well plate. Plates were sealed and frozen at -20 °C prior to MS analysis. LC-MS/MS was used to quantify the peak area response of each compound before and after incubation with liver microsomes using MS tune settings established and validated for each compound. These peak intensity measurements were used to calculate the % remaining after incubation with microsomes for each hit compound.

## 6.6. Cellular 11 $\beta$ -HSD1 enzyme inhibition assay

The cellular 11 $\beta$ -HSD1 enzyme inhibition assay was performed using HEK293 cells stably transfected with the human 11 $\beta$ -HSD1 gene. Cells were incubated with substrate (cortisone) and product (cortisol) was determined by LC/MS. Cells were plated at  $2 \times 10^4$  cells/well in a 96-well poly-D-lysine coated tissue culture microplate (Greiner Bio-one) and incubated overnight at 37 °C in 5% CO<sub>2</sub> 95% O<sub>2</sub>. Compounds to be tested were solubilised in 100% DMSO at 10 mM and serially diluted in water and 10% DMSO to final concentration of 10  $\mu$ M in 10% DMSO. 10  $\mu$ L of each test dilution and 10  $\mu$ L of 10% DMSO (for low and high control) were dispensed into the well of a new 96-well microplate (Greiner Bio-one).

Medium was removed from the cell assay plate and 100  $\mu\text{L}$  of DMEM solution (containing 1% penicillin, 1% streptomycin and 300 nM cortisone) added to each well. Cells were incubated for 2 h at 37  $^{\circ}\text{C}$  in 5%  $\text{CO}_2$  95%  $\text{O}_2$ . Following incubation, medium was removed from each well into an eppendorf containing 500  $\mu\text{L}$  of ethyl acetate, mixed by vortex and incubated at rt for 5 min. A calibration curve of known concentrations of cortisol in assay medium was also set up and added to 500  $\mu\text{L}$  of ethyl acetate, vortexed and incubated as above. The supernatant of each eppendorf was removed to a 96-deep-well plate and dried down under liquid nitrogen at 65  $^{\circ}\text{C}$ . Each well was solubilised in 100  $\mu\text{L}$  70:30  $\text{H}_2\text{O}$ :ACN and removed to a 96-well V-bottomed plate for LC/MS analysis. Separation was carried out on a sunfire 150  $\times$  2.1 mm, 3.5  $\mu\text{M}$  column using a  $\text{H}_2\text{O}$ :ACN gradient profile. Typical retention times were 2.71 min for cortisol and 2.8 min for cortisone. The peak area was calculated and the concentration of each compound determined from the calibration curve.

#### 6.7. Cellular 11 $\beta$ -HSD2 enzyme inhibition assay

For measurement of inhibition of 11 $\beta$ -HSD2, HEK293 cells stably transfected with the full-length gene coding for human 11 $\beta$ -HSD2 were used. The protocol was the same as for the cellular 11 $\beta$ -HSD1 enzyme inhibition assay, only changing the substrate, this time cortisol, and the concentrations of the tested compounds, 10, 1 and 0.1  $\mu\text{M}$ .

#### 6.8. Parallel Artificial Membrane Permeation Assays- Blood-Brain Barrier (PAMPA-BBB)

To evaluate the brain penetration of the different compounds, a parallel artificial membrane permeation assay for blood-brain barrier was used, following the method described by Di [50]. The *in vitro* permeability ( $P_e$ ) of fourteen commercial drugs through lipid extract of porcine brain membrane together with the test compounds were determined. Commercial drugs and assayed compounds were tested using a mixture of PBS:EtOH (70:30). Assay validation was made by comparing the experimental permeability with the reported values of the commercial drugs by bibliography and lineal correlation between experimental and reported permeability of the fourteen commercial drugs using the parallel artificial membrane permeation assay was evaluated ( $y = 1.5366x - 0.9672$ ;  $R_2 = 0.9382$ ). From this equation and taking into account the limits established by Di et al. for BBB permeation [50], we established the ranges of permeability as compounds of high BBB permeation (CNS +):  $P_e$  ( $10^{-6} \text{ cm s}^{-1}$ )  $> 5.179$ ; compounds of low BBB permeation (CNS -):  $P_e$  ( $10^{-6} \text{ cm s}^{-1}$ )  $< 2.106$  and compounds of uncertain BBB permeation (CNS  $\pm$ ):  $5.179 > P_e$  ( $10^{-6} \text{ cm s}^{-1}$ )  $> 2.106$ .

#### 6.9. Pharmacokinetic study

All the animal experiments were performed according to the protocols approved by the Animal Experimentation Ethical Committee of Universitat Autònoma de Barcelona and by the Animal Experimentation Commission of the Generalitat de Catalunya (Catalan Government). Male CD-1 mice (20–25 g) purchased from Envigo Laboratories were used. Compound **23** was dissolved in cyclodextrin 10% at 3 mg/mL to give a clear solution. After oral administration (21 mg/kg, 10 mL/kg), blood (0.6 mL) was collected from cava vein using a syringe (23G needle) rinsed with 5% EDTA(K2) at 0, 0.5, 1, 3, 5 and 24 (3 animals/point). Each blood sample was immediately transferred to a tube containing 40  $\mu\text{L}$  of water with 5% EDTA. Blood samples were centrifuged at 10000 g for 5 min and plasma samples were stored at  $-20^{\circ}\text{C}$  until analysis of compound concentration by UPLC-MS/MS. Brains were transcardially perfused with 10 mL of saline,

removed, frozen in liquid  $\text{N}_2$  and stored at  $-80^{\circ}\text{C}$  until analysis of the compound concentration by UPLC-MS/MS.

#### 6.10. In vivo study

##### 6.10.1. Animals

SAMP8 mice 12 months old ( $n = 12$ ) were randomized in 2 experimental groups (control,  $n = 4$ ; treated,  $n = 8$ ), and additional group 2 months old ( $n = 4$ ) were planned as a young population. Mice were used with free access to food and water, under standard temperature conditions ( $22 \pm 2^{\circ}\text{C}$ ) and 12-h:12-h light-dark cycles (300 lx/0 lx). Compound **23** was administered dissolved in tap water and PEG400 (2% final concentration) yielding a dose of 21 mpk for 4 weeks. The dose was selected based on the  $\text{IC}_{50}$  value of **23** and our previous expertise in *in vivo* studies with other 11 $\beta$ -HSD1 inhibitors [20,21]. To maintain the correct dose along the treatment period, once a week the weight of the animals and the quantity of water that they drank were measured. Therefore, we adjusted the concentration (mg/mL) of the compound **23** in the drink bottle to achieve the correct dose of compound (mpk) to be administered to mice. Studies were performed in accordance with the institutional guidelines for the care and use of laboratory animals established by the Ethical Committee for Animal Experimentation at the University of Barcelona.

##### 6.10.2. Novel Object Recognition Test (NORT)

The test was conducted in a 90-degree, two-arm, 25-cm-long, 20-cm-high maze. Light intensity in the middle of the field was 30 lux. The objects to be discriminated were plastic figures (object A, 5.25-cm-high, and object B, 4.75-cm-high). First, mice were individually habituated to the apparatus for 10 min per day during 3 days. On day 4, they were submitted to a 10-min acquisition trial (first trial), during which they were placed in the maze in the presence of two identical novel objects (A + A or B + B) placed at the end of each arm. A 10-min retention trial (second trial) occurred 2 h (short term memory) or 24 h (long term memory) later. During this second trial, objects A and B were placed in the maze, and the times that the animal took to explore the new object (tn) and the old object (to) were recorded. A Discrimination index (DI) was defined as  $(tn - to) / (tn + to)$ . In order to avoid object preference biases, objects A and B were counterbalanced so that one half of the animals in each experimental group were first exposed to object A and then to object B, whereas the other one half first saw object B and then object A was presented. The maze, the surface, and the objects were cleaned with 96% ethanol between the animals' trials so as to eliminate olfactory cues.

##### 6.10.3. Brain isolation and western blot analysis

Mice were euthanized 1 day after the last NORT trial was conducted, and brain quickly removed from the skull. Hippocampus were dissected and frozen in powdered dry ice and maintained at  $-80^{\circ}\text{C}$  for further use. Tissue samples were homogenized in lysis buffer containing phosphatase and protease inhibitors (Cocktail II, Sigma), and cytosol and nuclear fractions were obtained as described elsewhere. Protein concentration was determined by the Bradford method. 20  $\mu\text{g}$  of protein were separated by Sodium dodecyl sulfate-Polyacrylamide gel electrophoresis (SDS-PAGE) (8–15%) and transferred onto Polyvinylidene difluoride (PVDF) membranes (Millipore). The membranes were blocked in 5% non-fat milk in Tris-buffered saline containing 0.1% Tween 20 (TBS-T) for 1 h at rt, followed by overnight incubation at 4  $^{\circ}\text{C}$  with primary antibodies against PSD95 (1:1,000, ab18258/Abcam), IDE (1:1,000, ab32216/Abcam) and APP C-Terminal Fragment (1:1,000, C1/6.1/Covance) diluted in TBS-T and 5% bovine serum albumin (BSA). GAPDH (1:2,000, Millipore) was used as a control protein charge. Membranes were then washed and incubated with secondary antibodies for 1 h at

rt. Immunoreactive proteins were visualized utilizing an Enhanced chemiluminescence-based detection kit (ECL kit; Millipore) and digital images were acquired employing a ChemiDoc XRS + System (BioRad). Band intensities were quantified by densitometric analysis using Image Lab software (BioRad) and values were normalized to GAPDH.

#### 6.10.4. RNA extraction and gene expression determination

Total RNA isolation was carried out by means of Trizol reagent following the manufacturer's instructions. RNA content in the samples was measured at 260 nm, and sample purity was determined by the A260/280 ratio in a NanoDrop™ ND-1000 (Thermo Scientific). Samples were also tested in an Agilent 2100B Bioanalyzer (Agilent Technologies) to determine the RNA integrity number. Reverse transcription-Polymerase chain reaction (RT-PCR) was performed as follows: 2 µg of messenger RNA (mRNA) was reverse-transcribed using the High Capacity complementary DNA (cDNA) Reverse Transcription kit (Applied Biosystems). Real-time quantitative PCR (qPCR) was utilized to quantify the mRNA expression of inflammatory genes Interleukin 6 (*IL-6*) and inducible nitric oxide synthase (*iNOS*). Normalization of expression levels was performed with *Actin* for SYBER Green. The primers were as follows: for *IL-6*, forward 5'-ATCCAGTTGCCTTCTGGGACTGA-3' and reverse 5'-TAAGCCTCCGACTTGTGAAGTGGT-3', for *iNOS*, forward 5'-GGCAGCCTGTGAGACCTTG-3' and reverse 5'-GAAGCGTTTCGGGATCTGAA-3', for *Actin*, forward 5'-CAACGAGCGGTTCCGAT-3' and reverse 5'-GCCACAGGTCCATACCA-3'.

Real-time PCR was performed on the Step One Plus Detection System (Applied Biosystems) employing the SYBR Green PCR Master Mix (Applied Biosystems). Each reaction mixture contained 7.5 µL of cDNA, whose concentration was 2 µg/µL, 0.75 µL of each primer (whose concentration was 100 nM), and 7.5 µL of SYBR Green PCR Master Mix (2X).

Data were analysed utilizing the comparative Cycle threshold (Ct) method ( $\Delta\Delta C_t$ ), where the actin transcript level was utilized to normalize differences in sample loading and preparation. Each sample ( $n = 4-8$ ) was analysed in triplicate, and the results represented the  $n$ -fold difference of transcript levels among different samples.

#### 6.10.5. Data analysis

Data are expressed as the mean  $\pm$  Standard Error of the Mean (SEM). Data analysis was conducted using GraphPad Prism® ver. 6 statistical software. Means were compared with one-way Analysis of Variance (ANOVA) and Tukey post hoc analysis.

#### Acknowledgements

We thank financial support from *Ministerio de Economía y Competitividad* and FEDER (Project SAF2014-57094-R) and the *Generalitat de Catalunya* (grants 2014-SGR-00052 and 2014-SGR-1189) and the *Consorci de Serveis Universitaris de Catalunya* for computational resources. R. L. thanks the Spanish *Ministerio de Educación Cultura y Deporte* for a PhD Grant (FPU program) and the *Fundació Universitària Agustí Pedro i Pons* for a Travel Grant. E. V. thanks the Institute of Biomedicine of the University of Barcelona (IBUB) for a PhD Grant. F. J. L. acknowledges the support from ICREA Academia. We thank ACCIÓ (*Generalitat de Catalunya*) and CIDQO 2012 SL for financial support (*Programa Nuclis*, RD14-1-0057, SAFNAD).

#### Appendix A. Supplementary data

Supplementary data related to this article can be found at <http://dx.doi.org/10.1016/j.ejmech.2017.08.003>.

#### References

- [1] M.J. Meaney, D. O'Donnell, W. Rowe, B. Tannenbaum, A. Steverman, M. Walker, N.P.V. Nair, S. Lupien, Individual differences in hypothalamic-pituitary-adrenal activity in later life and hippocampal aging, *Exp. Gerontol.* 30 (1995) 229–251.
- [2] J.L. Yau, T. Olsson, R.G. Morris, M.J. Meaney, J.R. Seckl, Glucocorticoids, hippocampal corticosteroid receptor gene expression and antidepressant treatment: relationship with spatial learning in young and aged rats, *Neuroscience* 66 (1995) 571–581.
- [3] S.J. Lupien, M. de Leon, S. de Santi, A. Convit, C. Tarshish, N.P.V. Nair, M. Thakur, B.S. McEwen, R.L. Hauger, M.J. Meaney, Cortisol levels during human aging predict hippocampal atrophy and memory deficits, *Nat. Neurosci.* 1 (1998) 69–73.
- [4] R.M. Reynolds, Glucocorticoid excess and the developmental origins of disease: two decades of testing the hypothesis, *Psychoneuroendocrinology* 38 (2013) 1–11.
- [5] E.R. Peskind, C.W. Wilkinson, E.C. Petrie, G.D. Schellenberg, M.A. Raskind, Increased CSF cortisol in AD is a function of APOE genotype, *Neurology* 56 (2001) 1094–1098.
- [6] J.G. Cernansky, H. Dong, A.M. Fagan, L. Wang, C. Xiong, D.M. Holtzman, J.C. Morris, Plasma cortisol and progression of dementia in subjects with Alzheimer-type dementia, *Am. J. Psychiatry* 163 (2006) 2164–2169.
- [7] K.N. Green, L.M. Billings, B. Roozendaal, J.L. McLaugh, F.M. LaFerla, Glucocorticoids increase amyloid- $\beta$  and tau pathology in a mouse model of Alzheimer's disease, *J. Neurosci.* 26 (2006) 9047–9056.
- [8] M.C. Holmes, J.L. Yau, Y. Kotelevtsev, J.J. Mullins, J.R. Seckl, 11 beta-hydroxysteroid dehydrogenases in the brain: two enzymes two roles, *Ann. N.Y. Acad. Sci.* 1007 (2003) 357–366.
- [9] M.C. Holmes, J.R. Seckl, The role of 11 beta-hydroxysteroid dehydrogenases in the brain, *Mol. Cell. Endocrinol.* 248 (2006) 9–14.
- [10] C.S. Wyrwoll, M.C. Holmes, J.R. Seckl, 11 $\beta$ -Hydroxysteroid dehydrogenases and the brain: from zero to hero, a decade of progress, *Front. Neuroendocrinol.* 32 (2011) 265–286.
- [11] M.-P. Moisan, J.R. Seckl, C.R.W. Edwards, 11 $\beta$ -hydroxysteroid dehydrogenase bioactivity and messenger RNA expression in rat forebrain: localization in hypothalamus, hippocampus and cortex, *Endocrinology* 127 (1990) 1450–1455.
- [12] G. Pelletier, V. Luu-The, S. Li, G. Bujold, F. Labrie, Localization and glucocorticoid regulation of 11beta-hydroxysteroid dehydrogenase type 1 mRNA in the male mouse forebrain, *Neuroscience* 145 (2007) 110–115.
- [13] T.C. Sandeep, J.L. Yau, A.M. MacLulich, J. Noble, L.J. Deary, B.R. Walker, J.R. Seckl, 11Beta-hydroxysteroid dehydrogenase inhibition improves cognitive function in healthy elderly men and type 2 diabetics, *Proc. Natl. Acad. Sci. U. S. A.* 101 (2004) 6734–6739.
- [14] R.W. Brown, R. Diaz, A.C. Robson, Y.V. Kotelevtsev, J.J. Mullins, M.H. Kaufman, J.R. Seckl, The ontogeny of 11 beta-hydroxysteroid dehydrogenase type 2 and mineralocorticoid receptor gene expression reveal intricate control of glucocorticoid action in development, *Endocrinology* 137 (1996) 794–797.
- [15] R.W. Brown, Y. Kotelevtsev, C. Leckie, R.S. Lindsay, V. Lyons, P. Murad, J.J. Mullins, K.E. Chapman, C.R.W. Edwards, J.R. Seckl, Isolation and cloning of human placental 11 $\beta$ -hydroxysteroid dehydrogenase-2 cDNA, *Biochem. J.* 313 (1996) 1007–1017.
- [16] C. Wyrwoll, M. Keith, J. Noble, P.L. Stevenson, V. Bomball, S. Crombie, L.C. Evans, M.A. Bailey, E. Wood, J.R. Seckl, M.C. Holmes, Fetal brain 11 $\beta$ -hydroxysteroid dehydrogenase type 2 selectively determines programming of adult depressive-like behaviors and cognitive function, but not anxiety behaviors in male mice, *Psychoneuroendocrinology* 59 (2015) 59–70.
- [17] M.C. Holmes, R.N. Carter, J. Noble, S. Chitnis, A. Dutia, J.M. Paterson, J.J. Mullins, J.R. Seckl, J.L. Yau, 11 $\beta$ -hydroxysteroid dehydrogenase type 1 expression is increased in the aged mouse hippocampus and parietal cortex and causes memory impairments, *J. Neurosci.* 30 (2010) 6916–6920.
- [18] J.L. Yau, J. Noble, C.J. Kenyon, C. Hibberd, Y. Kotelevtsev, J.J. Mullins, J.R. Seckl, Lack of tissue glucocorticoid reactivation in 11beta-hydroxysteroid dehydrogenase type 1 knockout mice ameliorates age-related learning impairments, *Proc. Natl. Acad. Sci. U. S. A.* 98 (2001) 4716–4721.
- [19] K. Sooy, S.P. Webster, J. Noble, M. Binnie, B.R. Walker, J.R. Seckl, J.L. Yau, Partial deficiency or short-term inhibition of 11 $\beta$ -hydroxysteroid dehydrogenase type 1 improves cognitive function in aging mice, *J. Neurosci.* 30 (2010) 13867–13872.



- [20] N. Wheelan, S.P. Webster, C.J. Kenyon, S. Caughey, B.R. Walker, M.C. Holmes, J.R. Seckl, J.L.W. Yau, Short-term inhibition of 11 $\beta$ -hydroxysteroid dehydrogenase type 1 reversibly improves spatial memory but persistently impairs contextual fear memory in aged mice, *Neuropharmacol* 91 (2015) 71–76.
- [21] K. Sooy, J. Noble, A. McBride, M. Binnie, J.L.W. Yau, J.R. Seck, B.R. Walker, S.P. Webster, Cognitive and disease-modifying effects of 11 $\beta$ -hydroxysteroid dehydrogenase type 1 inhibition in male Tg2576 mice, a model of Alzheimer's Disease, *Endocrinology* 156 (2015) 4592–4603.
- [22] E.G. Mohler, K.E. Browman, V.A. Roderwald, E.A. Cronin, S. Markosyan, R.S. Bitner, M.I. Strakhova, K.U. Drescher, W. Hornberger, J.J. Rohde, M.E. Brune, P.B. Jacobson, L.E. Rueter, Acute inhibition of 11 $\beta$ -hydroxysteroid dehydrogenase type-1 improves memory in rodent models of cognition, *J. Neurosci.* 31 (2011) 5406–5413.
- [23] J.L.W. Yau, J.R. Seckl, Local amplification of glucocorticoids in the aging brain and impaired spatial memory, *Front. Aging Neurosci.* 4 (2012) 24.
- [24] J.E. Morley, S.A. Farr, V.B. Kumar, H.J. Armbrecht, The SAMP8 mouse: a model to develop therapeutic interventions for Alzheimer's disease, *Curr. Pharm. Des.* 18 (2012) 1123–1130.
- [25] J.E. Morley, H.J. Armbrecht, S.A. Farr, V.B. Kumar, The senescence accelerated mouse (SAMP8) as a model for oxidative stress and Alzheimer's disease, *Biochim. Biophys. Acta* 1822 (2012) 650–656.
- [26] S. Olson, S.D. Aster, K. Brown, L. Carbin, D.W. Graham, A. Hermanowski-Vosatka, C.B. LeGrand, S.S. Mundt, M.A. Robbins, J.M. Schaeffer, L.H. Slossberg, M.J. Szymonifka, R. Thieringer, S.D. Wright, J.M. Balkovec, Adamantyl triazoles as selective inhibitors of 11 $\beta$ -hydroxysteroid dehydrogenase type 1, *Bioorg. Med. Chem. Lett.* 15 (2005) 4359–4362.
- [27] B. Sorensen, J. Rohde, J. Wang, S. Fung, K. Monzon, W. Chiou, L. Pan, X. Deng, D. Stolarik, E.U. Frevert, P. Jacobson, J.T. Link, Adamantane 11 $\beta$ -HSD-1 inhibitors: application of an isocyanide multicomponent reaction, *Bioorg. Med. Chem. Lett.* 16 (2006) 5958–5962.
- [28] C.L. Becker, K.M. Engstrom, F.A. Kerdesky, J.C. Tolle, S.H. Wagaw, W. Wang, A convergent process for the preparation of adamantane 11 $\beta$ -HSD1 inhibitors, *Org. Process Res. Dev.* 12 (2008) 1114–1118.
- [29] J.S. Scott, P. Barton, S.N.L. Bennett, J. deSchoolmeester, L. Godfrey, E. Kilgour, R.M. Mayers, M.J. Packer, A. Rees, P. Schofield, N. Selmi, J.G. Swales, P.R.O. Whittamore, Reduction of acyl glucuronidation in a series of acidic 11 $\beta$ -hydroxysteroid dehydrogenase type 1 (11 $\beta$ -HSD1) inhibitors: the discovery of AZD6925, *Med. Chem. Commun.* 3 (2012) 1264–1269.
- [30] J.S. Scott, J. deSchoolmeester, E. Kilgour, R.M. Mayers, M.J. Packer, D. Hargreaves, S. Gerhardt, D.J. Ogg, A. Rees, N. Selmi, A. Stocker, J.G. Swales, P.R.O. Whittamore, Novel acidic 11 $\beta$ -hydroxysteroid dehydrogenase type 1 (11 $\beta$ -HSD1) inhibitor with reduced acyl glucuronide liability: the discovery of 4-[4-(2-adamantylcarbonyl)-5-tert-butyl-pyrazol-1-yl]benzoic acid (AZD8329), *J. Med. Chem.* 55 (2012) 10136–10147.
- [31] O. Venier, C. Pascal, A. Braun, C. Namane, P. Mougénot, O. Crespín, F. Paquet, C. Mougénot, C. Monseau, B. Onofri, R. Dadjji-Fahun, C. Leger, M. Ben-Hassine, T. Van-Pham, J.-L. Ragot, C. Philippo, G. Farjot, L. Noah, K. Maniani, A. Boutarfa, E. Nicolai, E. Guillot, M.-P. Pruniaux, S. Güssregen, C. Engel, A.-L. Coutant, B. de Miguel, A. Castro, Discovery of SAR184841, a potent and long-lasting inhibitor of 11 $\beta$ -hydroxysteroid dehydrogenase type 1, active in a physiopathological animal model of T2D, *Bioorg. Med. Chem. Lett.* 23 (2013) 2414–2421.
- [32] S.B. Park, W.H. Jung, N.S. Kang, J.S. Park, G.H. Bae, H.Y. Kim, S.D. Rhee, S.K. Kang, J.H. Ahn, H.G. Jeong, K.Y. Kim, Anti-diabetic and anti-inflammatory effect of a novel selective 11 $\beta$ -HSD1 inhibitor in the diet-induced obese mice, *Eur. J. Pharmacol.* 721 (2013) 70–79.
- [33] S. Okazaki, T. Takahashi, T. Iwamura, J. Nakaki, Y. Sekiya, M. Yagi, H. Kumagai, M. Sato, S. Sakami, A. Nitta, K. Kawai, M. Kainoh, HIS-388, a novel orally active and long-acting 11 $\beta$ -hydroxysteroid dehydrogenase type 1 inhibitor, ameliorates insulin sensitivity and glucose intolerance in diet-induced obesity and nongenetic type 2 diabetic murine models, *J. Pharmacol. Exp. Ther.* 351 (2014) 181–189.
- [34] S.Y. Byun, Y.J. Shin, K.Y. Nam, S.P. Hong, S.K. Ahn, A novel highly potent and selective 11 $\beta$ -hydroxysteroid dehydrogenase type 1 inhibitor, UI-1499, *Life Sci.* 120 (2015) 1–7.
- [35] J.P. Gibbs, M.G. Emery, I. McCaffery, B. Smith, M.A. Gibbs, A. Akrami, J. Rossi, K. Paweletz, M.R. Gastonguay, E. Bautista, M. Wang, R. Perfetti, O. Daniels, Population pharmacokinetic/pharmacodynamic model of subcutaneous adipose 11 $\beta$ -hydroxysteroid dehydrogenase type 1 (11 $\beta$ -HSD1) activity after oral administration of AMG 221, a selective 11 $\beta$ -HSD1 inhibitor, *J. Clin. Pharmacol.* 51 (2011) 830–841.
- [36] S. Shah, A. Hermanowski-Vosatka, K. Gibson, R.A. Ruck, G. Jia, J. Zhang, P.M.T. Hwang, N.W. Ryan, R.B. Langdon, P.U. Feig, Efficacy and safety of the selective 11 $\beta$ -HSD1 inhibitors MK-0736 and MK-0916 in overweight and obese patients with hypertension, *J. Am. Soc. Hypertens.* 5 (2011) 166–176.
- [37] M.D. Duque, P. Camps, L. Profire, S. Montaner, S. Vázquez, F.X. Sureda, J. Mallol, M. López-Querol, L. Naesens, E. De Clercq, S.R. Prathalingam, J.M. Kelly, Synthesis and pharmacological evaluation of (2-oxaadamantan-1-yl)amines, *Bioorg. Med. Chem.* 17 (2009) 3198–3206.
- [38] M.D. Duque, C. Ma, E. Torres, J. Wang, L. Naesens, J. Juárez-Jiménez, P. Camps, F.J. Luque, W.F. DeGrado, R.A. Lamb, L.H. Pinto, S. Vázquez, Exploring the size limit of templates for inhibitors of the M2 ion channel of influenza A virus, *J. Med. Chem.* 54 (2011) 2646–2657.
- [39] M. Rey-Carrizo, E. Torres, C. Ma, M. Barniol-Xicota, J. Wang, Y. Wu, L. Naesens, W.F. DeGrado, R.A. Lamb, L.H. Pinto, S. Vázquez, 3-Azetetracyclo[5.2.1.1<sup>5,8</sup>.0<sup>1,5</sup>]undecane derivatives: from wild-type inhibitors of the M2 ion channel of influenza A virus to derivatives with potent activity against the V27A mutant, *J. Med. Chem.* 56 (2013) 9265–9274.
- [40] M. Rey-Carrizo, M. Barniol-Xicota, C. Ma, M. Frigolé-Vivas, E. Torres, L. Naesens, S. Llabrés, J. Juárez-Jiménez, F.J. Luque, W.F. DeGrado, R.A. Lamb, L.H. Pinto, S. Vázquez, Easily accessible polycyclic amines that inhibit the wild-type and amantadine-resistant mutants of the M2 channel of the influenza A virus, *J. Med. Chem.* 57 (2014) 5738–5747.
- [41] E. Torres, R. Leiva, S. Gazzarrini, M. Rey-Carrizo, M. Frigolé-Vivas, A. Moroni, L. Naesens, S. Vázquez, Azapropellanes with anti-influenza A virus activity, *ACS Med. Chem. Lett.* 5 (2014) 831–836.
- [42] R. Leiva, S. Gazzarrini, R. Esplugas, A. Moroni, L. Naesens, F.X. Sureda, S. Vázquez, Ritter reaction-mediated syntheses of 2-oxaadamantan-5-amine, a novel amantadine analog, *Tetrahedron Lett.* 56 (2015) 1272–1275.
- [43] M.D. Duque, P. Camps, E. Torres, E. Valverde, F.X. Sureda, M. López-Querol, A. Camins, S.R. Prathalingam, J.M. Kelly, S. Vázquez, New oxapolycyclic cage amines with NMDA receptor antagonist and trypanocidal activities, *Bioorg. Med. Chem.* 18 (2010) 46–57.
- [44] E. Torres, M.D. Duque, M. López-Querol, M.C. Taylor, L. Naesens, C. Ma, L.H. Pinto, F.X. Sureda, J.M. Kelly, S. Vázquez, Synthesis of benzopolycyclic cage amines: NMDA receptor antagonist, trypanocidal and antiviral activities, *Bioorg. Med. Chem.* 20 (2012) 942–948.
- [45] E. Valverde, F.X. Sureda, S. Vázquez, Novel benzopolycyclic amines with NMDA receptor antagonist activity, *Bioorg. Med. Chem.* 22 (2014) 2678–2683.
- [46] E. Valverde, C. Seira, A. McBride, M. Binnie, F.J. Luque, S.P. Webster, A. Bidon-Chanal, S. Vázquez, Searching for novel applications of the benzohomadamantane scaffold in medicinal chemistry: synthesis of novel 11 $\beta$ -HSD1 inhibitors, *Bioorg. Med. Chem.* 23 (2015) 7607–7617.
- [47] H. Cheng, J. Hoffman, P. Le, S.K. Nair, S. Cripps, J. Matthews, C. Smith, M. Yang, S. Kupchinsky, K. Dress, M. Edwards, B. Cole, E. Walters, C. Loh, J. Ermolieff, A. Fanjul, G.B. Bhat, J. Herrera, T. Paily, N. Hosea, G. Paderes, P. Rejto, The development and SAR of pyrrolidine carboxamide 11 $\beta$ -HSD1 inhibitors, *Bioorg. Med. Chem. Lett.* 20 (2010) 2897–2902.
- [48] R. Leiva, C. Seira, A. McBride, M. Binnie, A. Bidon-Chanal, F.J. Luque, S.P. Webster, S. Vázquez, Novel 11 $\beta$ -HSD1 inhibitors: effects of the C-1 vs C2-substitution and of the introduction of an oxygen atom in the adamantane scaffold, *Bioorg. Med. Chem. Lett.* 25 (2015) 4250–4253.
- [49] During the writing of this manuscript it has been reported the discovery and the results of Phase I clinical trials of UE2343, a brain-penetrant 11 $\beta$ -HSD1 inhibitor featuring a pyrrolidine unit embedded in a tropane core. The compound is being developed by Actinogen Medical for the treatment of Alzheimer's disease. See, Webster, S. P.; McBride, A.; Binnie, M.; Sooy, K.; Seckl, J. R.; Andrew, R.; Pallin, T. D.; Hunt, H. J.; Perrior, T. R.; Ruffles, V. S.; Ketelbey, J. W.; Boyd, A.; Walker, B. R. Selection and early clinical evaluation of the brain-penetrant 11 $\beta$ -hydroxysteroid dehydrogenase type 1 (11 $\beta$ -HSD1) inhibitor UE2343 (Xanamem™), *British J. Pharmacol.* 2017, 174, 396–408.
- [50] L. Di, E.H. Kerns, K. Fan, O.J. McConnell, G.T. Carter, High throughput artificial membrane permeability assay for blood-brain barrier, *Eur. J. Med. Chem.* 38 (2003) 223–232.
- [51] T. Takeda, Senescence-accelerated mouse (SAM) with special references to neurodegeneration models, SAMP8 and SAMP10 mice, *Neurochem. Res.* 34 (2009) 639–659.
- [52] M. Pallás, Senescence-accelerated mice P8: a tool to study brain aging and Alzheimer's disease in a Mouse Model, *ISRN Cell Biol.* (2012) 917167.
- [53] C. Griñan-Ferré, V. Palomera-Ávalos, D. Puigoriol-Illamola, A. Camins, D. Porquet, V. Plá, F. Aguado, M. Pallás, Behaviour and cognitive changes correlated with hippocampal neuroinflammation and neuronal markers in female SAMP8, a model of accelerated senescence, *Exp. Gerontol.* 80 (2016) 57–69.
- [54] M. Antunes, G. Biala, The novel object recognition memory: neurobiology, test procedure, and its modifications, *Cogn. Process.* 13 (2012) 93–110.
- [55] M.P. Murphy, H. LeVine III, Alzheimer's disease and the amyloid-beta peptide, *J. Alzheimers Dis.* 19 (2010) 311–323.
- [56] M. Kim, L.B. Hersh, M.A. Leissring, M. Ingelsson, T. Matsui, W. Farris, A. Lu, B.T. Hyman, D.J. Selkoe, L. Bertram, R.E. Tanzi, Decreased catalytic activity of the insulin-degrading enzyme in chromosome 10-linked Alzheimer Disease families, *J. Biol. Chem.* 282 (2007) 7825–7832.
- [57] J.E. Morley, S.A. Farr, J.F. Flood, Antibody to amyloid beta protein alleviates impaired acquisition, retention, and memory processing in SAMP8 mice, *Neurobiol. Learn. Mem.* 78 (2002) 125–138.

- [58] C.F. Culberson, P. Wilder Jr., The synthesis of 2-aza-1,2-dihydrocyclopentadienes, *J. Org. Chem.* 25 (1960) 1358–1362.
- [59] M. Fumimoto, K. Okabe, Nouvelle méthode de synthèse des dérivés d'ethano-4,7 polyhydroisoindoline, *Chem. Pharm. Bull.* 10 (1962) 714–718.
- [60] R.A. Friesner, R.B. Murphy, M.P. Repasky, L.L. Frye, J.R. Greenwood, T.A. Halgren, P.C. Sanschagrin, D.T. Mainz, Extra precision Glide: docking and scoring incorporating a model of hydrophobic enclosure for protein-ligand complexes, *J. Med. Chem.* 49 (2006) 6177–6196.
- [61] F.W. Goldberg, A.G. Leach, J.S. Scott, W.L. Snelson, S.D. Groombridge, C.S. Donald, S.N.L. Bennett, C. Bodin, P.M. Gutierrez, A.C. Gyte, Free-Wilson and structural approaches to co-optimising human and rodent isoform potency for 11 $\beta$ -hydroxysteroid dehydrogenase type 1 (11 $\beta$ -HSD1) inhibitors, *J. Med. Chem.* 55 (2012) 10652–10661.
- [62] W.L. Jorgensen, J. Chandrasekhar, J.D. Madura, R.W. Impey, M.L. Klein, Comparison of simple potential functions for simulating liquid water, *J. Chem. Phys.* 79 (1983) 926–935.
- [63] V. Hornak, R. Abel, A. Okur, B. Strockbine, A. Roitberg, C. Simmerling, Comparison of multiple Amber force fields and development of improved protein backbone parameters, *Proteins* 65 (2006) 712–725.
- [64] K. Lindorff-Larsen, S. Piana, K. Palmo, P. Maragakis, J.L. Klepeis, R.O. Dror, D.E. Shaw, Improved side-chain torsion potentials for the Amber ff99SB force field, *Proteins* 78 (2010) 1950–1958.
- [65] J. Wang, R.M. Wolf, J.W. Caldwell, P.A. Kollman, D.A. Case, Development and testing of a general force field, *J. Comp. Chem.* 25 (2004) 1157–1174.
- [66] J.L.W. Yau, N. Wheelan, J. Noble, B.R. Walker, S.P. Webster, C.J. Kenyon, M. Ludwig, J.R. Seckl, Intrahippocampal glucocorticoids generated by 11 $\beta$ -HSD1 affect memory in aged mice, *Neurobiol. Aging* 36 (2015) 334–343.

UNCORRECTED PROOF



## SUPPLEMENTARY MATERIAL FOR

### **Design, synthesis and *in vivo* study of novel pyrrolidine-based 11 $\beta$ -HSD1 inhibitors for age-related cognitive dysfunction**

Rosana Leiva<sup>1</sup>, Christian Griñan-Ferré<sup>2</sup>, Constantí Seira<sup>3</sup>, Elena Valverde<sup>1</sup>, Andrew McBride<sup>4</sup>, Margaret Binnie<sup>4</sup>, Belén Pérez<sup>5</sup>, F. Javier Luque<sup>3</sup>, Mercè Pallàs<sup>2</sup>, Axel Bidon-Chanal<sup>3</sup>, Scott P. Webster<sup>\*4</sup>, and Santiago Vázquez<sup>\*1</sup>

<sup>1</sup>*Laboratori de Química Farmacèutica (Unitat Associada al CSIC), Facultat de Farmàcia i Institut de Biomedicina (IBUB), Universitat de Barcelona, Av. Joan XXIII, 27-31, 08028 Barcelona, Spain.*

<sup>2</sup>*Unitat de Farmacologia, Farmacognòsia i Terapèutica, Facultat de Farmàcia i Institut de Neurociències, Universitat de Barcelona, Av. Joan XXIII, 27-31, 08028 Barcelona, Spain.*

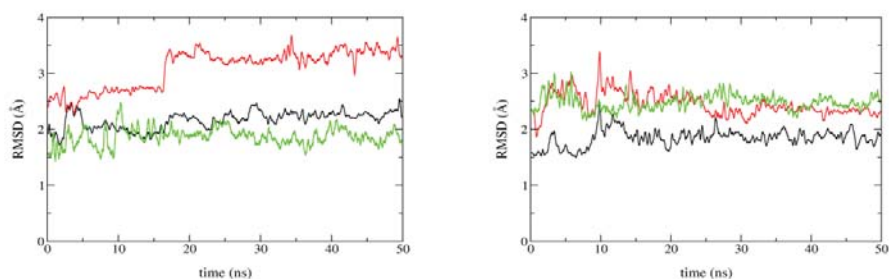
<sup>3</sup>*Department of Nutrition, Food Science and Gastronomy, Faculty of Pharmacy and Institute of Biomedicine (IBUB), University of Barcelona, Av. Prat de la Riba, 171, 08921 Santa Coloma de Gramenet, Spain.*

<sup>4</sup>*Centre for Cardiovascular Science, University of Edinburgh, Queen's Medical Research Institute, EH16 4TJ, United Kingdom.*

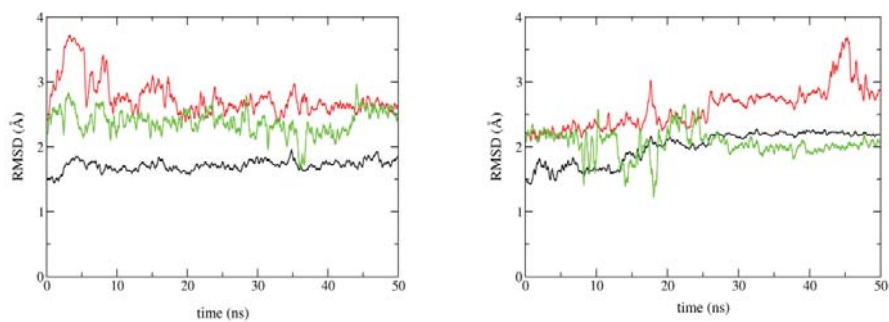
<sup>5</sup>*Departament de Farmacologia, Terapèutica i Toxicologia, Universitat Autònoma de Barcelona, 08193 Bellaterra, Barcelona, Spain.*

## Table of contents

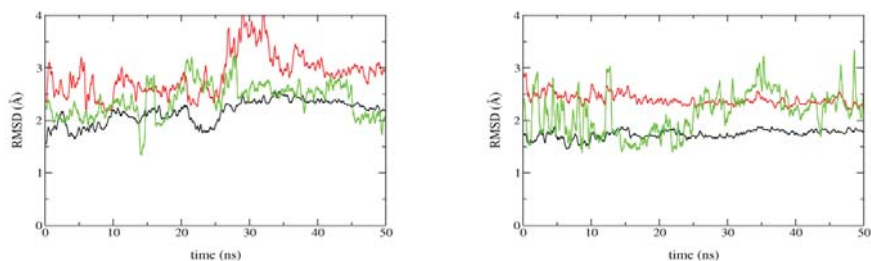
Figure S1	Page S3
Figure S2	Page S3
Figure S3	Page S4
Figure S4	Page S4
Table S1	Page S5
Figure S5	Page S5
Table S2	Page S6
Figure S6	Page S7
$^1\text{H}$ and $^{13}\text{C}$ NMR spectra of new compounds	Page S8



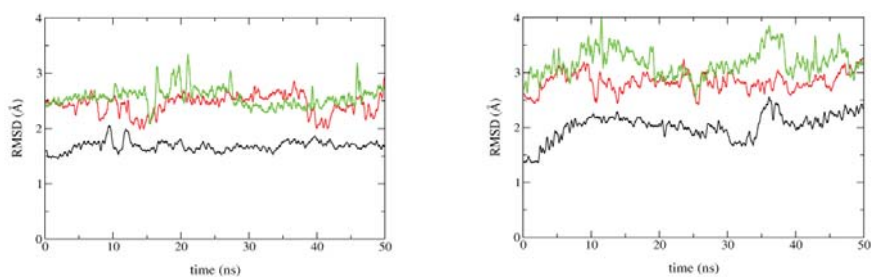
**Figure S1.** Representation of the root-mean square deviation (RMSD; Å) along the simulation time (ns) for the two independent MD simulations run for the complex between 11 $\beta$ -HSD1 and compound **12**. The RMSD was determined for the backbone atoms of the whole protein (black), the heavy atoms of the residues in the binding site (red), and the ligand (green).



**Figure S2.** Representation of the root-mean square deviation (RMSD; Å) along the simulation time (ns) for the two independent MD simulations run for the complex between 11 $\beta$ -HSD1 and compound **14**. The RMSD was determined for the backbone atoms of the whole protein (black), the heavy atoms of the residues in the binding site (red), and the ligand (green).



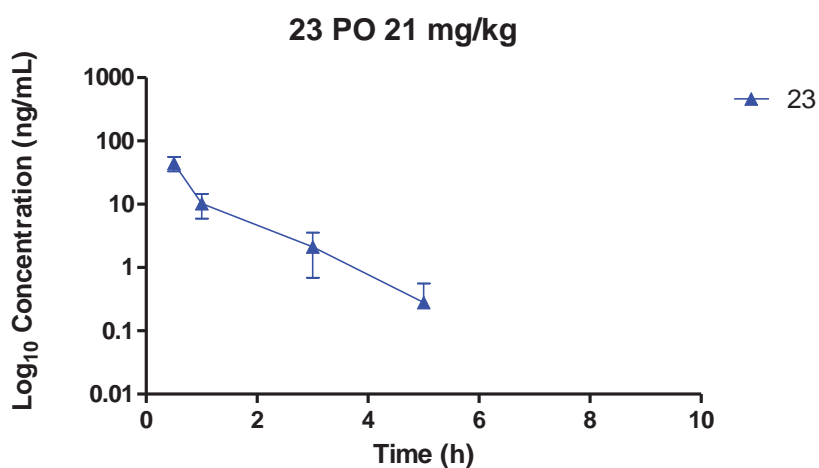
**Figure S3.** Representation of the root-mean square deviation (RMSD; Å) along the simulation time (ns) for the two independent MD simulations run for the complex between 11 $\beta$ -HSD1 and compound **8**. The RMSD was determined for the backbone atoms of the whole protein (black), the heavy atoms of the residues in the binding site (red), and the ligand (green).



**Figure S4.** Representation of the root-mean square deviation (RMSD; Å) along the simulation time (ns) for the two independent MD simulations run for the complex between 11 $\beta$ -HSD1 and compound **23**. The RMSD was determined for the backbone atoms of the whole protein (black), the heavy atoms of the residues in the binding site (red), and the ligand (green).

23 PO 21 mg/kg				
Time	ID	Total concentration (ng/mL)	Mean (ng/mL)	SD (ng/mL)
0h	Mouse 31	0	0	0
	Mouse 32	0		
	Mouse 33	0		
0.5h	Mouse 1	47.05	44.58	11.50
	Mouse 2	32.05		
	Mouse 3	54.65		
1h	Mouse 4	10.13	10.26	4.32
	Mouse 5	6.01		
	Mouse 6	14.65		
3h	Mouse 7	3.73	2.12	1.43
	Mouse 8	0.97		
	Mouse 9	1.67		
5h	Mouse 10	0.10	0.28	0.28
	Mouse 11	0.15		
	Mouse 12	0.60		
24h	Mouse 13	0.00	0.00	0.00
	Mouse 14	0.00		
	Mouse 15	0.00		

**Table S1.** Concentrations of **23** in mouse plasma at different times after oral administration at 21 mg/kg.

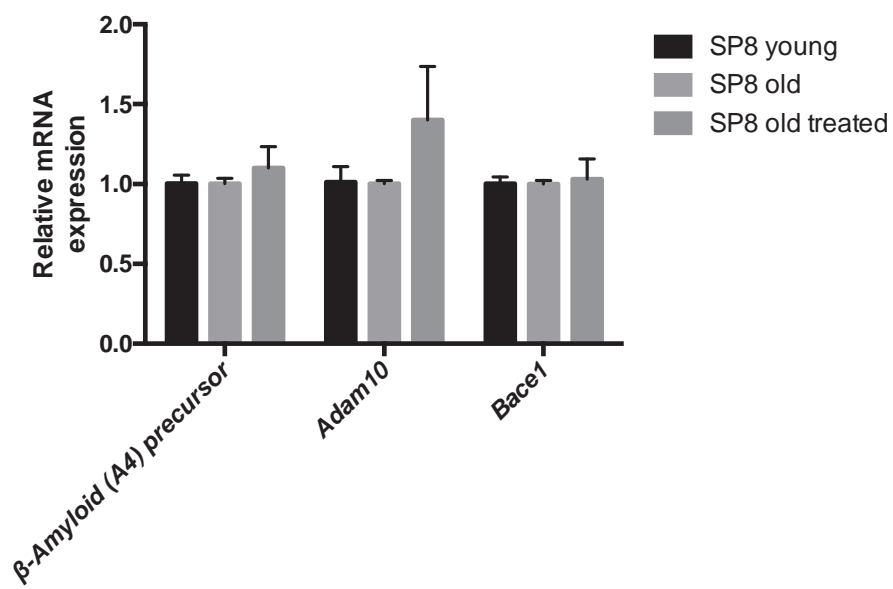


**Figure S5.** Concentration ( $\log_{10}$ ) vs time for oral administration at 21 mg/kg of **23**.

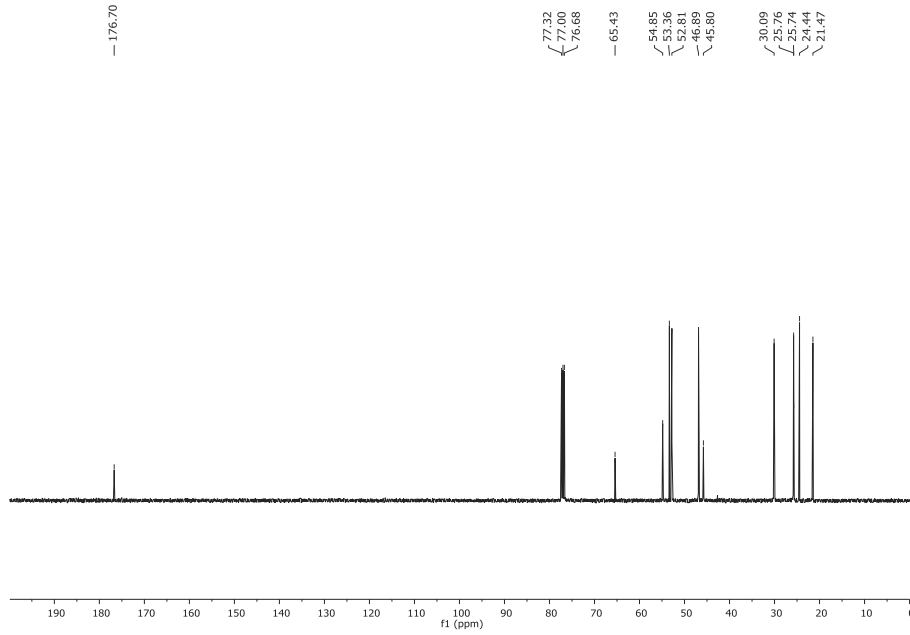
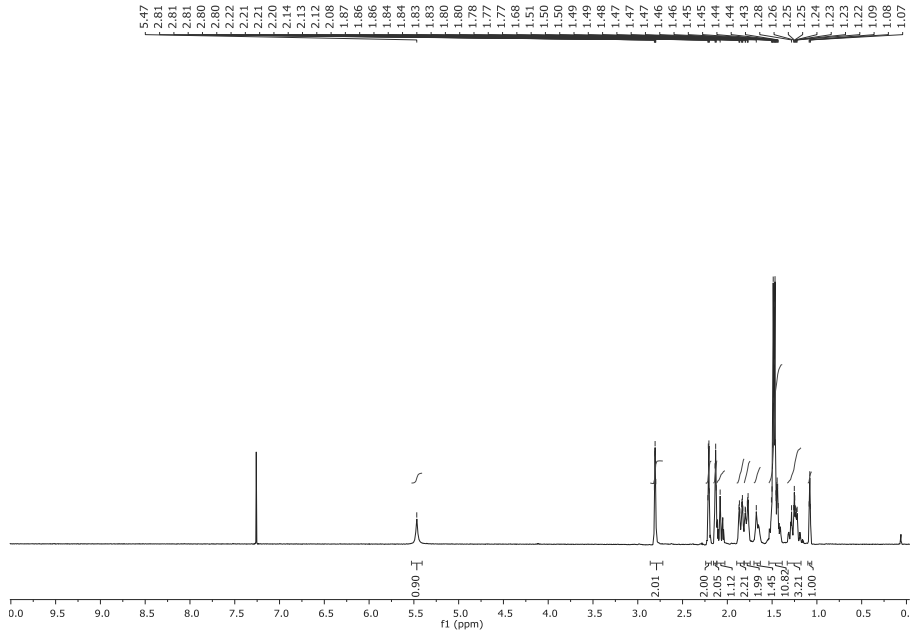
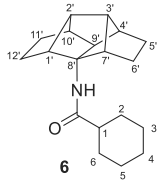


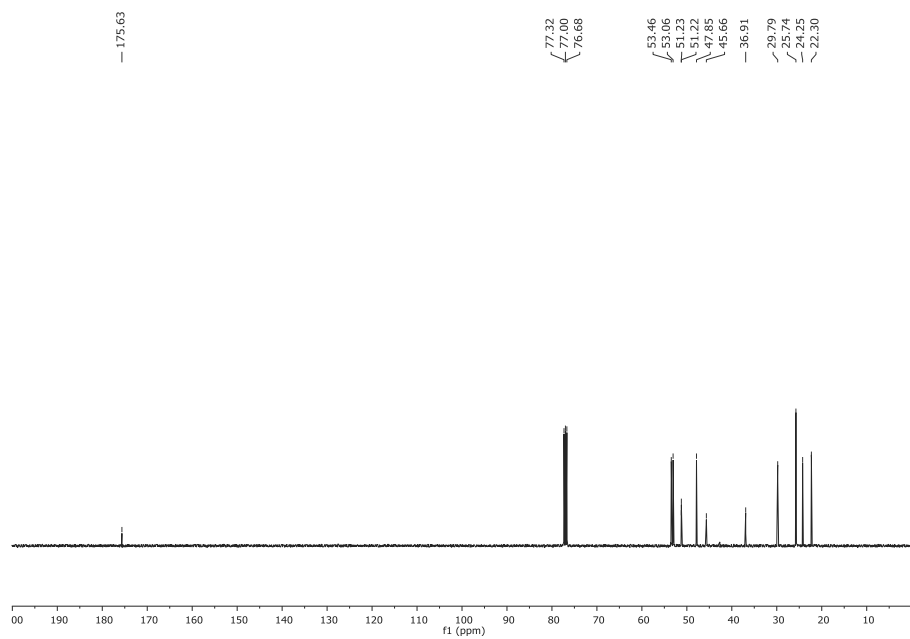
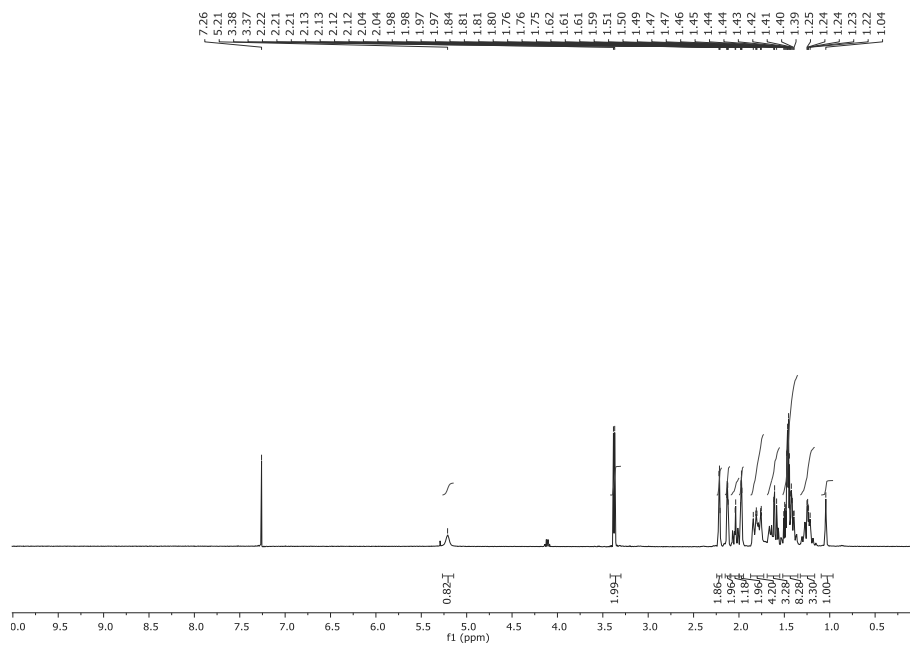
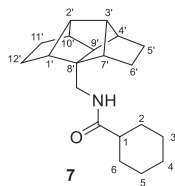
Parameter	Units	Estimate
<b>Lambda_z</b>	1/h	0.899
<b>HL_Lambda_z</b>	h	0.771
<b>Tmax</b>	h	0.500
<b>Cmax</b>	ng/mL	44.583
<b>Cmax_D</b>	kg* ng/mL/mg	2.123
<b>AUClast</b>	h* ng/mL	39.721
<b>AUCINF_obs</b>	h* ng/mL	40.036
<b>AUCINF_D_obs</b>	h* kg* ng/mL/mg	1.906
<b>AUC_%Extrap_obs</b>	%	0.787
<b>Vz_F_obs</b>	L/kg	583.499
<b>Cl_F_obs</b>	L/h/kg	524.522

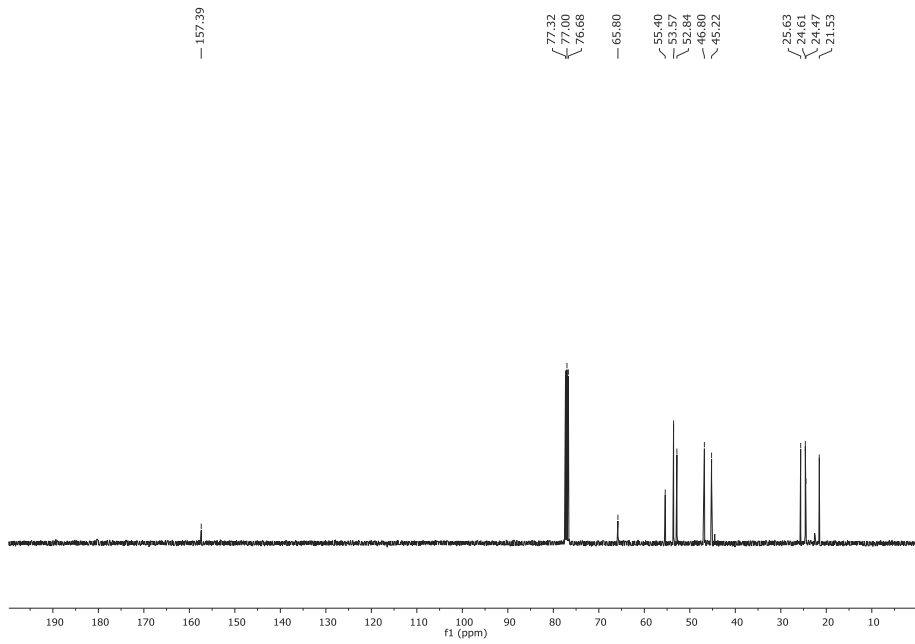
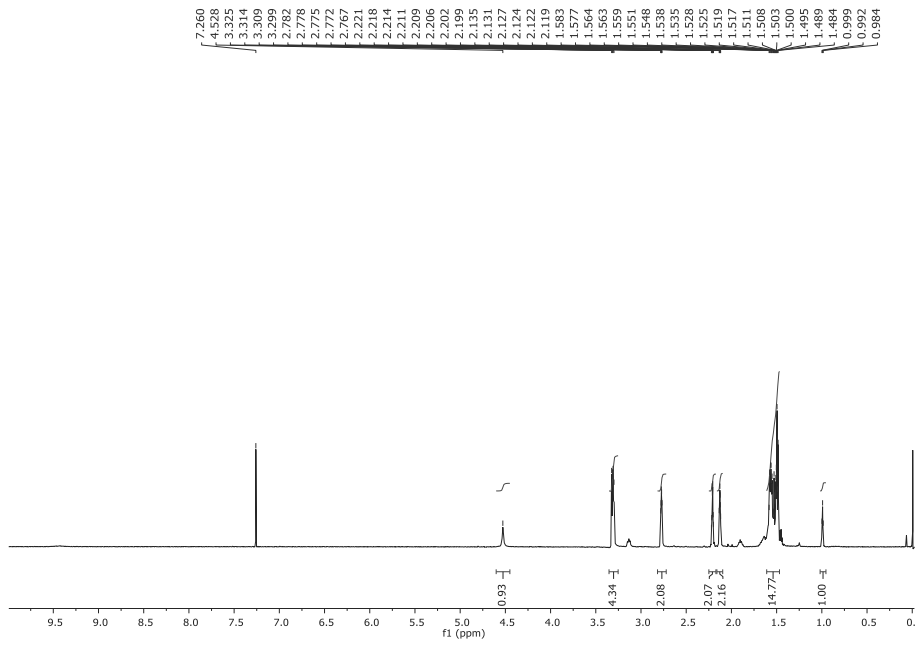
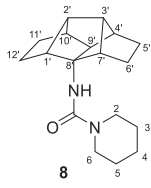
**Table S2.** Pharmacokinetic parameters of the pharmacokinetic study calculated by a Non Compartmental Analysis with Phoenix 7.0 Winnolin software.

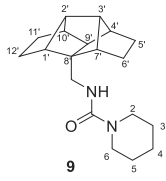


**Figure S6.** Lack of effects of amide **23** (at 21 mg/kg) on Pre-APP, Adam10 or Bace1 gene expression.



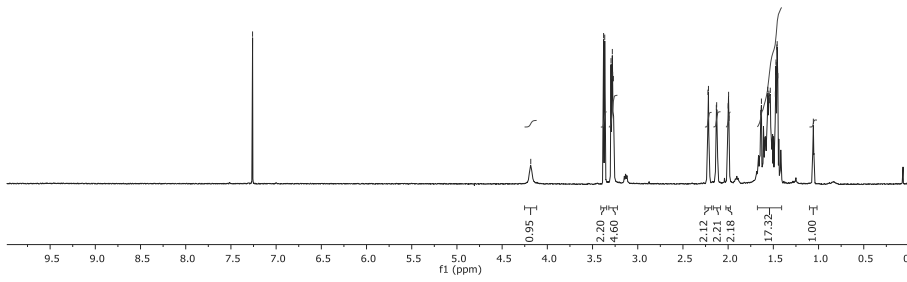






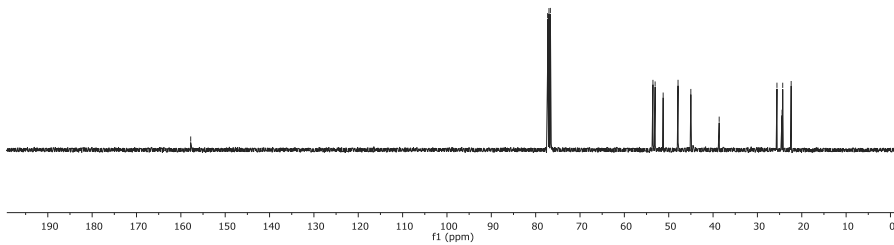
— 7.26

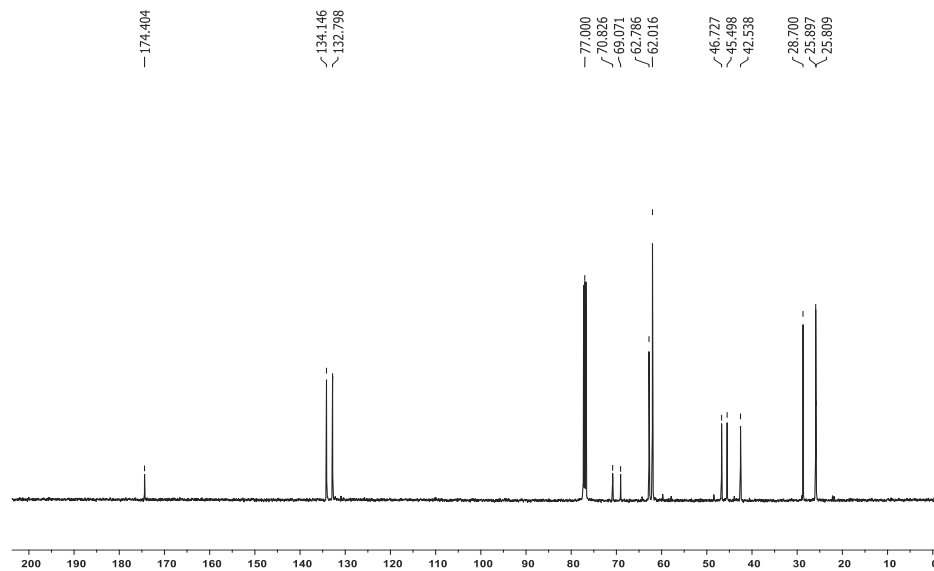
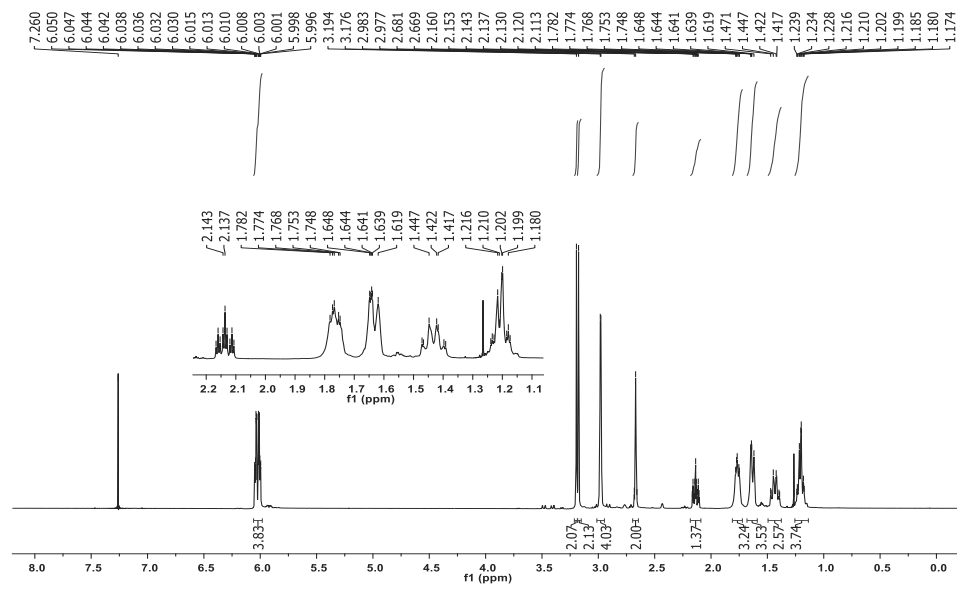
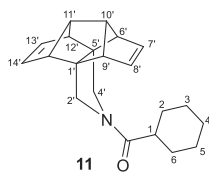
4.18  
3.38  
3.37  
3.30  
3.28  
3.28  
3.28  
3.27  
2.22  
2.12  
2.13  
2.12  
2.00  
2.00  
1.99  
1.64  
1.63  
1.57  
1.56  
1.55  
1.55  
1.54  
1.53  
1.53  
1.48  
1.47  
1.46  
1.46  
1.45  
1.45  
1.06

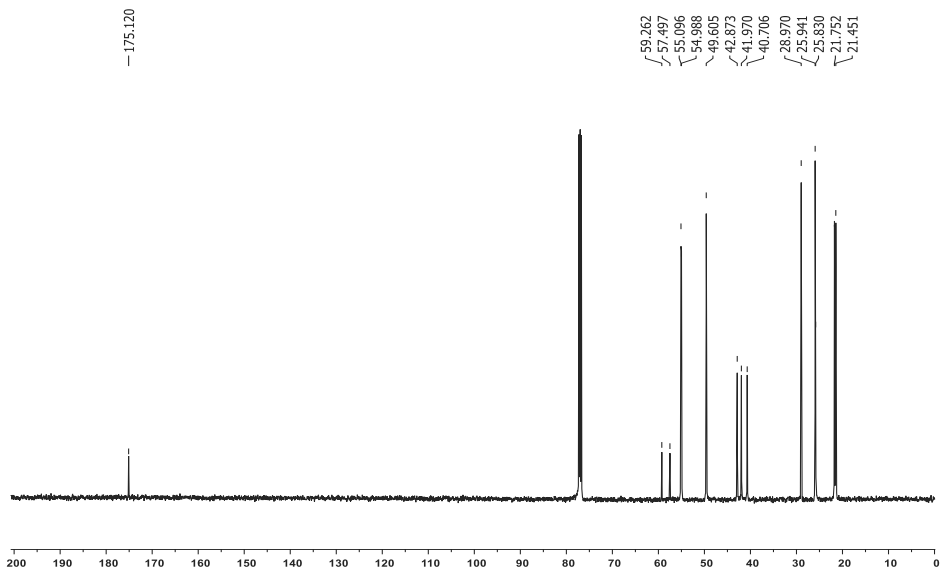
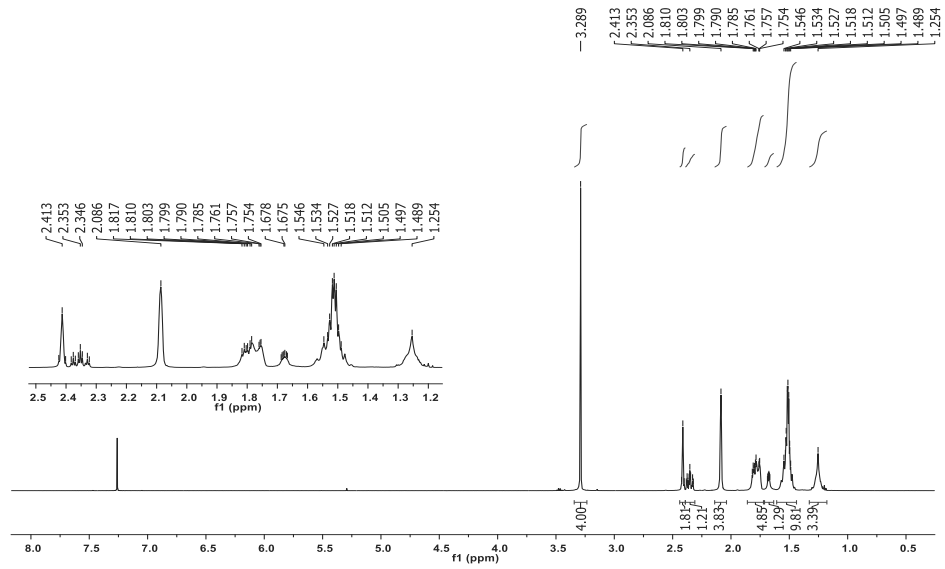
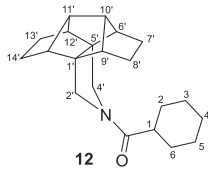


— 157.78

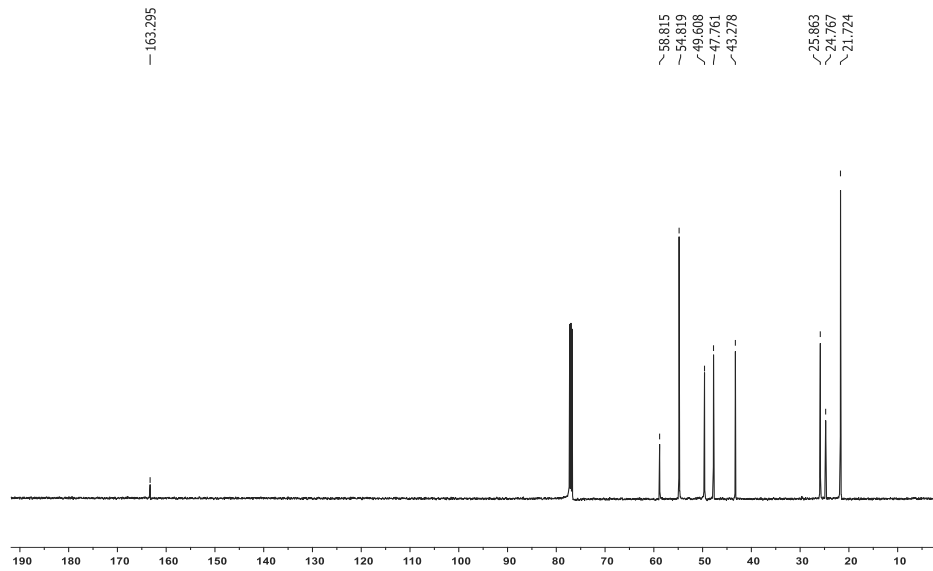
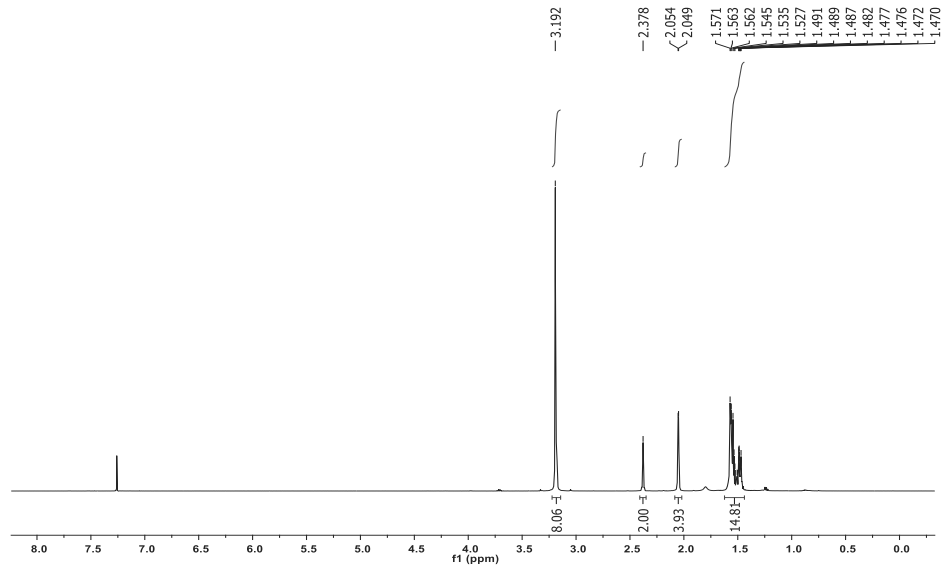
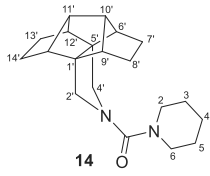
77.32  
77.00  
76.68  
53.56  
53.06  
51.25  
47.90  
45.01  
38.62  
25.60  
24.45  
24.30  
22.39

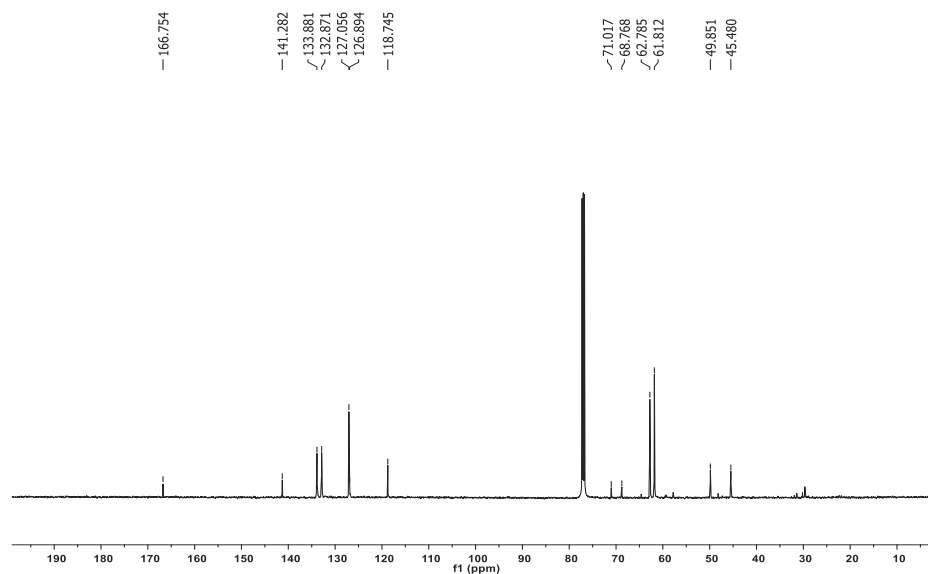
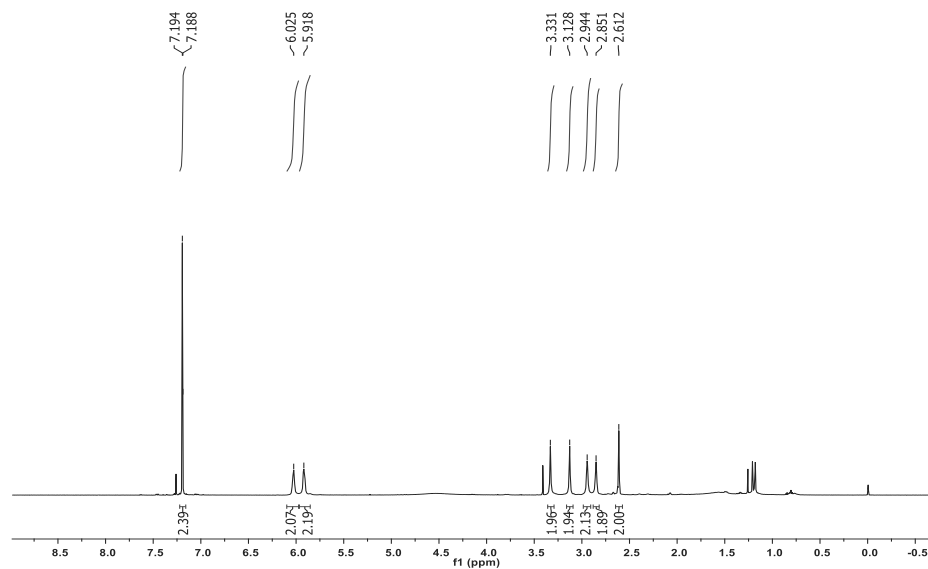
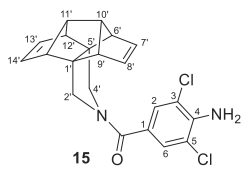


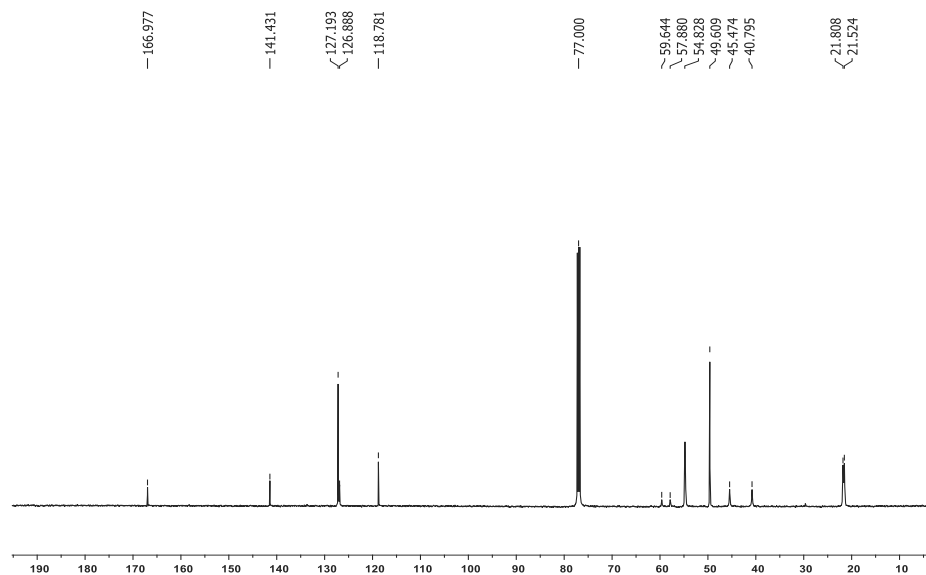
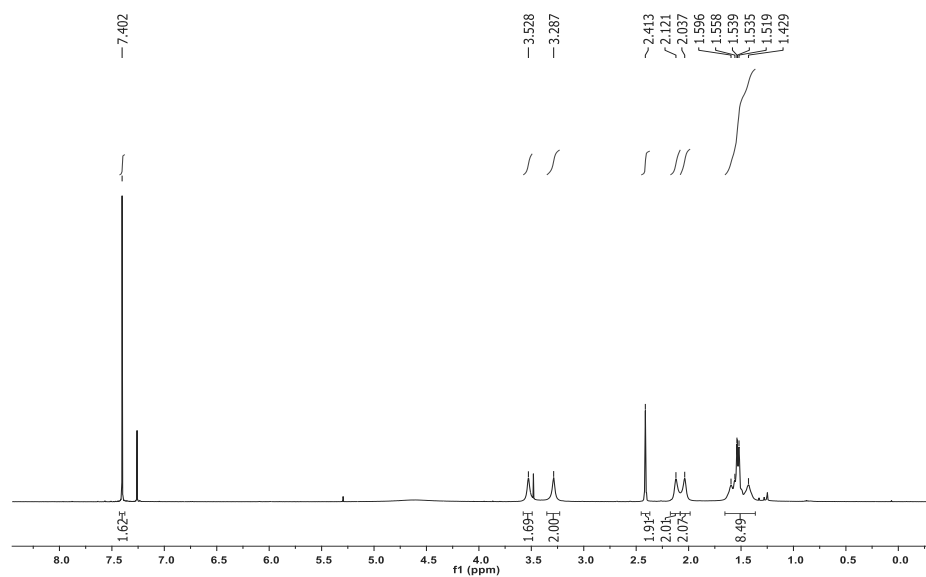
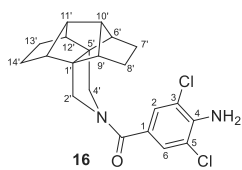


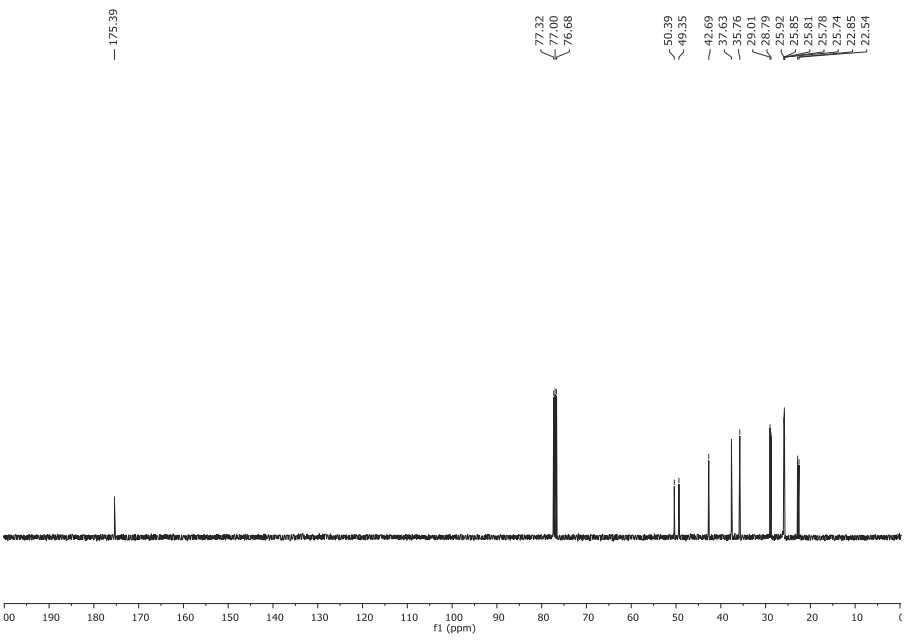
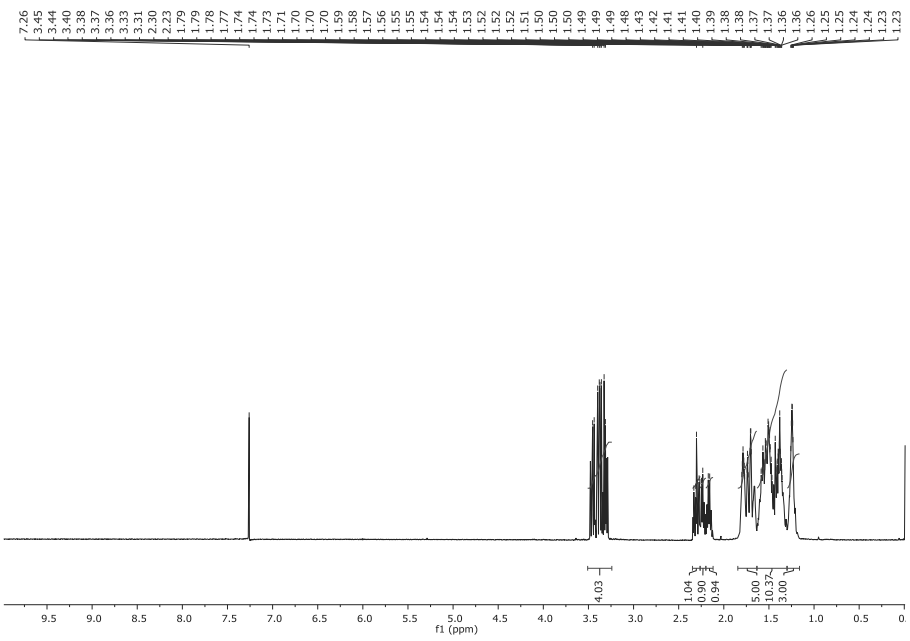
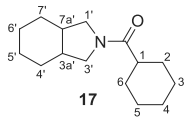


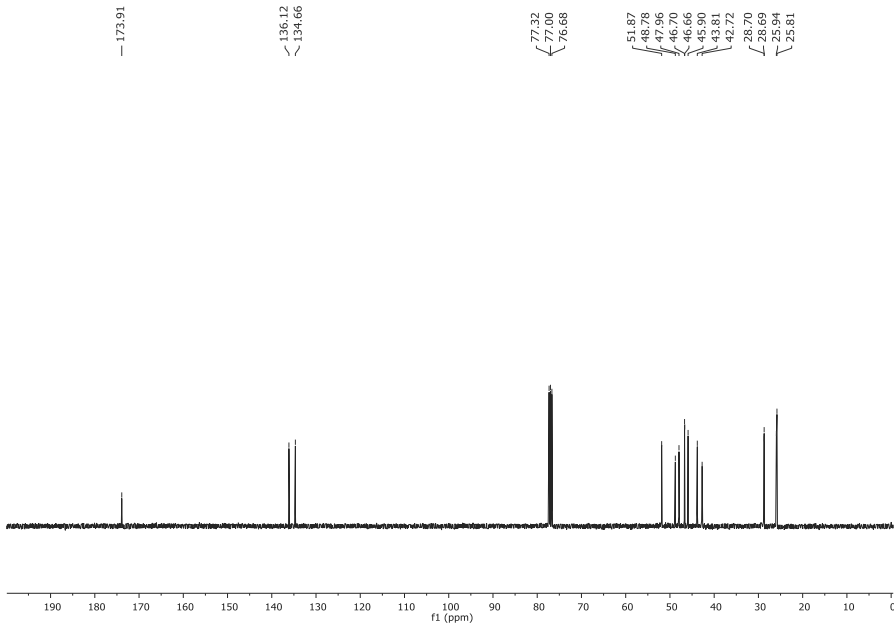
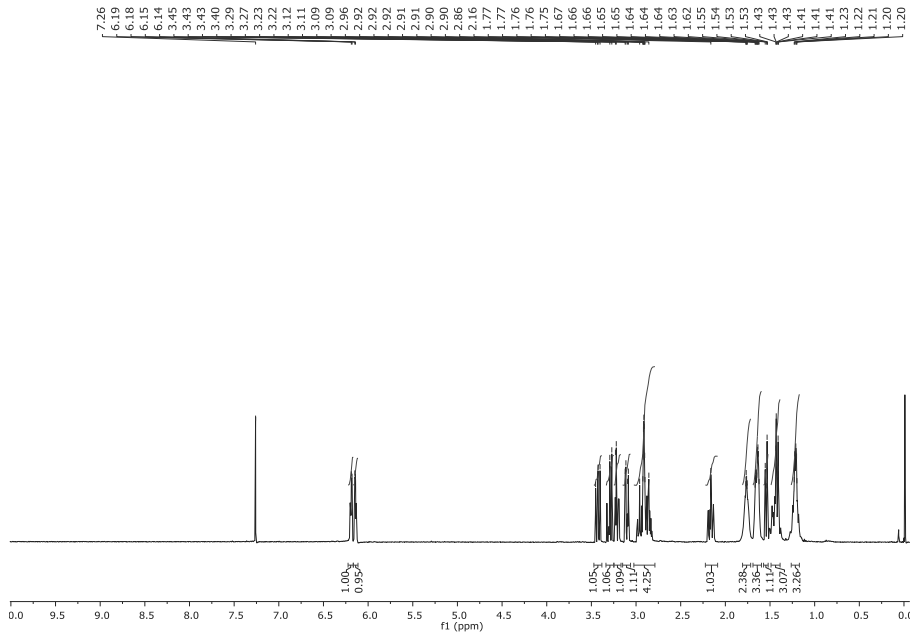
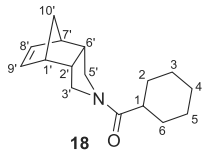




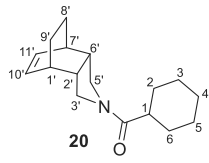




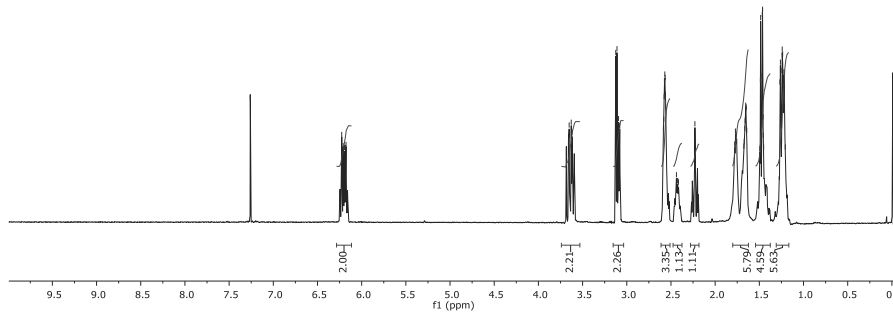




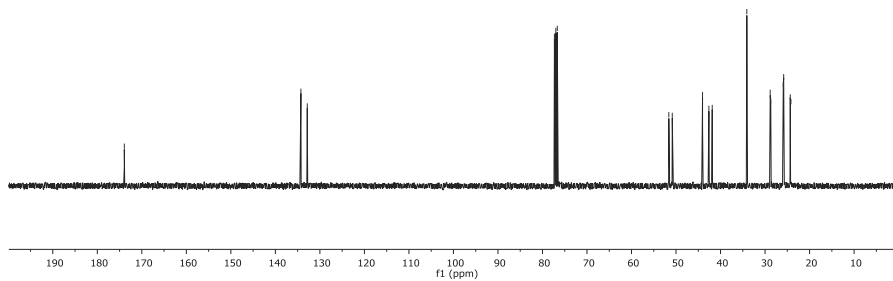


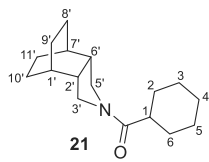


7.26  
6.73  
6.21  
6.21  
6.21  
6.19  
6.18  
6.18  
3.65  
3.63  
3.52  
3.12  
3.11  
3.09  
3.08  
3.08  
2.59  
2.58  
2.58  
2.57  
2.57  
2.57  
2.56  
2.56  
2.44  
2.44  
2.43  
2.42  
2.42  
2.38  
1.79  
1.77  
1.76  
1.76  
1.68  
1.67  
1.66  
1.66  
1.65  
1.65  
1.64  
1.64  
1.49  
1.49  
1.48  
1.48  
1.47  
1.47  
1.46  
1.46  
1.45  
1.45  
1.27  
1.27  
1.26  
1.25  
1.24  
1.24  
1.24  
1.24  
1.22  
1.22  
1.22  
1.21

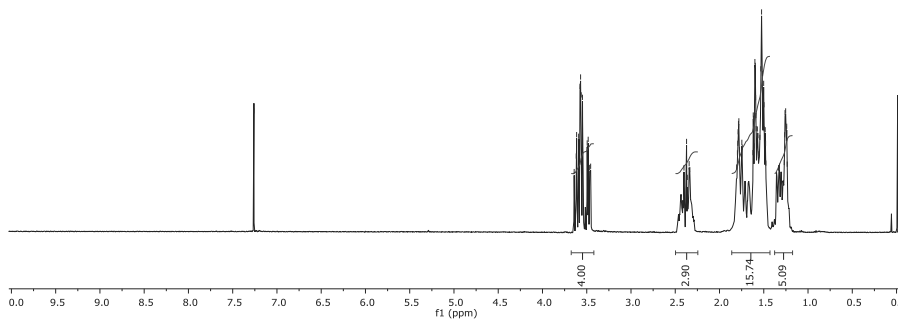


173.94  
134.27  
132.84  
77.32  
77.00  
76.68  
51.62  
50.85  
44.05  
42.62  
41.87  
34.10  
33.65  
28.72  
25.91  
25.85  
25.82  
24.34  
24.19





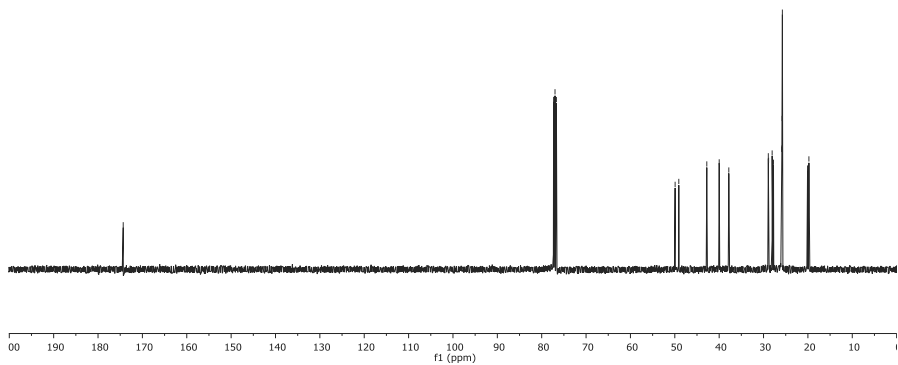
7.26  
3.62  
3.61  
3.59  
3.58  
3.57  
3.55  
3.50  
3.48  
3.47  
3.46  
2.40  
2.37  
2.34  
1.80  
1.80  
1.79  
1.79  
1.78  
1.78  
1.77  
1.75  
1.75  
1.74  
1.62  
1.62  
1.61  
1.60  
1.60  
1.60  
1.59  
1.59  
1.59  
1.57  
1.57  
1.56  
1.55  
1.54  
1.53  
1.53  
1.52  
1.50  
1.50  
1.49  
1.48  
1.48  
1.48  
1.33  
1.33  
1.32  
1.27  
1.26  
1.26  
1.25  
1.25  
1.24  
1.24



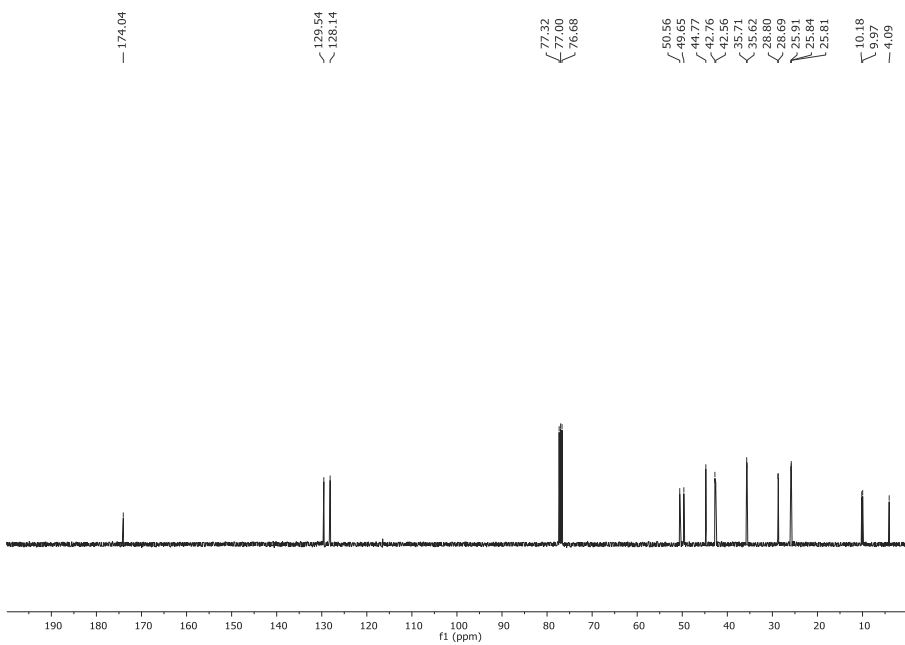
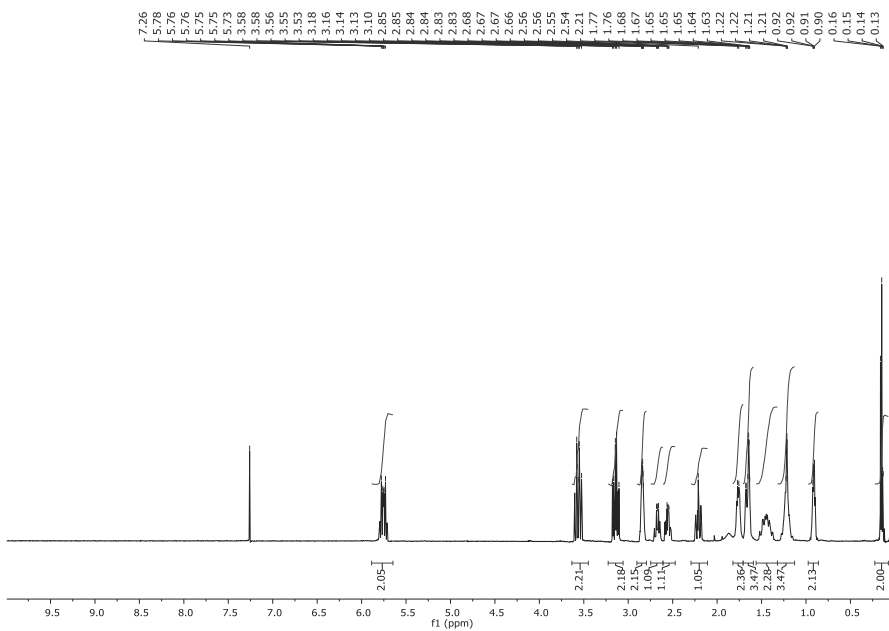
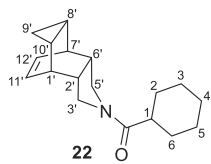
— 174.32

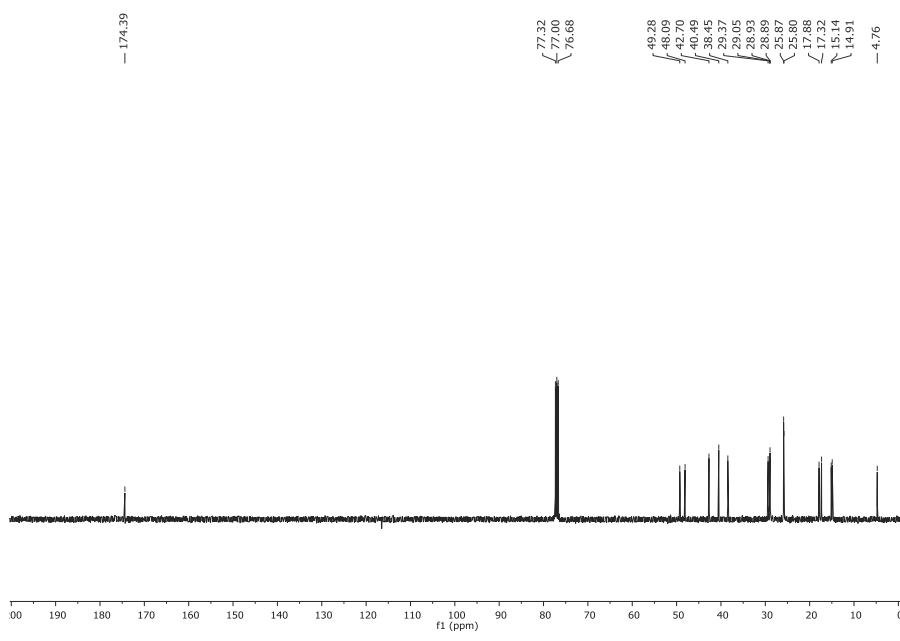
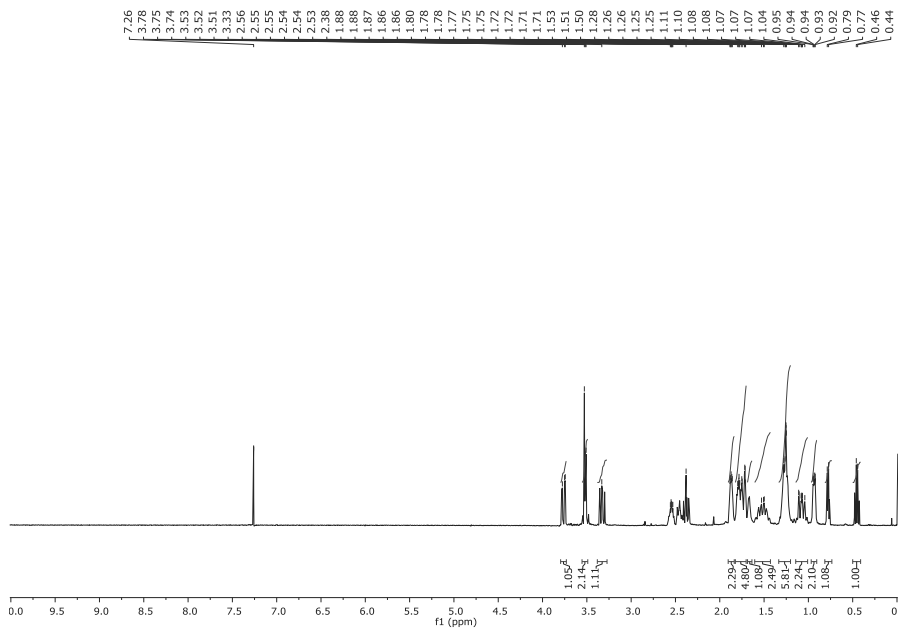
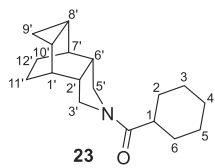
77.32  
77.00  
76.68

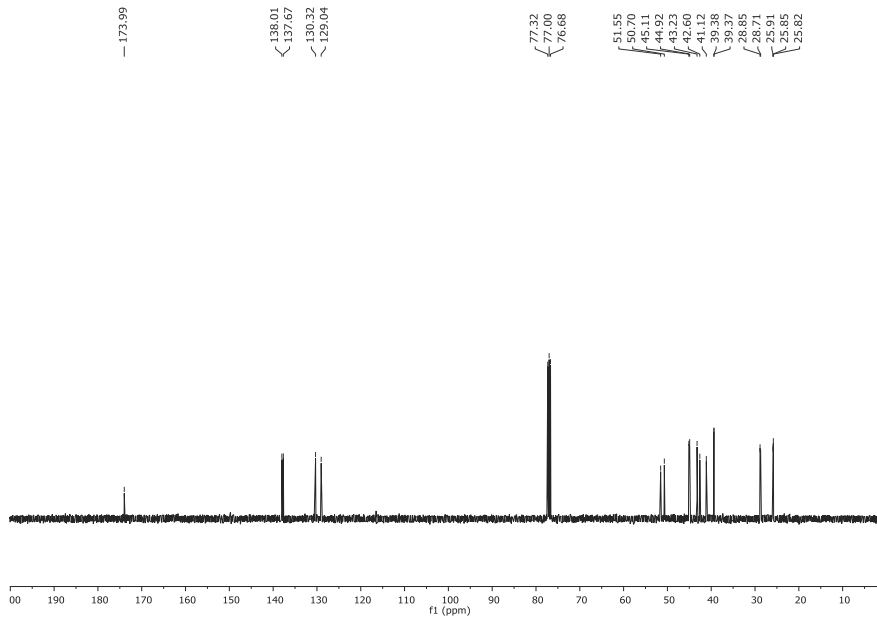
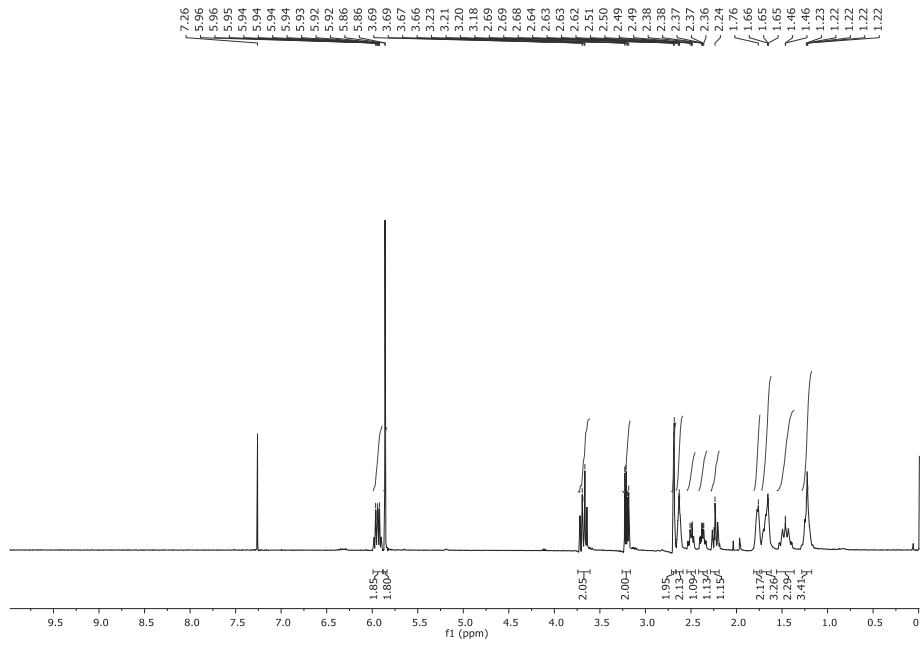
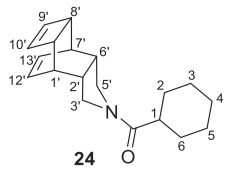
49.93  
42.70  
39.99  
37.83  
28.92  
28.86  
28.06  
27.76  
25.91  
25.81  
25.75  
20.08  
19.77

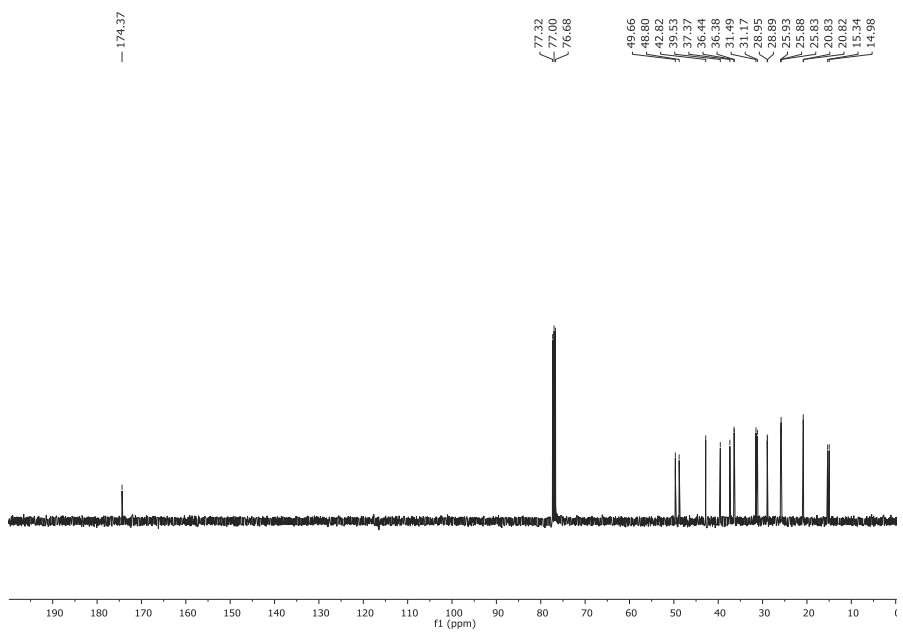
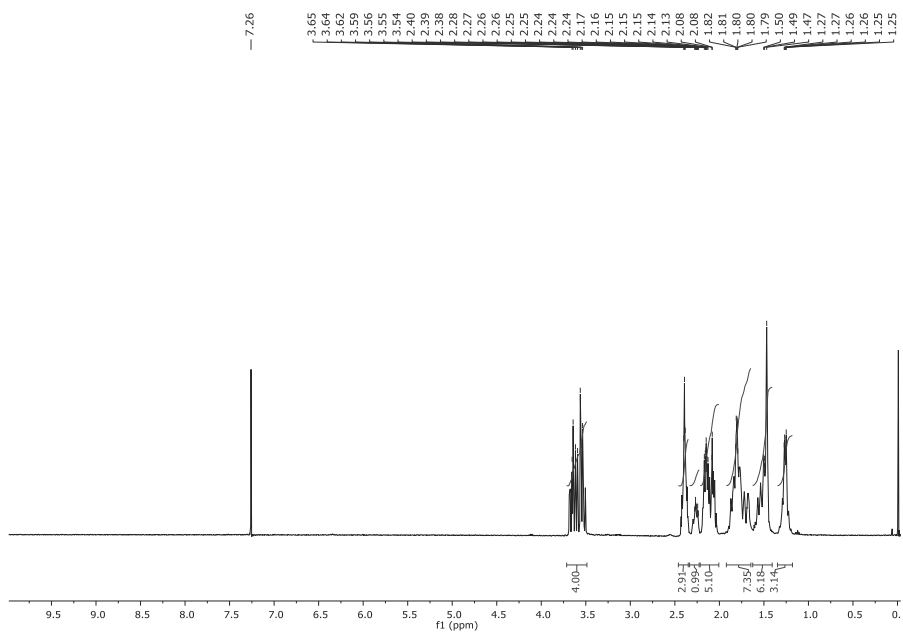
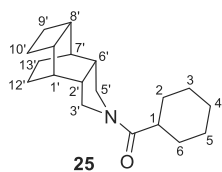


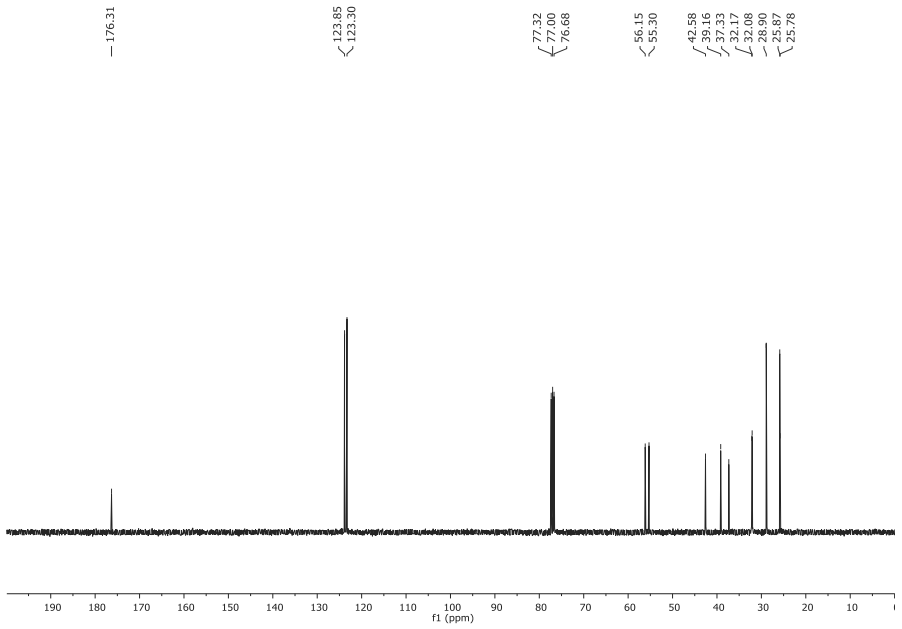
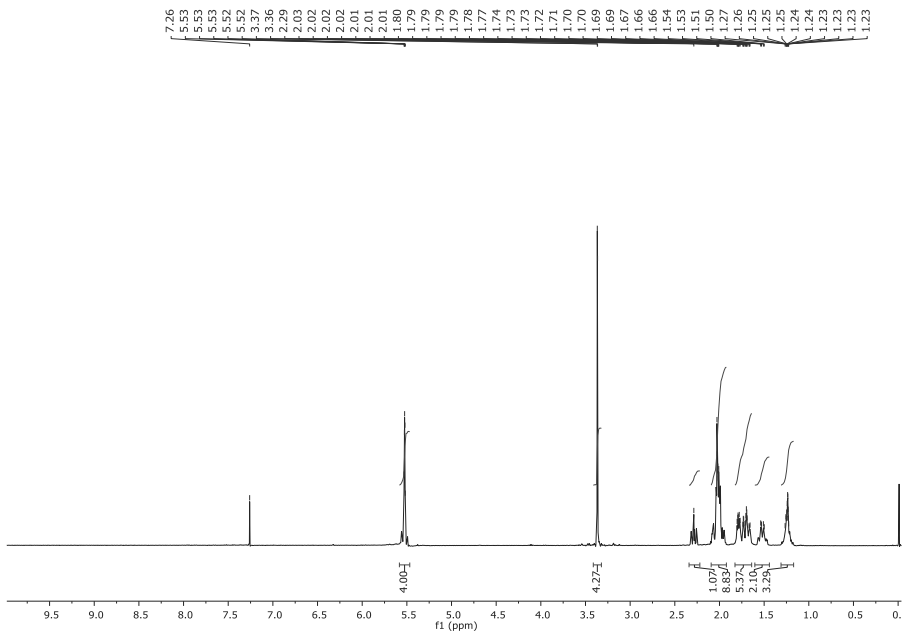
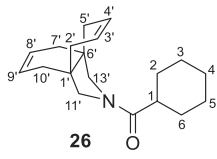


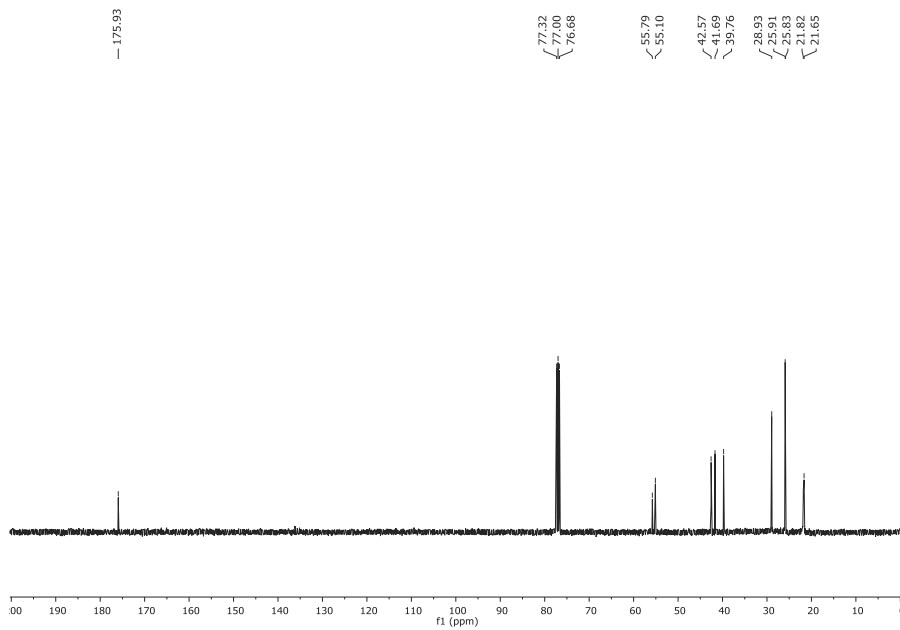
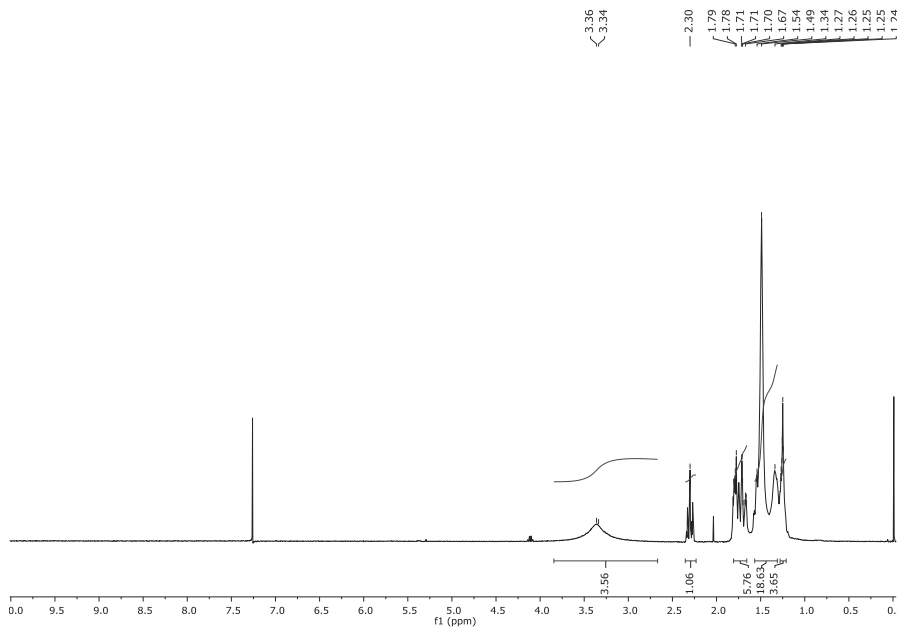
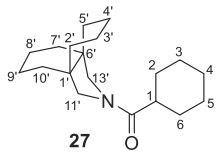


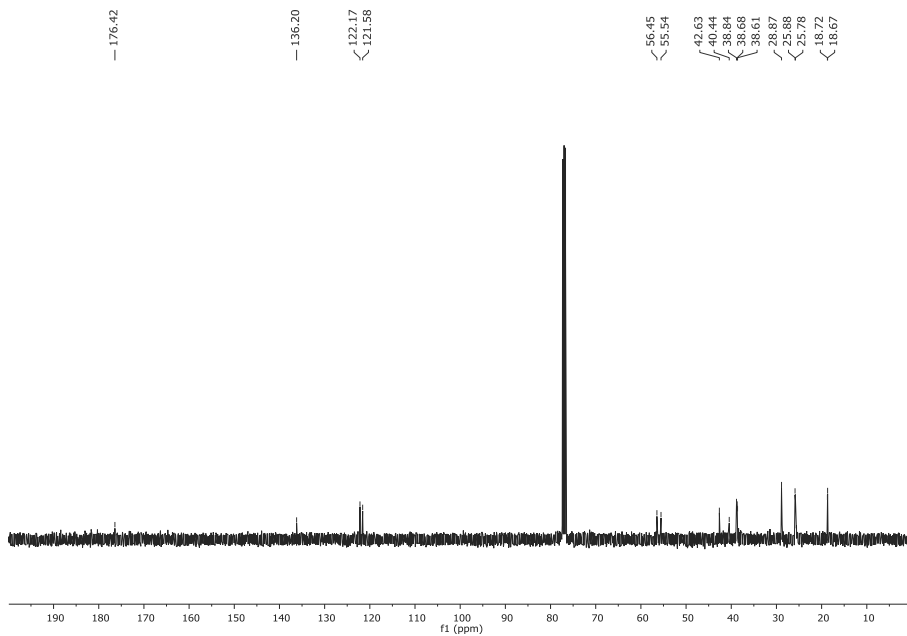
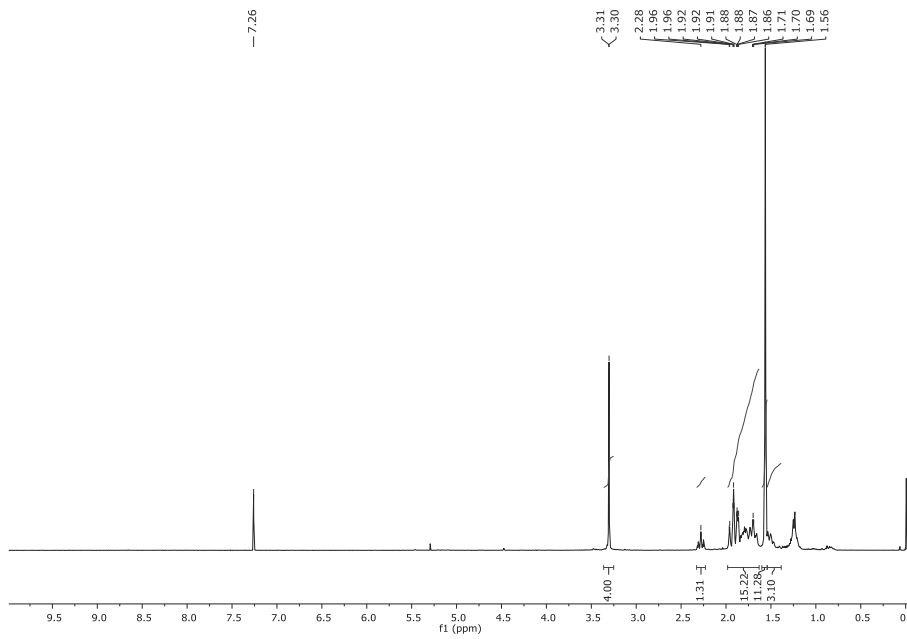
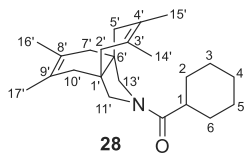


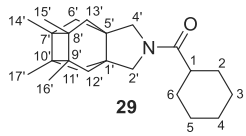




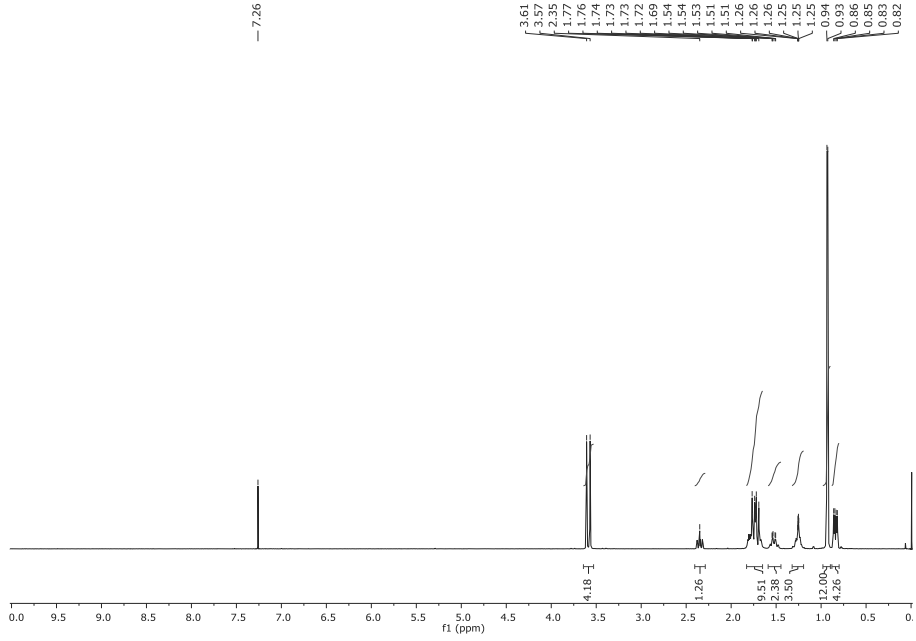




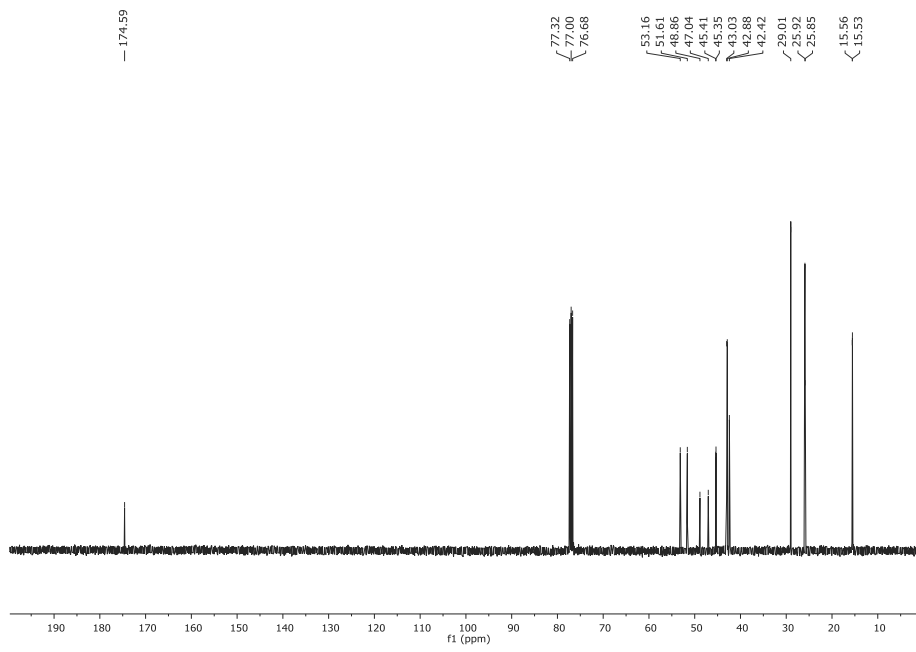




— 7.26



— 174.59







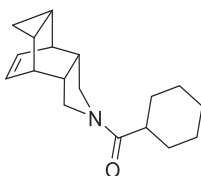
## CHAPTER 6

# **Exploring novel 11 $\beta$ -HSD1 inhibitors containing the optimized 4- azatetracyclo[5.3.2.0<sup>2,6</sup>.0<sup>8,10</sup>]dodec- 11-ene polycycle**



### 6.1 Rationale and previous work

The project discussed in this chapter aims to synthesize and evaluate novel compounds containing the 4-azapentacyclo[5.3.2.0<sup>2,6</sup>.0<sup>8,10</sup>]dodec-11-ene polycycle discovered in the previous project to have the optimal size and shape for filling the hydrophobic cavity in the 11 $\beta$ -HSD1 binding site. Although the high potency of compound **33**, the selectivity over 11 $\beta$ -HSD2 and the metabolic stability in HLM are far away from desirable values (Chart 8).<sup>238</sup>



**33**

hHSD1 IC<sub>50</sub> = 19 nM  
hHSD2 (10  $\mu$ M) = 69% inh  
HLM (30 min) = 27%

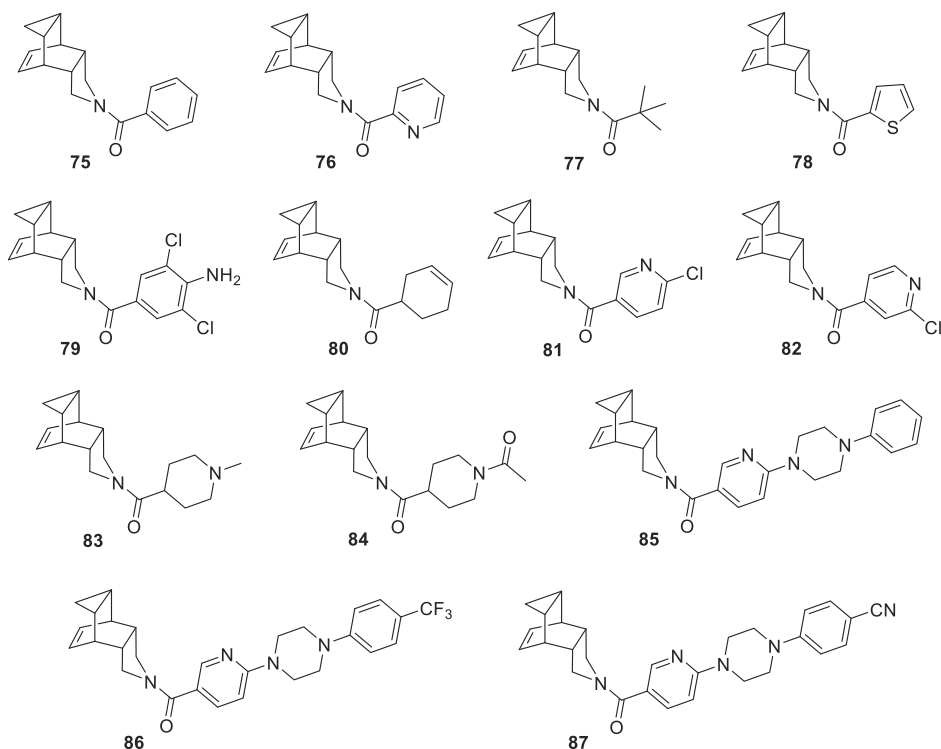
**Chart 8.** Structure of the previously described compound **33** and its pharmacological profile.<sup>238</sup>

Herein, there is the report of the exploration of different substituents in the right-hand side (RHS) of the molecule while maintaining the pyrrolidine-based polycycle of **33** in order to address the abovementioned issues. The endeavor started integrating different aromatic, heteroaromatic (electron-rich and -deficient rings), cycloalkenyl, heterocycloalkyl and branched alkyl substituents in order to generate diversity to build some SAR information.

Then, specifically, the target molecules were those outlined in the following chart.

<sup>238</sup> Leiva, R.; Griñan-Ferré, C.; Seira, C.; Valverde, E.; McBride, A.; Binnie, M.; Pérez, B.; Luque, F. J.; Pallàs, M.; Bidon-Chanal, A.; Webster, S. P.; Vázquez, S. *Eur. J. Med. Chem.* **2017**, *139*, 412-428.

*Polycyclic group optimization in 11 $\beta$ -HSD1 inhibitors and their pharmacological evaluation*



**Chart 9.** Designed novel compounds containing the 4-azapentacyclo[5.3.2.0<sup>2,6</sup>.0<sup>8,10</sup>]dodec-11-ene polycycle and varying the RHS substituent of the structure.

## 6.2 Theoretical discussion

All the compounds described in the following manuscript were prepared in the context of this Thesis. Their design, synthesis and pharmacological results are discussed in the manuscript, together with the experimental procedures and methods for the synthesis, characterization and biological evaluation.

In addition to the synthesis of the compounds, I also participated in its pharmacological evaluation during my research stay in the Dr Webster's laboratory (University of Edinburgh) in the same way as described in the previous project reported in Chapter 5.



## Exploring *N*-acyl-4-azatetracyclo[5.3.2.0<sup>2,6</sup>.0<sup>8,10</sup>]dodec-11-enes as 11 $\beta$ -HSD1 inhibitors

Rosana Leiva<sup>a</sup>, Andrew McBride<sup>b</sup>, Margaret Binnie<sup>b</sup>, Scott P. Webster<sup>b</sup>, and Santiago Vázquez<sup>a,\*</sup>

<sup>a</sup> *Laboratori de Química Farmacèutica (Unitat Associada al CSIC), Facultat de Farmàcia i Ciències de l'Alimentació, and Institute of Biomedicine (IBUB), Universitat de Barcelona, Av. Joan XXIII, 27-31, Barcelona, E-08028, Spain*

<sup>b</sup> *Centre for Cardiovascular Science, University of Edinburgh, Queen's Medical Research Institute, EH16 4TJ, United Kingdom*

### ARTICLE INFO

#### Article history:

Received  
Received in revised form  
Accepted  
Available online

#### Keywords:

Drug discovery  
Enzyme inhibitors  
Polycyclic substituents  
SAR investigation  
11 $\beta$ -HSD1

### ABSTRACT

Recently we found that a cyclohexylcarboxamide derived from 4-azatetracyclo[5.3.2.0<sup>2,6</sup>.0<sup>8,10</sup>]dodec-11-ene displayed low nanomolar inhibition of 11 $\beta$ -HSD1. In continuation of our efforts to discover potent and selective 11 $\beta$ -HSD1 inhibitors, herein we explored several replacements for the cyclohexyl ring. While some derivatives demonstrated potent inhibitory activity against human 11 $\beta$ -HSD1, low selectivity against isoenzyme 11 $\beta$ -HSD2 and poor microsomal stability could not be addressed.

2017 Elsevier Ltd. All rights reserved.

### 1. Introduction

Glucocorticoids (GCs) are hormones that play a major role in the modulation of inflammatory and immune responses, metabolism regulation, cardiovascular homeostasis and the body's response to stress.<sup>1,2</sup> It is well accepted that the local GC concentration in peripheral tissues depends not only on the circulating levels from adrenal secretion but also on the intracellular metabolism performed by activating and deactivating enzymes. 11 $\beta$ -hydroxysteroid dehydrogenase type 1 (11 $\beta$ -HSD1) catalyzes cortisol regeneration from its inactive form cortisone.<sup>3</sup> In contrast, 11 $\beta$ -HSD2 catalyzes the opposite reaction by oxidizing cortisol to cortisone.<sup>4</sup> 11 $\beta$ -HSD1 predominates in tissues mainly expressing glucocorticoid receptors, such as liver, adipose and brain, whereas 11 $\beta$ -HSD2 is found in tissues mainly expressing mineralocorticoid receptors, such as kidney, colon and salivary glands.<sup>5</sup> Selectivity against the desired 11 $\beta$ -HSD isoform is a key factor to avoid side effects of novel 11 $\beta$ -HSD1 inhibitors in development.

In recent years, both academia and industry have made great efforts to determine the role of this enzyme in diseases in which elevated cortisol plays an important role.<sup>6</sup> As a result, 11 $\beta$ -HSD1 activity in tissues has been found to be important in type 2 diabetes and metabolic syndrome,<sup>7</sup> in Alzheimer's disease (AD),<sup>8</sup> in osteoporosis,<sup>9</sup> and in glaucoma.<sup>10</sup> In light of this evidence, 11 $\beta$ -HSD1 has been explored as a therapeutic target to decrease cortisol concentrations in target tissues.

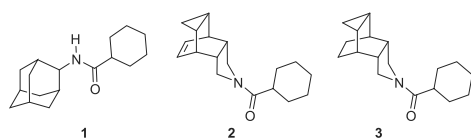
### 2. Results and discussion

#### 2.1. Design of new inhibitors

Our previous work on polycyclic substituent optimization of *N*-(2-adamantyl)amide **1**<sup>11</sup> led to the identification of pyrrolidine-based amides **2** and **3** as potent 11 $\beta$ -HSD1 inhibitors (Table 1). When tested against the 11 $\beta$ -HSD2 isoform, **2** had a selectivity index of at least 50-fold (IC<sub>50</sub> = 1–10  $\mu$ M), while **3** showed poor selectivity (IC<sub>50</sub> = 0.1–1  $\mu$ M). However, **3** possessed high metabolic stability in human liver microsomes (HLM, 94% of remaining compound after 30-min incubation), whereas **2** was rapidly metabolized (27%). In light of these results, and with the aim of prioritizing the microsomal stability, **3** was further *in vitro* characterized in terms of murine enzyme inhibition (mHSD1 IC<sub>50</sub> = 81 nM) and metabolic stability in murine liver microsomes (MLM, 93%). Subsequently, we performed an *in vivo* study with **3** in the Senescence-Accelerated Mouse Prone 8 (SAMP8) model of cognitive dysfunction in order to support the neuroprotective effect of 11 $\beta$ -HSD1 inhibition in cognitive decline related to the aging process. We found that **3**, administered to 12-month-old SAMP8 mice for four weeks, prevented memory deficits and displayed a neuroprotective action.<sup>12</sup>

These promising results with an early lead without optimal selectivity and DMPK properties led us to investigate additional potent 11 $\beta$ -HSD1 inhibitors that maintained the optimized polycycle of compound **2** while modifying the right-hand side (RHS) substituent of the structure.

\* Corresponding author. Tel.: +34-934-024-533; e-mail: [svazquez@ub.edu](mailto:svazquez@ub.edu)

**Table 1.** Previous 11 $\beta$ -HSD1 inhibitors reported by the group.<sup>a,b,11,12</sup>

Cp	hHSD1 IC <sub>50</sub> (nM)	HEK hHSD2 % inh 10 $\mu$ M or IC <sub>50</sub> <sup>c</sup>	HLM % parent <sup>d</sup>	mHSD1 IC <sub>50</sub> (nM)	MLM % parent <sup>d</sup>
1	86	88%	74	ND	ND
2	19	1-10 $\mu$ M	27	ND	ND
3	29	0.1-1 $\mu$ M	94	81	93

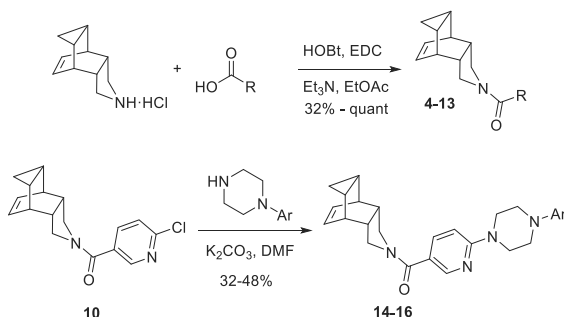
<sup>a</sup>See Experimental section for further details. <sup>b</sup>Percentage inhibition was determined relative to a no inhibitor control. <sup>c</sup>HEK293 cells stably transfected with the full-length gene coding for human 11 $\beta$ -HSD2 were used. <sup>d</sup>The microsomal stability of each compound was determined using either human or murine liver microsomes.

A series of different substituents were integrated into the RHS moiety, while the amido linker was retained to enable the key hydrogen bonds in the binding site.<sup>12</sup> A diversity of substituents was generated including aromatic, heteroaromatic (electron-rich and -deficient rings), branched alkyl, cycloalkenyl, heterocycloalkyl and other groups inspired in previously reported 11 $\beta$ -HSD1 inhibitors from Abbott (a series of dichloroaniline amides,<sup>13</sup> and ABT-384, which contains a 4-(pyridin-2-yl)piperazin-1-yl ring system.<sup>14</sup>

## 2.2. Chemistry

The novel compounds were synthesized according to Scheme 1. From 4-azapentacyclo[5.3.2.0<sup>2,6</sup>.0<sup>8,10</sup>]dodec-11-ene hydrochloride and the corresponding carboxylic acid in combination with 1-hydroxybenzotriazole (HOBT) and *N*-(3-dimethylaminopropyl)-*N'*-ethylcarbodiimide (EDC), amides **4-13** were prepared in moderate to excellent yields. For the synthesis of compounds **14-16**, the chloropyridinyl-containing analogue **10** was used as starting material in a nucleophilic aromatic substitution with the appropriate *N*-arylpiperazine delivering the desired compounds in moderate yields.

**Scheme 1.** Synthesis of amides **4-16** (for R and Ar motifs, see Table 2).



## 2.3. In vitro pharmacological evaluation

A preliminary screen was performed using a human microsome assay with compounds at 10  $\mu$ M in order to assess their potential inhibition of the target enzyme. Eight of the thirteen compounds presented 100% inhibition of the human 11 $\beta$ -HSD1 in this single concentration assay, so dose-response curves were performed to get their IC<sub>50</sub> values.

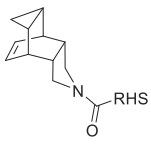
The analysis of these potencies showed some structure-activity relationships (SAR). Firstly, the introduction of a double bond in the cyclohexyl substituent of **2** delivered compound **9** which maintained nanomolar (IC<sub>50</sub> = 0.056  $\mu$ M). Secondly, introduction of a phenyl group on the RHS of the molecule was deleterious for the activity of the amide **4** (IC<sub>50</sub> = 0.546  $\mu$ M), which was replaced without success by either electron-rich (2-thiophenyl, **7**, 49% inhibition at 10  $\mu$ M) or electron-deficient (2-pyridinyl, 4-chloro-3-pyridinyl, 3-chloro-4-pyridinyl, **5**, **10** and **11**, IC<sub>50</sub> = 4.3  $\mu$ M, 0 and 23% inhibition at 10  $\mu$ M, respectively) heteroaromatic rings. Fortunately, when the phenyl group was substituted by a previously reported dichloroaniline group,<sup>13</sup> the potency was substantially increased to deliver a low nanomolar inhibitor (**8**, IC<sub>50</sub> = 0.045  $\mu$ M). Thirdly, introduction of *N*-substituted piperidinyl groups was again deleterious for the 11 $\beta$ -HSD1 inhibitory activity (**12** and **13**, 3 and 0% inhibition at 10  $\mu$ M, respectively). Fourthly, a branched alkyl substituent, such as the *tert*-butyl group, delivered amide **6** with a moderate potency (IC<sub>50</sub> = 0.666  $\mu$ M). Finally, compounds **14-16** containing a 6-(4-phenylpiperazin-1-yl)pyridin-3-yl system showed interesting SAR while completely inhibiting the target enzyme at 10  $\mu$ M. Compound **14**, featuring a terminal non-substituted phenyl ring in its structure, displayed an IC<sub>50</sub> of 5.44  $\mu$ M. Surprisingly, introduction of the trifluoromethyl group in *para* position mimicking the ABT-384 structure was deleterious for the activity (compound **15**, IC<sub>50</sub> = 11.60  $\mu$ M), while replaced by a cyano group increased the potency (compound **16**, IC<sub>50</sub> = 0.377  $\mu$ M).

Those compounds with submicromolar IC<sub>50</sub> values (**4**, **6**, **8**, **9** and **16**) were further evaluated in terms of cellular potency, selectivity over 11 $\beta$ -HSD2 and metabolic stability.

Cellular potency was assessed using Human Embryonic Kidney 293 (HEK293) cells stably transfected with the 11 $\beta$ -HSD1 gene. The results were in line with the previous results obtained in the microsomal assay. The most potent compounds (**8**, **9** and **16**, IC<sub>50</sub> = 0.045, 0.056 and 0.377  $\mu$ M, respectively) presented complete inhibition at 10  $\mu$ M in the cell-based assay, whereas compounds with IC<sub>50</sub> values between 0.5 and 1  $\mu$ M, **4** and **6**, showed a moderate cellular potency (77 and 41%, respectively).

Selectivity over 11 $\beta$ -HSD2 was also assessed in a cell-based assay using the same methodology as before (HEK293 stably transfected with the 11 $\beta$ -HSD2 gene). Although all the tested compounds presented a poor selectivity (>50% inhibition at 10  $\mu$ M), it must be highlighted that compound **16** (IC<sub>50</sub> = 0.377  $\mu$ M) presented a 54% inhibition, indicating that its IC<sub>50</sub> against 11 $\beta$ -HSD2 is approximately 10  $\mu$ M, having a selectivity index of 30-fold.

Finally, metabolic stability was determined using HLM, which are widely used to predict the degree of primary metabolic clearance in the liver. Compounds **6** and **4** displayed moderate to high microsomal stabilities (60 and 85% of remaining compound after 30-min incubation, respectively), while **8**, **9** and **16** presented low stabilities (13, 44 and 13%, respectively).

**Table 2.** Novel 11 $\beta$ -HSD1 inhibitors featuring the 4-azapentacyclo[5.3.2.0<sup>2,6</sup>.0<sup>8,10</sup>]dodec-11-ene polycycle.<sup>a,b</sup>


**4-16**

Cp	RHS	hHSD1 % inh at 10 $\mu$ M	hHSD1 IC <sub>50</sub> ( $\mu$ M)	HEK hHSD1 % inh at 10 $\mu$ M	HEK hHSD2 % inh at 10 $\mu$ M	HLM % parent <sup>d</sup>
2		100	0.019	100	69	27
4		100	0.546	77	84	85
5		100	4.265	ND	ND	ND
6		100	0.666	41	71	60
7		49	ND	ND	ND	ND
8		100	0.045	100	86	13
9		100	0.056	100	87	44
10		0	ND	ND	ND	ND
11		23	ND	ND	ND	ND
12		3	ND	ND	ND	ND
13		0	ND	ND	ND	ND
14		100	5.441	ND	ND	ND
15		100	11.560	ND	ND	ND
16		100	0.377	100	53	13

<sup>a</sup>See Experimental section for further details. <sup>b</sup>Percentage inhibition was determined relative to a no inhibitor control. <sup>c</sup>HEK293 cells stably transfected with the full length gene coding for human either 11 $\beta$ -HSD1 or 11 $\beta$ -HSD2 were used. <sup>d</sup>Percentage of remaining compound after 30-min incubation period in human liver microsomes. ND, not determined.

### 3. Conclusions

In summary, we have designed, synthesized and described SAR for a novel series of 11 $\beta$ -HSD1 inhibitors featuring the optimized polycyclic substituent 4-azapentacyclo[5.3.2.0<sup>2,6</sup>.0<sup>8,10</sup>]dodec-11-ene. Nanomolar potencies were achieved for compounds **8** and **9**, although selectivity and metabolic stabilities were suboptimal. The discovery of inhibitors with desirable

selectivity and DMPK properties is a key step for the development of successful 11 $\beta$ -HSD1 inhibitors for the treatment of GC-related disorders such as diabetes and AD. Clear SAR in this new family of HSD1 inhibitors was found; a double bond was tolerated in the initial cyclohexyl unit (**9**, IC<sub>50</sub> = 0.056  $\mu$ M), but the inclusion of heterocycloalkyl and heteroaromatic groups very detrimental for the inhibitory activity (**5**, IC<sub>50</sub> = 4.265  $\mu$ M, and **7**, **10**, **11**, **12** and **13**, <50% inhibition at 10  $\mu$ M). The



introduction of a phenyl group as RHS of the molecule was also detrimental for the potency (**4**, 0.546  $\mu\text{M}$ ); however, the introduction of a previously reported substitution pattern on the aryl unit delivered again a low nanomolar inhibitor (**8**,  $\text{IC}_{50}$  = 0.045  $\mu\text{M}$ ). Future efforts will be focused on rational design of the substitution pattern of this aryl group to identify optimized compounds addressing the weaknesses of those described in this work.

## 4. Experimental

### 4.1. Chemistry

#### 4.1.1. General

Melting points were determined in open capillary tubes with a MFB 595010M Gallenkamp. 400 MHz  $^1\text{H}/100.6$  MHz  $^{13}\text{C}$  NMR spectra were recorded on a Varian Mercury 400. The chemical shifts are reported in ppm ( $\delta$  scale) relative to internal tetramethylsilane, and coupling constants are reported in Hertz (Hz). Assignments given for the NMR spectra of the new compounds have been carried out on the basis of COSY  $^1\text{H}/^{13}\text{C}$  (gHSQC sequences) experiments. IR spectra were run on Perkin-Elmer Spectrum RX I spectrophotometer. Absorption values are expressed as wave-numbers ( $\text{cm}^{-1}$ ); only significant absorption bands are given. High-resolution mass spectrometry (HRMS) analyses were performed with an LC/MSD TOF Agilent Technologies spectrometer. Column chromatography was performed either on silica gel 60  $\text{\AA}$  (35-70 mesh) or on aluminium oxide, neutral, 60  $\text{\AA}$  (50-200  $\mu\text{m}$ , Brockmann I). Thin-layer chromatography was performed with aluminum-backed sheets with silica gel 60 F254 (Merck, ref 1.05554), and spots were visualized with UV light and 1% aqueous solution of  $\text{KMnO}_4$ . The analytical samples of all of the new compounds which were subjected to pharmacological evaluation possessed purity  $\geq 95\%$  as evidenced by their elemental analyses. The elemental analyses were carried out in a Flash 1112 series Thermofinnigan elemental microanalyzer (A5) to determine C, H and N.

#### 4.1.2. (4-azatetracyclo[5.3.2.0<sup>2.6</sup>.0<sup>8.10</sup>]dodec-11-en-4-yl)(phenyl)methanone, **4**

To a solution of 4-azapentacyclo[5.3.2.0<sup>2.6</sup>.0<sup>8.10</sup>]dodec-11-ene hydrochloride (400 mg, 2.07 mmol) in EtOAc (20 mL) were added benzoic acid (230 mg, 1.88 mmol), HOBt (381 mg, 2.82 mmol), EDC (437 g, 2.82mmol) and triethylamine (1.2 mL, 8.27 mmol). The reaction mixture was stirred at room temperature overnight. To the resulting suspension was then added water (20 mL) and the phases were separated. The organic phase was washed with saturated aqueous  $\text{NaHCO}_3$  solution (20 mL) and brine (20 mL), dried over anh.  $\text{Na}_2\text{SO}_4$  and filtered. Evaporation *in vacuo* of the organics gave **4** as an orange oil (479 mg, 96% yield). Column chromatography (Hexane/Ethyl acetate mixture) gave **4** as a white solid (385 mg), mp 65-66°C. IR (ATR)  $\nu$ : 660, 700, 715, 763, 794, 814, 847, 986, 1029, 1135, 1170, 1231, 1378, 1423, 1572, 1618, 2845, 2865, 2921, 2946  $\text{cm}^{-1}$ .  $^1\text{H-NMR}$  (400 MHz,  $\text{CDCl}_3$ )  $\delta$ : 0.10-0.18 (complex signal, 2 H, 9'-H<sub>2</sub>), 0.82-0.98 (complex signal, 2 H, 8'-H and 10'-H), 2.50-2.66 (complex signal, 2 H, 2'-H and 6'-H), 2.71 (m, 1 H, 1'-H or 7'-H), 2.91 (m, 1 H, 7'-H or 1'-H), 3.09 (dd,  $J = 11.6$  Hz,  $J' = 4.4$  Hz, 1 H, 3'-H<sub>a</sub> or 5'-H<sub>a</sub>), 3.42-3.56 (complex signal, 2 H, 5'-H<sub>a</sub> or 3'-H<sub>a</sub> and 3'-H<sub>b</sub> or 5'-H<sub>b</sub>), 3.74 (dd,  $J = 13.0$  Hz,  $J' = 8.6$  Hz, 1 H, 5'-H<sub>b</sub> or 3'-H<sub>b</sub>), 5.70 (m, 1 H, 11'-H or 12'-H), 5.86 (m, 1 H, 12'-H or 11'-H), 7.32-7.41 (complex signal, 5 H, Ar-H).  $^{13}\text{C-NMR}$  (100.5 MHz,  $\text{CDCl}_3$ )  $\delta$ : 3.9 ( $\text{CH}_2$ , C9'), 9.2 (CH, C8' or C10'), 10.2 (CH, C10' or C8'), 35.5 (CH, C1' or C7'), 35.6 (CH, C7' or C1'), 42.8 (CH, C2' or C6'), 44.8 (CH, C6' or C2'), 49.3 ( $\text{CH}_2$ , C3' or C5'), 53.3 ( $\text{CH}_2$ , C5' or C3'), 126.8 [CH, C2(6)], 128.1

[CH, C3(5)], 128.2 (CH, C11' or C12'), 129.2 (CH, C12' or C11'), 129.4 (CH, C4), 137.4 (C, C1), 168.9 (C, CO). Calcd for  $\text{C}_{18}\text{H}_{19}\text{NO}$ : C, 81.47; H, 7.22; N, 5.28. Found: C, 81.52; H, 7.34; N 5.25.

#### 4.1.3. (4-azatetracyclo[5.3.2.0<sup>2.6</sup>.0<sup>8.10</sup>]dodec-11-en-4-yl)(pyridin-2-yl)methanone, **5**

To a solution of 4-azapentacyclo[5.3.2.0<sup>2.6</sup>.0<sup>8.10</sup>]dodec-11-ene hydrochloride (400 mg, 2.07 mmol) in EtOAc (20 mL) were added picolinic acid (231 mg, 1.88 mmol), HOBt (381 mg, 2.82 mmol), EDC (437 mg, 2.82 mmol) and triethylamine (1.2 mL, 8.27 mmol). The reaction mixture was stirred at room temperature overnight. To the resulting suspension was then added water (20 mL) and the phases were separated. The organic phase was washed with saturated aqueous  $\text{NaHCO}_3$  solution (20 mL) and brine (20 mL), dried over anh.  $\text{Na}_2\text{SO}_4$  and filtered. Evaporation *in vacuo* of the organics gave **5** as an orange oil (466 mg, 93% yield). Column chromatography (Hexane/Ethyl acetate mixture) gave **5** as a white solid (326 mg), mp 110-111°C. IR (ATR)  $\nu$ : 682, 720, 753, 796, 814, 844, 912, 988, 1041, 1082, 1142, 1165, 1201, 1226, 1269, 1294, 1302, 1340, 1378, 1400, 1441, 1474, 1562, 1585, 1618, 2850, 2870, 2926, 3007, 3048  $\text{cm}^{-1}$ .  $^1\text{H-NMR}$  (400 MHz,  $\text{CDCl}_3$ )  $\delta$ : 0.10-0.19 (complex signal, 2 H, 9'-H<sub>2</sub>), 0.84-0.97 (complex signal, 2 H, 8'-H and 10'-H), 2.57-2.69 (complex signal, 2 H, 2'-H and 6'-H), 2.75 (m, 1 H, 1'-H or 7'-H), 2.90 (m, 1 H, 7'-H or 1'-H), 3.31 (dd,  $J = 12.4$  Hz,  $J' = 4.8$  Hz, 1 H, 3'-H<sub>a</sub> or 5'-H<sub>a</sub>), 3.42 (dd,  $J = 13.0$  Hz,  $J' = 4.8$  Hz, 1 H, 5'-H<sub>a</sub> or 3'-H<sub>a</sub>), 3.82 (dd,  $J = 13.6$  Hz,  $J' = 8.8$  Hz, 1 H, 3'-H<sub>b</sub> or 5'-H<sub>b</sub>), 3.85 (dd,  $J = 12.8$  Hz,  $J' = 8.8$  Hz, 1 H, 5'-H<sub>b</sub> or 3'-H<sub>b</sub>), 5.71 (m, 1 H, 11'-H or 12'-H), 5.83 (m, 1 H, 12'-H or 11'-H), 7.30 (ddd,  $J = 12.4$  Hz,  $J' = 4.8$  Hz,  $J'' = 1.6$  Hz, 1 H, 5-H), 7.67-7.80 (complex signal, 2 H, 4-H and 3-H), 8.54 (ddd,  $J = 4.8$  Hz,  $J' = 1.6$  Hz,  $J'' = 1.0$  Hz, 1 H, 6-H).  $^{13}\text{C-NMR}$  (100.5 MHz,  $\text{CDCl}_3$ )  $\delta$ : 4.1 ( $\text{CH}_2$ , C9'), 10.0 (CH, C8' or C10'), 10.2 (CH, C10' or C8'), 35.4 (CH, C1' and C7'), 42.5 (CH, C2' or C6'), 45.2 (CH, C6' or C2'), 50.2 ( $\text{CH}_2$ , C3' or C5'), 52.8 ( $\text{CH}_2$ , C5' or C3'), 123.6 (CH, C3), 124.3 (CH, C5), 128.6 (CH, C11' or C12'), 129.1 (CH, C12' or C11'), 136.7 (CH, C4), 147.9 (CH, C6), 154.8 (C, C2), 165.8 (C, CO). Calcd for  $\text{C}_{17}\text{H}_{18}\text{N}_2\text{O}$ : C, 76.66; H, 6.81; N, 10.52. Found: C, 76.47; H, 7.01; N, 10.21.

#### 4.1.4. (4-azatetracyclo[5.3.2.0<sup>2.6</sup>.0<sup>8.10</sup>]dodec-11-en-4-yl)(tert-butyl)methanone, **6**

To a solution of 4-azapentacyclo[5.3.2.0<sup>2.6</sup>.0<sup>8.10</sup>]dodec-11-ene hydrochloride (200 mg, 1.03 mmol) in EtOAc (10 mL) were added pivalic acid (105 mg, 0.94 mmol), HOBt (190mg, 1.41 mmol), EDC (218 mg, 1.41 mmol) and triethylamine (0.6 mL, 4.14 mmol). The reaction mixture was stirred at room temperature overnight. To the resulting suspension was then added water (10 mL) and the phases were separated. The organic phase was washed with saturated aqueous  $\text{NaHCO}_3$  solution (10 mL) and brine (10 mL), dried over anh.  $\text{Na}_2\text{SO}_4$  and filtered. Evaporation *in vacuo* of the organics gave **6** as a yellowish solid (216 mg, 94% yield). The analytical sample was obtained by crystallization from hot EtOAc (69 mg), mp 91-92°C. IR (ATR)  $\nu$ : 720, 756, 766, 809, 829, 849, 912, 943, 988, 1036, 1069, 1094, 1165, 1193, 1239, 1274, 1340, 1362, 1380, 1405, 1461, 1476, 1507, 1610, 2870, 2896, 2936, 2951, 2992  $\text{cm}^{-1}$ .  $^1\text{H-NMR}$  (400 MHz,  $\text{CDCl}_3$ )  $\delta$ : 0.10-0.18 (complex signal, 2 H, 9'-H<sub>2</sub>), 0.91 [m, 2 H, 8'(10')-H], 1.18 [s, 9 H, C( $\text{CH}_3$ )<sub>3</sub>], 2.56 [m, 2 H, 2'(6')-H], 2.84 [m, 2 H, 1'(7')-H], 3.27 [dd,  $J = 11.8$  Hz,  $J' = 4.2$  Hz, 2 H, 3'(5')-H<sub>a</sub>], 3.63 [m, 2 H, 3'(5')-H<sub>b</sub>], 5.74 [t,  $J = 4.0$  Hz, 2 H, 11'(12')-H].  $^{13}\text{C-NMR}$  (100.5 MHz,  $\text{CDCl}_3$ )  $\delta$ : 3.9 ( $\text{CH}_2$ , C9'), 10.1 [CH, C8'(10')], 27.5 [ $\text{CH}_3$ , C( $\text{CH}_3$ )<sub>3</sub>], 35.6 [CH, C1'(7')], 38.6 [C, C( $\text{CH}_3$ )<sub>3</sub>], 51.7 [ $\text{CH}_2$ , C3'(5')], 128.6 [CH, C11'(12')], 175.7 (C, CO). The signal of C2'(6') was not observed. Anal.

Calcd for C<sub>16</sub>H<sub>23</sub>NO: C, 78.32; H, 9.45; N, 5.71. Found: C, 78.16; H, 9.52; N, 5.86.

#### 4.1.5. (4-azatetracyclo[5.3.2.0<sup>2,6</sup>.0<sup>8,10</sup>]dodec-11-en-4-yl)(thien-2-yl)methanone, 7

To a solution of 4-azapentacyclo[5.3.2.0<sup>2,6</sup>.0<sup>8,10</sup>]dodec-11-ene hydrochloride (200 mg, 1.03 mmol) in EtOAc (10 mL) were added 2-thiophenecarboxylic acid (121 mg, 0.94 mmol), HOBt (190mg, 1.41 mmol), EDC (218 mg, 1.41 mmol) and triethylamine (0.6 mL, 4.14 mmol). The reaction mixture was stirred at room temperature overnight. To the resulting suspension was then added water (10 mL) and the phases were separated. The organic phase was washed with saturated aqueous NaHCO<sub>3</sub> solution (10 mL) and brine (10 mL), dried over anhydrous Na<sub>2</sub>SO<sub>4</sub> and filtered. Evaporation *in vacuo* of the organics gave **7** as a yellowish solid (219 mg, 86% yield). The analytical sample was obtained by crystallization from hot EtOAc (87 mg), mp 104-105°C. IR (ATR)  $\nu$ : 667, 703, 720, 738, 786, 814, 849, 890, 915, 950, 1008, 1031, 1057, 1087, 1132, 1239, 1254, 1279, 1312, 1352, 1380, 1403, 1431, 1519, 1580, 1598, 2921, 2936, 3002, 3037 cm<sup>-1</sup>. <sup>1</sup>H-NMR (400 MHz, CDCl<sub>3</sub>)  $\delta$ : 0.12-0.20 (complex signal, 2 H, 9'-H<sub>2</sub>), 0.86-1.02 (complex signal, 2 H, 8'-H and 10'-H), 2.63 (m, 1 H, 2'-H or 6'-H), 2.73 (m, 1 H, 6'-H or 2'-H), 2.81-2.98 (complex signal, 2 H, 1'-H and 7'-H), 3.36-3.48 (complex signal, 2 H, 3'-H<sub>a</sub> and 5'-H<sub>a</sub>), 3.72-3.96 (complex signal, 2 H, 3'-H<sub>b</sub> and 5'-H<sub>b</sub>), 5.75 (m, 1 H, 11'-H or 12'-H), 5.83 (m, 1 H, 12'-H or 11'-H), 7.03 (dd,  $J = 5.0$  Hz,  $J' = 3.4$ , 1 H, 4-H), 7.40 (dd,  $J = 3.4$  Hz,  $J' = 1.0$ , 1 H, 3-H or 5-H), 7.43 (dd,  $J = 5.0$  Hz,  $J' = 1.0$ , 1 H, 5-H or 3-H). <sup>13</sup>C-NMR (100.5 MHz, CDCl<sub>3</sub>)  $\delta$ : 4.1 (CH<sub>2</sub>, C9'), 10.0 (CH, C8' or C10'), 10.1 (CH, C10' or C8'), 35.6 (broad s, CH, C1' and C7'), 42.1 (CH, C2' or C6'), 45.4 (CH, C6' or C2'), 50.9 (CH<sub>2</sub>, C3' or C5'), 52.9 (CH<sub>2</sub>, C5' or C3'), 126.8 (CH, C3), 128.3 (broad s, CH, C11' or C12'), 129.1 (CH, C4), 129.3 (CH, C5), 129.4 (broad s, CH, C12' or C11'), 139.4 (C, C2), 161.2 (C, CO). Anal. Calcd for C<sub>16</sub>H<sub>17</sub>NOS: C, 70.81; H, 6.31; N, 5.16. Found: C, 70.70; H, 6.28; N, 5.12.

#### 4.1.6. (4-amino-3,5-dichlorophenyl)(4-azatetracyclo[5.3.2.0<sup>2,6</sup>.0<sup>8,10</sup>]dodec-11-en-4-yl)methanone, 8

To a solution of 4-azapentacyclo[5.3.2.0<sup>2,6</sup>.0<sup>8,10</sup>]dodec-11-ene hydrochloride (200 mg, 1.03 mmol) in EtOAc (10 mL) were added 3,5-dichloro-4-aminobenzoic acid (194 mg, 0.94 mmol), HOBt (190mg, 1.41 mmol), EDC (218 mg, 1.41 mmol) and triethylamine (0.6 mL, 4.14 mmol). The reaction mixture was stirred at room temperature overnight. To the resulting suspension was then added water (10 mL) and the phases were separated. The organic phase was washed with saturated aqueous NaHCO<sub>3</sub> solution (10 mL) and brine (10 mL), dried over anhydrous Na<sub>2</sub>SO<sub>4</sub> and filtered. Evaporation *in vacuo* of the organics gave **8** as a yellowish solid (322 mg, 89% yield). The analytical sample was obtained by crystallization from hot EtOAc, mp 186-187°C. IR (ATR)  $\nu$ : 680, 718, 743, 763, 783, 809, 844, 864, 892, 915, 955, 991, 1034, 1097, 1173, 1223, 1246, 1297, 1347, 1416, 1469, 1501, 1537, 1595, 2875, 2921, 3194, 3240, 3301, 3458 cm<sup>-1</sup>. <sup>1</sup>H-NMR (400 MHz, CDCl<sub>3</sub>)  $\delta$ : 0.10-0.19 (complex signal, 2 H, 9'-H<sub>2</sub>), 0.84-0.98 (complex signal, 2 H, 8'-H and 10'-H), 2.52-2.64 (complex signal, 2 H, 2'-H and 6'-H), 2.76 (m, 1 H, 1'-H or 7'-H), 2.88 (m, 1 H, 7'-H or 1'-H), 3.16 (m, 1 H, 3'-H<sub>a</sub> or 5'-H<sub>a</sub>), 3.44 (m, 1 H, 5'-H<sub>a</sub> or 3'-H<sub>a</sub>), 3.58 (m, 1 H, 3'-H<sub>b</sub> or 5'-H<sub>b</sub>), 3.68 (m, 1 H, 5'-H<sub>b</sub> or 3'-H<sub>b</sub>), 4.63 (s, 2 H, NH<sub>2</sub>), 5.70 (m, 1 H, 11'-H or 12'-H), 5.83 (m, 1 H, 12'-H or 11'-H), 7.30 [s, 2 H, 2(6)-H]. <sup>13</sup>C-NMR (100.5 MHz, CDCl<sub>3</sub>)  $\delta$ : 4.0 (CH<sub>2</sub>, C9'), 10.0 (CH, C8' or C10'), 10.1 (CH, C10' or C8'), 35.5 (CH, C1' and 7'), 42.6 (CH, C2' or C6'), 45.0 (CH, C6' or C2'), 49.6 (CH<sub>2</sub>, C3' or C5'), 53.6 (CH<sub>2</sub>, C5' or C3'), 118.7 [C, C3(5)], 126.8 (C, C1), 127.2

[CH, C2(6)], 128.2 (CH, C11' or C12'), 129.3 (CH, C12' or C11'), 141.3 (C, C4), 166.4 (C, CO). Anal. Calcd for C<sub>18</sub>H<sub>18</sub>Cl<sub>2</sub>N<sub>2</sub>O: C, 61.90; H, 5.20; N, 8.02. Found: C, 62.10; H, 5.20; N, 7.92.

#### 4.1.7. (4-azatetracyclo[5.3.2.0<sup>2,6</sup>.0<sup>8,10</sup>]dodec-11-en-4-yl)(cyclohex-3-en-1-yl)methanone, 9

To a solution of 4-azapentacyclo[5.3.2.0<sup>2,6</sup>.0<sup>8,10</sup>]dodec-11-ene hydrochloride (200 mg, 1.03 mmol) in EtOAc (10 mL) were added 3-cyclohexene carboxylic acid (119 mg, 0.94 mmol), HOBt (190mg, 1.41 mmol), EDC (218 mg, 1.41 mmol) and triethylamine (0.6 mL, 4.14 mmol). The reaction mixture was stirred at room temperature overnight. To the resulting suspension was then added water (10 mL) and the phases were separated. The organic phase was washed with saturated aqueous NaHCO<sub>3</sub> solution (10 mL) and brine (10 mL), dried over anhydrous Na<sub>2</sub>SO<sub>4</sub> and filtered. Evaporation *in vacuo* of the organics gave **9** as a white solid (199 mg), mp 78-79°C. IR (ATR)  $\nu$ : 682, 710, 763, 816, 839, 854, 887, 915, 940, 981, 1016, 1034, 1087, 1135, 1168, 1203, 1221, 1274, 1292, 1332, 1355, 1380, 1431, 1620, 1651, 2870, 2926, 3022 cm<sup>-1</sup>. <sup>1</sup>H-NMR (400 MHz, CDCl<sub>3</sub>)  $\delta$ : 0.10-0.19 (complex signal, 2 H, 9'-H<sub>2</sub>), 0.86-0.96 (complex signal, 2 H, 8'-H and 10'-H), 1.56-2.38 (complex signal, 6 H, 2-H<sub>ax</sub>, 5-H<sub>ax</sub>, 6-H<sub>ax</sub>, 2-H<sub>eq</sub>, 5-H<sub>eq</sub>, 6-H<sub>eq</sub>), 2.47 (m, 1 H, 1-H), 2.56 (m, 1 H, 2'-H or 6'-H), 2.67 (m, 1 H, 6'-H or 2'-H), 2.81-2.89 (complex signal, 2 H, 1'-H and 7'-H), 3.11-3.24 (complex signal, 2 H, 3'-H<sub>a</sub> and 5'-H<sub>a</sub>), 3.52-3.64 (complex signal, 2 H, 3'-H<sub>b</sub> and 5'-H<sub>b</sub>), 3.50-3.64 (complex signal, 2 H, 3'-H<sub>b</sub> and 5'-H<sub>b</sub>), 5.61-5.84 (complex signal, 4 H, 11'-H, 12'-H, 3-H and 4-H). <sup>13</sup>C-NMR (100.5 MHz, CDCl<sub>3</sub>)  $\delta$ : 4.03 and 4.06 (CH<sub>2</sub>, C9'), 9.9 (CH, C8' or C10'), 10.1 (CH, C10' or C8'), 24.96 and 24.99 (CH<sub>2</sub>, C5 or C6), 25.1 and 25.2 (CH<sub>2</sub>, C6 or C5), 27.40 and 27.43 (CH<sub>2</sub>, C2), 35.6 (CH, C1' or C7'), 35.7 (CH, 7' or C1'), 38.36 and 38.38 (CH, C1), 42.7 (CH, C2' or C6'), 44.72 and 44.73 (CH, C6' or C2'), 49.68 and 49.74 (CH<sub>2</sub>, C3' or C5'), 50.6 (CH<sub>2</sub>, C5' or C3'), 125.88 and 125.94 (CH, C3 or C4), 126.3 and 126.4 (CH, C4 or C3), 128.1 (CH, C11' or C12'), 129.5 and 129.6 (CH, C12' or C11'), 173.66 and 173.69 (C, CO). Anal. Calcd for C<sub>18</sub>H<sub>23</sub>NO: C, 80.26; H, 8.61; N, 5.20. Found: C, 80.24; H, 8.73; N 5.19.

#### 4.1.8. (4-azatetracyclo[5.3.2.0<sup>2,6</sup>.0<sup>8,10</sup>]dodec-11-en-4-yl)(6-chloropyridin-3-yl)methanone, 10

To a solution of 4-azapentacyclo[5.3.2.0<sup>2,6</sup>.0<sup>8,10</sup>]dodec-11-ene hydrochloride (500 mg, 2.58 mmol) in EtOAc (25 mL) were added 6-chloropyridin-3-yl carboxylic acid (370 mg, 2.35 mmol), HOBt (477 mg, 3.53 mmol), EDC (547 mg, 3.53 mmol) and triethylamine (1.4 mL, 10.34 mmol). The reaction mixture was stirred at room temperature overnight. To the resulting suspension was then added water (25 mL) and the phases were separated. The organic phase was washed with saturated aqueous NaHCO<sub>3</sub> solution (25 mL) and brine (25 mL), dried over anhydrous Na<sub>2</sub>SO<sub>4</sub> and filtered. Evaporation *in vacuo* of the organics gave **10** as a yellowish solid (664 mg, 86% yield). Column chromatography (Hexane/Ethyl acetate mixture) gave **10** as a white solid (457 mg), mp 101-102°C. IR (ATR)  $\nu$ : 712, 736, 759, 793, 814, 835, 924, 940, 985, 1030, 1097, 1129, 1156, 1174, 1215, 1239, 1251, 1271, 1283, 1350, 1372, 1430, 1455, 1563, 1583, 1612, 2914, 2948, 3002 cm<sup>-1</sup>. <sup>1</sup>H-NMR (400 MHz, CDCl<sub>3</sub>)  $\delta$ : 0.12-0.20 (complex signal, 2 H, 9'-H<sub>2</sub>), 0.85-0.98 (complex signal, 2 H, 8'-H and 10'-H), 2.54-2.68 (complex signal, 2 H, 2'-H and 6'-H), 2.75 (m, 1 H, 1'-H or 7'-H), 2.92 (m, 1 H, 7'-H or 1'-H), 3.10 (dd,  $J = 10.8$  Hz,  $J' = 3.2$  Hz, 1 H, 5'-H<sub>a</sub> or 3'-H<sub>a</sub>), 3.42-3.58 (complex signal, 2 H, 3'-H<sub>a</sub> or 5'-H<sub>a</sub> and 5'-H<sub>b</sub> or 3'-H<sub>b</sub>), 3.71 (m, 1 H, 3'-H<sub>b</sub> or 5'-H<sub>b</sub>), 5.69 (t,  $J = 7.2$  Hz, 1 H, 11'-H or 12'-H), 5.86 (t,  $J = 7.2$  Hz, 1 H, 12'-

H or 11'-H), 7.35 (dd,  $J = 8.4$  Hz,  $J' = 0.8$  Hz, 1 H, 5-H), 7.71 (dd,  $J = 8.4$  Hz,  $J' = 2.6$  Hz, 1 H, 4-H), 8.43 (dd,  $J = 2.6$  Hz,  $J' = 0.8$  Hz, 1 H, 2-H).  $^{13}\text{C-NMR}$  (100.5 MHz,  $\text{CDCl}_3$ )  $\delta$ : 3.9 ( $\text{CH}_2$ , C9'), 9.8 ( $\text{CH}$ , C8' or C10'), 10.1 ( $\text{CH}$ , C10' or C8'), 35.5 ( $\text{CH}$ , C1' or C7'), 35.6 ( $\text{CH}$ , C7' or C1'), 42.7 ( $\text{CH}$ , C2' or C6'), 44.8 ( $\text{CH}$ , C6' or C2'), 49.7 ( $\text{CH}_2$ , C3' or C5'), 53.4 ( $\text{CH}_2$ , C5' or C3'), 124.1 ( $\text{CH}$ , C5), 128.1 ( $\text{CH}$ , C11' or C12'), 129.4 ( $\text{CH}$ , C12' or C11'), 131.8 (C, C3), 137.7 ( $\text{CH}$ , C4), 148.1 ( $\text{CH}$ , C2), 152.3 (C, C6), 165.2 (C, CO). Anal. Calcd for  $\text{C}_{17}\text{H}_{17}\text{ClN}_2\text{O}$ : C, 67.88; H, 5.70; N, 9.31. Found: C, 68.14; H, 5.84; N, 9.00.

#### 4.1.9. (4-azatetracyclo[5.3.2.0<sup>2,6</sup>.0<sup>8,10</sup>]dodec-11-en-4-yl)(2-chloropyridin-4-yl)methanone, **11**

To a solution of 4-azapentacyclo[5.3.2.0<sup>2,6</sup>.0<sup>8,10</sup>]dodec-11-ene hydrochloride (500 mg, 2.58 mmol) in EtOAc (25 mL) were added 6-chlororonicotinic acid (370 mg, 2.35 mmol), HOBt (477 mg, 3.53 mmol), EDC (547 mg, 3.53 mmol) and triethylamine (1.4 mL, 10.34 mmol). The reaction mixture was stirred at room temperature overnight. To the resulting suspension was then added water (25 mL) and the phases were separated. The organic phase was washed with saturated aqueous  $\text{NaHCO}_3$  solution (25 mL) and brine (25 mL), dried over anhydrous  $\text{Na}_2\text{SO}_4$  and filtered. Evaporation *in vacuo* of the organics gave **11** as a yellowish solid (614 mg, 79% yield). Column chromatography (Hexane/Ethyl acetate mixture) gave **11** as a white solid (445 mg), mp 135-136°C. IR (ATR)  $\nu$ : 669, 708, 720, 741, 753, 771, 817, 844, 915, 942, 987, 1041, 1091, 1118, 1163, 1176, 1203, 1232, 1245, 1269, 1287, 1342, 1373, 1437, 1464, 1476, 1530, 1593, 1632, 2868, 2932, 3003, 3057  $\text{cm}^{-1}$ .  $^1\text{H-NMR}$  (400 MHz,  $\text{CDCl}_3$ )  $\delta$ : 0.12-0.22 (complex signal, 2 H, 9'-H<sub>2</sub>), 0.85-1.00 (complex signal, 2 H, 8'-H and 10'-H), 2.56-2.70 (complex signal, 2 H, 2'-H and 6'-H), 2.76 (m, 1 H, 1'-H or 7'-H), 2.92 (m, 1 H, 7'-H or 1'-H), 3.01 (dd,  $J = 11.0$  Hz,  $J' = 3.8$  Hz, 1 H, 5'-H<sub>a</sub> or 3'-H<sub>a</sub>), 3.40-3.52 (complex signal, 2 H, 3'-H<sub>a</sub> or 5'-H<sub>a</sub> and 5'-H<sub>b</sub> or 3'-H<sub>b</sub>), 3.68 (m, 1 H, 3'-H<sub>b</sub> or 5'-H<sub>b</sub>), 5.71 (m, 1 H, 11'-H or 12'-H), 5.87 (m, 1 H, 12'-H or 11'-H), 7.18 (dd,  $J = 5.0$  Hz,  $J' = 1.4$  Hz, 1 H, 5-H), 7.30 (dd,  $J = 1.4$  Hz,  $J' = 0.8$  Hz, 1 H, 3-H), 8.42 (dd,  $J = 5.0$  Hz,  $J' = 0.8$  Hz, 1 H, 6-H).  $^{13}\text{C-NMR}$  (100.5 MHz,  $\text{CDCl}_3$ )  $\delta$ : 4.0 ( $\text{CH}_2$ , C9'), 9.8 ( $\text{CH}$ , C8' or C10'), 10.1 ( $\text{CH}$ , C10' or C8'), 35.5 ( $\text{CH}$ , C1' or C7'), 35.6 ( $\text{CH}$ , C7' or C1'), 42.7 ( $\text{CH}$ , C2' or C6'), 44.6 ( $\text{CH}$ , C6' or C2'), 49.6 ( $\text{CH}_2$ , C3' or C5'), 53.1 ( $\text{CH}_2$ , C5' or C3'), 119.8 ( $\text{CH}$ , C5), 121.9 ( $\text{CH}$ , C3), 128.2 ( $\text{CH}$ , C11' or C12'), 129.4 ( $\text{CH}$ , C12' or C11'), 147.6 (C, C4), 150.1 ( $\text{CH}$ , C6), 151.9 (C, C2), 164.8 (C, CO). Anal. Calcd for  $\text{C}_{17}\text{H}_{17}\text{ClN}_2\text{O}$ : C, 67.88; H, 5.70; N, 9.31. Found: C, 67.98; H, 5.77; N, 9.09.

#### 4.1.10. (4-azatetracyclo[5.3.2.0<sup>2,6</sup>.0<sup>8,10</sup>]dodec-11-en-4-yl)(1-methylpiperidin-4-yl)methanone, **12**

To a solution of 4-azapentacyclo[5.3.2.0<sup>2,6</sup>.0<sup>8,10</sup>]dodec-11-ene hydrochloride (200 mg, 1.03 mmol) in EtOAc (10 mL) were added 1-methylpiperidine-4-carboxylic acid (135 mg, 0.94 mmol), HOBt (190 mg, 1.41 mmol), EDC (218 g, 1.41 mmol) and triethylamine (0.6 mL, 4.14 mmol). The reaction mixture was stirred at room temperature overnight. To the resulting suspension was then added water (10 mL) and the phases were separated. The organic phase was washed with saturated aqueous  $\text{NaHCO}_3$  solution (10 mL) and brine (10 mL), dried over anhydrous  $\text{Na}_2\text{SO}_4$  and filtered. Evaporation *in vacuo* of the organics gave a yellowish solid (129 mg). Column chromatography (Hexane/Ethyl acetate/Methanol mixture) gave **12** as a yellowish solid (86 mg, 32% yield). The analytical sample was obtained by crystallization from hot EtOAc (50 mg), mp 100-101°C. IR (ATR)  $\nu$ : 718, 767, 819, 835, 850, 876, 915, 987, 1013, 1041, 1067, 1090, 1129, 1150, 1191, 1214, 1250, 1276, 1305, 1359, 1374, 1431, 1447, 1625, 2780, 2857, 2914, 2940, 3328  $\text{cm}^{-1}$ .  $^1\text{H-NMR}$  (400 MHz,  $\text{CDCl}_3$ )  $\delta$ : 0.10-0.18 (complex signal, 2 H, 9'-H<sub>2</sub>), 0.86-0.96 (complex signal, 2 H, 8'-H and 10'-H), 1.58-1.68

(complex signal, 2 H, 3-H<sub>ax</sub> and 5-H<sub>ax</sub>), 1.71-1.87 (complex signal, 2 H, 3-H<sub>eq</sub> and 5-H<sub>eq</sub>), 1.88-1.98 (complex signal, 2H, 2-H<sub>ax</sub> and 6-H<sub>ax</sub>), 2.18 (tt,  $J = 11.2$  Hz,  $J' = 3.6$  Hz, 1 H, 1-H), 2.24 (s, 3 H, N-CH<sub>3</sub>), 2.55 (m, 1 H, 2'-H or 6'-H), 2.66 (m, 1 H, 6'-H or 2'-H), 2.81-2.96 (complex signal, 4 H, 1'-H, 7'-H, 2-H<sub>eq</sub> and 6-H<sub>eq</sub>), 3.11 (dd,  $J = 11.0$  Hz,  $J' = 5.0$  Hz, 1 H, 3'-H<sub>a</sub> or 5'-H<sub>a</sub>), 3.16 (dd,  $J = 13.0$  Hz,  $J' = 5.0$  Hz, 1 H, 5'-H<sub>a</sub> or 3'-H<sub>a</sub>), 3.50-3.64 (complex signal, 2 H, 3'-H<sub>b</sub> and 5'-H<sub>b</sub>), 5.74 (complex signal, 2 H, 11'-H and 12'-H).  $^{13}\text{C-NMR}$  (100.5 MHz,  $\text{CDCl}_3$ )  $\delta$ : 4.1 ( $\text{CH}_2$ , C9'), 9.4 ( $\text{CH}$ , C8' or C10'), 10.2 ( $\text{CH}$ , C10' or C8'), 27.9 ( $\text{CH}_2$ , C3 or C5), 28.0 ( $\text{CH}_2$ , C5 or C3), 35.6 ( $\text{CH}$ , C1' or C7'), 35.7 ( $\text{CH}$ , C7' or C1'), 39.9 ( $\text{CH}$ , C4), 42.7 ( $\text{CH}$ , C2' or C6'), 44.8 ( $\text{CH}$ , C6' or C2'), 46.4 ( $\text{CH}_3$ , N-CH<sub>3</sub>), 49.8 ( $\text{CH}_2$ , C3' or C5'), 50.6 ( $\text{CH}_2$ , C5' or C3'), 55.2 ( $\text{CH}_2$ , C2 or C6), 55.3 ( $\text{CH}_2$ , C6 or C2), 128.1 ( $\text{CH}$ , C11' or C12'), 129.6 ( $\text{CH}$ , C12' or C11'), 172.9 (C, CO). HRMS-ESI+  $m/z$   $[\text{M}+\text{H}]^+$ : Calcd for  $[\text{C}_{18}\text{H}_{26}\text{N}_2\text{O}+\text{H}]^+$ : 287.2118, found: 287.2113.

#### 4.1.11. 1-[4-(4-azatetracyclo[5.3.2.0<sup>2,6</sup>.0<sup>8,10</sup>]dodec-11-en-4-yl)carbonyl]piperidin-1-yl]ethan-1-one, **13**

To a solution of 4-azapentacyclo[5.3.2.0<sup>2,6</sup>.0<sup>8,10</sup>]dodec-11-ene hydrochloride (200 mg, 1.03 mmol) in EtOAc (10 mL) were added 1-acetyl-4-piperidinecarboxylic acid (161 mg, 0.94 mmol), HOBt (190 mg, 1.41 mmol), EDC (218 g, 1.41 mmol) and triethylamine (0.6 mL, 4.14 mmol). The reaction mixture was stirred at room temperature overnight. To the resulting suspension was then added water (10 mL) and the phases were separated. The organic phase was washed with saturated aqueous  $\text{NaHCO}_3$  solution (10 mL) and brine (10 mL), dried over anhydrous  $\text{Na}_2\text{SO}_4$  and filtered. Evaporation *in vacuo* of the organics gave a yellowish solid (182 mg). Column chromatography (Hexane/Ethyl acetate mixture) gave **13** as a white solid (134 mg, 45% yield), mp 134-135°C. IR (ATR)  $\nu$ : 605, 703, 762, 814, 829, 920, 956, 977, 997, 1041, 1098, 1116, 1168, 1222, 1271, 1307, 1356, 1426, 1620, 1640, 2852, 2925, 2992  $\text{cm}^{-1}$ .  $^1\text{H-NMR}$  (400 MHz,  $\text{CDCl}_3$ )  $\delta$ : 0.11-0.19 (complex signal, 2 H, 9'-H<sub>2</sub>), 0.88-0.98 (complex signal, 2 H, 8'-H and 10'-H), 1.50-1.84 (complex signal, 4 H, 3-H<sub>2</sub>, 5-H<sub>2</sub>), 2.06 (s, 3 H, COCH<sub>3</sub>), 2.46 (tt,  $J = 10.6$  Hz,  $J' = 4.0$  Hz, 1 H, 4-H), 2.52-2.74 (complex signal, 3 H, 2'-H, 6'-H and 2-H<sub>ax</sub> or 6-H<sub>ax</sub>), 2.81-2.89 (complex signal, 2 H, 1'-H and 7'-H), 3.05 (m, 1 H, 6-H<sub>ax</sub> or 2-H<sub>ax</sub>), 3.11-3.22 (complex signal, 2 H, 3'-H<sub>a</sub> and 5'-H<sub>a</sub>), 3.50-3.64 (complex signal, 2 H, 3'-H<sub>b</sub> or 5'-H<sub>b</sub>), 3.84 (dm,  $J = 13.6$  Hz, 1 H, 2-H<sub>eq</sub> or 6-H<sub>eq</sub>), 4.54 (dm,  $J = 13.6$  Hz, 1 H, 6-H<sub>eq</sub> or 2-H<sub>eq</sub>), 5.75 (complex signal, 2 H, 11'-H and 12'-H).  $^{13}\text{C-NMR}$  (100.5 MHz,  $\text{CDCl}_3$ )  $\delta$ : 4.1 ( $\text{CH}_2$ , C9'), 9.9 ( $\text{CH}$ , C8' or C10'), 10.1 ( $\text{CH}$ , C10' or C8'), 21.4 ( $\text{CH}_3$ , COCH<sub>3</sub>), 27.6 and 27.7 ( $\text{CH}_2$ , C3 or C5), 28.1 and 28.2 ( $\text{CH}_2$ , C5 or C3), 35.6 ( $\text{CH}$ , C1' or C7'), 35.7 ( $\text{CH}$ , C7' or C1'), 40.1 ( $\text{CH}$ , C4), 40.9 and 41.0 ( $\text{CH}_2$ , C2 or C6), 42.62 and 42.64 ( $\text{CH}$ , C2' or C6'), 44.69 and 44.70 ( $\text{CH}$ , C6' or C2'), 45.7 and 45.8 ( $\text{CH}_2$ , C6 or C2), 49.8 ( $\text{CH}_2$ , C3' or C5'), 50.63 and 50.64 ( $\text{CH}_2$ , C5' or C3'), 128.0 ( $\text{CH}$ , C11' or C12'), 129.65 and 129.68 ( $\text{CH}$ , C12' or C11'), 168.8 (C, COCH<sub>3</sub>), 171.82 and 171.85 (C, CO). Anal. Calcd for  $\text{C}_{19}\text{H}_{26}\text{N}_2\text{O}_2$ : C 72.58; H, 8.34; N, 8.91. Found: C, 72.65; H 8.60; N 8.48.

#### 4.1.12. (4-azatetracyclo[5.3.2.0<sup>2,6</sup>.0<sup>8,10</sup>]dodec-11-en-4-yl)[6-(4-phenylpiperazin-1-yl)pyridin-3-yl]methanone, **14**

To a solution of **10** (100 mg, 0.33 mmol) and 1-phenylpiperazine (60 mg, 0.37 mmol) in DMF (0.5 mL) was added solid  $\text{K}_2\text{CO}_3$  (82 mg, 0.59 mmol). The resulting suspension was stirred at 90 °C for 48 hours. Water (5 mL) and DCM (5 mL) were added and the phases were separated. The aqueous phase was then extracted with further DCM (2 x 5 mL). The organics were dried over anhydrous  $\text{Na}_2\text{SO}_4$ , filtered and evaporated *in vacuo* to

give a yellowish solid (137 mg). Column chromatography (Hexane/Ethyl acetate mixture) gave **14** as a white solid (56 mg, 39% yield). The analytical sample was obtained by washing this solid with cold pentane (45 mg), mp 90-91°C. IR (ATR) v: 661, 695, 739, 754, 814, 822, 845, 948, 987, 1013, 1028, 1041, 1095, 1152, 1227, 1310, 1349, 1349, 1395, 1413, 1491, 1594, 1617, 2847, 2919, 2997 cm<sup>-1</sup>. <sup>1</sup>H-NMR (400 MHz, CDCl<sub>3</sub>) δ: 0.12-0.20 (complex signal, 2 H, 9-H<sub>2</sub>), 0.86-1.00 (complex signal, 2 H, 8-H and 10-H), 2.54-2.66 (complex signal, 2 H, 2-H and 6-H), 2.76 (m, 1 H, 1-H or 7-H), 2.90 (m, 1 H, 7-H or 1-H), 3.18-3.36 [complex signal, 6 H, 3-H<sub>a</sub>, 5-H<sub>a</sub>, 2''(6'')-H<sub>2</sub>], 3.38-3.84 [complex signal, 6 H, 3-H<sub>b</sub>, 5-H<sub>b</sub>, 3''(5'')-H<sub>2</sub>], 5.70 (m, 1 H, 11-H or 12-H), 5.84 (m, 1 H, 12-H or 11-H), 6.66 (d, *J* = 8.8 Hz, 1 H, 5'-H), 6.90 (t, *J* = 7.2 Hz, 1 H, 4'''-H), 6.97 [d, *J* = 8.6 Hz, 2 H, 2'''(6''')-H], 7.28 [dd, *J* = 8.6 Hz, *J'* = 7.2 Hz, 2 H, 3'''(5''')-H], 7.66 (dd, *J* = 8.8 Hz, *J'* = 2.4 Hz, 1 H, 4'-H), 8.31 (d, *J* = 2.4 Hz, 1 H, 2'-H). <sup>13</sup>C-NMR (100.5 MHz, CDCl<sub>3</sub>) δ: 3.9 (CH<sub>2</sub>, C9), 10.2 (broad s, CH, C8 and C10), 35.5 (CH, C1 and C7), 42.6 (CH, C2 or C6), 44.9 [CH<sub>2</sub>, C3''(5'')], 45.0 (CH, C6 or C2), 49.1 [CH<sub>2</sub>, C2''(6'')], 49.6 (CH<sub>2</sub>, C3 or C5), 53.6 (CH<sub>2</sub>, C5 or C3), 105.8 (CH, C5'), 116.4 [CH, C2'''(6''')], 120.2 (CH, C4'''), 121.9 (C, C3'), 128.2 (CH, C11 or C12), 129.19 [CH, C3'''(5''')], 129.24 (CH, C12 or C11), 137.5 (CH, C4'), 147.5 (CH, C2'), 151.1 (C, C1'''), 159.3 (C, C6'), 167.1 (C, CO). HRMS-ESI+ *m/z* [M+H]<sup>+</sup> calcd for [C<sub>27</sub>H<sub>30</sub>N<sub>4</sub>O+H]<sup>+</sup>: 427.2494, found: 427.2492.

#### 4.1.13. (4-azatetracyclo[5.3.2.02,6.08,10] dodec-11-en-4-yl)[6-[4-(4-trifluoromethyl)phenylpiperazin-1-yl]pyridin-3-yl]methanone, **15**

To a solution of **10** (100 mg, 0.33 mmol) and 1-(4-trifluoromethylphenyl)piperazine (85 mg, 0.37 mmol) in DMF (0.5 mL) was added solid K<sub>2</sub>CO<sub>3</sub> (82 mg, 0.59 mmol). The resulting suspension was stirred at 90 °C for 48 hours. Water (5 mL) and DCM (5 mL) were added and the phases were separated. The aqueous phase was then extracted with further DCM (2 x 5 mL). The organics were dried over anh. Na<sub>2</sub>SO<sub>4</sub>, filtered and evaporated *in vacuo* to give a yellowish solid (161 mg). Column chromatography (Hexane/Ethyl acetate mixture) gave **15** as a white solid (52 mg, 32% yield). The analytical sample was obtained by washing with cooled pentane (38 mg), mp 157-158°C. IR (ATR) v: 667, 711, 721, 744, 770, 806, 824, 909, 951, 971, 984, 1039, 1070, 1106, 1157, 1199, 1230, 1330, 1354, 1390, 1429, 1493, 1522, 1594, 1615, 2847, 2919 cm<sup>-1</sup>. <sup>1</sup>H-NMR (400 MHz, CDCl<sub>3</sub>) δ: 0.10-0.18 (complex signal, 2 H, 9-H<sub>2</sub>), 0.84-0.98 (complex signal, 2 H, 8-H and 10-H), 2.54-2.66 (complex signal, 2 H, 2-H and 6-H), 2.75 (m, 1 H, 1-H or 7-H), 2.90 (m, 1 H, 7-H or 1-H), 3.26 (m, 1 H, 3-H<sub>a</sub> or 5-H<sub>a</sub>), 3.41 [t, *J* = 5.4 Hz, 4 H, 2''(6'')-H<sub>2</sub>], 3.48 (m, 1 H, 5-H<sub>a</sub> or 3-H<sub>a</sub>), 3.56-3.82 [complex signal, 6 H, 3-H<sub>b</sub>, 5-H<sub>b</sub>, 3''(5'')-H<sub>2</sub>], 5.69 (m, 1 H, 11-H or 12-H), 5.85 (m, 1 H, 12-H or 11-H), 6.65 (d, *J* = 8.8 Hz, 1 H, 5'-H), 6.95 [d, *J* = 8.6 Hz, 2 H, 2'''(6''')-H], 7.50 [d, *J* = 8.6 Hz, 2 H, 3'''(5''')-H], 7.66 (dd, *J* = 8.8 Hz, *J'* = 2.2 Hz, 1 H, 4'-H), 8.31 (d, *J* = 2.2 Hz, 1 H, 2'-H). <sup>13</sup>C-NMR (100.5 MHz, CDCl<sub>3</sub>) δ: 3.9 (CH<sub>2</sub>, C9), 10.2 (broad s, CH, C8 and C10), 35.6 (CH, C1 and C7), 42.7 (CH, C2 or C6), 44.5 [CH<sub>2</sub>, C3''(5'')], 45.1 (CH, C6 or C2), 47.7 [CH<sub>2</sub>, C2''(6'')], 49.6 (CH<sub>2</sub>, C3 or C5), 53.6 (CH<sub>2</sub>, C5 or C3), 105.8 (CH, C5'), 114.6 [CH, C2'''(6''')], 120.8 (q, *J* = 32 Hz, C, C4'''), 122.1 (C, C3'), 124.6 (q, *J* = 269 Hz, C, CF<sub>3</sub>), 126.4 [q, *J* = 4 Hz, CH, C3'''(5''')], 128.1 (CH, C11 or C12), 129.3 (CH, C12 or C11), 137.5 (CH, C4'), 147.5 (CH, C2'), 153.0 (C, C1'''), 159.1 (C, C6'), 167.0 (C, CO). HRMS-ESI+ *m/z* [M+H]<sup>+</sup> calcd for [C<sub>28</sub>H<sub>29</sub>F<sub>3</sub>N<sub>4</sub>O+H]<sup>+</sup>: 495.2396, found: 495.2369.

#### 4.1.14. 4-[[4-[5-(4-azatetracyclo[5.3.2.02,6.08,10] dodec-11-en-4-yl)carbonyl]pyridin-2-yl]piperazin-1-yl]benzotrile, **16**

To a solution of **10** (100 mg, 0.33 mmol) and 4-piperazinobenzotrile (69 mg, 0.37 mmol) in DMF (0.5 mL) was added solid K<sub>2</sub>CO<sub>3</sub> (82 mg, 0.59 mmol). The resulting suspension was stirred at 90°C for 48 hours. Water (5 mL) and DCM (5 mL) were added and the phases were separated. The aqueous phase was then extracted with further DCM (2 x 5 mL). The organics were dried over anh. Na<sub>2</sub>SO<sub>4</sub>, filtered and evaporated *in vacuo* to give a yellowish solid (181 mg). Column chromatography (Hexane/Ethyl acetate mixture) gave **16** as a white solid (72 mg, 48% yield), mp 160-161°C. IR (ATR) v: 656, 692, 713, 742, 773, 811, 912, 951, 1008, 1039, 1176, 1235, 1312, 1392, 1426, 1511, 1537, 1555, 1599, 1648, 1666, 2847, 2925 cm<sup>-1</sup>. <sup>1</sup>H-NMR (400 MHz, CDCl<sub>3</sub>) δ: 0.10-0.22 (complex signal, 2 H, 9''-H<sub>2</sub>), 0.84-1.00 (complex signal, 2 H, 8'''-H and 10'''-H), 2.54-2.66 (complex signal, 2 H, 2'''-H and 6'''-H), 2.75 (m, 1 H, 1'''-H or 7'''-H), 2.90 (m, 1 H, 7'''-H or 1'''-H), 3.15-3.56 [complex signal, 6 H, 3'''-H<sub>a</sub>, 5'''-H<sub>a</sub>, 3'(5')-H<sub>2</sub>], 3.58-3.84 [complex signal, 6 H, 3'''-H<sub>b</sub>, 5'''-H<sub>b</sub>, 2'(6')-H<sub>2</sub>], 5.69 (m, 1 H, 11'''-H or 12'''-H), 5.84 (m, 1 H, 12'''-H or 11'''-H), 6.63 (d, *J* = 8.8 Hz, 1 H, 3'''-H), 6.87 [dm, *J* = 8.8 Hz, 2 H, 3(5)-H], 7.51 [dm, *J* = 8.8 Hz, 2 H, 2(6)-H], 7.67 (dd, *J* = 8.8 Hz, *J'* = 2.2 Hz, 1 H, 4'''-H), 8.31 (d, *J* = 2.2 Hz, 1 H, 6'''-H). <sup>13</sup>C-NMR (100.5 MHz, CDCl<sub>3</sub>) δ: 3.9 (CH<sub>2</sub>, C9'''), 10.1 (broad singlet, CH, C8''' and C10'''), 35.5 (CH, C1''' and C7'''), 42.7 (CH, C2''' or C6'''), 44.2 [CH<sub>2</sub>, C2'(6')], 45.0 (CH, C6''' or C2'''), 46.6 [CH<sub>2</sub>, C3'(5')], 49.6 (CH<sub>2</sub>, C3''' or C5'''), 53.5 (CH<sub>2</sub>, C5''' or C3'''), 100.5 (C, C1), 105.7 (CH, C3'''), 114.0 [CH, C3(5)], 119.9.2 (C, CN), 122.2 (C, C5'''), 128.1 (CH, C11''' or C12'''), 129.3 (CH, C12''' or C11'''), 133.5 [CH, C2(6)], 137.6 (CH, C4'''), 147.4 (CH, C6'''), 152.9 (C, C4), 158.8 (C, C2'''), 166.9 (C, CO). HRMS-ESI+ *m/z* [M+H]<sup>+</sup> calcd for [C<sub>28</sub>H<sub>29</sub>N<sub>5</sub>O+H]<sup>+</sup>: 452.2445, found: 452.2444.

#### 4.2. 11β-HSD1 Enzyme Inhibition Assay

11β-HSD1 activity was determined in mixed sex, human liver microsomes (Celsis In-vitro Technologies) by measuring the conversion of <sup>3</sup>H-cortisone to <sup>3</sup>H-cortisol. Percentage inhibition was determined relative to a no inhibitor control. 5 μg of human liver microsomes were pre-incubated at 37°C for 15 min with inhibitor and 1 mM NADPH in a final volume of 90 μL Krebs buffer. 10 μL of 200 nM <sup>3</sup>H-cortisone was then added followed by incubation at 37°C for a further 30 min. The assay was terminated by rapid freezing on dry ice and <sup>3</sup>H-cortisone to <sup>3</sup>H-cortisol conversion determined in 50 μL of the defrosted reaction by capturing liberated <sup>3</sup>H-cortisol on anti-cortisol (HyTest Ltd)-coated scintillation proximity assay beads (protein A-coated YSi, GE Healthcare).

#### 4.3. Cellular 11β-HSD1 Enzyme Inhibition Assay

The cellular 11β-HSD1 enzyme inhibition assay was performed using HEK293 cells stably transfected with the human 11β-HSD1 gene. Cells were incubated with substrate (cortisone) and product (cortisol) was determined by LC/MS. Cells were plated at 2 x 10<sup>4</sup> cells/well in a 96-well poly-D-lysine coated tissue culture microplate (Greiner Bio-one) and incubated overnight at 37°C in 5% CO<sub>2</sub> 95% O<sub>2</sub>. Compounds to be tested were solubilized in 100% DMSO at 10 mM and serially diluted in water and 10% DMSO to final concentration of 10 μM in 10% DMSO. 10 μL of each test dilution and 10 μL of 10% DMSO (for low and high control) were dispensed into the well of a new 96-well microplate (Greiner Bio-one). Medium was removed from the cell assay plate and 100 μL of DMEM solution (containing 1% penicillin, 1% streptomycin and 300 nM cortisone) added to each well. Cells were incubated for 2 h at

37°C in 5% CO<sub>2</sub> 95% O<sub>2</sub>. Following incubation, medium was removed from each well into an eppendorf containing 500 µL of ethyl acetate, mixed by vortex and incubated at rt for 5 min. A calibration curve of known concentrations of cortisol in assay medium was also set up and added to 500 µL of ethyl acetate, vortexed and incubated as above. The supernatant of each eppendorf was removed to a 96-deep-well plate and dried down under liquid nitrogen at 65°C. Each well was solubilised in 100 µL 70:30 H<sub>2</sub>O:ACN and removed to a 96-well V-bottomed plate for LC/MS analysis. Separation was carried out on a sunfire 150 x 2.1 mm, 3.5 µM column using a H<sub>2</sub>O:ACN gradient profile. Typical retention times were 2.71 min for cortisol and 2.80 min for cortisone. The peak area was calculated and the concentration of each compound determined from the calibration curve.

#### 4.4. Cellular 11β-HSD2 Enzyme Inhibition Assay

For measurement of inhibition of 11β-HSD2, HEK293 cells stably transfected with the full-length gene coding for human 11β-HSD2 were used. The protocol was the same as for the cellular 11β-HSD1 enzyme inhibition assay, only changing the substrate, this time cortisol, and the concentrations of the tested compounds, 10, 1 and 0.1 µM.

#### 4.5. Microsomal Stability Assay

The microsomal stability of each compound was determined using human liver microsomes (Celsis In-vitro Technologies). Microsomes were thawed and diluted to a concentration of 2 mg/mL in 50 mM NaPO<sub>4</sub> buffer pH 7.4. Each compound was diluted in 4 mM NADPH (made in the phosphate buffer above) to a concentration of 10 µM. Two identical incubation plates were prepared to act as a 0 minute and a 30 minute time point assay. 30 µL of each compound dilution was added in duplicate to the wells of a U-bottom 96-well plate and warmed at 37°C for approximately 5 min. Verapamil, lidocaine and propranolol at 10 µM concentration were utilised as reference compounds in this experiment. Microsomes were also pre-warmed at 37°C before the addition of 30 µL to each well of the plate resulting in a final concentration of 1 mg/mL. The reaction was terminated at the appropriate time point (0 or 30 min) by addition of 60 µL of ice-cold 0.3 M trichloroacetic acid (TCA) per well. The plates were centrifuged for 10 min at 112 x g and the supernatant fraction transferred to a fresh U-bottom 96-well plate. Plates were sealed and frozen at -20°C prior to MS analysis. LC-MS/MS was used to quantify the peak area response of each compound before and after incubation with human liver microsomes using MS tune settings established and validated for each compound. These peak intensity measurements were used to calculate the % remaining after incubation with human microsomes for each hit compound.

#### Acknowledgements

We thank financial support from *Ministerio de Economía y Competitividad* and FEDER (Project SAF2014-57094-R) and ACCIÓ (*Generalitat de Catalunya*) and CIDQO 2012 SL (*Programa Nuclis*, RD14-1-0057, SAFNAD). R. L. thanks the *Ministerio de Educación Cultura y Deporte* for a PhD Grant (FPU program) and the *Fundació Universitària Agustí Pedro i Pons* for a Travel Grant.

#### References and notes

1. Dallman, M. F.; Strack, A. M.; Akana, S. F.; Bradbury, M. J.; Hanson, E. S.; Scribner, K. A.; Smith, M. *Front. Neuroendocrinol.* **1993**, *14*, 303-347.
2. Sapolsky, R. M.; Romero, L. M.; Munck, A. U. *Endocr. Rev.* **2000**, *21*, 55-89.
3. Seckl, J. R.; Walker, B. R. *Endocrinology* **2001**, *142*, 1371-1376.
4. Brown, R. W.; Diaz, R.; Robson, A. C.; Kotelevtsev, Y. V.; Mullins, J. J.; Kaufman, M. H.; Seckl, J. R. *Endocrinology* **1996**, *137*, 794-797.
5. a) Stavreva, D. A.; Wiench, M.; John, S.; Conway-Campbell, B. L.; McKenna, M. A.; Pooley, J. R.; Johnson, T. A.; Voss, T. C.; Lightman, S. L.; Hager, G. L. *Nat. Cell Biol.* **2009**, *11*, 1093-1102. b) Hardy, R. S.; Seibel, M. J.; Cooper, M. S. *Curr. Opin. Pharmacol.* **2013**, *13*, 440-444.
6. Wamil, M.; Seckl, J. R. *Drug Discov. Today* **2007**, *12*, 504-520.
7. Masuzaki, H.; Yamamoto, H.; Kenyon, C. J.; Elmquist, J. K.; Morton, N. M.; Paterson, J. M.; Shinyama, H.; Sharp, M. G. F.; Fleming, S.; Mullins, J. J.; Seckl, J. R.; Flier, J. S. *J. Clin. Invest.* **2003**, *112*, 83-90.
8. Holmes, M. C.; Carter, R. N.; Noble, J.; Chitnis, S.; Dutia, A.; Paterson, J. M.; Mullins, J. J.; Seckl, J. R.; Yau, J. L. *J. Neurosci.* **2010**, *30*, 6916-6920.
9. Park, J. S.; Bae, S. J.; Choi, S.-W.; Son, Y. H.; Park, S. B.; Rhee, S. D.; Kim, H. Y.; Jung, W. H.; Kang, S. K.; Ahn, J. H.; Kim, S. H.; Kim, K. Y. *J. Mol. Endocrinol.* **2014**, *52*, 191-202.
10. Rauz, S.; Cheung, C. M. G.; Wood, P. J.; Coca-Prados, M.; Walker, E. A.; Murray, P. I.; Stewart, P. M. *QJM: Monthly Journal of the Association of Physicians* **2003**, *96*, 481-490.
11. Leiva, R.; Seira, C.; McBride, A.; Binnie, M.; Bidon-Chanal, A.; Luque, F. J.; Webster, S. P.; Vázquez, S. *Bioorg. Med. Chem. Lett.* **2015**, *25*, 4250-4253.
12. Leiva, R.; Griñan-Ferré, C.; Seira, C.; Valverde, E.; McBride, A.; Binnie, M.; Pérez, B.; Luque, F. J.; Pallás, M.; Bidon-Chanal, A.; Webster, S. P.; Vázquez, S. *Eur. J. Med. Chem.* **2017**, *139*, 412-428.
13. Richards, S.; Sorensen, B.; Jae, H.; Winn, M.; Chen, Y.; Wang, J.; Fung, S.; Monzon, K.; Frevort, E. U.; Jacobson, P.; Sham, H. L.; Link, J. T. *Bioorg. Med. Chem. Lett.* **2006**, *16*, 6241-6245.
14. Yeh, V. S. C.; Kurukulasuriya, R.; Madar, D.; Patel, J. R.; Fung, S.; Monzon, K.; Chiou, W.; Wang, J.; Jacobson, P.; Sham, H. L.; Link, J. T. *Bioorg. Med. Chem. Lett.* **2006**, *16*, 5408-5413.

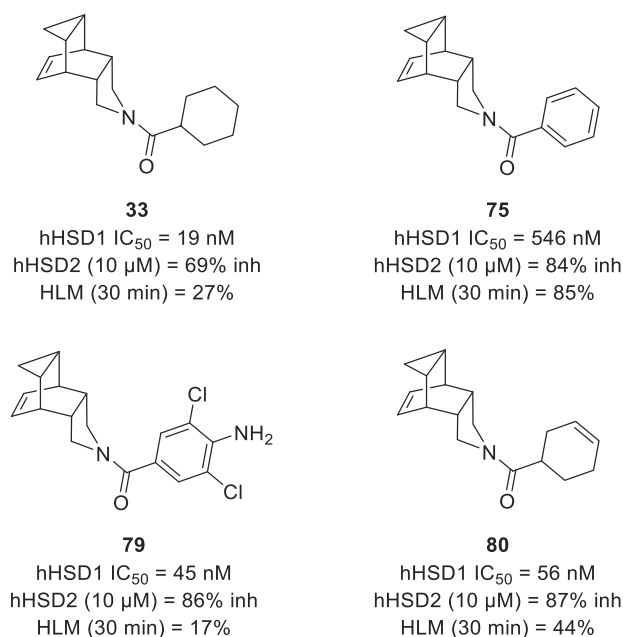
## CHAPTER 7

# **Rationally designed 4- azatetracyclo[5.3.2.0<sup>2,6</sup>.0<sup>8,10</sup>]dodec- 11-ene-containing derivatives as 11 $\beta$ -HSD1 inhibitors**



### 7.1 Rationale and previous work

The project reported in this chapter is the follow-up work of the previous project presented in Chapter 6. As previously discussed, the introduction of different substituents in the RHS of the molecule delivered some potent inhibitors, albeit with suboptimal results regarding selectivity and microsomal stability (Chart 10).<sup>239</sup>



**Chart 10.** Structures of the previously described compounds **33**, **75**, **79** and **80**, and their pharmacological profiles.<sup>239</sup>

Compounds **79** and **80** presented nanomolar potencies against the human 11β-HSD1 enzyme, but could not improve the selectivity of the previous cyclohexyl analog **33**, presenting high inhibition of the isoenzyme 11β-HSD2 (86% and 87% inhibition at 10 μM, respectively). Regarding the microsomal stability of the new compounds, cyclohexenyl derivative, **80**, slightly improved the performance of **33**, with a 44%

<sup>239</sup> Leiva, R.; McBride, A.; Binnie, M.; Webster, S. P.; Vázquez, S. Exploring *N*-acyl-4-azatetracyclo[5.3.2.0<sup>2,6</sup>.0<sup>8,10</sup>]dodec-11-enes as 11β-HSD1 inhibitors. *Bioorg. Med. Chem.* (submitted).



remaining compound after 30-min incubation with HLM vs the previous 17%. To our surprise, the unsubstituted phenyl derivative, **75**, presented a high microsomal stability, 85%, although being less potent (Chart 10).

These observations made us envisage new substitution patterns in the aryl moiety that would combine the good points of compounds **79** and **75**, as well as improving the selectivity over 11 $\beta$ -HSD2. For doing so, we implemented a structure-based design in order to establish additional interactions of the molecule RHS within the binding site that would deliver more potent and selective inhibitors.

## **7.2 Theoretical discussion**

Stemming from the computational work carried out by Constantí Seira in the context of his PhD Thesis, directed by Prof. F. J. Luque and Dr A. Bidon-Chanal (*Departament de Nutrició, Ciències de l'Alimentació i Gastronomia, Facultat de Farmàcia i Ciències de l'Alimentació, Universitat de Barcelona*), several compounds were targeted as putative 11 $\beta$ -HSD1 inhibitors with improved selectivity. All these compounds described in the following manuscript were prepared in the context of the present Thesis. Their rational design, synthesis and pharmacological evaluation are discussed in the manuscript that follows.

# Rational design as an ally to discover novel *N*-acylpyrrolidine-based 11 $\beta$ -HSD1 inhibitors

*Rosana Leiva<sup>1</sup>, Constantí Seira<sup>2</sup>, Andrew McBride<sup>3</sup>, Margaret Binnie<sup>3</sup>, F. Javier Luque<sup>2</sup>, Axel Bidon-Chanal<sup>2</sup>, Scott P. Webster<sup>3</sup>, and Santiago Vázquez<sup>\*1</sup>*

<sup>1</sup>Laboratori de Química Farmacèutica (Unitat Associada al CSIC), Facultat de Farmàcia i Ciències de l'Alimentació and Institut of Biomedicine (IBUB), Universitat de Barcelona, Av. Joan XXIII, 27-31, 08028 Barcelona, Spain.

<sup>2</sup>Department of Nutrition, Food Science and Gastronomy, Facultat de Farmàcia i Ciències de l'Alimentació and Institute of Biomedicine (IBUB), Universitat de Barcelona, Av. Prat de la Riba, 171, 08921 Santa Coloma de Gramenet, Spain.

<sup>3</sup>Centre for Cardiovascular Science, University of Edinburgh, Queen's Medical Research Institute, EH16 4TJ, United Kingdom.

## **Abstract:**

Structure-based drug design contributed to the discovery of potent 11 $\beta$ -HSD1 inhibitors containing the previously reported *N*-acylpyrrolidine structure. Biaryl derivatives **11** and **17** were identified as low nanomolar inhibitors with greater metabolic stabilities than the earlier hit dichloroaniline **7**, although better selectivity over the isoenzyme 11 $\beta$ -HSD2 remains to be achieved.

## **Keywords:**

Glucocorticoids, 11 $\beta$ -HSD1 inhibitors, rational drug design, polycyclic substituents.

## 1. Introduction

Cushing's syndrome is caused by increased circulating levels of cortisol, the glucocorticoid (GC) hormone. This elevated and sustained cortisol levels causes the characteristic clinical symptomatology, namely central obesity, hyperglycaemia, dyslipidaemia and hypertension by its action in key metabolic tissues, and depression and cognitive impairments by acting in the CNS.<sup>1</sup> Thus, from these observations and some mechanistic investigations elevated cortisol seems to be key in metabolic syndrome and age-related diseases such as cognitive decline.<sup>2-5</sup>

11 $\beta$ -Hydroxysteroid dehydrogenase (11 $\beta$ -HSD) enzymes are responsible for the interconversion of cortisone and cortisol (or 11-dehydrocorticosterone and corticosterone in rodents, respectively) in target tissues, being an enzymatic barrier gating GC access to intra-cellular receptors.<sup>6,7</sup> 11 $\beta$ -HSD presents two isoforms: 11 $\beta$ -HSD1 with a predominantly reductase activity is present in the liver, adipose tissue and in the hippocampus and cortex of the brain, where it regenerates the active cortisol from cortisone; and 11 $\beta$ -HSD2, present in mineralocorticoid tissues such as the kidney, with an oxidative activity on cortisol to inactivate it to cortisone, protecting by this way mineralocorticoid receptors from GC activation.<sup>8</sup>

The expected promising effects have been found both in metabolic and cognitive disorders in numerous studies using 11 $\beta$ -HSD1 knockout mice. Global knockout of 11 $\beta$ -HSD1 causes enhanced hepatic insulin sensitivity and reduced gluconeogenesis and glycogenolysis, indicating a potential use of 11 $\beta$ -HSD1 inhibitors for type 2 diabetes.<sup>9</sup> These same mice also present low serum triglycerides and increased HDL cholesterol and apo-lipoprotein A1 levels, suggesting a positive effect of 11 $\beta$ -HSD1 inhibition in atherosclerosis prevention.<sup>10</sup> In addition to this, 11 $\beta$ -HSD1 knockout mice are also protected against age-related cognitive impairment, encouraging the use of that inhibitors in cognitive dysfunction-related diseases, such as Alzheimer's disease.<sup>11</sup>

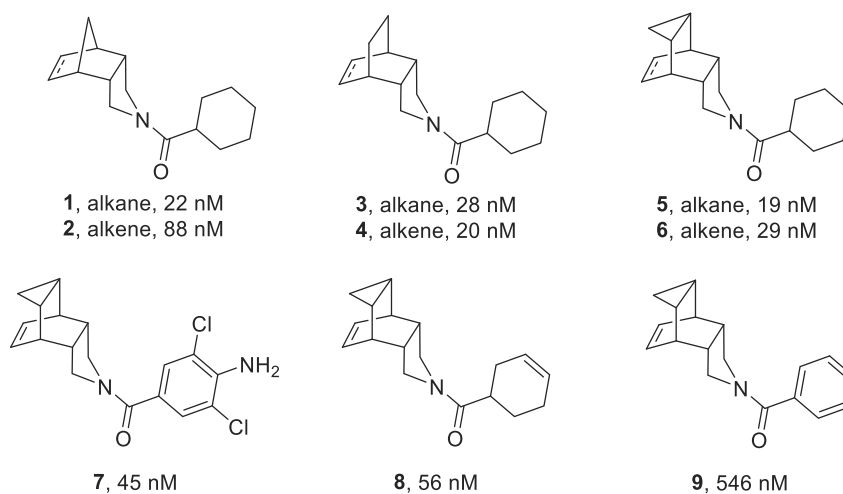
Very encouraging results have also been obtained in several *in vitro* and *in vivo* models of both cognitive and metabolic disorder using a myriad of 11 $\beta$ -HSD1 inhibitors.<sup>12</sup> Notwithstanding, the efficacy of 11 $\beta$ -HSD1 inhibitors in clinics has still to be proven since no compounds have progressed beyond phase II, with insufficient efficacy being the main cause of attrition. Regarding metabolic indications, the failure to achieve primary efficacy endpoints such as glycaemic control or blood pressure were disappointing.<sup>13</sup> Although Abbott's compound ABT-384 failed in demonstrating efficacy in phase II clinical trial,<sup>14</sup> central 11 $\beta$ -HSD1 inhibition seems a promising approach to

deal with cognitive dysfunction associated with AD, since sub-maximal inhibition of the target in the brain seems enough to reverse memory impairment in ageing and AD.<sup>15</sup> Indeed, inhibitors from Actinogen Medical (UE2343) and Astellas (ASP3662) are still in active development, both of them in phase II trials, in relation to age-associated cognitive impairment and AD.<sup>15,16</sup>

## 2. Previous work

We have previously described novel series of 11 $\beta$ -HSD1 inhibitors featuring polycyclic *N*-acylpyrrolidines. Our first efforts were focused on the optimization of the polycyclic substituent to replace the adamantyl nucleus broadly used in 11 $\beta$ -HSD1 inhibitors.<sup>17</sup> After working on the polycyclic group and finding potent enzyme inhibitors (**1-6**) (Chart 1), we moved forward to explore the right-hand side (RHS) substituent of the molecule in order to improve selectivity and DMPK properties maintaining the potency. This work led us to establish some clear structure-activity relationships (SAR) of our molecules and the discovery of new nanomolar inhibitors containing the 4-azapentacyclo[5.3.2.0<sup>2,6</sup>.0<sup>8,10</sup>]dodec-11-ene polycycle (**7** and **8**).<sup>18</sup>

The replacement of the cyclohexyl moiety of compound **6** by a phenyl group was detrimental for the potency (**6**, IC<sub>50</sub> = 29 nM vs **9**, 546 nM); however, the introduction of a previously reported substitution pattern on the aryl unit delivered again a low nanomolar inhibitor (**7**, IC<sub>50</sub> = 45 nM). Despite the potent inhibitory activity of **7**, its low metabolic stability (13% remaining compound after 30-min incubation with human liver microsomes, HLM), the sub-optimal selectivity over 11 $\beta$ -HSD2 (71% inhibition at 1  $\mu$ M) and the aromatic amine as a structural alert of mutagenicity –even though the *ortho*-disubstitution is expected to hinder its metabolic activation– made this compound not an ideal lead for our medicinal chemistry program.



**Figure 1. Previous 11 $\beta$ -HSD1 inhibitors reported by the group with their IC<sub>50</sub> values.**<sup>17,18</sup>

### 3. Design of the new inhibitors

In light of these findings, we focused our efforts on a rational design of new substitution patterns of this RHS aryl group in order to establish additional interactions in the binding site that would deliver more potent and selective inhibitors using docking coupled to molecular dynamics simulations.

Our endeavor started with the search of different crystalized 11 $\beta$ -HSD1 potent inhibitors and its superposition with the docking generated complex of our (best) hit, compound **7**. For each case, visual inspection of the superposed ligands led to a ligand inspired new compound that was proposed also taking into account its synthetic accessibility. A docking experiment was carried out with each proposed ligand in order to build a ligand–receptor complex for each of them. In every case, the best prediction was selected as the highest scored pose where the ligand preserved the orientation of compound **7** and the hydrogen bond interaction with the crucial residues Ser170 and/or Tyr183. Afterwards, at least three independent 50 ns molecular dynamics (MD) simulations were run to obtain a relaxed structure of the selected docking pose in the binding site. The MD run for compound **7** was used as a reference system to compare with the different proposals. The root-mean square deviation (RMSD) profiles were similar in all cases. Thus, the RMSD of the protein backbone varied from 1.35–2.0 Å, whereas the residues in the binding site showed a larger RMSD (2.05 to 2.60 Å) due to

the enhanced flexibility of the loops that surround it. The proximity of the binding site to the C-terminal endpoint of the protein has also an influence in its instability in both chains<sup>19</sup>.

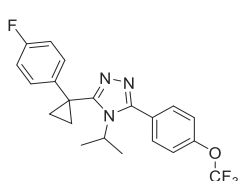
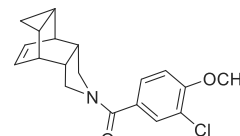
In the first case, compound **7** was superposed to the 3D5Q crystal ligand featuring a trifluoromethoxy group on its RHS phenyl moiety (Table 1).<sup>20</sup> The scores obtained for both molecules in the docking experiment were similar (-8.72 and -8.67, respectively). The proposed substitution pattern inspired in this crystal ligand was a methoxy group in *para* position to replace the amino group and maintaining one chloro substituent in order to fill a small hydrophobic cavity present in the binding site (residues Leu152, Gly197, Leu198, Val212, Met214). The score for this new compound **10** was the same as for the crystal ligand (-8.67), so we expected a similar potency. The binding mode was also the usual with the central amide carbonyl group making a hydrogen bond interaction with the hydroxyl groups of Ser170 and Tyr183. The binding pose obtained with the docking experiment was taken as the starting point to run three independent 50 ns unrestrained MD simulations of the enzyme complex with compound **10**. The ligand was placed in both chains of the crystal structure and the obtained trajectories confirmed the stability of the binding mode in the standard V-shaped conformation. However, due to the enhanced flexibility of the loops and the C-terminal part, the ligand was kept in both binding sites throughout the whole simulation only in one trajectory. For the cases where the ligand was kept in the binding site, the mean hydrogen bond distances with the critical residue Ser170 were 2.89 Å, 3.69 Å and 2.76 Å respectively.

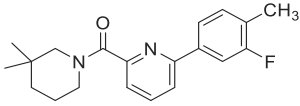
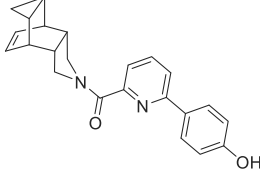
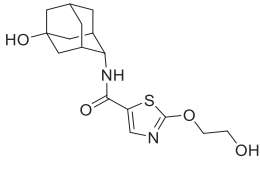
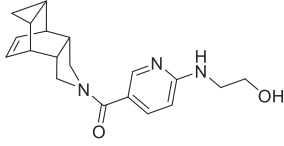
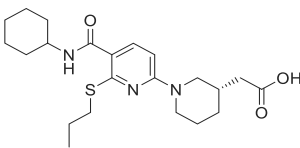
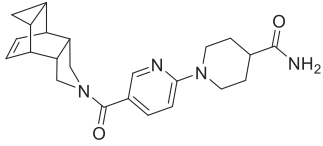
In the second case, we did not observe a significant difference between the scores of the 3CH6 crystal ligand and our compound **7** (-10.90 vs -10.20).<sup>21</sup> Our proposal was compound **11**, mimicking the biaryl structure of the crystal ligand but substituting the methyl group in *para* position by a hydroxyl group to interact through a hydrogen bond with Pro178. Docking calculations corroborated our expectations predicting a higher score for **11** (-12.08). Again, three independent 50 ns unrestrained MD simulations were run with the ligand placed in both chains of the crystal structure. In this case, the ligand was kept in the binding site of the chain B in all the cases, however it was only stable in one of the trajectories for the chain A. In the cases where the ligand was kept in the binding site, the mean hydrogen bond distances of the central amide carbonyl group with the side chain of Ser170 were 2.81 Å, 3.51 Å, 3.54 Å and 2.69 Å.

The next case was using the 4C7J crystal ligand to superpose our compound **7** on it.<sup>22</sup> After docking calculations, the score obtained for the crystal ligand was similar to the

calculated for **7** (-10.71 and -10.17, respectively), despite of the additional interaction of the hydroxyl group of the ethylene chain with the side chain of Asp259. The proposed new compound, **12**, replicating the lateral chain of the crystal ligand, presented an even higher score (-11.13) in the docking and a good consistency of the binding mode in the three independent 50 ns unrestrained MD simulation runs. In this case, the mean hydrogen bond distances of the central amide carbonyl group with the hydroxyl group of Ser170 for those simulations in which the ligand was kept in the binding site were 2.66 Å, 2.73 Å and 3.54 Å.

In the last case, the superposition of **7** with the crystal ligand of 4HFR was suitable.<sup>23</sup> Again, the crystal ligand showed a higher docking score than **7** (-10.65 vs -10.39) and established an additional interaction between the carboxylic acid moiety and the amide group of Leu217. Our proposal was to reproduce the two-ring structure of the crystal ligand with a different final hydrogen bond donor to seek the interaction with Asp259. The proposed compound **13** presented a high score (-11.49) in the docking calculations although this predicted additional interaction between the amino group of the distal amide and the Asp259 was not observed in the docking calculations without losing the principal interactions of the central amide carbonyl group. Furthermore, the ligand was kept in the binding site only in two simulations with mean hydrogen bond distances between the central amide carbonyl group and the side chain hydroxyl group of Ser170 of 2.91 Å and 2.95 Å.

Crystal	Compound	Score
3D5Q	<b>7</b>	-8.72
	Crystal ligand <sup>20</sup>	-8.67
		-8.67
	Proposed compound <b>10</b>	-8.67
		

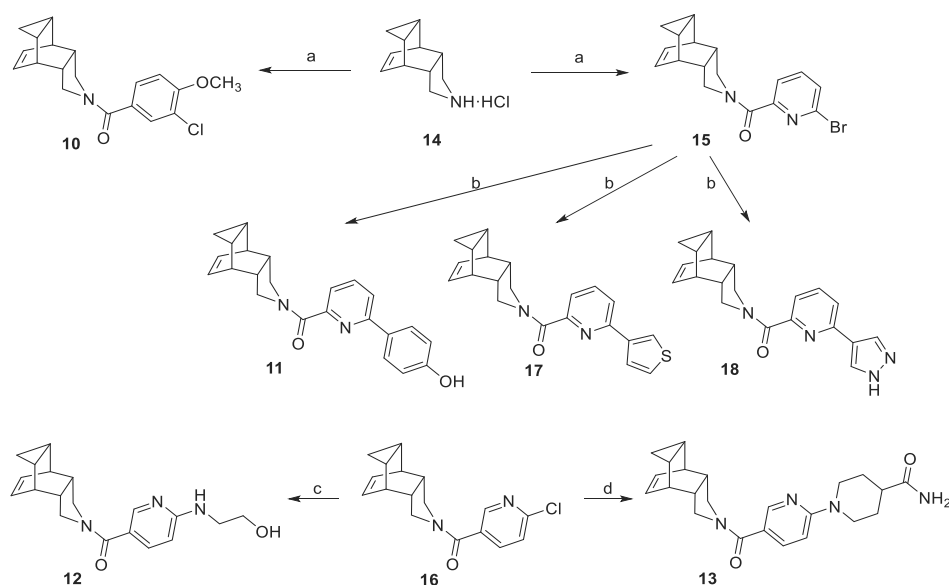
<b>3CH6</b>	<b>7</b>	-10.20
	Crystal ligand <sup>21</sup>	-10.90
		
	Proposed compound <b>11</b>	-12.08
		
<b>4C7J</b>	<b>7</b>	-10.17
	Crystal ligand <sup>22</sup>	-10.71
		
	Proposed compound <b>12</b>	-11.13
		
<b>4HFR</b>	<b>7</b>	-10.39
	Crystal ligand <sup>23</sup>	-10.65
		
	Proposed compound <b>13</b>	-11.49
		

**Table 1. Reference crystal ligands, new designed compounds and their docking scores.**



#### 4. Synthesis

The novel compounds were synthesized according to the Scheme 1. Compound **10** was obtained in quantitative yield from the coupling reaction between 4-azapentacyclo[5.3.2.0<sup>2,6</sup>.0<sup>8,10</sup>]dodec-11-ene hydrochloride,<sup>24</sup> **14**, and 3-chloro-4-methoxybenzoic acid using 1-hydroxybenzotriazole (HOBt) and *N*-(3-dimethylaminopropyl)-*N*'-ethylcarbodiimide (EDC). For the preparation of compound **11**, was first necessary the synthesis of the 6-bromopyridin-2-yl-containing intermediate **15** using the previous methodology for the amide formation, followed by a Suzuki-Miyaura cross-coupling with 4-hydroxyphenylboronic acid which proceeded with moderate yield. Finally, compounds **12** and **13** were obtained by a nucleophilic aromatic substitution using the chloropyridine derivative **16** previously described by our group as the starting material.<sup>18</sup> Amide **16** was dissolved in ethanolamine and heated at 120 °C for 24 hours to give compound **12** in moderate yield. Besides, compound **13** was obtained in high yield heating a solution of the starting material **16**, piperidine-4-carboxamide and potassium carbonate in DMF at 90 °C for 2 days.



**Scheme 1. Syntheses of compound 10-14 and 16-17.** a) HOBt, EDC, Et<sub>3</sub>N, EtOAc, rt, 24 h, 3-chloro-4-methoxybenzoic acid for **10** (quant. yield), 6-bromopyridine-2-carboxylic acid for **15** (73% yield). b) Pd(Ph<sub>3</sub>)<sub>4</sub>, K<sub>2</sub>CO<sub>3</sub>, dioxane, water, 4-hydroxyphenylboronic acid for **11** (59%

yield), thiophene-3-boronic acid for **17** (79% yield), 1*H*-pirazole-4-boronic acid for **18** (28% yield). c) Ethanolamine, 120 °C, 24 h, 61% yield. d) 4-piperidinecarboxamide, DMF, 90 °C, 2 d, 85% yield.

## 5. Pharmacological evaluation

Target compounds **10-13** together with the intermediate amide **15** were tested to determine their human 11 $\beta$ -HSD1 inhibitory activity using a microsomal assay as the preliminary screen. Compounds **12** and **13** presented 20% and 21% inhibition at 10  $\mu$ M concentration, respectively, so they were not further examined to get their IC<sub>50</sub> values. However, **10**, **11** and **15** presented high inhibition of the enzyme, exhibiting diverse potencies. The 3-chloro-4-methoxybenzoyl derivative, **10**, showed a discrete IC<sub>50</sub> value (1003 nM), while the bromopyridine analog, **15**, presented a submicromolar value (200 nM). The IC<sub>50</sub> value of the biaryl **11** (14 nM) was lower than that of our early hit dichloroaniline **7** (45 nM) (Table 2).

As compounds **12** and **13** showed poor inhibition, one may hypothesize that we could not obtain the designed compounds interacting with the Asp259 that was expected to deliver more potent compounds. However, we cannot feel confident with this statement since the performed assay uses a cellular fraction (HLM) instead of the purified enzyme, which introduces more factors to consider besides the mere interaction between the ligand and the target protein.

The most potent compounds **10**, **11** and **15** were further evaluated in terms of cellular potency and selectivity over 11 $\beta$ -HSD2.

Cellular potency was assessed using Human Embryonic Kidney 293 (HEK293) cells stably transfected with the 11 $\beta$ -HSD1 gene. Results for compounds **11** and **15** were in line with those derived from the microsomal assay (cellular IC<sub>50</sub> = 2 and 208 nM, respectively). Surprisingly, compound **10** showed to be more potent in cells than in microsomes presenting an IC<sub>50</sub> value one order of magnitude below of the previously obtained (82 *vs* 1003 nM). This fact could be explained by high metabolism in microsomes that would clear the compound not permitting to perform its activity in the microsomal assay.

Selectivity over 11 $\beta$ -HSD2 was also assessed in a cell-based assay using HEK293 stably transfected with the 11 $\beta$ -HSD2 gene. Regretfully, none of the tested compounds improved the selectivity of **7**, since they presented moderate to high inhibition of the isoenzyme at 10 and 1  $\mu$ M concentration.

Since compound **11** was the most promising inhibitor in terms of potency against the target enzyme, we envisage the preparation of few biaryl analogs in order to explore the SAR of these compounds. To this end, the pyridinyl-containing polycyclic *N*-acylpyrrolidine structure was kept unchanged, and the aromatic group was varied. Doing so we synthesized the 3-thienyl and 1*H*-4-pirazolyl analogs, **17** and **18**, using the Suzuki-Miyaura cross-coupling as previously applied for the preparation of compound **11** (Scheme 1). These new compounds were tested for 11 $\beta$ -HSD1 inhibitory activity both in HLM and HEK cells, being the 3-thiophenyl derivative one order of magnitude more potent than the 1*H*-4-pirazolyl analog (cellular IC<sub>50</sub> = 28 vs 344 nM, respectively).

Diminished activity vs the murine enzyme was not desirable since the mouse was our most accessible *in vivo* animal model to further study these inhibitors. Thus, these biaryl inhibitors were assayed for their mouse 11 $\beta$ -HSD1 inhibitory activity in murine liver microsomes (MLM). Surprisingly, substituent effects on the inhibitory activity of the murine 11 $\beta$ -HSD1 were more pronounced than on the human enzyme. The promising phenol-containing derivative, **11**, displayed almost no 11 $\beta$ -HSD1 inhibition with an IC<sub>50</sub> in the high micromolar range (77.75  $\mu$ M). By contrast, compound **18** that had displayed a modest submicromolar IC<sub>50</sub> in the human enzyme was the most potent inhibitor against the murine 11 $\beta$ -HSD1 (IC<sub>50</sub> = 84 nM), while the 3-thienyl derivative, **17**, presented a potency in between the other two biaryl analogs (IC<sub>50</sub> = 774 nM).

Finally, their metabolic stability was also measured using both human and mouse liver microsomes. Not surprisingly, the three compounds were more stable in HLM than in MLM. Compared with the microsomal stability of our earlier hit compound **7** (13% remaining compound after 30-min incubation in HLM), the new biaryl derivatives were far more stable, presenting good to excellent stabilities (77, 93 and 100% for **11**, **18** and **17**, respectively).

Cp	hHSD1 IC <sub>50</sub> (nM)	HEK hHSD1 IC <sub>50</sub> (nM) <sup>c</sup>	HEK hHSD2 % inh at 10 and 1 μM <sup>c</sup>	mHSD1 IC <sub>50</sub> (nM)	HLM % parent <sup>d</sup>	MLM % parent <sup>d</sup>
<b>7</b>	45	ND	86% 71%	ND	13%	ND
<b>10</b>	1003	82	94% 88%	ND	ND	ND
<b>11</b>	14	2	96% 92%	77750	77%	47%
<b>15</b>	200	208	81% 64%	ND	ND	ND
<b>17</b>	39	28	96% 92%	774	100%	37%
<b>18</b>	333	344	91% 83%	84	93%	23%

**Table 2.** *In vitro* biological profiling of the new 11β-HSD1 inhibitors.<sup>a,b</sup>

<sup>a</sup>See Experimental section for further details. <sup>b</sup>Percentage inhibition was determined relative to a no inhibitor control. <sup>c</sup>HEK293 cells stably transfected with the full-length gene coding for human either 11β-HSD1 or 11β-HSD2 were used. <sup>d</sup>The microsomal stability of each compound was determined using either human or mouse liver microsomes. ND, not determined.

## 6. Conclusions

We have reported the rational design, synthesis and pharmacological evaluation of novel 11β-HSD1 inhibitors featuring a polycyclic *N*-acylpyrrolidine previously described by our group. The designed compounds inspired in reported inhibitors crystalized in complex with the enzyme delivered potent compounds against the human 11β-HSD1. Particularly interesting were the biaryl derivatives, that were further characterized, with the phenol-containing analog, **11**, being the most active compound in the human enzyme with a low nanomolar IC<sub>50</sub>, despite not corresponding with a potent murine activity. The polarity of the compounds conferred them a higher microsomal stability in HLM, one

parameter aimed to be improved in our early hit compound **7**. Unfortunately, the additional substituents introduced to establish potential interactions and to provide selectivity over 11 $\beta$ -HSD2 were not successful, presenting all the compounds undesirable high inhibition at micromolar concentrations. This selectivity issue should be further addressed before moving forward to *in vivo* efficacy studies.

## **7. Experimental section**

### **7.1. Chemistry**

#### **7.1.1. General Methods.**

Melting points were determined in open capillary tubes with a MFB 595010M Gallenkamp. 400 MHz <sup>1</sup>H/100.6 MHz <sup>13</sup>C NMR spectra were recorded on a Varian Mercury 400 spectrometer. The chemical shifts are reported in ppm ( $\delta$  scale) relative to internal tetramethylsilane, and coupling constants are reported in Hertz (Hz). Assignments given for the NMR spectra of the new compounds have been carried out on the basis of COSY <sup>1</sup>H/<sup>13</sup>C (gHSQC sequences) experiments. IR spectra were run on Perkin-Elmer Spectrum RX I spectrophotometer. Absorption values are expressed as wave-numbers (cm<sup>-1</sup>); only significant absorption bands are given. High-resolution mass spectrometry (HRMS) analyses were performed with an LC/MSD TOF Agilent Technologies spectrometer. Column chromatography was performed either on silica gel 60 Å (35–70 mesh) or on aluminium oxide, neutral, 60 Å (50-200  $\mu$ m, Brockmann I). Thin-layer chromatography was performed with aluminum-backed sheets with silica gel 60 F<sub>254</sub> (Merck, ref 1.05554), and spots were visualized with UV light and 1% aqueous solution of KMnO<sub>4</sub>. The elemental analysis of compound **15** was carried out in a Flash 1112 series Thermofinnigan elemental microanalyzer (A5) to determine C, H and N. HPLC/MS were determined with a HPLC Thermo Ultimate 3000SD (Thermo Scientific Dionex) coupled to a photodiode array detector DAD-3000 (Thermo Scientific Dionex) and mass spectrometer LTQ XL ESI-ion trap (Thermo Scientific) with Xcalibur v2.2 acquisition software (Thermo Scientific) (HPLC-PDA-MS). 5  $\mu$ L of sample 0.5 mg/mL in methanol were injected, using a ZORBAX Extend-C18 3.5  $\mu$ m 2.1x50 mm column at 30 °C. The mobile phase was a mixture of A = formic acid 0.05% in water and B = formic acid 0.05% in acetonitrile with the method described as follows: flow 0.6 mL/min, 5%B-95%A 3 min, 100%B 4 min, 95%B-5%A 8 min. Purity is given as % of absorbance at 254 nm; UV-Vis spectra were collected every 0.2 s between 650 and 275 nm; data from

mass spectra were analysed by electrospray ionization in positive mode every 0.3 s between 50 and 1000 Da.

7.1.2. (4-azatetracyclo[5.3.2.0<sup>2,6</sup>.0<sup>8,10</sup>]dodec-11-en-4-yl)(3-chloro-4-methoxyphenyl) methanone, (**10**).

To a solution of 4-azapentacyclo[5.3.2.0<sup>2,6</sup>.0<sup>8,10</sup>]dodec-11-ene hydrochloride (200 mg, 1.03 mmol) in EtOAc (10 mL) were added 3-chloro-4-methoxybenzoic acid (176 mg, 0.94 mmol), HOBt (190 mg, 1.41 mmol), EDC (218 mg, 1.41 mmol) and triethylamine (0.6 mL, 4.14 mmol). The reaction mixture was stirred at room temperature overnight. To the resulting suspension was then added water (10 mL) and the phases were separated. The organic phase was washed with saturated aqueous NaHCO<sub>3</sub> solution (10 mL) and brine (10 mL), dried over anh. Na<sub>2</sub>SO<sub>4</sub> and filtered. Evaporation in *vacuo* of the organics gave **10** as an orange semisolid (329 mg, quantitative yield). IR (ATR)  $\nu$ : 615, 651, 692, 708, 754, 814, 835, 850, 891, 915, 946, 1018, 1059, 1095, 1142, 1183, 1232, 1256, 1294, 1349, 1387, 1418, 1501, 1560, 1599, 1617, 2868, 2925, 3002 cm<sup>-1</sup>. <sup>1</sup>H-NMR (400 MHz, CDCl<sub>3</sub>)  $\delta$ : 0.10-0.18 (complex signal, 2 H, 9'-H<sub>2</sub>), 0.82-0.98 (complex signal, 2 H, 8'-H and 10'-H), 2.54-2.64 (complex signal, 2 H, 2'-H and 6'-H), 2.74 (m, 1 H, 1'-H or 7'-H), 2.90 (m, 1 H, 7'-H or 1'-H), 3.12 (broad d,  $J = 11.2$  Hz, 1 H, 5'-H<sub>a</sub> or 3'-H<sub>a</sub>), 3.45 (broad d,  $J = 11.2$  Hz, 1 H, 3'-H<sub>a</sub> or 5'-H<sub>a</sub>), 3.54 (m, 1 H, 5'-H<sub>b</sub> or 3'-H<sub>b</sub>), 3.71 (m, 1 H, 3'-H<sub>b</sub> or 5'-H<sub>b</sub>), 3.91 (s, 3 H, OCH<sub>3</sub>), 5.69 (m, 1 H, 11'-H or 12'-H), 5.85 (m, 1 H, 12'-H or 11'-H), 6.90 (d,  $J = 8.8$  Hz, 1 H, 5-H), 7.31 (dd,  $J = 8.8$  Hz,  $J' = 2.4$  Hz, 1 H, 6-H), 7.45 (d,  $J = 2.4$  Hz, 1 H, 2-H). <sup>13</sup>C-NMR (100.5 MHz, CDCl<sub>3</sub>)  $\delta$ : 3.9 (CH<sub>2</sub>, C9'), 9.9 (CH, C8' or C10'), 10.1 (CH, C10' or C8'), 35.5 (CH, C1' and C7'), 42.7 (CH, C2' or C6'), 44.9 (CH, C6' or C2'), 49.5 (CH<sub>2</sub>, C3' or C5'), 53.5 (CH<sub>2</sub>, C5' or C3'), 56.2 (CH<sub>3</sub>, OCH<sub>3</sub>), 111.3 (CH, C5), 122.1 (C, C3), 127.1 (CH, C6), 128.2 (CH, C11' or C12'), 129.25 (CH, C12' or C11'), 129.31 (CH, C2), 130.3 (C, C1), 155.9 (C, C4), 167.2 (C, CO). HPLC-PDA-MS: RT = 3.63 min;  $\lambda_{\max} = 209$  nm; purity 98.5% (254 nm). HRMS-ESI+  $m/z$  [M+H]<sup>+</sup>: Calcd for [C<sub>19</sub>H<sub>20</sub>ClNO<sub>2</sub>+H]<sup>+</sup>: 330.1255, found: 330.1251.

7.1.3. (4-azatetracyclo[5.3.2.0<sup>2,6</sup>.0<sup>8,10</sup>]dodec-11-en-4-yl)[6-(4-hydroxyphenyl)pyridin-2-yl] methanone, (**11**).

A mixture of **15** (300 mg, 0.87 mmol), 4-hydroxyphenylboronic acid (132 mg, 0.96 mmol), tetrakis(triphenylphosphine)palladium(0) (10 mg, 0.009 mmol) and K<sub>2</sub>CO<sub>3</sub> (240 mg, 1.74 mmol) in 1,4-dioxane (3 mL) and H<sub>2</sub>O (1.5 mL) was heated at 100 °C for 2 h. EtOAc (10 mL) was added and then washed with H<sub>2</sub>O (10 mL). The aqueous phase was extracted with further EtOAc (10 mL). The organics were dried over anh. Na<sub>2</sub>SO<sub>4</sub>, filtered

and evaporated in *vacuo* to give a brownish solid (461 mg). Column chromatography (Hexane/Ethyl acetate mixture) gave **11** as a white solid (184 mg, 59% yield), mp 221-222 °C. IR (ATR)  $\nu$ : 630, 654, 711, 754, 822, 840, 915, 946, 992, 1039, 1085, 1103, 1173, 1230, 1276, 1297, 1346, 1380, 1400, 1429, 1460, 1516, 1558, 1586, 1604, 2930, 3002, 3126  $\text{cm}^{-1}$ .  $^1\text{H-NMR}$  (400 MHz,  $\text{CDCl}_3$ )  $\delta$ : 0.10-0.20 (complex signal, 2 H, 9'-H<sub>2</sub>), 0.84-0.98 (complex signal, 2 H, 8'-H and 10'-H), 2.58-2.74 (complex signal, 2 H, 2'-H and 6'-H), 2.77 (m, 1 H, 1'-H or 7'-H), 2.93 (m, 1 H, 7'-H or 1'-H), 3.47 (dd,  $J = 12.4$  Hz,  $J' = 4.0$  Hz, 1 H, 5'-H<sub>a</sub> or 3'-H<sub>a</sub>), 3.54 (dd,  $J = 13.2$  Hz,  $J' = 4.0$  Hz, 1 H, 3'-H<sub>a</sub> or 5'-H<sub>a</sub>), 3.83 (dd,  $J = 13.2$  Hz,  $J' = 8.6$  Hz, 1 H, 3'-H<sub>b</sub> or 5'-H<sub>b</sub>), 3.97 (dd,  $J = 12.4$  Hz,  $J' = 8.6$  Hz, 1 H, 5'-H<sub>b</sub> or 3'-H<sub>b</sub>), 5.73 (m, 1 H, 11'-H or 12'-H), 5.85 (m, 1 H, 12'-H or 11'-H), 6.94 [dm,  $J = 8.6$  Hz, 2 H, 3''(5'')-H], 7.56 (dd,  $J = 8.0$ ,  $J' = 0.8$  Hz, 1 H, 5-H), 7.63 (dd,  $J = 8.4$  Hz,  $J' = 0.8$  Hz, 1 H, 3-H), 7.74 (dd,  $J = 8.4$  Hz,  $J' = 8.0$  Hz, 1 H, 4-H), 7.83 [dm,  $J = 8.6$  Hz, 2 H, 2''(6'')-H], 7.91 (broad singlet, 1 H, OH).  $^{13}\text{C-NMR}$  (100.5 MHz,  $\text{CDCl}_3$ )  $\delta$ : 4.0 ( $\text{CH}_2$ , C9'), 10.0 (CH, C8' or C10'), 10.2 (CH, C10' or C8'), 35.6 (CH, C1' and C7'), 42.4 (CH, C2' or C6'), 45.1 (CH, C6' or C2'), 50.6 ( $\text{CH}_2$ , C3' or C5'), 53.2 ( $\text{CH}_2$ , C5' or C3'), 115.9 [CH, C3''(5'')], 120.2 (CH, C3), 120.9 (CH, C5), 128.2 [CH, C2''(6'')], 128.6 (CH, C11' or C12'), 129.1 (CH, C12' or C11'), 130.5 (C, C1'), 137.5 (CH, C4), 153.7 (C, C6), 155.7 (C, C2), 158.0 (C, C4''), 166.4 (C, CO). HPLC-PDA-MS: RT = 3.28 min;  $\lambda_{\text{max}} = 215, 269, 287$  nm; purity > 99.5% (254 nm). HRMS-ESI+  $m/z$  [ $\text{M}+\text{H}$ ]<sup>+</sup>: Calcd for  $[\text{C}_{23}\text{H}_{22}\text{N}_2\text{O}_2+\text{H}]^+$ : 359.1754, found: 359.1750.

**7.1.4** (4-azatetracyclo[5.3.2.0<sup>2,6</sup>.0<sup>8,10</sup>]dodec-11-en-4-yl)[6-((2-hydroxyethyl)amino)pyridine-3-yl]methanone, (**12**).

A mixture of **16** (100 mg, 0.33 mmol) and ethanolamine (0.36 mL, 6 mmol) was heated at 120 °C for 24 h. Water (10 mL) and EtOAc (10 mL) were added and the phases were separated. The organic phase was dried over anhydrous  $\text{Na}_2\text{SO}_4$ , filtered and evaporated in *vacuo* to give an orange oil (65 mg). Crystallization from hot EtOAc gave **12** as a yellowish solid (59 mg, 55% yield), mp 87-88 °C. IR (ATR)  $\nu$ : 636, 716, 731, 767, 811, 832, 909, 943, 984, 1010, 1044, 1070, 1150, 1232, 1274, 1302, 1343, 1423, 1460, 1488, 1527, 1591, 1612, 2868, 2914, 3002, 3064, 3136, 3271  $\text{cm}^{-1}$ .  $^1\text{H-NMR}$  (400 MHz,  $\text{CDCl}_3$ )  $\delta$ : 0.10-0.22 (complex signal, 2 H, 9'-H<sub>2</sub>), 0.84-1.00 (complex signal, 2 H, 8'-H and 10'-H), 2.51-2.65 (complex signal, 2 H, 2'-H and 6'-H), 2.76 (m, 1 H, 1'-H or 7'-H), 2.88 (m, 1 H, 7'-H or 1'-H), 3.22 (m, 1 H, 5'-H<sub>a</sub> or 3'-H<sub>a</sub>), 3.34-3.53 (complex signal, 2 H, 3'-H<sub>a</sub> or 5'-H<sub>a</sub>), 3.48 (m, 1 H, 1''-H<sub>2</sub>), 3.61 (m, 1 H, 5'-H<sub>b</sub> or 3'-H<sub>b</sub>), 3.69 (m, 1 H, 3'-H<sub>b</sub> or 5'-H<sub>b</sub>), 3.77 (t,  $J = 4.6$  Hz, 2 H, 2''-H<sub>2</sub>), 5.36 (m, 1 H, NH), 5.68 (m, 1 H, 11'-H or 12'-H),

5.82 (m, 1 H, 12'-H or 11'-H), 6.35 (d,  $J = 8.6$  Hz, 1 H, 5-H), 7.51 (d,  $J = 8.6$  Hz, 1 H, 4-H), 8.14 (s, 1 H, 2-H).  $^{13}\text{C}$ -NMR (100.5 MHz,  $\text{CDCl}_3$ )  $\delta$ : 3.9 ( $\text{CH}_2$ , C9'), 9.99 (CH, C8' or C10'), 10.01 (CH, C10' or C8'), 35.5 (CH, C1' and C7'), 42.6 (CH, C2' or C6'), 44.9 (CH, C6' or C2' and C1''), 49.5 ( $\text{CH}_2$ , C3' or C5'), 53.6 ( $\text{CH}_2$ , C5' or C3'), 62.8 ( $\text{CH}_2$ , C2''), 107.6 (CH, C5), 121.6 (C, C3), 128.2 (CH, C11' or C12'), 129.2 (CH, C12' or C11'), 137.2 (CH, C4), 147.1 (CH, C2), 159.3 (C, C6), 167.1 (C, CO). HPLC-PDA-MS: RT = 2.27 min;  $\lambda_{\text{max}} = 196, 258, 312$  nm; purity 96.1% (254 nm). HRMS-ESI+  $m/z$   $[\text{M}+\text{H}]^+$ : Calcd for  $[\text{C}_{19}\text{H}_{23}\text{N}_3\text{O}_2+\text{H}]^+$ : 326.1863, found: 326.1867.

7.1.5. 1-[[5-(4-azatetracyclo[5.3.2.0<sup>2,6</sup>.0<sup>8,10</sup>] dodec-11-en-4-yl)carbonyl]pyridin-2-yl] piperidine-4-carboxamide, (**13**).

To a solution of **16** (100 mg, 0.33 mmol) and 4-piperidinecarboxamide (85 mg, 0.66 mmol) in DMF (0.5 mL) was added solid  $\text{K}_2\text{CO}_3$  (82 mg, 0.59 mmol). The resulting suspension was stirred at 120 °C for 48 hours. Water (5 mL) and DCM (5 mL) were added and the phases were separated. The aqueous phase was then extracted with further DCM (2 x 5 mL). The organics were dried over anhydrous  $\text{Na}_2\text{SO}_4$ , filtered and evaporated *in vacuo* to give **13** as a yellowish solid (110 mg, 85% yield), mp 162-163 °C. IR (ATR)  $\nu$ : 630, 692, 723, 773, 811, 845, 943, 982, 1010, 1028, 1041, 1095, 1129, 1178, 1219, 1238, 1312, 1351, 1367, 1408, 1431, 1501, 1540, 1584, 1599, 1687, 1736, 2919, 3152, 3307  $\text{cm}^{-1}$ .  $^1\text{H}$ -NMR (400 MHz,  $\text{CDCl}_3$ )  $\delta$ : 0.10-0.20 (complex signal, 2 H, 9''-H<sub>2</sub>), 0.84-1.00 (complex signal, 2 H, 8''-H and 10''-H), 1.72 [m, 2 H, 3(5)-H<sub>ax</sub>], 1.92 [m, 2 H, 3(5)-H<sub>eq</sub>], 2.39 (m, 1 H, 2''-H or 6''-H), 2.59 (m, 1 H, 6''-H or 2''-H), 2.75 (m, 1 H, 1''-H or 7''-H), 2.82-2.98 [complex signal, 3 H, 7''-H or 1''-H and 2(6)-H<sub>ax</sub>], 3.24 (m, 1 H, 5''-H<sub>a</sub> or 3''-H<sub>a</sub>), 3.46 (m, 1 H, 5''-H<sub>b</sub> or 3''-H<sub>b</sub>), 3.56-3.80 (complex signal, 2 H, 3''-H<sub>a</sub> or 5''-H<sub>a</sub> and 3''-H<sub>b</sub> or 5''-H<sub>b</sub>), 4.35 [dm,  $J = 12.8$  Hz, 2 H, 2(6)-H<sub>eq</sub>], 5.55-6.00 (complex signal, 4 H, 11'-H, 12'-H and NH<sub>2</sub>), 6.60 (d,  $J = 9.0$  Hz, 1 H, 3'-H), 7.59 (d,  $J = 9.0$  Hz, 1 H, 4'-H), 8.26 (s, 1 H, 6'-H).  $^{13}\text{C}$ -NMR (100.5 MHz,  $\text{CDCl}_3$ )  $\delta$ : 3.9 ( $\text{CH}_2$ , C9''), 10.1 (broad singlet, CH, C8'' and C10''), 28.2 [ $\text{CH}_2$ , C3(5)], 35.5 (CH, C1'' and C7''), 42.6 (CH, C2'' and C6''), 44.6 [ $\text{CH}_2$ , C2(6)], 45.0 (CH, C4), 49.6 ( $\text{CH}_2$ , C3'' or C5''), 53.6 ( $\text{CH}_2$ , C5'' or C3''), 105.8 (CH, C3'), 121.3 (C, C5'), 128.2 (CH, C11'' or C12''), 129.2 (CH, C12'' or C11''), 137.3 (CH, C4'), 147.5 (CH, C6'), 159.1 (C, C2'), 167.2 (C, CO), 176.9 (C, CONH<sub>2</sub>). HPLC-PDA-MS: RT = 2.49 min;  $\lambda_{\text{max}} = 195, 268, 318$  nm; purity 95.3% (254 nm). HRMS-ESI+  $m/z$   $[\text{M}+\text{H}]^+$ : Calcd for  $[\text{C}_{23}\text{H}_{28}\text{N}_4\text{O}_2+\text{H}]^+$ : 393.2285, found: 393.2285.

7.1.6. (4-azatetracyclo[5.3.2.0<sup>2,6</sup>.0<sup>8,10</sup>]dodec-11-en-4-yl)(6-bromopyridin-2-yl) methanone, (**15**).



To a solution of 4-azapentacyclo[5.3.2.0<sup>2,6</sup>.0<sup>8,10</sup>]dodec-11-ene hydrochloride (200 mg, 1.03 mmol) in EtOAc (10 mL) were added 6-bromopyridine-2-carboxylic acid (190 mg, 0.94 mmol), HOBt (190 mg, 1.41 mmol), EDC (218 g, 1.41 mmol) and triethylamine (0.6 mL, 4.14 mmol). The reaction mixture was stirred at room temperature overnight. To the resulting suspension was then added water (10 mL) and the phases were separated. The organic phase was washed with saturated aqueous NaHCO<sub>3</sub> solution (10 mL) and brine (10 mL), dried over anh. Na<sub>2</sub>SO<sub>4</sub> and filtered. Evaporation in *vacuo* of the organics gave **15** as a white solid (235 mg, 73% yield), mp 185-186 °C. IR (ATR)  $\nu$ : 643, 659, 705, 734, 762, 814, 827, 850, 912, 935, 984, 1044, 1080, 1119, 1165, 1199, 1225, 1245, 1274, 1305, 1341, 1392, 1405, 1454, 1545, 1576, 1617, 2857, 2925, 3002, 3043, 3059 cm<sup>-1</sup>. <sup>1</sup>H-NMR (400 MHz, CDCl<sub>3</sub>)  $\delta$ : 0.11-0.19 (complex signal, 2 H, 9'-H<sub>2</sub>), 0.86-0.98 (complex signal, 2 H, 8'-H and 10'-H), 2.61 (m, 1 H, 2'-H or 6'-H), 2.68 (m, 1 H, 6'-H or 2'-H), 2.81 (m, 1 H, 1'-H or 7'-H), 2.91 (m, 1 H, 7'-H or 1'-H), 3.34 (dd,  $J = 12.2$  Hz,  $J' = 5.2$  Hz, 1 H, 5'-H<sub>a</sub> or 3'-H<sub>a</sub>), 3.42 (dd,  $J = 13.2$  Hz,  $J' = 5.2$  Hz, 1 H, 3'-H<sub>a</sub> or 5'-H<sub>a</sub>), 3.77 (dd,  $J = 13.2$  Hz,  $J' = 9.2$  Hz, 1 H, 3'-H<sub>b</sub> or 5'-H<sub>b</sub>), 3.92 (dd,  $J = 12.2$  Hz,  $J' = 9.2$  Hz, 1 H, 5'-H<sub>b</sub> or 3'-H<sub>b</sub>), 5.72 (m, 1 H, 11'-H or 12'-H), 5.82 (m, 1 H, 12'-H or 11'-H), 7.50 (dd,  $J = 8.0$  Hz,  $J' = 1.0$  Hz, 1 H, 5-H), 7.62 (dd,  $J = J' = 8.0$  Hz, 1 H, 4-H), 7.72 (dd,  $J = 8.0$  Hz,  $J' = 1.0$  Hz, 1 H, 3-H). <sup>13</sup>C-NMR (100.5 MHz, CDCl<sub>3</sub>)  $\delta$ : 4.1 (CH<sub>2</sub>, C9'), 10.0 (CH, C8' or C10'), 10.2 (CH, C10' or C8'), 35.52 (CH, C1' or C7'), 35.54 (CH, C7' or C1'), 42.3 (CH, C2' or C6'), 45.2 (CH, C6' or C2'), 50.6 (CH<sub>2</sub>, C3' or C5'), 52.8 (CH<sub>2</sub>, C5' or C3'), 122.7 (CH, C3), 128.7 (CH, C11' or C12'), 129.0 (CH, C5), 129.1 (CH, C12' or C11'), 139.1 (CH, C4), 140.1 (C, C6), 155.2 (C, C2), 163.8 (C, CO). Anal. Calcd for C<sub>17</sub>H<sub>17</sub>BrN<sub>2</sub>O: C, 59.14; H, 4.96; N, 8.11. Found: C, 59.31; H, 4.92; N, 7.87.

7.1.7. (4-azatetracyclo[5.3.2.0<sup>2,6</sup>.0<sup>8,10</sup>]dodec-11-en-4-yl)[6-(thien-3-yl)pyridin-2-yl]methanone, (**17**).

A mixture of **15** (230 mg, 0.67 mmol), 3-thiopheneboronic acid (93 mg, 0.73 mmol), tetrakis(triphenylphosphine)palladium(0) (8 mg, 0.007 mmol) and K<sub>2</sub>CO<sub>3</sub> (185 mg, 1.34 mmol) in 1,4-dioxane (2.3 mL) and H<sub>2</sub>O (1.2 mL) was heated at 100 °C for 2 h. EtOAc (10 mL) was added and then washed with H<sub>2</sub>O (10 mL). The aqueous phase was extracted with further EtOAc (10 mL). The organics were dried over anh. Na<sub>2</sub>SO<sub>4</sub>, filtered and evaporated in *vacuo* to give a brownish semisolid (238 mg). Column chromatography (Hexane/Ethyl acetate mixture) gave **17** as a brownish semisolid (184 mg, 79% yield), mp 48-49 °C. IR (ATR)  $\nu$ : 615, 646, 703, 716, 752, 791, 829, 845, 863, 915, 948, 987, 1036, 1095, 1178, 1235, 1274, 1343, 1418, 1431, 1460, 1566, 1581, 1617, 2000, 2051,

2175, 2325, 2868, 2919, 2997  $\text{cm}^{-1}$ .  $^1\text{H-NMR}$  (400 MHz,  $\text{CDCl}_3$ )  $\delta$ : 0.11-0.20 (complex signal, 2 H, 9'-H<sub>2</sub>), 0.86-1.00 (complex signal, 2 H, 8'-H and 10'-H), 2.59-2.74 (complex signal, 2 H, 2'-H and 6'-H), 2.79 (m, 1 H, 7'-H or 1'-H), 2.93 (m, 1 H, 1'-H or 7'-H), 3.43-3.57 (complex signal, 2 H, 3'-H<sub>a</sub> and 5'-H<sub>a</sub>), 3.81 (dd,  $J = 13.0$  Hz,  $J' = 8.6$  Hz, 1 H, 3'-H<sub>b</sub> or 5'-H<sub>b</sub>), 4.01 (dd,  $J = 11.8$  Hz,  $J' = 8.2$  Hz, 1 H, 5'-H<sub>b</sub> or 3'-H<sub>b</sub>), 5.74 (m, 1 H, 11'-H or 12'-H), 5.86 (m, 1 H, 12'-H or 11'-H), 7.40 (dd,  $J = 5.2$  Hz,  $J' = 3.2$  Hz, 1 H, 4''-H), 7.61-7.68 (complex signal, 3 H, 5-H, 3-H and 5''-H), 7.77 (dd,  $J = 8.0$  Hz,  $J' = 7.6$  Hz, 1 H, 4-H), 7.89 (dd,  $J = 3.2$  Hz,  $J' = 1.4$  Hz, 1 H, 2''-H).  $^{13}\text{C-NMR}$  (100.5 MHz,  $\text{CDCl}_3$ )  $\delta$ : 4.0 ( $\text{CH}_2$ , C9'), 10.0 ( $\text{CH}$ , C8' or C10'), 10.2 ( $\text{CH}$ , C10' or C8'), 35.6 ( $\text{CH}$ , C1' or C7'), 35.7 ( $\text{CH}$ , C7' or C1'), 42.4 ( $\text{CH}$ , C2' or C6'), 45.3 ( $\text{CH}$ , C6' or C2'), 50.5 ( $\text{CH}_2$ , C3' or C5'), 53.0 ( $\text{CH}_2$ , C5' or C3'), 120.7 ( $\text{CH}$ , C3), 121.9 ( $\text{CH}$ , C5), 123.8 ( $\text{CH}$ , C2''), 126.2 ( $\text{CH}$ , C4''), 126.4 ( $\text{CH}$ , C5''), 128.6 ( $\text{CH}$ , C11' or C12'), 129.1 ( $\text{CH}$ , C12' or C11'), 137.5 ( $\text{CH}$ , C4), 141.8 (C, C3''), 151.5 (C, C6), 154.3 (C, C2), 165.5 (C, CO). HPLC-PDA-MS: RT = 3.78 min;  $\lambda_{\text{max}} = 218, 259$  nm; purity 99.3%. HRMS-ESI+  $m/z$   $[\text{M}+\text{H}]^+$ : Calcd for  $[\text{C}_{21}\text{H}_{20}\text{N}_2\text{OS}+\text{H}]^+$ : 349.1369, found: 349.1374.

7.1.8. (4-azatetracyclo[5.3.2.0<sup>2,6</sup>.0<sup>8,10</sup>]dodec-11-en-4-yl)[6-(1H-pyrazol-4-yl)pyridin-2-yl]methanone, (**18**).

A mixture of **15** (285 mg, 0.83 mmol), 1H-pyrazole-4-boronic acid (102 mg, 0.91 mmol), tetrakis(triphenylphosphine)palladium(0) (9 mg, 0.008 mmol) and  $\text{K}_2\text{CO}_3$  (229 mg, 1.66 mmol) in 1,4-dioxane (2.8 mL) and  $\text{H}_2\text{O}$  (1.4 mL) was heated at 100 °C for 2 h. EtOAc (10 mL) was added and then washed with  $\text{H}_2\text{O}$  (10 mL). The aqueous phase was extracted with further EtOAc (10 mL). The organics were dried over anhyd.  $\text{Na}_2\text{SO}_4$ , filtered and evaporated in *vacuo* to give a brown solid (300 mg). Column chromatography (Hexane/Ethyl acetate mixture) gave **18** as a brownish solid (78 mg, 28% yield), mp 164-165 °C. IR (ATR)  $\nu$ : 623, 646, 708, 729, 762, 809, 845, 868, 928, 974, 1026, 1041, 1085, 1145, 1176, 1219, 1238, 1276, 1307, 1336, 1367, 1377, 1413, 1431, 1460, 1558, 1581, 1917, 1940, 1987, 2935, 3162  $\text{cm}^{-1}$ .  $^1\text{H-NMR}$  (400 MHz,  $\text{CDCl}_3$ )  $\delta$ : 0.10-0.21 (complex signal, 2 H, 9'-H<sub>2</sub>), 0.84-1.00 (complex signal, 2 H, 8'-H and 10'-H), 2.58-2.72 (complex signal, 2 H, 2'-H and 6'-H), 2.77 (m, 1 H, 1'-H or 7'-H), 2.92 (m, 1 H, 7'-H or 1'-H), 3.40-3.54 (complex signal, 2 H, 3'-H<sub>a</sub> and 5'-H<sub>a</sub>), 3.82 (dd,  $J = 13.0$  Hz,  $J' = 8.6$  Hz, 1 H, 3'-H<sub>b</sub> or 5'-H<sub>b</sub>), 3.94 (dd,  $J = 12.2$  Hz,  $J' = 8.6$  Hz, 1 H, 5'-H<sub>b</sub> or 3'-H<sub>b</sub>), 5.73 (m, 1 H, 11'-H or 12'-H), 5.84 (m, 1 H, 12'-H or 11'-H), 7.47 (d,  $J = 8.0$  Hz, 1 H, 3-H), 7.54 (d,  $J = 7.4$  Hz, 5-H), 7.72 (dd,  $J = 8.0$  Hz,  $J' = 7.4$  Hz, 1 H, 4-H), 8.09 (s, 2 H, 3''-H and 5''-H).  $^{13}\text{C-NMR}$  (100.5 MHz,  $\text{CDCl}_3$ )  $\delta$ : 4.0 ( $\text{CH}_2$ , C9'), 10.0 ( $\text{CH}$ , C8' or C10'), 10.2 ( $\text{CH}$ ,

C10' or C8'), 35.58 (CH, C1' or C7'), 35.62 (CH, C7' or C1'), 42.4 (CH, C2' or C6'), 45.2 (CH, C6' or C2'), 50.5 (CH<sub>2</sub>, C3' or C5'), 53.0 (CH<sub>2</sub>, C5' or C3'), 120.2 (CH, C3), 121.0 (CH, C5), 122.7 (C, C4''), 128.6 (CH, C11' or C12'), 129.1 (CH, C12' or C11'), 132.5 (broad singlet, CH, C3'' and C5''), 137.4 (CH, C4), 150.4 (C, C6), 154.3 (C, C2), 165.9 (C, CO). HPLC-PDA-MS: RT = 2.90 min;  $\lambda_{\text{max}}$  = 196, 253, 292 nm; purity 99.4% (254 nm). HRMS-ESI+ m/z [M+H]<sup>+</sup>: Calcd for [C<sub>20</sub>H<sub>20</sub>N<sub>4</sub>O+H]<sup>+</sup>: 333.1710, found: 333.1716.

### 7.2. 11 $\beta$ -HSD1 *in vitro* Enzyme Inhibition Assay

11 $\beta$ -HSD1 activity was determined in mixed sex, human or murine liver microsomes (Celsis In-vitro Technologies) by measuring the conversion of cortisone to cortisol by LC/MS. Percentage inhibition was determined relative to a no inhibitor control. 5  $\mu$ g of human liver microsomes were pre-incubated at 37°C for 15 min with inhibitor and 1 mM NADPH in a final volume of 90  $\mu$ L Krebs buffer. 10  $\mu$ L of 2  $\mu$ M cortisone was then added followed by incubation at 37°C for a further 30 min. The assay was terminated by rapid freezing on dry ice and subsequent extraction with acetonitrile on thawing. Samples dried down under nitrogen at 65°C and solubilised in 100  $\mu$ L 70:30 H<sub>2</sub>O:ACN and removed to a 96-well V-bottomed plate for LC/MS analysis. Separation was carried out on a sunfire 150 x 2.1 mm, 3.5  $\mu$ M column using a H<sub>2</sub>O:ACN gradient profile. Typical retention times were 2.71 min for cortisol and 2.80 min for cortisone. The peak area was calculated and the concentration of each compound determined from the calibration curve.

### 7.3. Cellular 11 $\beta$ -HSD1 Enzyme Inhibition Assay

The cellular 11 $\beta$ -HSD1 enzyme inhibition assay was performed using HEK293 cells stably transfected with the human 11 $\beta$ -HSD1 gene. Cells were incubated with substrate (cortisone) and product (cortisol) was determined by LC/MS. Cells were plated at 2 x 10<sup>4</sup> cells/well in a 96-well poly-D-lysine coated tissue culture microplate (Greiner Bio-one) and incubated overnight at 37°C in 5% CO<sub>2</sub> 95% O<sub>2</sub>. Compounds to be tested were solubilized in 100% DMSO at 10 mM and serially diluted in water and 10% DMSO to final concentration of 10  $\mu$ M in 10% DMSO. 10  $\mu$ L of each test dilution and 10  $\mu$ L of 10% DMSO (for low and high control) were dispensed into the well of a new 96-well microplate (Greiner Bio-one). Medium was removed from the cell assay plate and 100  $\mu$ L of DMEM solution (containing 1% penicillin, 1% streptomycin and 300 nM cortisone) added to each well. Cells were incubated for 2 h at 37 °C in 5% CO<sub>2</sub> 95% O<sub>2</sub>. Following incubation, medium was removed from each well into an eppendorf containing 500  $\mu$ L

of ethyl acetate, mixed by vortex and incubated at rt for 5 min. A calibration curve of known concentrations of cortisol in assay medium was also set up and added to 500  $\mu$ L of ethyl acetate, vortexed and incubated as above. The supernatant of each eppendorf was removed to a 96-deep-well plate and dried down under liquid nitrogen at 65°C. Each well was solubilised in 100  $\mu$ L 70:30 H<sub>2</sub>O:ACN and removed to a 96-well V-bottomed plate for LC/MS analysis. Separation was carried out on a sunfire 150 x 2.1 mm, 3.5  $\mu$ M column using a H<sub>2</sub>O:ACN gradient profile. Typical retention times were 2.71 min for cortisol and 2.80 min for cortisone. The peak area was calculated and the concentration of each compound determined from the calibration curve.

#### **7.4. Cellular 11 $\beta$ -HSD2 Enzyme Inhibition Assay**

For measurement of inhibition of 11 $\beta$ -HSD2, HEK293 cells stably transfected with the full-length gene coding for human 11 $\beta$ -HSD2 were used. The protocol was the same as for the cellular 11 $\beta$ -HSD1 enzyme inhibition assay, only changing the substrate, this time cortisol, and the concentrations of the tested compounds, 10 and 1  $\mu$ M.

#### **7.5. Microsomal Stability Assay**

The microsomal stability of each compound was determined using either human or mouse liver microsomes (Celsis In-vitro Technologies). Microsomes were thawed and diluted to a concentration of 2 mg/mL in 50 mM NaPO<sub>4</sub> buffer pH 7.4. Each compound was diluted in 4 mM NADPH (made in the phosphate buffer above) to a concentration of 10  $\mu$ M. Two identical incubation plates were prepared to act as a 0 minute and a 30 minute time point assay. 30  $\mu$ L of each compound dilution was added in duplicate to the wells of a U-bottom 96-well plate and warmed at 37°C for approximately 5 min. Verapamil, lidocaine and propranolol at 10  $\mu$ M concentration were utilised as reference compounds in this experiment. Microsomes were also pre-warmed at 37°C before the addition of 30  $\mu$ L to each well of the plate resulting in a final concentration of 1 mg/mL. The reaction was terminated at the appropriate time point (0 or 30 min) by addition of 60  $\mu$ L of ice-cold 0.3 M trichloroacetic acid (TCA) per well. The plates were centrifuged for 10 min at 112 x g and the supernatant fraction transferred to a fresh U-bottom 96-well plate. Plates were sealed and frozen at -20°C prior to MS analysis. LC-MS/MS was used to quantify the peak area response of each compound before and after incubation with human liver microsomes using MS tune settings established and validated for each compound. These peak intensity measurements were used to calculate the % remaining after incubation with human microsomes for each hit compound.

## 7.6. Computational Methods

Docking calculations were performed using Glide,<sup>25</sup> with the X-ray structures of the human enzymes with PDB ID: 3D5Q, 3CH6, 4C7J and 4HFR.<sup>26</sup> The geometry of each ligand was energy minimized and the centroids of the inhibitors cocrystallized in each of them were used to generate the docking cavity by selecting all the residues located within 20 Å from the ligand. 100 poses were generated for each ligand, and the best-scored poses fitting the expected arrangement within the binding pocket were chosen as starting structures for MD simulations.

For each ligand-protein complex three independent 50 ns MD simulations were run to check the consistency of the binding mode. To this end, the ligand-protein complex was located inside an octahedral box of TIP3P<sup>27</sup> water molecules and sodium ions were added to neutralize the system. The force field ff99SBildn<sup>28,29</sup> was used for the protein parameters, and RESP charges at the HF/6-31G (d) together with the gaff<sup>30</sup> force field were used to generate the ligand and the NADP parameters. All systems were refined through a three-step energy minimization procedure (entailing first hydrogen atoms, water molecules, and finally the entire system) and a six-step equilibration (heating the system from 0 K to 300 K in 6 steps of 20 ps, the first, 50 ps the next four, and 5 ns the last one). The resulting structures were used as initial structures for MD production runs.

## Acknowledgements

We thank financial support from *Ministerio de Economía y Competitividad* and FEDER (Project SAF2014-57094-R) and the *Generalitat de Catalunya* (grants 2014-SGR-00052 and 2014-SGR-1189) and the *Consorci de Serveis Universitaris de Catalunya* for computational resources. R. L. thanks the Spanish *Ministerio de Educación Cultura y Deporte* for a PhD Grant (FPU program). F. J. L. acknowledges the support from ICREA Academia. We thank ACCIÓ (*Generalitat de Catalunya*) and CIDQO 2012 SL for financial support (*Programa Nuclis*, RD14-1-0057, SAFNAD).

## References

1. Arnaldi, G.; Angeli, A.; Atkinson, A. P.; Bertagna, X.; Cavagnini, F.; Chrousos, G. P.; Fava, G. A.; Findling, J. W.; Gaillard, R. C.; Grossman, A. B.; Kola, B.; Lacroix, A.; Mancini, T.; Mantero, F.; Newell-Price, J.; Nieman, L. K.; Sonino, N.; Vance, M. L.; Giustina, A.; Boscaro, M. *J. Clin. Endocrinol. Metab.* **2003**, *88*, 5593-5602.
2. Walker, B. R. *Eur. J. Endocrinol.* **2007**, *157*, 545-559.
3. Van Raalte, D. H.; Ouwens, D. M.; Diamant, M. *Eur. J. Clin. Invest.* **2009**, *39*, 81-93.
4. Swabb, D. F.; Bao, A. M.; Lucassen, P. J. *Ageing Res. Rev.* **2005**, *4*, 141-194.
5. Meaney, M. J.; O'Donnell, D.; Rowe, W. *Exp. Gerontol.* **1995**, *30*, 229-251.
6. Seckl, J. R.; Walker, B. R. *Endocrinology* **2001**, *142*, 1371-1376.
7. Morton, N. M.; Seckl, J. R. *Front. Horm. Res.* **2008**, *36*, 146-164.
8. Brown, R. W.; Chapman, K. E.; Edwards, C. R.; Seckl, J. R. *Endocrinology* **1993**, *132*, 2614-2621.
9. Kotelevtsev, Y.; Holmes, M. C.; Burdell, A.; Houston, P. M.; Schmall, D.; Jamieson, P.; Best, R.; Brown, R.; Edwards, C. R. W.; Seckl, J. R.; Mullins, J. J. *Proc. Natl. Acad. Sci. U.S.A.* **1997**, *94*, 14924-14929.
10. Morton, N. M.; Holmes, M. C.; Fievet, C.; Staels, B.; Tailleux, A.; Mullins, J. J. *J. Biol. Chem.* **2001**, *276*, 41293-41300.
11. Yau, J. L. W.; Noble, J.; Kenyon, C. J.; Hibberd, C.; Kotelevtsev, Y.; Mullins, J. J.; Seckl, J. R. *Proc. Natl. Acad. Sci. U.S.A.* **2001**, *98*, 4716-4721.
12. Scott, J. S.; Goldberg, F. W.; Turnbull, A. V. *J. Med. Chem.* **2014**, *57*, 4466-4486.
13. Feig, P. U.; Shah, S.; Hermanowski-Vosatka, A.; Plotkin, D.; Springer, M. S.; Donahue, S.; Thach, C.; Klein, E. J.; Lai, E.; Kaufman, K. D. *Diabetes, Obesity Metab.* **2011**, *13*, 498-504.
14. Marek, G. J.; Katz, D. A.; Meier, A.; Greco, N.; Zhang, W.; Liu, W.; Lenz, R. A. *Alzheimers Dement.* **2014**, *10*, (5 Suppl), S364-S373.
15. Webster, S. P.; McBride, A.; Binnie, M.; Sooy, K.; Seckl, J. R.; Andrew, R.; Pallin, T. D.; Hunt, H. J.; Perrior, T. R.; Ruffles, V. S.; Ketelbey, J. W.; Boyd, A.; Walker, B. R. *British J. Pharmacol.* **2017**, *174*, 396-408.
16. <https://www.astellas.com/en/ir/library/medical.html>. Accessed June 2017.

17. Leiva, R.; Griñan-Ferré, C.; Seira, C.; Valverde, E.; McBride, A.; Binnie, M.; Pérez, B.; Luque, F. J.; Pallàs, M.; Bidon-Chanal, A.; Webster, S. P.; Vázquez, S. *Eur. J. Med. Chem.* **2017**, *139*, 412-428.
18. Leiva, R.; McBride, A.; Binnie, M.; Webster, S. P.; Vázquez, S. *Bioorg. Med. Chem.* (submitted).
19. Liang, J.; Naveed, H.; Jimenez-Morales, D.; Adamian, L., & Lin, M. *Biochim. Biophys. Acta* **2012**, *1818*, 927–941.
20. Tu, H.; Powers, J. P.; Liu, J.; Ursu, S.; Sudom, A.; Yan, X.; Xu, H.; Meininger, D.; DeGraffenreid, M.; He, X.; Jaen, J. C.; Sun, D.; Labelle, M.; Yamamoto, H.; Shan, B.; Walker, N. P. C.; Wang, Z. *Bioorg. Med. Chem.* **2008**, *16*, 8922-8931.
21. Wang, H.; Ruan, Z.; Li, J. J.; Simpkins, L. M.; Smirk, R. A.; Wu, S. C.; Hutchins, R. D.; Nirschl, D. S.; Kirk, K. V.; Cooper, C. B.; Sutton, J. C.; Ma, Z.; Golla, R.; Seethala, R.; Salyan, M. E. K.; Nayeem, A.; Krystek Jr., S. R.; Sheriff, S.; Came, D. M.; Morin, P. E.; Carpenter, B.; Robl, J. A.; Zahler, R.; Gordon, D. A.; Hamann, L. G. *Bioorg. Med. Chem. Lett.* **2008**, *18*, 3168-3172.
22. Goldberg, F. W.; Dossetter, A. G.; Scott, J. S.; Robb, G. R.; Boyd, S.; Groombridge, S. D.; Kemmitt, P. D.; Sjögren, T.; Moretin Gutiérrez, P.; deSchoolmeester, J.; Swales, J. G.; Turnbull, A. V.; Wild, M. J. *J. Med. Chem.* **2014**, *57*, 970-986.
23. Scott, J. S.; Bowker, S. S.; deSchoolmeester, J.; Gerhardt, S.; Hargreaves, D.; Kilgour, E.; Lloyd, A.; Mayers, R. M.; McCoull, W.; Newcombe, N. J.; Ogg, D.; Packer, M. J.; Rees, A.; Revill, J.; Schofield, P.; Selmi, N.; Swales, J. G.; Whittamore, P. R. O. *J. Med. Chem.* **2012**, *55*, 5951-5964.
24. Rey-Carrizo, M.; Barniol-Xicotá, M.; Ma, C.; Frigolé-Vivas, M.; Torres, E.; Naesens, L.; Llabrés, S.; Juárez-Jiménez, J.; Luque, F. J.; DeGrado, W. F.; Lamb, R. A.; Pinto, L. H.; Vázquez, S. *J. Med. Chem.* **2014**, *57*, 5738–5747.
25. Friesner, R. A.; Murphy, R. B.; Repasky, M. P.; Frye, L. L.; Greenwood, J. R.; Halgren, T. A.; Sanschagrin, P. C.; Mainz, D. T. *J. Med. Chem.* **2006**, *49*, 6177–6196.
26. Goldberg, F. W.; Leach, A. G.; Scott, J. S.; Snelson, W. L.; Groombridge, S. D.; Donald, C. S.; Bennett, S. N. L.; Bodin, C.; Gutierrez, P. M.; Gyte, A. C. *J. Med. Chem.* **2012**, *55*, 10652–10661.
27. Jorgensen, W. L.; Chandrasekhar, J.; Madura, J. D.; Impey, R. W.; Klein, M. L. *J. Chem. Phys.* **1983**, *79*, 926–935.

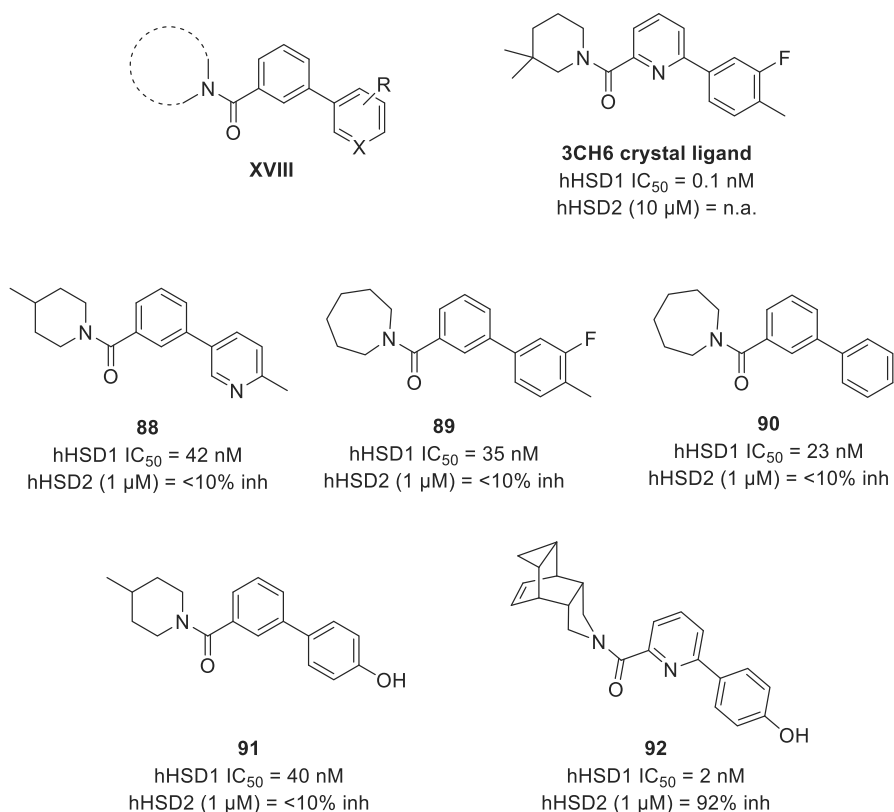
28. Hornak, V.; Abel, R.; Okur, A.; Strockbine, B.; Roitberg, A.; Simmerling, C. *Proteins* **2006**, *65*, 712–725.
29. Lindorff-Larsen, K.; Piana, S.; Palmo, K.; Maragakis, P.; Klepeis, J. L.; Dror, R. O.; Shaw, D. E. *Proteins* **2010**, *78*, 1950–1958.
30. Wang, J.; Wolf, R. M.; Caldwell, J. W.; Kollman, P. A.; Case, D. A. *J. Comput. Chem.* **2004**, *25*, 1157–1174.





#### 7.4 Additional results: Dealing with selectivity. Synthesis and evaluation of additional biaryl amides

During the writing of the present Thesis, a PCT application by the company DSM Nutritional Products was published describing biaryl amides with potent and selective inhibitory activity against 11 $\beta$ -HSD1 over 11 $\beta$ -HSD2.<sup>240</sup> Shortly thereafter, the same company published a collaborative paper with the University of Basel with further details.<sup>241</sup> The general structure of these novel compounds, **XVIII**, and some examples, **88-91**, are depicted in the following chart.

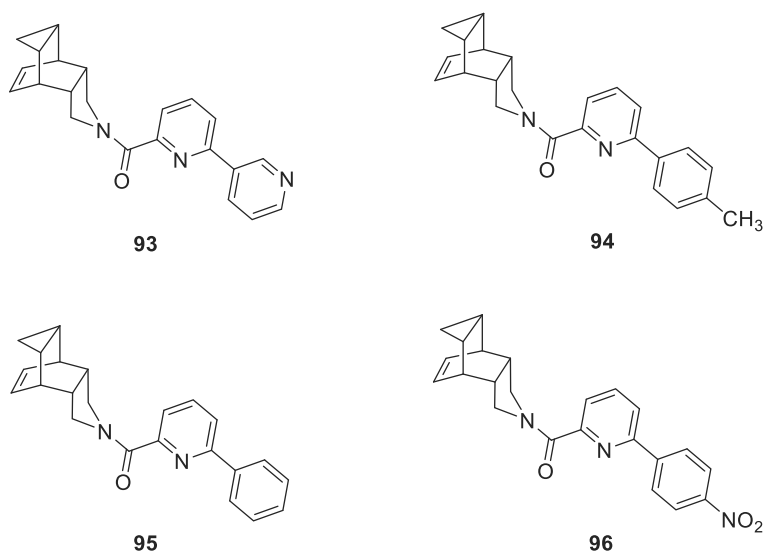


**Chart 11.** General structure of the novel compounds, **XVIII**, (X = N, CH), some examples together with their cellular IC<sub>50</sub> and our compound **92**. n.a., no activity.<sup>240-242</sup>

<sup>240</sup> Boudon, S. M.; Geotti-Bianchini, P.; Heidl, M.; Jackson, E.; Schlifke-Poschalko, A. WO Patent Application, WO2017012890, 2017.

<sup>241</sup> Boudon, S. M.; Vuorinen, A.; Geotti-Bianchini, P.; Wandeler, E.; Kratschmar, D. V.; Heidl, M.; Campiche, R.; Jackson, E.; Odermatt, A. *PLoS ONE* **2017**, *12*, e0171079.

The compounds from DSM Nutritional Products and the University of Basel containing a biaryl amide core and a cyclic secondary amine reminded us the structure of the 3CH6 crystal ligand<sup>242</sup> that inspired us to design the last compounds prepared in this Thesis (Chapter 7), our potent *but non-selective* *N*-(biaryl)acylpyrrolidines (e.g. see **92** in Chart 11). All together let us think about the preparation of some additional compounds bearing the same –or similar- aryl groups of the second ring of DSM compounds in order to confirm the lack of selectivity of our similar inhibitors attributable to *our* lipophilic polycycle. Thus, compounds **93-96** were envisaged to this end as additional biaryl amides worthy to synthesize to test our hypothesis (Chart 12).



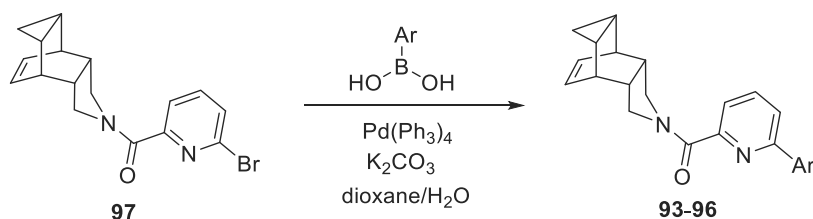
**Chart 12.** Envisaged compounds **93-96**.

Docking calculations of these compounds were carried out by Constantí Seira in order to check their accommodation in the binding site of the 11 $\beta$ -HSD1. The obtained results were positive since the docking scores were in the same range than the previous from

<sup>242</sup> Wang, H.; Ruan, Z.; Li, J. J.; Simpkins, L. M.; Smirk, R. A.; Wu, S. C.; Hutchins, R. D.; Nirschl, D. S.; Kirk, K. V.; Cooper, C. B.; Sutton, J. C.; Ma, Z.; Golla, R.; Seethala, R.; Salyan, M. E. K.; Nayeem, A.; Krystek, S. R.; Sheriff, S.; Camac, D. M.; Morin, P. E.; Carpenter, B.; Robl, J. A.; Zahler, R.; Gordona, D. A.; Hamann, L. G. *Bioorg. Med. Chem. Lett.* **2008**, *18*, 3168-3172.

the potent biaryl derivatives (-11.25, -11.49, -11.28 and -9.53 for **93-96**, respectively, vs -12.08 for **92**).

The new compounds were planned to be prepared with the same methodology used for the previous synthesized biaryl amides, the Suzuki-Miyaura cross-coupling between the bromopyridin-containing amide derivative, **97**, and the corresponding arylboronic acids (Scheme 16).

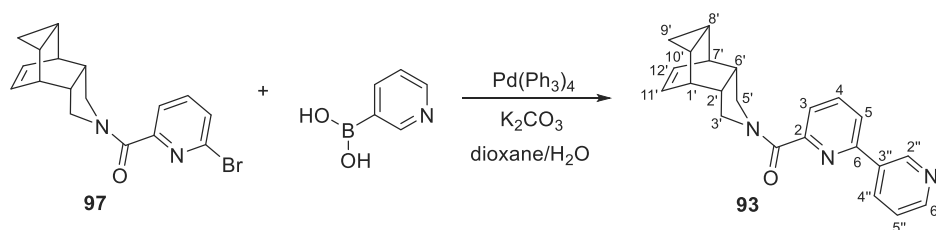


**Scheme 16.** General procedure of the preparation of the novel biaryl amides **93-96**.

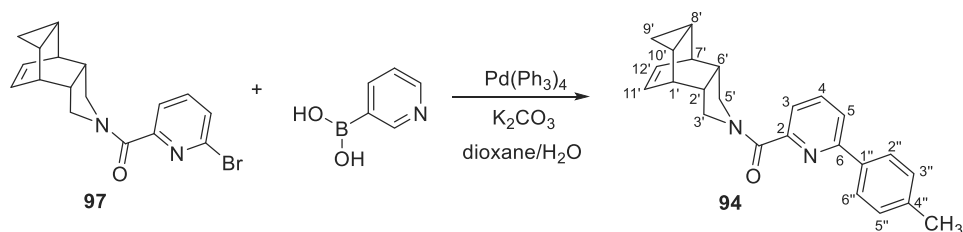
The synthesis of the compounds was straightforward and the desired products were obtained and fully characterized (see below). At the presentation of this Thesis, the compounds are being tested by the group of Dr Scott P. Webster, so the pharmacological results are not yet available for further discussion.

#### 7.4 Experimental data of the unpublished work

(4-azatetracyclo[5.3.2.0<sup>2,6</sup>.0<sup>8,10</sup>]dodec-11-en-4-yl)[6-(pyridin-3-yl)pyridin-2-yl]methanone, **93**.



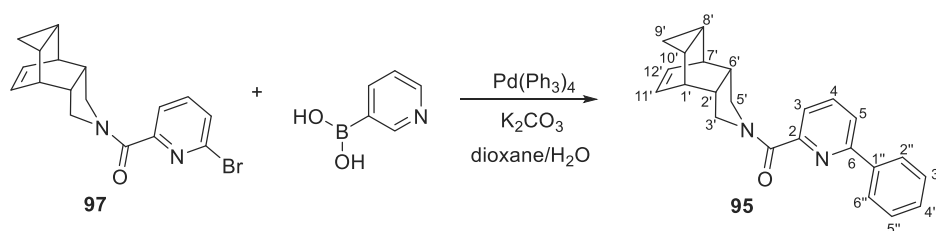
A mixture of **97** (200 mg, 0.58 mmol), 3-pyridinylboronic acid (79 mg, 0.64 mmol), tetrakis(triphenylphosphine)palladium(0) (69 mg, 0.06 mmol) and K<sub>2</sub>CO<sub>3</sub> (160 mg, 1.16 mmol) in 1,4-dioxane (2 mL) and H<sub>2</sub>O (1.1 mL) was heated at 100 °C for 2 h. EtOAc (10 mL) was added and then washed with H<sub>2</sub>O (10 mL). The aqueous phase was extracted with further EtOAc (10 mL). The organics were dried over anh. Na<sub>2</sub>SO<sub>4</sub>, filtered and evaporated in *vacuo* to give an orange oil (223 mg). Column chromatography (Hexane/Ethyl acetate mixture) gave **93** as a yellowish solid (108 mg, 54% yield), mp 146–148 °C. IR (NaCl)  $\nu$ : 2924, 2854, 1739, 1628, 1589, 1572, 1462, 1422, 1388, 1348, 1235, 1193, 1088, 1021, 991, 807, 755, 708, 665 cm<sup>-1</sup>. <sup>1</sup>H-NMR (400 MHz, CDCl<sub>3</sub>)  $\delta$ : 0.12–0.20 (complex signal, 2 H, 9'-H<sub>2</sub>), 0.86–1.00 (complex signal, 2 H, 8'-H and 10'-H), 2.60–2.74 (complex signal, 2 H, 2'-H and 6'-H), 2.80 (m, 1 H, 1'-H or 7'-H), 2.94 (m, 1 H, 7'-H or 1'-H), 3.46–3.56 (complex signal, 2 H, 3'-H<sub>a</sub> and 5'-H<sub>a</sub>), 3.82 (dd,  $J = 13.0$  Hz,  $J' = 8.4$  Hz, 1 H, 3'-H<sub>b</sub> or 5'-H<sub>b</sub>), 4.03 (dd,  $J = 12.2$  Hz,  $J' = 8.4$  Hz, 1 H, 5'-H<sub>b</sub> or 3'-H<sub>b</sub>), 5.74 (m, 1 H, 11'-H or 12'-H), 5.87 (m, 1 H, 12'-H or 11'-H), 7.42 (ddd,  $J = 8.0$  Hz,  $J' = 4.8$  Hz,  $J'' = 0.8$  Hz, 5''-H), 7.78 (dd,  $J = 7.6$  Hz,  $J' = 1.2$  Hz, 1 H, 3-H or 5-H), 7.79 (dd,  $J = 8.0$  Hz,  $J' = 1.2$  Hz, 1 H, 3-H and 5-H), 7.88 (dd,  $J = 8.0$  Hz,  $J' = 7.6$  Hz, 1 H, 4-H), 8.29 (ddd,  $J = 8.0$ ,  $J' = 2.4$  Hz,  $J'' = 1.6$  Hz, 1 H, 4''-H), 8.67 (dd,  $J = 4.8$  Hz,  $J' = 1.6$  Hz, 1 H, 6''-H), 9.25 (dd,  $J = 2.4$  Hz,  $J' = 0.8$  Hz, 1 H, 2''-H). <sup>13</sup>C-NMR (100.5 MHz, CDCl<sub>3</sub>)  $\delta$ : 4.1 (CH<sub>2</sub>, C9'), 10.1 (CH, C8' or C10'), 10.2 (CH, C10' or C8'), 35.64 (CH, C1' or C7'), 35.67 (CH, C7' or C1'), 42.4 (CH, C2' or C6'), 45.3 (CH, C6' or C2'), 50.6 (CH<sub>2</sub>, C3' or C5'), 53.1 (CH<sub>2</sub>, C5' or C3'), 121.0 (CH, C3 or C5), 123.0 (CH, C5 or C3), 123.6 (CH, C5''), 128.6 (CH, C11' or C12'), 129.2 (CH, C12' or C11'), 134.2 (CH, C4''), 134.3 (C, C3''), 137.9 (CH, C4), 148.4 (CH, C2''), 150.1 (CH, C6''), 152.9 (C, C6), 154.8 (C, C2), 165.2 (C, CO). HPLC-PDA-MS: RT = 2.86 min;  $\lambda_{\text{max}}$  = 197, 235, 267 nm; purity > 98.5% (254 nm). HRMS-ESI+ m/z [M+H]<sup>+</sup>: Calcd for [C<sub>22</sub>H<sub>21</sub>N<sub>3</sub>O+H]<sup>+</sup>: 344.1757, found: 344.1751.

**(4-azatetracyclo[5.3.2.0<sup>2,6</sup>.0<sup>8,10</sup>]dodec-11-en-4-yl)[6-(4-methylphenyl)pyridin-2-yl]methanone, **94**.**

A mixture of **97** (200 mg, 0.58 mmol), 4-methylphenylboronic acid (87 mg, 0.64 mmol), tetrakis(triphenylphosphine)palladium(0) (69 mg, 0.06 mmol) and  $K_2CO_3$  (160 mg, 1.16 mmol) in 1,4-dioxane (2 mL) and  $H_2O$  (1.1 mL) was heated at 100 °C for 2 h. EtOAc (10 mL) was added and then washed with  $H_2O$  (10 mL). The aqueous phase was extracted with further EtOAc (10 mL). The organics were dried over anhydrous  $Na_2SO_4$ , filtered and evaporated in *vacuo* to give a yellowish oil (266 mg). Column chromatography (Hexane/Ethyl acetate mixture) gave **94** as a white solid (132 mg, 64% yield), 126–128 °C. IR (NaCl)  $\nu$ : 430, 587, 623, 636, 655, 709, 758, 813, 832, 850, 893, 916, 948, 991, 1019, 1038, 1065, 1087, 1099, 1186, 1211, 1233, 1276, 1302, 1347, 1417, 1514, 1633, 1799, 1910, 1977, 2327, 2731, 2872, 2929, 3003, 3240, 3466  $cm^{-1}$ .  $^1H$ -NMR (400 MHz,  $CDCl_3$ )  $\delta$ : 0.12–0.20 (complex signal, 2 H, 9'-H<sub>2</sub>), 0.84–1.00 (complex signal, 2 H, 8'-H and 10'-H), 2.42 (s, 3 H, Ar-CH<sub>3</sub>), 2.60–2.72 (complex signal, 2 H, 2'-H and 6'-H), 2.79 (m, 1 H, 1'-H or 7'-H), 2.94 (m, 1 H, 7'-H or 1'-H), 3.48–3.56 (complex signal, 2 H, 3'-H<sub>a</sub> and 5'-H<sub>a</sub>), 3.82 (dd,  $J = 13.2$  Hz,  $J' = 8.8$  Hz, 1 H, 3'-H<sub>b</sub> or 5'-H<sub>b</sub>), 4.03 (dd,  $J = 12.5$  Hz,  $J' = 8.8$  Hz, 1 H, 5'-H<sub>b</sub> or 3'-H<sub>b</sub>), 5.74 (m, 1 H, 11'-H or 12'-H), 5.86 (m, 1 H, 12'-H or 11'-H), 7.29 [dm,  $J = 8.0$  Hz, 2 H, 3''(5'')-H], 7.67 (dd,  $J = 7.8$ ,  $J' = 1.2$  Hz, 1 H, 5-H), 7.73 (dd,  $J = 8.0$  Hz,  $J' = 1.2$  Hz, 1 H, 3-H), 7.80 (dd,  $J = 8.0$  Hz,  $J' = 7.8$  Hz, 1 H, 4-H), 7.91 [dm,  $J = 8.0$  Hz, 2 H, 2''(6'')-H].  $^{13}C$ -NMR (100.5 MHz,  $CDCl_3$ )  $\delta$ : 4.0 (CH<sub>2</sub>, C9'), 10.1 (CH, C8' or C10'), 10.2 (CH, C10' or C8'), 21.3 (CH<sub>3</sub>, Ph-CH<sub>3</sub>), 35.6 (CH, C1' or C7'), 35.7 (CH, C7' or C1'), 42.4 (CH, C2' or C6'), 45.3 (CH, C6' or C2'), 50.5 (CH<sub>2</sub>, C3' or C5'), 53.0 (CH<sub>2</sub>, C5' or C3'), 120.6 (CH, C3), 121.9 (CH, C5), 126.7 [CH, C2''(6'')], 128.6 (CH, C11' or C12'), 129.1 (CH, C12' or C11'), 129.5 [CH, C3''(5'')], 136.1 (C, C4''), 137.4 (CH, C4), 139.2 (C, C1''), 154.3 (C, C6), 155.4 (C, C2),

165.7 (C, CO). HPLC-PDA-MS: RT = 4.05 min;  $\lambda_{\text{max}}$  = 195, 213, 258 nm; purity > 98.5% (254 nm). HRMS-ESI+ m/z [M+H]<sup>+</sup>: Calcd for [C<sub>24</sub>H<sub>24</sub>N<sub>2</sub>O+H]<sup>+</sup>: 357.1961, found: 357.1957.

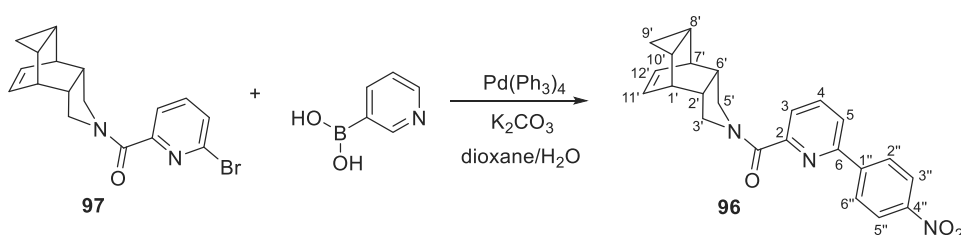
**(4-azatetracyclo[5.3.2.0<sup>2,6</sup>.0<sup>8,10</sup>]dodec-11-en-4-yl)[6-(phenyl)pyridin-2-yl]methanone, 95.**



A mixture of **97** (200 mg, 0.58 mmol), phenylboronic acid (78 mg, 0.64 mmol), tetrakis(triphenylphosphine)palladium(0) (69 mg, 0.06 mmol) and K<sub>2</sub>CO<sub>3</sub> (160 mg, 1.16 mmol) in 1,4-dioxane (2 mL) and H<sub>2</sub>O (1.1 mL) was heated at 100 °C for 2 h. EtOAc (10 mL) was added and then washed with H<sub>2</sub>O (10 mL). The aqueous phase was extracted with further EtOAc (10 mL). The organics were dried over anh. Na<sub>2</sub>SO<sub>4</sub>, filtered and evaporated in *vacuo* to give a yellowish oil (259 mg). Column chromatography (Hexane/Ethyl acetate mixture) gave **95** as a yellowish solid (131 mg, 66% yield), mp 94–96 °C. IR (NaCl)  $\nu$ : 623, 666, 694, 725, 751, 829, 990, 1027, 1088, 1184, 1233, 1300, 1347, 1398, 1424, 1463, 1573, 1587, 1628, 2873, 2927, 3003, 3043 cm<sup>-1</sup>. <sup>1</sup>H-NMR (400 MHz, CDCl<sub>3</sub>)  $\delta$ : 0.10–0.22 (complex signal, 2 H, 9'-H<sub>2</sub>), 0.86–1.02 (complex signal, 2 H, 8'-H and 10'-H), 2.60–2.72 (complex signal, 2 H, 2'-H and 6'-H), 2.79 (m, 1 H, 1'-H or 7'-H), 2.94 (m, 1 H, 7'-H or 1'-H), 3.46–3.58 (complex signal, 2 H, 3'-H<sub>a</sub> and 5'-H<sub>a</sub>), 3.82 (dd,  $J$  = 13.4 Hz,  $J'$  = 8.6 Hz, 1 H, 3'-H<sub>b</sub> or 5'-H<sub>b</sub>), 4.03 (dd,  $J$  = 12.2 Hz,  $J'$  = 8.6 Hz, 1 H, 5'-H<sub>b</sub> or 3'-H<sub>b</sub>), 5.74 (m, 1 H, 11'-H or 12'-H), 5.87 (m, 1 H, 12'-H or 11'-H), 7.40–7.55 [complex signal, 3 H, 3''(5'')-H and 4''-H], 7.70 (d,  $J$  = 7.8, 1 H, 5-H), 7.76 (d,  $J$  = 7.8 Hz, 1 H, 3-H), 7.83 (dd,  $J$  = 7.8 Hz,  $J'$  = 7.8 Hz, 1 H, 4-H), 8.00 [dm,  $J$  = 8.0 Hz, 2 H, 2''(6'')-H]. <sup>13</sup>C-NMR (100.5 MHz, CDCl<sub>3</sub>)  $\delta$ : 4.0 (CH<sub>2</sub>, C9'), 10.1 (CH, C8' or C10'), 10.2 (CH, C10' or C8'), 35.65 (CH, C1' or C7'), 35.68 (CH, C7' or C1'), 42.4 (CH, C2' or C6'), 45.3 (CH, C6' or C2'), 50.5 (CH<sub>2</sub>, C3' or C5'), 53.0 (CH<sub>2</sub>, C5' or C3'), 120.9 (CH, C3), 122.2 (CH, C5), 126.9 [CH, C2''(6'')], 128.6

(CH, C11' or C12'), 128.8 [CH, C3''(5'')], 129.09 (CH, C12' or C11'), 129.14 (C, C4''), 137.5 (CH, C4), 138.8 (C, C1''), 154.4 (C, C6), 155.4 (C, C2), 165.7 (C, CO). Anal. Calcd for C<sub>23</sub>H<sub>22</sub>N<sub>2</sub>O: C, 80.67; H, 6.48; N, 8.18. Found: C, 80.36; H, 6.53; N, 7.81.

**(4-azatetracyclo[5.3.2.0<sup>2,6</sup>.0<sup>8,10</sup>]dodec-11-en-4-yl)[6-(4-nitrophenyl)pyridin-2-yl]methanone, **96**.**



A mixture of **97** (200 mg, 0.58 mmol), 4-nitrophenylboronic acid (107 mg, 0.64 mmol), tetrakis(triphenylphosphine)palladium(0) (69 mg, 0.06 mmol) and K<sub>2</sub>CO<sub>3</sub> (160 mg, 1.16 mmol) in 1,4-dioxane (2 mL) and H<sub>2</sub>O (1.1 mL) was heated at 100 °C for 2 h. EtOAc (10 mL) was added and then washed with H<sub>2</sub>O (10 mL). The aqueous phase was extracted with further EtOAc (10 mL). The organics were dried over anh. Na<sub>2</sub>SO<sub>4</sub>, filtered and evaporated in *vacuo* to give a yellowish oil (329 mg). Column chromatography (Hexane/Ethyl acetate mixture) gave **96** as a yellowish solid (132 mg, 59% yield), mp 174–175 °C. IR (NaCl)  $\nu$ : 644, 665, 727, 749, 825, 857, 948, 992, 1012, 1039, 1108, 1185, 1235, 1276, 1347, 1390, 1422, 1463, 1519, 1570, 1582, 1627, 1729, 2873, 2927, 3003, 3045 cm<sup>-1</sup>. <sup>1</sup>H-NMR (400 MHz, CDCl<sub>3</sub>)  $\delta$ : 0.12–0.22 (complex signal, 2 H, 9'-H<sub>2</sub>), 0.84–1.02 (complex signal, 2 H, 8'-H and 10'-H), 2.60–2.74 (complex signal, 2 H, 2'-H and 6'-H), 2.78 (m, 1 H, 1'-H or 7'-H), 2.95 (m, 1 H, 7'-H or 1'-H), 3.47 (dd,  $J = 12.0$  Hz,  $J' = 4.2$  Hz, 1 H, 5'-H<sub>a</sub> or 3'-H<sub>a</sub>), 3.53 (dd,  $J = 13.4$  Hz,  $J' = 4.2$  Hz, 1 H, 3'-H<sub>a</sub> or 5'-H<sub>a</sub>), 3.82 (dd,  $J = 13.4$  Hz,  $J' = 8.4$  Hz, 1 H, 3'-H<sub>b</sub> or 5'-H<sub>b</sub>), 3.98 (dd,  $J = 12.0$  Hz,  $J' = 8.4$  Hz, 1 H, 5'-H<sub>b</sub> or 3'-H<sub>b</sub>), 5.73 (m, 1 H, 11'-H or 12'-H), 5.88 (m, 1 H, 12'-H or 11'-H), 7.79 (dd,  $J = 7.8$  Hz,  $J' = 1.2$  Hz, 1 H, 5-H), 7.84 (dd,  $J = 8.0$  Hz,  $J' = 1.2$  Hz, 1 H, 3-H), 7.91 (dd,  $J = 8.0$  Hz,  $J' = 7.8$  Hz, 1 H, 4-H), 8.18 [dm,  $J = 8.8$  Hz, 2 H, 3''(5'')-H], 8.34 [dm,  $J = 8.8$  Hz, 2 H, 2''(6'')-H]. <sup>13</sup>C-NMR (100.5 MHz, CDCl<sub>3</sub>)  $\delta$ : 4.0 (CH<sub>2</sub>, C9'), 10.0 (CH, C8' or C10'), 10.2 (CH, C10' or C8'), 35.66



*Polycyclic group optimization in 11 $\beta$ -HSD1 inhibitors and their pharmacological evaluation*

(CH, C1' or C7'), 35.71 (CH, C7' or C1'), 42.4 (CH, C2' or C6'), 45.3 (CH, C6' or C2'), 50.5 (CH<sub>2</sub>, C3' or C5'), 53.0 (CH<sub>2</sub>, C5' or C3'), 121.6 (CH, C3), 123.6 (CH, C5), 124.0 [CH, C2''(6'')], 127.6 [CH, C3''(5'')], 128.5 (CH, C11' or C12'), 129.2 (CH, C12' or C11'), 138.0 (CH, C4), 144.6 (C, C1''), 148.2 (C, C4''), 152.9 (C, C6), 155.0 (C, C2), 165.1 (C, CO). Anal. Calcd for C<sub>23</sub>H<sub>21</sub>N<sub>3</sub>O<sub>3</sub> · 0.2 C<sub>6</sub>H<sub>14</sub>: C, 71.83; H, 5.93; N, 10.38. Found: C, 71.88; H, 5.91; N, 10.29.

## CHAPTER 8

# **Conclusions**



Fulfilling the objectives of the present Thesis, numerous 11 $\beta$ -HSD1 inhibitors with different polycyclic substituents so far unexplored in the context of this topic have been designed, synthesized and pharmacologically evaluated. In addition, work on the rest of the molecule gave us valuable SAR information to secure potent inhibitors.

Besides, the *in vitro* biological characterization permitted us to select a suitable compound to study the neuroprotection of 11 $\beta$ -HSD1 inhibition in rodent models of cognitive dysfunction, stress and cognitive impairment aggravated with a given high-fat diet.

In detail the main findings and conclusions that have arisen from each chapter are the following:

### **Chapter 3. Synthesis and evaluation of the novel 2-oxadamantane-5-amine**

- The target cage amine was successfully prepared applying consecutive Criegee rearrangements on 2-methyl-2-adamantanol to deliver the 2-oxadamantane, which was then functionalized by C-H activation using phase-transfer catalysis. Finally, a Ritter reaction followed by deprotection with thiourea delivered the desired 2-oxadamantane-5-amine.
- The novel heteroanalog of amantadine was tested against two of its well-known targets, the M2 channel of the Influenza A virus and the NMDA receptor, in order to assess its behavior as an isostere of amantadine.
- Unfortunately, the 2-oxadamantane-5-amine showed low inhibition of the M2 channel activity, in the wild type as well as in the amantadine-resistant mutants (9-21% inhibition), resulting in a lack of antiviral activity.
- The new oxadamantadine presented discreet antagonistic activity of the NMDA receptor, being 2.5 fold less potent than amantadine.

**Chapter 4. Study of C-1 vs C-2 substitution in adamantyl derivatives and introduction of oxaadamantyl groups in 11 $\beta$ -HSD1 inhibitors**

- Three pairs of 1- and 2-adamantyl derivatives featuring fragments of proven 11 $\beta$ -HSD1 inhibitors were prepared and characterized as well as three oxaanalogs.
- All the compounds were pharmacologically evaluated to test their inhibition of the human 11 $\beta$ -HSD1 enzyme. Among them, three new 2-adamantyl derivatives displayed submicromolar potency.
- Some robust SAR information was disclosed, since all the C-1 substituted adamantyl derivatives lack of 11 $\beta$ -HSD1 inhibition, while their C-2 substituted counterparts presented nanomolar to submicromolar IC<sub>50</sub>s.
- Docking studies together with molecular dynamics simulations help us to rationalize the experimental results. 1-Adamantyl derivatives showed higher fluctuation in the binding site compared to C-2 substituted inhibitors, suggesting a poorer fit due to the larger steric hindrance of the adamantyl cage oriented to the cofactor comparing with the C2-H unit in their C-2 derived counterparts.
- Unpleasantly, oxaadamantyl derivatives were inactive as 11 $\beta$ -HSD1 inhibitors. From these results, the introduction of an oxygen seems detrimental for the activity, although one could also blame the C-1 substitution of these compounds for the lack of inhibition.

**Chapter 5. Polycycle optimization in 11 $\beta$ -HSD1 inhibitors. Evaluation of unexplored pyrrolidine-based polycyclic hydrocarbons**

- To begin with, four *N*-pentacyclo[6.4.0.0<sup>2,10</sup>.0<sup>3,7</sup>.0<sup>4,9</sup>]dodec-8-yl-containing amides were successfully prepared and evaluated to be compared with their pyrrolidine-based hexacyclic analogs. 11 $\beta$ -HSD1 inhibitory potencies revealed the preferred *N*-acylpyrrolidine motif versus the opened structure in a few pairs of comparable compounds.
- Docking studies were combined with molecular dynamics simulations to shed light into this SAR. The fused pyrrolidine ring seems to reduce the contribution

of the conformational penalty to the binding affinity of pyrrolidine-containing compounds compared to the more flexible compounds.

- To further explore and optimize the pyrrolidine-based polycycle, thirteen new compounds with different polycyclic substituents featuring a common cyclohexyl moiety as RHS of the molecule were prepared and evaluated as 11 $\beta$ -HSD1 inhibitors. The vast majority were potent inhibitors, with some of them presenting low nanomolar potencies. The SAR trends revealed that smaller polycycles led to an increase in the inhibitory activity due to the better fit in the binding site, which was supported by computational studies.
- The more potent inhibitors were characterized in terms of cellular potency, selectivity over 11 $\beta$ -HSD2, human metabolic stability and predicted brain permeability.
- This *in vitro* profiling permitted us to select a potent, metabolically stable and predicted BBB-permeable inhibitor to perform the first *in vivo* study of an 11 $\beta$ -HSD1 inhibitor in the rodent model of cognitive dysfunction SAMP8. The selected compound was orally administered to old SAMP8 mice that presented cognitive impairment, being able to reverse the cognition status to that of the control young SAMP8 mice.
- These results provide further support for the neuroprotective effect of 11 $\beta$ -HSD1 inhibition in cognitive decline, through reduction of neuroinflammation and oxidative stress, and increased proteases removing proamiloidogenic species.
- Besides, a second analysis studied the implication of the autophagy process in the observed neuroprotective effect. An increase in the removal of abnormal proteins was detected, which could be important on the basis of the pharmacological effects of 11 $\beta$ -HSD1 inhibition.

#### **Chapter 6. Exploring novel 11 $\beta$ -HSD1 inhibitors containing the optimized 4-azatetracyclo[5.3.2.0<sup>2,6</sup>.0<sup>8,10</sup>]dodec-11-ene polycycle**

- Thirteen new compounds containing the polycycle 4-azatetracyclo[5.3.2.0<sup>2,6</sup>.0<sup>8,10</sup>]dodec-11-ene were successfully prepared and evaluated as 11 $\beta$ -HSD1 inhibitors.

- SAR information on the RHS of the molecule was disclosed, being that: (i) the introduction of a double bond in the cyclohexyl substituent maintained the nanomolar activity in the same range of magnitude; (ii) a phenyl group was deleterious for the activity as well as either electron-rich or electron-deficient heteroaromatic rings; (iii) a previously reported dichloroaniline group restored the inhibitory activity to deliver a low nanomolar inhibitor; (iv) *N*-substituted piperidinyl groups were deleterious for the activity; (v) a branched alkyl substituent, such as the *tert*-butyl group, was also deleterious for the activity, but conferring a modest potency; (vi) compounds containing the 6-(4-phenylpiperazin-1-yl)pyridin-3-yl system presented varying potencies depending on the *para* substitution of the phenyl ring, being the cyano group preferred over the hydrogen and the trifluoromethyl.
- Those compounds with submicromolar IC<sub>50</sub> values were further evaluated in terms of cellular potency, selectivity over 11 $\beta$ -HSD2 and metabolic stability.
- 11 $\beta$ -HSD2 inhibition as well as metabolic stability presented discouraging values to further characterize these compounds *in vivo*.

#### **Chapter 7. Rationally designed 4-azatetracyclo[5.3.2.0<sup>2,6</sup>.0<sup>8,10</sup>]dodec-11-ene-containing derivatives as 11 $\beta$ -HSD1 inhibitors**

- A few compounds containing the 4-azatetracyclo[5.3.2.0<sup>2,6</sup>.0<sup>8,10</sup>]dodec-11-ene polycycle were rationally designed using different crystal ligands as reference compounds.
- These new compounds were successfully prepared and evaluated as 11 $\beta$ -HSD1 inhibitors, presenting varying activities. The biaryl-containing derivative was the most promising compound, displaying a low nanomolar cellular potency.
- To further explore the biaryl motif and its SAR, a series of biaryl analogs were synthesized and pharmacologically evaluated. The introduction of different substituents in the phenyl ring and its substitution by heteroaromatic rings revealed some SAR trends.

To sum up, in this PhD Thesis, we have discovered potent, brain-penetrant 11 $\beta$ -HSD1 inhibitors. We have obtained compounds with low nanomolar activities, reasonable metabolic stabilities and we have successfully performed *in vivo* studies with a selected compound. However, selectivity over the isoenzyme 11 $\beta$ -HSD2 remains a challenge to be accomplished. This will be the goal of further work by the multidisciplinary team involved in this project.





**ABBREVIATIONS**

11 $\beta$ -HSD – 11 $\beta$ -hydroxysteroid dehydrogenase	Et <sub>3</sub> N – triethylamine
Ac – acetyl	EtOAc – ethyl acetate
Ac <sub>2</sub> O – acetic anhydride	EtOH – ethanol
ACTH – pituitary corticotropin	GC/MS – gas chromatography-mass spectrometry
AD – Alzheimer's disease	GCs – glucocorticoids
ADAS-Cog – Alzheimer's disease assessment scale-cognitive subscale	GH – growth hormone
AME – apparent mineralocorticoid excess	GM-CSF – granulocyte macrophage colony-stimulating factor
AMPK – AMP-activated protein kinase	GnRH – hypothalamic gonadotropin-releasing hormone
Anh. – anhydrous	GR – glucocorticoid receptor
Aq. – aqueous	H <sub>2</sub> – hydrogen
Asn – asparagine	H <sub>2</sub> O <sub>2</sub> – hydrogen peroxide
AVP – arginine vasopressin	H <sub>2</sub> SO <sub>4</sub> – sulfuric acid
BTEAC – benzyltriethylammonium chloride	H6PDH – hexose-6-phosphate dehydrogenase
C/EBP – CCAAT/enhancer binding protein	hBA1c – body weight and haemoglobin A1C
CBr <sub>4</sub> – carbon tetrabromide	HCl – hydrochloric acid
CNS – central nervous system	HgO – mercury(II) oxide
Concd – concentrated	HLM – human liver Microsomes
CRH – corticotropin-releasing hormone	HOBt – 1-hydroxybenzotriazole
CSF – cerebral spinal fluid	HPA – hypothalamic-pituitary-adrenal
DCI – diabetes cognitive impairment	I <sub>2</sub> – iodine
DCM – dichloromethane	IFN- $\gamma$ – interferon gamma
DMPK – drug metabolism and pharmacokinetics	IL – interleukin
EDC·HCl – N-(3-Dimethylaminopropyl)-N'-ethylcarbodiimide hydrochloride	KOH – potassium hydroxide
Et <sub>2</sub> O – diethyl ether	LAP – liver activator protein
	LC3B – light chain 3 B

LDL – low-density lipoprotein	PDPN – painful diabetic peripheral neuropathy
LH – luteinizing hormone	PRL – prolactin
LIP – liver inhibitory protein	PTSD – post-traumatic stress disorder
Me <sub>3</sub> SiN <sub>3</sub> – azidotrimethylsilane	RHS – right-hand side
MeMgBr – methylmagnesium bromide	RT – room temperature
MeOH – methanol	SAMP8 – Senescence Accelerated Mouse-Prone 8
MeONa – sodium methoxide	sAPP $\alpha$ – secreted amyloid precursor protein- $\alpha$
MR – mineralocorticoid receptor	SAR – structure-activity relationship
mTOR – mammalian target of rapamycin	SET – single-electron-transfer
NaBH <sub>4</sub> – sodium borohydride	SnCl <sub>4</sub> – tin(IV) chloride
NADP – nicotinamide adenine dinucleotide phosphate	SNS – sympathetic nervous system
NAFLD – non-alcoholic fatty liver disease	SOBr <sub>2</sub> – thionyl bromide
NaN <sub>3</sub> – sodium azide	SOCl <sub>2</sub> – thionyl chloride
NaOH – sodium hydroxide	T2DM – type 2 diabetes mellitus
<i>n</i> -Bu <sub>3</sub> P – tributylphosphine	<i>t</i> -BuSH – tert-butylthiol
NMDA – N-methyl-D-aspartate	TFAA – trifluoroacetic acid
pAMPK – phosphorylated AMP-activated protein kinase	TFAAn – trifluoroacetic anhydride
Pd/C – palladium on carbon	TFPAA – trifluoroperacetic acid
	THF – tetrahydrofuran
	TNF- $\alpha$ – tumor necrosis factor alfa

## REFERENCES

1. Sapolsky, R.M.; Romero, L.M.; Munck, A.U. *Endocr. Rev.* **2000**, *21*, 55–89.
2. Galosy, R. A.; Clarke, L. K.; Vasko, M. R.; Crawford, I. L. *Neurosci. Biobehav. Rev.* **1981**, *5*, 137–175.
3. Krakoff, L. *Cardiol. Clin.* **1988**, *6*, 537–545.
4. Little, G. The adrenal cortex. **1981** In: Wilson J., Foster D. (eds) Williams Textbook of Endocrinology, ed. 7. W. B. Saunders Co., Philadelphia, 249–292.
5. Orth, D.; Kovacs, W.; DeBold, C. The adrenal cortex. **1992** In: Wilson J., Foster D. (eds) Williams Textbook of Endocrinology, ed. 8. W. B. Saunders Co., Philadelphia, 518–519.
6. Hayamizu, S.; Kanda, K.; Ohmori, S.; Murata, Y.; Seo, H. *Endocrinology* **1994**, *135*, 2459–2464.
7. Jain, R.; Zwickler, D.; Hollander, C.; Brand, H.; Saperstein, A.; Hutchinson, B.; Brown, C.; Audhya, T. *Endocrinology* **1991**, *128*, 1329–1336.
8. Pawlikowski, M.; Zelazowski, P.; Dohler, K.; Stepien, H. *Brain. Behav. Immun.* **1988**, *2*, 50–56.
9. Sapolsky, R.; Rivier, C.; Yamamoto, G.; Plotsky, P.; Vale, W. *Science* **1987**, *238*, 522–524.
10. Bernton, E.; Beach, J.; Holaday, J.; Smallridge, R.; Fein, H. *Science* **1987**, *238*, 519–521.
11. Munck, A.; Guyre, P.M.; Holbrook, N. J. *Endocr. Rev.* **1984**, *5*, 25–44.
12. Wick, G.; Hu, Y.; Schwarz, S.; Kroemer, G. *Endocr. Rev.* **1993**, *14*, 539–563.
13. Barber, A. E.; Coyle, S. M.; Marano, M. A.; Fischer, E.; Calvano, S. E.; Fong, Y.; Moldawer, L. L.; Lowry, S. F. *J. Immunol.* **1993**, *150*, 1999–2006.
14. De Kloet, E. R.; Vreugdenhil, E.; Oitzl, M. S.; Joels, M.; *Endocr. Rev.* **1998**, *19*, 269–301.
15. Munck, A.; Naray-Fejes-Toth, A. Glucocorticoid action. Physiology. **1995** In: DeGroot L. J. (ed) Endocrinology. W.B. Saunders Co., Philadelphia, 1642–1656.
16. Eigler, N.; Sacca, L.; Sherwin, R. S. *J. Clin. Invest.* **1979**, *63*, 114–123.
17. DeFronzo, R.; Sherwin, R.; Felig, P. *Acta. Chir. Scand.* [Suppl] **1980**, *498*, 33–39.
18. Doyle, P.; Guillaume-Gentile, C.; Rohner-Jeanrenaud, F.; Jeanrenaud, B. *Brain Res.* **1994**, *645*, 225–230.
19. Horner, H. C.; Packan, D. R.; Sapolsky, R. M. *Neuroendocrinology* **1990**, *52*, 57–63.
20. Arase, K.; York, D.; Shimizu, H.; Shargill, N.; Bray, G. *Am. J. Physiol.* **1988**, *255*, E255–259.
21. Pavlides, C.; Kimura, A.; Magarinos, A. M.; McEwen, B. S. *Neuroreport* **1994**, *5*, 2673–2677.
22. Kerr, D. S.; Campbell, L. W.; Thibault, O.; Landfield, P. W. *Proc. Natl. Acad. Sci. USA* **1992**, *89*, 8527–8531.
23. Sirinathsinghji, D.; Rees, L.; Rivier, J.; Vale, W. *Nature* **1983**, *305*, 232–235.
24. Bambino, T.; Hsueh, A. *Endocrinology* **1981**, *108*, 2142–2147.
25. Sapolsky, R. *Endocrinology* **1985**, *116*, 2273–2278.
26. Selye, H.; Tuchweber, B. Stress in relation to aging and disease. **1976** In: Everitt A, Burgess J (eds) Hypothalamus, Pituitary and Aging. Charles C Thomas, Springfield, IL, 557–573.
27. Pearl, R. The Rate of Living. **1929** Alfred Knopf, New York.
28. Curtis, H. *Science* **1963**, *141*, 686–694.
29. Pare, W. *J. Gerontol.* **1965**, *20*, 78–84.
30. Sapolsky, R.; Krey, L.; McEwen, B. *Exp. Gerontol.* **1983**, *18*, 55–64.
31. Krieger, D. Cushing's Syndrome In: Monographs in Endocrinology. **1982** Springer-Verlag, Berlin, vol 22.
32. Sapolsky, R. M.; Krey, L. C.; McEwen, B. S. *Endocr. Rev.* **1986**, *7*, 284–301.
33. Bauer, M. E. *Stress* **2005**, *8*, 69–83.
34. Rosmond, R.; Dallman, M. F.; Bjorntorp, P. *J. Clin. Endocrinol. Metab.* **1998**, *83*, 1853–1859.
35. McEwen, B. S.; Magarinos, A. M. *Hum. Psychopharmacol.* **2001**, *16*, S7–S19.
36. Hench, P. S.; Kendall, E. C.; et al., *Proc. Staff Meet. Mayo Clin.* **1949**, *24*, 181–197.
37. Amelung, D.; Hubener, H. J.; Roka, L.; Meyerheim, G. *J. Clin. Endocrinol. Metab.* **1953**, *13*, 1125–1126.
38. Lakshmi, V.; Monder, C. *Endocrinology*, **1988**, *123*, 2390–2398.
39. Agarwal, A. K.; Monder, C.; Eckstein, B.; White, P. C. *J. Biol. Chem.* **1989**, *264*, 18939–18943.
40. Stewart, P. M.; Corrie, J. E.; Shackleton, C. H. Edwards, C. R. *J. Clin. Invest.* **1988**, *82*, 340–349.
41. Arriza, J. L.; Weinberger, C.; Cerelli, G.; Glaser, T. M.; Handelin, B. L.; Housman, D. E.; Evans, R. M. *Science* **1987**, *237*, 268–275.
42. Edwards, C. R.; Stewart, P. M.; Burt, D.; Brett, L.; McIntyre, M. A.; Sutanto, W. S.; de Kloet, E. R.; Monder, C. *Lancet* **1988**, *2*, 986–989.

43. Funder, J. W.; Pearce, P. T.; Smith, R.; Smith, A. I. *Science* **1988**, *242*, 583–585.
44. Stewart, P. M.; Wallace, A. M.; Valentino, R.; Burt, D.; Shackleton, C. H.; Edwards, C. R. *Lancet* **1987**, *2*, 821–824.
45. Gereben, B.; Zavacki, A. M.; Ribich, S.; Kim, B. W.; Huang, S. A.; Simonides, W. S.; Zeold, A.; Bianco, A. C. *Endocr. Rev.* **2008**, *29*, 898–938.
46. Chapman, K.; Holmes, M.; Jonathan Seckl, J. R. *Physiol. Rev.* **2013**, *93*, 1139–1206.
47. Brown, R. W.; Chapman, K. E.; Edwards, C. R.; Seckl, J. R. *Endocrinology* **1993**, *132*, 2614–2621.
48. Rusvai, E.; Naray-Fejes-Toth, A. *J. Biol. Chem.* **1993**, *268*, 10717–10720.
49. Albiston, A. L.; Obeyesekere, V. R.; Smith, R. E.; Krozowski, Z. S. *Mol. Cell Endocrinol.* **1994**, *105*, R11–R17.
50. Agarwal, A. K.; Mune, T.; Monder, C.; White, P. C. *J. Biol. Chem.* **1994**, *269*, 25959–25962.
51. Rajan, V.; Chapman, K. E.; Lyons, V.; Jamieson, P.; Mullins, J. J.; Edwards, C. R.; Seckl, J. R. *J. Steroid Biochem. Mol. Biol.* **1995**, *52*, 141–147.
52. Roland, B. L.; Krozowski, Z. S.; Funder, J. W. *Mol. Cell Endocrinol.* **1995**, *111*, R1–R7.
53. Whorwood, C. B.; Ricketts, M. L.; Stewart, P. M. *Endocrinology* **1994**, *135*, 2533–2541.
54. Roland, B. L.; Funder, J. W. *Endocrinology* **1996**, *137*, 1123–1128.
55. Kenouch, S.; Lombes, M.; Delahaye, F.; Eugene, E.; Bonvalet, J.P.; Farman, N. *J. Clin. Endocrinol. Metab.* **1994**, *79*, 1334–1341.
56. Dave-Sharma, S.; Wilson, R. C.; Harbison, M. D.; Newfield, R.; Azar, M. R.; Krozowski, Z. S.; Funder, J. W.; Shackleton, C. H.; Bradlow, H. L.; Wei, J. Q.; Hertecant, J.; Moran, A.; Neiberger, R. E.; Balfe, J. W.; Fattah, A.; Daneman, D.; Akkurt, H. I.; De Santis, C.; New, M. I. *J. Clin. Endocrinol. Metab.* **1998**, *83*, 2244–2254.
57. Jamieson, P. M.; Chapman, K. E.; Edwards, C. R.; Seckl, J. R. *Endocrinology* **1995**, *136*, 4754–4761.
58. Dzyakanchuk, A. A.; Balazs, Z.; Nashev, L. G.; Amrein, K. E.; Odermatt, K. *Mol. Cell Endocrinol.* **2009**, *301*, 137–141.
59. Bruley, C.; Lyons, V.; Worsley, A. G.; Wilde, M. D.; Darlington, G. D.; Morton, N. M.; Seckl, J. R.; Chapman, K. E. *Endocrinology* **2006**, *147*, 2879–2885.
60. Moisan, M. P.; Edwards, C. R.; Seckl, J. R. *Mol. Endocrinol.* **1992**, *6*, 1082–1087.
61. Williams, L. J.; Lyons, V.; MacLeod, I.; Rajan, V.; Darlington, G. J.; Poli, V.; Seckl, J. R.; Chapman, K. E. *J. Biol. Chem.* **2000**, *275*, 30232–30239.
62. Yang, Z.; Zhu, X.; Guo, C.; Sun, K. *Endocrine* **2009**, *36*, 404–411.
63. Ignatova, I. D.; Kostadinova, R. M.; Goldring, C. E.; Nawrocki, A. R.; Frey, F. J.; Frey, B. M. *Am. J. Physiol. Endocrinol. Metab.* **2009**, *296*, E367–E377.
64. Sai, S.; Esteves, C. L.; Kelly, V.; Michailidou, Z.; Anderson, K.; Coll, A. P.; Nakagawa, Y.; Ohzeki, T.; Seckl, J. R.; Chapman, K. E. *Mol. Endocrinol.* **2008**, *22*, 2049–2060.
65. Gout, J.; Tirard, J.; Thevenon, C.; Riou, J. P.; Begeot, M.; Naville, D. *Biochimie* **2006**, *88*, 1115–1124.
66. Arai, N.; Masuzaki, H.; Tanaka, T.; Ishii, T.; Yasue, S.; Kobayashi, N.; Tomita, T.; Noguchi, M.; Kusakabe, T.; Fujikura, J.; Ebihara, K.; Hirata, M.; Hosoda, K.; Hayashi, T.; Sawai, H.; Minokoshi, Y.; Nakao, K. *Endocrinology* **2007**, *148*, 5268–5277.
67. Arizmendi, C.; Liu, S.; Croniger, C.; Poli, V.; Friedman, J. E. *J. Biol. Chem.* **1999**, *274*, 13033–13040.
68. Esteves, C. L.; Kelly, V.; Begay, V.; Man, T. Y.; Morton, N. M.; Leutz, A.; Seckl, J. R.; Chapman, K. E. *PLoS One* **2012**, *7*, e37953.
69. <http://www.rcsb.org/pdb/results/results.do?tabtoshow=Current&grid=48A0266>, Accessed April 2017.
70. Thomas, M. P.; Potter, B. V. L. *Future Med. Chem.* **2011**, *3*, 367–390.
71. Sandeep, T. C.; Walker, B. R. *Trends Endocrinol. Metab.* **2001**, *12*, 446–453.
72. Persson, B.; Kallberg, Y.; Bray, J. E.; Bruford, E.; Dellaporta, S. L.; Favia, A. D.; Duarte, R. G.; Jornvall, H.; Kavanagh, K. L.; Kedishvili, N.; Kisiela, M.; Maser, E.; Mindnich, R.; Orchard, S.; Penning, T. M.; Thornton, J. M.; Adamski, J.; Oppermann, U. *Chem. Biol. Interact.* **2009**, *178*, 94–98.
73. Obeid, J.; White, P. C. *Biochem. Biophys. Res. Commun.* **1992**, *188*, 222–227.
74. Schuster, D.; Maurer, E. M.; Laggner, C.; Nashev, L. G.; Wilckens, T.; Langer, T.; Odermatt, A. *J. Med. Chem.* **2006**, *49*, 3454–3466.

75. Kavanagh, K.; Wu, X.; Svensson, S.; Elleby, B.; Von Delft, F.; Debreczeni, J. E.; Sharma, S.; Bray, J.; Edwards, A.; Arrowsmith, C.; Sundstrom, M.; Abrahmsen, L.; Oppermann, U. PDB 2BEL, 2006. doi:10.2210/pdb2bel/pdb.
76. Moisan, M. P.; Seckl, J. R.; Edwards, C. R. *Endocrinology* **1990**, *127*, 1450–1455.
77. Tannin, G. M.; Agarwal, A. K.; Monder, C.; New, M. I.; White, P. C. *J. Biol. Chem.* **1991**, *266*, 16653–16658.
78. Bujalska, I. J.; Kumar, S.; Stewart, P. M. *Lancet* **1997**, *349*, 1210–1213.
79. Davani, B.; Khan, A.; Hult, M.; Martensson, E.; Okret, S.; Efendic, S.; Jornvall, H.; Oppermann, U. *C. J. Biol. Chem.* **2000**, *275*, 34841–34844.
80. Walker, B. R.; Yau, J. L.; Brett, L. P.; Seckl, J. R.; Monder, C.; Williams, B. C.; Edwards, C. R. W. *Endocrinology* **1991**, *129*, 3305–3312.
81. Benediktsson, R.; Yau, J. L. W.; Low, S.; Brett, L. P.; Cooke, B. E.; Edwards, C. R. W.; Seckl, J. R. *J. Endocrinol.* **1992**, *135*, 53–58.
82. Phillips, D. M.; Lakshmi, V.; Monder, C. *Endocrinology* **1989**, *125*, 209–216.
83. Lakshmi, V.; Sakai, R. R.; McEwen, B. S.; Monder, C. *Endocrinology* **1991**, *128*, 1741–1748.
84. Moisan, M. P.; Seckl, J. R.; Brett, L. P.; Monder, C.; Agarwal, A. K.; White, P. C.; Edwards, C. R. *J. Neuroendocrinol.* **1990**, *2*, 853–858.
85. Burton, P. J.; Krozowski, Z. S.; Waddell, B. J. *Endocrinology* **1998**, *139*, 376–382.
86. Waddell, B. J.; Benediktsson, R.; Brown, R. W.; Seckl, J. R. *Endocrinology* **1998**, *139*, 1517–1523.
87. Gilmour, J. S.; Coutinho, A. E.; Cailhier, J. F.; Man, T. Y.; Clay, M.; Thomas, G.; Harris, H. J.; Mullins, J. J.; Seckl, J. R.; Savill, J. S.; Chapman, K. E. *J. Immunol.* **2006**, *176*, 7605–7611.
88. Stewart, J. D.; Sienko, A. E.; Gonzalez, C. L.; Christensen, H. D.; Rayburn, W. F. *Am. J. Obstet. Gynecol.* **1998**, *179*, 1241–1247.
89. Speirs, H. J.; Seckl, J. R.; Brown, R. W. *J. Endocrinol.* **2004**, *181*, 105–116.
90. Kotelevtsev, Y.; Holmes, M. C.; Burchell, A.; Houston, P. M.; Schmoll, D.; Jamieson, P.; Best, R.; Brown, R.; Edwards, C. R. W.; Seckl, J. R.; Mullins, J. J. *Proc. Natl. Acad. Sci. USA* **1997**, *94*, 14924–14929.
91. <sup>1</sup>Lavery, G. G.; Zielinska, A. E.; Gathercole, L. L.; Hughes, B.; Semjonous, N.; Guest, P.; Saqib, K.; Sherlock, M.; Reynolds, G.; Morgan, S. A.; Tomlinson, J. W.; Walker, E. A.; Rabbitt, E. H.; Stewart, P. M. *Endocrinology* **2012**, *153*, 3236–3248.
92. <sup>1</sup>Odermatt, A.; Da Cunha, T.; Penno, C. A.; Chandsawangbhuwana, C.; Reichert, C.; Wolf, A.; Dong, M.; Baker, M. E. *Biochem. J.* **2011**, *436*, 621–629.
93. <sup>1</sup>Ackermann, D.; Vogt, B.; Escher, G.; Dick, B.; Reichen, J.; Frey, B. M.; Frey, F. J. *Hepatology* **1999**, *30*, 623–629.
94. <sup>1</sup>Diederich, S.; Grossmann, C.; Hanke, B.; Quinkler, M.; Herrmann, M.; Bahr, V.; Oelkers, W. *Eur. J. Endocrinol.* **2000**, *142*, 200–207.
95. Rose, A. J.; Diaz, M. B.; Reimann, A.; Klement, J.; Walcher, T.; Kronen-Herzig, A.; Strobel, O.; Werner, J.; Peters, A.; Kleyman, A.; Tuckermann, J. P.; Vegiopoulos, A.; Herzig, S. *Cell Metab.* **2011**, *14*, 123–130.
96. Hughes, K. A.; Reynolds, R. M.; Andrew, R.; Critchley, H. O.; Walker, B. R. *J. Clin. Endocrinol. Metab.* **2010**, *95*, 4696–4702.
97. Morton, N. M.; Paterson, J. M.; Masuzaki, H.; Holmes, M. C.; Staels, B.; Fievet, C.; Walker, B. R.; Flier, J. S.; Mullins, J. J.; Seckl, J. R. *Diabetes* **2004**, *53*, 931–938.
98. Goedecke, J. H.; Wake, D. J.; Levitt, N. S.; Lambert, E. V.; Collins, M. R.; Morton, N. M.; Andrew, R.; Seckl, J. R.; Walker, B. R. *Clin. Endocrinol.* **2006**, *65*, 81–87.
99. Paulmyer-Lacroix, O.; Boullu, S.; Oliver, C.; Alessi, M. C.; Grino, M. *J. Clin. Endocrinol. Metab.* **2002**, *87*, 2701–2705.
100. Rask, E.; Walker, B. R.; Soderberg, S.; Livingstone, D. E.; Eliasson, M.; Johnson, O.; Andrew, R.; Olsson, T. *J. Clin. Endocrinol. Metab.* **2002**, *87*, 3330–3336.
101. Masuzaki, H.; Paterson, J.; Shinyama, H.; Morton, N. M.; Mullins, J. J.; Seckl, J. R.; Flier, J. S. *Science* **2001**, *294*, 2166–2170.
102. Masuzaki, H.; Yamamoto, H.; Kenyon, C. J.; Elmquist, J. K.; Morton, N. M.; Paterson, J. M.; Shinyama, H.; Sharp, M. G.; Fleming, S.; Mullins, J. J.; Seckl, J. R.; Flier, J. S. *J. Clin. Invest.* **2003**, *112*, 83–90.
103. Gremlich, S.; Roduit, R.; Thorens, B. *J. Biol. Chem.* **1997**, *272*, 3216–3222.
104. Lambillotte, C.; Gilon, P.; Henquin, J. C. *J. Clin. Invest.* **1997**, *99*, 414–423.

105. Duplomb, L.; Lee, Y.; Wang, M. Y.; Park, B. H.; Takaishi, K.; Agarwal, A. K.; Unger, R. H. *Biochem. Biophys. Res. Commun.* **2004**, *313*, 594–599.
106. Turban, S.; Liu, X.; Ramage, L.; Webster, S. P.; Walker, B.; Dunbar, D.; Mullins, J.; Seckl, J. R.; Morton, N. *Diabetes* **2012**, *61*, 642–652.
107. Morton, N. M.; Ramage, L. *Endocrinology* **2004**, *145*, 2707–2712.
108. Ichikawa, Y.; Yoshida, K.; Kawagoe, M.; Saito, E.; Abe, Y.; Arikawa, K.; Homma, M. *Metabolism* **1977**, *26*, 989–997.
109. Antoniv, T. T.; Ivashkiv, L. B. *Arthritis Rheum.* **2006**, *54*, 2711–2721.
110. Sakai, R. R.; Lakshmi, V.; Monder, C.; McEwen, B. S. *J. Neuroendocrinol.* **1992**, *4*, 101–106.
111. Gottfried-Blackmore, A.; Sierra, A.; McEwen, B. S.; Ge, R.; Bulloch, K. *Glia* **2010**, *58*, 1257–1266.
112. Densmore, V. S.; Morton, N. M.; Mullins, J. J.; Seckl, J. R. *Endocrinology* **2006**, *147*, 4486–4495.
113. Thaler, J. P.; Yi, C. X.; Schur, E. A.; Guyenet, S. J.; Hwang, B. H.; Dietrich, M. O.; Zhao, X.; Sarruf, D. A.; Izgur, V.; Maravilla, K. R.; Nguyen, H. T.; Fischer, J. D.; Matsen, M. E.; Wisse, B. E.; Morton, G. J.; Horvath, T. L.; Baskin, D. G.; Tsch, M. H.; Schwartz, M. W. *J. Clin. Invest.* **2012**, *122*, 153–162.
114. Swaab, D. F.; Bao, A. M.; Lucassen, P. J. *Ageing Res. Rev.* **2005**, *4*, 141–194.
115. Meaney, M. J.; O'Donnell, D.; Rowe, W.; Tannenbaum, B.; Steverman, A.; Walker, M.; Nair, N. P. V.; Lupien, S. *Exp. Gerontol.* **1995**, *30*, 229–251.
116. Yau, J. L.; Olsson, T.; Morris, R. G.; Meaney, M. J.; Seckl, J. R. *Neuroscience* **1995**, *66*, 571–581.
117. Lupien, S. J.; de Leon, M.; de Santi, S.; Convit, A.; Tarshish, C.; Nair, N. P. V.; Thakur, M.; McEwen, B. S.; Hauger, R. L.; Meaney, M. J. *Nat. Neurosci.* **1998**, *1*, 69–73.
118. Seckl, J. R. *Front. Neuroendocrinol.* **1997**, *18*, 49–99.
119. Yau, J. L.; McNair, K. M.; Noble, J.; Brownstein, D.; Hibberd, C.; Morton, N.; Mullins, J. J.; Morris, R. G.; Cobb, S.; Seckl, J. R. *J. Neurosci.* **2007**, *27*, 10487–10496.
120. Yau, J. L.; Noble, J.; Kenyon, C. J.; Hibberd, C.; Kotelevtsev, Y.; Mullins, J. J.; Seckl, J. R. *Proc. Natl. Acad. Sci. USA* **2001**, *98*, 4716–4721.
121. Sooy, K.; Webster, S. P.; Noble, J.; Binnie, M.; Walker, B. R.; Seckl, J. R.; Yau, J. L. *J. Neurosci.* **2010**, *30*, 13867–13872.
122. Dhingra, D.; Parle, M.; Kulkarni, S. K. *J. Ethnopharmacol.* **2004**, *91*, 361–365.
123. Peskind, E. R.; Wilkinson, C. W.; Petrie, E. C.; Schellenberg, G. D.; Raskind, M. A. *Neurology* **2001**, *56*, 1094–1098.
124. Cernansky, J. G.; Dong, H.; Fagan, A. M.; Wang, L.; Xiong, C.; Holtzman, D. M.; Morris, J. C. *Am. J. Psychiatry* **2006**, *163*, 2164–2169.
125. Green, K. N.; Billings, L. M.; Roozendaal, B.; McGaugh, J. L.; LaFerla, F. M. *J. Neurosci.* **2006**, *26*, 9047–9056.
126. Scott, J. S.; Goldberg, F. W.; Turnbull, A. V. *J. Med. Chem.* **2014**, *57*, 4466–4486.
127. Boyle, C. D.; Kowalski, T. J. *Expert Opin. Ther. Pat.* **2009**, *19*, 801–825.
128. Gathercole, L. L.; Lavery, G. G.; Morgan, S. A.; Cooper, M. S.; Sinclair, A. J.; Tomlinson, J. W.; Stewart, P. M. *Endocr. Rev.* **2013**, *34*, 525–555.
129. Abrahmsen, L.; Nilsson, J.; Opperman, U.; Svensson, S. WO Patent Application, WO2005068646, 2005.
130. Gibbs, J. P.; Emery, M. G.; McCaffery, I.; Smith, B.; Gibbs, M. A.; Akrami, A.; Rossi, J.; Paweletz, K.; Gastonguay, M. R.; Bautista, E.; Wang, M.; Perfetti, R.; Daniels, O. *J. Clin. Pharmacol.* **2011**, *51*, 830–841.
131. Wyszynski, M. WO Patent Application, WO2012/051139A1, 2012.
132. Courtney, R.; Stewart, P. M.; Toh, M.; Ndongo, M. N.; Calle, R. A.; Hirshberg, B. *J. Clin. Endocrinol. Metab.* **2008**, *93*, 550–556.
133. No safety issues were involved in the termination decision. See <http://clinicaltrials.gov/ct2/show/NCT00427401>, Accessed March 2017.
134. Rosenstock, J.; Banarer, S.; Fonseca, V. A.; Inzucchi, S. E.; Sun, W.; Yao, W.; Hollis, G.; Flores, R.; Levy, R.; Williams, W. V.; Seckl, J. R.; Huber, R. *Diabetes Care* **2010**, *33*, 1516–1522.
135. Hollis, G.; Huber, R. *Diabetes, Obesity Metab.* **2011**, *13*, 1–6.
136. <https://www.incyte.com/what-we-do/develop.aspx>, Accessed March 2017.
137. Feig, P. U.; Shah, S.; Hermanowski-Vosatka, A.; Plotkin, D.; Springer, M. S.; Donahue, S.; Thach, C.; Klein, E. J.; Lai, E.; Kaufman, K. D. *Diabetes, Obesity Metab.* **2011**, *13*, 498–504.
138. Shah, S.; Hermanowski-Vosatka, A.; Gibson, K.; Ruck, R. A.; Jia, G.; Zhang, J.; Hwang, P. M. T.; Ryan, N. W.; Langdon, R. B.; Feig, P. U. *J. Am. Soc. Hypertens.* **2011**, *5*, 166–176.

139. Bauman, D. R.; Whitehead, A.; Contino, L. C.; Cui, J.; Garcia- Calvo, M.; Gu, X.; Kevin, N.; Ma, X.; Pai, L.; Shah, K.; Shen, X.; Stribling, S.; Zokian, H. J.; Metzger, J.; Shevell, D. E.; Waddell, S. T. *Bioorg. Med. Chem. Lett.* **2013**, *23*, 3650–3653.
140. <https://clinicaltrials.gov/ct2/results?term=BMS-770767&Search=Search>, Accessed March 2017.
141. <http://www.bms.com/research/pipeline/Pages/default.aspx>, Accessed March 2017.
142. Wang, H.; Robl, J. A.; Hamann, L. G.; Simpkins, L.; Golla, R.; Li, Y.; Seethala, R.; Zvyaga, T.; Gordon, D. A.; Li, J. J. *Bioorg. Med. Chem. Lett.* **2011**, *21*, 4146–4149.
143. Xiang-Yang, Y.; Chen, S. Y.; Wu, S.; Yoon, D. S.; Wang, H.; Hong, Z.; O'Connor, S. P.; Li, J.; Li, J. J.; Kennedy, L. L.; Walker, S. J.; Nayeem, A.; Sheriff, S.; Camac, D. M.; Ramamurthy, V.; Morin, P. E.; Zebo, R.; Taylor, J. R.; Morgan, N. N.; Ponticello, R. P.; Harrity, T.; Apedo, A.; Golla, R.; Seethala, R.; Wang, M.; Harper, T. W.; Slecza, B. G.; He, B.; Kirby, M.; Leahy, D. K.; Li, J.; Hanson, R. L.; Guo, Z.; Li, Y.; DiMarco, J. D.; Scaringe, R.; Maxwell, B. D.; Moulin, F.; Barrish, J. C.; Gordon, D. A.; Robl, J. A. *J. Med. Chem.* **2017**, *60*, 4932–4948.
144. <https://clinicaltrials.gov/ct2/show/NCT00979368?term=BMS-816336&rank=1>, Accessed March 2017.
145. <http://adisinsight.springer.com/drugs/800027626>, Accessed March 2017.
146. Zhuang, L.; Tice, C. M.; Xu, Z.; Zhao, W.; Cacatian, S.; Ye, Y. J.; Singh, S. B.; Lindblom, P.; McKeever, B. M.; Krosky, P. M.; Zhao, Y.; Lala, D.; Kruk, B. A.; Meng, S.; Howard, L.; Johnson, J. A.; Bukhtiyarov, Y.; Panemangalore, R.; Guo, J.; Guo, R.; Himmelsbach, F.; Hamilton, B.; Schuler-Metz, A.; Schauerte, H.; Gregg, R.; McGeehan, G. M.; Leftheris, K.; Claremon, D. A. *Bioorg. Med. Chem.* **2017**, *25*, 3649–3657.
147. <https://clinicaltrials.gov/ct2/results?term=BI-135585&Search=Search>, Accessed March 2017.
148. Freude, S.; Heise, T.; Woerle, H. J.; Jungnik, A.; Rauch, T.; Hamilton, B.; Schölch, C.; Huang, F.; Graefe-Mody, U. *Diabetes Obes. Metab.* **2016**, *18*, 483–490.
149. Report of Medicines in Development for Diabetes 2012, America's Biopharmaceutical Research Companies.
150. Report of Medicines in Development for Diabetes 2014, America's Biopharmaceutical Research Companies.
151. <http://ir.vitaepharm.com/phoenix.zhtml?c=219654&p=irol-newsArticle&ID=2123771>, Accessed March 2017.
152. <http://adisinsight.springer.com/drugs/800036000>, Accessed March 2017.
153. <https://clinicaltrials.gov/ct2/show/NCT00791752?term=AZD4017&rank=5>, Accessed March 2017.
154. <https://clinicaltrials.gov/ct2/show/NCT01173471?term=AZD4017&rank=6>, Accessed March 2017.
155. <http://adisinsight.springer.com/drugs/800029324>, Accessed March 2017.
156. <https://www.clinicaltrialsregister.eu/ctr-search/trial/2013-003387-32/GB>, Accessed March 2017.
157. <https://www.clinicaltrialsregister.eu/ctr-search/trial/2013-003643-31/GB>, Accessed March 2017.
158. <https://clinicaltrials.gov/ct2/show/NCT02017444?term=AZD4017&rank=1>, Accessed March 2017.
159. <https://clinicaltrials.gov/ct2/results?term=AZD8329&Search=Search>, Accessed March 2017.
160. <http://adisinsight.springer.com/drugs/800030582>, Accessed March 2017.
161. Scott, J. S.; Chooramun, J. RSC Drug Discovery Series No. 27, 2012. New Therapeutic Strategies for Type 2 Diabetes: Small Molecule Approaches. Chapter 5: 11 $\beta$ -Hydroxysteroid Dehydrogenase Type 1 (11 $\beta$ -HSD1) Inhibitors in Development.
162. <https://clinicaltrials.gov/ct2/show/NCT00823680?term=RO5027838&rank=1>, Accessed March 2017.
163. Te. Heisel, L.; Morrow, M.; Hompesch, H.-U.; Häring, C.; Kapitza, M.; Abt, M.; Ramsauer, M. C.; Magnone, S.; Fuerst-Recktenwald, S. *Diabetes Obes. Metab.* **2014**, *16*, 1070–1077.
164. Roche presentation, October 14, 2010, slide 37. See <http://www.roche.com/irp3q10e.pdf>.
165. Roche presentation, October 16, 2012, p 47. See <http://www.roche.com/irp3q12e.pdf>.
166. <https://clinicaltrials.gov/ct2/show/NCT01277094?term=RO5093151&rank=4>, Accessed March 2017.
167. Stefan, N.; Ramsauer, M.; Jordan, P.; Nowotny, B.; Kantartzis, K.; Machann, J.; Hwang, J.; Nowotny, P.; Kahl, S.; Harreiter, J.; Hornemann, S.; Sanyal, A. J.; Stewart, P. M.; Pfeiffer, A. F.;



- Kautzky-Willer, A.; Roden, A.; Häring, H.; Fürst-Recktenwald, S. *Lancet Diabetes Endocrinol.* **2014**, *2*, 406-416.
168. Ratziu, V. *Lancet Diabetes Endocrinol.* **2014**, *2*, 354-356.
169. <https://clinicaltrials.gov/ct2/show/NCT01493271?term=RO5093151&rank=1>, Accessed March 2017.
170. <https://clinicaltrials.gov/ct2/show/NCT02622334?term=RO5093151&rank=2>, Accessed March 2017.
171. Roche presentation, April 19, 2016, page 50. <http://www.roche.com/dam/jcr:2a156912-eff5-4257-9547-fbd0623d9429/en/irp1q16e-a.pdf>.
172. Roche presentation, October 20, 2016, page 50. <http://www.roche.com/dam/jcr:70f6e9e4-80d5-431c-9e78-eb12cf5ce087/en/irp161020-a.pdf>
173. <https://clinicaltrials.gov/ct2/results?term=HSD016&Search=Search>, Accessed March 2017.
174. Lilly presentation 2Q 2013, page 12. [http://files.shareholder.com/downloads/LLY/2073248133x0x678669/d90dc9fa-da40-4bb3-82f6-02acaa752eb7/Q2\\_2013\\_Slides.pdf](http://files.shareholder.com/downloads/LLY/2073248133x0x678669/d90dc9fa-da40-4bb3-82f6-02acaa752eb7/Q2_2013_Slides.pdf).
175. <https://clinicaltrials.gov/ct2/show/NCT01674348?term=P2202&rank=1>, Accessed March 2017.
176. <http://www.ctri.nic.in/Clinicaltrials/pmaindet2.php?trialid=2394>, Accessed March 2017.
177. <https://clinicaltrials.gov/ct2/show/NCT00997152?term=JTT-654&rank=1>, Accessed March 2017.
178. Japan Tobacco presentation of the Consolidated Financial Results for the six months ended September 30, 2010, page 10. [http://www.jti.com/files/2713/2818/3505/JTs\\_Consolidated\\_Financial\\_Results\\_for\\_the\\_6\\_months\\_ended\\_September\\_30\\_2010.pdf](http://www.jti.com/files/2713/2818/3505/JTs_Consolidated_Financial_Results_for_the_6_months_ended_September_30_2010.pdf).
179. <http://www.businesswire.com/news/home/20101104007514/en/TransTech-Pharma-High-Point-Pharmaceuticals-Awarded-1.96>, Accessed March 2017.
180. Katz, D. A.; Liu, W.; Locke, C.; Jacobson, P.; Barnes, D. M.; Basu, R.; An, G.; Rieser, M. J.; Daszkowski, D.; Groves, F.; Heneghan, G.; Shah, A.; Gevorkyan, H.; Jhee, S. S.; Ereshefsky, L.; Marek, G. J. *Transl. Psychiatry* **2013**, *3*, e295, 1-7.
181. <https://clinicaltrials.gov/ct2/show/NCT01009216?term=ABT-384&rank=1>, Accessed March 2017.
182. <https://clinicaltrials.gov/ct2/show/NCT01137526?term=ABT-384&rank=2>, Accessed March 2017.
183. Marek, G. J.; Katz, D. A.; Meier, A.; Greco, N.; Zhang, W.; Liu, W.; Lenz, R. A. *Alzheimers Dement.* **2014**, *10*, (5 Suppl), S364-S373.
184. <https://wellcome.ac.uk/press-release/promising-drug-candidate-reverses-age-related-memory-loss-mice>, Accessed March 2017.
185. <https://clinicaltrials.gov/ct2/show/NCT01770886?term=UE2343&rank=1>, Accessed March 2017.
186. <https://beta.companieshouse.gov.uk/company/SC478733>, Accessed March 2017.
187. <http://www.asx.com.au/asxpdf/20140827/pdf/42rs6xh1sx5rsm.pdf>
188. <http://www.edinburghbioquarter.com/news/item/actinogen-limited-to-acquire-corticine-limited/>, Accessed March 2017.
189. <https://clinicaltrials.gov/ct2/show/NCT02616445?term=UE2343&rank=2>, Accessed March 2017.
190. Webster, S. P.; McBride, A.; Binnie, M.; Sooy, K.; Seckl, J. R.; Andrew, R.; Pallin, T. D.; Hunt, H. J.; Perrior, T. R.; Ruffles, V. S.; Ketelbey, J. W.; Boyd, A.; Walker, B. R. *British J. Pharmacol.* **2017**, *174*, 396-408.
191. <https://clinicaltrials.gov/ct2/show/NCT02727699?term=UE2343&rank=3>, Accessed March 2017.
192. <http://actinogen.com.au/research/#current>, Accessed March 2017.
193. <https://clinicaltrials.gov/ct2/show/NCT02194491?term=ASP+3662&rank=1>, Accessed March 2017.
194. <https://clinicaltrials.gov/ct2/show/NCT02372578?term=ASP+3662&rank=2>, Accessed March 2017.
195. [https://www.astellas.com/en/ir/library/pdf/3q2017\\_rd\\_en.pdf](https://www.astellas.com/en/ir/library/pdf/3q2017_rd_en.pdf).

196. Harno, E.; Cottrell, E. C.; Yu, A.; DeSchoolmeester, J.; Gutierrez, P. M.; Denn, M.; Swales, J. G.; Goldberg, F. W.; Bohlooly-Y, M.; Andersén, H.; Wild, M. J.; Turnbull, A. V.; Leighton, B.; White, A. *Endocrinology* **2013**, *154*, 4580-4593.
197. Rey-Carrizo, M.; Barniol-Xicota, M.; Ma, C.; Frigolé-Vivas, M.; Torres, E.; Naesens, L.; Llabrés, S.; Juárez-Jiménez, J.; Luque, F. J.; DeGrado, W. F.; Lamb, R. A.; Pinto, L. H.; Vázquez, S. *J. Med. Chem.* **2014**, *57*, 5738–5747.
198. Valverde, E.; Sureda, F. X.; Vázquez, S. *Bioorg. Med. Chem.* **2014**, *22*, 2678-2683.
199. Vázquez S.; Valverde, E.; Leiva, R.; Vázquez-Carrera, M.; Codony, S. PCT Patent Application, WO2017017048.
200. Barniol-Xicota, M.; Kwak, S.-H.; Lee, S.-D.; Caseley, E.; Valverde, E.; Jiang, L.-H.; Kim, Y.-C.; Vázquez, S. *Bioorg. Med. Chem. Lett.* **2017**, *27*, 759-763.
201. Valverde, E.; Seira, C.; McBride, A.; Binnie, M.; Luque, F. J.; Webster, S. P.; Bidon-Chanal, A.; Vázquez, S. *Bioorg. Med. Chem.* **2015**, *23*, 7607-7617.
202. Duque, M. D.; Camps, P.; Profire, L.; Montaner, S.; Vázquez, S.; Sureda, F. S.; Mallol, J.; López-Querol, M.; Naesens, L.; De Clercq, E.; Prathalingam, S. R.; Kelly, J. M. *Bioorg. Med. Chem.* **2009**, *17*, 3198–3206.
203. Dong, G.; Peng, C.; Luo, J.; Wang, C.; Han, L.; Wu, B.; Ji, G. & He, H. *PLoS One* **2015**, *10*, e0119115.
204. Thomaston, J. L.; DeGrado, W. F. *Protein Science* **2016**, *25*, 1551-1554.
205. Wu, Y.; Canturk, B.; Jo, H.; Ma, C.; Gianti, E.; Klein, M. L.; Pinto, L. H.; Lamb, R. A.; Fiorin, G.; Wang, J.; DeGrado, W. F. *J. Am. Chem. Soc.* **2014**, *136*, 17987–17995.
206. Stetter, H.; Tacke, P.; Gaertner, J. *Chem. Ber.* **1964**, *97*, 3480-3487.
207. Camps, P.; El Achab, R.; Font-Bardia, M.; Görbig, D. M.; Morral, J.; Muñoz-Torrero, D.; Solans, X.; Simon, M. *Tetrahedron* **1996**, *52*, 5867-5880.
208. Mc Donald, I. A.; Dreiding, A. S.; Hutmacher, H.; Musso, H. *Helv. Chim. Acta* **1973**, *56*, 1385-1395.
209. Krasutsky, P. A.; Kolomitsyn, I. V.; Kiprof, P.; Carlson, R. M.; Forkin, A. A. *J. Org. Chem.* **2000**, *65*, 3926-3933.
210. Alder, R. W.; Carta, F.; Reed, C. A.; Stoyanova, I.; Willis, C. L. *Org. Biomol. Chem.* **2010**, *8*, 1551-1559.
211. Sugimoto, H.; Yamada, S. *Synthesis* **1986**, *9*, 741-743.
212. After finishing this work, it has been recently reported a two-step synthesis of **8** from **6** in 36% overall yield, see Benneche, T.; Tius, M. A. *Tetrahedron Lett.* **2016**, *57*, 3150-3151.
213. a) Schreiner, P. R.; Lauenstein, O.; Kolomitsyn, I. V.; Nadi, S.; Fokin, A. A. *Angew. Chem. Int. Ed.* **1998**, *37*, 1895-1897; b) Schreiner, P. R.; Lauenstein, O.; Butova, E. D.; Gunchenko, P. A.; Kolomitsyn, I. V.; Wittkopp, A.; Feder, F.; Fokin, A. A. *Chem. Eur. J.* **2001**, *7*, 4997-5003.
214. Davis, M. C.; Nissan, D. A. *Synth. Commun.* **2006**, *36*, 2113-2119.
215. Leiva, R.; Gazzarrini, S.; Esplugas, R.; Moroni, A.; Naesens, L.; Sureda, F. X.; Vázquez, S. *Tetrahedron Lett.* **2015**, *56*, 1272-1275.
216. Webster, S. P.; Ward, P.; Binnie, M.; Craigie, E.; McConnell, K. M. M.; Sooy, K.; Vinter, A.; Seckl, J. R.; Walker, B. R. *Bioorg. Med. Chem. Lett.* **2007**, *17*, 2838-2843.
217. Xia, G.; Liu, L.; Liu, H.; Yu, J.; Xu, Z.; Chen, Q.; Ma, C.; Li, P.; Xiong, B.; Liu, X.; Shen, J. *Chem. Med. Chem.* **2013**, *8*, 577-581.
218. Leiva, R.; Seira, C.; McBride, A.; Binnie, M.; Bidon-Chanal, A.; Luque, F. J.; Webster, S. P.; Vázquez, S. *Bioorg. Med. Chem. Lett.* **2015**, *25*, 4250-4253.
219. Cheng, H.; Hoffman, J.; Le, P.; Nair, S. K.; Cripps, S.; Matthews, J.; Smith, C.; Yang, M.; Kupchinsky, S.; Dress, K.; Edwards, M.; Cole, B.; Walters, E.; Loh, C.; Ermolieff, J.; Fanjul, A.; Bhat, G. B.; Herrera, J.; Pauly, T.; Hosea, N.; Paderes, G.; Rejto, P. *Bioorg. Med. Chem. Lett.* **2010**, *20*, 2897-2902.
220. Elena Valverde, PhD Thesis, Universitat de Barcelona 2015.
221. Marta Barniol-Xicota, PhD Thesis, Universitat de Barcelona 2017.
222. Duque, M. D.; Ma, C.; Torres, E.; Wang, J.; Naesens, L.; Juárez-Jiménez, J.; Camps, P.; Luque, F. J.; DeGrado, W. F.; Lamb, R. A.; Pinto, L. H.; Vázquez, S. *J. Med. Chem.* **2011**, *54*, 2646–2657.
223. Paquette, L. A.; Wyvrat, M. J. *J. Am. Chem. Soc.* **1974**, *96*, 4671-4673.
224. McNeil, D.; Vogt, B. R.; Sudol, J. J.; Theodoropoulos, S.; Hedaya, E. J. *Am. Chem. Soc.* **1974**, *96*, 4673-4674.
225. Taylor, R. J.; Welter, M. W.; Paquette, L. A. *Org. Synth. Coll. VIII* **1993**, 298-302.
226. Camps, P.; Pujol, X.; Rossi, R. A.; Vázquez, S. *Synthesis* **1999**, 854-858.

227. Recently, our group has found that hemiester **50** can be obtained more easily just boiling anhydride **49** in methanol, without need of sodium methoxide neither anhydrous solvent.
228. Barton, D. H. R.; Crich, D.; Motherwell, W. B. *Tetrahedron*. **1985**, *41*, 3901-3924.
229. Barton, D. H. R.; Samadi, M. *Tetrahedron* **1992**, *48*, 7083-7090.
230. Curtius, T. J. *Prakt. Chem.* **1894**, *50*, 275-294.
231. Culberson, C. F.; Wilder Jr., P. J. *Org. Chem.* **1960**, *25*, 1358-1362.
232. Fumimoto, M.; Okabe, K. *Chem. Pharm. Bull.* **1962**, *10*, 714-718.
233. Abou-Gharbia, M.; Patel, U. R.; Webb, M. B.; Moyer, J. A.; Andree, T. H.; Muth, E. A. *J. Med. Chem.* **1988**, *31*, 1382-1392.
234. Torres, E.; Leiva, R.; Gazzarrini, S.; Rey-Carrizo, M.; Frigolé-Vivas, M.; Moroni, A.; Naesens, L.; Vázquez, S. *ACS Med. Chem. Lett.* **2014**, *5*, 831-836.
235. Vázquez, S.; Leiva, R.; Valverde, E. PCT Patent Application, PCT/EP2017/059178, 2017.
236. Boyle, C. D.; Kowalski, T. J. *Expert Opin. Ther. Patents* **2009**, *19*, 801-825.
237. Puigoriol-Illamola, D.; Vasilopoulou, F.; Griñan-Ferre, C.; Leiva, R.; Vázquez, S.; Pallàs, M. Neuroprotective effect of RL-118, an 11b-HSD1 inhibitor: implication in autophagy and inflammaging processes in SAMP8 mouse model. *Neuropharmacology* (submitted).
238. Leiva, R.; Griñan-Ferré, C.; Seira, C.; Valverde, E.; McBride, A.; Binnie, M.; Pérez, B.; Luque, F. J.; Pallàs, M.; Bidon-Chanal, A.; Webster, S. P.; Vázquez, S. *Eur. J. Med. Chem.* **2017**, *139*, 412-428.
239. Leiva, R.; McBride, A.; Binnie, M.; Webster, S. P.; Vázquez, S. Exploring *N*-acyl-4-azatetracyclo [5.3.2.0<sup>2,6</sup>.0<sup>8,10</sup>]docec-11-enes as 11β-HSD1 inhibitors. *Bioorg. Med. Chem.* (submitted).
240. Boudon, S. M.; Geotti-Bianchini, P.; Heidl, M.; Jackson, E.; Schlifke-Poschalko, A. WO Patent Application, WO2017012890, 2017.
241. Boudon, S. M.; Vuorinen, A.; Geotti-Bianchini, P.; Wandeler, E.; Kratschmar, D. V.; Heidl, M.; Campiche, R.; Jackson, E.; Odermatt, A. *PLoS ONE* **2017**, *12*, e0171079.
242. Wang, H.; Ruan, Z.; Li, J. J.; Simpkins, L. M.; Smirk, R. A.; Wu, S. C.; Hutchins, R. D.; Nirschl, D. S.; Kirk, K. V.; Cooper, C. B.; Sutton, J. C.; Ma, Z.; Golla, R.; Seethala, R.; Salyan, M. E. K.; Nayeem, A.; Krystek, S. R.; Sheriff, S.; Camac, D. M.; Morin, P. E.; Carpenter, B.; Robl, J. A.; Zahler, R.; Gordona, D. A.; Hamann, L. G. *Bioorg. Med. Chem. Lett.* **2008**, *18*, 3168-3172.